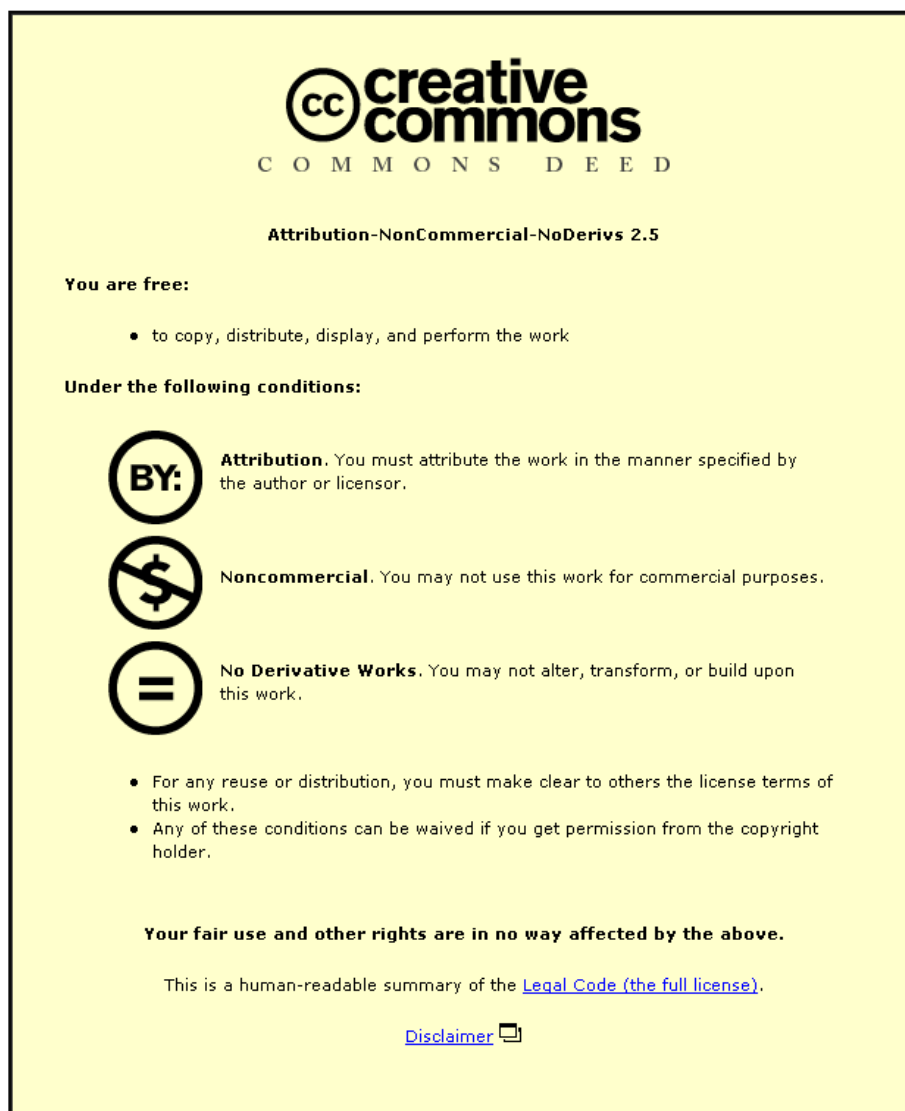


This item was submitted to Loughborough University as a PhD thesis by the author and is made available in the Institutional Repository (<https://dspace.lboro.ac.uk/>) under the following Creative Commons Licence conditions.



For the full text of this licence, please go to:
<http://creativecommons.org/licenses/by-nc-nd/2.5/>

**ALTERNATIVE FILTER MEDIA IN RAPID GRAVITY
FILTRATION OF POTABLE WATER**

By

PHILLIP D. DAVIES

A Doctoral Thesis Submitted in Partial Fulfillment of the Requirements for the
Award of Doctor of Philosophy of Loughborough University

June 2012

© By Phillip D. Davies (2012)

1 ABSTRACT

Sand has been the main filter media used in rapid gravity filtration since their emergence in the 19th century. This dominance is due to its low cost, availability and extensive experience which has led to dependable and predictable performance. Over recent years multi-media filters have become the typical filter arrangement. Sand still remains the preferred filter medium in the lower layer with typically anthracite used in the upper layer.

A limitation to match previous work has been the emphasis on overall performance but mechanistic analysis as to the reasons for the variations compared to sand has been rare. The fundamental effects of particle size and consolidation on filtration performance and headloss are known but were not often accounted for in the reported research. This has limited the academic contribution of previous work and made it more difficult to compare with the data for this thesis.

At an average treatment works the highest costs are associated with the use of chemicals (30 %) and power (60 %) required mainly for pumping. Rapid gravity filters are one of the least energy demanding stages in this system, only requiring pumping for backwashing and air scour, assuming gravity feed was incorporated into the design.

Energy efficiency of water treatment has become more important and the research was conducted to determine if the use of novel new media could be used to improve the performance of the filters with regards to turbidity and headloss. For example, the result presented within this thesis demonstrates through the use of angular media improved performance to benefit both turbidity and headloss performance. This was obtained from slate having a sphericity of 0.49 compared to sand at 0.88.

In addition the use of novel materials with different physical properties has allowed an extension to analysis of performance using fundamental filtration mechanisms. The greater range of properties available from the novel media used in this thesis compared to sand has suggested additions to this theory. The use of surface reactive materials, including limestone, has shown the removal of additional contaminants such as phosphorus, iron, aluminium and manganese not typically associated with rapid gravity filtration. An assessment of the impact these reactions had on typical filter performance criteria, for

example turbidity, headloss and life expectancy. The results showed an 97 % removal of Fe in the limestone compared to 13 % for sand. This was brought about by the precipitation of hydroxide, coagulation, a pH change and consequent co-precipitation. In the case of iron and aluminium removal this pH induced change was theorized as the most likely cause of coagulation within the filter bed itself leading to improved turbidity removal performance.

Filter media chosen for laboratory and pilot study in this work was firstly assessed using British Standards tests, but additional tests were added that could provide additional characterisation data. The media were selected based on an individual fundamental property that differed from the other media selected whilst retaining the standard RGF size. Filtralite for example offered a high surface area, limestone a more active surface and slate a plate-like particle shape. Glass had a very smooth surface texture and as a recycled material better sustainability. Four of these filter media (Sand (control), Glass, Filtralite and Slate) were then selected for further on-site pilot plant studies, based on results from the laboratory work.

Both the laboratory and pilot study suggested that turbidity and headloss performance could be improved by changes in media specification. The results showed that after particle size, angularity of the media was the most important factor affecting turbidity and headloss performance. A greater angularity led to improvements in filter run time with for example a doubling of filter run time with the slate compared to sand for the same turbidity removal in the pilot plant. Previous literature had suggested an improvement in turbidity performance but that head loss would deteriorate but this was not seen in the data from this research, with slate (sphericity of 0.49) offering improved headloss performance. This improvement was attributed to the varied packing of the filter bed and associated porosity variations throughout the filter.

The objectives of the pilot study were to provide understanding of scale-up factors and adjust these theories with real variable clarified water. Real water chemistry is too complex to model and enabled experiments more typical of the variation that a rapid gravity filter would encounter. The pilot plant is 0.07 % the plan area of a full scale filter compared to the 0.01 % of the laboratory columns. Results corroborated the laboratory work on the effect of extreme particle shapes on filter performance.

The pilot study also highlighted problems from floc carry over with the use of clarified water and quantified the impact it had on filtration performance. In this case floc carryover changed the performance of the pilot plant results significantly. Thus an overall conclusion from the work was that an integrated design approach to filters, to account for the clarifier type the likelihood of floc carryover and raw water anticipated could be further researched. There were also limitations to the current monitoring equipment that could not quantitatively measure the floc carryover because of large particle size.

CONTENTS

1	Abstract	1
2	Acknowledgements	7
3	Introduction	14
4	Literature Review	18
4.1	Studies on Alternative Filter Media	18
4.1.1	Pumice	20
4.1.2	Glass	27
4.1.3	Expanded Aluminosilicate (Filtralite®)	39
4.1.4	Limestone	53
4.1.5	Other	59
4.2	Filtration Mechanisms	61
4.2.1	Particle Transportation	63
4.2.2	Attachment Mechanisms	68
4.3	Analysis and Objectives	74
5	Media Characterisation Results and discussion	76
5.1	Density	77
5.1.1	Theory	77
5.1.2	Testing	81
5.2	Sphericity and Particle Shape	82
5.2.1	Theory	82
5.2.2	Testing	83
5.3	Particle Size Distribution	85
5.3.1	Theory	85
5.3.2	Testing	88
5.4	Bed Porosity	97
5.4.1	Theory	97
5.4.2	Testing	99
5.5	Friability and Mechanical Durability of Media	102
5.5.1	Theory	102
5.5.2	Testing	105
5.6	Acid Solubility	106

5.6.1	Theory.....	106
5.6.2	Testing	109
5.7	Surface Area Determination.....	112
5.7.1	Theory.....	112
5.7.2	Testing	115
5.8	Scanning Electron Microscopy (SEM).....	117
5.8.1	Sand	118
5.8.2	Glass.....	119
5.8.3	LimestoNe.....	121
5.8.4	Filtralite.....	122
5.8.5	Slate	124
5.8.6	Steel and Furnace Slag.....	125
5.8.7	Phosphorus Slag	126
5.8.8	Pumice (Techfil [®]).....	126
5.8.9	Pumice (Pumex [®])	127
5.9	Batch Adsorption Testing	128
5.9.1	Methodology	128
5.9.2	Testing	129
5.10	Initial Characterization recommendations.....	137
6	Laboratory Scale Trials	139
6.1	Raw Water.....	140
6.2	Filter Bed Specifications	143
6.2.1	Supporting Media	143
6.2.2	Filter Media	146
6.3	Apparatus	148
6.3.1	Raw Water Storage and Delivery.....	149
6.3.2	Filter Columns.....	151
6.3.3	Pressure ports.....	158
6.4	Filter Run Results.....	162
6.4.1	Steady State Turbidity	166
6.4.2	Headloss	180
6.4.3	Backwashing	188

6.5	Summary and Conclusions	190
7	Pilot Scale Trials.....	194
7.1	Methodology	194
7.1.1	Water Treatment Works.....	194
7.1.2	Pilot Plant	197
7.1.3	Clarified Water Quality	200
7.1.4	Mudballing + Backwashing	205
7.2	Results	207
7.2.1	Summary of Testing.....	207
7.2.2	Turbidity Removal.....	209
7.2.3	Headloss	212
7.2.4	Analysis	220
8	Summarising Discussion and Conclusions	224
9	Further Work.....	227
10	References.....	229

2 ACKNOWLEDGEMENTS

Firstly, I would like to thank my supervisor Professor Andrew Wheatley who has supported me throughout the project. I am grateful for his guidance on the topic of my PhD and also the wealth of additional knowledge I was provided with, sometimes without requesting it on a broad range of subjects. Thanks also to Christine Barton for organizing Andrew's time so well that he was always available when I needed his time to query another idea.

My thanks go out to all the technicians in the civil engineering laboratories at Loughborough for their contributions both great and small. More specifically, I would like to thank both Mick Barker and Mick Shonk for their assistance in constructing the equipment, without their skills and advice I would have made very slow progress. In addition, I must thank Geoffrey Russell and Jayshree Bhuptani for their help in sample analysis, general advice and their often interesting conversation. Thanks must also go to the technicians over in materials engineering for their analysis of samples and answering any questions I had.

Thanks go to Severn Trent Water for allowing me access to one of their sites to carry out a pilot study, and especially to Bernadette Ryan, Jessie Roe, Lizz Brookes, Keiron Maher, Mick Carvell and the numerous operators on site who offered assistance and guidance throughout the project. Also thanks to those who have helped and taken an interest in my work from United Utilities and especially to David Watson.

Thanks also to my co-workers in the hub who constantly ensured I never got too far ahead of myself and the members of the cycling club who made sure I was sufficiently distracted from work to never get too stressed. For those I have not mentioned I offer simple thanks.

Figure 1 - Head loss and Turbidity removal charts from Farizoglu et al (2002)	22
Figure 2 - Typical turbidity (a) and headloss (b) curves from pilot plant study	24
Figure 3 - Expanded bed height versus backwash velocity (initial bed height of 104 cm) from Soyer et al (2010)	28
Figure 4 - Sieve analysis of sand and glass from Rutledge and Gagnon (2002)	30
Figure 5 - Scanning electron microscopy imaging of sand (a) and glass (b) by Rutledge and Gagnon (2002).....	31
Figure 6 - Pilot plant process stream - filtration mode from Evans et al (2002).....	32
Figure 7 - Particle counts for a filter run in the crushed glass summer period from Rutledge and Gagnon (2002)	35
Figure 8 - Particle counts from a filter run in the sand filter summer period from Rutledge and Gagnon (2002)	35
Figure 9 - Average size distribution of effluent particles from the crushed glass and silica sand (error bars represent one standard deviation) from Rutledge and Gagnon (2002)	36
Figure 10 - Log removal of total particle counts for the sand and crushed-glass filter from Rutledge and Gagnon (2002).....	36
Figure 11 - Effect of filtration rate on headloss accumulation rate from Evans et al (2002).....	37
Figure 12 - Head loss and bed expansion data from crushed green glass (0.5 - 1.0 mm) from Fitzpatrick (2005)	38
Figure 13 - Comparison of settling velocity of filter materials from Eikebrokk & Saltnes (2001).....	42
Figure 14 - Comparison of particle size distribution after filter operation from Eikebrokk and Saltnes (2001)....	43
Figure 15 - Turbidity results from Saltnes et al (2002) – F1 (Filtralite), F2 (Anthracite/Sand), F1+ (Filtralite at deeper bed depth)	44
Figure 16 - Head loss build-up in filters from Mitrouli et al (2009)	48
Figure 17 - Turbidity removal efficiency through filtration beds made of LCA 0.5/3 mm sieved fraction and variable depth (L); Co = 42 - 44.7 NTU, flow rate = 4.43 m/h from Albuquerque & Labrincha (2008).....	50
Figure 18 - Turbidity removal efficiency through filtration beds made of LCA 0/3 mm sieved fraction and variable depth (L); Co = 37 - 58 NTU, variable flow rate from Albuquerque & Labrincha (2008).....	50
Figure 19 - Turbidity removal efficiency through filtration beds made of LCA 0/0.5 mm sieved fraction with variable depth (L); Co = 37 - 48.3 NTU, variable flow rate from Albuquerque & Labrincha (2008)	51
Figure 20 - Comparison of turbidity removal for flow rate of 4.43 m/h and bed depth of 30 form data in Albuquerque & Labrincha (2008).....	51
Figure 21 – Turbidity, TS and TSS removal in basalt, dolomite and calcite roughing filters from Rooklidge et al (2002).....	54
Figure 22 – Configuration of Spraystab unit from Mackintosh & de Villiers (1999)	56
Figure 23 - Relationship of particle size pore size from Ives (1987)	64
Figure 24 - Diagram of electrostatic force acting around a colloid Zeta Meter Inc (1997).....	70
Figure 25 - Change in ion concentration and charge density (Zeta Meter Inc. (1997))	71
Figure 26 - Change in Zeta Potential with distance (Zeta Meter Inc. (1997))	72

Figure 27 - Sphericity of tested media	84
Figure 28 - Particle Size Distribution of Sand (0.5 – 1.0 mm)	89
Figure 29 - Particle Size Distribution of Glass (0.7 – 1.0 mm)	89
Figure 30 - Particle Size Distribution of Limestone (0.6 – 1.2 mm).....	90
Figure 31 - Particle Size Distribution of Filtralite (0.8 – 1.6 mm)	91
Figure 32 - Particle Size Distribution of Slate (0.425 – 1.4).....	92
Figure 33 - Particle Size Distribution of Pumice (Pumex) (0.4 – 1.4 mm)	92
Figure 34 - Particle Size Distribution of Pumice (Techfil) (0.4 – 1.0 mm).....	93
Figure 35 - Particle Size Distribution of Steel Slag (0.5 – 1.0 mm)	94
Figure 36 - Particle Size Distribution of Furnace Slag (0.5 – 1.0 mm)	94
Figure 37 - Particle Size Distribution of Phosphorus Slag (0.5 – 1.0 mm)	94
Figure 38 - Overall comparison of Particle Size Distribution curves from all media.....	96
Figure 39 - Small backwashing rig for cleaning small amounts of media for laboratory testing	99
Figure 40 - Micrometrics Tristar 3000 BET surface area and porosimetry analyzer.....	115
Figure 41 - Specific Surface Area results for all filter media	116
Figure 42 - Carl Zeiss (Leo / Cambridge) Stereoscan 360 SEM.....	118
Figure 43 - SEM image of Sand at 85x, 500x and 1500x magnification	118
Figure 44 - SEM image of Glass at 85x, 500x and 1500x magnification	119
Figure 45 - SEM image of Limestone at 80x, 500x and 1500x magnification	121
Figure 46 - SEM image of Filtralite at 80x, 500x and 1500x magnification	122
Figure 47 - Image showing effect of particles surface on flow around media.....	123
Figure 48 - SEM image of Slate at 80x, 500x and 1500x magnification	124
Figure 49 - SEM image of Steel Slag at 90x, 500x and 1500x magnification.....	125
Figure 50 - SEM image of Furnace Slag at 110x, 500x and 1500x magnification	125
Figure 51 - SEM image of Phosphorus Slag at 85x, 500x and 1500x magnification.....	126
Figure 52 - SEM image of Pumice (Techfil) at 85x, 500x and 1500x magnification	126
Figure 53 - SEM image of Pumice (Pumex) at 85x, 500x and 1500x magnification	127
Figure 54 - Chart showing the amount of each metal removed per unit mass of media	130
Figure 55 - Chart of Aluminium (Al) removal for each filter media in batch adsorption tests	131
Figure 56 - Log concentration charts for both ferric-iron and alum species	132
Figure 57 - Chart of Iron (Fe) removal for each filter media in batch adsorption tests.....	133
Figure 58 - Chart of Manganese (Mn) removal for each filter media in batch adsorption tests	134

Figure 59 - Chart of Phosphorus (P) removal for each filter media in batch adsorption tests	135
Figure 60 - Particle Size Distribution of kaolin solution at different settlement times.....	142
Figure 61 - Supporting media in laboratory filter columns.....	145
Figure 62 - Photograph of filter columns and associated pipework	148
Figure 63 - Raw water storage tank showing delivery pump and mixing system.....	149
Figure 64 - Constant head tank internal (a) and connecting pipework (b).....	150
Figure 65 - Filter columns in place with media installed	152
Figure 66 - Filter column top-section design drawing	154
Figure 67 - Filter column section joint flange layout (a) and top cap design (b) diagrams.....	155
Figure 68 - Filter column middle section showing the location of pressure ports along its length.....	156
Figure 69 - Filter column bottom-section	157
Figure 70 - Pressure transducer and air removal loop.....	159
Figure 71 - Diagram of pressure port design	160
Figure 72 - Images of pressure port on filter column	160
Figure 73 - Variation in turbidity removal with flow rate for all media at 9 NTU	166
Figure 74 - Variation in turbidity removal with flow rate for all media at 35 NTU.....	167
Figure 75 - Difference in interaction of flow streams between angular and spherical filter media.....	169
Figure 76 - Summary results for turbidity removal from an initial concentration of 9 NTU at a flow rate of 8.6 m/h	170
Figure 77 - Chart showing variation of retention time relative to flow rate (m/h) and porosity	173
Figure 78 - Chart showing variation in filter performance (C/C_0) against retention time	175
Figure 79 - Retention time and C/C_0 relationship with Filtralite results included	177
Figure 80 - Diagram of contact between three spherical filter media grains	178
Figure 81 - Relationship between particle sizes and void areas between contacting spherical filter media grains	179
Figure 82 - Initial headloss for various flow rates at a raw water turbidity of 9 NTU.....	181
Figure 83 - Initial headloss for various flow rates at a raw water turbidity of 35 NTU.....	181
Figure 84 - Head loss accumulation at 9 NTU for various flowrates.....	184
Figure 85 - Head loss accumulation at 35 NTU for various flowrates.....	185
Figure 86 - Relationship between initial headloss and sphericity.....	186
Figure 87 - Relationship between bed expansion and backwash flowrate	188
Figure 88 - Change in TSS during backwashing	189
Figure 89 - Raw water sources to water works.....	195

Figure 90 - Water works treatment train.....	196
Figure 91 - Image and diagram of pilot plant design	198
Figure 92 - Re-design of de-bubbler on pilot plant.....	200
Figure 93 - Floc entering the pilot plant filter columns	202
Figure 94 - View of glass and sand saturated by iron in the upper layer, other media are darker and so mat is less visible	203
Figure 95 - Floc shown above the sludge blanket.....	204
Figure 96 – Mudballs settled at the base of the filter column.....	205
Figure 97 - Overview of turbidity results for packed bed pilot trials	210
Figure 98 - Overview of turbidity results for un-packed bed pilot trials.....	211
Figure 99 - Example of turbidity variation during test run 12	212
Figure 100 – Example of flowrate change after 2000 mm headloss during test 13	213
Figure 101 - Overview of initial headloss results for packed bed pilot trials.....	214
Figure 102 - Overview of initial headloss results for un-packed bed pilot trials.....	215
Figure 103 – Example headloss variation during filter test run 12	217
Figure 104 - Filter run-time results for packed bed pilot trials.....	218
Figure 105 - Filter run-time results for un-packed filter bed pilot trials.....	218
Figure 106 - Relationship between initial headloss and retention time for packed bed trials	219
Figure 107 - Impact of sphericity on rate of change in initial headloss	220
Table 1 - Summary of results from pilot plant column during summer period from Ghebremichael (2004)	23
Table 2 - Summary of results from pilot plant column during summer period from Ghebremichael (2004)	24
Table 3 - Attrition loss of pumice and expanded slate after 50 h backwashing from Morgeli & Ives (1979).....	26
Table 4 - Filter media configurations compared in testing from Evans et al (2002).....	29
Table 5 - Particle size parameter comparison.....	30
Table 6 - Feed water quality summary from Evans et al (2002)	32
Table 7 - Summary of pilot plant runs undertaken from Evans et al (2002).....	33
Table 8 - Typical turbidities and particle counts during pilot testing from Evans et al (2002)	34
Table 9 - Comparison of media and bed depth	40
Table 10 - Comparison of filter media and bed depth.....	41
Table 11 - Parameters of raw water from Mitrouli et al (2009)	45
Table 12 - Filter media properties from Mitrouli et al (2009).....	46

Table 13 - Measured parameters at various run criteria from Mitrouli et al (2009)	47
Table 14 - Raw and effluent water quality at sites A and B from Mackintosh & de Villiers (1999)	57
Table 15 - Selected filter media for characterization testing.....	76
Table 16 Range of densities for materials covered in British Standards for approved filter media	79
Table 17 Specific densities for a range of filter media from Ives (1990)	79
Table 18 - Values for bulk density packed of tested filter media	81
Table 19 - Specific Particle Density for media as tested according to Ives (1990).....	82
Table 20 - Tested settling velocity of media grains tested according to the procedure of Ives (1990).....	83
Table 21 - Particle Size Properties found for all media	95
Table 22 - Values for bed porosity of filter media used in laboratory scale experiments.....	100
Table 23 - Porosity values for a range of media tested by previous authors (UC – Unconsolidated)	100
Table 24 - Limits for guidance on friability from Degremont (1979)	103
Table 25 - Results of tests carried out by Suthaker et al (1995) on friability.....	104
Table 26 - Results for attrition testing of filter media	105
Table 27 - Acid solubility limits from British Standards	107
Table 28 - Acid solubility test results based on BS EN 12902:2004	109
Table 29 - Flow rates used in laboratory scale testing.....	140
Table 30 - Previous studies using synthetic water for filtration studies.....	140
Table 31 - Particle size gradation for supporting media from Kawamura (2000).....	144
Table 32 - Filter media bed depth specifications from Kawamura (2000).....	146
Table 33 - Sampling frequency used during laboratory scale testing.....	163
Table 34 - Parameters altered for each test carried out in laboratory filter columns.....	163
Table 35 - Summary of results for lab testing of the 9 NTU suspensions, showing average turbidity vales	164
Table 36 - Summary of results for lab testing of the 35 NTU suspensions, showing average turbidity vales	165
Table 37 - Turbidity removal performance change with flowrate from Figure 73	168
Table 38 - Turbidity removal performance in laboratory scale testing	168
Table 39 - Retention time related to flow rate and bed porosity of various filter media	171
Table 40 - Comparison of calculated values of initial headloss against test results	182
Table 41 - Clarified water turbidity values fed to the unpacked filter beds	201
Table 42 - Initial backwashing procedure	205
Table 43 - Backwashing procedure used during trials	206

Table 44 – Overview of results from all packed bed testing (C1 – Slate, C2 – Filtralite, C3 – Glass and C4 – Sand)	207
Table 45 - Overview results from all settled bed testing (C1 – Slate, C2 – Filtralite, C3 – Glass and C4 – Sand).	208
Table 46 - Comparison of initial headloss between laboratory and pilot studies at approx. 8.6 m/h.....	214
Equation 1 - Equation to determine interception parameter between particles and filter media from Ives (1970)	64
Equation 2 - Equation for calculating bulk density from BS EN 12902:2004	78
Equation 3 - Equation to determine ratio of C_D/Re from Ives (1990)	84
Equation 4 - Determination of porosity of the filter bed.....	97
Equation 5 - Calculation of percentage loss of media from Degremont (1979)	103
Equation 6 - Mass fraction equation for acid solubility	107
Equation 7 - Calculation of bed depth from Kawamura (2000)	146
Equation 8 - Equation for calculating retention time in the filter bed	172
Equation 9 - Trend line equations for C/C_o against retention time from test data	175
Equation 10 - Retention time equation (Equation 8) substituted into Equation 9.....	175
Equation 11 - Equation showing variation in filter performance related to retention time in the filter bed.....	176
Equation 12- Carman-Kozeny Equation from McCabe et al (2004)	182

3 INTRODUCTION

Rapid gravity filtration (RGF) has been in use since the 1880s and was developed into a widely adopted and generic treatment process in the 1920s. Hendricks (2005, p. 529) gives one of the most comprehensive overviews of the history and development of rapid gravity filtration from its inception to modern practice. Throughout the history of its use rapid gravity filtration has been combined with solid/liquid separation processes by coagulation, flocculation and subsequent settlement (or flotation) with iron or aluminium salts. In recent times large molecular weight charged polymers have also been used to aid in solids removal and this will have an impact on the filters (See sections 7.1.3 & 7.1.4).

Rapid gravity filtration as part of a treatment train is currently the most widespread type of filtration used in drinking water processes that supply most major populations with safe drinking water. RGF processes play a vital role in removing micron sized particles, the most common size of bacterial pathogens. RGF is used to improve water quality to produce safe, clean drinking water. In recent times drinking water standards have become more stringent, leading to the addition of new processes such as granular activated carbon (GAC) for pesticides removal, intermediate ozone to remove soluble ammonia, nitrate and deal with cryptosporidium. RGF is seen as a process that can be optimized to deal with these contaminants reducing the need for additional costly and energy intensive processes. The literature review will establish that filtration is a low energy process, and improvements made to rapid gravity filtration performance can lead to quality benefits where cryptosporidium is the main risk, but also there are possible benefits through reducing the dependence on other processes such as chemical coagulation and GAC.

Rapid gravity filtration has seen little development over the last 90 years, with the main areas for change being the use of dual or multi-media filters. Dual-media filtration using anthracite above sand only became widespread during the 1960's (McNamee et al, 1956). The use of garnet as a third layer creating a multi-media filter also became more common during this time. These developments allowed the filters to treat at higher hydraulic loading rates of up to 12.24 m/h and sometimes higher flowrates. The coarser anthracite removed the residual floc that remained after settlement, while finer particles passed through into the finer sand media that was more susceptible to clogging, this led to longer runtimes.

Anthracite was selected as its lower density allowed for it to consistently settle back into a segregated upper layer after backwashing. Other problems noted by the early pioneers in filtration which were described as follows taken from Hendricks (2000):

- Maintaining effective coagulation
- Lack of laboratory control
- Education of operators
- Under-drain design
- Inadequate backwash design associated with control of mudballs and surface cracking

Surface wash techniques in addition to standard backwashing were developed by Baylis after it was observed that clogging predominantly occurred in the upper 150 mm of the filter bed. This would be expected if there was residual floc present in the water after clarification, and if the sedimentation process was not totally effective the floc would enter the filters leading to a number of problems listed above. These problems associated with rapid gravity filtration identified in its early days remain to this day. There has been research conducted into improving backwashing to attempt to alleviate a number of these but in practice filters still exhibit the same problems as this research confirms (see section 7.1.4). Problems with floc carryover from clarification highlight the need for further development to increase the performance of coagulation which can have a significant impact on filter performance. More practical research into rapid gravity filtration could potentially lead to small changes in operation but give improved magnitudes of performance. For example, research concentrating on backwashing of filters has often been limited to pilot studies and when applied to full scale filters the hydraulics lead to variations that cause operational problem. This highlights problems with using laboratory and pilot scale experiments when testing these aspects of filtration and in applying findings to scale-up.

The purpose of this thesis is to describe the research undertaken to investigate the use of alternative filter media. Improving filter performance was the aim, while also linking these changes in performance to the mechanisms. Through this method it is possible to contribute to fundamental knowledge on filtration, and understand variations between novel new media and sand. This work includes controlled laboratory scale tests of the media followed

by a pilot scale study carried out at a local water treatment works to apply theories gained from the laboratory study to the variability expected in coagulated/flocculated water.

In reporting the work this thesis has used findings from the physical characterization of the filter media compared against filter theory to form the basis of the conclusions drawn from the results found in the laboratory and pilot studies. Chapter two presents a review of previously published research of alternative filter media. This was to help design the experiments and highlight the knowledge gaps in the use of possible alternative media. A number of alternative filter media studies were found, including both at laboratory and pilot scale with a wide range of different water types. The research was however limited in number and scope as often the work does not attempt to detail the influence of fundamental properties of the filter media on performance. Typically papers attempt to present data comparison of the new media to sand. The review includes literature concerning the fundamental mechanisms of filtration used to discuss the performance to be related to the linked fundamental properties of the media. By understanding what properties of a filter media impact positively on filtration performance a greater understanding of what properties should enable better media design and appropriate experimental procedure can be gained.

Chapter three presents the results from characterization testing of the chosen filter media, these tests are used to determine the differences between the filter media that would lead to variances in performance. Testing was chosen based on the requirements of current filter media standards and also through consideration of the fundamental mechanisms and what properties would impact on these. Results were compared with previous findings where available to corroborate the conclusions. From these results five filter media were chosen to be tested in the laboratory scale filter columns.

Chapter four describes the laboratory scale testing of the filter media. These experiments were conducted under controlled conditions to allow for detailed comparison of the filter media and to understand how the variation in the properties of the media impacted on the fundamental mechanisms of filtration. The chapter details the design and development of the apparatus and the methods of the operation, this is followed by an analysis of the results and conclusions based on the observations carried out and how they impact on filter

practice. The conclusions from this chapter were then used to guide the scale up studies carried out in the pilot plant.

Chapter five presents the details of the pilot plant study carried out at a local water treatment works. The section details the issues that arose from the use of filters with real clarified water and the impact this had on filter performance. Results are compared with the conclusions found from the laboratory testing and any variations in performance between the two are discussed and explained. The impact of alternative filter media on the performance of the filters is discussed and the implications of changing to alternative media for water treatment works are investigated.

Chapter six presents the final summarising discussion and conclusions from all the studies carried out and makes recommendations for future research in the field and considerations for changes to accepted filter practice. The appendices contain the raw data and statistics with other associated relevant experimental results; some data sets e.g. from the on-line monitoring were too large and are not included in the thesis but can be requested from the author if required.

There have been two conference papers and a refereed journal paper published in Water Science and Technology output from this thesis so far.

4 LITERATURE REVIEW

Additional literature was encountered concerning waste water treatment, membrane filtration and from water filtration applied to Geotechnics. For example a wide variety of alternative media, mainly plastic, have been used for waste water treatment, but in these cases the mechanisms are mainly biological via biofilm formation and these have been excluded from critical review. Membrane processes are also now widely used for drinking water treatment; however these cases rely on sieve or pore size filtration not the deep bed mechanisms associated with rapid gravity filtration and therefore these were not reviewed. There is also geotechnical literature covering infiltration through gravels, sands and geotextiles. These sources do include some discussion of materials and mechanisms associated with rapid gravity filtration and examples have been reviewed. The literature directly associated with rapid gravity filtration of potable water is given in the following section. It is divided into overviews of current best practice, media size and shape and the current state of research into alternative media. The literature outlining the current understanding of the fundamental mechanisms directly applicable to RGF in potable drinking water treatment are also discussed.

4.1 STUDIES ON ALTERNATIVE FILTER MEDIA

There has not been a great deal of research into possible alternative filter materials for use in rapid gravity filtration of drinking water, therefore work carried out in other areas including the food industry, wastewater treatment and pre-treatment for multiple applications as well as alternative filtration methods were considered. Although these are not specifically drinking water treatment, the work will offer further information on the possible mechanisms involved in filtration and aid in developing the basic theory to validate the variations in performance of the filter media. In some cases the work was duplicating or did not offer any further understanding towards rapid gravity filtration of drinking water and was not included in the literature review. Some research papers were limited to simple reports on their solids removal, but due to the limited research availability were included in the literature review.

Sand has been the predominant filter media used in filtration since slow sand filters were initially designed by John Gibb in 1804 (Baker 1948) and finally implemented into drinking

water treatment in 1829 (Huisman & Wood, 1974). When Rapid Gravity Filtration came to prominence in the United States from 1896 (EPA 1990), sand was the predominant filter media and has remained so ever since although there have been attempts to find suitable alternatives. An example is pumice in Turkey and Italy. Recycled glass which is both robust and available in small enough sizes has also been used as possibly a more sustainable source.

Currently the specificity of the standards for filtration media requires very specific high quality silica sand which limits the use of alternative sands from other parts of the world. There was a recent case study (from personal communication with UKFilters) of rebuilding work in Iraq installing a number of pressure filters where importation of media was not practical. The sand media present in the local area was not suitable based on current standards due to additional calcium carbonate content which increased its solubility. $\text{Ca}(\text{CO}_3)_2$ was derived from the geology of the region originally from the bed of a large seawater body. The media failed on acid solubility and was deemed unsuitable for filtration. A great deal of effort would be required to remove the offending calcium carbonate. This is an extreme case that highlights how a variation in the quality of sand can lead to a great deal of problems, the original standards are based on a high silica content which is very robust over long periods of time. In the UK this type of sand is supplied by Garside Sands (Leighton Buzzard) to the UK filter market. A broader spectrum of standards associated with filter media would allow for innovative use of novel new media that may possibly lead to performance enhancements through energy/cost reduction and water quality improvements. Any improvements may also impact on the requirements of other treatment processes such as reduced chemical coagulation demands based on an improvement in solids removal in filters.

Sand has remained in this position through prolonged use in filtration, leading to a great deal of data available and confidence in its performance. However with changing requirements such as for cryptosporidium and persistent organic pollutants (POPs) removal and the higher costs of chemical coagulants and polymers a revisiting of sand should be carried out as well as the possibility of improving the standards. When building a filter into a new works design it is still considered best practice to carry out a pilot trial given the capital cost involved to determine the most suitable filter arrangements to provide suitable performance. The current media standards limit the possibility of innovation in this area by utilities hindering

further developments of a key treatment process. Further research is therefore required to drive innovation and provide proof that there is a benefit to pursue a better filter performance through an inclusion of novel media in filter media standards and best practice. If new media are to be embraced by industry and considered as suitable alternatives to sand then further research and development is required to drive forward the idea that innovation into rapid gravity filtration is worth pursuing within industry leading to new technologies and ideas.

4.1.1 PUMICE

Pumice is a textural term for a volcanic rock that is solidified frothy lava, typically created when super-heated, highly pressurized rock is violently ejected from a volcano. The characteristic properties of pumice, lightness and porous structure, are formed due to the simultaneous actions of rapid cooling and rapid depressurization. The depressurization creates bubbles by lowering the solubility of gases dissolved in the lava which rapidly exsolve. Simultaneous rapid cooling then traps these bubbles in the matrix of the pumice to form a sponge like structure.

Two of the main world suppliers of pumice are Italy and Turkey, which according to Farizoglu et al (2003) have a 44% and 9% share of the market respectively. This information poses some problems with regards to the use of pumice in filtration as it limits its availability to geologically active areas of the world increasing transport costs and reducing sustainability.

The internal structure of the pumice is irregular or oval shaped pores that are not usually connected to each other according to Farizoglu et al (2002), while Ghebremichael (2004) states that the pores can vary in size and form depending on the composition and extent of entrapped gas. Some types of pumice are characterized by elongated, tubular parallel vesicles, whereas others have more spherical cavities. Ghebremichael (2004) also states that when the vesicles are open and interconnected the pumice becomes easily water logged and sinks in water.

These two papers show that there is significant variation in the structure of pumice and to truly determine the basics affecting performance, trials would need to be conducted on a range of different types to understand the influence of pore structure. The structure of the

pores within the pumice can be studied by Scanning Electron Microscopy (SEM) which will show whether the pores are interconnected or not and if this will lead to problems of floating and also a reduced surface area as only the open external surface is available for attachment.

Ghebremichael (2004) considered the pumice to be an alternative to anthracite that is used in dual and multi-media filters and therefore the particle size of the pumice (Effective Size ES = 1.1 mm, Uniformity Coefficient UC = 1.6) reflects that closely matches that of the anthracite used (ES = 1.0 mm, UC = 1.42). In contrast Farizoglu et al (2002) considered the pumice as an alternative to sand, with a grading of 0.5 – 1.0 mm which is typical of rapid gravity filtration systems (Hendricks, 2005). Farizoglu et al (2002) looked at three gradings of pumice from Erciş, Turkey (0.5 – 1.0 mm, 1.0 – 2.0 mm and 2.0 – 5.0 mm).

Results for the pumice at the grading of 0.5 – 1.0 mm by Farizoglu et al (2002) give results that enable comparative performance to be measured independently of the particle size. Ghebremichael (2004) considered pumice as an alternative to anthracite and therefore its particle size was higher than that of the 0.5 – 1.0 mm typical for sand, as noted but the data could be comparable to the 1.0 – 2.0 mm results from Farizoglu et al (2002).

Ghebremichael (2004) does not provide any information on the influent water used in the laboratory scale trials and also there are no detailed results from these tests aside from the assertion that the results showed pumice to be a suitable alternative to anthracite. It was noted that the influent water was from the sedimentation tanks at Stretta Vaudetto, but no details of water quality.

Farizoglu et al (2002) used a 100 mm diameter, 1350 mm high Perspex column, within which the media was supported by 0.35 mm gauze above a stainless steel mesh. Ghebremichael (2004) had a larger diameter column of 120 mm but a shorter length of 500 mm, but in addition studies were conducted in a pilot plant using 200 – 250 mm diameter 2000 mm long columns at Stretta Vaudetto treatment works, Italy. Within the pilot plant columns a 100 mm bed of graded gravel was used as a bedding material to support the filter media,

Farizoglu et al (2002) prepared a controlled influent from mixing 26 g of clay with 350 l of clean water. The properties of this suspension aside from the turbidity (29 – 31 NTU) are not given in the paper and therefore it cannot be precisely reproduced. The feed suspension was

fed into the filter columns by a pump followed by a rotameter flow meter. Ghebremichael (2004) again does not give details of the method of rapid gravity filtration used; overall therefore there is insufficient information from either paper to reproduce the details of apparatus used.

Farizoglu et al (2002) showed that under identical operating conditions, flowrate of 7.64 m/h and a bed depth of 750 mm (typical RGF mono-media depth is 600 mm), the pumice was able to achieve a greater removal of turbidity with a lower head loss accumulation than the sand as shown in figure 1.

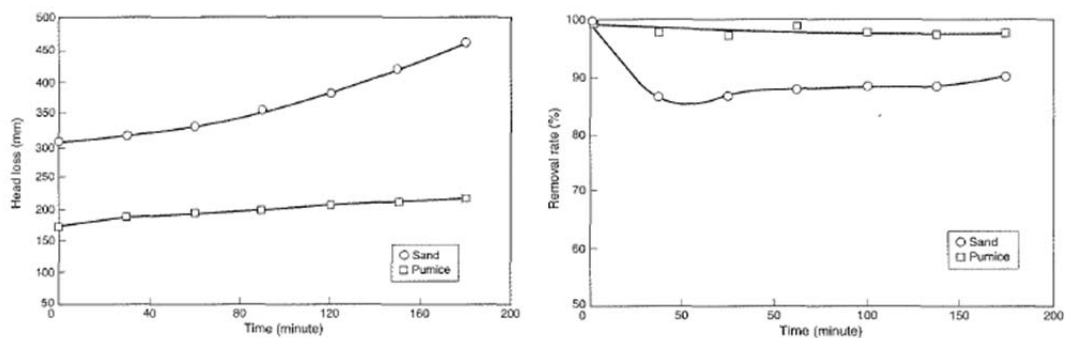


Figure 1 - Head loss and Turbidity removal charts from Farizoglu et al (2002)

As can be seen the initial head loss of the pumice is 100 mm less than the Sand, combined with the lower head loss accumulation rate the Pumice would be expected to maintain a longer filter run time than the sand. Farizoglu et al (2002) suggests that this was because sand is a non-porous material, and therefore particulate material can only be retained in the spaces between the grains in the filter bed. Pumice has two types of porosity, one of the pumice itself and the other of the filter bed as with the sand, with larger particles being retained in the filter bed and smaller particles in the pores of the pumice. This enables a greater retention of particles within the filter bed compared to bed retention alone.

Ghebremichael (2004) does not give as much information on results from the pilot study with only single values for turbidity and head loss that do not give an indication of the performance variation with time. The results given are provided in tables 1 and 2, with table 1 showing the summer period and table 2 the winter period:

Table 1 - Summary of results from pilot plant column during summer period from Ghebremichael (2004)

Flow rate m/h	No of runs	Influent turbidity (NTU)	Effluent turbidity (NTU)	Headloss (cm)	
				Clean	Terminal
Dual media (Pumice-sand)					
3.0	8	3.52 ± 0.4	0.68 ± 0.1	7.4 ± 0.9	53.5 ± 3.0
5.5	9	4.61 ± 1.6	1.32 ± 0.5	12.0 ± 3.2	55.2 ± 6.8
7.5	8	2.85 ± 0.7	0.77 ± 0.2	15.7 ± 2.0	58.9 ± 5.2
Mono medium (sand from existing filters)					
3.0	8	3.52 ± 0.4	0.74 ± 0.2	10.6 ± 0.7	80.5 ± 2.9
5.5	9	4.61 ± 1.6	1.37 ± 0.9	13.7 ± 4.2	77.3 ± 9.6
7.5	8	2.85 ± 0.7	0.59 ± 0.1	20.8 ± 2.1	81.0 ± 2.4

Results from the summer period (table 1) show an influent turbidity within the range expected of post clarified water although the method of clarification in these studies is not known. The winter period (table 2) shows a far higher influent turbidity above that which would be expected at this stage in the treatment process. Ghebremichael (2004) gives the reason for this higher turbidity to be due to poor pre-treatment prior to the filters in the treatment works. This level of NTU would be typical of a UK river water without any form of pretreatment. The filtered water quality as a consequence is not as good as might be expected.

It is noted also that the final turbidity was reduced at higher flowrates, this is related to the reduction in inflow turbidity showing that the clarified or raw water quality has a significant impact on results and must be carefully controlled to give reliable results in experiments. The comparison of dual-media to mono-media is not a good comparison as it would be expected to produce an improved turbidity result in the mono-media as the full depth of the filter is a finer media while the dual-media filter has a coarser media above the finer media, although headloss results show the benefits of using dual-media with lower corresponding headloss values.

Table 2 - Summary of results from pilot plant column during summer period from Ghebremichael (2004)

Flow rate m/h	No of runs	Influent turbidity (NTU)	Effluent turbidity (NTU)	Headloss (cm)	
				Clean	Terminal
Dual media (Pumice-sand)					
5.5	7	17.8 ± 3.1	6.04 ± 2.3	11.9 ± 1.8	31.4 ± 14.2
Mono medium (sand from existing filters)					
5.5	7	17.8 ± 3.1	6.44 ± 1.6	12.8 ± 3.1	49.9 ± 17.5

Results from these studies by Ghebremichael (2004) give very limited information with only an average value with an additional range related to that test. A single chart showing the change in turbidity and head loss with time was given for the summer phase 1 and is shown in figure 2:

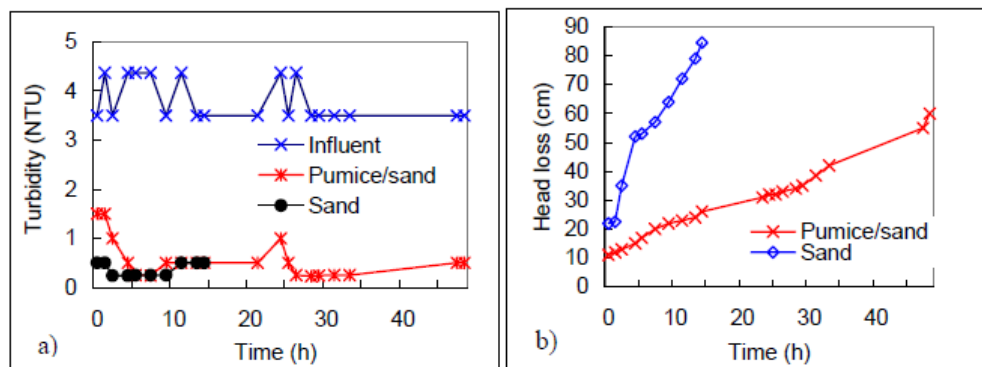


Figure 2 - Typical turbidity (a) and headloss (b) curves from pilot plant study

The performance variations between the mono-media sand filter and the dual-layer sand/pumice filter are to be expected from the increased voidage in the larger surface area media allowing for the greater accumulation of solids in voids across the bed. The increased performance with regard to head loss accumulation is to be expected from a dual-media filter based on previous knowledge with sand/anthracite filters around the world; it is one of the main reasons for the introduction of anthracite (Ives (1970)). The removal of turbidity is very similar between the two types of filter; any minor differences are likely to be due to the variation in filter depths of the sand present, with the mono-media likely having a greater depth of sand compared to the dual-media filter.

The work by Ghebremichael (2004) has also given information on increased performance from two different types of filter method (mono-media to dual-media). The comparison given in the paper is between a mono-media and dual-media system where a significant increase in mean time would be expected. There is no suggestion as to whether pumice may be a suitable alternative to sand as it was compared to anthracite as an upper layer in this study. The work by Ghebremichael (2004) did not provide any direct comp of anthracite and pumice in a dual-media configuration which would support why the author believes pumice to be a suitable alternative to anthracite.

Farizoglu et al (2002) were able to compare pumice to sand under identical conditions or particle size as possible, and were able to conclude that a pumice bed will show a lower head loss accumulation and greater turbidity removal than that of a sand filter. This is based on the observation that because of its greater porosity, pumice has a higher capacity for accumulation of particulate matter within the pores and on the external surfaces of the media.

There are concerns however regarding attrition of the pumice under backwashing (Morgeli & Ives, 1979). Farizoglu et al (2002) stated that pumice is fragile and may crumble during filtration compared to sand, but they did not observe any deformation or any quantitative losses that would be required to back this up.

Morgeli & Ives (1979) conducted a 50 hour continuous air and water backwash on two types of media (Pumice and Expanded Slate) with the results given in table 3. A 100 hour backwash according to Morgeli and Ives (1979) corresponds to a 0.5 – 3 years and so 50 hours would be around half this range. It is important to consider however that Morgeli & Ives (1979) studied media for wastewater treatment which has a far higher backwash frequency due to the higher particle load. The grain size is also larger (2.5 – 3.15 mm) than that used in drinking water treatment rapid gravity filtration (0.5 – 1.0 mm), which is likely to have a different rate of breakdown than the smaller particle size.

Table 3 - Attrition loss of pumice and expanded slate after 50 h backwashing from Morgeli & Ives (1979)

Initial fraction (mm)	Grain size after 50 h backwash (mm)	Percentage residue			
		Pumice		Expanded slate	
		1st test	2nd test	1st test	2nd test
2.5-3.15	3.15	0	0	0	0
	2.5-3.15	70	74	92	92
	2.0-2.5	26	24	8	8
	1.6-2.0	4	2	0	0
	1.6	0	0	0	0

Results given in table 3 show the particle size distribution for two duplicate tests. The original media had a range of 2.5 – 3.15 mm and any percentage outside of this range shows a change in the media. It can be seen that in the pumice a quarter of the media has shifted to the 2.0 – 2.5 mm size range corresponding to a loss of the media and since these losses have a significant impact on the porosity of the filter bed, the performance will be significantly altered if this occurred in a rapid gravity filter.

From handling of the two types of pumice in this study it became apparent that it was very easy to crumble and crush and this combined with the work carried out by Morgeli & Ives meant that pumice was rejected for the later continuous trials. This is supported by the Eurocodes where prolonged durability of the media is an important criterion. The sustainability of the material is also questioned by the closure of quarrying on the Italian island of Lipari due to environmental concerns. The sustainability of shipping in filter media from across Europe and the globe is a negative factor in comparison to sand.

The studies reviewed by Farizoglu et al (2002) and Ghebremichael (2004) have shown that positive head loss improvements, while maintaining suitable water quality, can be brought about by a more porous material. So suggesting that a material is able to retain a larger amount of solids per cubic metre and that fundamental properties have an impact on the performance leading to the conclusion that different materials will have varying positive performance enhancements.

4.1.2 GLASS

Recycled glass or cullet has been highlighted as a possible filtration media by WRAP (Waste & Resources Action Programme), an organization concerned with developing new markets for materials to help reduce waste and improve sustainability. This report was based on information provided and work carried out by Dryden Aqua Ltd & Entec Ltd. The information provided for this report is wholly commercial literature and has little academic value; this commercial literature lists the following benefits of using glass media:

- Resistance to biofouling – increased service life
- Improved flow rates – better overall performance
- Much better ‘backwash’ efficiency – stable and predictable

Dryden Aqua Ltd give an improvement in performance of between 30 – 80 % over sand, but without any data to support this comment. The three potential benefits listed above do not stem from any academic work that can be found, therefore they cannot be verified. Biofouling is not a problem in rapid gravity drinking water sand filters. Improved flow rates will mainly be linked to variations in particle size and shape and so can be achieved with any filter media type. Backwash trials carried out by Fitzpatrick (2005), Soyer et al (2010) and Evans et al (2002) for example show that although glass required a lower flow to achieve the same expansion, it was not significant.

The fluidization experiments carried out by Soyer et al (2010) were conducted in 100 mm diameter columns at a temperature of 18 – 19 °C. The chart from these experiments is shown in Figure 3 below:

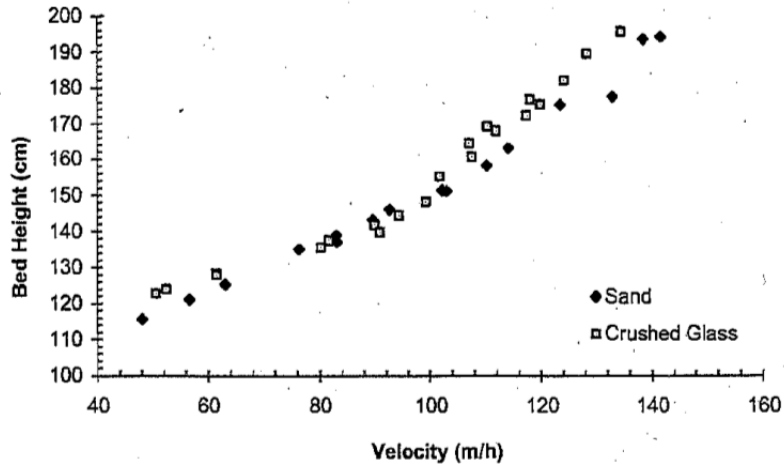


**Figure 3 - Expanded bed height versus backwash velocity (initial bed height of 104 cm)
from Soyer et al (2010)**

The results above show that for higher flow velocities, the glass bed will expand to a greater volume than the sand filter, however for the range of 25 – 45 % the bed expansion of the two media follow each other closely with the glass only showing improved fluidization at either lower or higher flowrates. Soyer et al (2010) state that bed expansion results from such tests are only applicable to the specific filter bed type tested and if the parameters of size distribution, density, sphericity and bed porosity vary then so will the results found above.

As glass media varies from manufacturers and source then the results of such testing will only be applicable to the specific media types being tested. Dryden Aqua Ltd's proprietary glass known as AFM however is the only current glass filter media that is approved by the Drinking Water Inspectorate (DWI) for use in treatment of potable drinking water.

Fitzpatrick (2005) states that crushed glass is now available as a potential filter medium to replace sand and in the UK is awaiting Drinking Water Inspectorate approval before it can be used in drinking water. At present the most recent information from the DWI only lists AFM as an approved glass filter medium, with some companies still attempting to gain this approval to bring their crushed glass to market for use as a filter medium.

There were three main papers on glass as a media rapid gravity filtration of drinking water, these are Evans et al (2002), Soyer et al (2010) and Rutledge and Gagnon (2002). Rutledge

and Gagnon (2002) studied the Canadian recycled glass market and concluded that even though the market for filter media is small compared to other possibilities it is still a possible avenue for its use. Rutledge and Gagnon (2002) used recycled glass as an alternative to sand in a dual-media configuration with anthracite above either the sand or glass. Soyer et al (2010) first analyzed the properties of the glass media to evaluate its suitability for use in rapid gravity filtration and then carried out pilot scale studies on the media compared to sand with varying coagulant types and dosages. In addition Fitzpatrick (2005) investigated the suitability for glass as a filter media based on its physical parameters.

Particle size is a key consideration with regard to how a filter media will perform and for effective comparison of media the particle sizing should be as close as possible to each other or ideally identical in size to help determine the reasons for performance variations. Evans et al (2002) selected glass media to closely match that of the sand as shown in table 5:

Table 4 - Filter media configurations compared in testing from Evans et al (2002)

	Sand media	Recycled glass media
Media identification	River sand	Bronze blast glass media
Supplier	Brisbane river sands	Visy recycling
Effective size (mm) (as measured by HWA La.)	0.97	0.98
Uniformity coefficient (as measured by HWA Lab.)	1.27	1.31
Depth installed in pilot plant column (mm)	900	900
Support gravel layers (mm) (effective size/layer depth)	2–3 mm/100 mm 3–6 mm/100 mm 6–12 mm/100 mm 12–24 mm/100 mm	2–3 mm/100 mm 3–6 mm/100 mm 6–12 mm/100 mm 12–24 mm/100 mm
Pilot plant filtration stream	Stream 1	Stream 2

The effective size of the media relates to the particle size that 10 % of the media passes through, this value combined with the Uniformity Coefficient which is a ratio between the sieve sizes that 60 % of the media passes through and the effective size. These parameters however do not account for any variation in grain shape which will also have an effect on the filtration performance of the media. Glass is thought to be more angular compared to the more rounded form of the sand grains.

Rutledge and Gagnon (2002) reported on the performance of recycled glass but were unable to source comparable media, as is shown in the particle size distribution (PSD) curve shown in figure 4:

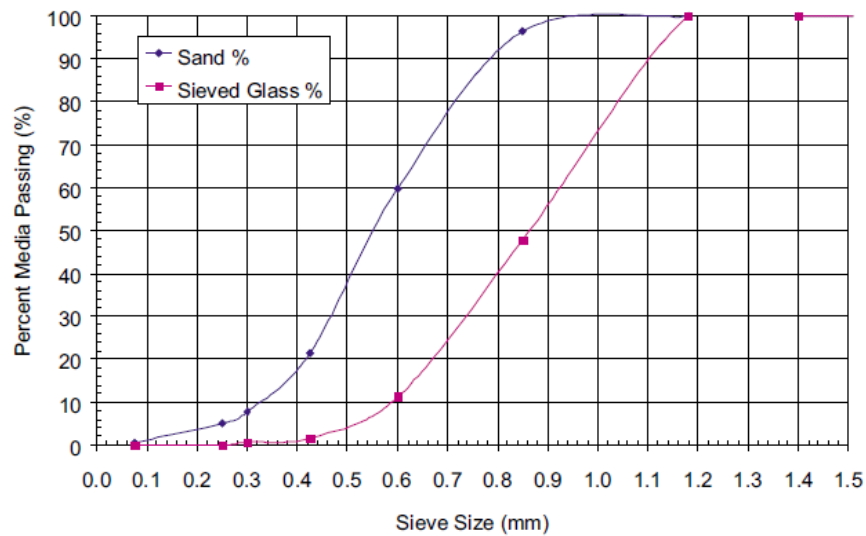


Figure 4 - Sieve analysis of sand and glass from Rutledge and Gagnon (2002)

Representation of this PSD given in the same form as Evans et al (2002) as shown in table 5 allows a better comparison between the three papers:

Table 5 - Particle size parameter comparison

	Evans et al (2002)		Rutledge and Gagnon (2002)		Soyer et al (2010)	
	Sand	Glass	Sand	Glass	Sand	Glass
Effective Size (d_{10})	0.97	0.98	0.33	0.59	0.79	0.77
Uniformity Coefficient (U)	1.27	1.31	1.82	1.58	1.33	1.41

The variation in the particle size in the work by Rutledge and Gagnon (2002) is significant and will impact on the performance of the filter media being tested. Taking these particle size properties into consideration the sand would be expected to perform more effectively for turbidity removal but less well for head loss than the Glass in the study by Rutledge and Gagnon (2002). Rutledge and Gagnon (2002) state that the bed porosity was expected to be higher in the glass media due to the materials angularity, however the increased particle size will also affect the porosity value.

The angularity of the glass (b) is shown in scanning electron microscopy images in figure 5 by Rutledge and Gagnon (2002), but of important note is the image of the sand (a) as it shows that although more rounded than the glass, the sand still exhibits a higher angularity than that seen in Leighton Buzzard Sand (See section 5.2). This can go some way to explain why the porosity of the beds is similar to that reported by Rutledge and Gagnon (2002) with sand being 0.47 and glass at 0.52.

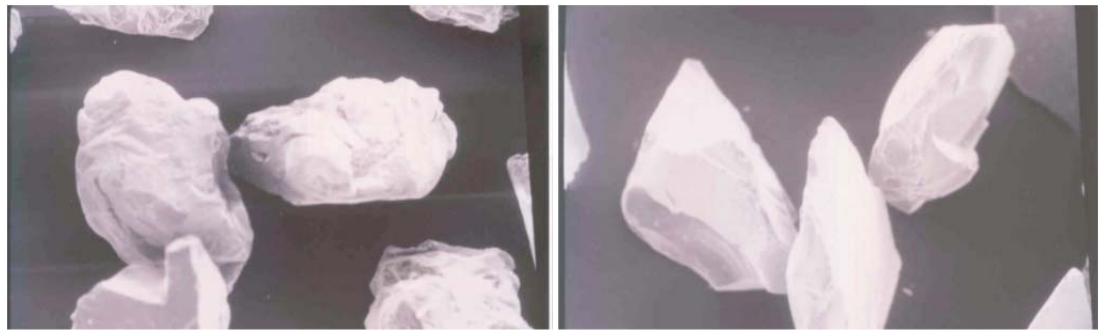


Figure 5 - Scanning electron microscopy imaging of sand (a) and glass (b) by Rutledge and Gagnon (2002)

As noted by Fitzpatrick (2005) the higher angularity of the glass media compared to sand gave a higher porosity than the sand even with similar particle size distributions. This is likely if the more angular media has higher bed porosity. When a range of particle size distributions are used, such as with Rutledge and Gagnon (2002) the porosity is also being governed by the particle size distribution, and the degree to which the angularity is affecting the porosity cannot easily be differentiated.

Evans et al (2002) used a pilot plant and therefore the water quality will have been variable and influenced by seasonal variation and other factors. Typical parameters of this feed water are given in table 6. The values for turbidity are as expected for post clarified water as shown by comparing with data from Severn Trent Water treatment works (See section 7.1.3) which show a range of primarily 1 – 2 NTU.

Table 6 - Feed water quality summary from Evans et al (2002)

Parameter	Units	Range during trials	
Turbidity	NTU	1.3–5.5	
Colour (true)	PtCo	5–10	
pH	–	6.9–7.7	
Particle count	Particles/mL	1,500–1,900	
Iron	– total	μg/L	320–1,700
	– soluble	μg/L	30–310
Manganese	– total	μg/L	32–51
	– soluble	μg/L	36–48
Aluminium	– total	μg/L	400–860
	– soluble	μg/L	40–80
Feed water temperature	°C	14–18	

Details of the pilot columns used for the Evans et al (2002) study are shown in Figure 6 below, with a constant head, constant flow arrangement. The flow is maintained by a float located in the control tank as shown in figure 6. Pressure head above the filter bed is kept constant but will vary within the bed during operation as solids become trapped within the bed.

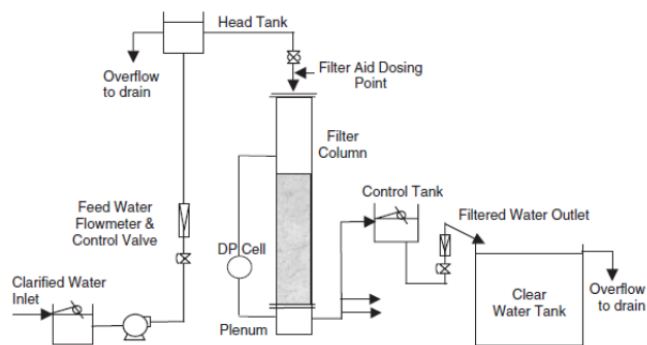


Figure 6 - Pilot plant process stream - filtration mode from Evans et al (2002)

In contrast Rutledge and Gagnon (2002) considered the use of recycled glass as an alternative to sand in a dual-media pressure filter combined with anthracite. The set-up of the pressure filters consisted of a 600 mm (24 inch) layer of anthracite overlaying either glass or sand of depth 400 mm (16 inch). Rutledge and Gagnon (2002) did not give a typical composition of the influent which may be synthetic or real which limits the ability to analyze the results.

Rutledge and Gagnon (2002) acknowledge that traditionally the performance of filters has been assessed by turbidity, and within industry this is still the primary method for performance evaluation. Particle counting however was noted by Rutledge and Gagnon

(2002) as to be more suitable for this task due to improved sensitivity especially at lower levels of turbidity in filter effluent. It has also been shown to detect particle breakthrough sooner and detect minor changes to the process by Hargesheimer et al (1998). Based on this information Rutledge and Gagnon (2002) used a HACH 2200 PCX (HACH Corp Loveland CO) particle counter to monitor raw water, filter influent and effluent water.

Evans et al (2002) used turbidity as the primary measure of performance of the filters which is more typical of the majority of studies carried out on filtration. But taking into account the improved performance of particle counters shown in previous studies (O’Leary et al 2003, Chowdhury et al 1997) a particle counter was also used for comparison with turbidity to highlight any specific variations in capture of particular particle size ranges.

Evans et al (2002) carried out a testing scheme with a range of filtration rates, polymer doses and runtimes based on termination criteria (Table 7). The type of polymer used in the study is not given by Evans et al (2002) other than noting it was a polymer.

Table 7 - Summary of pilot plant runs undertaken from Evans et al (2002)

Run No.	Start date	Filter No.	Filter media type	Filtration rate (m/h)	Filter aid dose (mg/L)	Run time (hours)	Reason run ended
CHC01	7/8/00	1	Sand	7.5	–	>25	Time
		2	Glass	7.5	–	>25	Time
CHC02	8/8/00	1	Sand	10	–	>25	Time
		2	Glass	10	–	>25	Time
CHC03	9/8/00	1	Sand	12.5	–	14.7	Tb>0.3
		2	Glass	12.5	–	14.6	Tb>0.3
CHC04	10/8/00	1	Sand	12.5	–	13.7	Tb>0.3
		2	Glass	12.5	–	13.6	Tb>0.3
CHC05	15/8/00	1	Sand	12.5	0.025/0.05	9.2	Tb>0.3
		2	Glass	12.5	0.025/0.05	9.2	Tb>0.3
CHC06	16/8/00	1	Sand	12.5	0.1	6.4	HL>3 m
		2	Glass	12.5	0.1	6.5	HL>3 m
CHC07	17/8/00	1	Sand	12.5	0.05	6.2	HL>3 m
		2	Glass	12.5	0.05	4.7	HL>3 m
CHC08	17/8/00	1	Sand	12.5	0.015/0.03	5.5	Tb 0.3
		2	Glass	12.5	0.015/0.03	5.5	Tb

The run termination criteria are given in Table 7 with time that the run was allowed to run for, turbidity (Tb) greater than 0.3 and a headloss (HL) greater than 3 metres. Basic results from these trials are given in Table 8 by Evans et al (2002). Further detail from the testing such as how the turbidity varied during the test run and ripening times are not available in the paper and therefore comparison between the filters during the run cannot be made without reliance on the author’s interpretation.

Table 8 - Typical turbidities and particle counts during pilot testing from Evans et al (2002)

Run No.	Media	Turbidity (NTU)		Particle counts	
		Filtered water	Raw water	Filtered water (P/mL)	Feed water (P/mL)
CHC01	Sand	0.04	2	–	1,500
	Glass	0.04		<10	
CHC02	Sand	0.07	1.9	–	1,900
	Glass	0.07		35	
CHC03	Sand	0.06	2.5	–	1,700
	Glass	0.07		20	
CHC04	Sand	0.09	2.7	45	1,500
	Glass	0.11		45	
CHC05	Sand	0.1	4.0	45	–
	Glass	0.1		37	
CHC06	Sand	0.05	4.3	20	–
	Glass	0.05		20	
CHC07	Sand	0.07	2.5	12	–
	Glass	0.04		11	
CHC08	Sand	0.09	2.5	15	–
	Glass	0.05		15	

These limited results from each of the tests are given in Table 8, the results are given in both turbidity and particle counts found. The results are typical values and therefore do not give the range that was found during the trials and it is not known if this is an average value or best case etc. The values for turbidity between the sand and glass are extremely similar showing that the performance between the media for the removal of particles is negligible until higher filtration rates are used and the glass begins showing better performance in turbidity and particle count. The filtration rate of 12.5 m/h however is higher than what would be expected to be used in a treatment works and the value of 7.5 and 10 m/h are closer to what would be expected and therefore the results at these rates show the negligible practical difference in removal.

Results from the work by Rutledge and Gagnon (2002) (Figure 7 and Figure 8) are only given in particle counts. The chart range also makes it difficult to interpret the results effectively and as can be seen in Figure 7 and Figure 8 the influent particle counts are not the same with the crushed glass having a typical influent count of 500 – 1000 counts/mL against 1000 – 1500 counts/mL in the sand.

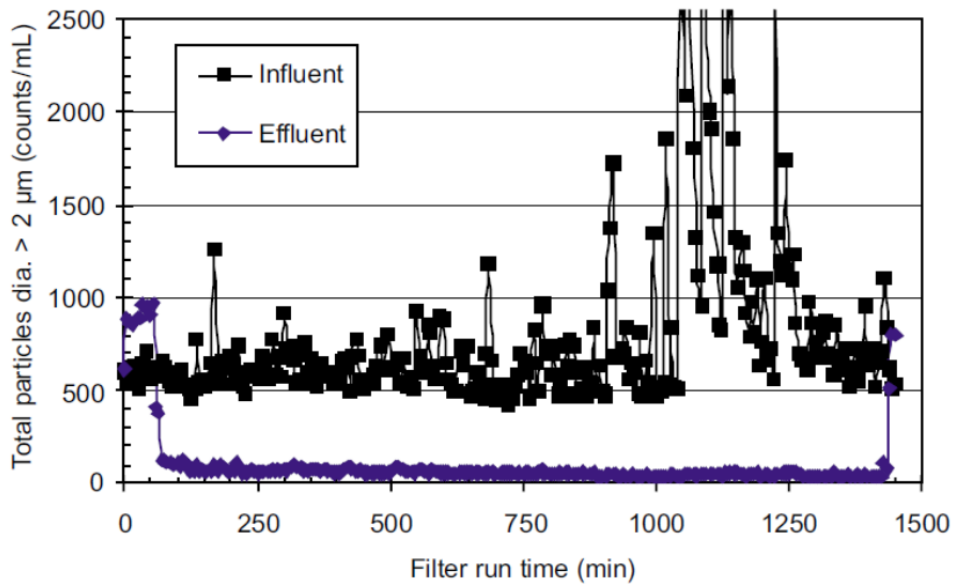


Figure 7 - Particle counts for a filter run in the crushed glass summer period from Rutledge and Gagnon (2002)

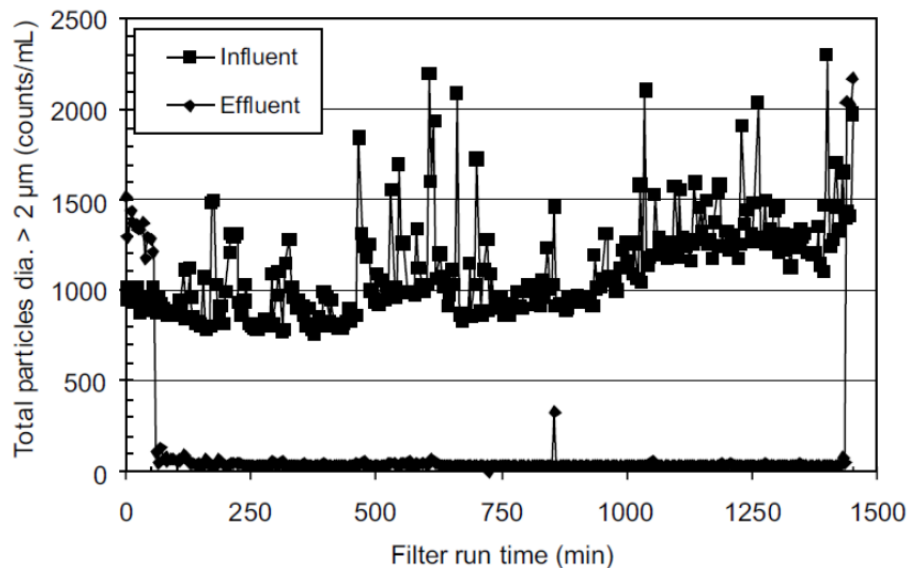


Figure 8 - Particle counts from a filter run in the sand filter summer period from Rutledge and Gagnon (2002)

From the effluent results however the sand removes a greater number of particles (figure 7 & 8). This performance variation with the sand performing better than the glass corresponds well to what would be expected since the glass has a larger particle size than the sand meaning that the sand should be able to remove a higher proportion of finer particles. This effect is shown in figure 9 below, with the sand removing a higher proportion of the finer particles in the range of 2 – 5 μm . Only in the range of 5 – 7 μm does the glass filter

outperform the sand. Rutledge and Gagnon (2002) conclude that the glass, due to its angular nature, is more effective at removal of finer particles than conventional media such as the sand, but this is not shown by their own results shown in figure 9:

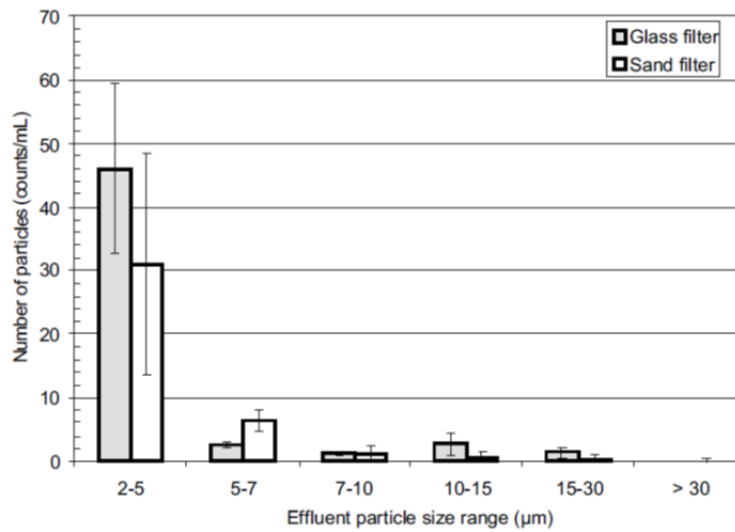


Figure 9 - Average size distribution of effluent particles from the crushed glass and silica sand (error bars represent one standard deviation) from Rutledge and Gagnon (2002)

Total Log removal of particles from the filters during the warm (summer) and cold (winter) periods (Figure 10) by Rutledge and Gagnon (2002) also show that overall the performance of the sand filter is better than that of the glass under either temperature condition.

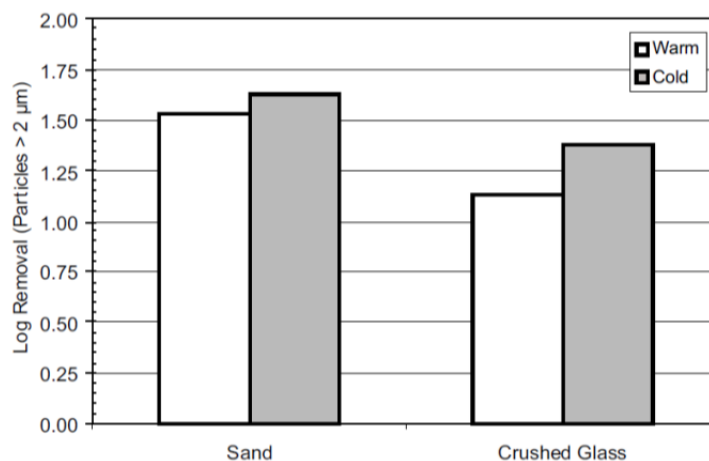


Figure 10 - Log removal of total particle counts for the sand and crushed-glass filter from Rutledge and Gagnon (2002)

Rutledge and Gagnon (2002) in their conclusion state that the initial performance of the glass was variable, and with time and use over a period of 6 months the performance of the

glass improved, this was suggested to be due to the wear on the media making it more rounded. The movement of the media wore down the particle size, bringing it closer to the size of the sand. Overall the performance variation between the glass and the sand can be explained by the larger particle size of the glass in the study by Rutledge and Gagnon (2002), they did not come to this conclusion as previously noted.

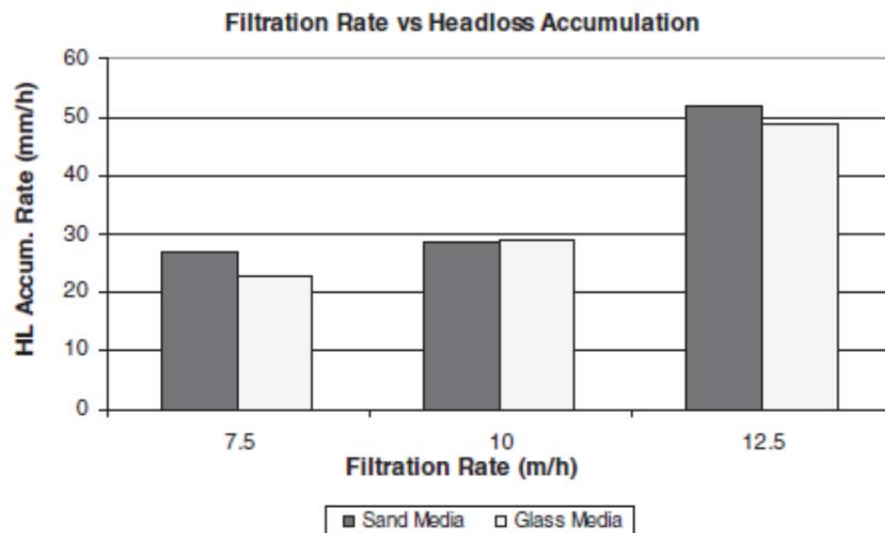


Figure 11 - Effect of filtration rate on headloss accumulation rate from Evans et al (2002)

Evans et al (2002), using similarly graded glass and sand, showed that the headloss between the two media was relatively similar but that overall the glass showed a slightly lower rate of accumulation (Figure 11). This would suggest a longer period between backwashing for the glass filter leading to full life cost savings but this would require further specific testing of various backwashing criteria to confirm. The long term effects of use of the new media are a new consideration regarding durability and predicting whether the filtration performance is affected by this.

Evans et al (2002) carried out backwashing trials on the media and concluded that the glass media expanded to between 10 - 20 % less than the sand for the same backwash rates. Fitzpatrick (2005) also carried out detailed analysis of backwashing with water but only for the glass and not in comparison with sand tested as shown in Figure 12.

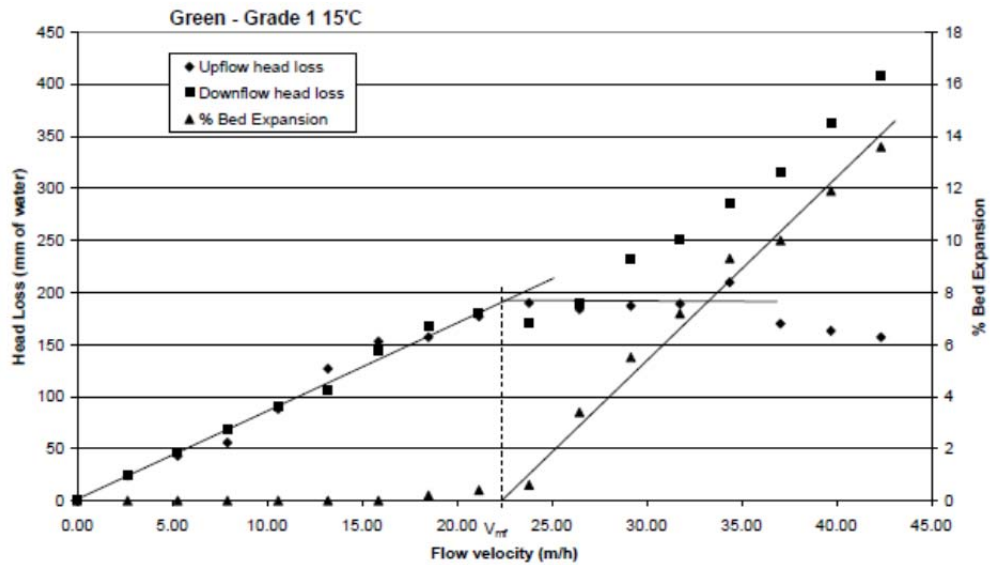


Figure 12 - Head loss and bed expansion data from crushed green glass (0.5 - 1.0 mm) from Fitzpatrick (2005)

To help determine if glass was suitable as a long term filter media, durability of the media was tested by Fitzpatrick (2005) using 100 hour long backwashing tests with air and water. Under these experiments it was shown that the glass released a slightly higher proportion of fines and these have showed a slightly higher media loss of 1.6 % compared to 0.4 % for the sand under identical conditions.

Overall previous work shows that glass offers similar performance to sand with a slightly lower headloss accumulation rate. This suggests glass might have an advantage with regard to headloss and by a contribution to sustainability of the filters without any detrimental effect on water quality. However Fitzpatrick (2005) has highlighted a potential issue of leaching of metals used for coloring of glass although AFM and DWI tests suggest this is not a problem, although further study with the most refined equipment is needed to determine whether this is of concern.

Further detailed understanding of the breakdown of the glass is also required to confirm the difference in usable lifetime of the filter bed. As pointed out by Rutledge and Gagnon (2002), over the period of 6 months of testing, the glass became more rounded which although increasing filter performance in their own trials, may not be satisfactory for long term operation if it continues to wear, and replacement of media may be required more frequently than sand.

The work by Rutledge and Gagnon (2002) is marred by the difference in particle size used between the glass and sand. The better performance of the sand noted by Rutledge and Gagnon (2002) although not explained can be attributed to the finer particle size of the sand retaining smaller particles and creating a larger headloss. The data itself is still useful and with the particle size variation taken into consideration the performance of the glass is very similar to the sand.

4.1.3 EXPANDED ALUMINOSILICATE (FILTRALITE®)

The British European Standard BS EN 12905:2005 allows the use of expanded aluminosilicate in drinking water treatment, allowing for its use in this application as long as the requirements laid out by BS EN 12905:2005 are met. There have been numerous studies (Saltnes et al, 2002 & Mitrouli et al, 2009) conducted into its use as a filter medium, the predominant material reported on was Filtralite®. Filtralite® is a commercial filter media that is produced from heating clay in an oven to expand the material and produce a lightweight porous particle that is then crushed and graded according to the required application.

Filtralite® is marketed as a dual-media solution replacement to current filter materials, and therefore it has been compared primarily to dual-media anthracite/sand filters. Mitrouli et al (2008) compared dual-media anthracite/sand to Filtralite®/sand, and then to a dual-media configuration of two grades of Filtralite® (Mitrouli et al, 2009). In these two papers the comparison is made by the pre-treatment of seawater prior to entering a desalination plant.

Saltnes et al (2002) compared dual-media anthracite/sand to a dual-media configuration of Filtralite® in a filter pilot plant for the treatment of raw water containing humics. Eikebrokk & Saltnes (2001) in earlier work investigated ions and suggested an improvement from the performance variation between anthracite/sand and Filtralite®/sand configurations for removal of Natural Organic Matter (NOM) in a pilot plant.

Albuquerque & Labrincha (2008) did not consider Filtralite® but looked at rejected material from the production of lightweight aggregates which is a similar expanded aluminosilicate material to Filtralite® with a lightweight porous structure. In the research Albuquerque & Labrincha (2008) compared different grades of the expanded aluminosilicate against each

other in laboratory scale mono-media configurations investigating metals and turbidity removal.

The work by Albuquerque & Labrincha (2008) is different as a rejected unregistered material from lightweight aggregate production and is therefore not a specifically marketed filter media product like Filtralite®. It would be expected that as Filtralite® is marketed for this specific purpose to particular grades and sizes its performance would be better for experimentation than rejected material. Also Albuquerque & Labrincha (2008) did not compare the performance of the lightweight aggregate to a control material such as sand or anthracite and sand. The study only looks at variations in performance of this single lightweight aggregate with different size fractions. These results can be compared with results from other studies but the conditions between them will be different leading to uncertainty when carrying out a critical comparison of the data.

In the Eikebrokk & Saltnes (2001) and Mitrouli et al (2008) papers dual-media configurations of Filtralite®/Sand are compared to Anthracite/Sand to demonstrate improvements in filtration performance between Anthracite and Filtralite®. The details of the specification of both the filter media and bed depths are given in Table 9 below:

Table 9 - Comparison of media and bed depth

Paper	Layer	Column 1		Column 2	
		Depth	Material	Depth	Material
Eikebrokk & Saltnes (2001)	Top	600 mm	Anthracite 0.8 – 1.6 mm	600 mm	Filtralite® NC 0.8 – 1.6 mm
	Bottom	350 mm	Sand 0.4 – 0.8 mm	350 mm	Sand 0.4 – 0.8 mm
Mitoruli et al (2008)	Top	700 mm	Anthracite 1.2 – 2.5	700 mm	Filtralite® MC 1.5 – 2.5 mm
	Bottom	500 mm	Sand 0.8 – 1.25 mm	500 mm	Sand 0.8 – 1.25 mm

The particle sizes of the Filtralite® and anthracite are kept relatively similar (Table 9) as is good practice when comparing filter media. The size range for Eikebrokk & Saltnes (2001) is similar to that of a typical sand grading (0.5 – 1.0 mm); while in the work by Mitrouli et al (2008) the size is over double that of sand. Using results from this work to help determine performance benefits over sand is difficult, as the final turbidity and removal of finer

particles in the two papers will be done by the finer bed of sand below the Filtralite® and improvements in water quality will only show that the Filtralite® is more effective as a media in the upper layer compared to Anthracite.

The later work by both Saltnes et al (2002) and Mitrouli et al (2009) is different as it compares a dual-media filter comprising of Anthracite/Sand as before against a combination of two different grades of Filtralite®. The specification of each filter is given in Table 10 below:

Table 10 - Comparison of filter media and bed depth

Paper	Layer	Column 1		Column 2	
		Depth	Material	Depth	Material
Saltnes et al (2002)	Top	600 mm	Anthracite 0.8 – 1.6 mm	480 mm	Filtralite® NC 1.6 – 2.5 mm
	Bottom	350 mm	Sand 0.4 – 0.8 mm	470 mm	Filtralite® HC 0.8 – 1.6 mm
Mitoruli et al (2009)	Top	700 mm	Anthracite 1.2 – 2.5	700 mm	Filtralite® NC 1.5 – 2.5 mm
	Bottom	500 mm	Sand 0.8 – 1.25 mm	500 mm	Filtralite® HC 0.8 – 1.6 mm

Albuquerque & Labrincha (2008) considered a 455 mm bed depth to give comparisons of performance between three grades of lightweight aggregate which were 0 / 0.5 mm, 0.5 / 3 mm and 0 / 3 mm. The final grading of 0 / 3 mm is confusing as it's naming shows a wide particle size range but looking at the results and images of the particles it appears to have a grading greater than 3 mm, meaning that the three are arranged as such; 0 – 0.5 mm, 0.5 – 3 mm and then > 3 mm. But this is contradictory to the description of results later in their work and a more likely size range to correspond with the results is one of; 0 – 0.5 mm, 0.5 – 3 mm and 0 – 3 mm.

The surface area of the three different gradings was determined by Albuquerque & Labrincha (2008) to be as follows:

- 0/0.5 – 2.4 m²/g
- 0/3 – 1.55 m²/g
- 0.5/3 – 2.76 m²/g

If the 0.5/3 fraction is considered the most coarse as described by the authors then its surface area should be lower than the other two, this is not the case and casts doubt as to the results given in the work.

With a porous material such as Filtralite® a concern is flotation of the material which would lead to higher losses from the filter. Also if air is trapped in pores then the flow required to wash away that particle will be lower than other fully saturated particles under backwashing conditions. Eikebrokk & Saltnes (2001) considered the stability of the material when stored in water as it would be in a filter and carried out testing on the settlement rates of different Filtralite® types against sand and anthracite to determine whether the density changes from adsorption of water or replacement of air entrapped in the material with water. Figure 13 shows this below and the type of Filtralite® that is considered a suitable alternative to sand as it has the smallest particle size available from the manufacturer is Filtralite® HC 0.8 – 1.6 mm:

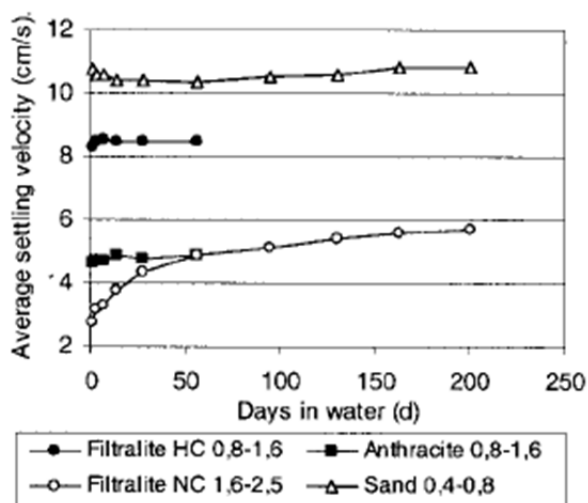


Figure 13 - Comparison of settling velocity of filter materials from Eikebrokk & Saltnes (2001)

Filtralite® HC shows that when in water the Filtralite® HC is more stable and does not absorb as much water as the NC material with time in the filter and thus its performance under backwashing will be more stable than that of the lighter version of Filtralite®.

A concern with the Filtralite® is that it is only available in a certain range of sizes and types, with the closest grading to sand being the Filtralite® HC with a particle size range of 0.8 – 1.6

mm which is greater than the typical 0.5 – 1.0 mm grading of filter sand. Eikebrokk & Saltnes (2001) show a grading curve (Figure 14) comparing sand and anthracite to Filtralite® with the upper layer comprising the lighter NC material and the bottom layer comprising of the denser HC material. The top and middle and bottom refers to the sample point in a filter and the grading of the top layer of Filtralite® is indicative of stratification of the media in the bed with the lighter particles migrating to the top after operation and numerous backwashing events. This is likely to reduce the number of flow paths as a result of clogging of the surface layers.

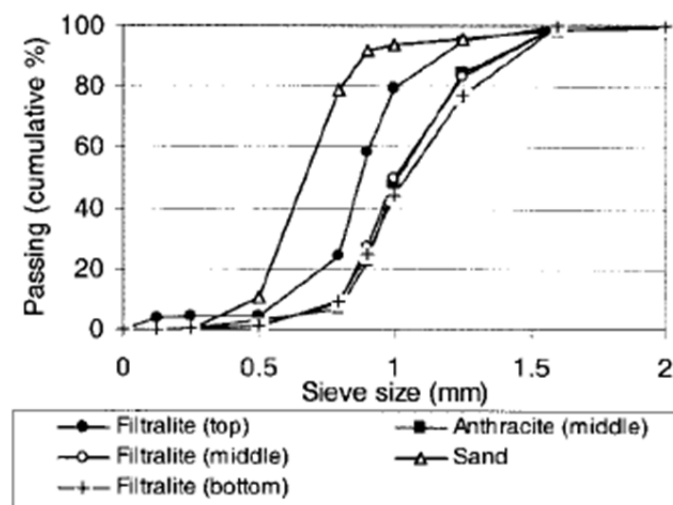


Figure 14 - Comparison of particle size distribution after filter operation from Eikebrokk and Saltnes (2001)

This variation in particle size with the Filtralite® being significantly larger than the sand will mean that the pores within the filter bed between individual filter media grains will be larger making transport of particulates in the water to the media surface unlikely to occur, and allowing for a greater number of particles to pass through the filter without filtration occurring meaning that a lower removal would be expected from a filter made entirely of Filtralite® when compared to a filter of identical dimensions made up of a sand or other filter media with a particle size grading of 0.5 – 1.0 mm. This variation in particle size will influence comparisons with materials with a different grading curve, as performance is strongly dependent on it (Kawamura, 2000).

Saltnes et al (2002) gave a range of results for the operation of the filters along with various raw water types, shown below in Figure 15 are the results for Raw Water 50/3 (RW50/3)

where the 50 denotes the mg Pt/l colour added and the /3 denotes the addition of bentonite (about 9 mg/l) to create a turbidity value of 3 NTU and RW50 where no bentonite was added. The type of coagulant added to the water is shown below the charts in Figure 15 with aluminium sulphate (AS), poly-aluminium chloride (PAC), iron chloride sulphate (ICS) and the bio-polymer chitosan (CHI).

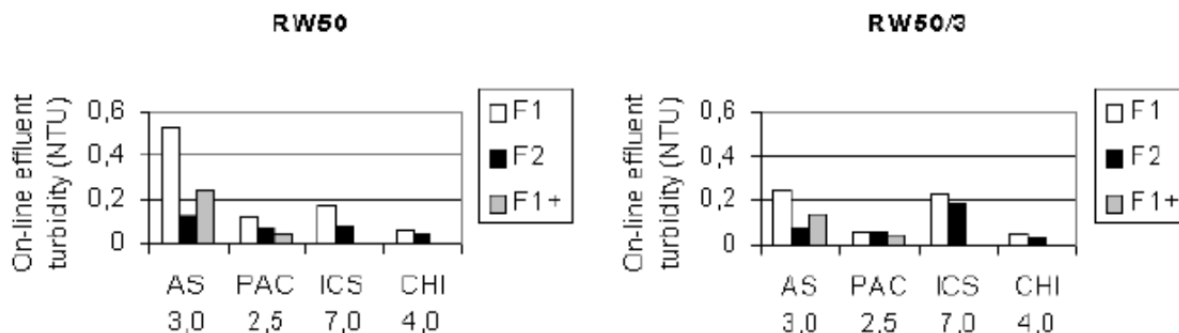


Figure 15 - Turbidity results from Saltnes et al (2002) – F1 (Filtralite), F2 (Anthracite/Sand), F1+ (Filtralite at deeper bed depth)

The results of prior turbidity values are not given and those given in figure 14 are only for the effluent turbidity from the filters operating at 7.5 m/h. Saltnes et al (2002) state that due to particulate aluminium hydroxide penetrating the filter there is a higher turbidity and this is shown in Figure 15. Also shown is how there is a lower turbidity in the anthracite / sand filter F2 than in the Filtralite® filter F1. The F1+ filter is a Filtralite filter with a deeper bed depth calculated to give similar performance to sand/anthracite. Typically across all results the turbidity is lower in the Anthracite / Sand filter although the PAC results for RW50/3 show a turbidity that is very similar if not higher in the sand / anthracite filter but this is not the norm looking at the other results. Higher turbidity in the Filtralite® filter is likely due to the larger particle size of the filter media compared to the lower layer of sand in the sand / anthracite filter as the sand being a finer particle size is allowing for a higher probability of transport and attachment to occur between particles in the water and the media grain surface. Regardless of the surface properties of the filter media if transport of the particles to the surface does not occur as frequently then the particles are more likely to pass through the filter.

Filter media grain size was shown to be an important characteristic by Saltnes et al (2002) and from the results shown it is likely that the variation in performance is primarily down to

the larger particle size in the 0.8 – 1.6 mm Filtralite® HC compared to the sand 0.4 -0.8 mm (typically 0.5 – 1.0 mm in filters according to Kawamura, 2000). In addition it was concluded by Saltnes et al (2002) that increasing bed depth can compensate for a lower turbidity removal. Also addition of coagulant and polymer as filter aid can also improve the effluent turbidity sufficiently and allow for the Filtralite® filter and larger media particle sizes potentially to be used.

Mitrouli et al (2009) looked at Filtralite® for dual-media filtration of seawater prior to desalination in reverse osmosis plant. The raw water was directly abstracted from an inlet in the Thermaikos Gulf and the parameters of the water from the study show in Table 11:

Table 11 - Parameters of raw water from Mitrouli et al (2009)

Parameter		Cations, mg/L	
pH	8.1	Na ⁺	12.8 x 10 ³
Conductivity, µS/cm	49 x 10 ³	K ⁺	533
TDS, mg/L	38 x 10 ³	Ca ²⁺	487
Total hardness, F	615.8	Mg ²⁺	1.2 x 10 ³
Carbonate hardness, F	15.3		
Non-carbonate hardness, F	600.5		
Alkalinity, M, mg/L CaCO ₃	152.5		
SDI _{2min} ^b	~38		
Trace elements, mg/L		Anions, mg/L	
B	4.8	Cl	21.2 x 10 ³
Cu	0.4	HCO ₃ ⁻	186
Fe	1.3	SO ₄ ²⁻	30 x 10 ²
Mn	0.5	NO ₃ ⁻	2.87
Zn	0.2	NO ₂ ⁻	<0.01
		PO ₄ ³⁻	<0.46

A number of parameters in this study are very different to those found in a typical water source that is treated for use as drinking water. For example the conductivity of 49000 µS/cm is far higher than a typical value of 500 µS/cm shown in data provided by Severn Trent Water Plc. Turbidity values of the raw water shown in the test results varied from 1.0 to 4.5 NTU which is on a higher range than expected from clarified water prior to entering a rapid gravity filter in a drinking water treatment plant. The results are from a hot climate and the water temperature reflects this with an average value of 27 °C, against UK temperatures again supplied by Severn Trent Water Plc. where the average over 3 years was shown to be 11 °C. This variation in temperature will bring about a variation in viscosity that has an

impact on the filtration performance of the filters. A combination of these various factors means that performance of the filters in the work carried out by Mitrouli et al (2009) and work carried out for this study will vary based on these water quality parameters.

Specific properties of the various media used by Mitrouli et al (2009) are given in Table 12, with the particle size between materials attempted to be matched as close as possible as discussed previously. Of interest in the table is the filter bed void fraction comparison between the two filters with the Filtralite® filters having a 20 % greater bed voidage than that of the anthracite/sand filter. This means that particles in the water will be less likely to attach to the media surface as the size of the void is far greater than the size of the particle to attach and transportation of the particle to the media's surface for attachment will be reduced with a greater voidage.

Table 12 - Filter media properties from Mitrouli et al (2009)

Parameter	Sand	Anthracite	Filtralite	Filtralite HC
Particle size range, mm	0.8 – 1.25	1.2 – 2.5	0.8 – 1.6	1.5 – 2.5
Bulk density, kg/m ³	1550	730	700 ± 75	235 ± 75
Particle density, kg/m ³	2650	1400	1650 ± 150	720 ± 150
Effective size (d ₁₀), mm	0.9	1.55	0.9	1.7 ± 0.3
Coefficient of uniformity	<1.5	1.3	<1.5	<1.5
Particle porosity, %	-	-	40	73
Filter bed void fraction, %	43	48	62	67

Due to the low turbidity of the raw water shown in Table 11 the turbidity of the effluent from the filters does not vary significantly between the two filter types as shown in Table 13 taken from Mitrouli et al (2009), the results are not very detailed with only a snapshot of results given for each test run.

Table 13 - Measured parameters at various run criteria from Mitrouli et al (2009)

Date	Turbidity (NTU)			Head build-up, MWC/d		
	F.W.	M/M	S/A	F.W.	M/M	S/A
U = 5 m/h and 1.8 mgAl/l						
31/07/07	1.7	0.1	0.1	-	0.41	0.53
01/08/07	1.7	0.1	0.1	-	0.40	0.47
02/08/07	2.0	0.1	0.1	-	0.27	0.29
03/08/07	1.3	0.1	0.1	-	0.22	0.27
U = 10 m/h and 1.8 mgAl/l						
24/07/07	0.7	0.1	0.1	-	0.64	1.42
25/07/07	0.7	0.1	0.1	-	-	-
26/07/07	1.8	0.1	0.1	-	0.87	1.26
27/07/07	0.9	0.1	0.1	-	0.86	1.23
U = 15 m/h and 1.8 mgAl/l						
07/08/08	3.3	0.1	0.2	-	2.05	3.00
08/08/07	4.6	0.1	0.3	-	-	-
09/08/07	3.8	0.1	0.1	-	2.46	3.42
10/08/07	2.5	0.1	0.1	-	2.96	3.13

The results from the 5 m/h and 10 m/h tests are the most valid when compared against current operating filters in the UK water industry. The results shown in Table 13 however give no indication of a variation between the two filters with regards to turbidity, of important note however is the very low influent turbidity of 0.7 in 2 and 0.9 in the third test out of the four tests at 10 m/h which mean that the percentage removal in the filter at this rate will be lower with the 24/07/07 test giving a percentage removal of 86 % compared with 94 % on the 31/07/07. Therefore the influent turbidity will affect the consistency of the true performance of the filters which cannot be determined with variability in the influent turbidity.

In addition to the results shown in Table 13 Mitrouli et al (2009) discuss earlier trials negating the use of any coagulant aids where the only details of results given are the influent turbidity which was reduced from a typical value of 1.4 NTU down to 0.4 NTU in both filters. SDI (Silt Density Index) a key criterion for RO desalination according to Mitrouli et al (2009) was higher than desired and therefore this led the authors to decide that coagulation aids were required and hence why the results for the main bulk of testing given in Table 13 include these.

The results at 15 m/h begin to show a variation in performance between the two filters, with the Filtralite® showing a higher effluent turbidity of 0.2 and 0.3 NTU in two of the tests while

the anthracite/sand filter retains the 0.1 NTU result as it has in all other tests shown. This may indicate that the performance of the Filtralite® for turbidity removal does not cover as wide a range as sand although these are only two results and the difference is still minimal and cannot be taken as a true indication of a poorer performance from the Filtralite® media.

The 10 m/h filter runs were operated for 24 hours and the authors state that there was no turbidity breakthrough during this time and considering the low influent turbidity this would be expected for a dual-media filter. The results do not give the details of the progress of turbidity removal in the filters and without further data it is difficult to conclude on the effectiveness of Filtralite® compared to sand. Of important consideration also is the fact that the sand and Filtralite® layers although of similar particle sizes (0.8 – 1.25 sand, 0.8 – 1.6 Filtralite®) the sand is significantly larger than the 0.5 – 1.0 mm used in most rapid gravity filters (Kawamura (2000)) and Filtralite® is not produced in a grade of exactly this size. It is primarily marketed as a dual-media solution of the configuration given by Mitrouli et al (2009).

Ripening time in both filters was observed to typically take less than 30 minutes in both filters with no discernible difference in their operation. Head build-up in the filters is where a difference in the filters became apparent and indicates that if Filtralite® was used, a longer runtime would be expected for the same filtration conditions as shown by Figure 16 below:

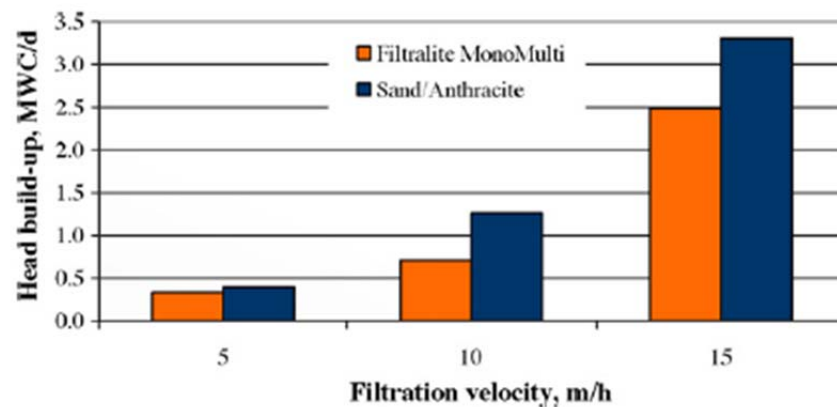


Figure 16 - Head loss build-up in filters from Mitrouli et al (2009)

By reducing the head build up through the use of Filtralite® it is shown by Figure 16 that filter run times could be increased which reduces the energy usage of the filters and requires less downtime for washing leading to substantial savings over the lifetime of a filter.

Silt Density Index (SDI) was a parameter used by Mitrouli et al (2009) and based on this criterion the authors conclude that the Filtralite® filter performs better than the anthracite/sand based filter. It was stated this is due to the greater particle porosities (of the media grains not the filter bed) that influences the grain shape and the surface texture of the filter media, which for the Filtralite® is very rough with a significant number of crevices. It is anticipated that the retention of deposited flocs within these crevices allow them to be shielded from flow shearing forces that can cause them to become re-suspended.

Issues with this work carried out by Mitrouli et al (2009) and also Mitrouli et al (2008) are that as mentioned by the authors the work was primarily concerned with paying attention to filtrate quality parameters relevant to feeding reverse osmosis (RO) membrane desalination systems. The SDI (Silt Density Index) was used to determine performance variations between the two filters. SDI is never used for assessing performance of a rapid gravity filtration plant for drinking water and therefore these results are not directly interchangeable. Mitrouli et al (2009) noted that the Filtralite® filter had a similar performance with regard to particulate removal from the feed water (NTU and SDI) with the major variation between the two filters being the rate of head build-up with Filtralite® exhibiting a lower rate of head build up as shown in Figure 16. Mitrouli et al (2009) concluded that this improved performance of the Filtralite® was due to its rough surface texture with crevices that better retain the flocs and protect them from flow shearing forces.

Work by Albuquerque & Labrincha (2008) on expanded aluminosilicate waste material from the manufacture of lightweight aggregates offers a different form of similar materials with similar physical characteristics compared to the commercial filter solution Filtralite®. The results for turbidity removal however were not consistent and are difficult to interpret as can be seen in the following charts showing turbidity removal (%) against volume (ml) of treated water but follow a trend to better performance at the shallowest depth and lowest flows:

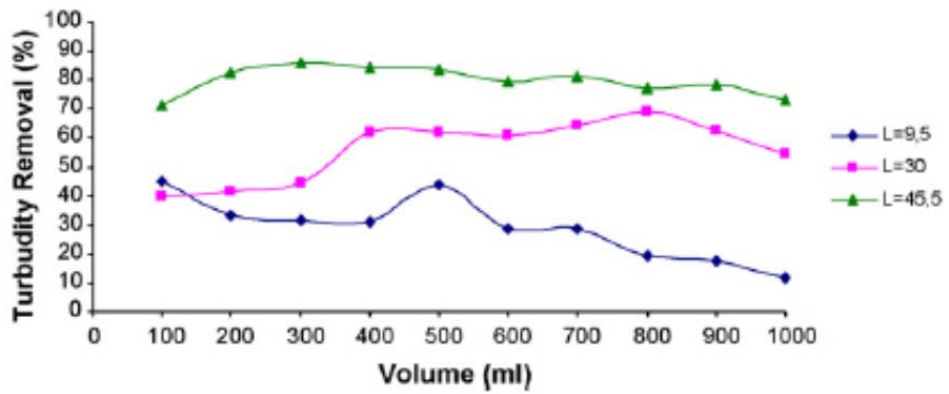


Figure 17 - Turbidity removal efficiency through filtration beds made of LCA 0.5/3 mm sieved fraction and variable depth (L); $C_o = 42 - 44.7$ NTU, flow rate = 4.43 m/h from Albuquerque & Labrincha (2008)

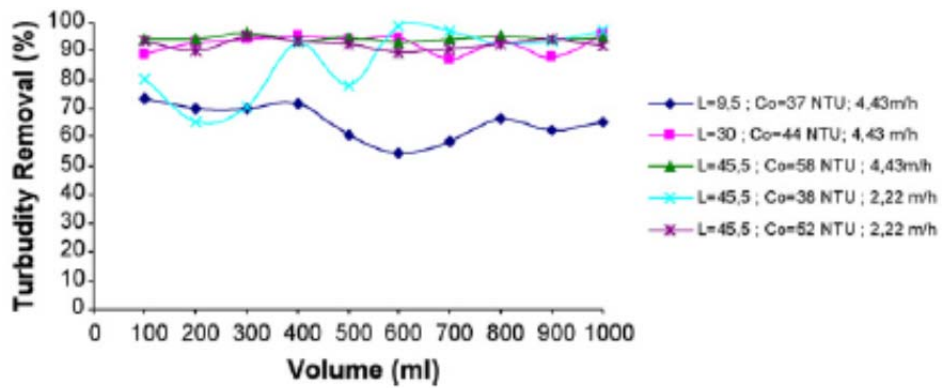


Figure 18 - Turbidity removal efficiency through filtration beds made of LCA 0/3 mm sieved fraction and variable depth (L); $C_o = 37 - 58$ NTU, variable flow rate from Albuquerque & Labrincha (2008)

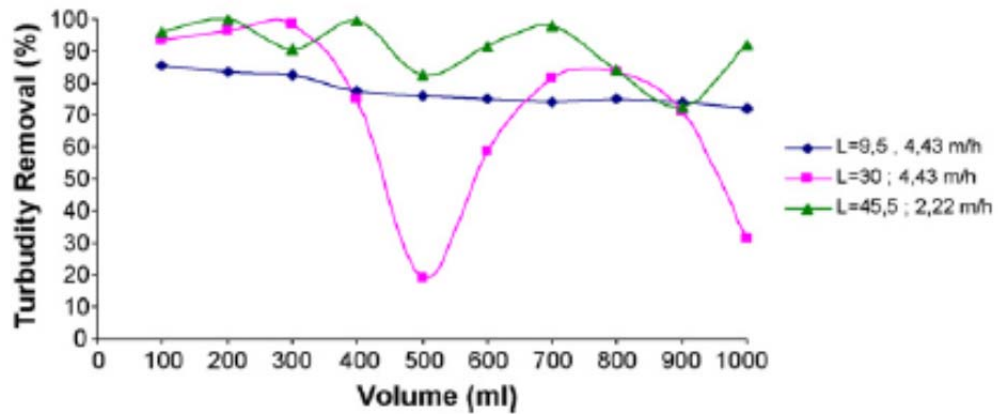


Figure 19 - Turbidity removal efficiency through filtration beds made of LCA 0/0.5 mm sieved fraction with variable depth (L); $C_o = 37 - 48.3$ NTU, variable flow rate from Albuquerque & Labrincha (2008)

Based on the data for a bed depth (L) of 30 and flow rate of 4.43 m/h from the three different fractions the results show a trend as shown in table below:

Figure 20 - Comparison of turbidity removal for flow rate of 4.43 m/h and bed depth of 30 form data in Albuquerque & Labrincha (2008)

Fraction Size	Turbidity Removal (%)
0/0.5	70 - 100
0.5/3	40 - 70
0/3	85 - 95

These results show that the removal is best in the finest fraction although not as stable as the other results as the chart in Figure 19 shows the value dropping to 20 % in some instances that indicates a breakthrough of particles. The results given for the 0/0.5 fraction gives the best turbidity removal as would be expected due to its lower bed porosity, while the material 0/3 again has small particles that are able to lower the bed porosity. Consequentially the 0.5/3 media will have a greater bed porosity and lower turbidity performance as is shown.

The data given by Albuquerque & Labrincha (2008) is limited with regards to turbidity and its application for determining performance in rapid gravity filters due to the off particle size ranges used that are not comparable with typical size range such as 0.5 - 1.0 mm used, although the work does show that lower particle sizes/reduction in bed porosity improves

turbidity performance. In addition the low flow rates being exceptionally low do not offer any clear conclusions for a comparison with current media used in rapid gravity filtration.

Overall the research conducted demonstrates benefits for the use of expanded materials such as aluminosilicate or natural pumice, clay and Filtralite® within filtration of potable water. The authors conclude the surface roughness, high surface area and high porosity of the filter media are the major contributing factors to better performance compared to sand. From an academic perspective the smallest size fraction that Filtralite® is available in is 0.8 – 1.60 mm is larger than the typical range of 0.5 – 1.0 mm found for filter sand which this study is looking to replace. Particle size and consequently porosity are major influences on performance of the filter bed. Where comparative testing is carried out, this larger particle size will bias the media from showing its true potential against the sand and other media that have a smaller particle size. Expanded aluminosilicates have a highly porous structure with a high surface area, both parameters correspond to a high roughness and this is considered to be a positive influence of filtration.

One area of significant improvement shown by the authors discussed was the reduction in head build-up within the filter being significantly lower in a Filtralite® based filter, as would be expected from the larger media. This can lead to greatly increased run-times that offer energy savings through reduction of backwashing frequency and the lightweight nature of the material also lends itself to reduced flow rate required for backwashing. Therefore if the media can be shown to be as good as sand because of its greater surface area then significant savings could be brought about through these reductions in backwashing flow rates and frequency that can help improve the sustainability of the plant.

The commercial media Filtralite will be used in the trial although the greater particle size compared to the other media being used will influence the results and it will be difficult to determine how much of an effect this will have. Careful consideration of the results in light of this variation is key to gain useful information and to provide accurate conclusions from the experimental data.

4.1.4 LIMESTONE

Hallsworth and Knox (1999) describe limestone as a sedimentary rock composed dominantly of calcium carbonate (CaCO_3), where the carbonate portion is usually composed of calcite.

There has been no research into the specific use of limestone as an alternative media to sand in rapid gravity filtration although it has been used as a media in roughing filters or specifically designed filters for removal of particular metal contaminants or to condition water to alter pH. There are papers that show the positive filter aspects of Limestone and these are described in the following section.

Work by Rooklidge et al (2002) for example determined the performance of limestone for removal of clay (smectite and kaolin) in horizontal roughing filters compared with dolomite and crushed basalt. Within this work Rooklidge et al (2002) states that dissolved calcite destabilizes colloidal clay, which is normally unaffected by simple mechanisms of sedimentation due to the small clay size and particle charge. Therefore as the limestone media is exchanged in the filter the calcium released destabilizes the clay particles increasing the amount of flocculation and sedimentation occurring within the filter bed. In addition Rooklidge et al (2002) also highlights the importance of particle surface-charge suppression in this process, which is the reduction in the intensity of the electric double layer that surrounds both the particles in suspension and the filter media. Ives (1970) also considers the surface charge to be an important consideration in the performance of filters as it hinders attachment in filters by repulsing particles from the surface of filter media because both surfaces carry a negative charge of typically -20 mV. In addition it is possible that interlayer cation exchange initiated by calcium and magnesium added from the dissolution of the limestone filter media can destabilize the clay promoting flocculation and sedimentation within the voids of the filter media as described by Rooklidge et al (2002) from van Olphen (1977).

Rooklidge et al (2002) considered three material types which were river rock composed mainly of basalt, dolomite limestone and high-calcium limestone. The authors note that there was no more than a 3 % change in alkalinity after passing through the limestone filters. Results from the work by Rooklidge et al (2002) is limited to roughing filters that have a different operation requirements to those of a rapid gravity filter although the fundamental

mechanisms for removal of particles are still standard for water treatment. Sacrificial use of limestone filter media assuming dissolution occurs can provide quantifiable benefit to the removal of clays by self-coagulation without the use of harmful chemicals to enhance the flocculation within the filter helps with the remit of trying to reduce the use of costly chemical coagulants and polymers to enhance the treatment process.

Destabilization of clay particles in the filter, due to interaction of released calcium and magnesium from the limestone media enhanced the deposition of the clay particles on to the media surface along the torturous path through the angular filter bed. This is seen as the primary removal mechanism in limestone beds by Rooklidge et al (2002). There is however a hint at the fact that the torturous path through the more angular filter bed may also enhance the transportation mechanisms (Ives, 1970) that increase the likelihood of a particle coming into contact with the media surface again increasing the likelihood of attachment occurring.

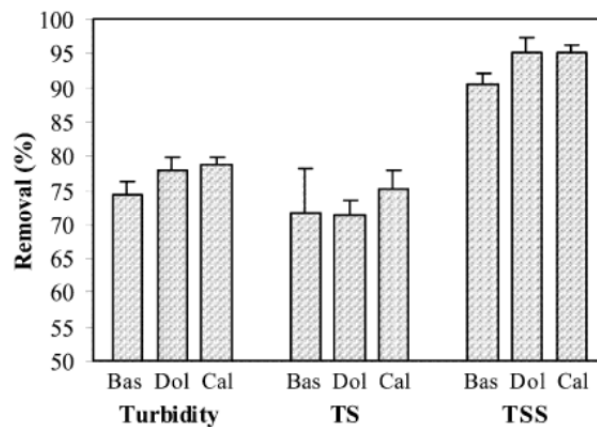


Figure 21 – Turbidity, TS and TSS removal in basalt, dolomite and calcite roughing filters from Rooklidge et al (2002)

Figure 21 shows the turbidity removal from the experiments carried out by Rooklidge et al (2002), however this is only a comparison between three different types of limestone with no comparison with other filter media, although it is noted that the performance was improved compared to river rock analyzed in previous work in Galvis et al (1998). Rooklidge et al (2002) state in conclusion that a limestone with a higher purity will enhance the removal of clays without adding harmful contaminants to the water which is an advantage over the addition of chemical coagulants and polymers to enhance filtration. The work also

highlights the importance of total suspended solids (TSS) to distinguish between the clay products and dissolution products. This is due to the dissolution products escaping the filter bed and adding to the value of turbidity measured in the filter effluent giving a lower performance than if these dissolution products were removed and only the clay particles removal was being analyzed. This is a risk that must be analyzed prior to use of this media and will be dependent on the quality of the limestone used.

Other work involving the use of limestone has centered on the removal of specific contaminants such as manganese which is a problem metal for many treatment works. Aziz & Smith (1996) have shown improved manganese removal through limestone filtration and Lipp et al (1997) investigated limestone as pretreatment before an ultra-filtration process where removal of manganese was the priority for the limestone stage in combination with pH adjustment of acidic natural waters to meet required drinking water standards.

The type of limestone used in a study will affect the results, and so information on the chemical composition and location of source would be preferential when looking at other studies that have used the material. The information given by Lipp et al (1997) is limited to the type of media which is described as dense calcium carbonate, while Aziz & Smith (1996) used Dolomite. The tests were not set-up like a rapid gravity filter and flow rates especially were lower than what would be expected in a rapid gravity filter. Aziz & Smith (1996) have a range of flow rates of 10 – 80 ml/min (0.000212 – 0.001698 m/h) which is lower than the range expected in an RGF filter (5 – 10 m/h for example). No details on the particle size of the media is given in the work and so it is difficult to make comparisons and with the variation in composition of different types of limestone available then it is unlikely that the work could be validated or give an indication as to how the limestone in this study will perform regarding manganese removal.

Lipp et al (1997) has shown removal of manganese in the water from values of 0.15 mg/L to around 0.01 mg/L to meet the German standards which are below the EU limit of 25 µg/l for drinking water that the study by Lipp et al (1997) was working to. However the study also showed an increase in pH of the effluent water to 9. Therefore CO₂ dosing was required to bring this value down below the upper limit of pH 8.

This pH variation will depend on the type of limestone filter media being used, if there is a lower release of CaCO_3 into the water as it flows through the filter, this will reduce the effect on the pH value of the effluent from the filter. However even with a reduced release of CaCO_3 , noted by Rooklidge et al (2002) to be below 8 mg/L that enhances the removal of smectite particles in a filter. Lipp et al (1997) showed a value of 70 mg/L in the effluent of the limestone filters. Release from limestone will be dependent on different types of limestone and water conditions, which will affect the removal of particles (clay in the cases of these studies). Dissolution of media is a concern for long term operations of a rapid gravity filter and this requires further study under these operating conditions.

Mackintosh & de Villiers (1999) considered the use of limestone filters for the treatment of soft, acidic and ferruginous groundwater. The authors describe the suitability for the use of limestone to meet these criteria in comparison to other methods such as lime dosing based on reduced costs of the material and how no CO_2 dosing is required and operators require less skill than with other methods. Mackintosh & de Villiers (1999) used a filter system known as a Spraystab[®] unit that operates differently to a typical rapid gravity filter, a diagram of the unit is shown below in Figure 22:

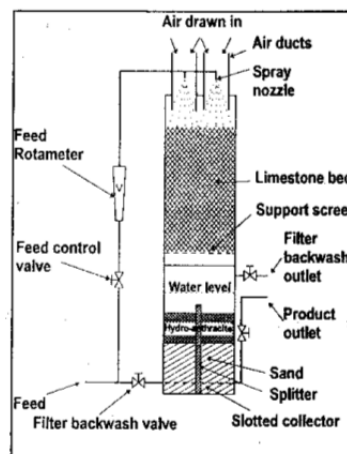


Figure 22 – Configuration of Spraystab unit from Mackintosh & de Villiers (1999)

This system consists of three units, an aeration unit to strip CO_2 from the water and dissolve oxygen into the water to enhance the oxidation of iron. A stabilization unit to hold the limestone media that increases the calcium, total alkalinity and pH of the water. The filtration unit then removes limestone fines and iron floc from within the stabilization unit. This filtration unit is made up of anthracite and filter sand as is typical in a dual-media filter.

This system from Mackintosh & de Villiers (1999) obviously differs from a typical rapid gravity filter and in this study the media will directly replace or supplement the sand in a filter. This will lead to performance variations with regard to the criteria chosen by the authors to a normal filter with limestone in place of sand. However as with the majority of the studies on limestone and other media where limited information on the specific use in a rapid gravity filter, the fundamentals and analysis of how the media might behave in RGF can be linked to what is occurring in studies for this research.

Mackintosh & de Villiers (1999) show that there is excellent performance (Table 14) from this system and it highlights the possibility of Limestone for removal of Iron and stabilization of pH and alkalinity of water, these are often problems for upland sources that are acidic from the surrounding environment.

Table 14 - Raw and effluent water quality at sites A and B from Mackintosh & de Villiers (1999)

Determinant	Unit	Site A		Site B	
		Raw	Treated	Raw	Treated
pH		4.7	8.2	6.0	8.5
Calcium as CaCO ₃	mg/l	0	39	6.5	26.25
Total alkalinity as CaCO ₃	mg/l	2	40	20	40
Conductivity	mS/m	18	75	22.5	26
CCDP as CaCO ₃	mg/l	207	2.3	87	1.7
Iron as Fe	mg/l	1.55	0.09	0	0
Manganese as Mn	mg/l	0	0	0	0

As the results show (Table 14) the removal of iron is highly effective when limestone is a filter media used. This method however has the limestone filter prior to the dual-media sand/anthracite filter that is there to remove the iron flocs created in the limestone filter. It will be interesting to see the performance of the limestone on its own as a filter in flocculating the residual iron and then removing it within its own bed. There is no discussion as to the mechanisms of the removal but it is likely due to the calcium destabilizing the iron

particles in the water and generating hydroxide precipitates allowing it to flocculate into larger particles that can be removed by filtration.

Therefore limestone has been shown in numerous studies to offer a benefit for the removal of metals such as iron and manganese, as well as adjustment of alkalinity and pH of the water to more beneficial values. In addition it was shown by Rooklidge et al (2002) that a small addition of CaCO_3 to the water of 8 mg/L or less can improve the removal of fine clays (smectite) from water which could be beneficial to rapid gravity filters and possibility may also improve removal through destabilization of the other particles from the water improving filter performance. The problem of dissolution and longevity of limestone filter media however must be understood more effectively to determine the economic viability of its use over a long period of time.

4.1.5 OTHER

A range of additional materials have been considered for use in filtration. These include the crushed shells of apricot stones as the upper layer in a dual-media filter by Aksogan et al (2003). Permeable collectors which typically consist of fibrous material arranged to form spheres described by Mulder & Gimbel (1991), Judd & Solt (1991) consider the use of fibrous collectors but for a specific application of aerosol removal by inducing an electric field on the media which is not a suitable solution for drinking water treatment. Gray & Learner (1984) considered the use of a dual-media percolating filters for waste water treatment consisting of a lower layer of blast furnace slag topped by a plastic media, and Sokolovic et al (2009) using expanded polystyrene particles.

Aksogan et al (2003) considered the replacement of anthracite with crushed apricot stone shells with silica sand placed below; this was carried out at laboratory scale using kaolin clay to produce the turbid water. The authors concluded from the work that the apricot shells produced a better turbidity performance than anthracite, the particle size of the media were given only as effective size (d_{10}) with the anthracite given as 0.85 and the crushed apricot shells were 0.70 mm and 1.80 mm for the fine and coarse version. In both tests carried out with either coarse or fine crushed apricot shells the performance was improved compared to the anthracite used. The paper does not discuss the reasons for this increased turbidity removal performance and it is not possible to ascertain from the research as limited information on the media's characteristics are given, such as a full particle size distribution curve.

Mulder & Gimbel (1991) state that conventional granular filter media have low collection efficiency and this is due to the fact that attachment can only occur on the external surface of the media, they therefore propose the use of a permeable media grains. The research carries out a numerical based approach to developing an argument for the use of permeable media over the more traditional impermeable grains and then moves on to carrying out experiments to corroborate the numerical analysis. The experiment involved placing a single plastic foam sphere (diameter – 13 mm) inside a tube with an identical internal diameter; polyethylene powder at a concentration of 100 g/m^3 (3 – 40 microns) was used to provide the turbidity. The suspension was fed into the tube filter for a specified time and then the

foam sphere was washed using distilled water and the retained particles of polyethylene powder were determined by total carbon analysis and turbidity measurements. The authors determined that the experimental results gave good correlation with theoretical results considering the difficulties in carrying out the experiment. The results however are only valid for a single collector (single media grain) and the impact at full scale is not known, in addition the impact of backwashing on what appear to be fragile permeable spheres were not considered and with a lifetime of over twenty years a typical filter media must be robust enough to resist any breakdown.

Gray and Learner (1984) used blast furnace slag and an upper plastic medium layer in a dual-media configuration; this however was for use in a waste water percolating filter. The work considered the removal of a range of metals including Fe, Cr, Cu, Ni, Zn, Cd and Pb, in addition suspended solids were also tested. The work did not compare the results directly with another media and only looked at the comparison between the dual-media filter and filters using the media separately. The bulk of the work concentrated on results that are not directly relevant to rapid gravity filtration of potable water such as Biological Oxygen Demand (BOD) and nitrification. It was concluded however that the dual-media filter did operate more effectively, with an upper layer of plastic acting as the coarse layer and the blast furnace slag lower layer achieving better water quality.

Sokolovic et al (2009) looked at the use of expanded polystyrene spheres for wastewater filtration. Density was determined to be key in affecting the performance of the polystyrene spheres by the author as more dense spheres had a smoother surface texture than the low density spheres. This however is a surrogate measurement for surface texture and highlights the importance of surface texture to removal and not density. Uniformity coefficient was also shown to have an impact on performance with a narrower particle size band showing poorer removal performance and greater headloss. It was concluded that the crucial parameter for optimizing filtration using expanded polystyrene spheres is the uniformity coefficient of the bed. This would be expected as an increase in finer particles would lead to increased removal while having a detrimental impact on headloss and run-times while the opposite is true for larger particles. The work shows that particle sizing is an important aspect to optimize filter media to the water quality that is to be treated, and that

consideration of surface roughness is important to turbidity removal performance within a filter bed.

Work analysing the removal of particles as they travel through porous rocks and soils has been conducted within the field of Geotechnics, examples includes work by Sherard et al (1984) who has written papers on the properties of gravel filters and the removal of silts and clays. The work considers gravels that have much larger particle sizes than would be expected within rapid gravity filtration with sizes up to 10 mm (compared to 0.5 mm). The work focusses on the impact of the hydraulic load through the filter affecting the grading and consolidation of the material than removal of particles. Neither are the clay particles in the size range expected within the drinking water filtration process. The application of this research considers the loss of fines from an earth dam that can lead to leaks and breakthroughs in the dam. Nevertheless the work considers the effect of hydraulics on mixtures of sands and gravels and could contribute to the knowledge of the behaviour of multimedia RGF, although there is literature on media mixtures reviewed within the field of drinking water filtration. The latter work does highlight the possibilities from mixed grading but notes this would be negated by the regular backwashing of normal RGF filters causing complete mixing of a bed of uniform density.

In conclusion there was limited research available on novel media for use in rapid gravity filtration, and much of this was commercially orientated. There was limited detail on the performance impact of the basic physical and chemical properties of media. Thus it was concluded that there was scope for further work to look at the performance of novel media in relation to fundamental theory of filtration and to provide an understanding of how to develop novel media to further improve its performance. In particular the literature review suggested there were possibilities to adapt media to optimize to incoming raw water quality and to contribute to the demands of future drinking water standards.

4.2 FILTRATION MECHANISMS

Fundamental mechanisms that impact the filtration performance are summarized by Ives (1970) and described by a number of other authors including O'Melia (1985) and Tobiasson & O'Melia (1982). These mechanisms were accepted as the fundamental methods of particle removal for deep bed filtration when operating correctly. In a full scale filter there will be a

variable impact from straining which occurs if the particles entering clog the pores between media grains.

Currently the proportion each of these mechanisms attributes to the overall removal performance of a filter is not fully understood but by comparing the physical and chemical differences between the filter media to each of these mechanisms helps develop an understanding of how each will vary based on the different media and an understanding as to why there is a variation in performance can be gained. Once a predominant mechanism has been determined then it could be enhanced by design to benefit from the physical or chemical variation of a media. Aspects required in an ideal filter media can then be determined and this can lead to an optimally “designed” filter media which is selected based on the raw water characteristics and upstream treatment processes allowing for an optimized design to be produced leading to improved filter performance and therefore improved water quality and possibly reduced operating costs.

Removal mechanisms fall into two primary categories, transportation and attachment. Transportation describes the mechanisms that move the suspended particles in the water and transport them closer to the media surface. An improvement in transportation does not lead to an improvement in attachment to the media surface but by increasing the amount of particles transported to the surface of the filter media there is a higher probability of a greater number of particles becoming attached. Attachment concerns the governing mechanisms that allow the particle to become attached to the surface of the media. It is important to note that not all of the mechanisms described offer a positive benefit. The electrostatic force for example offers a repulsive force to any particles attempting to attach to the media surface.

4.2.1 PARTICLE TRANSPORTATION

Ives (1970) notes a number of forces and effects that influence the transportation stage which move particles across streamlines to the grain surface where attachment can occur, these are:

1. Interception
2. Inertia
3. Sedimentation (Gravity)
4. Diffusion (Brownian Motion)
5. Hydrodynamic Action
6. Orthokinetic Flocculation

Authors, for example Yao et al (1971) and Ives (1987), note that transport to the boundary layer is the most important mechanism which includes interception, sedimentation and diffusion. Ives (1970) also notes straining but this is not considered to be a method of transportation and it is an undesirable occurrence since it may cause a reduction in flowpaths through the filter bed increasing headloss accumulation. This is because the full depth of the filter bed is not being utilized, and the relative size of the particles (< 20 microns) to the pore size (around 100 microns) is large, as can be seen in the diagram below (Figure 23) from Ives (1987):

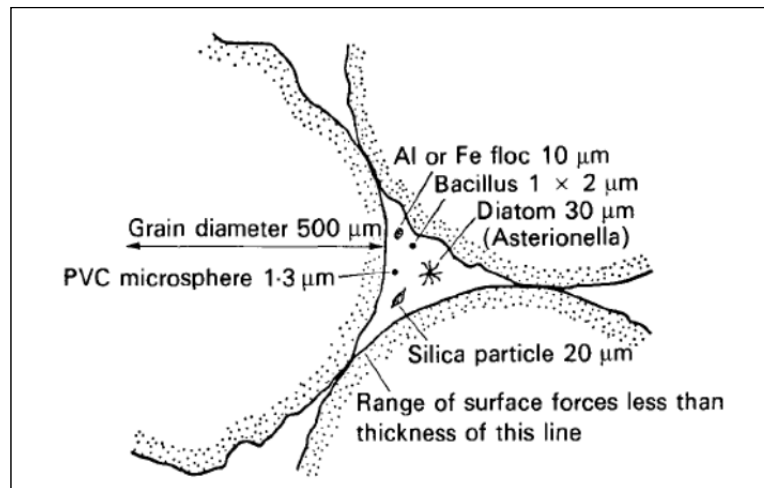


Figure 23 - Relationship of particle size pore size from Ives (1987)

For dilute aqueous suspensions inertia (for small particles < 20 microns) is considered unimportant (Ives (1970)), and would explain why it is not considered as a transportation mechanism by other authors. Orthokinetic flocculation is not considered as a mechanism for transportation but can improve the chance of particle removal through aggregation of particles, which produce larger groupings improving the rate of capture. Hydrodynamic forces are not used to describe the transportation process and authors such as Yao et al (1971) only note the effect of Interception, Sedimentation and Diffusion as the primary methods of transportation.

4.2.1.1 INTERCEPTION

Interception occurs when particles are located within a streamline that ensures the location of the particle is the same distance from the grain surface as the radius of the particle. Interception is the final step of the transportation method, and relies on other methods to move particles into streamlines that are adjacent to the grain surface. Ives (1970) states that the mechanism can be explained by the ratio of particle diameter to grain diameter given by Equation 1 below:

$$I = \frac{e}{d}$$

Equation 1 - Equation to determine interception parameter between particles and filter media from Ives (1970)

I = interception parameter, e = particle diameter, d = media grain diameter

A typical value for the interception parameter for cryptosporidium (4 μm) in a sand of 0.5 – 1.0 mm ($d_{60} = 0.74$) would give a value of $I = 0.0054$. Increasing particle size to $d_{60} = 1.0$ mm would give $I = 0.004$. As noted by Ison & Ives (1969), a reduction in the value of the interception parameter corresponds to a reduction in removal performance of the media as would be expected for a larger media grain.

4.2.1.2 INERTIA

A particle trapped in a streamline flowing around a particle can have sufficient inertia that they maintain their initial trajectory causing them to break free of the streamline and come into contact with the filter media grain so that attachment may occur. Ives (1970) states that in water, higher flow rates lead to lower collection efficiencies. This is expected as the higher flow rates would increase the shearing forces acting to detach particles from the surface of the filter media, while also reducing the effectiveness of attachment occurring.

Inertia will be affected by the flow path through the filter bed. If the path is variable and angular in nature then less inertial force is required for particles to break free. Angular particles would lead to sharp changes in direction and this flow state. While a more gradual path as would be expected with a spherical filter media would lead to a less varied flow path and therefore higher inertia forces would be required to allow the particles to break free of the streamlines.

4.2.1.3 SEDIMENTATION

Particles that are sufficiently large and have a greater density than the suspending water are subjected to a settling velocity, downwards in the direction of gravity. The extent as to which this will affect the particles so that they may come in contact with a grain surface depends on relative orientation (divergences) of the fluid streamline velocity vector and gravitational velocity vector (Ives (1970)). According to Ives (1970) the effect of sedimentation can be characterized by the dimensionless equation given below. This may be recognized as the ratio of Stokes settling velocity for the particle, to the fluid approach velocity (Ison & Ives (1969)):

$$S = \frac{(\rho_s - \rho)e^2 g}{18\mu v}$$

S = dimensionless sedimentation parameter, ρ_s = particle density, ρ = liquid density

e = particle diameter, g = gravitational acceleration,

μ = dynamic viscosity, v = approach velocity of filtration

4.2.1.4 DIFFUSION

Due to thermal energy of the water molecules surrounding a particle it exhibits a random movement as it travels through the streamlines due to collisions with the exited fluid molecules. For particles >1 micron in diameter this movement is restricted by viscous drag and the mean free path of the particle is at most one to two particle diameters (Ives (1970)). For particles less than 1 micron in diameter the movement becomes increasingly significant with reducing particle diameter.

The Peclet number P is used to give value to the ratio of movement due to Brownian diffusion, to advective motion of the fluid (Ives (1970)). This equation is:

$$P = \frac{dv}{D}$$

P = Peclet number, dv = change in approach velocity of filtration,

D = Stokes-Einstein diffusion coefficient

D is the Stokes-Einstein diffusion coefficient, this diffusion effect has been studied extensively in the field of air filtration but less so in water filtration although Yao (1968) indirectly studied diffusion in rapid filtration along with Ives and Sholji (1965).

4.2.1.5 HYDRODYNAMIC ACTION

Flow within filter pores is laminar with a velocity gradient, therefore a shear field exists. Within a uniform shear field a spherical particle would experience a rotation that would create a spherical flow field which would cause the particle to migrate across the field in a manner similar to that of a swerving ball in flight. In filter pores where the shear field is not uniform the particle will not migrate in a uniform or predictable way. The shape of the particle if not spherical will also create out of balance forces, moving it across the

streamlines. Combination of these factors creates a situation where the particle exhibits apparent random motion across streamlines to aid in transportation.

Ison & Ives (1969) demonstrated that this effect of hydrodynamic action was significant in the filtration of Kaolinite Clay suspension using an arrangement of multiple filter tubes with a range of different media sizes and clay suspension sizes to compare results against known filtration mechanisms described in this section. Ison & Ives concluded that a theoretical method of describing hydrodynamic action was not available, due to the complex and irregular nature of the streamlines within the filter pores causing too much complexity to calculate its impact on transportation.

4.2.1.6 ORTHOKINETIC FLOCCULATION

Camp (1964) suggested that orthokinetic flocculation could lead to aggregation of particles within the pores of the filter; this would lead to an improvement in the transportation of the particles according to the other transport mechanisms. Ives (1970) does not consider this a method of transportation as a consequence of changes in particle characteristics as this is promoted by the other mechanisms. Graham (1988) carried out computer model predictions and experimental tests which Ives (1970) had been unable to carry out to determine the impact of orthokinetic flocculation on filter performance. The results were based on numerical modeling, the prediction was that orthokinetic flocculation of particles in filter pores is appreciable but the improvement in filter performance through the increase in transport efficiency was small. When carrying out laboratory experiments, a cationic polymer was added along with the kaolin suspension, and it was shown that removal was higher than predicted in the model. The cationic polymer was added to aid with charge neutralization, however the addition of this polymer could explain the increased performance, as residual polymer present in the filter bed would lead to increased particle capture.

Graham (1988) concludes that filter pore particle flocculation is a minority mechanism and that based on observations from the study the two flocculation mechanisms altered were the particle-grain attachment efficiency and the preferential deposition of suspended particles onto the previously deposited matrix of particles. This second mechanism of preferential deposition onto already attached particles is considered the primary reason

behind the ripening time of a filter; that is as particles become attached the performance improves as particles will preferentially attach to other particles already attached to the media, this overcomes the electrostatic charge repulsion of the media surface. Therefore to understand how a filter media impacts on a number of fundamental removal mechanisms a comparison of the ripening time is important.

4.2.1.7 COMBINED TRANSPORTATION MECHANISMS

Ives (1970) explains that it is unlikely that any of these mechanisms acts uniquely. This would be expected and any experiments set-up to analyze improvement in any single mechanism in isolation would be extremely difficult if not impossible using currently available equipment. However by understanding the variations of all mechanisms and physical properties of the filter media, a better judgment can be made as to which mechanisms are likely to benefit from the change in filter media. Ison & Ives (1969) carried out laboratory experiments that showed interception, sedimentation and hydrodynamic mechanisms were the most significant for kaolinite in water. However these experiments were carried out under highly controlled conditions where the media used were spherical glass beads known as balitini. This would have reduce the impact of some mechanisms such as inertia that rely on changes in direction to allow for the inertia of the suspended particle to break it free and move towards the media surface.

4.2.2 ATTACHMENT MECHANISMS

Attachment mechanisms can be broken down into four key mechanisms; these vary in their significance according to the media's influence on the retention of the particulates from the water. The four considered to affect the attachment by Ives (1987) are:

1. Electrostatic Force
2. Van Der Waals Force
3. Polyelectrolyte bridging
4. Hydrodynamic Thinning

The electrostatic force or electrokinetic potential of the media grains and the particles suspended in the water are important factors in the attachment mechanism. They are typically repulsive between the particles and sand, and typically negative in water (Ives, 1987). Under rare circumstances the electrostatic force can be beneficial when the charge sign of both the grain and particles are opposite creating an attractive force to aid attachment (Ives, 1970).

It is unlikely that with real particles this would happen as perfectly or homogeneously ideal behavior as Ives suggests. As media particles have a very varied surface profile and the movement of the particles through the filter bed could alter the shape of the electric double layer. These effects would likely alter the charge density on different positions around both the media and particles moving through the bed.

The Van Der Waals force is a universally attractive molecular force between atoms and molecules, but is really only effective over very short distances i.e. inter-atomic distances on the order of 50 nm (Ives (1970)).

Polyelectrolyte bridging is where additional chemicals typically added during the coagulation phase of the water treatment process pass through into the filter. These provide bridges between both the particles themselves, and also between particles and media grains (Ives (1970)).

Hydrodynamic thinning resists the particles as they get closer to the surface of the media grain. As the particle approaches the surface the fluid between it and the surface of the grain must be displaced to allow attachment to occur. Displaced fluid creates a radial flow which experiences viscous resistance, this slows down the approach of the particle making it more susceptible to being swept away by the pore water flow.

Of the four mechanisms of attachment, the electrostatic force is discussed in further detail below. Hydrodynamic thinning and Van Der Waals are considered beyond the scope of this research at present and even testing for zeta potential is limited by the large cost of apparatus (Streaming Potential method), meaning available laboratories to carry out the tests are limited and often charge greatly for their use.

4.2.2.1 ELECTROSTATIC FORCE (ZETA POTENTIAL)

The model used to visualize the ionic environment in the vicinity of a charged colloid and also the surface area in the vicinity of a filter media particle is the electric double layer. The model helps to explain how electrical repulsion (or rarely attraction in natural circumstances) forces occur in the area surrounding the colloid or particle. Information in this section is taken from Elimelech et al (1995), Tien & Ramaro (1989) and Zeta Meter Inc. (1997).

Attraction caused by the negative colloid causes some of the positive ions to form a highly attached layer around colloids surface; this is known as the Stern Layer. Additional positive ions are still attracted to the negative colloid but repulsion is also caused by the already attached positive ions within the Stern Layer and also by other freely available positive ions that are simultaneously being attracted to the surface of the colloid (H^+ , Fe^+ etc). This dynamic equilibrium results in the formation of the diffuse layer of counter ions. The concentration of ions is greatest nearest the Stern layer and gradually reduces with distance until it reaches equilibrium with the counter-ion concentration in the solution. The diagram below (Fig. 4) gives a visual representation of this:

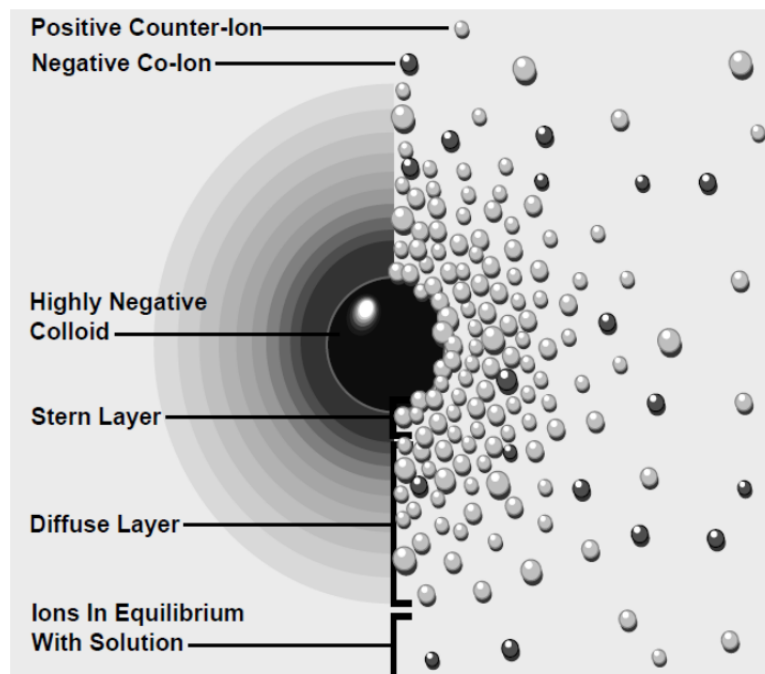


Figure 24 - Diagram of electrostatic force acting around a colloid Zeta Meter Inc (1997)

The concentration of negative ions will gradually increase with distance as the repulsive forces of the negative colloid are diffused by the positive ions surrounding it until equilibrium is reached with the surrounding solution as with the positive counter-ions (Figure 25). This relationship between positive and negative ions from the surface of the colloid to equilibrium with the surrounding solution follows a distribution similar to that shown in the chart below (Figure 25):

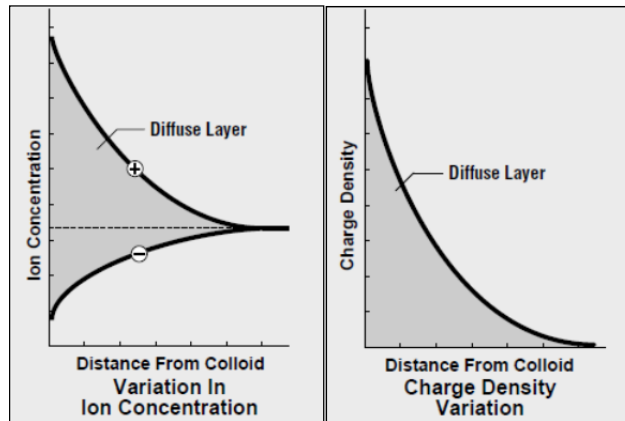


Figure 25 - Change in ion concentration and charge density (Zeta Meter Inc. (1997))

Charge density at any distance from the surface of the colloid is equal to the difference in concentration of positive and negative ions at that point. Charge density is therefore greatest near the colloid, where there are only positive ions (for this case) within the Stern layer. The density then gradually reduces to zero where there are an equal number of positive and negative ions within the equilibrium of the solution. The typical change in charge density against distance from the surface of the colloid is shown in the second figure above (Figure 26).

The double layer is formed as a consequence of the Stern and diffuse layers in order to neutralize the charged colloid and therefore in turn causes an electrokinetic potential between the surface of the colloid and any point in the mass of the suspending liquid. This difference is measured in millivolts and is referred to as the surface potential. The magnitude of the surface potential is related to the surface charge and the thickness of the double layer. The potential drops linearly from the surface inside the Stern layer and then exponentially through the diffuse layer approaching zero at the boundary of the double layer to the surrounding solution as shown in the diagram below (Figure 27):

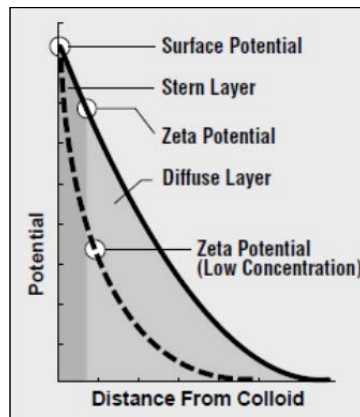


Figure 26 - Change in Zeta Potential with distance (Zeta Meter Inc. (1997))

A charged particle will move with a fixed velocity in a voltage field (the basis for zeta potential calculation). This phenomenon is called electrophoresis which is one method of determining the Zeta Potential of particles suspended in a liquid such as water. The Zeta Potential is typically used as a method of estimating the surface potential of the colloids as the surface potential is experimentally immeasurable, the zeta potential is therefore the best method of getting an indication of the value of the particle potential.

The zeta potential is a measure of the potential at the shear plane which is located at the boundary between the fixed and mobile part of the double layer (Elimelech et al (1995)). The exact location of this plane is not known and therefore uncertainty exists but it is often taken to be the boundary between the Stern layer and the diffuse layer as the Stern layer is considered to be where ions are strongly attached to the particle surface and move with the particles as a highly attached layer.

Applying these theories to filtration, O'Melia & Ali (1978) suggests that as the particle approaches the surface of the media grain the two diffuse layers begin to interact. The distance at which this interaction begins to occur will depend on the ionic strength of the solution, salts concentration and pH value but in water treatment a distance of 50 nm is considered to be the usual according to O'Melia & Ali (1978). This interaction is nearly always a repulsive force and for attachment to occur the Van Der Waals force must begin to attract the particle to the surface of the media grain before the repulsive force becomes significant enough to restrict the particle from interacting by attractive Van Der Waals forces.

Suthaker et al (1995) describes how charge concentration occurs along the sharp edges of an angular filter media. As electrostatic charge is typically negative (-20 mV according to Ives (1990) for sand) which repels the negatively charged particles attempting to attach to the media surface. Therefore these charge concentrated zones will be more difficult to attach to than other areas assuming the predominant surface charge of natural particles for removal is negative and repulsion occurs. Suthaker et al (1995) states that this increased charge concentration will increase particle attachment in these zones, this is counter to the theory that electrostatic charge from the media repels the media attempting to attach to the surface. Suthaker et al (1995) does not elaborate on this or show how this was determined, and was uncorroborated by experimental work and remains theoretical and does not compare well with what is currently known about the electrostatic force and its repulsive impact as stated by Ives (1990).

Work on understanding and describing the fundamental mechanisms that govern attachment of particles within a filter were well developed by previous authors, the above is a summation of the work that outlines the current understanding of the mechanisms. This information will be used to discern links with performance of novel filter media to understand why there was a variation in performance between the media and help understand the most important mechanisms.

In conclusion the literature review has suggested the fundamental mechanisms of RGF are well known but the contribution of each to filter performance operating under different conditions is less well understood. The quantitative link between physical (surface area, roughness, shape) and chemical properties of filter media to enhancement or reduction in the performance of each mechanism is not well understood. This is an aspect that the work within this thesis has tried to overcome. It was incorporated into an experimental design to include steady state well controlled synthetic raw water and variable real waters to develop the application of these fundamental filtration mechanisms.

4.3 ANALYSIS AND OBJECTIVES

A review of the currently available literature on the use of alternative filter media in rapid gravity filtration has revealed a limited amount of published research on the subject and a limited number of alternative media suggested. The media found to dominate the literature when specifically looking at rapid gravity filtration were glass, pumice and expanded aluminosilicate. Additional materials found to be rarely considered included limestone, slags, permeable spheres and biological materials such as apricot stones which all have only a single research paper related to them or are considered for use in different treatment processes.

The previous research is limited as each test is carried out using different apparatus and water qualities and this limits the cross comparison of the different alternative filter media being analyzed in each paper. In addition the work does not provide a comparison of the results with fundamental filter theory which would enable filter media to be chosen based on predicted performance, based on the water quality to be treated. An analysis of a range of alternative filter media under identical conditions will give a better indication of the mechanisms involved. A lack of research conducted at pilot or demonstration scale at operating water works limits the ability of industry to make decisions on the possible use of alternative filter media for rapid gravity filtration.

To overcome these limitations of the currently available literature, this study will aim to meet the following objectives and further the understanding of filtration mechanisms and to determine suitability of alternative media.

- Explore the advantages and disadvantages of alternative filter media
- Report on the fundamental properties of the alternative filter media compared to the traditional sand
- Report on how the fundamental mechanisms of filtration are impacted upon by variations in media properties of the alternative media.

- Carry out comparative analysis of suitable filter media at pilot scale at an operating water works to confirm findings and determine what benefits can be made.

5 MEDIA CHARACTERISATION RESULTS AND DISCUSSION

Materials that had been highlighted as possible alternative filter media from previous research and those that may have beneficial properties are shown in Table 15. Maintaining a similar particle size was a key consideration of selecting the alternative filter media, however manufacturers produce these materials for a wide range of applications and therefore sourcing a particle size similar to the 0.5 – 1.0 mm of sand was difficult. In instances where it was not possible, the nearest appropriate sample was provided by the supplier and this was tested and consideration made of how this variation would have influenced conclusions. A variation in particle size, however, is the most important criterion for optimization of filtration and a comparison of this would enable detailed analysis of the impact of PSD, although often ignored in some previous literature.

Table 15 - Selected filter media for characterization testing

Media	Source	Size
Sand	Garside Sands (Aggregate)	0.5 – 1.0 mm
Glass	Garside Sands (Aggregate)	0.7 – 1.0 mm
Limestone	Tarmac Quarry Materials	0.6 – 1.18 mm (Trucal 25)
Filtralite	AMT Systems Ltd	0.8 – 1.6 mm (Type HC)
Slate	Delabole Slate	0.425 – 1.4 mm (Type S12)
Pumice	Pumex	0.2 – 1.4 mm (NMP 9)
Pumice	Techfil Europe Ltd	0.6 – 2.0 mm (Type No. 4)
Steel Slag	Pelt & Hooykaas	0.5 – 1.0 mm
Phosphorus Slag	Pelt & Hooykaas	0.5 – 1.0 mm
Furnace Slag	Pelt & Hooykaas	0.5 – 1.0 mm

Characterization testing would allow for the variations in the alternative filter media to be compared to traditional sand and quantified against changes in performance. In addition some testing was carried out to possibly determine if there was additional benefit for the

removal of common soluble metal contaminants to be gained from filtration helping to reduce the load on other additional systems that are used.

Tests were predominantly based on British Standards (noted in each test) to compare alternative media with the current requirements for filter media. This was considered important in selecting media for further testing at laboratory and pilot scale. Alternative or new criteria were also included in the testing for media that obviously fail to meet the required British Standards. These standards are based predominantly on the use of sand, which would limit the development of novel new solutions. These additional tests were based on the literature review and an understanding of what properties would impact on fundamental transportation and attachment mechanism. They were Scanning Electron Microscopy and particle shape analysis to understand the surface properties of the filter media and the flow paths through the filter bed.

5.1 DENSITY

5.1.1 THEORY

Ives (1990) suggests that the density of the filter media does not directly affect its performance as a filter media; but it is generally vital information used to help determine the backwashing/fluidization behavior of the filter grains. For the design of multi-layer filters, different densities between the media ensure that the desired stratification is maintained after backwashing has been completed; in a rapid gravity filter the denser materials will settle to the base of the filter with lower densities nearer the surface.

BS EN 12902:2004 Products used for the treatment of water intended for human consumption – Inorganic supporting and filtering materials – Methods of test gives the procedure for determining the bulk density of a filter material with a particle size that is less than 4 mm. The method determines the density of dried filter media in loose or packed form by weighing a known volume in a measuring cylinder.

The sample is prepared by drying a sufficient volume of media in an oven at 105 ± 2 °C to constant mass, the media is then returned to ambient temperature in a desiccator. For a porous material the temperature should be raised to 150 ± 2 °C to ensure no liquid remains within the media.

For loose material the measuring cylinder is weighed to the nearest 1 g. With the measuring cylinder positioned on the balance the media sample is poured in and the volume is noted along with the mass of the media. When determining the density of the packed material the procedure is the same except for the use of a glass rod covered by a rubber sleeve to tap the walls of the measuring cylinder until the media reaches a constant volume.

When calculating the density the following Equation 2 is used:

$$\rho = \frac{m_1 - m_0}{V_1} \times 1000$$

Equation 2 - Equation for calculating bulk density from BS EN 12902:2004

Where:

m_0 - The mass of the measuring cylinder, in grams.

m_1 – The mass of the sample of media and the measuring cylinder, in grams.

V_1 – The volume of the media in the measuring cylinder, in millilitres.

The British and European Standards give limits ranges of density that certain filter materials should fall within for both loose and packed bulk density. Filter media covered by these limits include Silica Sand (BS EN 12904:2005), Pumice (BS EN 12906:2005), Expanded Aluminosilicate (BS EN 12905:2005), Pyrolyzed Coal Material (BS EN 12907:2009), Anthracite (BS EN 12909:2005), Garnet (BS EN 12910:2005), and Barite (BS EN 12912:2005). The values given by these standards are shown in Table 16 below:

Table 16 Range of densities for materials covered in British Standards for approved filter media

Filter Media	Bulk Density Loose		Bulk Density Packed	
	Lower Bound (kg/m ³)	Upper Bound (kg/m ³)	Lower Bound (kg/m ³)	Upper Bound (kg/m ³)
Silica Sand	1400	1700	1500	1900
Expanded Aluminosilicate	300	900	320	950
Pumice	300	650	320	750
Pyrolyzed Coal Material	450	560	460	580
Anthracite	650	800	670	820
Garnet (Almandite)	2150	2250	2350	2400
Garnet (Andradite)	1850	2000	1950	2250
Barite	2200	2400	2500	2600

Ives (1990) gives values for typical specific (particle) densities of various common filter media (Table 17), these values discount the pore spaces that occur in the media when placed in a volume and are used as more effective determinations of the densities for backwashing calculations.

Table 17 Specific densities for a range of filter media from Ives (1990)

Filter Material	Origin	Density (kg/m ³)
Quartz Sand	UK	2650
Anthracite	UK	1400
Hydranthracite	FRG	1740
Pumice	Sicily	1180
Expanded Slate	FRG	1500
Garnet	USA	3950

The method for determining the particle density is given by Ives (1990) from which Table 17 is derived. This more precise method uses standard density bottles and was described as follows:

- a) Weigh empty bottle and record value (A) in grams.
- b) Weigh bottle full of water and record value (B) in grams.
- c) Weigh bottle with dry filter media sample and record value (C) in grams.
- d) Weigh bottle with filter media sample and water filled to original water level and record value (D) in grams.
- e) Determine volume of bottle (E) in cm^3 by subtraction of (B) from (A).
- f) Mass of sample (F) recorded in grams is found by subtracting (C) from (A)
- g) The volume of water present in the flask (G) with the sample of filter media and expressed in cm^3 is found by subtracting (D) from (C).
- h) The volume of the sample (H) in cm^3 is therefore found by subtracting (E) from (G).
- i) Finally the density of the sample in kg/m^3 is found by dividing (F) by (H)

For porous media such as anthracite or pumice, soaking for 24 hours and slow stirring may be required to remove all of the air bubbles from within the pores of the media to enable an accurate determination of the particle density excluding the air space in pores using the above method as described by Ives (1990).

The buoyancy effect of the filter media being placed in water must be taken into consideration when being placed under water within a filter (Ives (1990)) and as the density of water is typically taken as $1000 \text{ kg}/\text{m}^3$ this is the value by which the density is reduced to give the effective density of the filter grains when placed in a submerged working filter and also under backwash conditions for calculation of the flow rates.

The particle density is used to determine the sphericity of the particles as described in 5.2, and is a useful method of comparing the filter media density more accurately as it negates the voids between the particles and considers only the density of the media itself. Effects of the density on backwashing and the determination of suitable materials to avoid stratification require knowledge of the particle density of the various media (although in combination with settlement tests).

5.1.2 TESTING

Results from testing of the filter media selected in the laboratory are given in Table 18. These were determined using the method given in BS EN 12902:2004 used along with Equation 2 as noted. Packed bulk density is calculated only as this is the more useful value as the material will not be used in its loose state, the hydraulics will compact the media.

Table 18 - Values for bulk density packed of tested filter media

Media	Mass (g)	Volume (ml)	Bulk Density Packed (kg/m³)
Glass	341.1	250	1364.4
Pumice (Pumex)	98.9	250	395.6
Pumice (Techfil)	102.7	250	410.6
Filtralite	200.2	250	800.8
Limestone	331.1	250	1324.5
Slate	335.0	250	1340.0
Steel Slag	394.0	250	1576.0
Furnace Slag	288.3	250	1153.2
Phosphorus Slag	313.2	250	1252.8
Sand	391.1	250	1564.4

The results shown in Table 18 show that as expected Pumice and Filtralite have the lowest bulk density thanks to their porous structure. It is interesting to note that glass and slate have virtually identical values for bulk density, with the phosphorous and furnace slag also having a similar bulk density. It was also noted that sand and steel slag had the highest density with only a slight difference between them.

The values for the materials fall within the range expected by the British Standards shown in Table 16 however with the lack of standard for limestone, slate and slags then these cannot be compared. Bulk density however is not as effective as the specific density for determining the likely settlement and backwashing characteristics of the media. Particle shape will also have an effect on these two criteria, packing and backwashing as well as specific density.

Specific density was calculated using the method outlined by Ives (1990) and the results for the filter media tested are shown below in Table 19. The media selected for this test are the ones that were used in the laboratory studies and the tests were not carried out until after backwashing results to compare the data.

Table 19 - Specific Particle Density for media as tested according to Ives (1990)

Media	Measured Specific Density (kg/m³)
Sand	2582
Glass	2497
Limestone	2651
Filtralite	1713
Slate	2886

The values found above compare favorably with either data from manufacturers (Filtralite – 1700 kg/m³), and from previous studies such as Ives (1990) which shows sand to be 2650 kg/m³ and Fitzpatrick (2005) who tested glass to be 2511 kg/m³. These correlations show good confidence in the testing of the media for its specific particle density.

Of the five media tested, they were ranked in descending order as Slate, Limestone, Sand, Glass and Filtralite. As with the BS test the Filtralite was shown as the least dense material as the structure is made up of a significant number of pores. Although the method of determining the specific particle density requires removal of all air pockets from the media this was not possible in practice. Some of the pores of Filtralite are within the internal structure of the media and not open to the external environment and therefore the water cannot penetrate into the media sufficiently and hence the particle density is reduced. However the result given for Filtralite is applicable to filtration as the closed areas will not be entirely filled with water when the media is in use. The other filter media all fall within a range of 2500 to 2900 kg/m³.

5.2 SPHERICITY AND PARTICLE SHAPE

5.2.1 THEORY

Ives (1975) highlighted that a more spherical filter media would lead to improved turbidity removal due to the torturous flow path through the media that would need to be navigated by suspended particles. However a limit of 0.6 as a lower limit on sphericity was set as below this value the filter bed would have a very low undesirable permeability. Slate falls below this value with a sphericity of 0.49 and will offer an insight into the impact of this on headloss performance which according to Ives (1975) will not be desirable.

Fitzpatrick (2005) found sphericity of 0.7 for glass (0.5 – 1.0 mm) using the settling velocity method given by Ives (1990) which has been used for this study, and is outlined in the following test results. This value given by Fitzpatrick (2005) however will be dependent on the type of processing used to crush the glass cutlet down into the required grading for filtration and it would not be unexpected to see a range of different values for glass used in this study compared to that in Fitzpatrick's. It is important to note however that the studies by Evans et al (2002) and Rutledge and Gagnon (2002) do not give a value for sphericity and therefore it is more difficult to compare results with this study if the sphericity is the dominant variable for performance of the media. Sphericity is determined to have a key impact on the physical characteristics of the filter bed, and therefore should be included in any future studies on filter media to enable for more effective comparison.

5.2.2 TESTING

Testing was carried out according to the method described by Ives (1990) and described previously. Settling velocities (Table 20) were calculated from an average of 10 grain particles of the media being tested as per the procedure designed by Ives (1990), with the grains selected to give a representation across the size range of the media. Particles that impacted or were near the walls of the glass cylinder were discounted and only those that fell impeded through the water were used to calculate the average settling velocity.

Table 20 - Tested settling velocity of media grains tested according to the procedure of Ives (1990)

Media	Avg. Settling Velocity (mm/s)	Standard Deviation
Sand	108	11.6
Glass	98	14.1
Limestone	104	13.3
Filtralite	89	12.9
Slate	79	11.9

The settling velocity was then applied to the method given by Ives (1990) which uses the following equation (Equation 3) to determine the ratio of drag coefficient to Reynolds number (C_D/Re):

$$\frac{C_D}{Re} = \frac{4g(\rho_s - \rho)\mu}{3\rho^2V^3}$$

Equation 3 - Equation to determine ratio of C_D/Re from Ives (1990)

Once the ratio of C_D/Re has been calculated then the Camp Curves can be used to obtain the corresponding Reynolds number value which is then input into the following equation to determine the hydraulic diameter of an equivalent spherical particle that would settle at the same rate as the tested particle:

$$d = \frac{\mu Re}{\rho V}$$

Sphericity of the tested particle is then determined by the division of the calculated hydraulic diameter by the average diameter of the particles being tested:

$$Sphericity (\psi) = \frac{d}{d_s}$$

The calculated values for sphericity are shown in Figure 27 below:

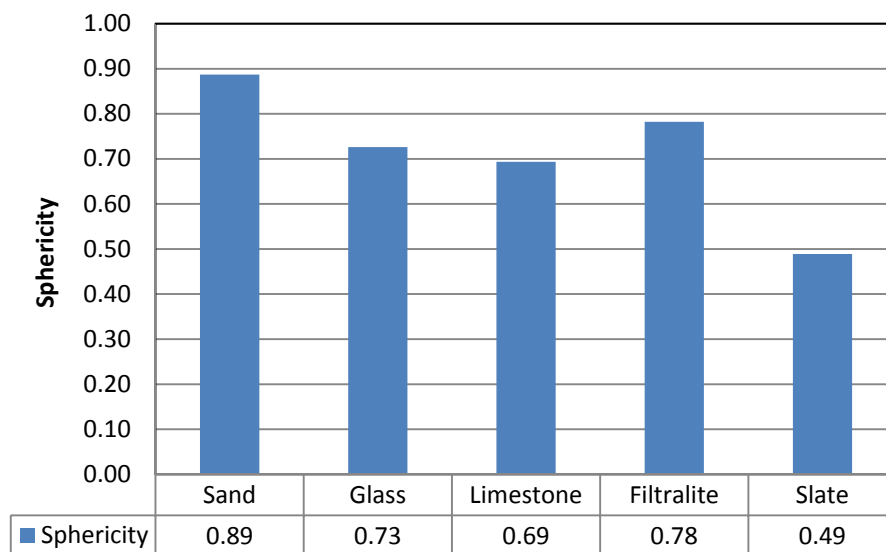


Figure 27 - Sphericity of tested media

The sphericity of the sand is close to the expected value of 0.85, confirming previous data given by Ives (1970). As can be seen all other media are less spherical than the sand. The slate falls below the 0.6 limit given by Ives (1975). It would be expected therefore that the slate would produce an undesirable headloss based on this theory. All other media are

above this 0.6 limit and therefore should be suitable. It is predicted that an increase in angularity would lead to improved headloss performance as the angularity reduces close packing leading to greater bed porosity that reduces resistance to flow through the bed. Comparison of the bed porosity results to angularity with headloss results is key to understanding this relationship.

5.3 PARTICLE SIZE DISTRIBUTION

5.3.1 THEORY

BS EN 12904:2005 Products used for the treatment of water intended for human consumption – Silica sand and silica gravel states that the particle size distribution will be described by either:

- a) Effective size: (d_{10}), with a maximum deviation of $\pm 5\%$

Uniformity coefficient: (U), shall be less than 1.5;

Minimum size: (d_1), with a maximum deviation of $\pm 5\%$

or

- b) Particle size range and mass fraction of oversize and undersize particles according to application. The maximum contents of oversize and undersize shall be a mass fraction of 5% for the application of the product in multi-media filters and a mass fraction of 10% in single media filters.

This allows two options for the acceptance of a particular Particle Size Distribution by mass with option (b) allowing for the media to not match the requirements of option (a), so long as the amount of material outside of the required particle size range is within the accepted 5% or 10% limits stated and that the media is suitable for the use intended. This therefore does give some freedom for the media based on the “suitable for the use intended” phrase which allows for the use of any material as long as it meets the performance required, does not alter water chemistry negatively and is economically viable.

The Degremont (1979) manual gives an alternative list of physical properties by which a filter media should generally be defined. Within this list those relating specifically to the particle size distribution include:

- a) Grain Size – A particle size distribution curve of the percentage of material passing each standard sieve size.
- b) Effective Size – Is the mesh size at which only 10% of the sample material is able to pass through.
- c) Coefficient of Uniformity – A ratio of sizes corresponding to the percentages 60 and 10 determined from the Particle Size Distribution (PSD) curve.

Guidance on determination of the particle size distribution are given by *BS EN 12902:2004 Products used for the treatment of water intended for human consumption – Inorganic supporting and filtering materials – Methods of test*. Under clause 5.1.1 it states:

The particle size distribution of granular materials shall be determined by sieving; this is applicable to distributions measured using sieves of nominal aperture size of 0.025 mm and above. Original details of the procedure are given in ISO 2591-1 Test sieving – Part 1: Methods using test sieves of woven wire cloth and perforated metal plate.

BS EN 12902:2004 (under 5.1.5 and 5.1.6) also gives guidance to how the information should be presented. It requires a cumulative particle size distribution curve in accordance with ISO 9276-1 and to also report the following parameters from the curve:

- a) Effective size (d_{10}) – 10 % passing
- b) Uniformity coefficient (U) - ratio of 60 % passing to 10 % passing
- c) Minimum size (d_1) – 1% passing
- d) Oversize percentage
- e) Undersize percentage

The value of the uniformity coefficient is a measure as to how much the media size varies (Ives (1990)); the closer the value is to unity the narrower the range giving more consistent

the performance throughout the bed depth but less versatile in dealing with finer particles. The guidelines set-out by BS EN 12902:2004 and standard textbooks (Degremont (1979) & Kawamura (2000)) typically give a range of between around 1.4 and 1.8. Although BS EN 12902:2004 does state that the media need not be excluded by this parameter alone but as it is a key indicator of the type of material being analyzed it does give an indication as to the variation in particle size of the media. If there is a significant range of particle sizes then stratification of the filter bed will occur affecting the overall filter performance.

Kawamura (2000) *Table 3.2.7-1* gives typical ranges of effective size and uniformity coefficient for filter sand used in a mono-media rapid gravity filter:

- a) Effective size: 0.45 – 0.65
- b) Uniformity coefficient: 1.4 – 1.7

These values are recommended for a mono-media sand filter. Degremont (1979) gives a range of uniformity coefficient between 1.2 and 1.6 with some measured practical instances up to 1.8, these uniformity coefficients vary compared to the value of < 1.5 specified by BS EN 12904:2005. This European standard also gives a second option for limits to the specification of filter media and it is not surprising therefore that different Uniformity Coefficients are reported in the literature. Therefore uniformity can be taken as a guideline value but care is still needed to ensure the medium has other suitable characteristics and is still suitable for use in rapid gravity filtration.

Ives (1990) states that there is no size specification that is best for all cases of water filtration. Therefore the size specification should be appropriate to the water quality to be filtered, e.g. pre-treatment, the flow rate and the desired filtrate quality, length of filter run and backwash conditions. To this end, the values stated above are not absolute design standards but they can be adjusted based on these operational requirements. This is one of the objectives of this project, to determine if alternative filter media sizes may be used to reduce dependence on chemical coagulation and GAC. Although media with a greater particle size range may incur these stratification problems suggested during backwashing where the smaller media would arrange itself at the surface and increase the risk of clogging. To reduce this effect the uniformity coefficient would as noted be as low as possible, although the ranges specified are based on years of operating experience with sand. There

may be advantages to removal by less uniform media and this is a reason for the consideration of a wider range of particle sizes in this project.

5.3.2 TESTING

All testing was carried out in accordance with ISO 2591-1, charts and results are shown here with the detailed Particle Size Distribution results sheets given in Appendix I. Other authors have published PSD curves of media, these include Rutledge & Gagnon (2002) who did not consider the difference between the PSD curves of the recycled glass and sand which is important to their interpretation of the results. PSD is often used as a direct comparison by authors of the media they are testing or a determination of an effect of mechanical degradation of the media after a friability test (Fitzpatrick, 2005). Fitzpatrick (2005) is an example; she compared the PSD of the glass and sand before and after an attrition test to determine the friability of the materials and its possible effect on filtration performance. Farizoglu et al (2003) determined the PSD of their filtration pumice.

PSD is an important consideration when analyzing the results from filtration trials as the impact of particle size on turbidity and headloss performance is known. However PSD is dependent on the selection of the media itself and can be altered depending on the specification required by the end user. As noted by Ives (1990) a media size specification is not appropriate to all situations and therefore the decision should be based on the raw water to be treated. In this study the media were chosen to match the standard 0.5 – 1.0 mm sand supplied by Garside Sands (UK) which has a UC of 1.27 and is commonly used throughout the UK for rapid gravity filtration of potable drinking water.

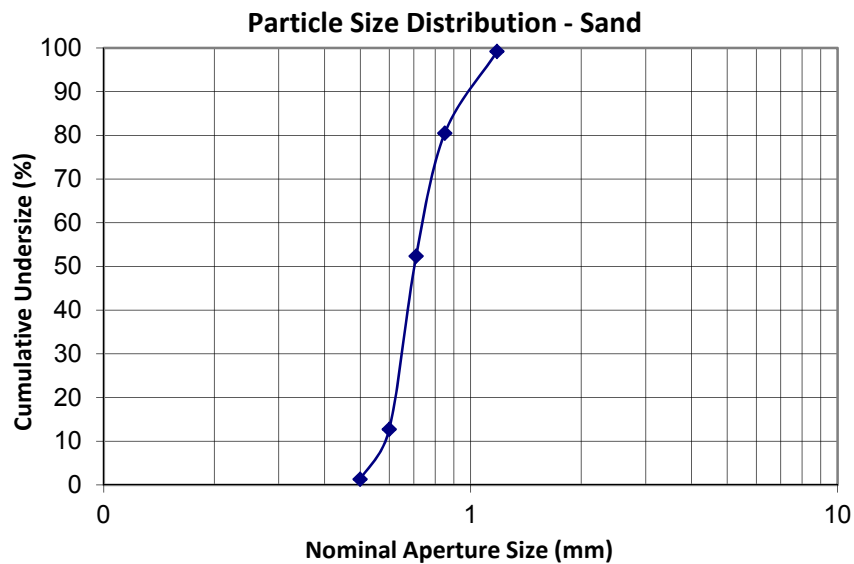


Figure 28 - Particle Size Distribution of Sand (0.5 – 1.0 mm)

As the current standard filter media in both mono and multi-layered filters then the results for sand are what the other media will attempt to be matched and compared against. Differences in filter performance between the media should be compared against these particle size distribution (PSD) curves to determine or eliminate the significance of the particle size. As noted however particle shape must also be considered simultaneously as this will affect the packing and therefore the effective porosity of the bed of potentially equal importance to the particle size.

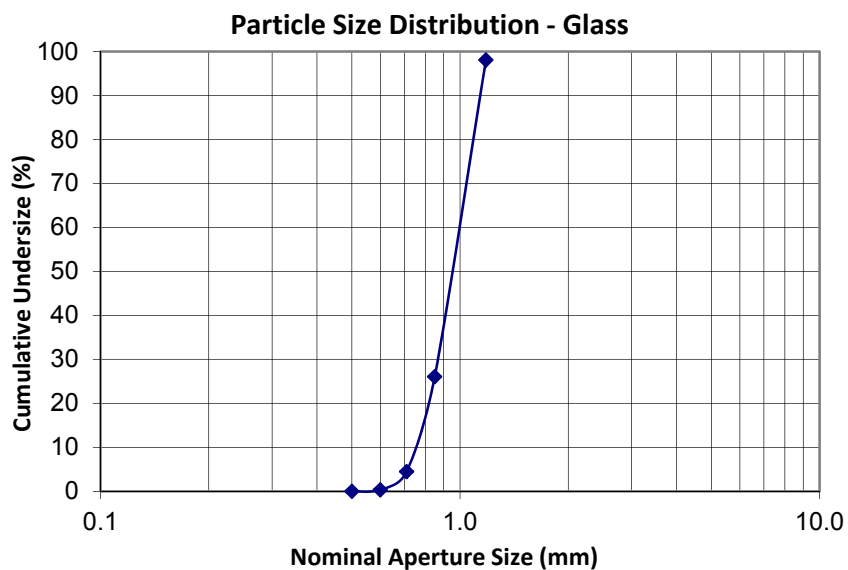


Figure 29 - Particle Size Distribution of Glass (0.7 – 1.0 mm)

The glass (Figure 29) has a larger overall particle size than the Sand (Figure 28), also the range of particle size of the glass is wider shown by its uniformity coefficient of 1.21 compared to a value of 1.27 for the sand (Table 21). Therefore there is a possibility that glass would show less effective turbidity performance than the sand due to its larger particle size but lower headloss. This does not however take into consideration the particle shape of the two media and its effect on porosity of the filter bed.

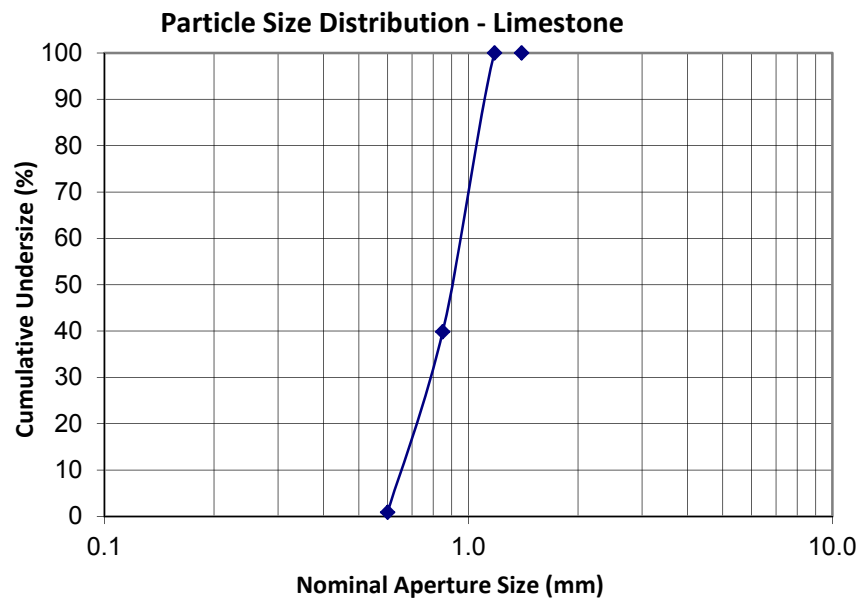


Figure 30 - Particle Size Distribution of Limestone (0.6 – 1.2 mm)

Limestone has a similar PSD (Figure 30) to glass (Figure 29) although the values as shown in Table 21 show that the variation in size is 0.05 mm smaller than the glass, with a higher uniformity coefficient meaning the range of particle size is larger than the glass. The particle shape of the limestone is less plate like than that of the glass and this may lead to the more uniform particle size, as a more rounded (but still angular) material is less likely to present a different profile to the sieves compared to a plate like material such as glass even though the medias particle sizes are similar. This is a further demonstration of the importance in understanding both the particle shape, as well as size when comparing media.

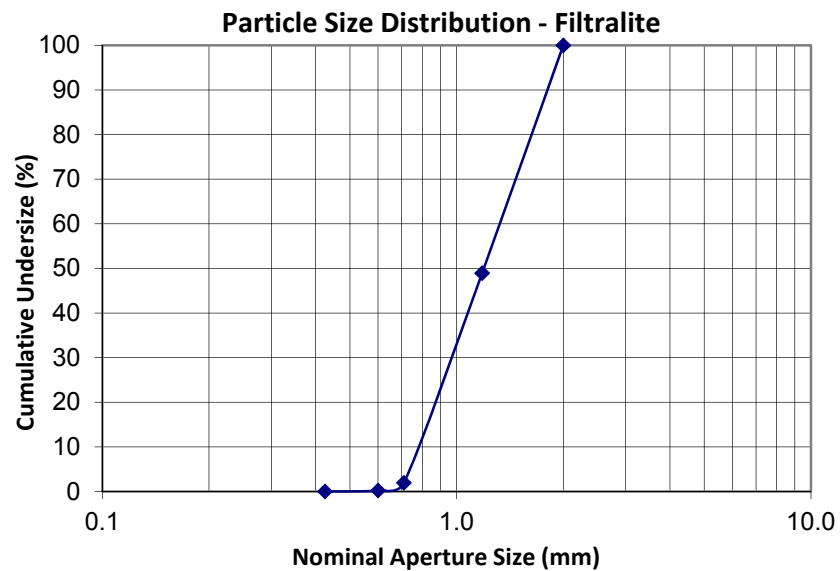


Figure 31 - Particle Size Distribution of Filtralite (0.8 – 1.6 mm)

Filtralite as can be seen in the PSD (Figure 31) has a larger particle size than standard sand and the other media tested. The manufacturer was unable to supply the media in a particle size more closely matching that of the sand for the purposes of this study. The effects of this larger particle shape will be an influence throughout the work. Other characteristics of the media such as surface area may be able to overcome this larger bed porosity to retain similar turbidity removal performance.

Filtralite is an angular material, not a plate like structure such as the slate or glass, and so the packing of the media will not be as close as that of the slate and glass. The porosity is expected to be high in comparison to these other media leading to poor turbidity removal performance but reduced head loss characteristics as noted for limestone. The manufacturers recommend Filtralite in a dual-layer arrangement with two grades of Filtralite to give optimum turbidity removal performance while benefiting from the reduced headloss.

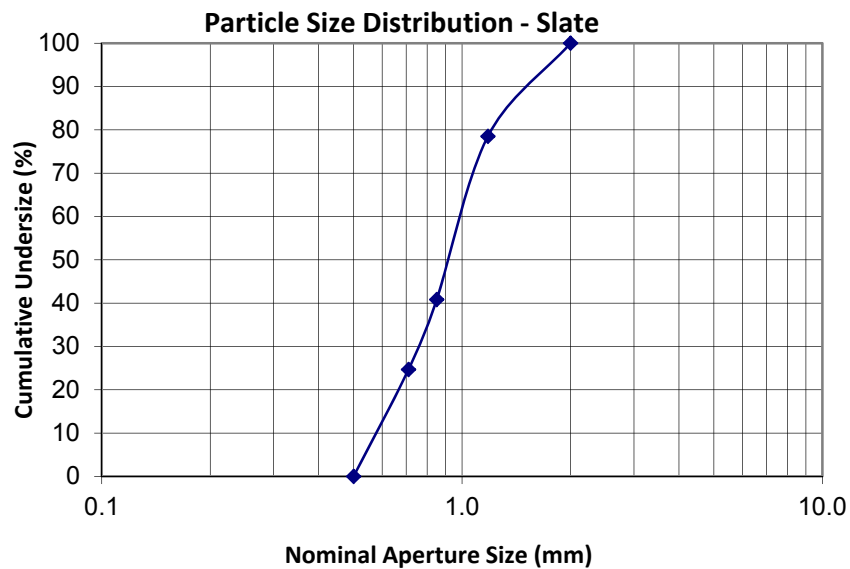


Figure 32 - Particle Size Distribution of Slate (0.425 – 1.4)

Slate exhibits a larger particle size according to the PSD (Figure 32) than standard sand, however due to its plate-like particle shape the packing of the filter will be quite different to that which would be expected if just looking at PSD results alone. There are problems measuring particle shape as a single dimension when the media is so markedly different in two dimensions and this will be discussed further in the section covering particle shape.

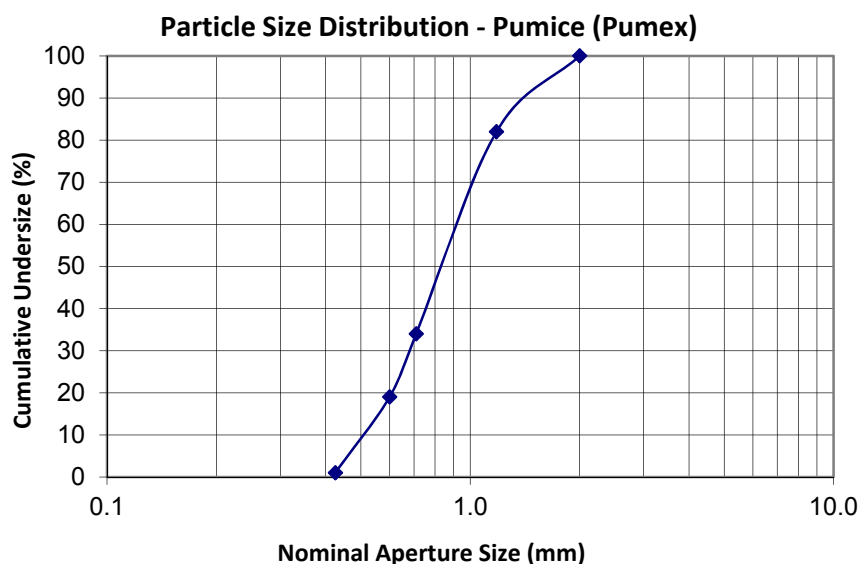


Figure 33 - Particle Size Distribution of Pumice (Pumex) (0.4 – 1.4 mm)

Pumice provided by the Pumex company (Figure 33) has a similar particle size distribution to that of the slate however the media is less plate like in shape and similar to the angularity of

limestone and Filtralite. The range of particle sizes as shown by the value of the uniformity coefficient (1.75) is high and the friability of the media reported by Fitzpatrick (2005) suggest that the value could change with time.

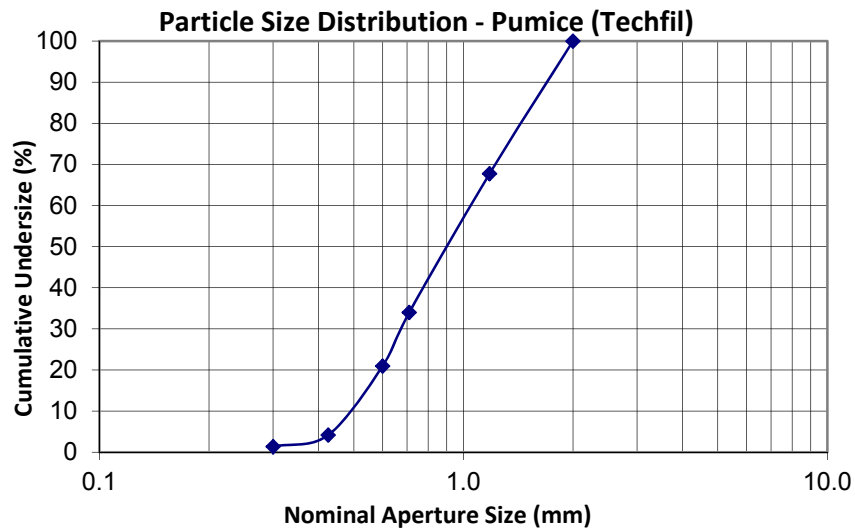


Figure 34 - Particle Size Distribution of Pumice (Techfil) (0.4 – 1.0 mm)

Pumice is supplied by an alternative company to Pumex (Figure 33) as Techfil (Figure 34) and this has a low uniformity (high UC value of 2.16) which was the highest value on test. This media therefore with a large range of particle sizes could stratify into different sizes in the bed leading to less effective performance as the finer grains will move to the top and clog the upper filter layers more readily. Lower particle sizes in the PSD curve (Figure 34) also show that there is a proportion outside the manufacturer specification suggesting that there has already been breakdown in transit highlighting a friability issue with pumice.

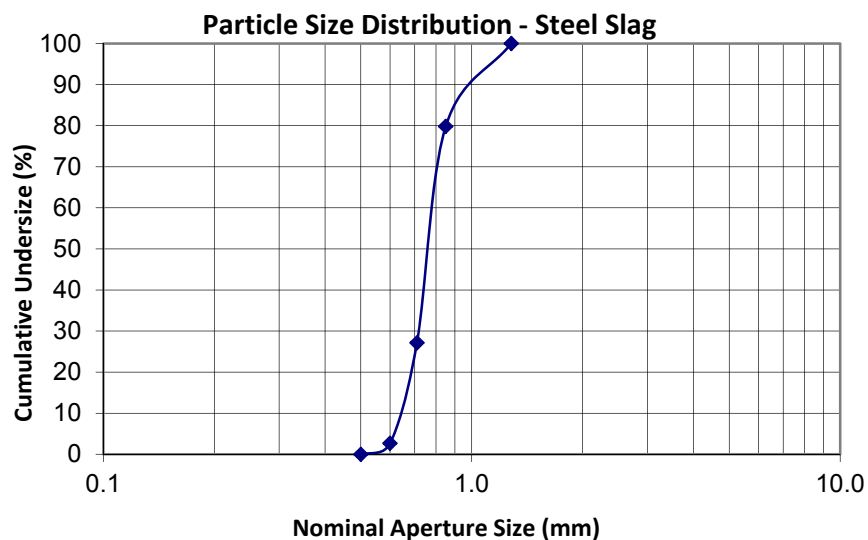


Figure 35 - Particle Size Distribution of Steel Slag (0.5 – 1.0 mm)

Steel slag (Figure 35) has similar size properties and uniformity to that of the sand as shown in Table 21, therefore any variation in performance will not likely be due to particle size, and experiments with steel slag should help differentiate the effects of shape and chemical interaction at the surface of the media

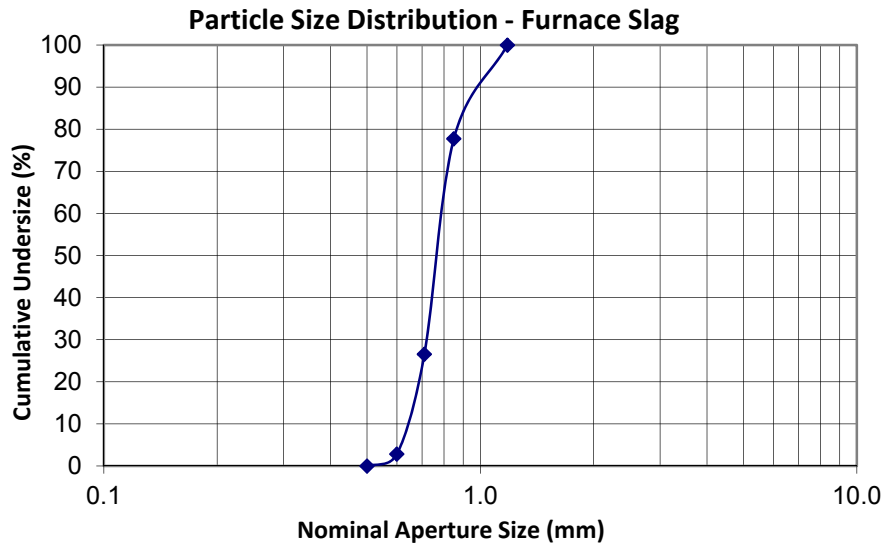


Figure 36 - Particle Size Distribution of Furnace Slag (0.5 – 1.0 mm)

Furnace slag (Figure 36) similarly has a PSD curve like sand and steel slag which provides control data for comparison of the fundamental reasons behind performance variation.

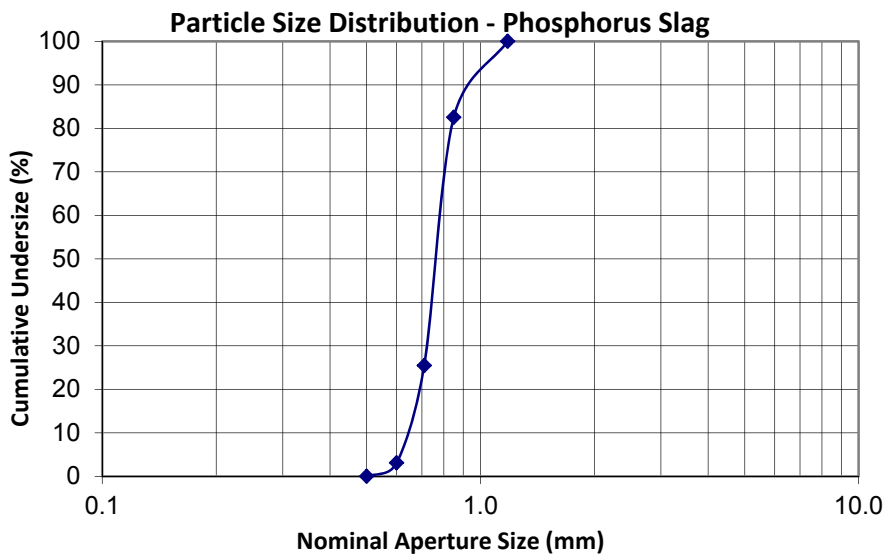


Figure 37 - Particle Size Distribution of Phosphorus Slag (0.5 – 1.0 mm)

Phosphorus slag (Figure 37) is similar if not equal to sand and the other slag. These slags are deliberately produced to a specific grade and client requirements. There were no limits as to what grading could be produced.

An overall summary of results from analysis of the PSD curves are shown in Table 21, together with a comparison of BS EN 12904:2005.

Table 21 - Particle Size Properties found for all media

Media	d₁₀	d₅₀	d₆₀	Uniformity Coefficient
Sand	0.59	0.75	0.75	1.27
Glass	0.76	0.92	1.00	1.21
Limestone	0.65	0.90	0.95	1.46
Filtralite	0.77	1.20	1.40	1.82
Slate	0.58	0.92	1.00	1.72
Pumice (Pumex)	0.52	0.83	0.91	1.75
Pumice (Techfil)	0.49	0.89	1.06	2.16
Steel Slag	0.65	0.75	0.78	1.20
Furnace Slag	0.64	0.76	0.79	1.23
Phosphorus Slag	0.65	0.75	0.78	1.20

Based on BSEN option (a) whereby the Uniformity Coefficient shall be less than 1.5, then Filtralite, Slate and both Pumice would fail this requirement. Using option (b) discussed in the previous section of no more than 5 % (multi-media filter application) of the media by mass fraction falls outside the specified particle size range or 10 % (mono-media), then for mono-media using the d₁₀ from the PSD charts and table above most media meet this requirement. Those that do not include glass (40 %), pumice (Techfil) (47 %) and Filtralite (45 %). The reason for these materials not meeting this part of the standard may be down to the sieve sizes and shape not giving suitably accurate retention points for the media. The glass is also a new material that has only just started to be produced by the supplier and therefore their checks on particle sizing may not be as stringent as what would be expected from the marketable product.

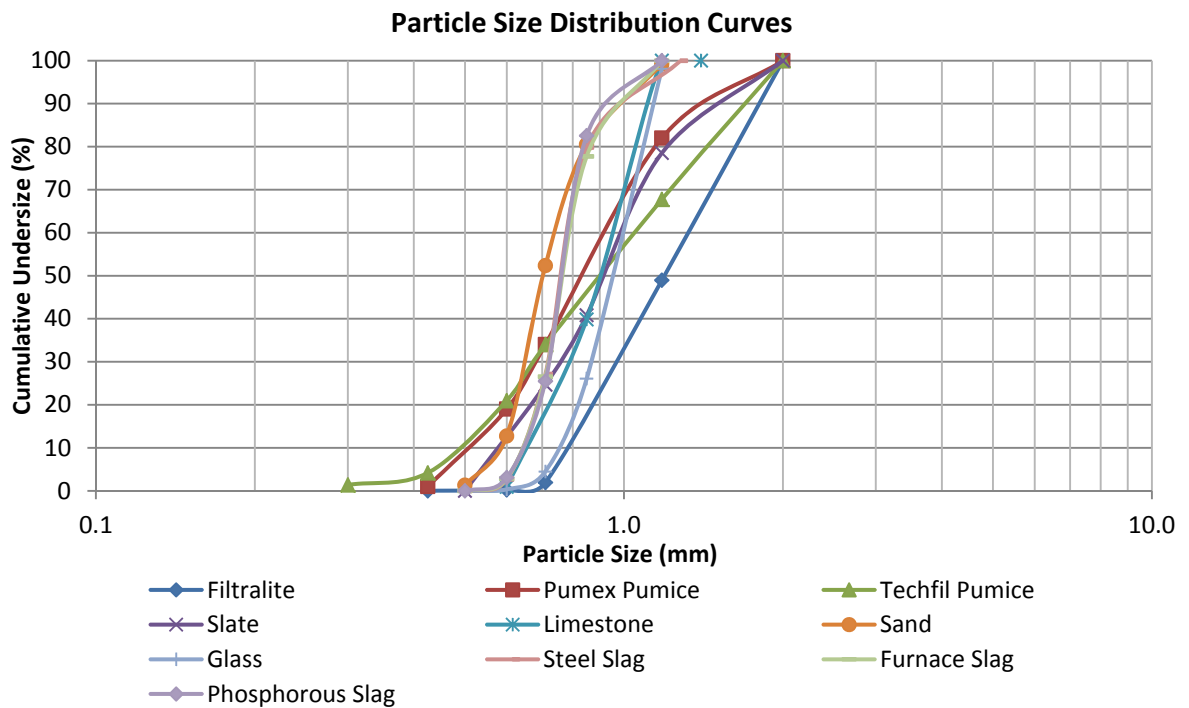


Figure 38 - Overall comparison of Particle Size Distribution curves from all media

Figure 38 shows all of the particle size distribution curves for all media together. This particle size distribution has been deliberately matched (steel slag, furnace slag and phosphorus slag), while in other cases the natural range of materials sizes offered has not matched the sand (Limestone, Pumice and Slate). Filtralite is confirmed well outside of the target range of particle size due to the fact the manufacturer is unable to supply it in a smaller grade.

These variations in particle size will be used to analyze the results from the filtration studies. It is expected that Filtralite will have the largest variation in performance due to its larger particle size, both with regard to headloss and turbidity performance. Other media such as slate (particle shape), limestone (calcium carbonate chemistry) and glass (smooth surface texture and low surface area) may exhibit other variations than those predicted from these different characteristics.

5.4 BED POROSITY

5.4.1 THEORY

Bed porosity is a measure of the percentage of empty space within the packed bed between the media grains. Porosity is determined by the two factors of particle shape and size. The more angular the material packing the less tightly or close packing within a bed and correlating to a larger value of porosity relative to a rounded material of the same diameter (Suthaker et al (1995)).

Mitrouli et al (2009) highlights how bed porosity is strongly linked to the increase in head loss across the filter bed. A higher value of bed porosity would indicate a lower initial headloss for the filter material and likely a lower head-loss accumulation rate. The porosity value measured is for initial porosity as the value will change with time as suspended particles become attached to the filter media which leads to a lower value of porosity and increased head-loss across the filter bed (Zamani & Maini (2009)).

Porosity is determined by calculating the volume of water that is retained within the total volume of the filter bed of combined water and media. The following equation (Equation 4) shows the calculation for determining the porosity of the media:

$$\varepsilon = \frac{V_w}{V_m}$$

Equation 4 - Determination of porosity of the filter bed

The procedure for determining the porosity of the bed is given below, an important consideration was to ensure that the packing of the filter bed matches that which occurs in the experimental columns as closely as possible, to achieve this a volumetric flask of the same or similar diameter to that of the columns is used.

1. A measuring cylinder of similar diameter to the test columns was filled with 500ml water.
2. 500ml of filter media was added to the measuring cylinder, by adding the media after the water this ensured there were no trapped air pockets within the bed.

3. Compaction of the media within the measuring cylinder by tapping the sides or vibration until there was no further settlement of the media.
4. The volume of water within the filter bed was calculated by subtracting the water volume above the filter bed from the initial value of 500 ml.
5. The values for bed volume and water volume were input into Equation 4 to determine the bed porosity.

Since values of porosity will depend on the compaction of the filter bed, ensuring similar packing between filter runs is important to maintain consistency in results. This was shown through initial operation of the filter as variability in the settlement of the filter media led to variation in filter performance. Also Glasgow (1998) highlights this problem in work on similar sized columns.

If the media was added prior to the water in the flask it would be difficult to remove the trapped pockets of air that occur if the experiment was operated in this order. The addition of the media into the water also ensures full saturation of all particles ensuring a compaction that matches more closely what is occurring in the filter columns.

However if the media has a larger bed porosity value, lower turbidity removal performance would be expected, because of the pass through of smaller turbidity particles unless other characteristics of the media offer enhancement of their removal to counteract the increased porosity. This has been noted by other authors such as Mitrouli et al (2009) and Farizoglu et al (2003) from, for example, more complex pore structures and surface activity. Therefore it is possible to have a media that offers improved head-loss performance while still offering the same or better turbidity removal performance.

Porosity of the filter bed is affected by both the particle size which is well documented and also the particle shape. Suthaker et al (1995) notes that the greater the angularity of the filter media, the higher the bed porosity value at similar overall media particle sizes.

Aside from these complications porosity therefore is a major influence in determining the performance of the filter and it is determined by the size of the filter media and packing. Standard porosity testing gives the combined effect of both of these media properties. This is important as measuring the particle shape of novel media (Slate) is difficult to carry out, with statistical rigour.

5.4.2 TESTING

Testing of the porosity of the filter media was carried out under wet conditions to better mimic the packing that would occur in the filter columns. As previously discussed a measuring cylinder of the same diameter as the laboratory filter columns (60 mm) was used to simulate the laboratory scale filter dimensions.

Prior to the determination of the porosity the media was cleaned to ensure there were no small particles of dust or broken media present that would affect the results. There is no standard method for washing and therefore a wash of 20 minutes was used and the outflow monitored to ensure no solids were still being released. Therefore a small washing rig was constructed to carry this out and this is shown in Figure 39 below:

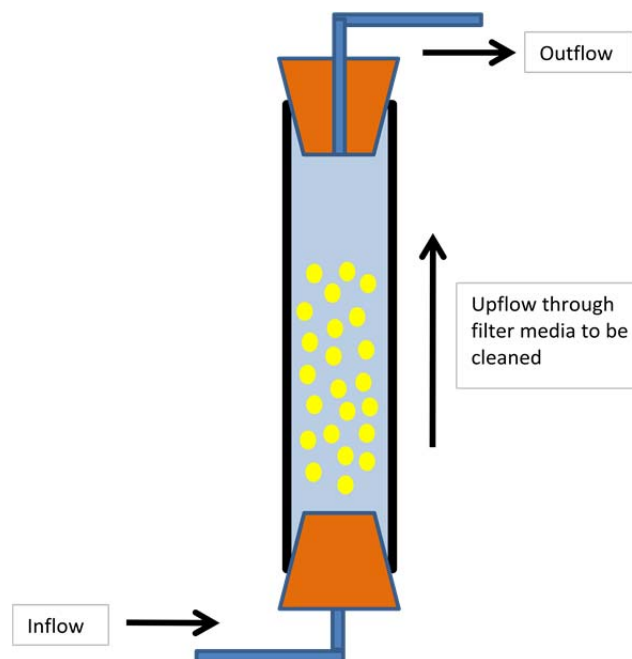


Figure 39 - Small backwashing rig for cleaning small amounts of media for laboratory testing

The backwashing rig shown in Figure 39 is constructed of a 60 mm acrylic column as are the operating lab filters with a bung at each end. Each bung has a small diameter (6 mm internal diameter) plastic acrylic tube inserted for flow through it. Tap water flows through from the base to top of the column as back washing removing any particles through the upper bung and out to waste. The wash was carried out for 20 minutes on each media to ensure they

were cleaned in a standardized way, the media was then air dried for a week at room temperature prior to the porosity test.

The procedure for determining the porosity followed that described in section 5.4.1; the results are summarized from these experiments in Table 22 shown below:

Table 22 - Values for bed porosity of filter media used in laboratory scale experiments

Media	Volume		
	V_w	V_m	ε
Sand	181	500	36.2
Glass	185	500	37.0
Limestone	217	500	43.4
Filtralite	240	500	48.0
Slate	217	500	43.4

The results show that sand has the lowest value of porosity; this is expected based on sphericity and confirms previous results, for example, by Suthaker et al (1995). Thus the more angular material has consistently higher porosity or greater particle size (Filtralite). The results shown in Table 22 correlate well with this idea.

Other previous works by a selected range of authors who have determined the porosity of the media that was being looked at are listed in Table 23 below:

Table 23 - Porosity values for a range of media tested by previous authors (UC – Unconsolidated)

Media	Author	Particle Size Range (mm)	Porosity (%)
Pumice	Farizoglu et al (2003)	0.5 – 1.0	69
Sand	Farizoglu et al (2003)	0.5 – 1.0	40
Sand	Rutledge & Gagnon (2002)	0.2 – 0.9	47
Glass	Rutledge & Gagnon (2002)	0.4 – 1.1	52
Glass	Fitzpatrick (2005)	0.5 – 1.0	50 (UC)
Filtralite MC	Mitrouli et al (2008)	1.5 – 2.5	58
Sand	Mitrouli et al (2009)	0.8 – 1.25	43
Filtralite HC	Mitrouli et al (2009)	0.8 – 1.6	62
Filtralite MC	Mitrouli et al (2009)	1.5 – 2.5	67
Anthracite	Mitrouli et al (2009)	1.2 – 2.5	48

Ives (1987) lists a typical expected porosity of sand to be 40 % for sand of 0.5 – 1.0 mm which fits in well with the results found by the other authors by experimentation shown in Table 23. Only Fitzpatrick (2005) discuss the method used to determine the porosity, which

limits the value of a comparison with the results in Table 22. Fitzpatrick (2005) notes the result as an unconsolidated value of porosity which is important since compacting during use would be anticipated. This would be an important factor in predicting full scale filter performance where consolidation would be increased because filters are less affected by wall effects that occur in small diameter columns as typically used in laboratory scale trials. The porosity of sand found in this study was 36.2 % which is lower than anticipated, however the packing of the media will have had an influence on this result and in this study the sand was consolidated as closely as possible within the filters by tapping and vibration, hence the slightly lower porosity value compared to previous studies.

Glass media in Table 23 show a higher value for porosity than the sand which is the same as the values found in this study however the results for this study show that the glass has a lower porosity than would be expected compared to these previous studies. This could be down to the consolidation method used in the testing to determine the porosity, being an angular material it would not initially pack as closely when tested in an unconsolidated state while if it was tested in a consolidated state then this angular material would demonstrate a significant change in porosity. This change to packing during consolidation could explain the lower porosity in this study. The Scanning Electron Microscopy (SEM) images in section 5.8 show the varying angularity of the media that causes this variation.

The Filtralite HC media used by Mitrouli et al (2009) is the same product as used in these trials and therefore a comparison of the porosity can directly be made. In this instance Mitrouli et al (2009) finds a porosity value of 62 % compared to 48 % for this study. This is a significant variation and it is believed that this is due again to the fact the results from previous studies are uncompacted or unconsolidated while the results in this study are consolidated to match the conditions that will be generated in the laboratory scale filters. Mitrouli et al (2008) and Mitrouli et al (2009) have the same Filtralite MC material in both studies, but interestingly show a different porosity for the same media (from 58 % to 67 % in the later paper). There is no explanation in either paper as to why this has occurred. It is not known if the porosity testing was carried out in the pilot rig, but if so the rig was identical between both studies. It is possible this variation is showing the differences in media consolidation between the tests, caused by possible vibration increasing consolidation in the

first test. Without further information on how the porosity was determined from the author then it is not possible to understand this variation fully.

5.5 FRIABILITY AND MECHANICAL DURABILITY OF MEDIA

5.5.1 THEORY

Friability and durability of the filter medium is a key consideration for identifying suitable alternative material for use in rapid gravity filtration. Media breakdown will produce fines in the treated water and in backwashing will lead to substantial losses of the media that will require replacement at a cost. The fines produced will also begin to clog the filter increasing head loss and significantly reducing the performance of the filter. Therefore standard accelerated wear tests have been developed to identify whether new filter media is likely to encounter these problems during its working life and to what degree these problems may occur.

Humby & Fitzpatrick (1996) carried out a comparison on the attrition of granular filter media (sand, GAC and anthracite) under extended accelerated backwashing under experimental conditions. It was shown that initial attrition was very high but reduced exponentially with time, due to the removal of sharp corners and edges from the media which were worn away more easily. This is a concern for any media that is angular in nature such as pumice and crushed glass which are in use as they have a large number of sharp edges and corners that could be lost early in their working life and reduce the performance.

Once these vulnerable edges are lost then the attrition will be negligible, but this period of time will be specific to the media being considered. For example Humby & Fitzpatrick (1996) showed this to be 30 hours backwashing for sand but 50 hours for the more angular and friable anthracite.

Morgeli & Ives (1979) compared various new filter media types for use in wastewater effluent filtration. The media size for this test was in the region of 1.6 to 3.15 mm which is higher than what is to be used in rapid gravity filtration. Pumice was found to be unsuitable in this application for wastewater recycling where more frequent backwashing is required, there was severe abrasion with all the sharp edges disappearing after 50 hours of continuous backwashing.

Due to the lower frequency of backwashing necessary in rapid gravity filtration of drinking water it would be more likely to survive for a longer period of time compared to effluent filtration. This effect may be countered by changes in size of the media. Different sizes of porous material such as pumice, for example, may be weakened compared to a larger particle size, and testing will be needed to satisfy users that the media does not physically alter over its expected lifetime.

The mechanical durability of filter media is covered by BS EN 12902:2004 *Products used for treatment of water intended for human consumption – Inorganic supporting and filtering materials – Methods of test* gives an informative in annex A of the document regarding the measurement of resistance to friability of filter media. This method is also the same as the one noted in Degremont (1979), but which in addition to a description of the test method also gives suitable limits for guidance as to whether the filter media should be accepted or rejected. These are reproduced in Table 24. The method involves placing samples of the media in a rotating cylinder with ball bearings and subjecting it to a specified number of revolutions:

Table 24 - Limits for guidance on friability from Degremont (1979)

	375 Revolutions	750 Revolutions
Very good	6 to 10 %	15 to 20 %
Good	10 to 15 %	20 to 25 %
Poor	15 to 20 %	25 to 35 %
Reject	Over 20 %	Over 35 %

Calculation of these percentages changes in size is carried out using Equation 5 below; Where X is the percentage of material smaller than the initial effective size (d_{10}):

$$Percentage\ Loss = \frac{10}{9}(X - 10)$$

Equation 5 - Calculation of percentage loss of media from Degremont (1979)

Suthaker et al (1995) reports on results using the Degremont (1979) method and carried out tests on crushed quartz, round sand, anthracite and existing media from the local plant in Bognor Regis which was silica sand. The results found from the friability test are as shown in Table 25:

Table 25 - Results of tests carried out by Suthaker et al (1995) on friability

Filter Media	Friability after 375 rev. (%)	Friability after 750 rev. (%)
Existing media	0.12	0.80
Crushed Quartz	2.61	4.08
Round Sand	1.07	1.98
Anthracite	18.90	24.30

All of these various media fall into the very good or good classification based on the 10 percentile size fraction given in Table 24 from Degremont (1979). It is noticeable however that there are higher values for anthracite indicating a higher degree of media breakdown comparison to the other media as might be predicted as it is an organic material and likely to be softer.

Extended backwashing tests have been carried out by Morgeli & Ives (1979), Humby & Fitzpatrick (1996) and Ives (1990), and it was concluded that this type of testing was more suitable and a better defined method of determining the attrition of filter media during its working life. It is argued this type of testing is more representative of the actual operating conditions for the filter media. Limits are given by Ives (1990) as >5% being unsatisfactory, 3-5% as undesirable, 1-3% as doubtful and <1% as satisfactory losses by total mass. The test was also published as an industry guideline BEWA (1993) accelerated backwash abrasion resistance test.

Continual monitoring of media loss through particle size distribution analysis during testing can give an indication of the loss of media through typical operations. Although the time required for this method is longer than the BS. This is especially important given the work by Humby & Fitzpatrick (1996). Alteration of the Particle Size Distribution at even small numbers of backwash cycles will give an idea of any trends that may begin to occur. Analytical techniques are now commonly available for PSD and particle shape and they can be used to monitor the alteration of the media with time in operation.

Of the three methods, the most representative is the extended backwashing. This method will involve the same forces as those to which the media will be subjected to in a real filter and will give a closer representation of the forces involved compared to the friability test. Continual monitoring of parameters during filter operations will also give an indication of the time series of the resistance of the media more accurately by avoiding the assumption of a

linear change with time. The time constraints and effort involved mean this will not be practical in operations at indicating total breakdown.

A combination of extended backwashing and PSD monitoring during operation of filters should allow for a prediction of the breakdown and therefore a prediction of the resistance of the media to be made. A key consideration will be its effect on the particle shape and also the performance of the filter as fines if released may begin to clog the filter and the change in grain shape may cause closer packing of the bed reducing the size of the voids. Shape change can be monitored by SEM analysis which will enable a better understanding of which performance critical parameters are affected, although it is accepted that this will be beyond the facilities of most laboratories.

5.5.2 TESTING

Testing was carried out using a 50 hour backwash attrition test; Morgeli & Ives (1979) noted that a 100 hr test was equivalent to a 0.5 – 3 year period of operation depending on the flow rates used for backwash. Morgeli & Ives (1979) then actually reduce the effort needed, using a 50 hour test to determine the durability of the media. Fitzpatrick (2005) carried out a 100 hr attrition test with water only at a 20% bed expansion based on the test described by Ives (1990).

The test carried out for this study was set at 50 hours but to gain a greater attrition and give a value more suitable for a longer period of use the expansion of the 600 mm bed was set to be 50 %. This is greater than the normal 15 – 25 % to account for this test running with just water while a combined air and water backwash is considered to be more aggressive. The higher bed expansion was used with the intention of better mimicking this aggressive air/water type of wash. The results from the attrition tests are shown in Table 26 below:

Table 26 - Results for attrition testing of filter media

	Volume Loss (%)
Sand	1.7
Glass	2.4
Limestone	1.2
Filtralite	0.4
Slate	2.2

Based on the criteria given by Ives (1990) the media would rank as follows, sand (doubtful), glass (doubtful), limestone (doubtful), Filtralite (satisfactory) and slate (unsatisfactory). These criteria are appropriate only to tested media done under identical conditions to the test carried out by Ives (1990) and other authors have used different criteria. This lack of distinct primary standard limits the ability to compare results across studies. However for this work the comparison with the work of Ives and the limits specified are the most suitable.

Based on a comparison of the media against standard sand which is commonly from the same source across the UK then slate and glass do perform less effectively but then the variation is very small with glass showing an attrition rate only 0.7 % worse than the sand. Filtralite is shown to be very low and this is determined to be due to the method of manufacture which fuses the clay at high temperatures into a strong ceramic like structure that clearly resists attrition very well.

This is important because of the previous work noted by Rutledge and Gagnon (2002) and Fitzpatrick (2005) that the angular protrusions of glass media are the first to be broken down; this would alter the shape of the particle and allow it to become more rounded with time. The testing carried out by comparing the media before and after the attrition test did not show any significant change in shape of the glass along the edges but when the lifetime of the filter is expected to be near 20 years for sand then it could pose a problem nearer the end of this timescale.

5.6 ACID SOLUBILITY

5.6.1 THEORY

The method of determining the acid solubility of the various media was carried out in accordance with *BS EN 12902:2004 Products used for treatment of water intended for human consumption – Inorganic supporting and filtering materials – Methods of test*, the method stated is as follows:

Weigh to the nearest 0.1 g, approximately 50 g of the filter media and transfer to a beaker. Note the mass as m_1 and then cover the ISFM sample with hydrochloric acid (Hydrochloric

acid solution mass fraction 20 %). Leave in contact for the 24 h at a temperature between 18 °C and 23 °C.

Undertake five washings with water avoiding loss of fines, and dry the sample in the oven at 105 °C to constant mass, then allow cooling in dessicator. Weigh the sample and note the mass m_2 .

Express the results as a mass fraction of lost material using the following Equation 6:

$$X_1 = \frac{(m_1 - m_2)}{m_1} \times 100$$

Equation 6 - Mass fraction equation for acid solubility

Where:

m_1 = mass fraction of media sample before the test (g)

m_2 = mass fraction of media sample after the test (g)

British Standards give limits for the content of acid-soluble material for the different approved filter media, these include silica sand (BS EN 12904:2005), sumice (BS EN 12906:2005) and expanded aluminosilicate (BS EN 12905:2005). Other filter material specifically anthracite, barite and garnet sand do not have a requirement for acid solubility specified in the British Standards. This could be because of the small proportion used in the filter but also it is likely the anthracite as an organic material would have a major acid weight loss. The values given in these standards are summarized in Table 27 below:

Table 27 - Acid solubility limits from British Standards

Filter Media	Mass fraction (%)
Silica Sand	< 2
Pumice	< 5
Expanded Aluminosilicate	< 7
Barite	< 3
Garnet Sand	Not Specified
Barite	Not Specified
Anthracite	Not Specified

Stevenson (1994) makes a reference to the acid solubility test in relation to silica sand. He notes that it is a reasonably quick measure of the calcium carbonate, which is a common contaminant in this type of filter media. No mention is made of the significance of test being an indication of the dissolution of the media itself. This work infers that some natural sands will fail the test but no data is presented to show such materials.

Ives (1990) indicates that the test is very severe with a high acid concentration. This ensures that the integrity of the grains is tested and that they are solid not aggregated. An aggregated particle is one that is cemented together with calcium complexes and if for example CaCO_3 resist the acid solubility test then they should not break down as easily in operation. The particle size and portion of fines in the media will be low. In the case of sand a reduction in weight will often indicate the presence of calcium carbonate that is generally due to the presence of shell fragments in the sand.

Ives (1990) makes mention of a 50% acid concentration which is a variant of the test carried out by University College London but suggests this is unnecessarily severe and therefore concludes that the method based on 20 % acid in the British Standard *BS EN 12902:2005* is more suitable, but makes no comment about the use of different types of acid..

50 % was also suggested by Suthaker et al (1995), who also used a different timing whereby determination of termination of dissolution was based on when gas bubbles were no longer observed. Results are still interpreted as a percentage mass loss as in other methods. This method is derived from the AWWA Standards for filtering material B100-89 (1989). The conclusion by Ives and also the more current British Standards mean that this method was adopted for determining the acid solubility of the filter media.

Pumice sourced from Turkey was shown to have an acid solubility of 4.8% according to Ghebremichael (2004) who carried out experiments, which falls within the recommended limit for pumice which is 5% given by the British Standards. Ghebremichael (2004) also compared the value to that for anthracite given by the AWWA (2010) standard for filtering materials ANSI/AWWA B100-09 which was, also 5%. Ghebremichael (2004) states that a material with a higher acid solubility is liable to material loss in low pH waters although to what degree this will be different to the much more severe conditions under which this test is carried out could be crucial is unknown. Considering the substantial difference between

the acid strengths reported by Ives and that experienced in typical inlet streams on average to rapid gravity filters that primarily range between a pH of 6 and 8, although upland water and high coagulant dosing could reduce this to 5. Therefore it is likely to take a significant amount of time for the 5% losses to occur in the filter, given the difference in the strengths of acid required to cause the breakdown.

5.6.2 TESTING

The result from testing undertaken as part of the research reported in this thesis is shown below in Table 28:

Table 28 - Acid solubility test results based on BS EN 12902:2004

Media	m₁ (g)	m₂ (g)	X₁	Liquid Color
Sand	49.9980	49.6955	0.61	Yellow
Glass	51.6269	51.5284	0.19	Yellow
Limestone	50.0154	5.9606	88.08	Brown
Filtralite	52.9819	52.4232	1.05	Dark Green to Yellow
Slate	52.5875	51.2318	2.58	Bright Orange Yellow
Pumice(Techfil)	50.0831	49.7336	0.70	Yellow
Pumice(Pumex)	50.1018	49.6466	0.91	Yellow

The results for sand falls below the limit set in the British Standards of < 2 % mass fraction loss as shown in Table 27. The yellow colour of the acid after addition of the media is due to the breakdown of the Fe₂O₃ by the acid and its release into solution. The amount released will affect the colour of the solution with a darker solution highlighting a greater release of Fe₂O₃.

Glass has no standard for acid solubility, but the value is the lowest of all the media and therefore its ability to resist acid attack is superior and it would easily meet the acid requirement if one existed. The manufacturing process of glass uses high temperatures which fuse the material together and enable it to resist acid attack more effectively than natural materials leading to the lower mass fraction loss as shown in Table 27. This is due to the amorphous nature of the material where all elements are tightly bound and not easily accessed.

Limestone is a media that was expected to fail this test because it is mainly calcium carbonate compared to the other media which are predominantly silica based. The calcium carbonate reacted violently with the acid used in the test as would be expected. The mass fraction loss of 88.08 % shown in Table 27 is lower than the true value as in reality the media was totally destroyed leaving only a residue that was weighed to give the mass fraction result for completeness. Based on this information, limestone fails the acid solubility requirement however this does not dismiss the media entirely. It was also noted that the acid test generated a brown solution, suggesting some nitrogen or iron possibly other metals co-precipitated with the limestone

The acid solubility test is a very aggressive and extreme test and under real conditions the pH value will be higher than that used here. Limestone has also been used in roughing filters before by Rooklidge et al (2002), Lipp et al (1997) and also for removal of metal contaminants from mine and raw water as shown by Aziz & Smith (1996), Mackintosh & de Villiers (1999) and Aziz et al (2008) as a selection. Therefore even with this risk of solubility it is still often used in waste water treatment for similar applications and there is possible benefit to water quality by acting as a sacrificial coagulant. Therefore it is envisaged that that limestone filter media may not be suitable under certain conditions (acid water) unless the more frequent replacement of the media is accepted and the benefits of using limestone outweigh this cost, but under other conditions it's benefits for improving water quality are worth the cost/risk of its continued loss due to acid solubility.

Filtralite meets the requirement for expanded aluminosilicate shown in Table 27, however the result is higher than the sand. Filtralite is a media produced under high temperatures of up to 1200 °C (greater than glass) and therefore is a man-made material. It is expected that the increased losses are possibly due to the increased surface area of the media allowing for greater access of the acid to a greater amount of the filter media leading to a slightly increased loss over others. The colour of the solution after addition of the Filtralite again shows that it was iron that could have been released into the solution. Although this would need further analysis it would be anticipated that the clay in Filtralite would contain less silica than sand and therefore be vulnerable to acids.

Slate has a higher mass fraction loss as shown in Table 28 than allowed for sand (< 2 %) but is comparable with other media which meet the standards shown in Table 27. If a standard

was produced for slate media based on experience with the other alternative media it would take this slightly increased acid solubility into account. The orange/yellow colour of the solution after addition of the slate points to a release of iron from the media as with others. This would need further work to fully investigate.

The two Pumice media (Techfil and Pumex), showed acid solubility values that met the requirements for silica sand and therefore it may be concluded that natural volcanic activity achieves the same sort of firing process compared to Filtralite (high temperatures in contact with water). Pumice meets the requirements of this stringent standard for filter media acid solubility very well.

Limestone when immersed in the acid solution showed darker colours compared to the yellows produced in the other media. This is likely to be due to the near total breakdown of the media releasing impurities into the solution. The slight green tint in the Filtralite solution could be attributed to copper or iron, as iron and other materials are used to colour glass bottles green. It is also important to note that although the Filtralite is a manufactured material it is produced from clay topsoil and the likelihood of additional chemicals and elements in its make-up is more likely compared to the other materials which are predominantly sourced from large rock formations that have been produced in a largely homogenous environment.

Overall the results show that the new media can meet the existing modified criteria for acid solubility for new materials except limestone. In this case it is important to highlight the possibility of using filter media to achieve different objectives, for example water quality, whereby the filter using Limestone is sacrificial, with more frequent media top-ups. The trade off against this increased cost is conditioning of the water by the limestone and improved removal of metal and other contaminants. Both of these generally require further treatment processes in the water works and if these could be reduced into one filter stage and cost savings achieved in GAC for example, this would possibly outweigh the negative implications of media loss. The media loss also will depend on the pH of the water entering the filters and hence a works by works analysis of the suitability of the limestone media would need to be carried out. Further work on analysis of the leachates from the media is required as all generated obviously coloured solutions.

5.7 SURFACE AREA DETERMINATION

5.7.1 THEORY

Little published research exists with regard to determining the specific surface area (area/unit mass, expressed as m^2/g) of filter media probably because the tests require complex equipment. Work carried out in other fields is available, primarily from Geotechnics and Chemical Engineering where work has been done comparing various methods of Specific Surface Area (SSA) determination. Work carried out by Arnepalli et al (2008) for example critically assessed methods to identify which was the most suitable method for use in determining the SSA. Arnepalli et al (2008) divided the experimental methods into three separate groups based on the equipment and method used:

- a) Gas or vapour adsorption techniques
 - a. Brunauer-Emmett-Teller (BET) nitrogen adsorption
 - b. Water vapour adsorption technique
- b) Adsorption of the polar liquids and dyes on the soil surface
 - a. Ethylene glycol (EG) method
 - b. Ethylene glycol monoethyl ether (EGME) method
 - c. *p*-Nitrophenol method
 - d. Methylene blue (MB) method
- c) Application of the state-of-the-art physical instrumentation
 - a. Mercury intrusion porosimetry (MIP)
 - b. Internal reflectance spectroscopy
 - c. X-Ray diffraction
 - d. Gas pycnometer

Arnepalli et al (2008) also noted that when deciding on the most effective method then consideration would be needed of the typical time taken to carry out the test, cost of the testing and the availability of skilled operators. Of primary academic concern however is the contribution to modeling performance adding generic knowledge and predicting the influence of the surrounding environment on the sample.

Both Arnepalli et al (2008) and Yukselen & Kaya (2006) indicate that only the methods based on the adsorption of polar liquids and dyes on the soil surface give the true total SSA of soil as other methods typically keep the soil in an un-natural dry state that limits access to the inter-layer surfaces. These methods would therefore give the external SSA of the soil which if applied to the case of filter media or wet environment would not give a true indication of the total area available for adsorption.

It is important to note that in the case of the larger filter media particles the inter-layer (the boundary between the minerals that make up the clay type) is not considered as important an area as it would in soils such as clay which have a particle size in the micron range. Therefore the other methods are still valid for the larger particle sizes as only the external surface area of the media and the inclusion of the pores themselves is considered. Adsorption of liquid into the inter-layers of clay materials is a key issue as this is what causes the swelling to occur in the material which is detrimental in construction. In filter media this is not considered to be likely as the mineral chemistry of the material is different to clay and is unlikely to swell and shrink under the presence of liquid. More work is needed in this area as internal pore size/surface is often quoted as a key performance indicator for GAC for example as noted in Hendricks (2000)

From the considerations made by Arnepalli et al (2008) then the number of the tests listed can be reduced based on a critical analysis of cost, time and availability. The following tests were available and required further analysis to determine their suitability:

- a) BET nitrogen adsorption
- b) Ethylene glycol (EG) method
- c) Ethylene glycol monoethyl ether (EGME) method
- d) Methylene blue (MB) method

Three of these methods are based on the adsorption of the polar liquids and dyes on to the soil surface, plus the BET nitrogen adsorption method where an entirely different principle non-polar gas is used and so will give different results.

Ethylene glycol monoethyl ether (EGME) method is an enhanced and developed form of the Ethylene glycol (EG) method reported on by Carter et al (1965) where EGME replaced EG as the polar liquid used in the experiment. For the media Carter concluded that EGME gave faster results thanks to its ability to reduce the time taken. It could be suggested that this might be due to the reduced polarity of the larger EGME compared to EG on its surface to reach mass equilibrium.

Arnepalli et al (2008) and Yukselen & Kaya (2006) have made different conclusions comparing EGME or MB methods for determining the SSA of soils. Yukselen & Kaya (2006) suggested that the MB method was the most suitable based on the idea that it was simpler and gave just as reliable results as the other method. They do note that the MB method gives slightly higher values than those from the EGME method but do not attempt to explain this discrepancy.

Arnepalli et al (2008) did attempt to explain this discrepancy by noting that the MB molecule has a prismoidal shape, which is adsorbed onto the surface of the soil in a way that the largest dimension is in-plane with the surface. In this orientation each MB molecule will cover a smaller area of the surface and over-predict the value of SSA when calculated against the average dimensions of the molecule. This they explained was not the case with EGME and therefore it is concluded this was the more reliable method which could be easily carried out with a low cost and time penalty.

Yukselen & Kaya (2006) also compared EGME with BET and in all cases the BET gave a lower value than the EGME method. They conclude that this is due to the fact that the EGME being a polar liquid is able to give the total specific surface area which is a combination of both the internal inter-layer surfaces and the external surfaces of the soils. While the BET method omits the internal inter-layer surfaces as the nitrogen did not easily pass into this area of the soils as a buoyant gas. For the filter media where primarily only the external surfaces are required then the BET method would still be valid while the EGME may give the research project an insight into whether there is any significant effect from inter-layers of the

material and polarity. This was thought unlikely as the materials were not expected to be susceptible to the shrinking and swelling that the clays with high inter-layer surface area are.

The work into analyzing the performance of novel filter media is only interested in the surface area that is available for the attachment of particles during filtration, this is known as the external surface area. Based on these needs BET was seen as the method of choice as EGME would over estimate this external surface area due to the inclusion of areas of the media that were not available for attachment during filtration. In addition, the BET method allows for the determination of the porosity of the media as well as the range of pore sizes on the media surface.

5.7.2 TESTING

The BET nitrogen adsorption testing was carried out using a Micrometrics Tristar 3000 as shown in Figure 40. The samples are prepared by washing in the same method as that used for the determination of the bed porosity using the apparatus shown in Figure 39, the media was then dried in an oven at 110 °C to remove any remaining water and then allowed to cool at room temperature prior to being placed in the analyzer.



Figure 40 - Micrometrics Tristar 3000 BET surface area and porosimetry analyzer

Results for Specific Surface Area (S.S.A.) are given in Figure 41 shown below in descending order.

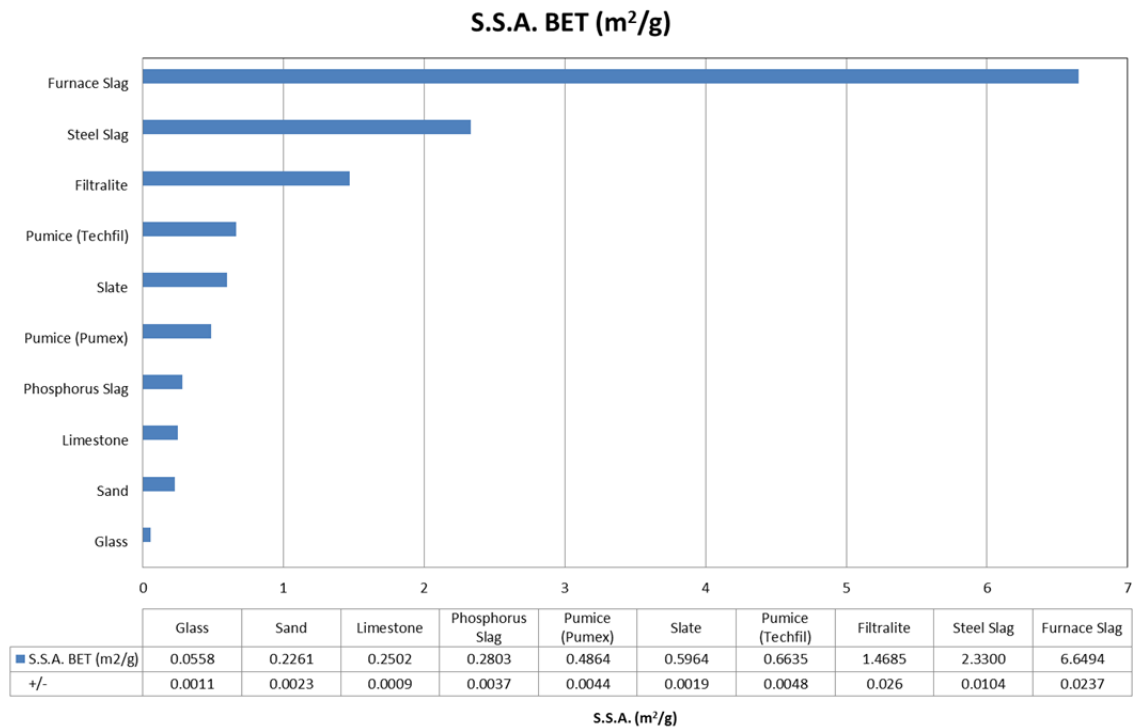


Figure 41 - Specific Surface Area results for all filter media

Experimentally Furnace Slag has a significantly higher surface area than all of the other tested filter media; compared to the sand it has a surface area 29.4 times greater than the sand. Glass had the lowest SSA which was expected based on its extremely smooth surface. Most other media fall into a range of 0.2 - 0.7 m²/g, It is interesting to see both Pumice media are lower than the Filtralite media as they are both marketed as having a high porosity due to their method of creation.

The reason for this variation is likely the way the two materials (Pumice and Filtralite) are produced. Pumice is formed due to the simultaneous actions of rapid cooling and rapid depressurization. The depressurization creates bubbles by lowering the solubility of gases dissolved in the lava which rapidly exsolve. Simultaneous rapid cooling then traps these bubbles in the matrix of the pumice. It is this trapping mechanism during the rapid cooling that likely reduces the surface area as, when tested by the BET method, the nitrogen cannot access the pores within the Pumice media and only has access to the ones on the surface that are open due to the action of crushing used to grade the pumice to the required size.

Filtralite however is manufactured from clay fed into long rotary kilns, the clay passes through the kiln over the time required where the clay is dried and expanded at

temperatures of 1200 °C. The expansion (formation of pores) occurs when organic matter in the clay combusts and the gas formation generates pores. In addition the material is crushed to the size required much like the pumice.

The variation in these two heat processes is the fact that the pumice is cooled sealing the pores within the material while in the expanded clay the organic matter expands the pores from within. This leads to a pathway between the pores of the Filtralite, allowing the nitrogen used in the BET test to penetrate into the filter media. This however poses problems if particulates for removal in filtration can become trapped within the media and cannot be removed by backwashing. The particles are then organics remaining present over the lifetime of the filter unless they are organic matter which could lead to their biological breakdown.

5.8 SCANNING ELECTRON MICROSCOPY (SEM)

Scanning Electron Microscopy (SEM) was used to study the surface characteristics of the filter media. Surface characteristics such as the shape and structure of this will influence the attachment of particles to the media surface (See Section 4.2.2).

A Carl Zeiss (Leo / Cambridge) Stereoscan 360 SEM was used for the SEM analysis of individual media grains. In addition the machine has an attached Oxford Instruments INCA system capable of X-Ray energy analysis, allowing mapping and line scans of most elements except Nitrogen and other very light elements. This gives an indication of the elemental make-up of the surface of the media only. It was not used during this work as it would not give an accurate determination of the chemical makeup of the media due to it being only able to penetrate a layer a few atoms thick on the media surface. To gain a true understanding of the chemical makeup of the media a combination of X-Ray Fluorescence and EDAX would be required to allow for accurate measurement of the internal and external structure of the media but this was prohibitively expensive per sample. However EDAX was used to analyse features on the media surface to understand their chemical makeup, as with the crystals shown to be “growing” on the surface of Limestone.

Preparation of the samples is required by coating with a thin layer of conducting gold onto the sample on a mounting stub. The machine used in these experiments is shown in Figure

42 below; the samples were inserted into the instrument below the grey tube that can be seen on the front of the instrument.



Figure 42 - Carl Zeiss (Leo / Cambridge) Stereoscan 360 SEM

Selected example images, of each media are shown with the magnifications of each image shown below each set of images. Larger and a greater number of SEM images of the media are given in Appendix II.

5.8.1 SAND

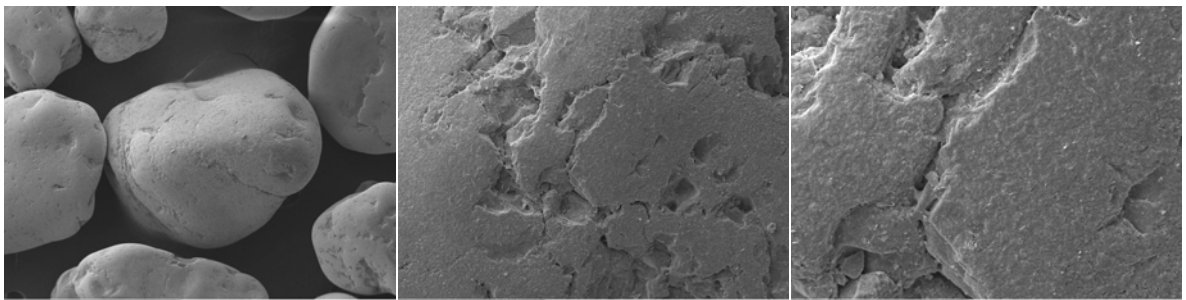


Figure 43 - SEM image of Sand at 85x, 500x and 1500x magnification

Sand (Figure 43) is rounded with a high sphericity; Ives (1990) noted a sphericity of 0.98 as typical for sand. As the magnification is increased crevices and surface features do become apparent, these increase the surface area compared to the calculated surface of an assumed

simple sphere. They are also not present in the fused silica of glass, shown in Figure 44. The surface features in the sand are not deep, and are unlikely to significantly affect the attachment and storage of particulates onto the media's surface significantly.

The sharper edges of these crevices in the sand may have an impact on the electrostatic charge as Suthaker et al (1995) noted that an increase in charge occurs along the sharp edges of an angular filter media. An average electrostatic charge, typically negative was -20 mV according to Ives (1990) for sand, which repels the negatively charged particles attempting to attach to the media surface. Therefore these charge concentrated zones will be more difficult to attach to than other areas assuming the predominant surface charge of particles for removal is also negative and repulsion occurs. Zeta potential measurements are reported in the literature which confirm that particle removal is enhanced by reducing the particle charge towards zero by addition of positive ions (Hendricks, 2000). Suthaker et al (1995) however states that this charge concentration will increase particle attachment in these zones, whereas most researchers report negative zeta potential or electrostatic charge from the media repels the also negative particles attempting to attach to the surface. The work by Suthaker et al (1995) does not elaborate on the number of measurements of this or show how these were determined, and not corroborated by any other experimental work and does not compare well with what is currently known about the electrostatic force and its repulsive impact as reviewed by Ives (1990).

5.8.2 GLASS

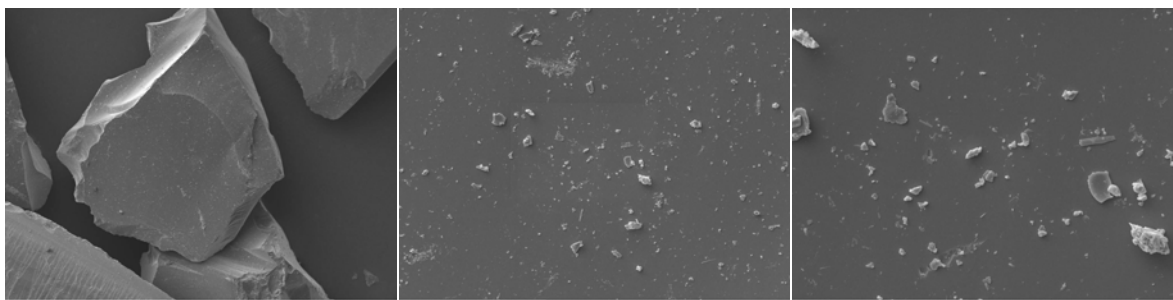


Figure 44 - SEM image of Glass at 85x, 500x and 1500x magnification

Comparison of images for glass (Figure 44) to the sand (Figure 43) show glass to be more angular and plate like due to the way the material breaks apart during crushing. Rutledge & Gagnon (2002), Evans et al (2002), Soyer et al (2010) and Fitzpatrick (2005). The higher

magnifications show smooth surface with no variations, except for scratches or rougher areas near the edge where the glass has been broken during the crushing process. The surface does show dust particles at the 500x and 1500x magnification, which are particles of dust that have fallen onto the surface of the media.

The edges of the glass are highly angular; with sharp edges and the earlier comments in section 5.8.1 discussing the charge concentration along edges by Suthaker et al (1995) could be applicable. The rest of the surface of the glass is very smooth with no surface features; therefore there is no shelter for attached particles potentially leading to a greater detachment of particles from greater shear forces passing over the smooth media. On the other hand the smooth surface could improve the removal of particles during backwashing, increasing the efficiency of the process. This is a characteristic observed in previous studies (See section 0) and noted as a benefit of using glass media. Sokolovic et al (2009) also noted that surface roughness improves filter performance for turbidity removal and therefore glass was expected to perform less effectively than other similarly sized media due to its smooth surface area.

The shape of the media grain is more flaky than the rounded sand, which combined with the angular nature of the filter media will positively influence the transportation mechanism for particles to the surface by inertia as discussed in more detail in section 5.2. Thus there could be advantages in turbidity removal from the angularity and disadvantages for the surface smoothness. The results for turbidity removal are described in section 0.

5.8.3 LIMESTONE

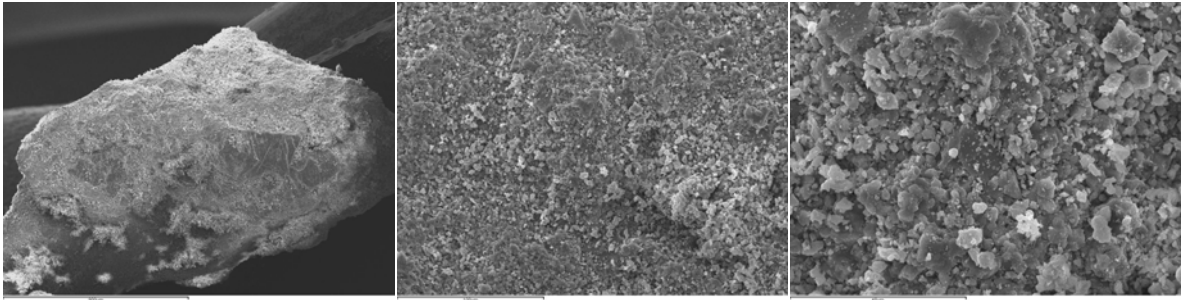


Figure 45 - SEM image of Limestone at 80x, 500x and 1500x magnification

The SEM of limestone at the lowest magnification shows a “furry” surface texture, whereas at the higher magnification the surface is shown to consist of stacks of crystals. These were analyzed as calcium carbonate crystals by EDAX. These crystals would provide a higher surface area and a rougher surface to allow particles to attach more securely and resist detachment. The surface texture of limestone is much rougher than either sand or glass but there are no clear crevices in the surface that would allow for particles to become trapped.

The generation and release of calcium carbonate into the water from the limestone leads to a zone of increased instability near the surface of the limestone media; this could contribute ion concentrations of calcium to assist binding and coagulation. Destabilization of contaminants such as colloidal clay particles were described by Rooklidge et al (2002), who concluded destabilization and coagulation improve transportation of particles to the surface of the media and also reduced the repulsive electrostatic force near the media surface increasing likelihood of attachment.

The surface texture of the limestone shown in Figure 45 will also give a greater surface area of at equivalent particle size compared to glass for example. This may however be dependent on the type of limestone, its origins and the solubility of calcium carbonate would vary. As the material is natural and unprocessed (unlike lime found in cement) it is less reactive and, this could have the benefit of ensuring the media has a longer lifespan in the filter. The resilience of limestone for different sources does need further work, there is little work reported in the literature.

Limestone has an angular particle shape, although not as much as the recycled glass (Figure 44 & Figure 45) which means the path through the filter bed will be less torturous than glass,

but more varied than with sand. The results for sphericity shown in Table 22 indicates limestone is similar to glass.

5.8.4 FILTRALITE

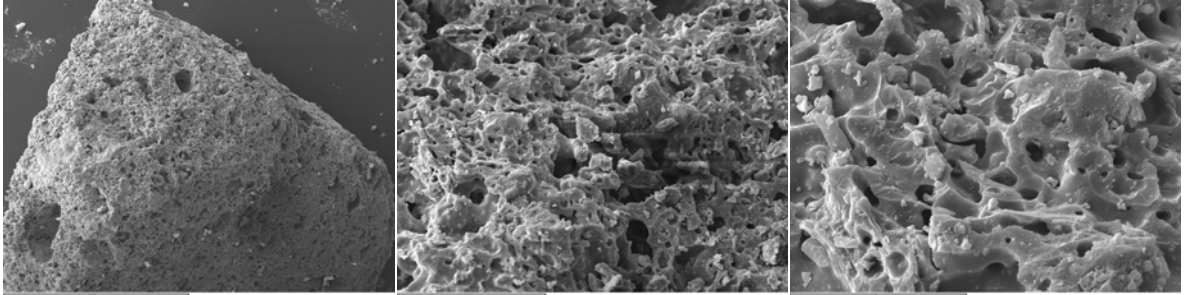


Figure 46 - SEM image of Filtralite at 80x, 500x and 1500x magnification

Filtralite has a large number of surface features (Figure 46); these consist of pores in varying sizes affecting the entire surface of the media. This open porous structure is responsible for its low particle density and suggested by the literature as leading to improved filter performance compared to sand. The surface of the media between these pores is smooth as might be expected due to the high temperatures used in the manufacture of the material but it constitutes a small portion of the surface area. This is the reason for improved durability compared to pumice (See section 5.5) which exhibits a similar open pore structure on its surface but suffers from durability problems

The media on the whole has angular edges much the same as limestone; the values for sphericity of the various media (Figure 27), show the variation in angularity between the tested filter media. The sphericity of Filtralite is between sand and glass, it is the second most spherical media after sand. The porous nature of the filter media however did not seem to improve the turbidity performance of the media. The performance of the Filtralite was not as good as glass/sand which would be expected from the greater surface area, this is discussed in Section 5.7. An explanation for this is suggested in Figure 47, which shows the smooth streamlines by-passing the porous structure and not contributing to the transport of particles to the media surface.

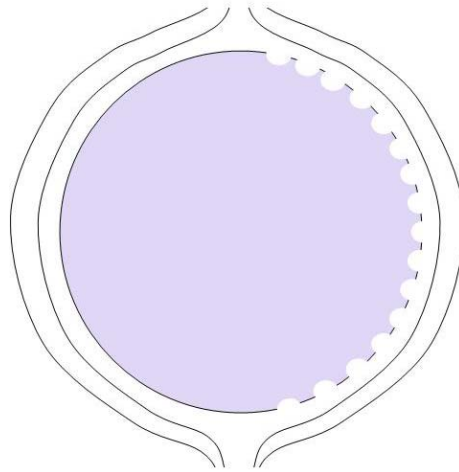


Figure 47 - Image showing effect of particles surface on flow around media

The flow around a media such as Filtralite, even though it is highly porous, its surface is not affected so as to impact upon the transportation of particles to the surface for attachment to occur. Figure 47 shows simply how the streamlines around the particle might be required to remain the same as if irrespective of either a smooth or porous surface. Particles already at the media surface may be captured and retained better as small particles may penetrate the pores. If attachment occurs it is predicted that the particles will be retained better by the Filtralite media as there will be shelter from shearing resulting from the flow around the media grains. The higher specific surface area of the media will allow a larger amount of particles to be retained per unit mass of media, with smaller particles attaching in the pores allowing larger particles to be retained on the external surfaces reducing the impact on head loss.

5.8.5 SLATE

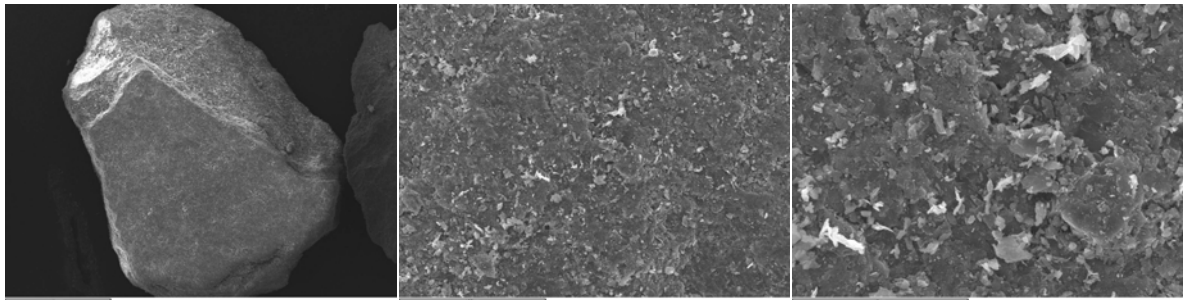


Figure 48 - SEM image of Slate at 80x, 500x and 1500x magnification

Slate has a flaky plate like particle shape with one dimension being smaller than the other two dimensions (Figure 48). This plate-like particle shape will pack in the filter bed differently to the traditional rounded or angular filter media. This plate shape and compaction will give a torturous flow path for particles moving through the filter bed. Data on performance in section 0 suggests this leads to more variable motion of the particles which gives a greater likelihood of particles attaching to the media surface as has been previously noted by Ives (1975) and discussed in section 0.

The surface detail seen in the higher magnification (Figure 48) images does not show any clear surface features other than the small flakes. The flakes or dust are all in a varying state of attachment to the surface, some look very fragile while others are fully attached and flat to the surface. It was envisaged that the number of these flakes would be reduced by breaking free during the first runs of the filter though backwashing and this was confirmed by the increased time to clean the media during initial uses as shown in section 5.5. However those flakes that remain firmly attached will offer a rough surface texture with flat plates protruding a short distance away from the media surface.

These surface features that protrude into the flow through the media bed will enhance filtration by offering a further attachment surface to particles, disturbance to the stream lines also offer shelter to attached particles from the shear forces that could cause detachment of particles from the media surface.

5.8.6 STEEL AND FURNACE SLAG

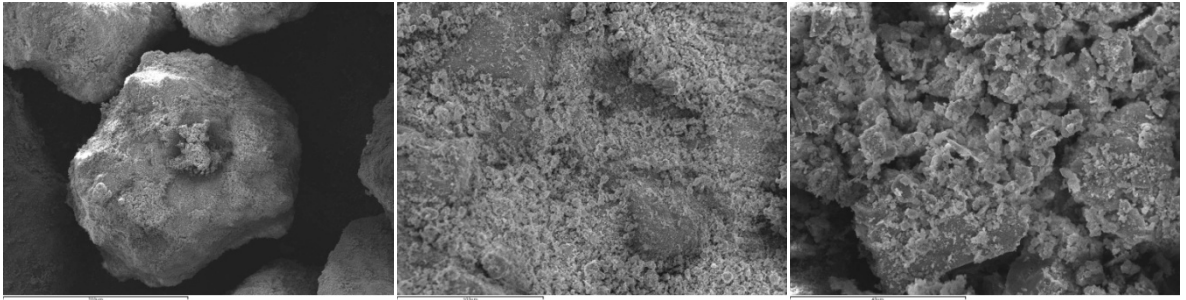


Figure 49 - SEM image of Steel Slag at 90x, 500x and 1500x magnification

Steel and Furnace slag has a similar surface texture, although arguably Steel slag has larger pores and a larger variation of surface features with deeper crevices and pits interpreted from Figure 49 and Figure 50. This broad range of pore size could allow for a range of particle sizes to attach to the media surface. The finer textures of the Steel or Furnace Slag having a high specific surface area may be too fine to aid in particle attachment.

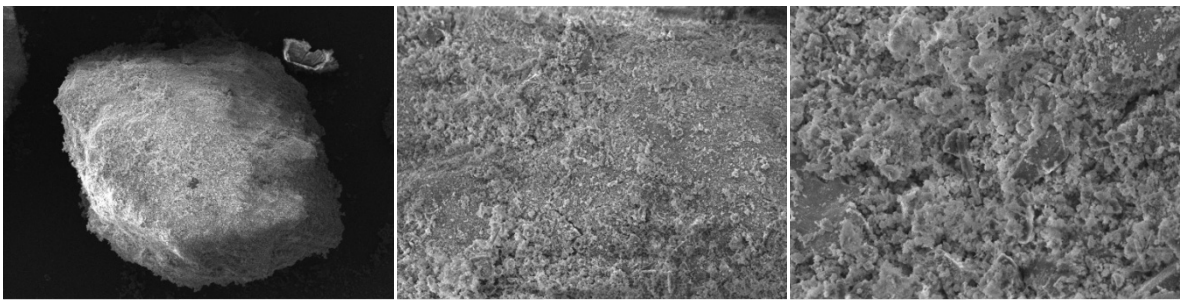


Figure 50 - SEM image of Furnace Slag at 110x, 500x and 1500x magnification

Furnace slag exhibited the highest specific surface area of any media tested; this is discussed in section 5.7. The reasons for this high surface area value can be seen in Figure 50, the surface is covered with fine pores (typically less than 1 μm). These pores are smaller than those seen in Filtralite, Pumice and Steel Slag. It is suggested that they will not have a significant impact on filtration performance as before as most particles in the water will not be able to enter these pores and the openings can easily be blocked by the larger particles in coagulated water. Furnace slag has a more rounded particle shape than the steel slag, although there is variation between particles with some having a more angular appearance. The steel or furnace slag is more angular than sand, with numerous edges around each

media grain but there is significant variation between particles with some being flatter and less rounded.

5.8.7 PHOSPHORUS SLAG

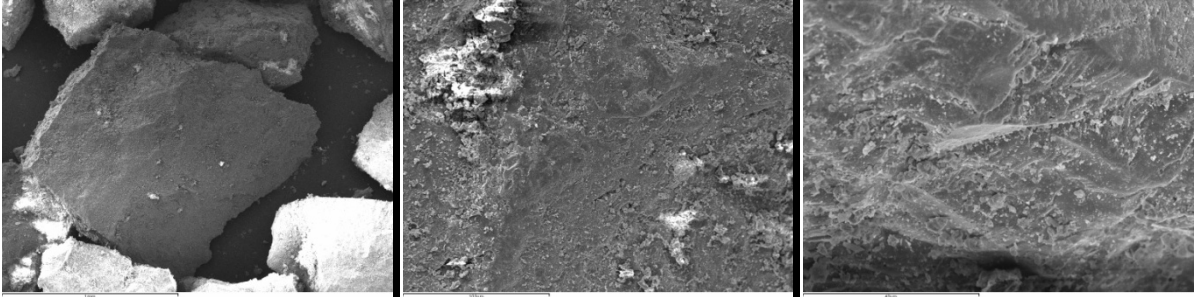


Figure 51 - SEM image of Phosphorus Slag at 85x, 500x and 1500x magnification

Phosphorus slag has a surface that is textured similarly to a fine powder (Figure 51). As discussed in section 5.7 the phosphorus slag has a low specific surface area and the SEM shows that the surface does not have pores unlike the other slag based materials. The main features are sharp changes in topography across the media surface. These types of features will not significantly impact on the specific surface area hence the low value for specific surface area in comparison with other media in Figure 41. The media shape is angular which will lead to improved head loss performance (from a variety of inter-pore dimensions) and improved turbidity removal.

5.8.8 PUMICE (TECHFIL®)

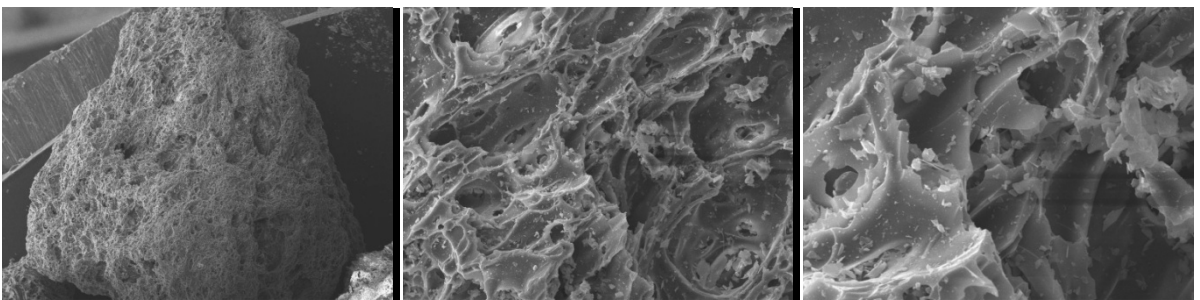


Figure 52 - SEM image of Pumice (Techfil) at 85x, 500x and 1500x magnification

Pumice is a highly porous naturally occurring material but from the images (Figure 52) it appears fragile. There are a number of sites along the edges of the pores that have broken off and fragments of these breakages can be seen across the surface of the media. This

highlights the issue first noted in section 5.5 and is a liability during use. The media will likely lose a significant amount of mass and pores during the lifetime of the filter and this will affect the performance assuming changes in porosity of the bed and a change in the effectiveness of the media in retaining particles on its surface.

The media has a wide range of pore sizes across the surface (1 – 100 μM). This is beneficial as the pores are large enough to trap particles in the pores and protect them from detachment forces that will be flowing over the surface of the media. Work by Farizoglu et al (2003) and Ghebremichael (2004) has suggested these features are beneficial features assisting performance compared to sand.

5.8.9 PUMICE (PUMEX[®])

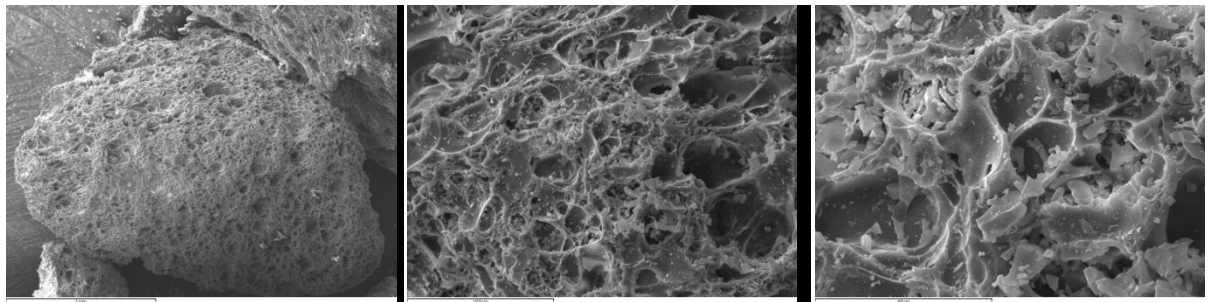


Figure 53 - SEM image of Pumice (Pumex) at 85x, 500x and 1500x magnification

Pumex[®] (Pumice) has the same surface structure as Techfil[®] (Figure 52) as they are both fundamentally the same material; however they are sourced from two different locations (Turkey & Italy). The media should therefore geologically perform exactly the same as Techfil[®] and would not overcome the problem of non-compliance with the durability standard.

5.9 BATCH ADSORPTION TESTING

5.9.1 METHODOLOGY

Batch Adsorption testing was carried out to give an indication of ion-adsorption of the commonly expected metals Iron (Fe), Manganese (Mn), Aluminium (Al) but also the non-metal Phosphorus (P) which was used as a model anion but is also a common pollutant found in water. Iron (Fe) and Aluminium (Al) salts are the most common coagulants and Manganese (Mn) is a common problematic contaminant. The testing procedure was based on a simple batch testing method described by Graetz & Nair (2000). The method was originally developed for phosphorus sorption isotherm determination but has been applied to metals as well. The Phosphate was chosen as the anion as it allowed the results to be compared with previous work and comparison with the performance of the filter media to soil samples in removing phosphate.

The procedure of the method described by Graetz & Nair (2000) is detailed below:

1. Air-dried samples were screened through an appropriate sized sieve to remove contaminating debris and non-standard particle sizes.
2. 2.0 g air-dried media sample was added to a shake flask.
3. 100mL of solution containing 50 mg P/L as KH_2PO_4 was added to the shake flask (Fe – $FeSO_4$, Al – $Al_2(SO_4)_3$ and Mn – $MnSO_4$ also in the same concentration) The P value being removed per gram of material would then indicate total removal if adsorption reached 25 mg P per gram of filter media.
4. The shake flasks were placed on a mechanical shaker for 24 hours at 25 ± 1 °C.
5. The suspension was then allowed to settle for an hour and the supernatant filtered through a 0.45 μ m membrane filter.
6. The filtrate was analyzed for the soluble reactive P, Fe, Al and Mn using an ICP.

The standard method is based on molybdate using a spectrophotometer to analyze the dyed filtrate samples. ICP was used as it was a more suitable precise modern method for analyzing the four contaminants during this testing, and the equipment was easily available. A single concentration of solution was used for each element of 50 mg/L. The standard test suggests a range of concentrations between 0.01 and 100 mg to cover non-linearity; in this case a

single initial concentration of 50 mg/L was used to simplify the comparison. The standard test does not represent the conditions in a filter, as the flow of water through the column is set at a lower contact time compared to the 24 hours that occurs in this test compared to 2 – 3 minutes in a filter.

Each of these metals is a problem for water treatment as the standards are now for the metals of 250 µg/L and it is normal now to add 1 mg/L of P as a corrosion inhibitor. Manganese and the anion phosphate also cause problems for removal using a typical treatment train with specific processes often used for their removal. Iron and Aluminium are the most common coagulants, they are also being dosed at higher concentrations than in the past due to increased problems from colour and turbidity spikes in raw water possibly caused by increased rainfall intensity and soil erosion and or algal blooms in the reservoir. They therefore must be effectively removed as soon as possible in the treatment process so as not to affect processes later in the treatment works.

5.9.2 TESTING

Figure 54 shows the mass removal of each metal in terms of unit mass of filter media (g/kg) the chart shows a predictable variation in specific adsorption potential. There was virtually total removal of the metals and P for the two metallic slags. This suggests a different removal mechanism between these two results. The results above 15 g/kg occur due to a change in speciation and precipitation of the metal from the solution. This was observed as floc particles settling to the bottom of the shake flask that was left overnight. In the cases of limestone, steel slag and blast furnace slag there was virtually instant floc development when the solution was brought into contact with the filter media in the shake flask. It was concluded that the metals were precipitated as the hydroxide polymers encouraged by the increase in pH. Measurement of the pH offers a confirmation of this theory since the hydroxides of Fe and Mn are insoluble, and therefore monitoring the pH of the media can give an indication of whether precipitation is the dominantly occurring process

The other filter media that show a removal lower than 15 g/kg exhibited no flocs, and it is likely the predominant removal mechanism was surface adsorption of the contaminants rather than precipitation onto the surface of the filter media.

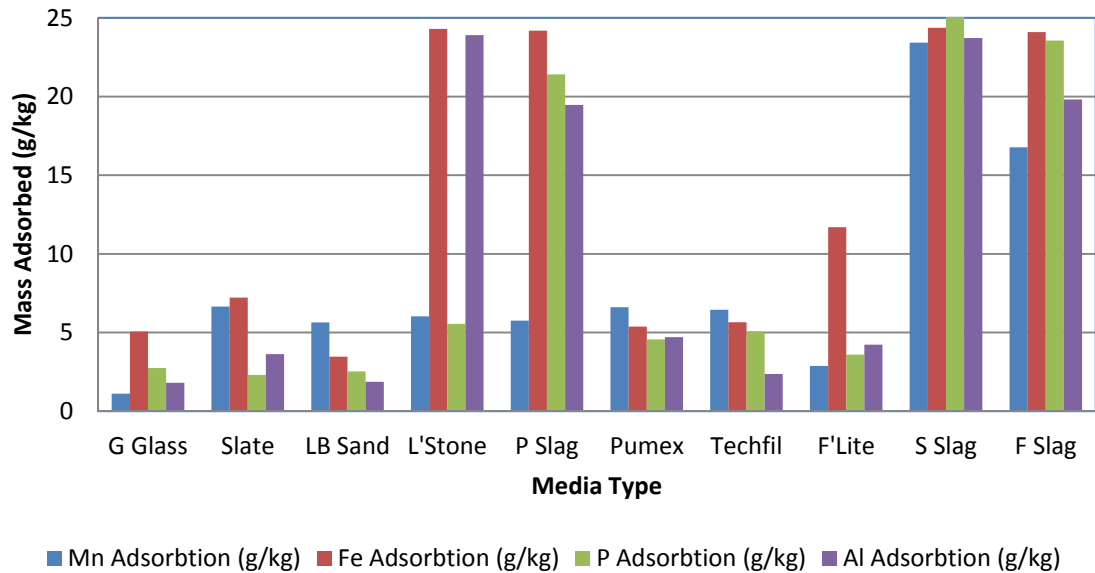


Figure 54 - Chart showing the amount of each metal removed per unit mass of media

This effect is shown in Figures Figure 55 (Al), Figure 57 (Fe), Figure 58 (Mn), and Figure 59 (P). Aluminium, Iron and Phosphate initially reduced the pH when dissolved to 4.0. Aluminium and Iron behave similarly as the pH increases as would be predicted by the theory of hydroxide formations. The pH from the slag columns would be expected to increase as a consequence of the high hydroxide content (or a cross reaction with the carbonates). In the results for aluminium removal in Figure 55 it is shown that the precipitation is limited to pH higher than the initial pH with the greater change in pH leading to greater aluminium removal. The change in pH is greatest in the Slag and Limestone.

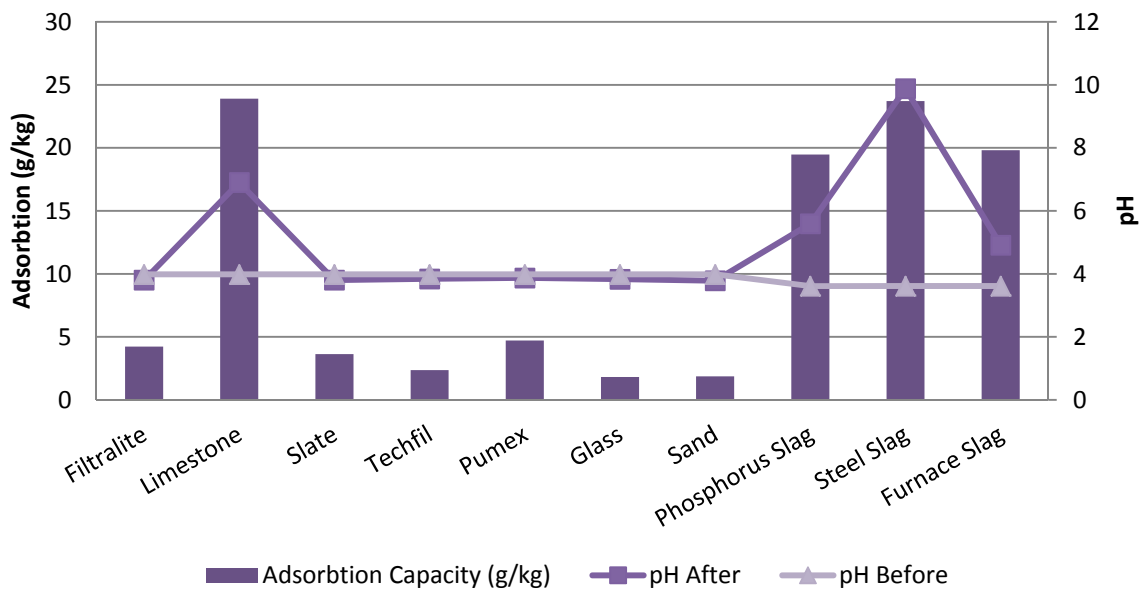


Figure 55 - Chart of Aluminium (Al) removal for each filter media in batch adsorption tests

The behavior of Iron (Figure 57) however was different to aluminium; there is no relationship between amount of precipitation and change in pH. A pH of over 7 causes complete removal of Iron from the solution. The base pH in this instance was around 5.7 increasing to a maximum value of 11.5 with the steel slag. Surprisingly limestone increased the pH to 7.5 which is a similar result to that seen with aluminium, but lower than the changes in the steel slag. This result ties in with charts for ion hydrolysis shown in Figure 56 below. The chart indicates that as the pH increases, the solubility of the Fe reduces as the pH nears 8 then increases. But by the time it starts increasing the precipitation of the Fe from solution has occurred and it is much slower to return to the soluble state leading to the total precipitation in the filter media once it reaches the pH of 7. The Limestone with the Fe however has not reached the pH of 8 but there is sufficient change for it to cause total precipitation at the pH of 7.5. The same mechanism can be seen in the Aluminium by looking at the associated chart in Figure 56, as the pH increases the solubility of the Al reduces and the material precipitates out, the pH in this case that most readily occurs is 7.0, which in the case of the Limestone and Steel slag is much higher than this and so total precipitation has occurred. For the Phosphorus Slag and the Furnace Slag there is not a total precipitation of all Al from solution and this is likely due to the fact that the pH only reaches a maximum of 5.8 and therefore it has not reached the point where precipitation occurs.

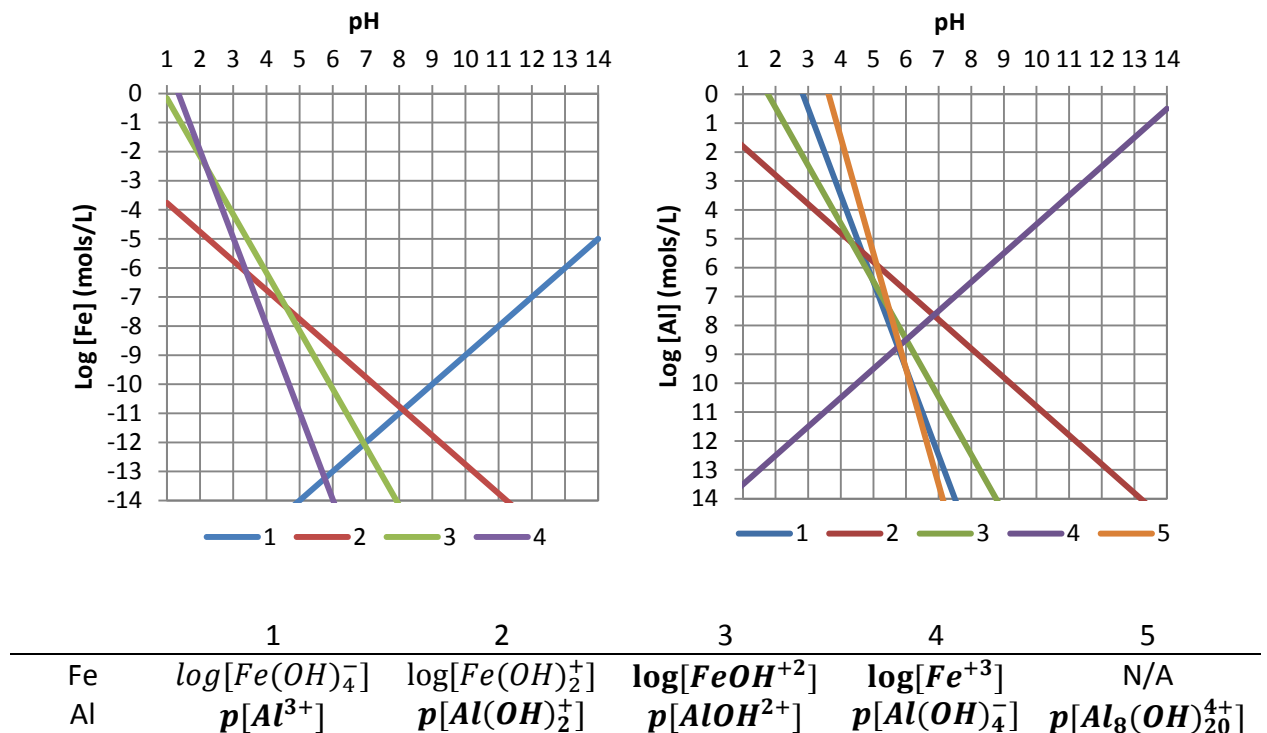


Figure 56 - Log concentration charts for both ferric-iron and alum species

The Fe adsorption by the media which did not influence the pH (that is Filtralite, slate, pumice, glass and sand) was influenced by surface area. Sand and glass showed similar removal values of 1.8 g/kg. Both these media have the lowest surface areas and this may be the major factor to their low performance, in addition to the reduction in pH suggesting a strong ionization and the need for an electrostatic reaction. The media with high surface areas such as the Pumice and Filtralite showed improved performance, although the Techfil Pumice only performed half as well as the Pumex derived material despite a greater surface area. This could be due to a variation in chemical composition according to the different origin the materials; this would be worth further investigation.

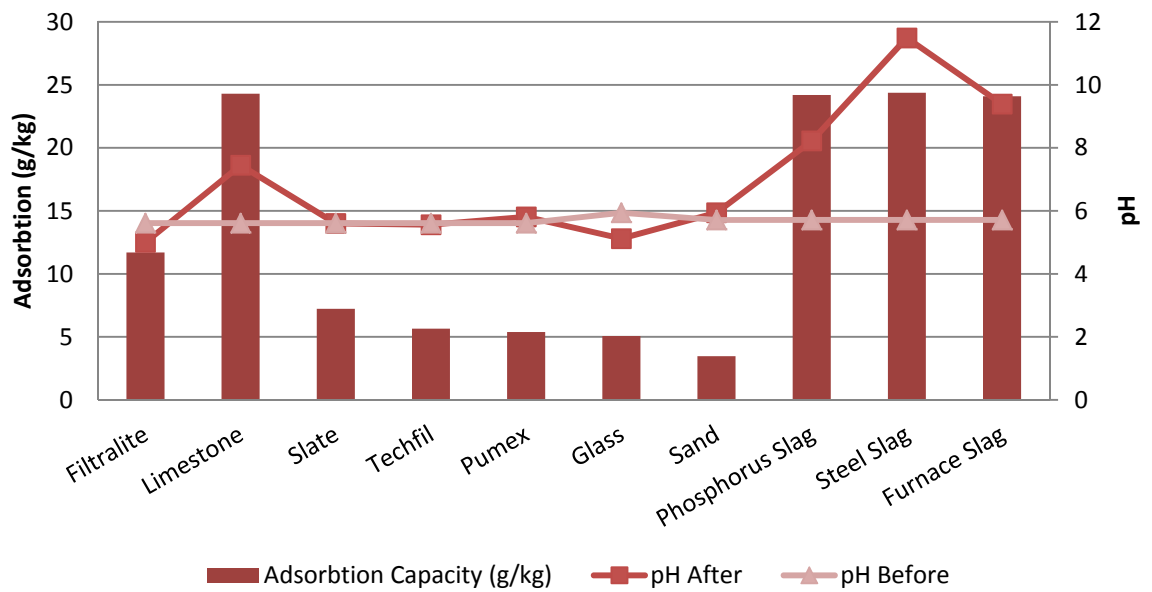


Figure 57 - Chart of Iron (Fe) removal for each filter media in batch adsorption tests

All the alternative media performed better than sand for iron adsorption including the glass media which was not expected due to its lower surface area. There was a reduction in pH caused by the Filtralite and Glass was also different to aluminium and other ions tested; the significance of this needs further work. Glass was expected to be an inert material particularly due to the high temperature method of manufacture leading to a fused surface. Removal of Iron was better than Aluminium (Figure 55) and this may be linked to their solubilities at the respective pH levels where Al was more acidic than the Fe.

The results for manganese (Figure 58) show little effect on pH, the pH of the solution being 7. The effect on limestone was therefore muted by the small change in pH from neutral, and therefore there is no significant dissolution of the limestone occurring to allow hydrolysis products to react with the solution. The phosphorus and furnace slag types also show no increased pH value, this could point to a similar mechanism to limestone with hydrolysis products only being released into solution when the pH is acidic. Neither was there a significant change in pH with the furnace slag but it still removes a significant portion of the manganese from solution. The steel slag however exhibits a high pH change up to 11.5 which has caused precipitation of the manganese from solution.

Furnace slag has the highest surface area of any of the filter media being tested and the surface is covered in fine pores that generate this high surface area (See section 5.7).

Considering there is no significant pH change in the solution with the media then it seems that furnace slag is highly effective at the removal of manganese by adsorption, this was corroborated by the lack of flocs seen in the solution after 24 hours compared to the Steel Slag. Thus it may be suggested that both mechanisms are possible, that is direct ion adsorption to the filter media and reaction and precipitation of insoluble salts.

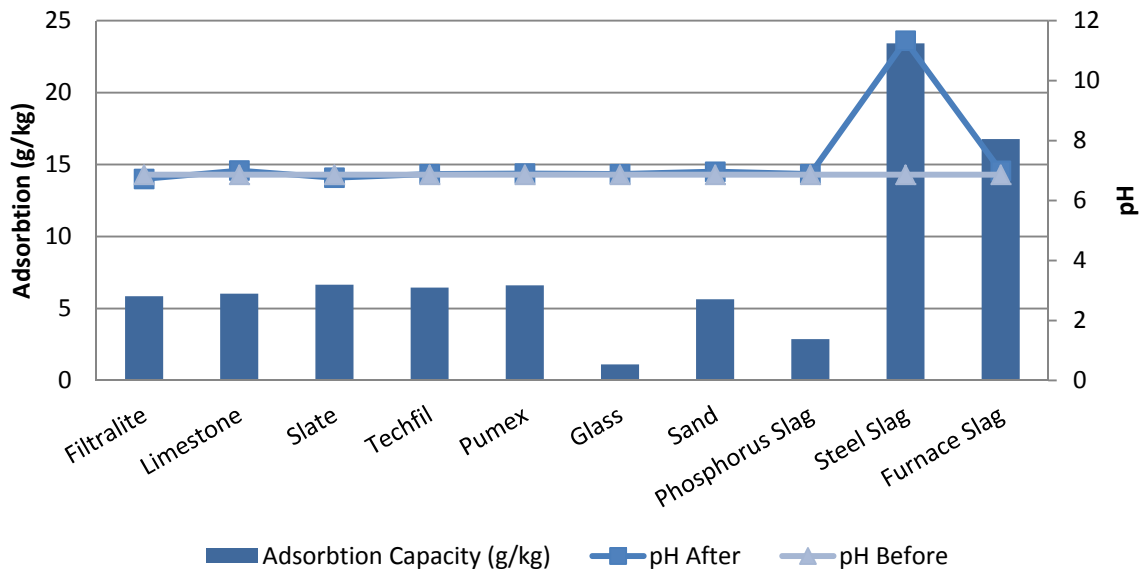


Figure 58 - Chart of Manganese (Mn) removal for each filter media in batch adsorption tests

The glass and phosphorus slag show poor removal of Manganese compared to other media. The glass is likely due to the low surface area of the media but the reason for the poor phosphorus slag performance may be due to the different surface chemistry. A possibility is the fact that manganese has more complicated oxidation states compared to iron and other metals tested and has a lower propensity to form hydroxides shown by the change in pH. This is supported by the reaction of limestone which also does not react or dissolve to form hydroxides.

The results for phosphorus do show the classical pattern of increasing pH increasing the binding to P. The results from the slag materials again show how a greater pH and potential for floc formation is able to remove dissolved ions from solution; this is as expected from the formation of hydroxide polymers (Hendricks, 2000). The removal by the limestone is less than expected but so is the increase in pH of 1.5. Limestone does have the largest removal of

PO₄ behind the slag materials although not significantly greater than the other media and no flocs were observed in the shake flask after 24 hours. Therefore a greater pH change is required to cause precipitation of floc and remove phosphorus from solution. In all other media there was no pH change that was significant enough to cause precipitation of hydroxide (OH) floc.

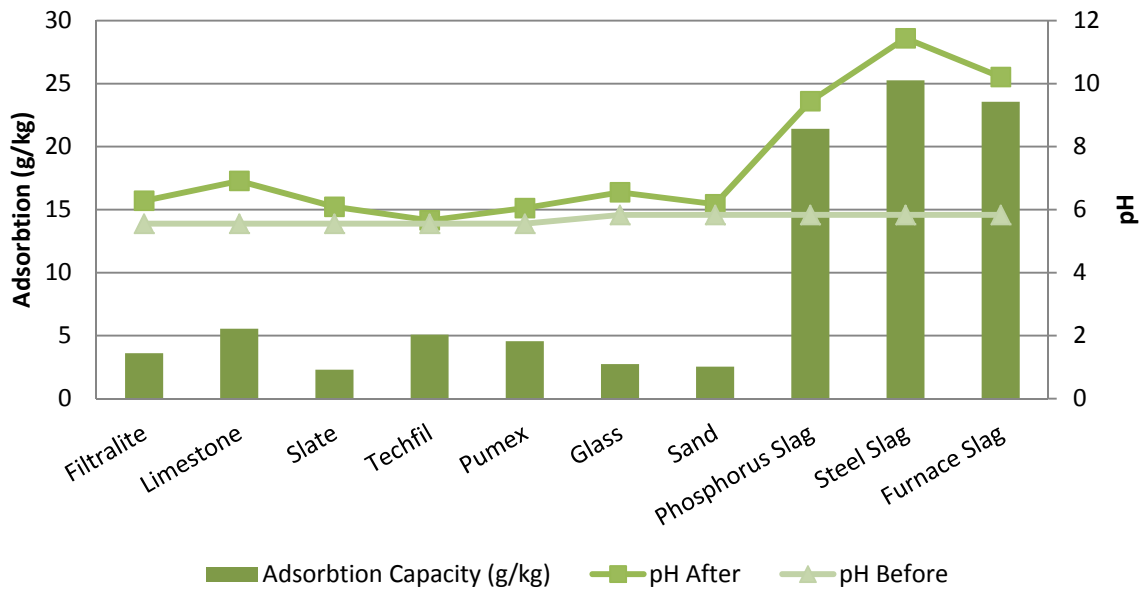


Figure 59 - Chart of Phosphorus (P) removal for each filter media in batch adsorption tests

The removal of phosphorus was therefore influenced by pH change causing precipitation. The adsorption was not as large as the cationic iron and aluminium, and it would be interesting to follow the speciation of the P involved in the precipitation.

In conclusion the precipitation of the metals and PO₄ from solution was the primary mechanism for removing the greatest amount of ions from solution as they were precipitated into large clearly visible flocs suspended or settled in the beakers. This was based on results from filtering through 0.45 micron filter paper and therefore was only measuring dissolved ions after the experiment was carried out and not that which had been precipitated. The increased precipitation in the slag materials compared to the limestone was assumed to be caused by the extra reactivity of the lime content of both. In the slag materials the calcium oxides are likely to be a more reactive type following heating as in the production of cement. This makes it more reactive and able to influence the pH of the

solution more rapidly and to a higher degree than the natural limestone that is mainly unprocessed limestone CaCO_3 or $\text{Ca}(\text{OH})_2$.

This reduced reactivity of the Limestone however ensures the activity is more subtle. There was no significant change in pH of the water and further treatment after filtration would not be required to deal with the increase of pH that would occur from using a slag material. Also as the lime in the slag media is more reactive, the effect would diminish more rapidly as the lime reacts over time and therefore removal of metal contaminants through precipitation would be reduced and media would require replacing or top-up to ensure constant removal of contaminant metals.

Formation of iron and aluminium flocs provide increased filtration performance (NTU) by collecting particles in the flow through the filter bed and then being larger they are more likely to attach to the filter media surface. The formation of these flocs within the filter bed itself also avoids limiting the effect to straining within the upper layer of the filter bed. Surface accumulation accelerates head loss and reduces filter run times. A reaction time is needed within the filter media to create the required pH increase for precipitation of the hydroxides and floc formation to occur within the filter pores.

The practical contact time in RGF filtration is however likely to reduce the impact of this effect, less than 10 minutes compared to the retention time of 24 hours for the standard isotherm shake flask tests. Contact times in RGF are measured in seconds or minutes at rapid gravity filter speeds of up to 8 m/hr (60 – 120 seconds in laboratory columns). The effect was instantaneous when observed with the steel slag (the most potent) with flocs forming a few seconds after the media came into contact with the metal solution. This needs further test work but potentially offers a type of reactive filter for some situations.

Metal concentration used in the tests was far higher than what would be typical at a water treatment works where, from data collected from Severn Trent Water Plc, the typical value for iron after clarification and prior to filtration is on average 0.23 mg/L which matches the 50 mg/L that was used in the test unrepresentative of drinking water filtration. This was to allow validation with other work in the laboratory on wastewater, but the results have confirmed the importance of pH and the potential to alter mechanisms of filtration with different potential sacrificial media.

5.10 INITIAL CHARACTERIZATION RECOMMENDATIONS

The information from all of the characterization testing carried out on the filter media was considered and a final list of filter media chosen to be used in laboratory scale tests was assessed as follows:

Sand – As the most common filter media used in rapid gravity filtration, sand was to be included as the standard and control against which all new filter media was judged.

Glass – Previous studies have shown glass to be a suitable alternative to sand as it is similar chemically (Silica Oxide). Characterization testing has shown it to be similar to sand against current requirements for a filter media. Fundamentally its smooth surface offers academic value to test how important surface roughness is to filter performance.

Limestone – Presents a different chemical structure to the silica based materials. The calcium carbonate that is leached from the media as water flows through it improves filtration through destabilization of particles in the water, improving transport and attachment mechanisms.

Filtralite –A commercially available filter media that has already been used in full scale filters, and which has a porous surface with a high surface area. The media is larger than other media chosen and the impact of this will need to be carefully considered in analysis.

Slate –Has the most angular particle shape compared to all other media. This will allow testing of the impact of angularity on headloss which previous research has suggested will lead to a low sphericity media, close packing and potentially better turbidity removal due to the increased torturous path.

The following media were discounted from these initial characterization tests:

Furnace Slag – With the highest specific surface of all the possible alternative filter media tested it was shown from the SEM images that this surface area was primarily due to a high density of very fine pores. These were deemed too fine to have any

significant impact on filtration and would clog rapidly. Thus combined with the alkaline pH it was discounted.

Steel Slag – It was discounted as when submerged in water the grains and precipitate began to fuse to one another producing large strongly iron precipitates bound media balls that backwashing would be unable to break apart and so it was removed from testing.

Phosphorus Slag –The high phosphorus content of the filter media could leach and could even be beneficial since P is added to drinking water to avoid metal solubility. In this case however limited resources and the pH effect precluded further work.

Pumice (Techfil / Pumex) – Previous research has shown Pumice to be a good alternative media for rapid gravity filtration, however there were issues of durability noted in the characterization tests. Therefore it was not chosen to be used in the laboratory scale filter columns.

Testing has shown that there is a large range of factors that must be considered when comparing performance, the zeta potential of the media would ideally have been included but the availability of suitable equipment meant it was not possible to include. The range of tests carried out enable a comparison of performance, fundamental mechanisms and media properties to be analyzed to determine the most desirable media properties and why they alter performance.

In addition the standard testing of turbidity removal and headloss, the leaching of soluble materials from the media has been shown to possibly be a benefit of using alternative filter media. Of the chosen media, limestone showed the best contaminant removal in the characterization testing; suggesting the formation of OH polymers with pH changes caused the precipitation of the metals. In a filter this would be expected to improve turbidity performance in the media, as soluble coagulants such as iron and alum are known to be precipitated within the filter bed.

The second phase of testing was carried out using laboratory scale filter columns; this section describes the design and construction of the filter columns. The laboratory scale filter columns were designed to operate as a real filter bed would, and offer an experiment operated as a small section of a standard rapid gravity filter. The small size of the filter column (60 mm internal diameter) does have limitations, especially with the wall effects that will become more evident at this scale.

The literature reviewed noted a range of flow rates for RGF and the laboratory unit needed to be able to represent this. Kawamura (2000) states that the filtration rate of rapid gravity filters when the media has an effective size $d_e = 0.45 - 0.65$ should be between 5 to 7.5 m/h with 7.5 m/h being the typical value used. In contrast Hammer (2007) gives a wider range of 5 to 24 m/h (the higher bound is extremely rare and for specialist applications) without a specification on the media size used along with a typical maximum design value of 12 m/h.

Hendricks (2005) gives a history of the variation of flow rate in rapid gravity filtration during its historical development, which he suggests took place from 1900 to 1950 where he reported the flow rate was 4.88 m/h. After 1950, Bayliss (1956) was able to recommend an increase in rate to 12.5 m/h. Hendricks (2005) also makes the point and states that from 1980 onwards flow rates of 25 m/h and above were used when conditions allowed. These high flow rates >10 m/h have not been found in the UK. From discussions with Utility companies in the UK, their typical flowrates are between 4– 12 m/h and often at the lower value as works rarely operate at their maximum capacity. Progressive loss of the anthracite in dual-media filters was quoted as the main reason for reduced flows.

The flow rates for this trial would ideally be designed to account for the likely conditions found in rapid gravity filters however it is well known (See section 4) that as flow rate decreases the turbidity removal improves and with increased flowrate the performance diminishes. Most utilities in the UK operate their filters at 5 – 10 m/h, which is lower than what is described in literature. It was decided that this study would look at higher rates to provide extra new data and determine if any increased performance could be gained with the new media.

Table 29 - Flow rates used in laboratory scale testing

Flow Rate (m/h)
8.6
11.1
13.6

Table 29 shows the chosen flow rates for the study, they cover the flow rates expected in a rapid gravity filter from the mid-range (from literature) to high range (from utilities) rate of 8.6 m/h up to a higher rate of 13.6 m/h. The lower rates were therefore excluded on the basis their performance was known. Flow rate was controlled by adjusting the outlet valve from the base of the filter column (Figure 69) and determining the flow rate by using a stop watch and measuring cylinder. These calibration measurements were checked every 30 minutes during a run to ensure the flowrate did not vary.

6.1 RAW WATER

It was decided to produce a controlled raw water suspension in the laboratory as this would enable the chemistry and quality to be carefully controlled and ensure repeatability between experimentation. The resources necessary to store and to transport and the changes likely in a real active raw water suggested synthetic water was the best option followed by scale up trials with real water. Table 30 shows the previous research studies used to develop synthetic water for the study. These were typically based on creating a known and repeatable turbidity value in the water as one of the main performance characteristics of filters and where noted in the papers the turbidity value used in the paper is given.

Table 30 - Previous studies using synthetic water for filtration studies

Author	Media	Synthetic Water	NTU
Farizoglu et al (2003)	Pumice	26 g Kaolin Clay to 350 L clean water	29 – 31
Albuquerque & Labrincha (2008)	Expanded Aluminosilicate	0.1486 g Kaolin Clay to 2 L water	37 - 57
Ives (1987)	Sand	Kaolin Clay noted to be commonly used in research studies on filter performance	
Glasgow (1998)	Sand	Latex beads	

Kaolin clay and latex beads were most commonly used to create turbidity in water. Glasgow (1998) noted latex beads have an advantage of being of a more consistent particle size allowing for studies to look at removal of particular particle sizes, in his case the relatively uniform protozoan oocysts. Kaolin clay on the other hand is a naturally occurring material that has a more realistic varied particle size distribution; it is these reasons that led to its use in the laboratory scale column experiments. The material is naturally occurring and present in raw water with measured concentrations up to 1000 mg/l, reducing to around 20 mg/l after coagulation noted by Ives (1987). Thus it was concluded kaolin was likely to interact more realistically with the various filter media, while synthetic latex beads are less polar when interacting with filter media giving biased filter performance than would be expected from real water.

The kaolin was added to tap water which had a consistent chemistry at Loughborough as it is from a large well buffered water supply grid for the East Midlands. The kaolin solution would be produced using Glasgow (1998)'s methodology that was used to produce the latex bead suspension; the details of this are given below:

1. 100 g Kaolin Clay added to 1 L of RO (reverse Osmosis) water, this solution was stirred overnight to ensure that it was well mixed.
2. The stirring was then stopped and the solution was allowed to settle for 4 hours before the top 800 ml of solution was siphoned off, this was the final solution used for the trials.
3. Prior to use the solution was thoroughly and continually stirred to ensure the kaolin was fully suspended in the solution and then it was added to a known volume of tap water in the raw water tank and allowed to mix before the test.

The settlement time was chosen after carrying out particle size analysis using the Malvern Mastersizer 2000. The results of three different settlement times with the kaolin solutions are shown in Figure 60:

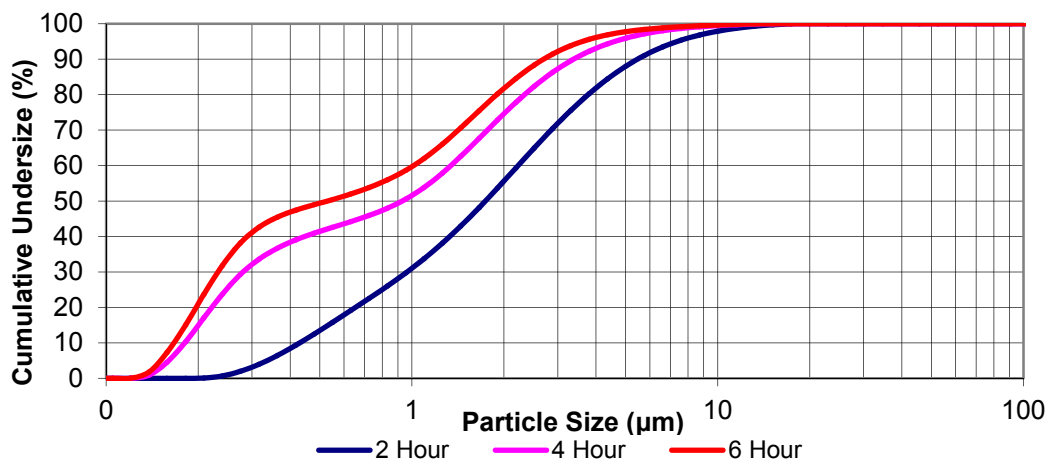


Figure 60 - Particle Size Distribution of kaolin solution at different settlement times

From this data the 4 hr settlement time was chosen, this split the particle size as 50 % greater than 1 µm and 50 % lower. Yao et al (1971) showed that for particles of 1 µm in size, filtration performance is at a minimum. For particles smaller than 1 µm diffusion plays an increasing role to enhance filtration, whereas for particles greater than 1 µm the mechanisms of inertia and gravity are more important. Work by O'Melia & Ali (1978) showed for that headloss was increased when a suspension contained smaller particle sizes. The removal of varying particle sizes is also influenced by other particle sizes in the suspension. The particle size typically expected to be treated in filters ranges from sub-micron to 20 µm in size according to Ives (1987) while Mackie & Bai (1992) used a suspension of 0 – 10 µm in size in studying particle size distribution and its impact on filtration performance..

Mackie & Bai (1992) showed that a filter bed does not treat equally the range of particle sizes that were present in the raw water suspension and it is possible that different areas of the filter are treating different particle sizes. Mackie & Bai (1992) also highlight that the removal of smaller particles is enhanced by the presence of larger particles in the suspension being filtered, which agrees with previous research in the area by Ives. Therefore it was concluded to keep PSD consistency that the preparation of the kaolin suspension to be added to the raw water for filtration is kept as identical as possible between batches.

Thus the 4 hour settlement time for the preparation of the suspension allows for the larger particles to be lost which would be removed by the coagulation stage while a wide range of particle sizes could be used. There were centered on the 1 µm particle size that Yao et al (1971) considered to be the size with the poorest removal in the filter. These sizes will

differentiate between mechanisms of removal that Yao et al (1971) suggested between the particles smaller and greater than 1 μm and the 2 – 4 hour settlement time match this work noted by previous authors.

The resulting turbidity values for the raw water were chosen to be either 35 and 9 NTU, which corresponded to an addition of 200 and 50 mL of the kaolin stock solution. These values were chosen to be higher than typical clarified water to accelerate the head loss during the 12 hour run-time for the filters. The increased turbidity would lead to a more rapid change in performance of the filter due to the increased solids load. Two raw water NTU values will also allow the variation of accumulating solids load to be compared from the two turbidities. The Pilot Plant trials were carried out on-site at a water treatment works then true clarified water with a low turbidity was to complement the controlled laboratory studies by representation of real-world results.

6.2 FILTER BED SPECIFICATIONS

The filter bed itself constitutes two parts, the supporting media that allows for backwash flow to be evenly distributed across the base of the filter bed and ensures no filter media is lost out of the filter during operation. The specification of the filter media and supporting bed was determined prior to final design of the filter test rig to ensure that the dimensions of the filter column were sufficient to be able to retain the media during use and backwash.

In practice the design was based on the worst case scenario, which was the largest and lightest media particle used, which was Filtralite. Applying retention criteria based on Filtralite then all other filter media were not likely to encounter any problems during use in the filter columns.

6.2.1 SUPPORTING MEDIA

A supporting bed is required to prevent filter media loss from the base of the column and to break-up the backwash water and air evenly throughout the cross-section of the filter bed. Kawamura (2000) gives a gradation of particle size and depth for a gravel support bed shown in Table 31 below. The support must meet the standards set out by BS EN 12904-2005 Products used for treatment of water intended for human consumption – typically Silica Sand and Silica Gravel.

Table 31 - Particle size gradation for supporting media from Kawamura (2000)

Layer Number	Passing Screen Size	Retaining Screen Size	Depth of Layer	Note
1	40 mm	20 mm	100 to 150 mm	Bottom Layer
2	20 mm	12 mm	75 mm	
3	12 mm	6 mm	75 mm	
4	6 mm	3 mm	75 mm	
5	3 mm	1.7 mm	75 mm	Top Layer

Glasgow (1998) noted that intermixing between the upper layers of the supporting gravel and the filter media occurred, to counter this problem a wire mesh was used to reduce this intermixing. This was adopted in the study reported here and worked well under most conditions, but under higher backwashing rates the smaller graded gravel particles began to lift. This in turn lifted the wire mesh and often unstable forces would cause the mesh to rotate within the column requiring dismantling of the filter column to rectify the problem and reposition the mesh.

To counter this problem a new design of support media was required to enable higher rates of backwash, and a series of experiments were carried out to perfect the design of supporting gravels. The solution was to restrain the graded gravel in a fabric mesh as shown in Figure 61. A smaller amount of finer graded gravel (1.7 – 3 mm) was then tightly held in a fabric mesh bag. The bag containing the finer material was installed to roughly 75 mm thickness recommended by Kawamura (2000) as in Table 31.



Figure 61 - Supporting media in laboratory filter columns

The gravel below the upper bag which again was enclosed in mesh was given a larger grading than specified by Kawamura (2000), the chosen grading was 6 – 12 mm and a depth of 100 mm. The fabric mesh would stop intermixing and so grading changes were not required as frequently and this size allows for a lower resistance to backwash. The design worked well with the weight of the larger gravel counteracting the effect of the backwash flow hitting the finer 1.7 – 3 mm particles (by wrapping the finer bag inside the other bag) and ensuring there was no lifting occurring. Below these two layers encompassed by fabric meshes was a layer of 12 – 20 mm gravel at a depth of 100 mm that was not held in a fabric mesh and was therefore loose. Mesh around this media was not required as the gravel was restrained by its increased mass and the enclosed supporting media above.

In summary the supporting media consisted of three layers, a lower layer of 100 mm deep 20 mm gravel, a middle layer also 100 mm deep of 6 – 12 mm in a mesh bag and an upper layer 75 mm deep of 1.7 – 3.0 mm also in a mesh bag. This was equivalent to a support of 275 mm. This variation did however still meet the two criteria of ensuring no loss of media and to distribute the backwash flow evenly across the bed.

6.2.2 FILTER MEDIA

To reduce the number of experimental variables it was decided to use mono-media filtration as dual media introduces ambiguity in the results by getting the different types of media to work together and differentiating the effect of each media. In addition it is believed that by comparing sand with the new media that if improved performance was noted, then the inclusion of anthracite to create a dual-media filter was likely to further benefit performance (Hendricks, 2005). Table 32 shows the equations for calculating the bed depth for a mono and dual-media in a range of flows from Kawamura (2000) which is also the method cited by Hendricks (2005). Kawamura (2000) notes that if a turbidity of the filtered water is to be less than 0.1 NTU without the use of polymer as addition to the filtration, it is recommended that the l/d_e (d_e = effective size, 10% passing) ratio be increased by 15 % altering the equation in Table 32 to $l/d_e \geq 1150$.

Table 32 - Filter media bed depth specifications from Kawamura (2000)

Bed Depth	Application
$l/d_e \geq 1000$	For ordinary mono-sand and dual-media beds
$l/d_e \geq 1250$	For regular tri-media (anthracite, sand and garnet) beds
$l/d_e \geq 1250$ to 1500	For most coarse deep mono-media beds (d_e is 1.2 to 1.4 mm)
$l/d_e \geq 1500$ to 2000	For very coarse deep mono-media beds (d_e is 1.5 to 2.0 mm)

The equation for mono-media in Table 32 was used to determine the bed depth for these experimental trials and this is calculated based on the effective size (d_e) of the sand which has been determined to be 0.59 mm and gives a value of 590 mm as a minimum bed depth to be used in these experiments shown in Equation 7 below:

$$\frac{l}{0.59} \geq 1000$$

$$l \geq 1000 \times 0.59 = 590 \text{ mm}$$

Equation 7 - Calculation of bed depth from Kawamura (2000)

For simplicity the bed depth was chosen as 600 mm. This was not based on increasing the l/d_e ratio to account for the fact no polymer aid as suggested by Kawamura (2000). This depth was based on the effective size of sand ($d_e = 0.59$) and some novel filter media did have higher values of d_e as shown in the particle distribution testing (see section 5.3). Section 5.3 shows the particle size distribution data for the filter media that was used in this study, Table 21 also shows the values found for all media. Where possible the media size was chosen to be as close to that of the sand as possible (0.5 – 1.0 mm) as this is the most common media size used in rapid gravity filtration (Ives (1990), Kawamura (2000)). Some suppliers however were unable to exactly meet this requirement and this is the reason for some variation from these criteria. These variations will be taken into consideration in the final analysis and their influence discussed. Filtralite showed the highest value of $d_e = 0.77$, however the average value for all media was $d_e = 0.63$ and bed depth was fixed to 600 mm in every filter column. This is within the range commonly used by the industry as specified by conversation with operators and in Hendricks (2005).

6.3 APPARATUS

The apparatus used is shown in Figure 62 below. The raw water storage tank is located in the lower left corner with the delivery pump located next to it at the base. Directly above the storage tank and obscured in this photograph is the constant head tank above the columns that ensured a constant pressure above the filter media, this drained directly into the six filter columns.

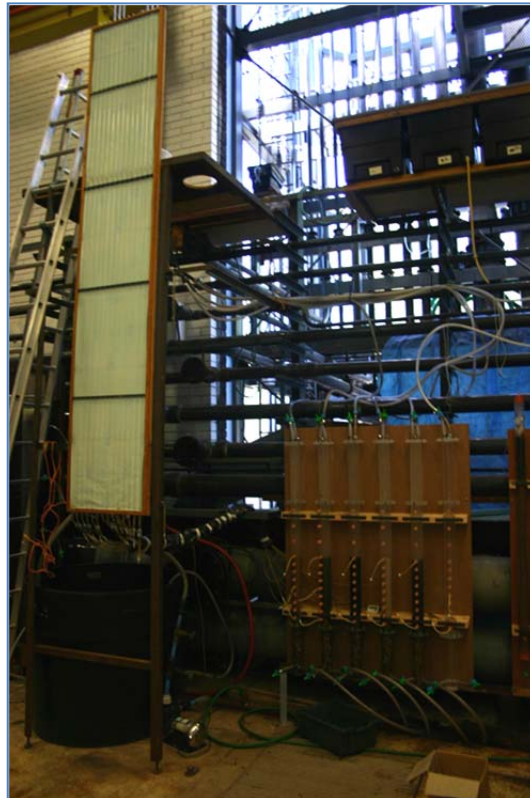


Figure 62 - Photograph of filter columns and associated pipework

Six filter columns were used so that simultaneous testing of the different media could take place. The columns were a standard design first reported by Glasgow (1998), construction was simple so that more columns could be made available if necessary to avoid stripping down columns between tests for further media

The filters were operated in a constant head / constant flow configuration and this called for the constant head tank to be used throughout the experimental period. This method was chosen as all external hydraulic factors between the filter media would be identical and variations would only occur as a result of changes within the filter bed itself. The constant

head tank was used for backwashing as it provided sufficient head to give sufficient bed expansion in each column after testing was completed. This also ensured that the delivery system was always cleaned thoroughly between test runs.

6.3.1 RAW WATER STORAGE AND DELIVERY

The raw water storage tank provided two functions, both to hold enough raw water for the maximum operating time of the filters (12 hours), and ensure the turbidity was evenly distributed throughout the tank. Multiple tanks were considered but even mixing would have been difficult to maintain and so a single tank (Figure 63) was chosen and the size required giving a 12 hour runtime at the maximum flowrate of 13.5 m³/h was 590 litres for a single column.



Figure 63 - Raw water storage tank showing delivery pump and mixing system

The mixing was carried out by diverting some of the flow from the delivery pump back into the tank via a hose which had the end bunged off and numerous holes drilled into its length. This provides a constant high velocity flow to mix the tank at varying levels. It was decided to use this over the original mechanical paddle system used by Glasgow (1998) due to the fact that the mechanical stirrers had dead-spots within tanks where settled particles were able to

build-up and alter the water quality throughout the test. Using pump mixing also avoided the additional mechanical device.

The flow not re-directed back into the tank was pumped into the constant head tank, this tank was placed 3 metres above the base of the filter media. This was based on typical design values from Kawamura (2000) who in line with industry practice (Severn Trent Water) gives the maximum allowable headloss from 2.5 to 3.0 m before backwashing is needed. The design of the constant head tank is shown in Figure 64 (a). The tank has a central weir that maintains the constant water level in the tank and drains the excess back into the low level storage tank below. The pipework connecting the weir to the storage tank and also to the columns themselves can be seen in Figure 64 (b).

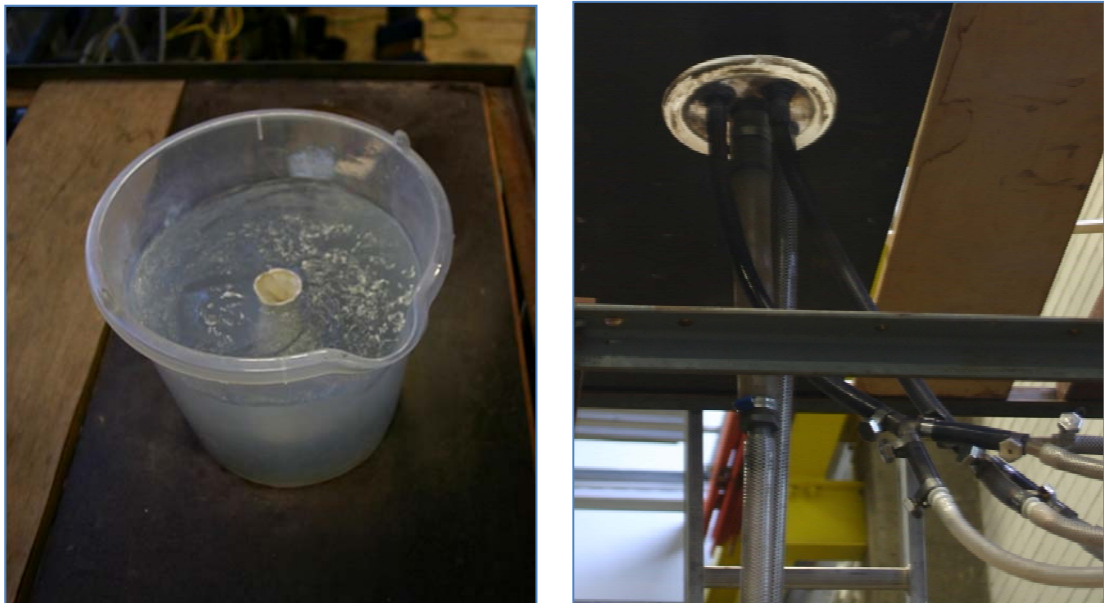


Figure 64 - Constant head tank internal (a) and connecting pipework (b)

All pipework connected to the filter columns from the constant head tank was covered in black plastic to reduce growth that can occur on the inner surface of pipes when the water was not flowing through the system. As the system was not run continuously biological growth was observed and can be seen at the base of the constant head tank in Figure 64 (b). This was rectified by carrying out testing in blocks to reduce standing time and draining the system when not in use. Regular cleaning was still carried out when required to ensure constant operating conditions.

6.3.2 FILTER COLUMNS

The filter columns (Figure 65) were manufactured from 60 mm internal diameter clear acrylic tubing, which allowed for visual monitoring of the media during various phases of filtration. Design of the columns was based on the work by Glasgow (1998) with modifications made to the support gravel and allow for variation in the requirements of the study which did not require sample of filtrate to be taken at a range of depths in the columns.

The filter columns were made up from four separate sections, a top-cap (Figure 67), top-section (Figure 66), middle-section (Figure 68) and bottom-section (Figure 69). Each section was representative of a different zone of the filter. The bottom-section containing the supporting media, the middle-section the filter media and the pressure ports for determining head loss. The top-section was to allow for increases in head and bed expansion during backwashing and the top-cap has the ports that connect to the inlet pipework.

Dimensions of the filter columns were originally based on information from Hendricks (2005) where it is stated that the diameter of a filter column must be no less than 50 times the grain diameter to ensure sidewall effects are not a consideration during operation. Using a 60 mm internal diameter column gives an allowable particle size of 1.20 mm which is above that of most media which are based on sand in the range of 0.5 – 1.0 mm. Filtralite was the largest grain used in this study and with an average particle size (d_{50}) of 1.20 mm which means an internal diameter of 60 mm is still suitable for this study.

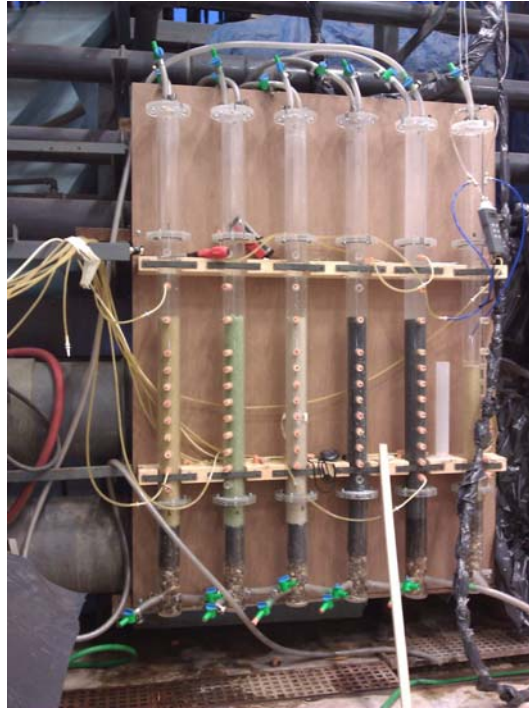


Figure 65 - Filter columns in place with media installed

The length of the columns is a summation of bed depth, support materials and void space used during backwashing. Calculation of the bed depth is given in section 6.2.2 and the supporting media in section 6.2.1. A void is also required above these to allow for sufficient bed expansion to take place during backwashing. It was decided to overdesign this area of the laboratory columns as the different media would mean varying bed expansion, Kawamura (2000) reported a value of 50% expansion that was needed to clean rapid gravity filters that do not employ a method of surface wash.

For the columns, a value of 80% was assumed to be sufficient to allow for backwashing to occur under likely worst case conditions and difficult media while still having a void space above the expansion zone (the void that the media expands into when under backwash conditions). This was to avoid media loss into the pipework and from the top of the filter columns. This extra space also allows consideration of the need to carry out an attrition tests by extended backwashing at a higher than normal bed expansion.

Therefore the final column length was 1490 mm, based on a supporting bed of 410 mm (See section 6.2.1), filter bed depth of 600 mm (See section 6.2.2) and an expansion zone of 470 mm.

Each section was joined to the next using a flange and rubber washer to ensure a watertight seal. The top section was 370 mm in length with the lower section being 320 mm. The middle section was the largest at 800 mm this was to ensure that there were no joints located within the filter bed and within the area that pressure ports were located (Figure 68). Drawings for each of the sections are given below:

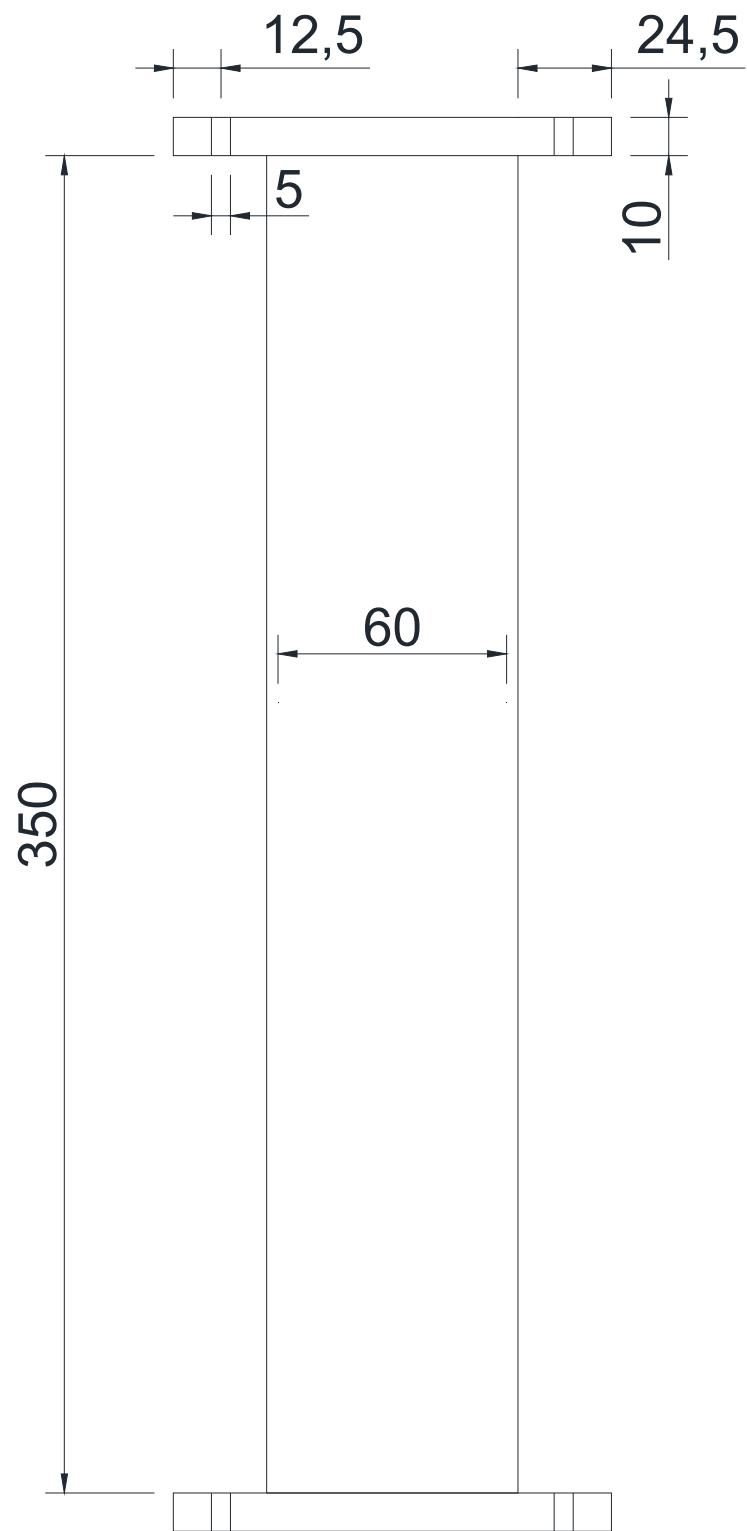


Figure 66 - Filter column top-section design drawing

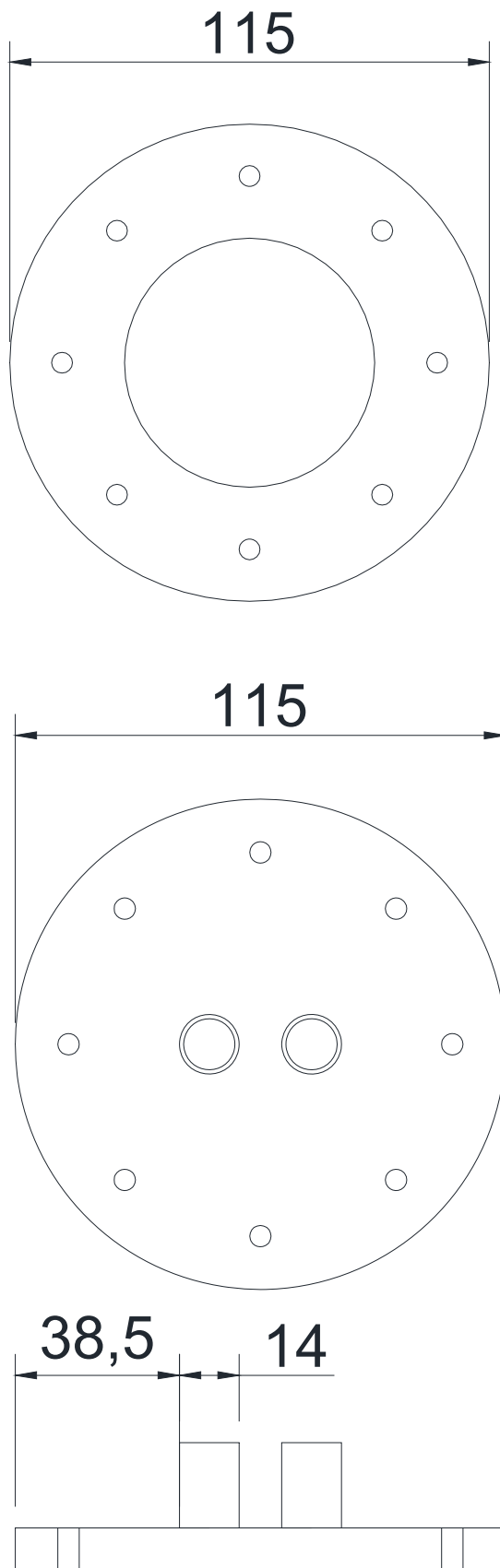


Figure 67 - Filter column section joint flange layout (a) and top cap design (b) diagrams

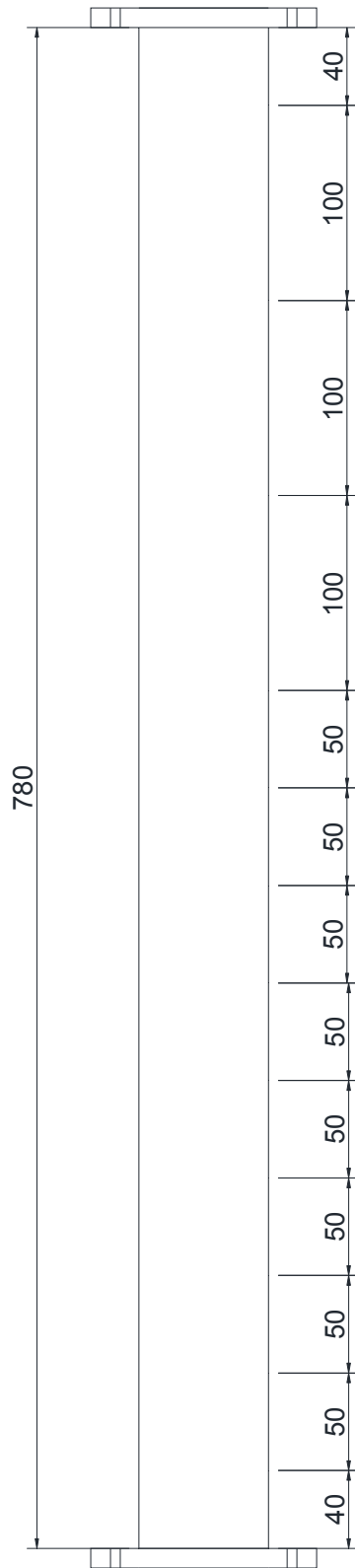


Figure 68 - Filter column middle section showing the location of pressure ports along its length

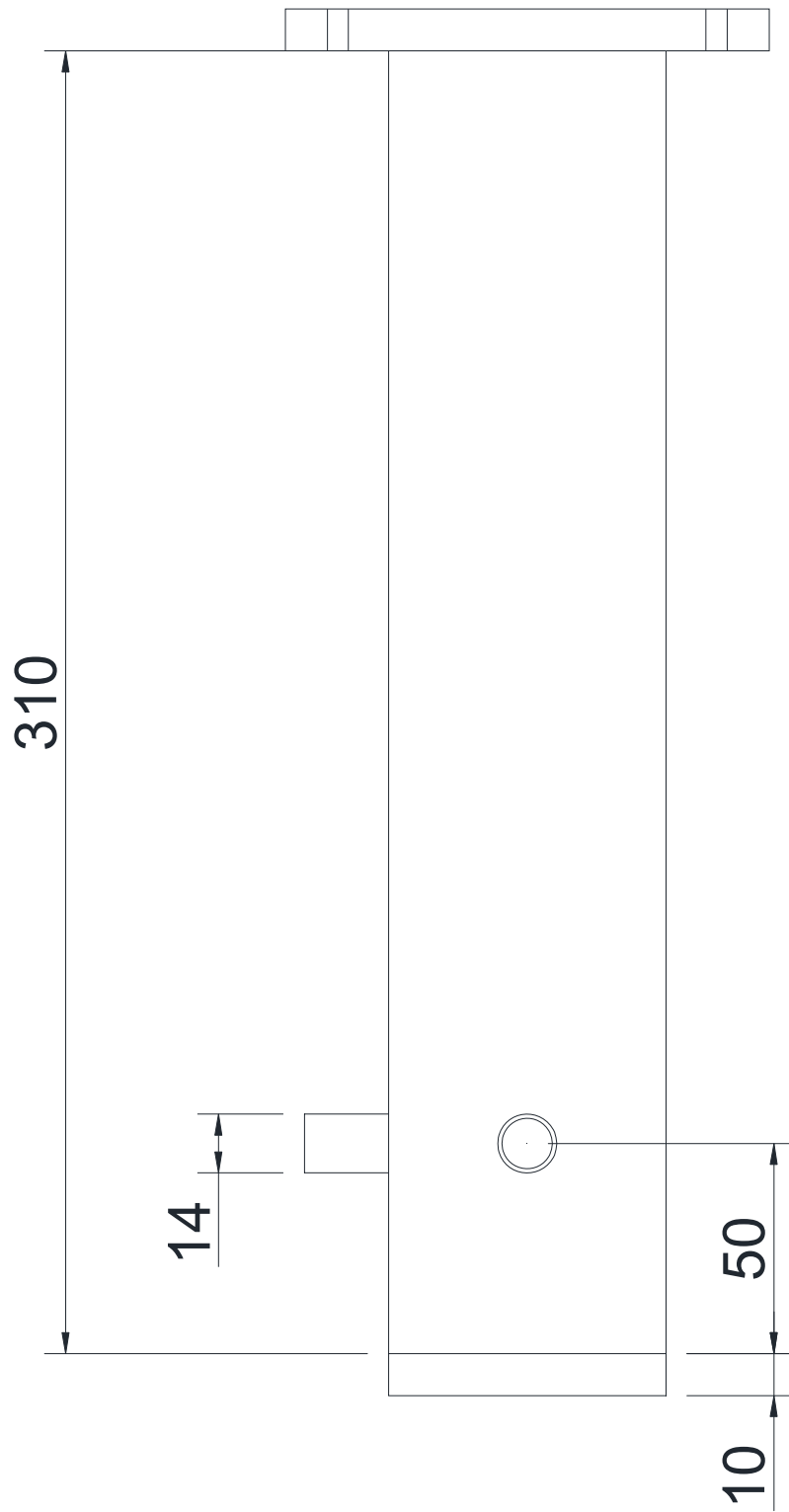


Figure 69 - Filter column bottom-section

With the filters operating with a constant head - constant flow system the flow was controlled by valves on the exit of the filters, these can be seen in Figure 65 (as the small green valves at the base of the filter columns). These were placed in-line within the pipework exiting the filters to waste (drain located directly below filter columns). The flow rate was set to the required value at the beginning of the filter run using a simple stop-watch and measuring cylinder, which was repeated three times to ensure the flow remained correct. The flow rate was also checked every 2 hours during the filter runs, but no variation in flow was noted during any experiment. This was due to the 12 hour run-time of the filters not allowing for a large enough solids load to accumulate in the filters to take the head-loss to near the maximum 3 metres allowed in the design. It was expected that the flow rate would vary as the filter head-loss increased near to the 3 metre maximum value but this was not approached in any of the experiments.

6.3.3 PRESSURE PORTS

Designs by Glasgow (1998) were used and adapted for this work; the key consideration was to ensure that wall effects had no impact on the pressure readings being taken. The brass tube ports were made to protrude into the filter bed from the wall to avoid this effect. Glasgow (1998) also determined whether scouring would occur around the end of the brass tube due to flow entering the piezometer's and concluded that the velocity was sufficiently low. With flow into the brass tubes being near zero and it was therefore concluded that scour would not occur. In the experiments reported here a differential pressure meter (Figure 70) was used instead of piezometers.



Figure 70 - Pressure transducer and air removal loop

The positioning of the pressure ports are shown in Figure 68 and the design of the brass tubing and bung is shown in Figure 71. The design uses the friction caused by forcing a bung into a Perspex tube that is located on the filter wall (see in Figure 72), the brass tube is then inserted through a hole in the side of the filter column and protrudes 15 mm into the filter bed. The wall effects are expected to occur only within 4 – 5 grain diameters away from the filter wall according to Leclerc (1975), which in the case of Filtralite is around 8 mm, which is the distance to the edge of the first slot on the brass tubing (Figure 71) and as this is the worst case expected thus 15 mm was suitable based on this evidence.

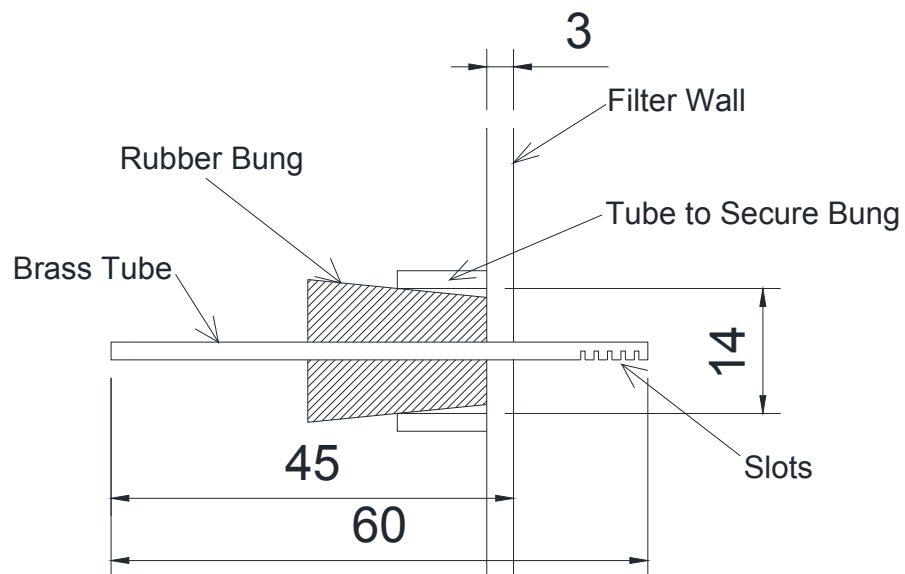


Figure 71 - Diagram of pressure port design

The slots were cut to be 0.5 mm in size and spaced at around 1 mm intervals along the tube. This slot size was below the minimum size of the media being tested to ensure no media can enter the brass tube and clog the system. The numerous slots were provided to ensure that the water was always able to enter the brass tube so that the pressure could be recorded. The slots were also orientated downward so that no settlement could occur in the tube from the turbidity in the water

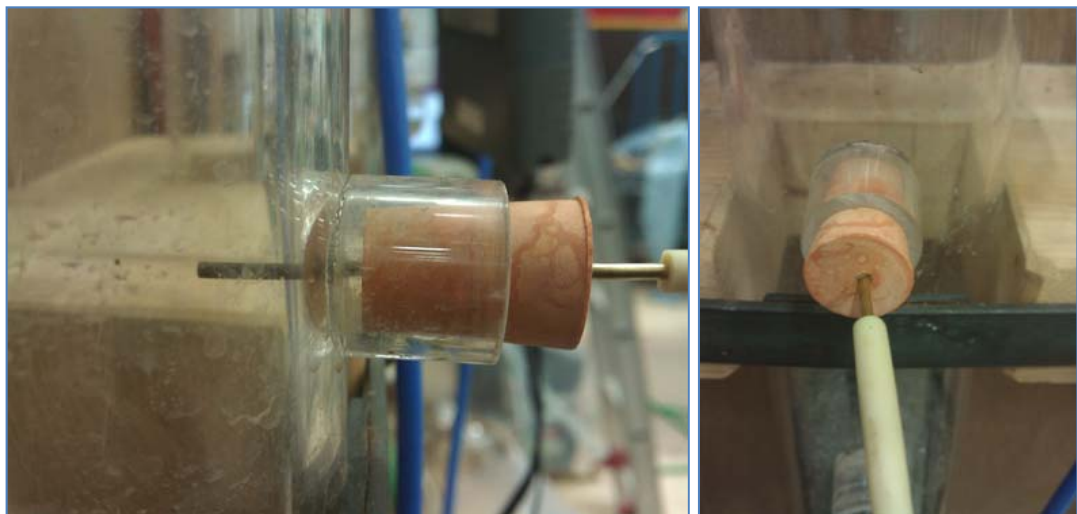


Figure 72 - Images of pressure port on filter column

Flexible tubing of 1.5 mm internal diameter was used to connect the end of the brass tube securely and then this was connected in turn to 4 mm internal diameter tubing to the

differential pressure meter. Air bubbles were an issue with this system and so the valve arrangement shown in Figure 70 was installed onto the differential pressure meter to allow flow between the higher and lower pressure ports and this flushed out any trapped air in the system; once air was removed the valve was closed to allow for normal operation.

6.4 FILTER RUN RESULTS

First step to conducting a test was to prepare the raw water in the low level storage tank, this was filled by hose to a known level using tap water. The temperature of the water was recorded but did not vary more than $\pm 1^{\circ}\text{C}$ but the water did warm in the laboratory environment and from pumping. The rate of temperature increase was very similar between test runs as long as the test was started as soon as possible after the tank was filled. After filling the pumping was started to fill and overflow the constant head tank, but the inlet valves to the filter columns remained closed so that the required concentration of kaolin could achieve steady state and complete mixing. The kaolin solution was added directly into the weir in the constant head tank. To confirm mixing and thorough even distribution in the constant head tank between 3 and 5 turbidity samples were taken to ensure confidence that the correct turbidity had been reached and that it was equally dispersed in the tank.

It is important to point out that after backwashing of the media the water level was not allowed to drop below the top of the filter media; this was to ensure that when the normal flow of water to the filter column was restarted there was no air trapped in the bed. Once the raw water suspension was confirmed to be well mixed, the inlet valves to the columns were opened and water flowed into the filters. Also the second backwash outlet drainage valve was opened and allowed the air trapped in the column to be removed and then this valve was closed. Once each column had the air purged and all inlet valves were fully opened the outlet valves were opened to allow the correct flowrate through the filter column, these were determined by timing a volume of water into a measuring cylinder. This was repeated three times with adjustments to ensure the flowrate was correct.

Once steady operation had been achieved then sampling and monitoring as noted in Table 33 was carried out. The sampling schedule was decided upon after analyzing results from several commissioning runs and performance of the filter columns.

Table 33 - Sampling frequency used during laboratory scale testing

Parameter	Sample Location	Frequency (minutes)
Temperature (°C)	Air	60
	Raw Water	60
	Filtered Water	60
Head Loss (m)	Across Filter	15
	Bed	
pH	Raw Water	60
	Filtered Water	60
Conductivity (µS)	Raw Water	60
	Filtered Water	60
Turbidity (NTU)	Raw Water	60
	Filtered Water	15

There were 30 tests runs in total at the three different flow rates (8.6 m/h, 11.1 m/h and 13.6 m/h) described in section 0, and two separate turbidities (9 and 35 NTU) as described in section 6.3.1. The tests carried out are shown and labeled in Table 34, the lettering of A – E corresponds to the filter media being tested with A – Sand, B – Glass, C – Limestone, D – Filtralite and E – Slate. The first test number in the table corresponds to either of the two turbidities and the second number the flowrates for each test.

Table 34 - Parameters altered for each test carried out in laboratory filter columns

Turbidity	Flowrate	Media	Test No.
9 NTU	8.6 m/h	A.1.1 –	A.1.1
		E.1.1	
	11.1 m/h	A.1.2 –	A.1.2
		E.1.2	
	13.5 m/h	A.1.3 –	A.1.3
		E.1.3	
35 NTU	8.6 m/h	A.2.1 –	A.2.1
		E.2.1	
	11.1 m/h	A.2.2 –	A.2.2
		E.2.2	
	13.5 m/h	A.2.3 –	A.2.3
		E.2.3	

A summary of the results from each of the tests carried out are given in Table 35 and Table 36, additional charts and further data collected from the experiments is presented in Appendix III. The tables present the turbidity as a full 12 hour average that includes ripening time, while the final 6 hour turbidity results present the average for only the last 6 hours of

the test to ensure ripening did not influence the results. Headloss is given as the initial and accumulate value, the combination of both which gives the final headloss recorded in each media for 12 hours.

Table 35 - Summary of results for lab testing of the 9 NTU suspensions, showing average turbidity vales

Flow (m/h)	Media	Turbidity					Headloss	
		Raw (NTU)	Full 12 (NTU)	Final 6 (NTU)	Full 12 (C/Co)	final 6 (C/Co)	Initial (mm)	Accu. (mm)
13.5	Sand	9.41	3.29	2.29	0.35	0.24	956	4
	Glass	9.81	3.97	3.05	0.40	0.31	480	5
	Limestone	9.82	2.60	2.03	0.26	0.21	548	11
	Filtralite	9.49	3.64	3.49	0.38	0.37	234	3
	Slate	9.13	2.31	2.13	0.25	0.23	421	7
11.1	Sand	9.38	2.11	1.56	0.22	0.17	749	5
	Glass	9.51	3.23	2.75	0.34	0.25	415	4
	Limestone	9.80	2.36	1.72	0.24	0.18	511	8
	Filtralite	9.42	3.16	3.06	0.34	0.32	193	4
	Slate	9.48	1.95	1.69	0.21	0.18	317	4
8.6	Sand	9.27	1.68	1.07	0.18	0.12	726	2
	Glass	9.13	2.38	1.65	0.26	0.18	358	3
	Limestone	9.22	1.37	0.99	0.15	0.11	360	1
	Filtralite	9.18	2.87	2.73	0.31	0.30	160	1
	Slate	9.63	1.33	1.05	0.14	0.11	258	5

Table 36 - Summary of results for lab testing of the 35 NTU suspensions, showing average turbidity vales

Flow (m/h)	Media	Turbidity					Headloss	
		Raw (NTU)	Full 12 (NTU)	Final 6 (NTU)	Full 12 (C/Co)	final 6 (C/Co)	Initial (mm)	Accu. (mm)
13.5	Sand	34.89	8.76	6.56	0.25	0.19	952	31
	Glass	34.86	10.56	8.74	0.30	0.25	467	24
	Limestone	34.91	9.26	7.48	0.27	0.21	205	70
	Filtralite	34.92	14.06	14.21	0.40	0.41	250	12
	Slate	34.77	9.14	7.64	0.26	0.22	400	27
11.1	Sand	34.82	6.57	4.08	0.19	0.12	938	32
	Glass	34.81	6.93	5.12	0.20	0.15	351	23
	Limestone	34.72	6.37	3.84	0.18	0.11	490	25
	Filtralite	34.62	9.16	9.36	0.26	0.27	169	11
	Slate	34.72	5.30	3.33	0.15	0.10	353	17
8.6	Sand	34.88	4.03	2.95	0.12	0.08	684	27
	Glass	34.58	4.90	3.65	0.14	0.11	360	16
	Limestone	34.43	6.26	3.22	0.18	0.09	367	18
	Filtralite	34.75	8.57	8.42	0.25	0.24	147	7
	Slate	35.04	2.60	2.23	0.07	0.06	276	13

6.4.1 STEADY STATE TURBIDITY

When discussing turbidity removal this is only considering the final 6 hours of the 12 hour filter run time, this was to ensure that the ripening period did not play a part as it will and this is discussed separately. Therefore the following charts (Figure 73 & Figure 74) show how the turbidity removal was affected by the type of media, varied flow rate and the two feed turbidity values of 9 and 35 tested:

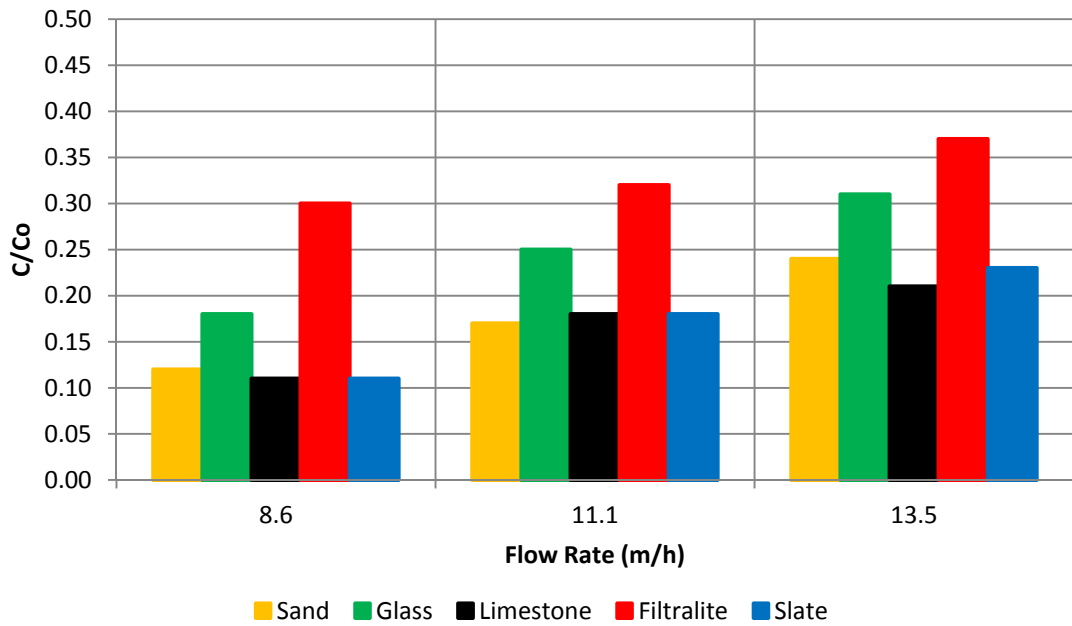


Figure 73 - Variation in turbidity removal with flow rate for all media at 9 NTU

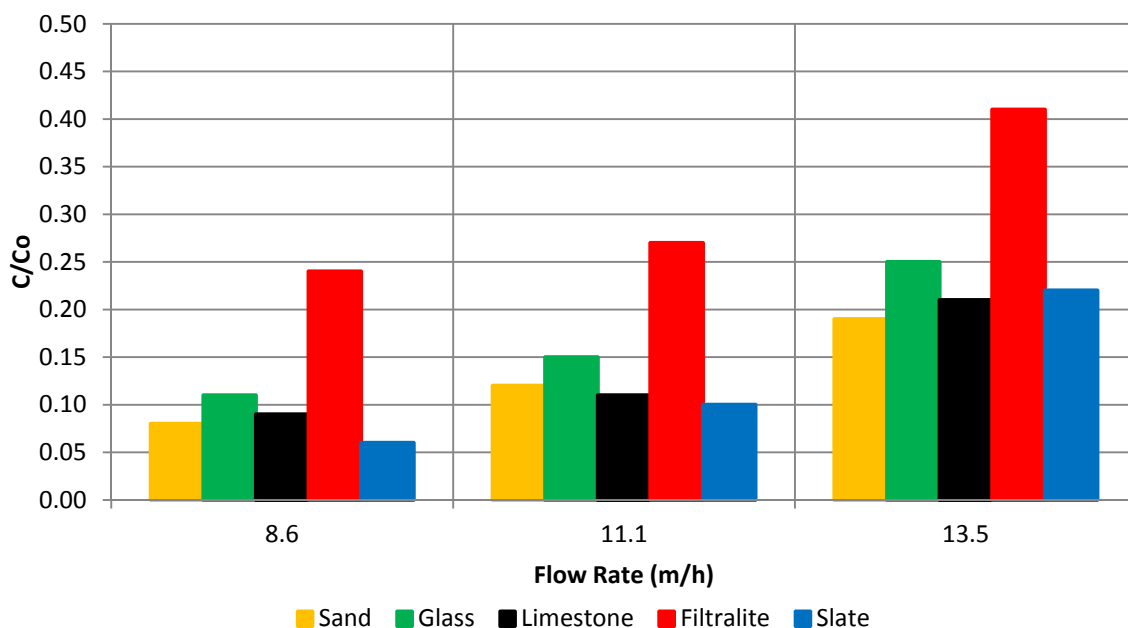


Figure 74 - Variation in turbidity removal with flow rate for all media at 35 NTU

The charts show that as would be expected more solids are retained at lower flowrates, the performance degrades as the flowrate increases. The amount that the performance reduces as the flowrate increases is equal between all filter media aside from Filtralite shown in Figure 73 for the turbidity of 9 NTU. There is the same pattern with the higher turbidity of 35 NTU shown in Figure 74, but at the highest flowrate of 13.5 m/h, all media show an increased rate of performance degradation (although sand is the least affected). This could be due to a limit of attachment performance in the filter media whereby the increased solids load maximises the amount of solids that can be attached to the media and particles that cannot attach move back into suspension and breakthrough the filter leading to the reduced performance. This suggests, in line with theory, that a saturation value exists which was not approached at the lower solids load.

Irrespective of media and initial turbidity the rate of deterioration shown in Table 37 is similar for all the media except the Filtralite. The overall performance of the Filtralite is also lower and both these effects are it is suggested due to the larger media particle size. The performance of Filtralite is poor across all test results due to its increased particle size, and even at the lowest flowrate only removing 70 % of the turbidity compared to the sand that is removing 88 %. The increased particle size means that a greater proportion of suspended particles will make their way through the larger pore sizes as they are too far from the media

surface for any mechanisms of transportation to take effect. Since these mechanisms are the most important and are already less effective, then flow rate will have less of an impact.

Table 37 - Turbidity removal performance change with flowrate from Figure 73

Media	Sand	Glass	Limestone	Filtralite	Slate
Rate of Performance Degradation (C/Co / m/h)	0.022	0.029	0.024	0.034	0.032

If Filtralite due to its greater particle size is omitted from the results the average change in turbidity performance as flowrate is increased is 0.06. Analysis of the changes at the higher turbidity of 35 NTU show that the rate of change in turbidity performance with flowrate is lower than that for the results at 9 NTU, and overall retention also better again suggesting void space is an important factor. These results are accelerated using higher turbidities and cannot be relied on to translate to longer run times and lower NTU.

When analysing the individual performance of the different filter media then variations are visible. Filtralite is consistently the poorest performing media with glass falling just below the other three filter media all of which follow the same performance pattern with regards to turbidity removal. The results for the mean value of turbidity removal over the final 6 hours of each 12 hours test are given in Table 38 below:

Table 38 - Turbidity removal performance in laboratory scale testing

Turbidity NTU	Flowrate m/h	Sand C/Co	Glass C/Co	Limestone C/Co	Filtralite C/Co	Slate C/Co
35	8.60	0.08	0.11	0.09	0.24	0.06
	11.10	0.12	0.15	0.11	0.27	0.10
	13.50	0.19	0.25	0.21	0.41	0.22
9	8.60	0.12	0.18	0.11	0.30	0.11
	11.10	0.17	0.25	0.18	0.32	0.18
	13.50	0.24	0.31	0.21	0.37	0.23

When the analysis takes into account shape then this would be expected to affect bed porosity. Sand is the most rounded media with a sphericity value of 0.89, compared to the limestone's 0.69 and the least spherical material Slate with a value of 0.49. The size of these three media is opposite, slate has the largest d_{60} at 1.0 mm (UC – 1.72), limestone with 0.95 mm (UC – 1.46) and sand the smallest particle size with 0.95 mm (UC – 1.27). Thus slate has

the largest particle size; sand has the smallest in size, the smallest variations in size and is very specific in its grading. Limestone falls between the two media in both size and uniformity coefficient. Therefore based on size and uniformity alone then sand would be expected to perform the best of the three media with limestone second followed by slate, but in fact the performance is similar between all media with slate virtually identical to sand.

By including the results for sphericity (sand is the most spherical (0.89) and slate (0.49) the most angular) then this could indicate why the particle size has not had the expected effect reported in literature. It is suggested as a particle become more angular the removal performance of the media will increase due to increased variability in the path suspended particles must take when flowing through the filter bed. Ives (1975) has discussed this previously, noting that a more angular media has a higher specific surface area for deposits to collect, but also that the angularity of particles creates a more torturous flow path through the media. Ives (1975) stated that the lowest angularity should be 0.6 as below this a more angular media offers low permeability in the direction of flow. The results with regards to Slate do not support this idea.

It is suggested that the torturous flow path leads to increased incidence of the transportation mechanisms based on inertia. This means suspended particles in the streamlines flowing around the media will be susceptible to greater angular changes in direction within a lower Sphericity filter media compared to a spherical filter media as is shown in Figure 75.

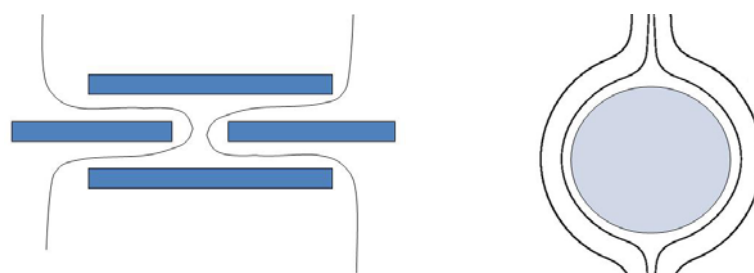


Figure 75 - Difference in interaction of flow streams between angular and spherical filter media

The angular change in the example on the left Figure 75(a) assuming an idealised packing arrangement for plates shows that the angular flow leads to paths that reduce the amount of inertial energy required for a particle to break free and move to the media surface for

attachment to occur, while the gradual changes of direction in a rounded media such as sand lead to higher inertial forces required to break free. The transportation mechanism is improved but attachment is still only as effective as before. The improvements in performance are only due to the increased proportion of suspended particles moving closer to the media surface increasing the probability of attachment occurring. It is recommended that this effect could be explored further with highly controlled studies with media designed with more subtle changes in sphericity to help understand numerically how influential the angularity is on turbidity removal.

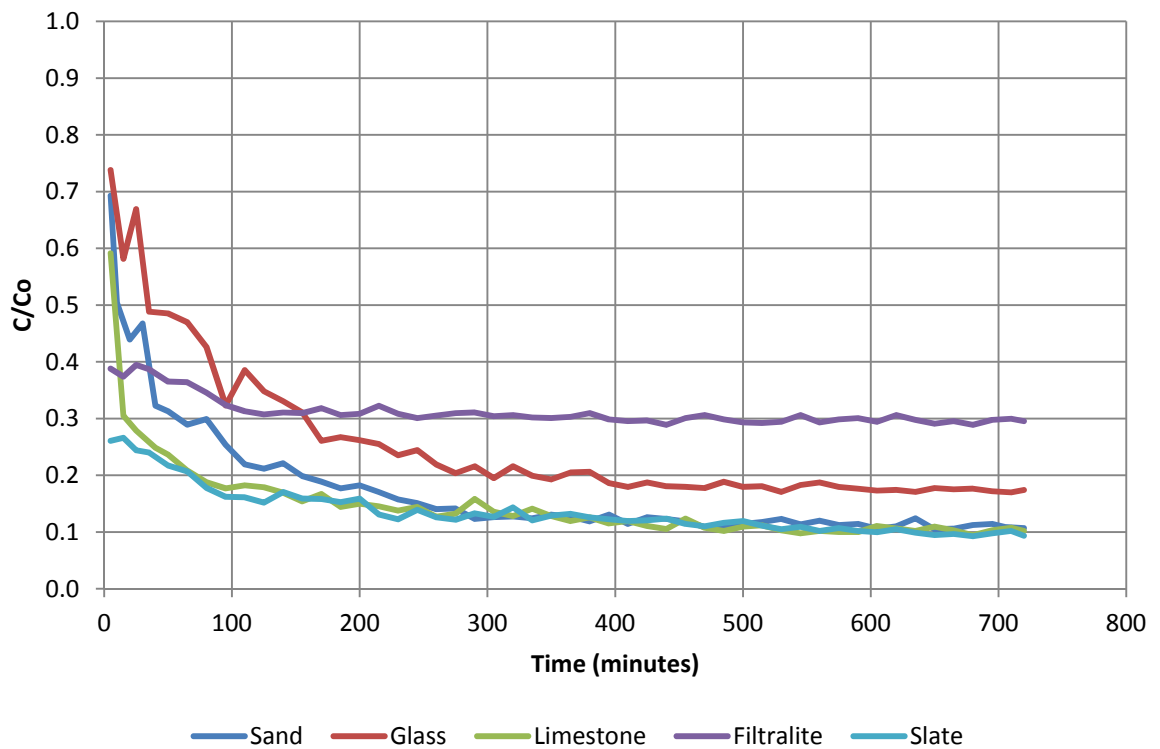


Figure 76 - Summary results for turbidity removal from an initial concentration of 9 NTU at a flow rate of 8.6 m/h

The ripening phase of the media follows a typical trend to that shown in Figure 76, where the Filtralite and slate do not have a high initial turbidity spike or the ripening is faster than the time it takes to take the first sample from the outlet water. Filtralite again however is impacted by its greater particle size and it is therefore difficult to offer suggestions in comparison with the other media. Slate however is closely followed by limestone and then sand with regards to C/Co performance. This follows the Sphericity values of the media with Slate (0.49) being the most angular followed by Limestone (0.69) then Sand (0.89). The

ripening stage is caused as suspended particles attach to the media surface they help improve the filter performance by reducing the repulsive effect of the electrostatic potential from the inorganic ions of the filter media and to a lesser extent the attached particles will also reduce the pore size in the media. These effects require the attachment of particles and this as described previous is improved by the torturous path caused by the angularity of the filter media. Therefore it was concluded that the more angular the filter media then also the faster the ripening time will be as it allows for better transportation to overcome the initial high repulsion of the electrostatic force.

Retention time is a parameter that is affected by the bed porosity, which is initiated by both particle size and angularity and therefore is a surrogate method of accounting for these media characteristics. Theoretical retention time for all filter media was calculated based on the bed porosity as in section 5.4. This is because the retention time is related only to the pore space between the media particles. Therefore a more porous material will have a larger retention time and therefore a lower velocity through the bed compared to a lower bed porosity media. The results for the calculated retention time for the experimental flow rates (m/h) used and bed porosities are given below in Table 39.

Table 39 - Retention time related to flow rate and bed porosity of various filter media

Media	Bed Porosity (ϵ)	Flow Rate (m/h)	Retention Time (sec)
Sand	0.362	8.6	91
		11.1	70
		13.6	57
Glass	0.370	8.6	93
		11.1	72
		13.6	59
Limestone	0.434	8.6	109
		11.1	84
		13.6	68
Filtralite	0.480	8.6	121
		11.1	93
		13.6	76
Slate	0.434	8.6	109
		11.1	84
		13.6	68

Bed porosity and flow rate are basic influences on the performance of the filter. Fundamentally the longer a particle is travelling through a filter and the lower the velocity

the more likely it is to be impacted upon by the fundamental mechanisms discussed in section 0.

A higher bed velocity will also lead to a higher instance of re-suspension of the particles after attachment and back into the flow through the bed. This is due to the higher shear forces linked to velocity flows that act upon the particles attached on the boundary of the media grains.

The retention time is calculated using

$$t_r = \frac{\varepsilon \cdot L_f A_f}{v}$$

Equation 8 - Equation for calculating retention time in the filter bed

Where:

t_r – retention time (seconds)

ε – bed porosity

L_f – Filter Bed Depth (m)

A_f – Filter Bed Area(m²)

v – flow velocity (m³/s)

Applying this equation to a range of values the following chart Figure 77 was produced showing the influences of flow rate and porosity have on the retention time of a filter, over a typical filtration range. For example the retention time of a typical RGF at 8 m/h would be 2 minutes. This however is the theoretical value and further work would be required to compare these results with real world tests using a range of media and porosities.

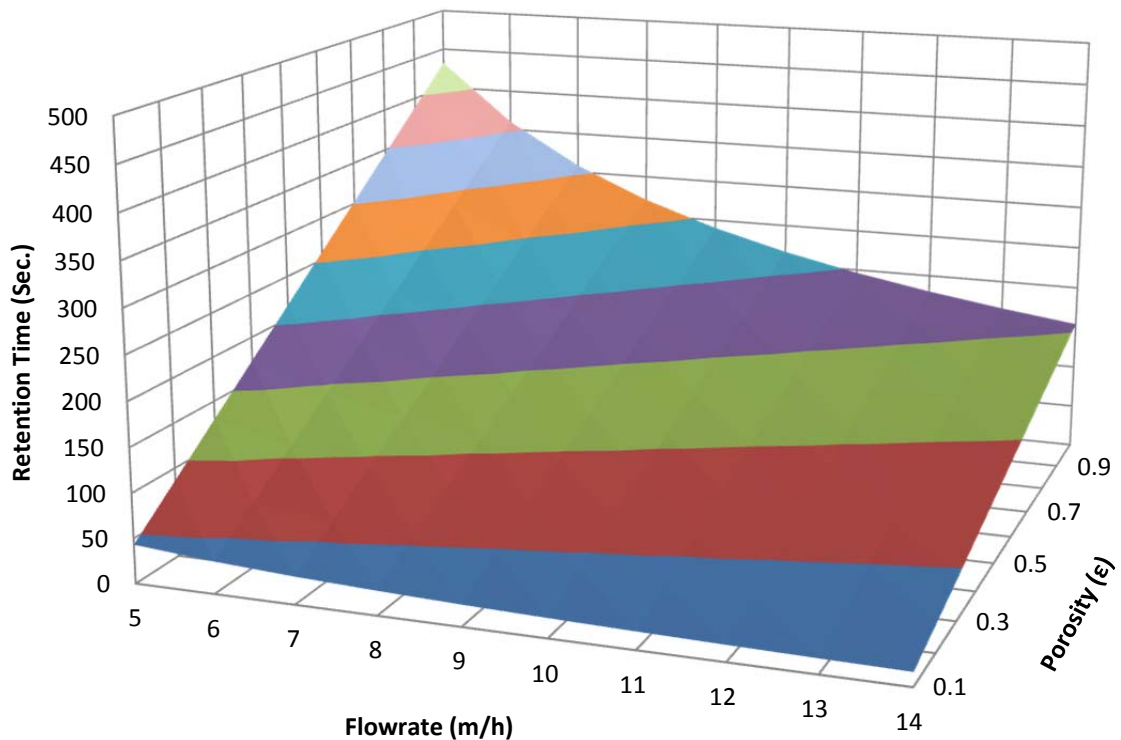


Figure 77 - Chart showing variation of retention time relative to flow rate (m/h) and porosity

Figure 77 visually confirms there is a linear relationship between the porosity that is directly proportional and linearly alters the retention time, while the flow rate has an inverse relationship which is what would be expected. The equation and graph predicts that there will be a point where performance of the filter will reach equilibrium, and beyond this point the degradation in removal performance will not be significant. Performance of the filter at such high flow rates would be unacceptable for typical rapid gravity filtration operations.

As the porosity increases the velocity of flow through the bed reduces to nearer the approach velocity. It is however generally accepted that a reduced value of porosity leads to improved filter performance, and this is generally true as a result of an increase in surface contact. This is despite being counteracted by the increased velocities and reduced retention time through the filter bed, these two factors therefore counteract each other in the filter bed to affect performance.

The theory is based on the reduced porosity leading to a closer packed filter bed leading to the particles in suspension always being closer to a media grain surface compared to a more

open structure associated with a larger porosity value. Lower voidage may cause straining of particles to become dominant in such cases. However the reduced retention time in low voidage filters leads to higher flow velocities in the pores and therefore a higher instance of attached particles being susceptible to shear forces that can cause detachment.

The typical design of filter plant is a bank of filter beds with contingency for backwashing, maintenance and population increases. Therefore they often do not operate at their design flow-rate. In this instance where flowrates are below design values, the retention time will be increased and performance will also generally be improved compared to what might be reported from academic studies.

A comparison of the retention time against filter performance (C/C_0) was carried out between the two tested turbidities and chart (Figure 78) of C/C_0 was produced, Filtralite however was omitted from the results as it was not of comparable size. It was therefore bound by its physical dimensions to give different results and the trials reports here confirm this. It is concluded that media used in this analysis must be of similar particle size to give a reasonable result; the details of this are discussed in later in this section (0).

The retention time was calculated from porosity data for each filter media at the various flow rates and plotted against a single C/C_0 turbidity removal performance which itself was calculated as the average value over the second half of each 12 hour filter run. This ensures that the result is not affected by the variable ripening times observed between filters. For simplicity given the deviation and linearity only the means are shown in the plot. Variation in turbidity results for the final 6 hours of the test was minimal and this is shown in the turbidity results presented in Appendix III.

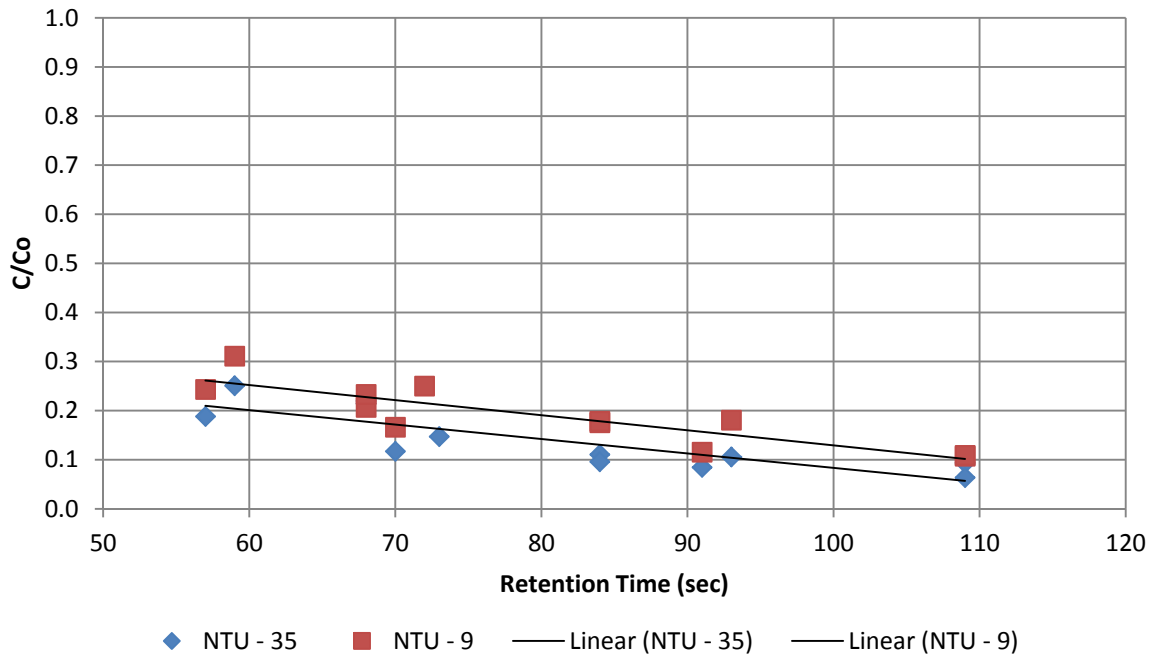


Figure 78 - Chart showing variation in filter performance (C/C_0) against retention time

The slope of the trend lines for both sets of data in Figure 78 above gives the following two equations (Equation 9), which are valid only for the case of this experiment and within the bounds of the retention time experienced within the experimental runs:

$$\frac{C}{C_0} = -0.0031 \cdot t_r + 0.4365$$

$$\frac{C}{C_0} = -0.0029 \cdot t_r + 0.3772$$

Equation 9 - Trend line equations for C/C_0 against retention time from test data

The slope at both turbidities for both trend lines is similar, with an average value of 0.003. By substituting in the equation for retention time (Equation 8) gives Equation 10 below:

$$\frac{C}{C_0} = \frac{-0.0031 \cdot \varepsilon \cdot L_f \cdot A_f}{v} + 0.4365$$

$$\frac{C}{C_0} = \frac{-0.0029 \cdot \varepsilon \cdot L_f \cdot A_f}{v} + 0.3772$$

Equation 10 - Retention time equation (Equation 8) substituted into Equation 9

By changing the subject of the equation to a change in filter performance ($\Delta C/C_o$) instead of determining the performance of a filter at those parameters and by assuming an average slope value of -0.003 Equation 11 is created:

$$\Delta \frac{C}{C_o} = -0.003 \left(\frac{\varepsilon_1 \cdot L_{f1} \cdot A_{f1}}{v_1} - \frac{\varepsilon_2 \cdot L_{f2} \cdot A_{f2}}{v_2} \right)$$

Equation 11 - Equation showing variation in filter performance related to retention time in the filter bed

Equation 11 allows for the determination of the variation in performance from a filter when the dimensions or porosity of the media are altered (the equation however is only valid for a known filter design where a performance at the current bed properties are known).

For example the performance variation of a filter that has lost media through backwashing can be determined by altering the depth of the filter bed, or the effect of porosity of the bed as it alters with time or the degradation or addition of media. The accumulation of particles in the filter affects porosity and therefore if this can be measured the equation can be used to help predict its impact on performance. However the equation does not consider the effect of varying sphericity from different filter media, and for many media this will have a direct impact on the porosity of the filter bed as particles are able to pack more densely as they become more rounded or flat and therefore there is some allowance for this in Equation 11, but it is a non-direct method of accounting for this.

The equation suggests any parameter that increases retention time in the filter bed leads to an increase in performance. The effect of bed depth is relatively straightforward, the increased retention time corresponds to the particles having to pass through a greater amount of filter media improving the likelihood of attachment occurring. Similarly filter area also increases performance as when the filter area is increased but the approach velocity remains the same then the velocity through the filter bed will reduce. This improves attachment due to the increased retention time in the filter and the lower flow velocities will also reduce shear forces that can detach attached particles back into the flow.

The inverse relationship of flow rate is expected as when flow rate is increased the retention time will reduce and so would the filter performance (Hendricks, 2005). This is well known and confirmed by the experiments reported here experimentally. Porosity is directly

proportional to retention time, showing that an increase in porosity leads to an increase in filter performance. This is not reported previously, and the generally held belief that a reduction in porosity would lead to tighter packing and improved performance due to reduced transportation distances to the media surface. On the other hand an increase in porosity would lead to a reduction in flow velocity through the filter bed and then an increase in performance would be expected.

To consider the impact of porosity the results for Filtralite are included in a re-plot of Figure 78 and shown in Figure 79. Filtralite was omitted from the linear analysis in Figure 79 as its particle size was larger than the other media being tested. Slate also had a larger particle size compared to standard 0.5 – 1.0 mm sand but the bed porosity and performance more closely resembled that of the other media and therefore this remained in the initial analysis.

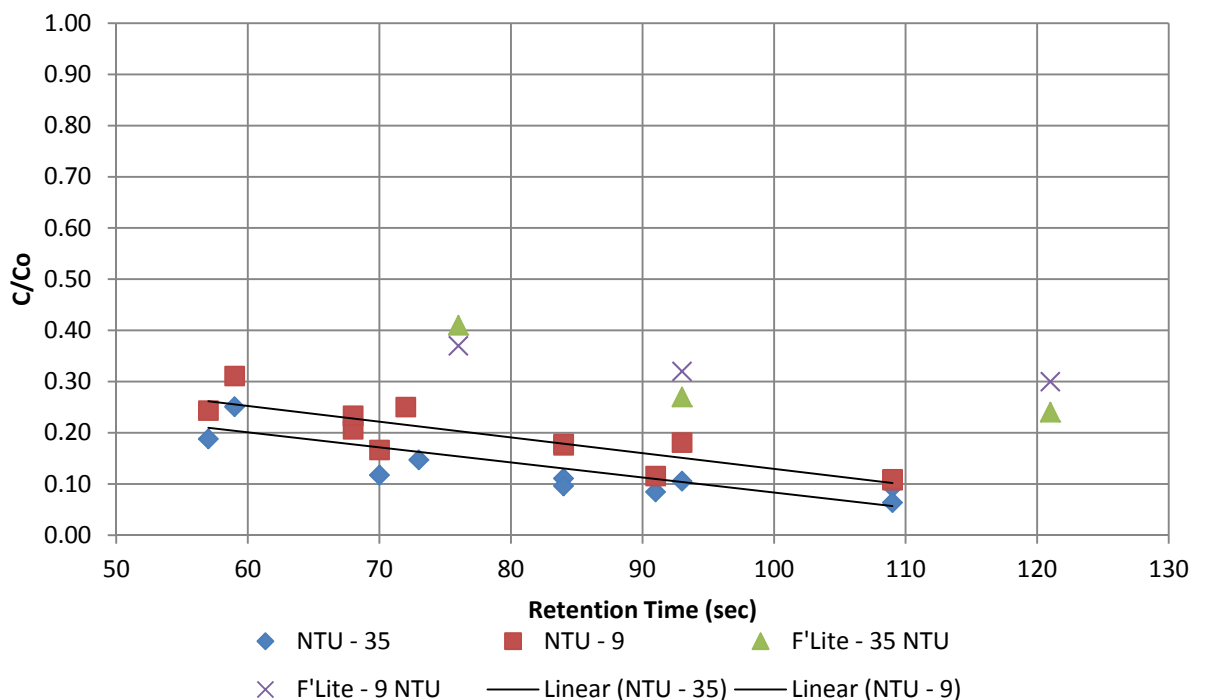


Figure 79 - Retention time and C/Co relationship with Filtralite results included

The slope for both the Filtralite turbidity results is similar to the -0.003 observed in the other media however the results do show a degree of leveling off as the retention time increases. The performance of the Filtralite is also poorer compared to all other filter media. This is due to the increased particle size of the media and generally this would be expected to be the case if increased porosity of the filter bed reduced transport and was more important than

retention time. Porosity alone as noted may not be a good indicator as it is the shape of the voids between particles that is considered as the important factor and for example the near spherical or angular media Filtralite would demonstrate that as particle size increases the distance between particles increases, reducing the effectiveness of transportation mechanisms. In the case of flatter media like slate where the plate like structure still allows the media to pack closely as particle size increases this cannot happen in Filtralite, this is further discussed below.

Figure 80 shows idealized packing of spheres, this shows that as the area between the media grains increases then the distance from the center of the void area to a grain surface will also increase. It is this increase in distance and the increase in the size of the area with larger filter media that leads to poorer performance as there is less likelihood of attachment occurring as the transportation mechanisms have greater distances to cover to give the opportunity for attachment to occur.

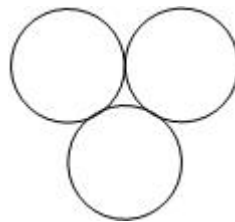


Figure 80 - Diagram of contact between three spherical filter media grains

Considering perfectly spherical filter media grains then the relationship between the filter grain size and the area of a pore space created when three grains contact each other as shown in Figure 80 is given in Figure 81 below:

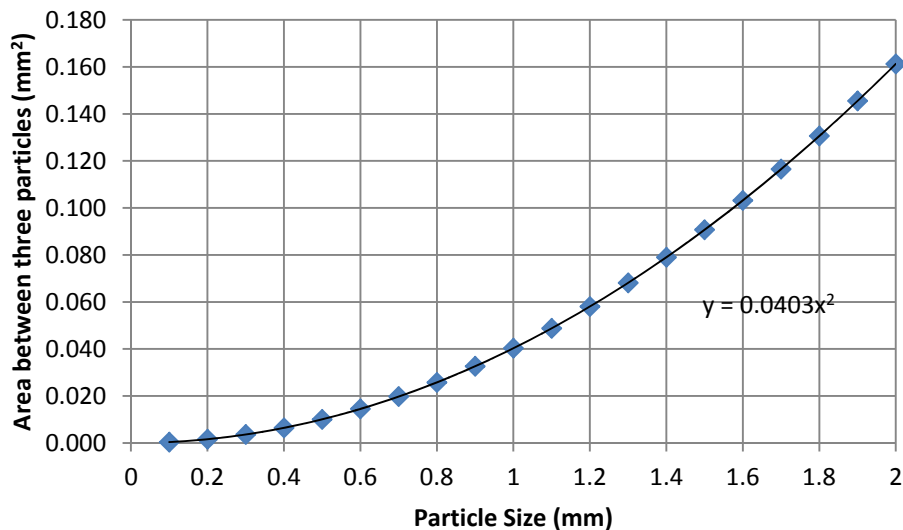


Figure 81 - Relationship between particle sizes and void areas between contacting spherical filter media grains

Filtralite has an average particle size (d_{50}) of 1.25 mm and sand is 0.7 mm. If both filter media were spherical then the exposed area between the particles for Filtralite would be 0.063 mm² and 0.020 mm² for sand (as it is, Filtralite is more angular which can lead to larger areas between connecting grains). This a three-fold increase in area between the media grains. It is suggested that that this is what is likely causing the discrepancy in the results between Filtralite and the other filter media and not the porosity values themselves, which as noted will be influenced by flow velocity.

It is concluded therefore that the porosity of the media alone is not a good indication of potential performance as it does not account for the variance in the size of the void. The reasons are summarized as media size increases then the voids will become larger but coincidentally there will be a lower number of voids across a specific plan area of the filter which accelerates velocity. Porosity calculations do not indicate filter performance as porosity does not account for the variation in the structure of the bed porosity caused by either the angularity size or compaction of the filter media.

It may also be concluded that Equation 11 would only be valid when comparing the same media shape with varying size or filter bed characteristics such as flow rate, depth and area. Different media with similar size can be compared, as shown in Figure 78 where the sand, glass and limestone all follow a similar trend. This is due to similar media size and also similar

void size between the various filter media, while Filtralite follows a different path due to its larger media size leading to increased void size between media grains reducing the effectiveness of the fundamental mechanisms of transportation. Slate, although a different shape, avoids close packing because of its low sphericity shape.

6.4.2 HEADLOSS

Headloss is an important performance indicator as it is a trigger for the need to backwash the filter, and therefore determines filter run-time. This is the most important factor affecting operating costs of the filter. Headloss can be divided into two, with initial headloss governed by the physical properties of the filter bed, together with flowrate and temperature of the water. Headloss accumulation is affected by the accumulation of solids in the filter bed as the filter is operating. How this solids retention impacts on headloss is determined by how the media retains the solids. It is therefore dependent upon the physical or operating characteristics of the filter bed, for example flowrate increases will lead to greater amounts of solids entering the filter per unit time.

Results for initial headloss are given in Figure 82 for the 9 NTU turbidity and Figure 83 for the 35 NTU turbidity. Each chart shows how as the flowrate increased so did the initial headloss except in the test with 35 NTU and a flowrate of 13.5 m/h for Limestone. This anomaly was determined to be from an error with the differential pressure meter for that test and it was determined that the information would not contribute. Unfortunately there were more pressing experiments and it was not possible to repeat this test.

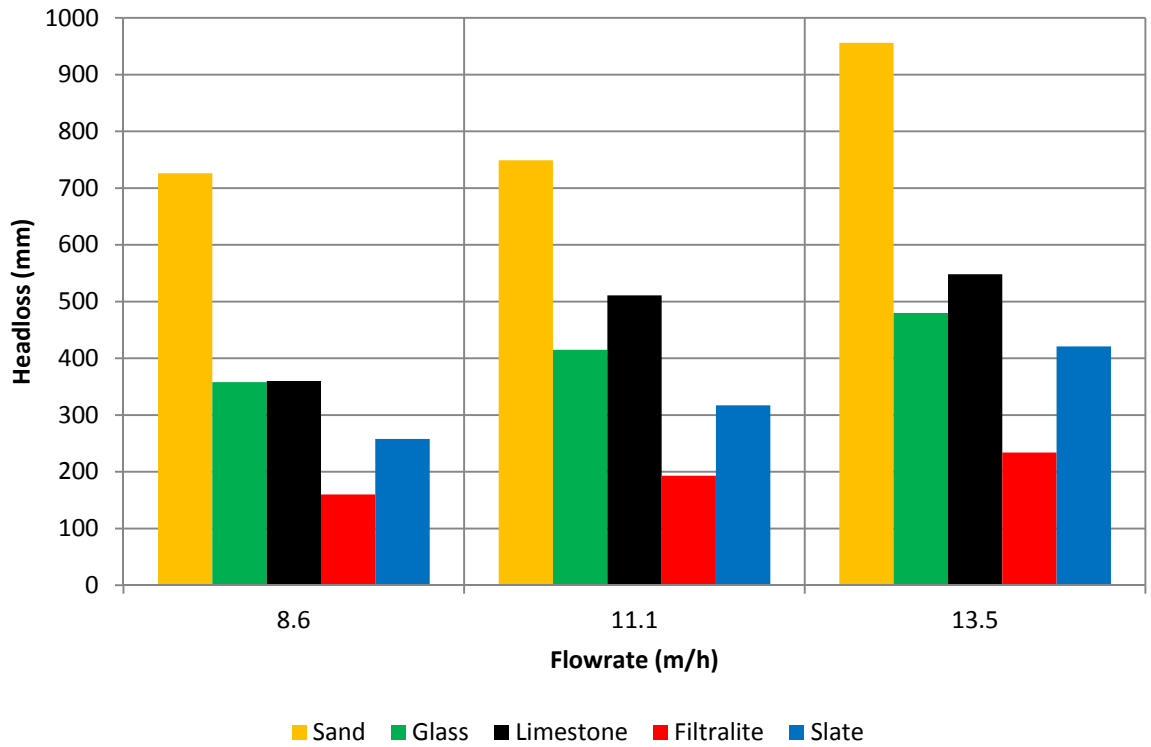


Figure 82 - Initial headloss for various flow rates at a raw water turbidity of 9 NTU

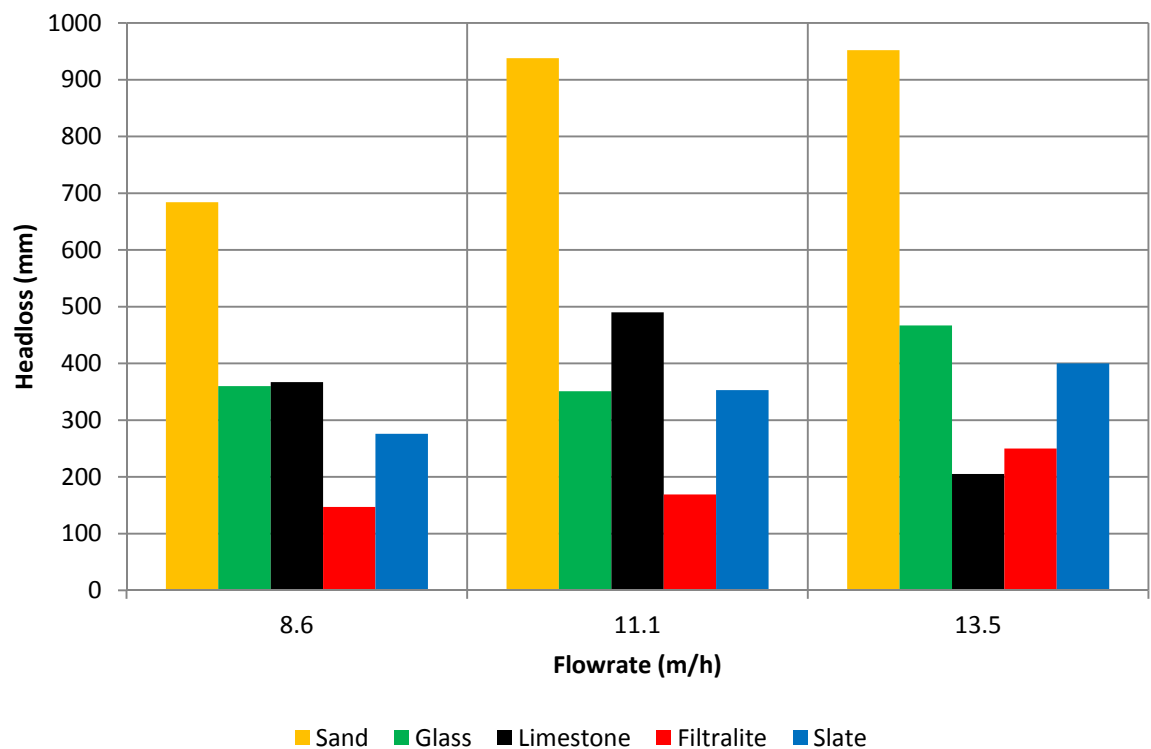


Figure 83 - Initial headloss for various flow rates at a raw water turbidity of 35 NTU

Ives (1975) states that a filter media with a sphericity value lower than 0.6 would be unsatisfactory due to its low permeability which would lead to high initial headloss values and reduced runtimes. Our data contradicts this, as can be seen in Figure 83. The slate with a sphericity value of 0.49 has a lower headloss than all the other media of similar bed porosity. Filtralite as expected shows the lowest initial headloss due to the media's greater particle size. Sand has an extremely high initial headloss, over twice that of comparatively sized filter media. Based on information from water treatment works the initial headloss would be expected to fall around 300 mm for sand but this is for a flowrate of around 5 m/h which is below that used in the laboratory studies. It could also suggest some problems with scale down from wall effects.

Data from the experimental work for initial headloss has been compared against theoretical values derived from the Carman-Kozeny (Equation 12) in Table 40 below:

Equation 12- Carman-Kozeny Equation from McCabe et al (2004)

$$\frac{\Delta p}{L} = \frac{180\bar{V}_0\mu(1-\epsilon)^2}{\Phi_s^2 D_p^2 \epsilon^3}$$

Δp = the pressure drop, L = total height of the bed,
 \bar{V}_0 = superficial velocity, μ = fluid viscosity, ϵ = bed porosity,
 Φ_s = sphericity of the particles, D_p = particle diameter.

Table 40 - Comparison of calculated values of initial headloss against test results

Flowrate (m/h)	Parameter	Initial Headloss (m)				
		Sand	Glass	Limestone	Filtralite	Slate
8.6	Calculated	0.662	0.597	0.349	0.096	0.663
	Tested (9 NTU)	0.726	0.358	0.360	0.160	0.258
	Tested (35 NTU)	0.684	0.360	0.367	0.147	0.276
11.1	Calculated	0.854	0.771	0.451	0.124	0.856
	Tested (9 NTU)	0.749	0.415	0.511	0.193	0.317
	Tested (35 NTU)	0.938	0.351	0.490	0.169	0.353
13.5	Calculated	1.039	0.937	0.548	0.150	1.041
	Tested (9 NTU)	0.956	0.480	0.548	0.234	0.421
	Tested (35 NTU)	0.952	0.467	0.205	0.250	0.400

The results show that there is a good correlation for the sand and limestone, while Filtralite, glass and slate show significant differences with values half that of the calculated value for

glass and 1.5 times less for the slate. This variation with theory for the slate is due to the low sphericity of the media, indicating that the packing behaviour of the media is an important consideration. Thus it was concluded that the idea from the literature review that a low sphericity media leads to detrimental headloss performance was incorrect, except when applied to near spherical media.

The result for glass was also unexpected as it has sphericity similar to limestone where the theoretical and measured values match well. The impact of the smoother surface of the glass combined with its lower sphericity and narrower particle size range may be leading to lower resistance to flow through the bed. While the limestone has a rough surface texture leading to greater headloss and closer match to the theoretical values.

The values for sand were expected to be a good match as it is spherical and also is the type of material that the theory was developed from. However it is important to note that accurate assessment of headloss performance for practical application in a full scale filter will require careful consideration of methodology. The wall effects and narrow but different sized columns used in this laboratory and pilot research were shown to have an impact on both the precision and accuracy of the result.

Headloss is typically the governing factor that determines the run-time of a filter; a limit is often set locally by operators as to what works best with the type of raw water. It is set to give an acceptable headloss for backwashing before turbidity breakthrough can occur (Severn Trent (March 2012) personally communicated their limit as 1.8 metres. The total headloss is a combination of both initial and accumulated headloss. In these studies where the filter run-time was limited to 12 hours the headloss accumulation was analysed from two shorter phases of filtration. These were called ripening and steady state. Pilot studies that continue to operate until failure which would offer a better indication of headloss accumulation. The laboratory experiments still enable differences between the media to be assessed and a combination of the accumulated and initial headloss was used to give an indication as to the likely performance of the filter media at pilot and full scale.

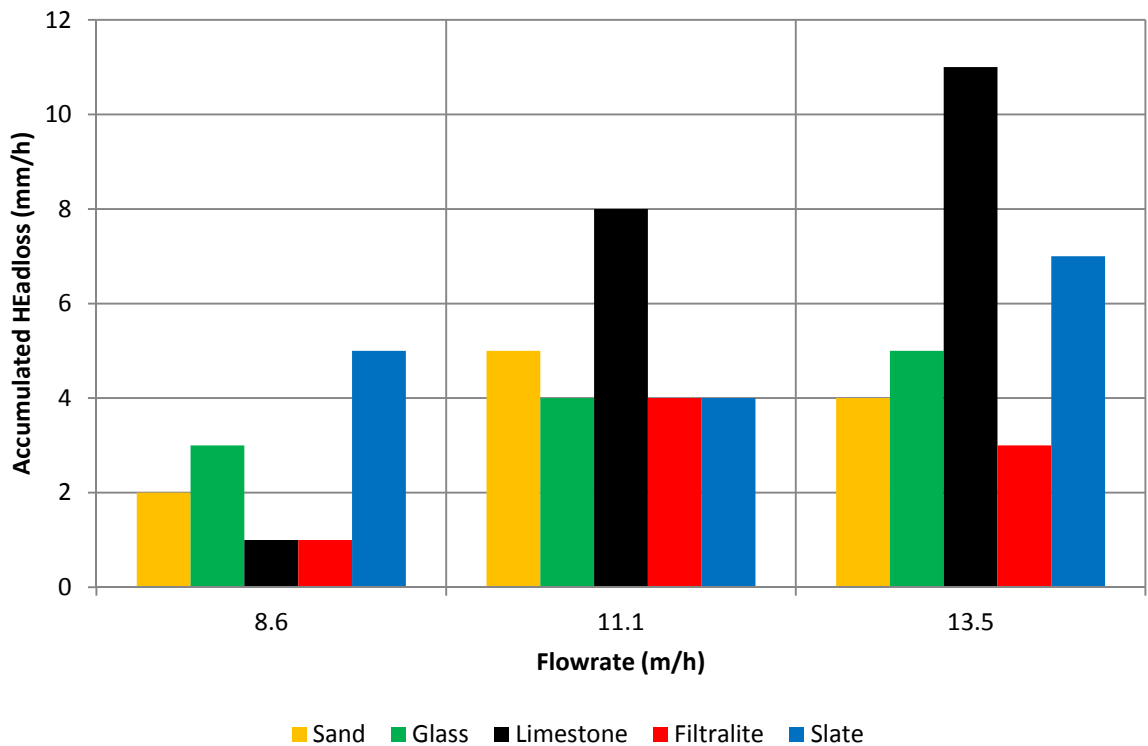


Figure 84 - Head loss accumulation at 9 NTU for various flowrates

Accumulated headloss (Figure 84) follows a less clear pattern compared to initial headloss. This is to be expected as the accumulated headloss will be dependent on the attachment and retention of suspended particles onto the media surface and it is unlikely that this would be reliably similar between the test runs. It can be seen in Figure 84 however that the rate of accumulation does increase with increasing flowrate, as would be expected due to the greater mass of particles passing into the filter per unit time. The headloss accumulation is for the three similar inert media sand, glass and slate. It was concluded that limestone was producing a precipitate which also increased headloss.

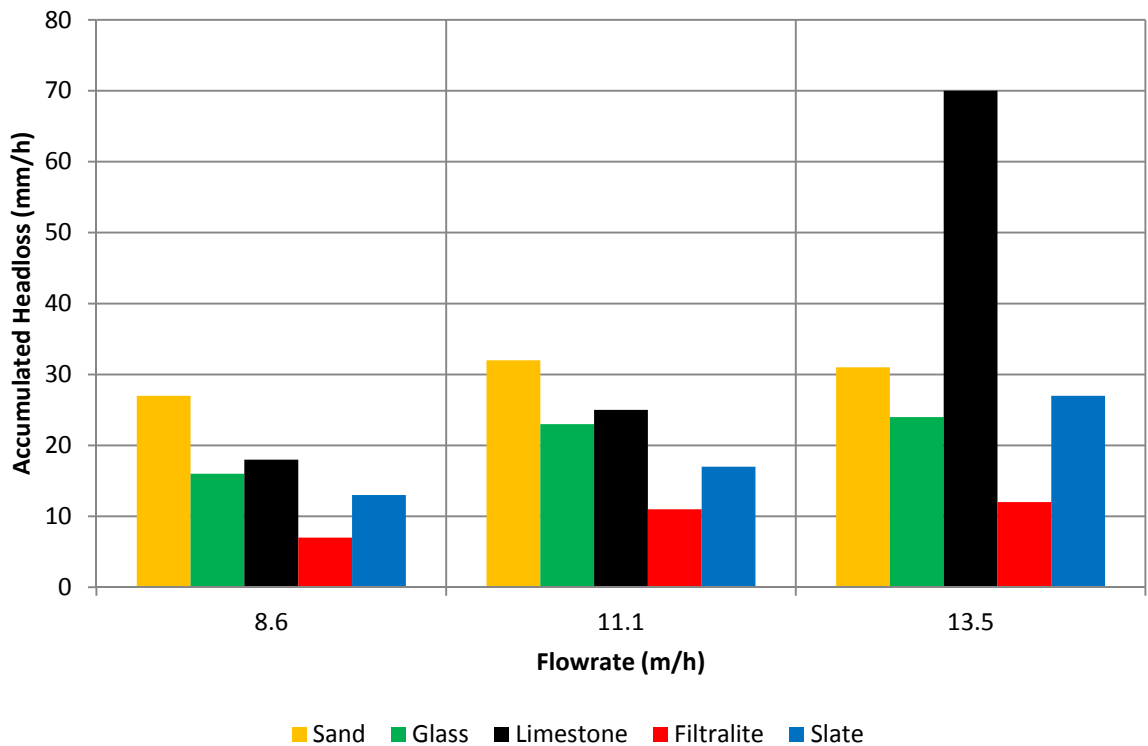


Figure 85 - Head loss accumulation at 35 NTU for various flowrates

The results from the higher turbidity of 35 NTU are shown in Figure 85 also show a degree of variability but the increase in accumulation with flowrate is clearer. The accumulation is an order of magnitude greater than the previous lower flowrate results. As with the initial headloss results the value for limestone at the highest flowrate of 13.5 m/h is not indicative of the true result, this is due to the problems described with the differential pressure meter. The results show that the Filtralite are also as expected and has the lowest accumulated headloss and this will be due to the greater particle size, larger bed porosity but also the reduced accumulation of solids retention within the bed and higher final water turbidity.

As the accumulated headloss results are variable and as the filters were not run to completion then these headloss results may only be indicative and are not valid for comparison with data from full length trials or full scale filters. However it is shown that the media that performed with the lowest initial headloss also has the lowest accumulated headloss and vice versa suggesting a principal measure of porosity. Results from initial headloss therefore give better scope for further analysis of the media.

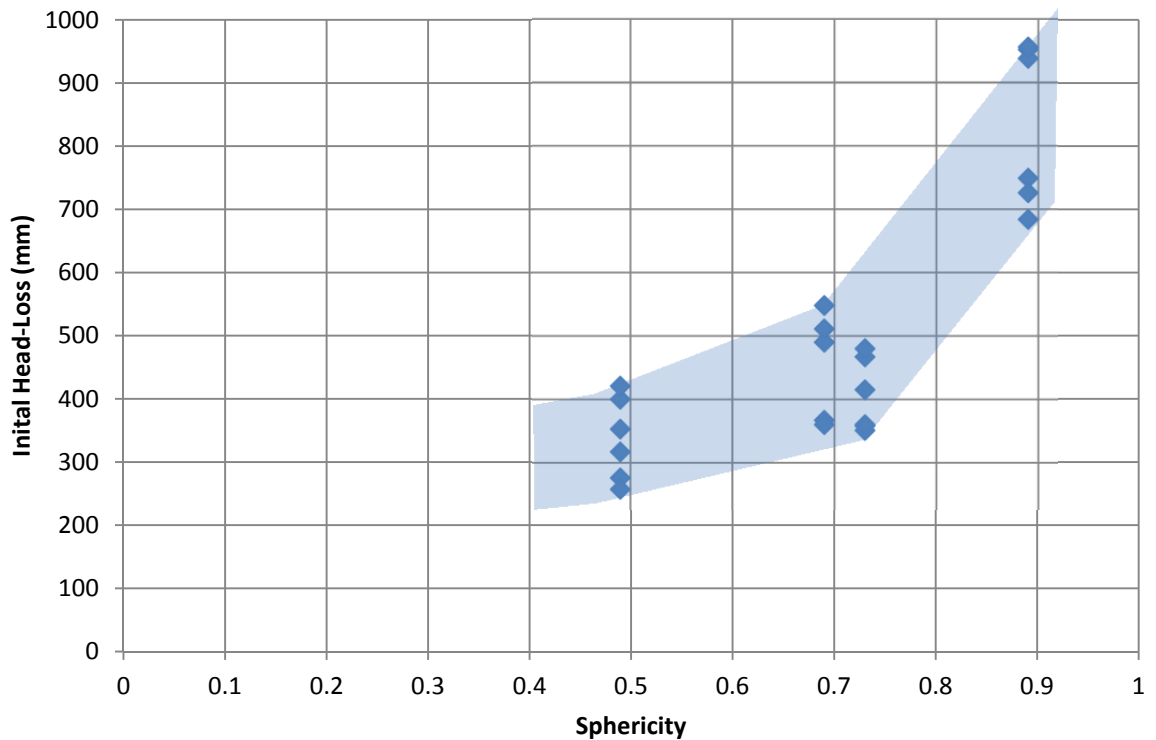


Figure 86 - Relationship between initial headloss and sphericity

Figure 86 shows the relationship between initial headloss and sphericity of the media, results for Filtralite have been omitted as the particle size has a greater impact than sphericity. Ives (1975) suggested that although there would be an improvement in turbidity removal for a media with a low sphericity, the permeability of the filter bed and therefore the headloss performance would be hindered by media with high angularity. Ives (1975) suggested a lower limit value for sphericity of 0.6. The results for slate in Figure 86 shows this is not the case, with the lower sphericity filter media (Slate) having the best initial headloss performance.

If the packing of the slate was considered to be orientated in such a way that the particles lay flat above one another then the limit of sphericity suggested by Ives (1975) could be demonstrated. However the slate has been shown by the SEM (Section 5.8.5) to have a highly varied packing leading to a varied permeability throughout the filter bed. In a sand bed the permeability is equal in all directions due to the packing arrangement being uniform with a spherical particle shape. As a media becomes more angular the packing arrangement becomes more random allowing for preferential and mixed flow paths to exist, this also helps with reducing headloss accumulation as particles will predominantly be transported to

areas of high permeability and these are the areas that attaching particles will have less impact on the flow of the filter.

Filtralite showed the lowest initial and accumulated headloss values and as previously discussed this is due to the increased particle size. The headloss accumulation however will also be impacted by the poorer turbidity removal as fewer particles will be retained in the filter bed to increase the headloss. Hudson (1963) and Glasgow (1998) demonstrated how a lower retention of solids in the bed due to surging of a filter will lengthen the filter runs where headloss is the limiting factor.

6.4.3 BACKWASHING

Tests were carried out to determine the backwashing properties of the filter media. This was carried out predominantly to compare the media and judge the impact of surface properties on retaining attached particles rather than to determine backwashing properties. The backwash was carried out using a constant up-flow flowrate to maintain a 20 % bed expansion which is typical (Hendricks, 2005 / Kawamura, 2000). The results are given in Figure 87 which shows the tests carried out to determine the required flowrate for 20 % bed expansion:

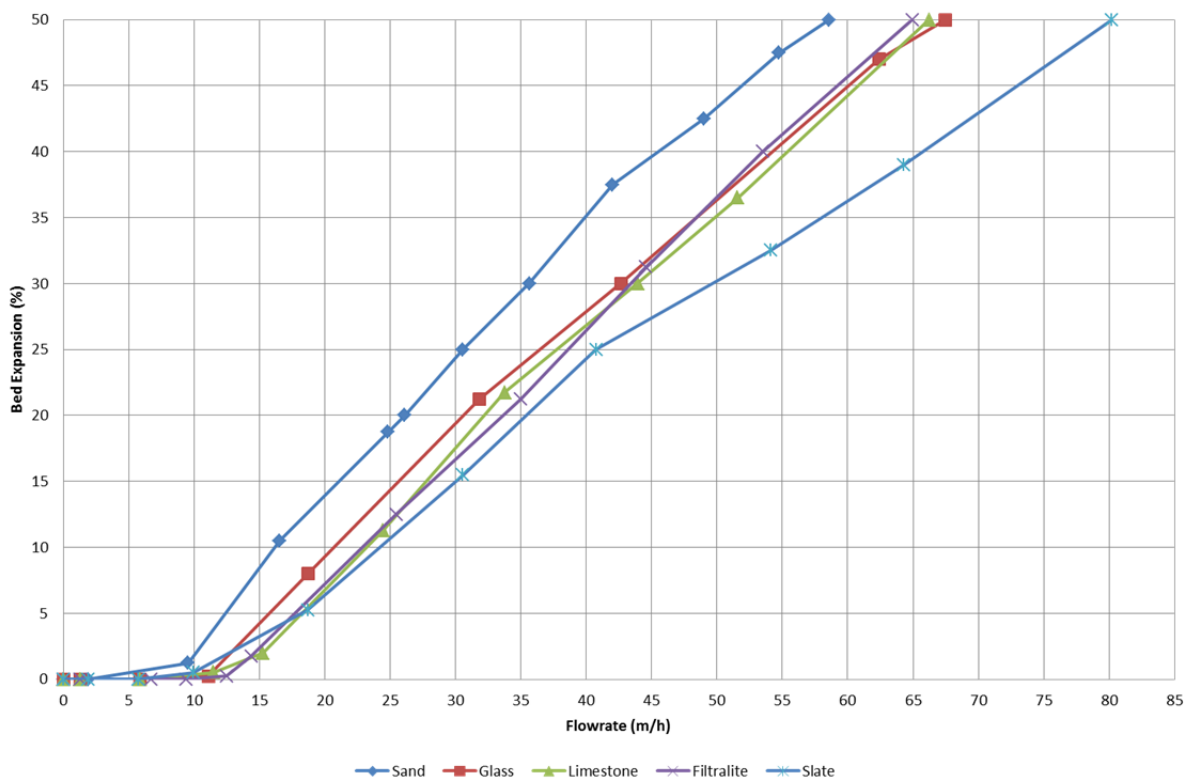


Figure 87 - Relationship between bed expansion and backwash flowrate

The results show that for a typical bed expansion of 20 %, sand required a lower flow than all other filter media including the lightweight Filtralite (S.G. = 1.7) which is noted in the manufacturer's literature (<http://www.filtralite.com/>) as requiring a lower flow rate. This was an unexpected result and is believed to be due to a combination of the hydraulics of the laboratory columns, both from the narrow diameter of the columns and the narrow backwash exit port at the top of the filters and the media size and shape. This highlights limitation in the use of small scale laboratory and pilot columns when carrying out

backwashing experiments. On a large scale filter the exit for wash water is typically a large weir the length of the one side of the filter. In the case of laboratory and pilot scale rigs the outflow is a small diameter port in the side or top of the filter column (See section 6.3.2) and this possibly impacts to require greater flow to maintain a similar bed expansion to a full scale filter. The media shape and surface features are possibly also impacting the result as the media with the highest headloss (sand) requires the lowest backwash flowrates to reach a 20% bed expansion, indicating high friction against flow. The impact of shape and the media's surface on backwashing requires further study using specially designed laboratory equipment to ensure accurate results.

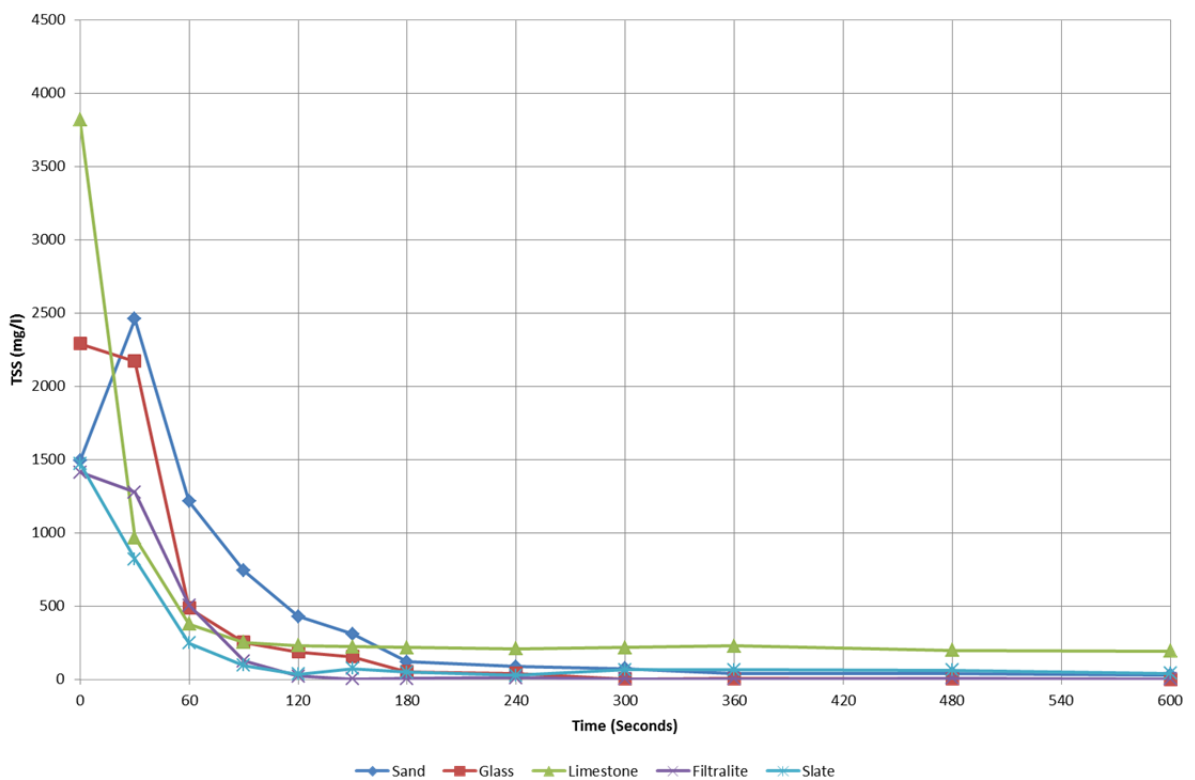


Figure 88 - Change in TSS during backwashing

Results for TSS removal (Figure 88) during backwashing show that all alternative filter media were cleaned at a faster rate than sand, this is possibly due to the lower flow velocities through the sand filter bed. The expansion of sand to 20 % required a 26 m/h backwash flow rate which is lower than the value of 31 m/h used for the next media (glass). Variation in solids removal between the media due to surface features (see section 5.8) such as the glass being smooth or Filtralite being very porous did not appear to offer any variation in solids removal with time of backwash according to the results shown. Further analysis of whether

solids remain attached to the media after backwashing is required to ensure that the media has been cleaned sufficiently.

Although testing of the filtered water from the limestone showed no calcium present, the results suggest dissolution did occur. The media generated a greater amount of solids during the backwashing procedure and it did not reach the same low values as the other media. These results show additional solids losses from the media during backwashing, but the durability testing in section 5.5 was 1.2 % for limestone compared to sand's 1.5 % at a more aggressive 50 % bed expansion. Further and more specific testing would be required to determine possible reasons for this additional turbidity release from the limestone. The results however did not impact on the filtration performance of the Limestone and the result does not discount the media from consideration.

6.5 SUMMARY AND CONCLUSIONS

Alternative media have been shown to offer improvements in the performance of rapid gravity filtration for both turbidity and headloss. Angularity was shown to be a key consideration. Lower sphericity improved both turbidity performance, and generated longer filter run times. This was attributed to the varied packing of the filter bed and flow paths. This was contrary to the more widely held belief that a rounded media such as sand is the most suitable, although no actual evidence in the literature was found to support this claim. The reason is due to the increasingly varied packing as sphericity reduces, creating areas of variable porosity which cause preferential flowpaths into the higher porosity zones where attached particles impact on headloss less.

Improved turbidity performance from the angular media was attributed to an improvement in the transportation mechanisms, specifically inertia. However the variation in performance between the limestone, sand and slate was not very large and with lower inflow turbidity from real clarified water (~0.3 NTU in the pilot study) any variation in turbidity performance will become less apparent. Angular media showed improved headloss performance; this was also contrary to the limestone expectations. Slate with a sphericity value of 0.49 was predicted by Ives (1975) to have a poorer headloss performance due to a reduction in permeability however this was not shown to be the case.

Previous research by Soyer et al (2010), Evans et al (2002) and Rutledge and Gagnon (2002) discussed in section 4.1.2 showed glass to typically perform near to sand. The detail experimental set-up however and choice of specific media will be different to this study and also there were a number of factors not considered in this previous research. Glass in this study's experiments showed turbidity removal that was not as good as sand and was between Filtralite and sand. Considering the greater angularity of glass, this was unexpected given the performance of slate noted previously. An explanation given could be particle size distribution which shows the uniformity coefficient to be narrower than the sand (for glass it is 0.7 – 1.0 mm) and this will lead to a larger pore size in the media much like Filtralite. Another area is the consideration that the surface area of the glass is 0.0558 m²/g while sand is 0.2261 m²/g indicating that glass is a very smooth media lacking in surface features as shown in section 5.8.

Limestone performed similarly to Sand and Slate for turbidity removal but headloss performance was improved compared to sand. Its suitability at continuously treating real water is still uncertain due to the risk of dissolution that may occur. During trials no significant reduction in filter media was found and limestone would also be expected to show poor turbidity removal due to these solids released from the dissolving filter but this also did not occur. Periodically a number of samples were taken from the filtered water to be tested for calcium in an ICP, no increased presence was detected and therefore during these trials dissolution of the media was inconclusive. It is expected that if there are acid raw waters (upland or residual coagulant) then there is the possibility of a problem occurring. As a sacrificial media as part of a dual or multi-media filter then it may offer additional benefits beyond turbidity removal. The characterization testing for adsorption of common metals (See section 0) shows that Limestone is an excellent media for causing precipitation of these common polluting metals which can then be collected within the filter itself for removal in backwashing. This may possibly be the only treatment required or it could help reduce the load on another system for the removal of the metal.

The turbidity performance of Filtralite was also unexpected; Filtralite would be less likely to be able to deal with an increase in smaller solids entering a filter compared to other media due to the increased bed porosity. Beard & Tanaka (1977) found that a threefold increase in particle concentration led to a 10 fold increase in the number of particles of 2.5 microns and

above. Longsdon et al (1981) found that an increase of 0.1 NTU in inflow turbidity increased the number of Giardia sp. cysts of 8 to 12 microns by between 10 and 50 times. Considering the importance of filtration in the removal potential of microbial pathogens such as cryptosporidium any reduction in turbidity performance reduces confidence that the media is working effectively. It is suggested that future work should consider the use of particle counting to compare media performance for removal of specifically sized particles to improve this confidence in this new media compared to the suitability of sand for removal of cryptosporidium. The results indicate that the larger media may still meet turbidity requirements if there is floc carry over or dual-media.

The variation in turbidity performance between the sand, limestone and slate was corroborated by considering both turbidity and headloss together, that is a media with a lower headloss accumulation would typically be expected to have a poorer turbidity removal. This was shown by the Filtralite media. Slate and Limestone show lower headloss than sand while also having the same turbidity performance meaning that the fundamental filtration mechanisms are more efficient at removing particles in these more angular media. The time for ripening to occur is reliant on these fundamental mechanisms alone as once ripening is completed the particles will become attached to the surface of the media and particles will preferentially attach to each other on the media surface rather than the media alone which is how ripening occurs. Slate shows the fastest ripening time again showing that the fundamental mechanisms (torturous paths) are more effective at removing particles in this angular filter media.

From the testing it is concluded that the key aspects of a filter media when considering filter performance are the impact of the physical properties on the packing arrangement. Sphericity reduces the packing variability increases leading to uniform filter performance. Media particle size was shown to be a key consideration and the choice of media size range and uniformity coefficient as noted by Sokolovic et al (2009). The results suggest the filter media size could be adjusted to suit clarified water quality and to optimize turbidity and head loss performance. The surface features of a media were also determined to be important to performance, surface roughness is possibly a better description. Glass, for example, was below expected performance. This was considered to be due to the virtually flawless surface of the media promoting detachment, as there is no shelter on the media

surface from flow. Based on this principle Filtralite should have performed well but because of its larger size transportation mechanisms are poorer and surface roughness only helps to shelter particles that are already attached.

7 PILOT SCALE TRIALS

7.1 METHODOLOGY

The trials conducted at pilot scale were designed to follow the same general principles of the laboratory study with mono-media filter beds at a depth of 600 mm. The selected media would ideally include sand, glass, limestone and slate as these gave the best turbidity performance and had similar particle size. Filtralite had too large a media size to give a fair comparison with these other media, but Filtralite is a commercial product with approval and was chosen in preference to limestone. Limestone was unsuitable due to possible dissolution problems. This was concluded as a risk rather than certainty from the previous research and limestone should still be considered as a possible alternative in future studies.

The objective of the pilot plant study was to carry out scale-up analysis of the alternative filter media and with real clarified water, continuing and corroborating the experiments carried out during the laboratory study. The pilot study continued with the same packing regime of tapping the sides of the columns until no further consolidation of the media occurred. Initial studies with unconsolidated beds were carried out to compare against consolidated tests and provide data to Severn Trent Water on filter performance. After initial installation and commissioning of the pilot plant, steady state data was collected continuously for a 2 month period (January – February 2012) which generated different filter cycle run-times.

7.1.1 WATER TREATMENT WORKS

The works is supplied from three primary sources (See Figure 89), an approximately 23,000 ML capacity reservoir and a smaller bankside balancing reservoir with an approximate capacity of 114 ML. Both of these reservoirs abstract water from the same river, typically water is predominantly taken from the smaller impoundment reservoir unless nitrate levels are high, in which case water is taken from the larger reservoir to blend and reduce the nitrate level. The water from the reservoirs is also mixed with water from two local boreholes. This water will have the preferential lowest solids content but abstraction is limited. The highest solids load would be when the water is predominantly being taken from the smaller reservoir with the lower retention time of approximately 4.8 days.

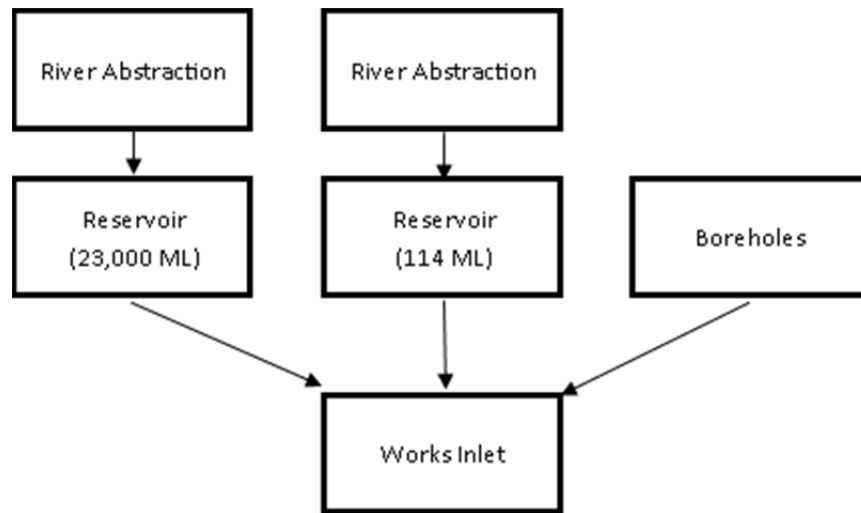


Figure 89 - Raw water sources to water works

The works itself has a maximum design capacity of 30 ML/day but due to a reduction in demand the works had been operating at a flow of 16 ML/day for several months and this included the duration of the pilot study. A single treatment train exists at the works and is detailed in Figure 90. The works operates an uncommon system of having two ozone treatment stages prior to filtration, and this is to deal with the high nitrate content of the water. One contact tank is located at the entrance to the works and the second is located directly between the clarification and filtration stages. To avoid the impact of the inter-ozone on the clarified water quality (possibly through reducing the solubility of any residual iron) the pilot plant was designed to take water directly from the clarified water channel that exited the hopper bottom clarifiers and prior to the second inter-ozone tank. This was considered important to ensure that results from the pilot study were more generally applicable for comparison with other works to highlight the benefits that alternative media could have at other works.

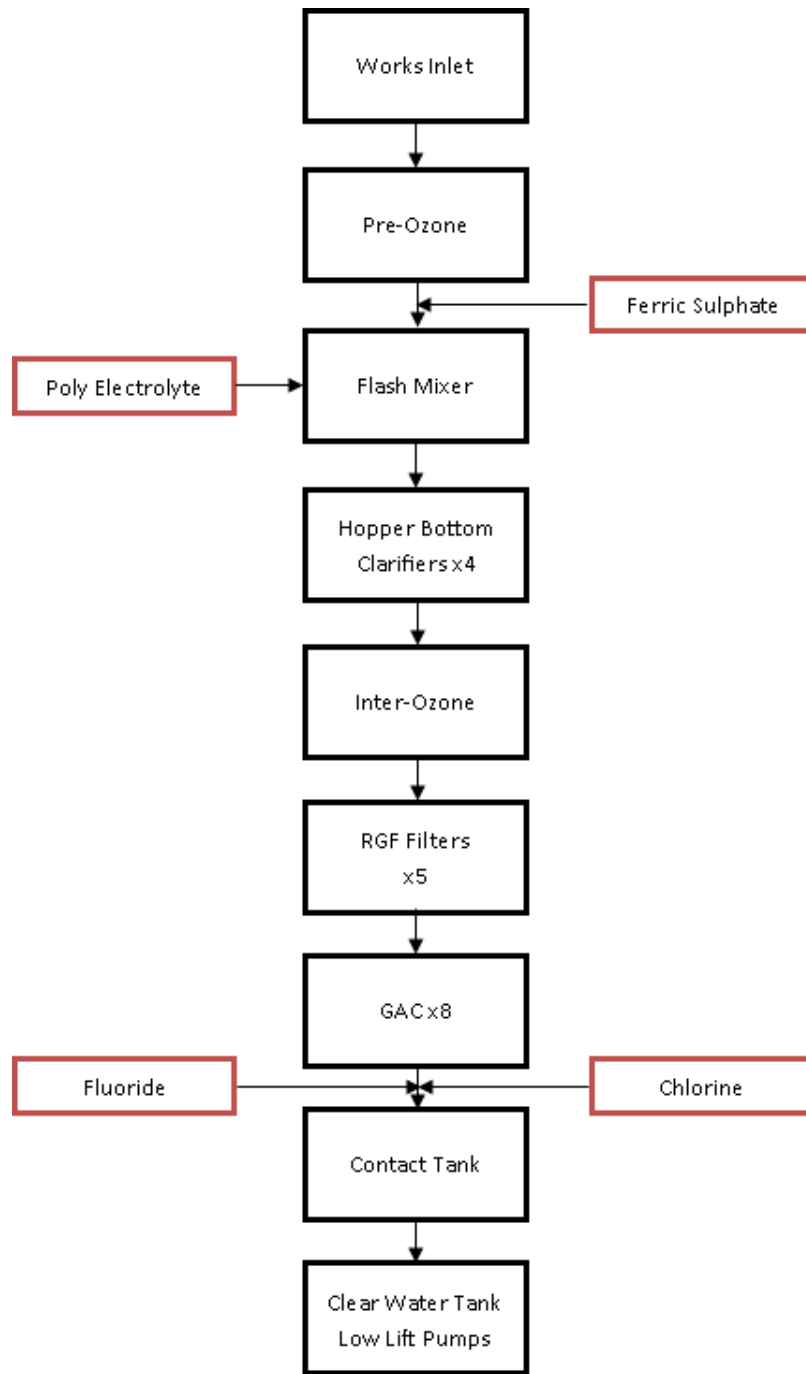


Figure 90 - Water works treatment train

The rapid gravity filters at the works consist of four original filters each having a plan area of 24 m². These filters were originally designed to use activated carbon as the filter media but have since been adapted to use a sand/antracite dual-media configuration. A fifth filter was added to the works at a later date and is larger with a surface area of 30.7 m² which was designed to use the dual-media configuration. The design filter media depth for all filters is 900 mm, the antracite layer should account for at least 150 mm of this. Previous work at

site and visual inspection showed that the anthracite layer had been reduced due to media loss from backwashing, core samples taken previously noted the depth to be approximately 75 mm. In addition, problems with media cracking and holes in the bed were noted previously in the filters on site; however the backwashing procedure had been altered prior to the pilot plant study and no filters showed signs of cracking during the study. The filter runs had been reduced and it was uncertain as to which change cured the problem.

The four original filters were backwashed every 48 hours while the fifth filter was washed every 36 hours. This was based on previous work that had highlighted the issues of cracking as being more severe in this filter. During the pilot study the run-time of the filter was slowly being increased to hopefully return to the 48 hours of the other four filters. Headloss was observed in the filters to reach approximately 1.4 metres for the four filters after 48 hours of run-time. The capacity of the works is for a maximum headloss of 1.8 metres but the filters are operated on time to ensure only one filter is out of operation at any time. The problems that have been observed on site are similar to the problems highlighted by Hendricks (2000) discussed in section 0. The conclusions of previous site work are that they were caused by inadequate backwashing which arises from the problems of using dual-media filters in a filter designed to use activated carbon as the media, however the results from the pilot study highlighted another factor.

7.1.2 PILOT PLANT

The inlet pipework was situated in a wet well at the base of a pair of Archimedes screws which transport the water to the inter-ozone. This area was suitable for abstraction from the clarified water channel as it offered a high level of turbulent flow due to the drop in level from the channel to the wet well, and also the mixing of the Archimedes screws possibly causing further coagulation of residual floc into larger particles. Increased turbulence reduces the likelihood of changes in water quality being due to changes in flow rate within the pilot plant disturbing sediment in the wet well. The wet well was also deeper than the channel and allowed the inlet pipework to be located further from the base. The pilot plant was located directly beneath the clarified water channel and the inlet to the pilot plant, this reduced the time from abstraction to entering the pilot plant ensuring water quality was not altered by long pipe runs.

The pilot plant consisted of four (Figure 91) filter columns with an internal diameter of 150 mm; the clear section of each column was 1.65 m high allowing sufficient space for the media support, and head accumulation. Unlike the laboratory columns where the backwash outlet was located at the top of the column there was a port located on the side of the pilot columns at 1.3 m above the base which allowed for sufficient backwashing head space with a 600 mm bed depth. The filter floor did not require the use of gravel as it had been designed to have the media placed directly above it. Gravity feed with constant head would have been the preferable method of operating the filters to keep these variations identical between laboratory and pilot studies, but the pilot plant had been designed for use at a wide range of sites which made the use of peristaltic pumps a more practical solution to ensuring the flowrate was constant.

The flowrate was constant although the head above the filters would increase in relation to the clogging of the filter. Peristaltic pumps would also limit damage to any fragile solids ensuring that the clarified water quality remained as it was in the channel. As the media became clogged and headloss increased the pressure above the filter bed would increase, to avoid damage, a pressure relief valve was installed at the top of each filter to a pressure of 0.3 bar which would allow the filters to operate up to this point which is equivalent to 3 metres head which is the same as the constantly maintained head in the laboratory filters.

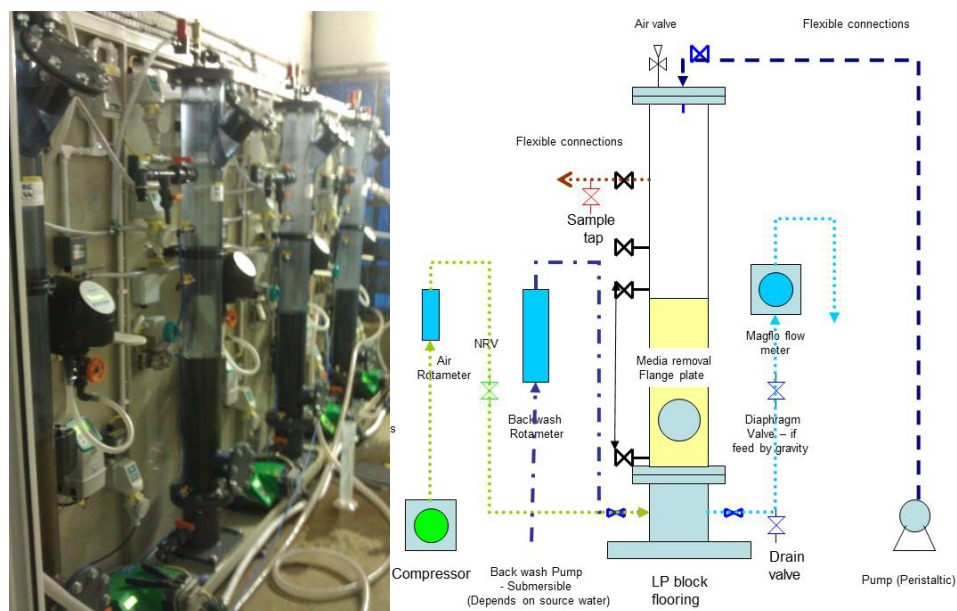


Figure 91 - Image and diagram of pilot plant design

All filtered water was collected in a storage tank which filled to a capacity of approximately 250 L which then overflowed to a wastewater drain on site. Water had to be removed to waste as the slate and glass were not approved filter media. This limited the choice of works for carrying out this study to those that had a connection to a mains wastewater collection system. The works chosen was also due for filter refurbishment and had a history of difficulties in operating filters and the study would feed important knowledge into the decision-making process in the future. The water stored in the tank was used for backwashing the filter media. This was carried out by using a submersible pump via a flow meter to enable accurate control of the backwashing. Measured volumes of compressed air were used for the air scour.

During commissioning of the pilot plant, a number of issues arose which could be used to improve the design, problems were expected as this was the first operational use of the pilot plant. A major problem was the design of the de-bubbler, which was used to ensure no air entered the turbidimeter and reduce the flow through the turbidimeter to its operational range. The tops of the de-bubblers were open to air and the placement of the overflow only 10 mm from the top lip meant that as the water rose in the de-bubbler there was an insufficient head of water to drive it through and water spilled over the top of the de-bubbler. The solution (see Figure 92) was to seal the top of the de-bubbler and install a T-piece on the overflow pipe with a length of open ended pipe to avoid a syphon that would otherwise occur as water flowed down out of the overflow (this would have reversed the flow through the turbidimeter).



Figure 92 - Re-design of de-bubbler on pilot plant

Turbidity was monitored continuously by an Aquascat P (Sigrist, Ely), operating at a range of 0 – 3 NTU, the range expected during operation and ripening. Headloss was monitored by a SITRANS P DS III (Siemens, Manchester); the output was in mmH₂O for headloss across the whole filter bed. Flowrate was monitored by a SITRANS F M MAGFLO MAG6000 (Siemens, Manchester) which was used to ensure there was no significant change in flow rate during operation. Data was collected by a Squirrel 2040 data logger (Grant Instruments, Cambridge). Readings for each of the monitored variables were taken every 10 seconds by the data logger, but the data was logged periodically based on an averaged reading for a 1 minute (turbidity/flowrate) or 2 minute period (headloss) which reduced the noise in the results and to give a more manageable volume of data. Data was downloaded onto a laptop using SquirrelView (Grant Instruments, Cambridge) software, this allowed the raw data to be formatted and read in Excel for analysis.

7.1.3 CLARIFIED WATER QUALITY

The pilot plant lacked the ability to continually monitor the clarified water quality, this data was supplied by the works SCADA system which provided turbidity and soluble iron results. It was not possible to provide the results in a downloadable format and therefore the results had to be printed for each test, these are provided in Appendix IV. Clarified water quality during the testing period ranged from 0.1 – 0.3 NTU except for 2 days of the study where the

reading increased to 0.3 – 0.4 NTU. Results for soluble iron for the same period typically fell between 0 – 0.2 µg/L and these are shown on the same plots as the turbidity in Appendix IV.

Samples of clarified water were also taken at the beginning and end of each test run, for wet analysis. In addition the laboratory’s ICP was not operating during the trial and total or soluble Iron was not corroborated with the SCADA values. A comparison of the average turbidity result for a typical test run and the associated grab samples is given in Table 41.

Table 41 - Clarified water turbidity values fed to the unpacked filter beds

Test	Date	Clarified Turbidity	
		Pilot Plant	Works Avg.
1	11/01/2012	0.173	0.16
2	13/01/2012	6.280	0.16
3	16/01/2012	0.168	0.19
4	18/01/2012	0.169	0.17
5	20/01/2012	0.206	0.15
6	23/01/2012	2.320	0.15
7	25/01/2012	0.721	0.16
8	27/01/2012	0.151	0.16
9	30/01/2012	0.144	0.16
10	01/02/2012	0.189	0.20
11	03/02/2012	0.310	0.24
12	10/02/2012	0.278	0.25
13	13/02/2012	0.320	0.28
14	16/02/2012	0.354	0.26
15	20/02/2012	0.332	0.28

There are 3 anomalies in the testing, the results for test 2, 6 and 7 which are all larger than the works average suggested. The result for tests 2 is due to accumulated solids in the inlet pipework being released when the flowrate was increased relative to the previous test run. Test 6 could also possibly be due to this. To counter this, at the end of a test run the pumps were increased to full output to clear solids out of the pipework and into the filter column, the columns were then backwashed and the next test run restarted as normal. This solution remedied the problem except in test runs 6 and 7 and as the results show (see Table 45) in test run 10 for the Slate media.

The Drinking Water Inspectorate states that the maximum turbidity value at a customer’s tap should not exceed 4 NTU, however most utilities strive for sub 0.1 NTU to reduce chlorine demand and to improve confidence in cryptosporidium removal. The quality of

water leaving the clarifiers according to turbidity readings taken would therefore be considered of good quality and also if this measured turbidity was replicated using clay as in the laboratory tests it would be difficult to determine any solids present by the naked eye. However visual inspection of the water entering the pilot plant for all test runs did have flocs and floc carry over not reliably indicated by the on-line turbidity measurements (both SCADA and manual samples). An example of the water quality observed in the pilot plant columns is given in Figure 93; a handheld torch was used to illuminate the 1-2 mm sized floc present in the water.

Floc carryover was observed throughout the 2 month trial. This was corroborated by the presence of a layer of iron that had settled onto the filter bed, also obvious in the upper layer of each filter media. This iron layer proved very difficult to effectively backwash and was also observed on the full scale filters and is possibly one of the causes of the cracking noted previously at the works. These cracks and holes were overcome by increasing the frequency of backwashing which did not allow the iron mat to consolidate.



Figure 93 - Floc entering the pilot plant filter columns

The depth of this iron saturated zone (See Figure 94) was dependent on the filter media size, the greater pore size of the Filtralite enabled the iron floc to travel deeper into the bed compared to the smaller particle size of the sand. These impact of this penetrating iron floc on filter performance was significant, with shorter than expected filter run-times and an improvement in turbidity removal. These are discussed in more detail in section 7.2,

however it is important to note in this methods section that floc carryover is likely to be common and should be taken into account during experimental design.



Figure 94 - View of glass and sand saturated by iron in the upper layer, other media are darker and so mat is less visible

An analysis of the possible reasons for floc entering the pilot plant was investigated. Initially it was thought that there was sediment being taken up from the wet well where the inlet was located but considering the turbulent flow and with a combined abstraction of up to 600 L/h maximum being taken from the main channel the possibility of this occurring was dismissed. If sediment was being abstracted then the solids would still need to be replenished continuously from another source. Visual monitoring of the hopper bottom clarifiers showed floc to be present throughout the depth of clear water above the sludge blanket as can be seen in Figure 95.

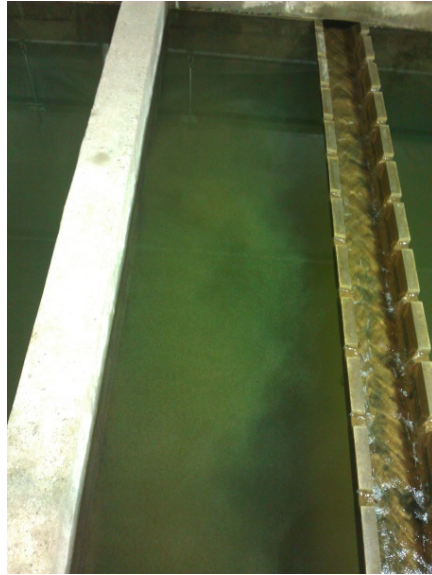


Figure 95 - Floc shown above the sludge blanket

During visual inspection it was observed that flow surges occasionally broke through the dense sludge blanket causing mushrooming above the surface, the particulates then move horizontally above the surface of the sludge blanket which was then directed or reflected off the walls into the launder weir before the flocs could resettle. This was observed predominantly in the first clarifier, and less frequently in the other three. This, it was suggested, could be due to the first clarifier receiving a greater portion of the flow.

The conclusion is that neither SCADA nor manual snap samples were able to confirm this and suggests further work is needed on monitoring methods to give a true indication of water quality before and after filtration. Conventional iron monitors analyze soluble iron and the snap samples to infringement while it is believed that the insoluble iron in the form of floc was not being detected. The works is unusual in using pre-ozone which could be reducing the solubility of the iron and this needs further analysis. Turbidity measurement is based on very small representative samples and often there are only a small and intermittent number of flocs present in the water. The site's on-line monitoring location was a significant distance from the sampling point and the particles may precipitate in the pipe runs and a representative sample may not be achieved. In the pilot plant and full scale however these individual floc particles are likely to accumulate together in the upper layers of the filter leading to the observed problems associated with reduced filter run-times.

7.1.4 MUDBALLING + BACKWASHING

The initial backwashing procedure (Table 42) was based on a backwashing procedure from a previous pilot plant which had been developed from work carried out by Severn Trent Water (Lizz Brooks). The floc carryover in this study from the HBC described in section 7.1.3 meant that the backwashing regime was found to be unsuitable, which also raised concerns as to the effectiveness of the full scale backwashing procedures under similar water quality conditions.

Table 42 - Initial backwashing procedure

Process	Duration	Flowrate
Air Scour	2 minutes	20 l/s
Water Wash	4 minutes	650 l/h
Water Wash	4 minutes	500 l/h

The air-scour broke the saturated iron mat down into smaller segments or in some cases pushed a plug of saturated media upwards in the column which then required tapping of the wall to break the mat and allow it to fall back down. The air-scour was turned off and then a water wash was begun which is supposed to assist in clearing out the solid material from the filter bed, however the higher density iron saturated media and agglomerates (mudballs) allowed them to fall downward against the up-flow of the wash water and through the fluidized bed until they settled on the base of the column (Figure 96).



Figure 96 – Mudballs settled at the base of the filter column

Based on these observations the backwashing procedure was altered to include a combined air/water scour shown in Table 43. The main criteria of the wash were to return all media to as clean a state as possible based on colour observations. Further optimisation of backwashing was required but given the time available it was made as vigorous as possible to ensure the mudballing did not occur and prejudice filter performance. The combined air/water wash allowed the mudballs to be further broken up as they fell mixed in the fluidized bed. The altered wash also cleared the mudballs already formed at the base of the columns down, however it was observed that due to the location of the inlet port on one side of the column that the majority of the force of the backwash flow was directed to one side of the base of the column and therefore there was an accumulation of solids on one side of the column base equally in all media.

Table 43 - Backwashing procedure used during trials

Process	Duration	Flowrate
Air Scour	2 minutes	20 l/s
Combined Air / Water	4 minutes	20 l/s + 400 l/h
Water Wash	2 minutes	650 l/h
Water Wash	2 minutes	500 l/h

The backwashing procedure is far more vigorous than what was being used in the full scale filters and the observations of mudballs sinking through the fluidized bed with the initial backwashing procedure copied from typical full scale filter wash. It is possible that mudballs are occurring in full scale filters but are not observed as they are hidden by dirty water initially during washing and then sink to the base of the filter bed. This is a risk to quality as mudballs will carry contaminants through the filter to the outlet and could include pathogens, and could release these contaminants. It is recommended that further work is needed on backwash since it could also address the problem of floc carryover affecting filter safety, however it will not address the impact of floc carryover on filter run-times.

In a full scale filter the weir that backwashed water exits the filter is often the length of one entire side of the filter, which should offer low resistance to the removal of solids. In this pilot plant the exit was a small 20 mm diameter hole which had a high resistance, this led to

a higher wash water velocity required to clear solids from the filter. Therefore the use of most practical pilot plant for designs of a suitable backwashing procedure for use in a full scale will likely be flawed. This testing will require a specific backwashing pilot rig to improve scalability.

7.2 RESULTS

7.2.1 SUMMARY OF TESTING

15 test runs were carried out between January and February (2012). The first 9 were with consolidated packing, done by tapping the side of the filter column until no more consolidation of the media could be seen. A further 6 test runs were carried out with an unpacked bed that was allowed to settle by its own weight after backwashing. A number of listed runs were excluded from the numerical analysis due to obvious irregularities in results of headloss or problems with operation that affected flowrates. These were most often caused by iron floc which accumulated in the inlet pipework prior to operation. This was most evident in test 1 (Table 44) where operational experience was being gained and used to address the problem through an altered methodology, where the accumulated headloss is much higher than other tests. There were no abnormal filtered turbidity results observed during any of the test runs.

Table 44 – Overview of results from all packed bed testing (C1 – Slate, C2 – Filtralite, C3 – Glass and C4 – Sand)

Test	Date	Flowrate (m/h)	Headloss								Turbidity (NTU)			
			Initial (mm)				Accumulation (mm/hr)				C1	C2	C3	C4
			C1	C2	C3	C4	C1	C2	C3	C4				
1	11/01/2012	9.34	309	153	352	689	194	110	169	200	0.030	0.036	0.033	0.034
2	13/01/2012	3.43	136	71	152	271	37	27	34	63	0.028	0.033	0.028	0.028
3	16/01/2012	8.73	313	189	401	775	129	68	99	166	0.029	0.034	0.031	0.032
4	18/01/2012	8.59	362	250	489	785	110	49	90	152	0.026	0.033	0.028	0.029
5	20/01/2012	4.32	183	102	234	295	49	27	43	71	0.027	0.034	0.027	0.027
6	23/01/2012	7.48	449	180	498	805	98	51	103	177	0.028	0.033	0.028	0.029
7	25/01/2012	6.47	272	142	370	540	95	44	91	127	0.028	0.034	0.028	0.029
8	27/01/2012	5.48	212	136	281	579	72	43	70	125	0.029	0.034	0.029	0.03
9	30/01/2012	7.54	310	172	371	697	132	49	118	154	0.031	0.035	0.033	0.033

Experiments 1 – 9 with packed beds (Table 44) are for comparison with the previous laboratory studies that used packed beds to provide scale up confirmation of the

fundamental filtration theory. The tests with no additional artificial consolidation are shown in Table 45, and these results offer a better opportunity for comparison with full scale rapid gravity filtration. The greater plan area of a full scale filter may lead to more consolidation than in the pilot plant due to the reduced wall effects.

Table 45 - Overview results from all settled bed testing (C1 – Slate, C2 – Filtralite, C3 – Glass and C4 – Sand)

Test	Date	Flowrate	Headloss								Turbidity (NTU)			
			Initial (mm)				Accumulation (mm/hr)							
			C1	C2	C3	C4	C1	C2	C3	C4	C1	C2	C3	C4
10	01/02/2012	8.56	514	107	192	385	86	36	70	135	0.034	0.038	0.035	0.035
11	03/02/2012	7.44	160	83	175	311	52	36	48	83	0.031	0.037	0.032	0.031
12	10/02/2012	6.51	136	73	151	268	52	30	57	76	0.030	0.039	0.032	0.031
13	13/02/2012	5.45	126	59	121	254	38	22	38	62	0.038	0.049	0.040	0.038
14	16/02/2012	4.46	106	51	105	174	25	17	30	47	0.040	0.054	0.042	0.039
15	20/02/2012	2.88	80	37	77	137	19	11	20	33	0.058	0.074	0.060	0.054

The results from the unconsolidated test runs 10 - 15 in Table 45 are consistent in pattern with the operating data in the previous consolidated trials (1 – 9), however test 10 showed an abnormally large initial and accumulated headloss value as a result of iron sediment that was dislodged from the inlet pipework into the filter and that had not been cleared sufficiently prior to operation.

The data shows that:

- Filtralite (C2) always has the lowest initial headloss, while the other alternative media (glass and slate) also show lower head loss compared to sand. The variation between sand and these media is greater in the packed bed; this is due to the angularity of the alternative media that reduces the impact of packing. The large pore size of the Filtralite is also proportionally less affected by consolidation than the other smaller sized media. Packing is important as the closer the media is packed the greater the influence of the entering floc particles. Filtralite with the largest pore size will be more capable of dealing with the floc than the other media.
- As predicted from laboratory testing, the accumulated headloss between the media follows a similar trend to the initial headloss results. Filtralite shows the best performance due to its increased particle size which is more suited to the water

being treated. The alternative media, as with the laboratory scale testing, again show improvements in performance over sand.

- A combination of improvements in the initial and accumulated headloss from the alternative filter media gave greater run times than sand, while maintaining turbidity values that were similar to sand (slate and glass) and below the 0.1 NTU performance limit imposed by the works (Filtralite). The lower head loss and larger run-times would save on operating costs while not leading to any degradation in water quality through the use of alternative filter media.
- Filtralite, as in the laboratory studies, exhibited the poorest turbidity performance, while the other media all performed similarly. It is suggested that the iron floc was having a significant impact on the results however and without the carryover of iron floc the results would be what was observed in the laboratory.

7.2.2 TURBIDITY REMOVAL

Figure 97 (packed bed) and Figure 98 (un-packed bed) show the average turbidity against flow rate for the duration of the filter run after ripening has occurred. The point at which ripening had been considered complete was when the turbidity fell below 0.1 NTU. For all test runs the turbidity was always below 0.1 NTU which suggests that all the media are suitable for use at full scale at this works, but the impact of floc carryover must also be considered. The results in both Figure 97 and Figure 98 show the effect of flowrate, due to the low inflow turbidity. It was likely that the floc caused extra straining of small particulates in the upper layer of the filter. The increase in outflow turbidity from the filters seen in Figure 98 as the flowrate decreases was due to an increase in clarified water turbidity during this period of time and not due to variations in flowrate.

The variation between the packed bed (Figure 97) and un-packed bed (Figure 98) is minimal, and is difficult to determine at the lower flowrates due to the increase in clarified water turbidity. However the results for the higher flowrates were conducted under similar clarified water turbidities and the results for the un-packed beds are marginally higher than the packed bed which would be expected due to the increased pore size in an un-packed

bed. As the clarified turbidity increased in the packed bed trials at the lower flow rates the performance of the Filtralite appears to deteriorate at a greater rate than the other media, this is similar to the results seen in the laboratory with the increase in turbidity from 9 to 35 NTU impacting the Filtralite more significantly. This would be expected to be more evident if a reduction in floc carryover occurred.

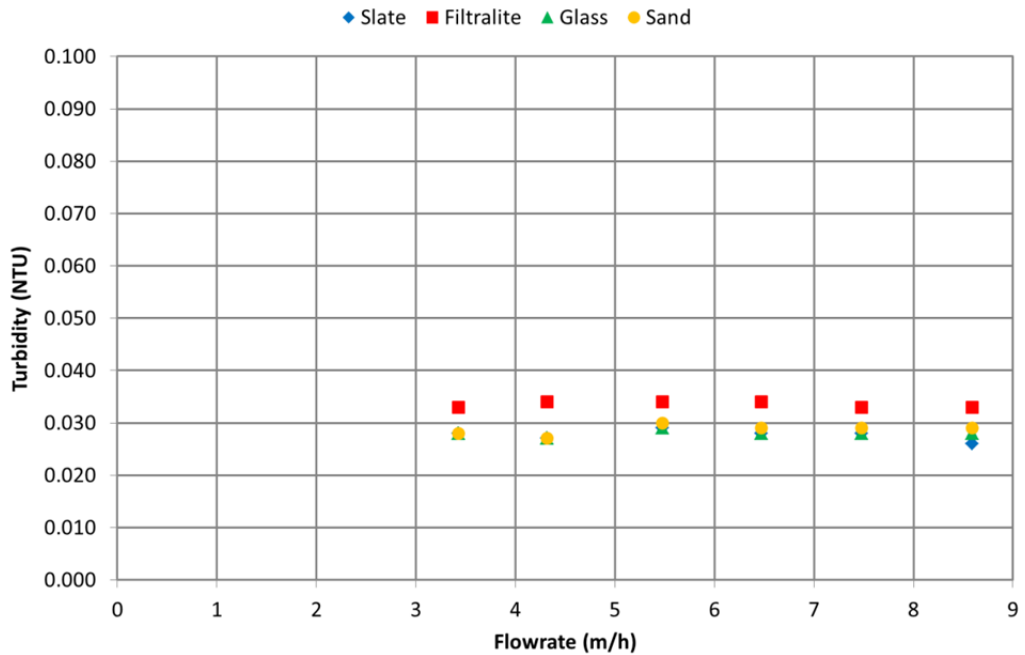


Figure 97 - Overview of turbidity results for packed bed pilot trials

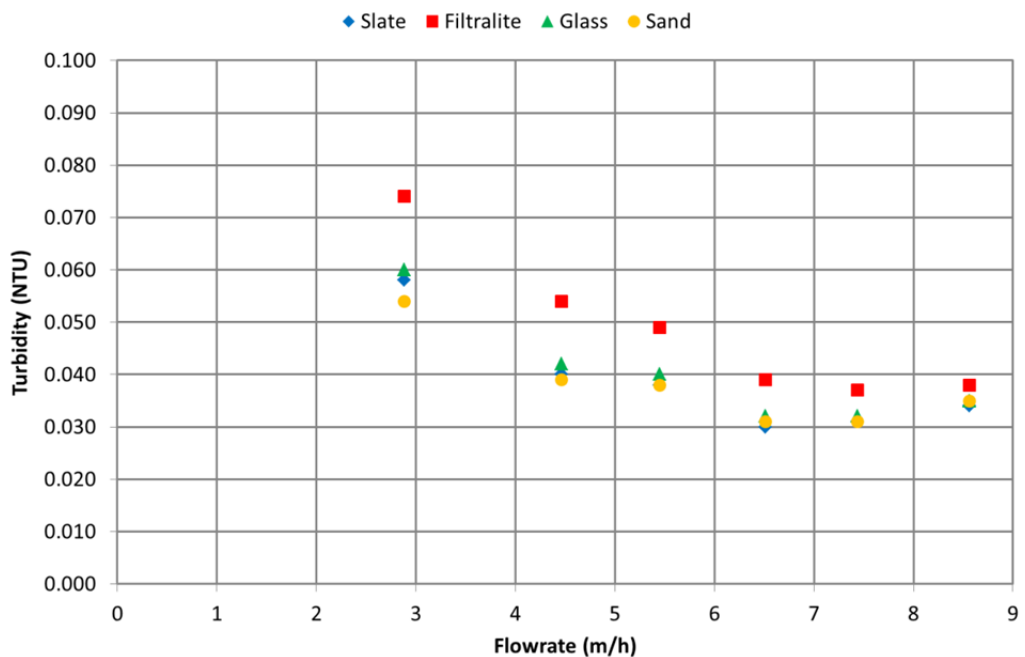


Figure 98 - Overview of turbidity results for un-packed bed pilot trials

The performance of the similarly sized media (sand, glass and slate) is identical in both packed and un-packed tests, considering the low clarified water turbidity (0.1 – 0.3 NTU) any variations between these media is within experimental error. Floc carryover is thought to be affecting the results as glass is performing better than the expectations from laboratory study. This is likely due to the fact that floc straining is occurring more as floc particles accumulate in each pore at the surface of the filter media and this will improve the removal of suspended particles. Filtralite, with its greater particle size and therefore porosity, is better able to accommodate the floc and so the straining that is occurring is having a lesser effect than in the smaller particle sized media which is why it performs not as well as the other three media. When floc is entering a filter as it was in this study, the turbidity performance of a filter will be impacted more by the filter media size and the associated pore size (angularity will also impact pore size). Thus it is suggested that improvements in turbidity removal by the fundamental mechanisms of deep bed filtration are not likely to have a significant impact on filter performance in this case, but in the absence of floc then they would become more dominant. Large media such as Filtralite would be expected not to perform as well as smaller more angular media such as slate. This behaviour was indicated by the more effective turbidity removal under controlled laboratory by the smaller media.

Figure 99 gives an example of typical turbidity results for a full filter run, the results corroborate the theory that iron floc straining is the dominant removal mechanism. Sand is shown to be the best performing media for turbidity removal but also shows the shortest filter run. The consistency of the performance of sand also improved due to progressive clogging of the smaller pore sizes and increased straining in the upper layer of the filter improving turbidity removal by effectively reducing the filter pore size. The same occurs in the glass and slate media with continually improving turbidity performance throughout the filter run. Filtralite shows improvement which does not reach the values of the smaller media.

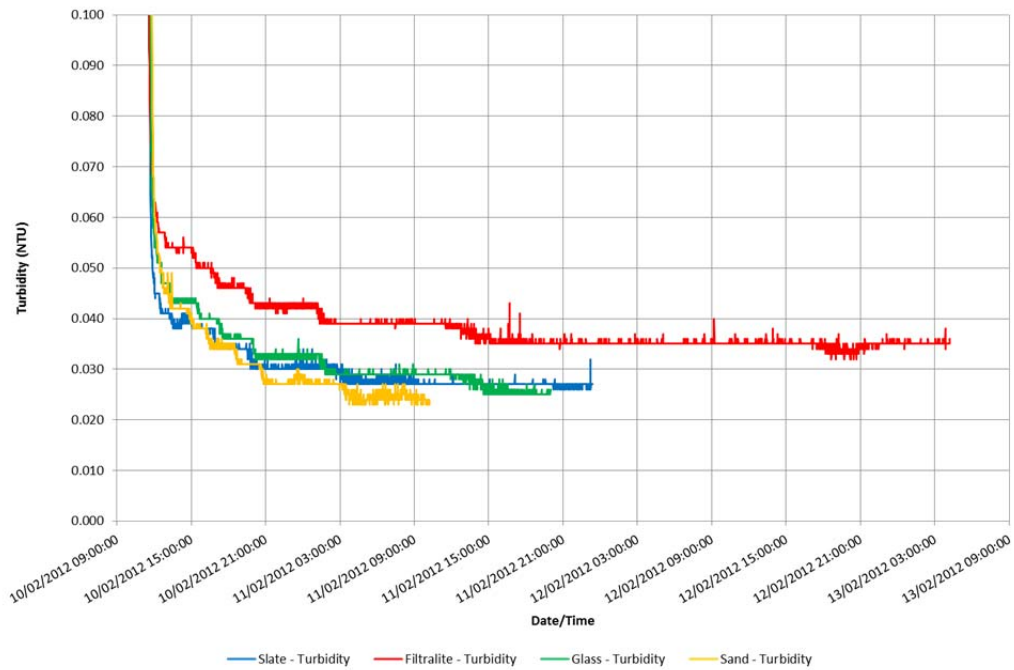


Figure 99 - Example of turbidity variation during test run 12

For consideration of improvements in fundamental flowpath removal mechanisms pointed to by the laboratory studies, only the ripening period can truly be considered as iron floc will have a lower impact during this period after which straining is more dominant. A media that shows a more effective ripening period can be expected to have improved fundamental mechanisms of removal and from laboratory studies this would be expected to be the media with the lowest sphericity which is the case with slate showing the lowest turbidity in ripening. Glass and sand follow similar trends, and although glass is angular the results from laboratory studies show that its performance is hindered by its narrow particle size band and smooth surface. The results do show that for the works the pilot plant was operating at all media were suitable considering the performance indicator is turbidity less than 0.1 NTU.

7.2.3 HEADLOSS

A maximum allowable headloss after which the filter run was considered complete was set at 2 metres, this was based on initial testing that showed beyond 2 metres headloss the flowrate through the filter media began to reduce, this can be seen in Figure 100. After 2 metres headloss part of the flow has begun to divert out of the pressure relief valve as the pressure above the filter bed has increased to near and above 0.3 bars. With a 2 metre headloss limit imposed there was no turbidity breakthrough observed during the study.

Beyond 2 metres there was also no breakthrough but the flowrate through the filter bed was gradually reducing and the results during this stage would not be considered representative.

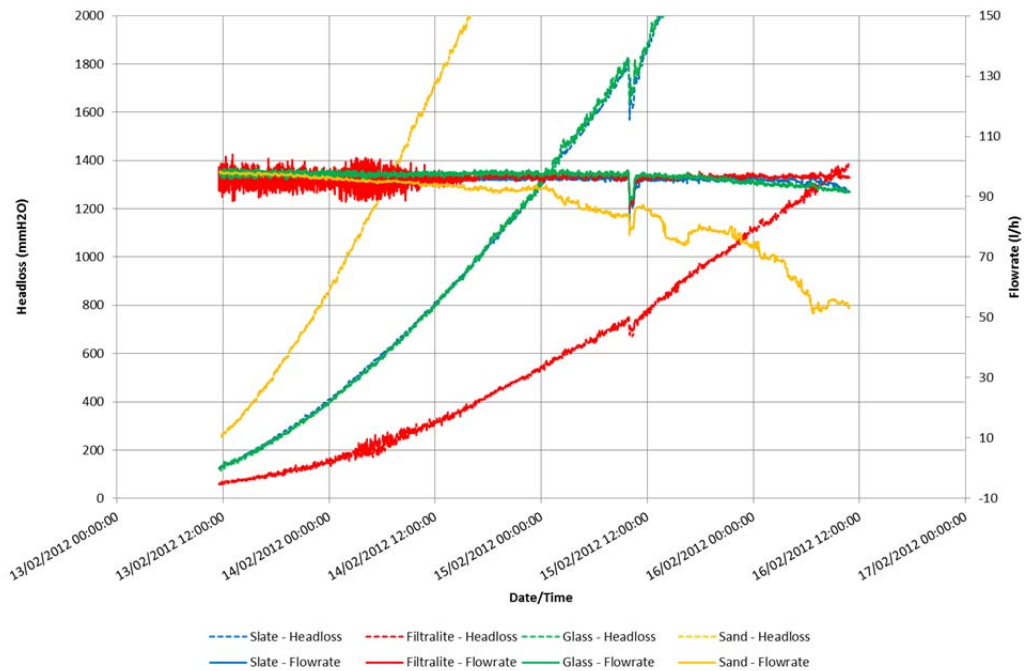


Figure 100 – Example of flowrate change after 2000 mm headloss during test 13

Filter run-time is governed by both the initial headloss and accumulated headloss, the initial headloss is governed by the bed characteristics and flowrate. Due to variations in clarified water quality between the laboratory and pilot study only the initial headloss can be compared directly and these results are shown in Table 46. Consideration must also be given for variations in water temperature between the various tests. The comparison between the packed bed pilot trials and the packed bed laboratory trials under similar consolidation show that the initial head loss is increased in the pilot plant compared to the laboratory columns. This increase is likely due to the impact of the smaller diameter (60 mm) columns in the laboratory leading to wall effects reducing the ability of the media to pack as tightly as was possible in the larger (150 mm) pilot columns. The reduction in the un-packed beds is to be expected although the result for slate is higher than anticipated due to an observed surge of accumulated solids entering the filter (time constraints limited the ability to re-run the test). The change in other media from packed to un-packed shows approximately a halving of the initial headloss. Packing of the pilot columns when allowed to consolidate naturally is expected to be nearer the packing expected in a full scale filter but not identical because of enhanced wall effects which will limit settlement.

Table 46 - Comparison of initial headloss between laboratory and pilot studies at approx. 8.6 m/h

	Laboratory		Pilot	
	35 NTU	9 NTU	Packed	Un-Packed
Slate	276	258	313	514
Filtralite	147	160	189	107
Glass	360	358	401	192
Sand	684	726	775	385

Results for initial headloss are given in Figure 101 (packed) and Figure 102 (un-packed), the results match those from the laboratory studies with sand showing the greatest headloss. The works was operating at an initial headloss of approximately 300 mm at a flowrate of 5.5 m/h in the 24 m² filters, this compares to a result of 260 mm found in the un-packed trials (Figure 102) in the pilot plant.

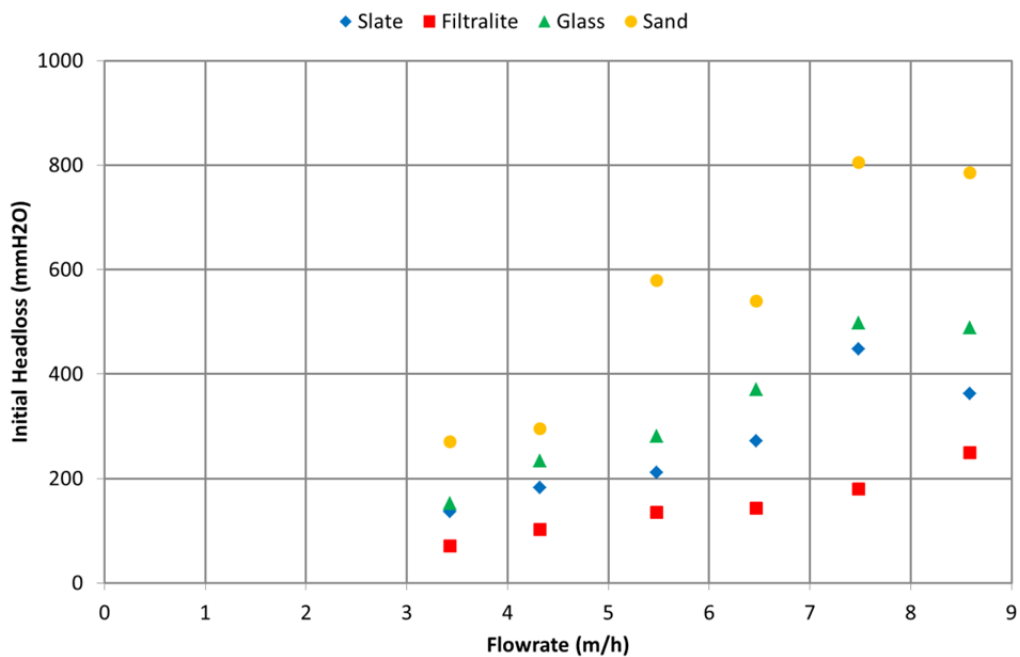


Figure 101 - Overview of initial headloss results for packed bed pilot trials

The sand also shows more erratic results in the packed bed trials (Figure 101) for the flowrates of 5.5 and 7.5 m/h. This is possibly due to the impact of mudballing previously described that was not fully cleared from the system until after a number of backwashes had been completed.

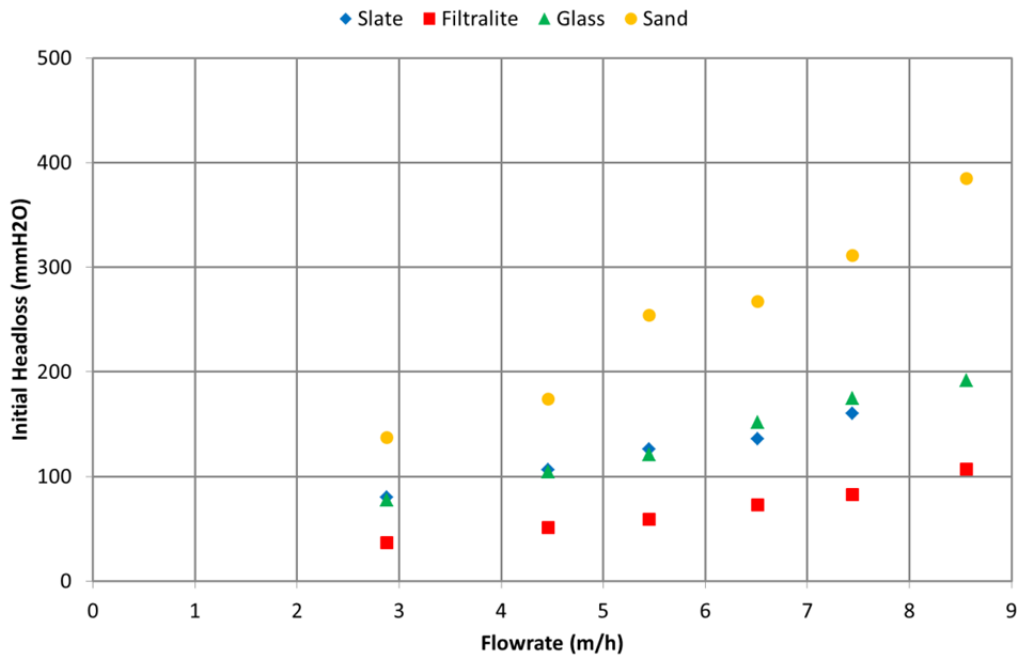


Figure 102 - Overview of initial headloss results for un-packed bed pilot trials

Figure 103 shows an example of how the headloss varies during a typical filter run (see Appendix IV). It is clear that as the filter run continues the headloss accumulation continues to increase. This effect is most prevalent in the sand, and this is due to the spherical shape and particle size giving rise to low pore sizes between the filter media combined with the impact of accumulating iron floc. This rounded media such as sand packs uniformly throughout the bed with an even pore distribution in all dimensions, whereas an angular media such as the slate and glass will pack with a less uniform pore distribution and therefore permeability will vary in all dimensions.

In typical filter operation, flow will seek out the path of least resistance. In sand no clear path exists while in slate there will be areas of preferential flow based on these areas of highest permeability and therefore the lower headloss. Ignoring the floc affecting these results, the area with the greater flow will also receive the greater proportion of suspended particles and if it is in these zones of high permeability where particles attach then their impact on the headloss will be low. Sand does not have areas of higher permeability and suspended particles will attach uniformly throughout the filter bed, combined with the lower permeability from the tighter packing of the spherical media this will create a greater headloss than an angular media such as slate or glass. Therefore the more angular filter

media the lower the accumulated headloss by attached particles and more prevalent areas of high porosity from variable packing of the filter media.

Glass shows similar headloss performance to the slate, it is an angular media too and gives similar headloss benefits to those discussed above. This is different to the previous laboratory studies where the head loss from glass was similar to sand. This may be attributed to floc carryover. Filtralite, with its greater particle size, has a high permeability throughout the bed and in all dimensions and therefore will always show the lowest headloss accumulation, especially when coupled with a poorer turbidity removal and therefore less solids accumulation within the bed which is the primary cause of headloss accumulation.

Iron floc entering the filter was observed to settle on the surface of the media and also was visible as an iron coloured layer up to 100 mm deep on the surface (Filtralite) and this shows that straining of this material was the dominant particle removal mechanism. Straining will lead to reduced filter headloss performance as there is a concentration of solids in the upper layers that are not distributed through the filter bed and increases the rate of headloss accumulation as solids concentrate at this point. This greater headloss can be seen by comparing the laboratory and pilot studies. The Filtralite shows significantly lower headloss over all other media, this is because its greater pore size reduces the likelihood of the floc clogging the pores on the surface of the media and this was corroborated by the observed thicker layer of iron saturated media.

Glass filter media has a smooth surface, lacking any features that would increase the resistance to flow (see Figure 44), and this, with a lower fines content than the sand (glass size grading of 0.7 – 1.0 mm), means it is better able to deal with the floc than similar sized sand. The angularity of slate and glass increases variability in permeability as discussed and will also aid in dealing with the floc carryover as it will be more likely to attach in areas of higher permeability where the impact of attached particles is less severe.

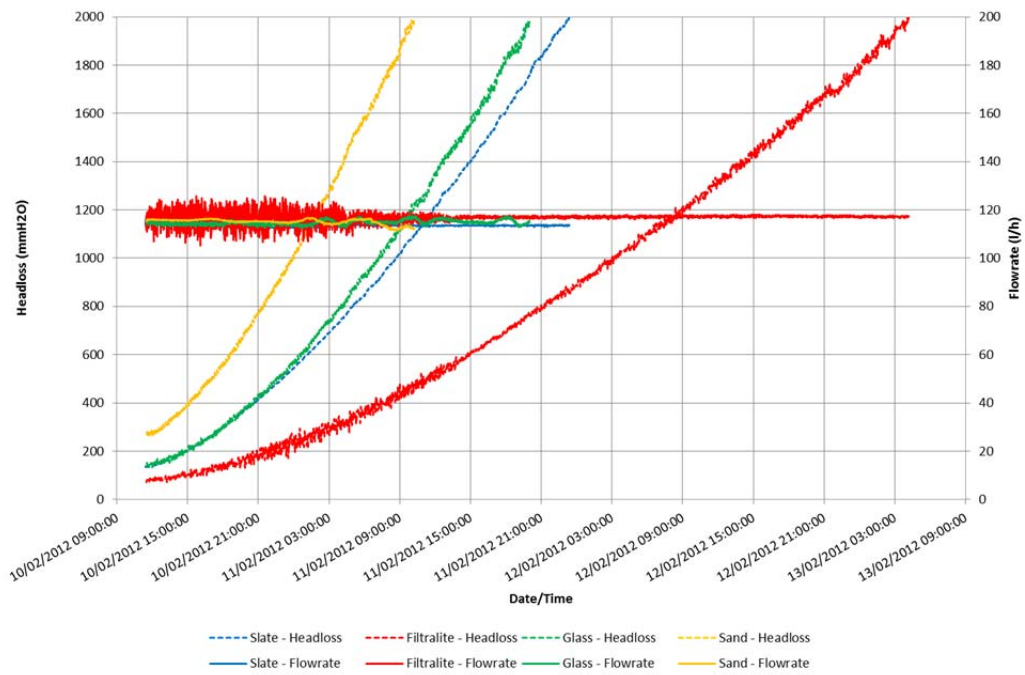


Figure 103 – Example headloss variation during filter test run 12

Headloss is often the determining factor ending a filter run and therefore the variation in filter run-time against flowrate with both Figure 104 (packed), and Figure 105 (un-packed), offer an insight into the run-times before a maximum headloss of 2 metres was reached. An increase in filter run time offers a reduction in operating costs by reducing the frequency of backwashing which requires pumping, while also reducing wastage of final treated water that is used to clean filters. An increased filter run time would also lead to a higher concentration of solids in the backwash water that would possibly improve optimisation of treating this waste water.

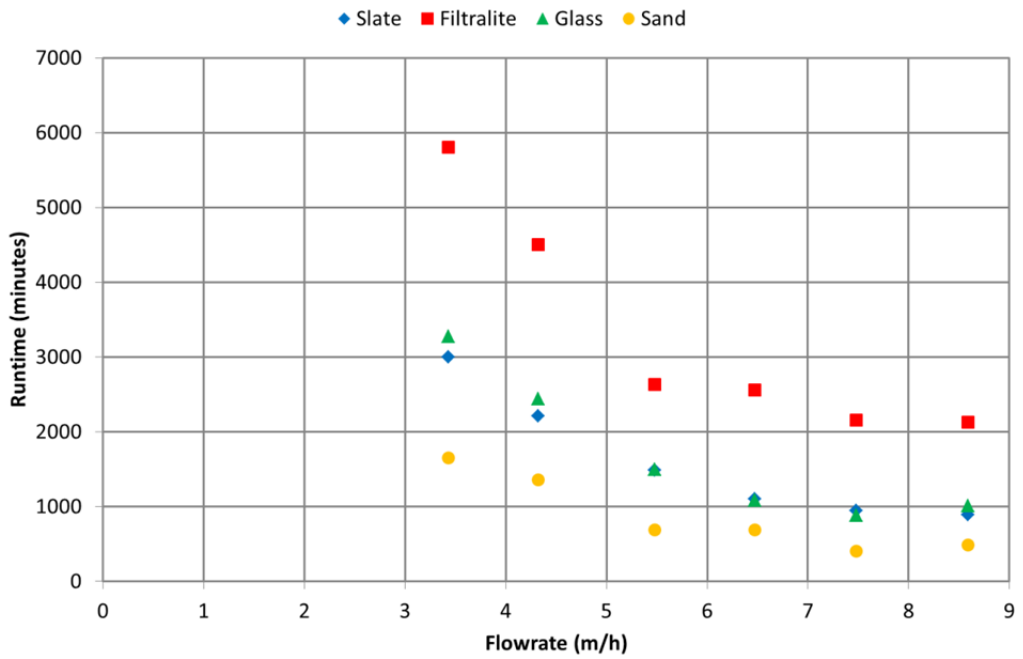


Figure 104 - Filter run-time results for packed bed pilot trials

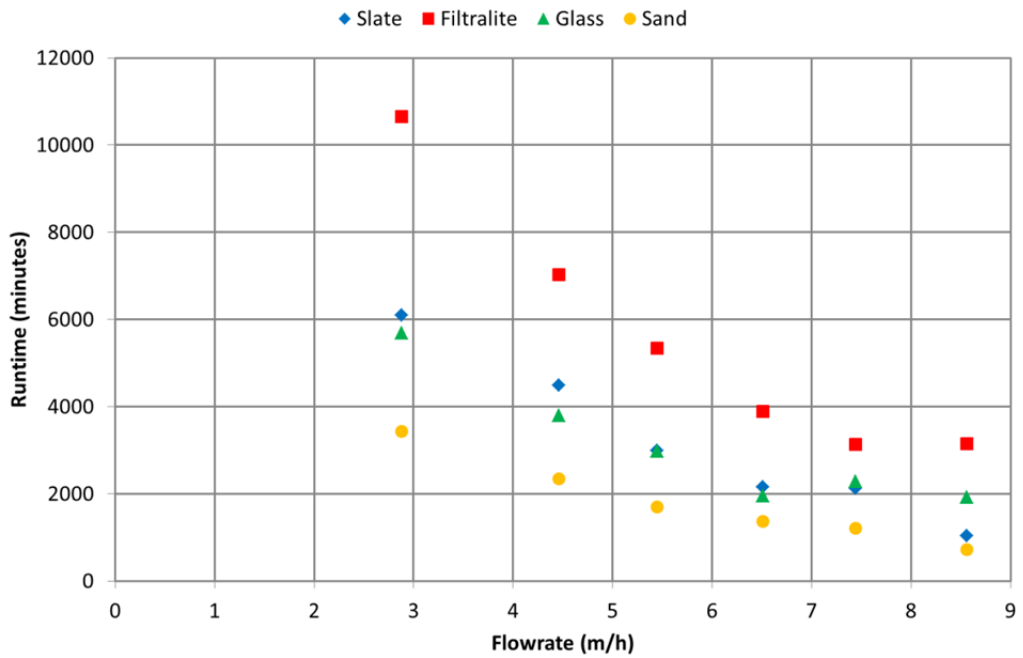


Figure 105 - Filter run-time results for un-packed filter bed pilot trials

Optimisation of the filter media used to match the clarified water quality or multi-media may be a method of achieving the greatest filter run time increase without compromising turbidity performance if the density can be varied. In this case the Filtralite offers the

greatest filter run-time, however without the iron floc the other media would be expected to show increased run-times, but this is speculation without further testing.

The impact of angularity on headloss can be analysed further by comparing initial headloss with the theoretical retention time of each filter media which is shown in Figure 106 below:

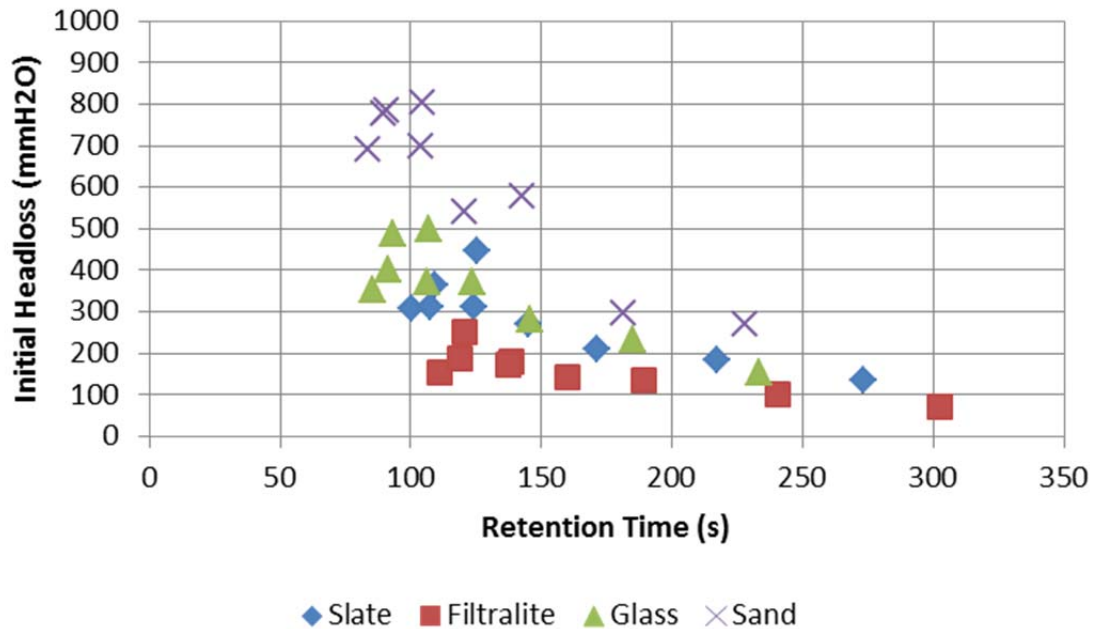


Figure 106 - Relationship between initial headloss and retention time for packed bed trials

It is well known that an increased flowrate will lead to a higher initial headloss and this is shown by the increased initial headloss in all media as their retention time reduces. The chart highlights the variation in the rate of change of headloss between the four filter media tested in the pilot plant. Based on the laboratory studies and these results, this has been attributed to the angularity of the filter media and therefore the rate of change as a slope of a linear trend line (from Figure 106) was plotted against the sphericity of each of the four media to produce the results shown in Figure 107.

Filtralite is plotted on the chart to show the impact of a significantly different particle size on the results, the other media follow a path that shows they are related and as sphericity increases to nearer 1.0 (perfectly spherical) the initial headloss will be affected by changes in retention time (which is a measure of all properties that impact on the flowrate through the filter bed). The reasons for this have previously been discussed as the close packing of spheres compared to the more variable packing arrangement of angular media. The results

show that as sphericity reduces the variability in permeability throughout the bed becomes greater to improve headloss performance while in turn helping to improve the transportation mechanisms.

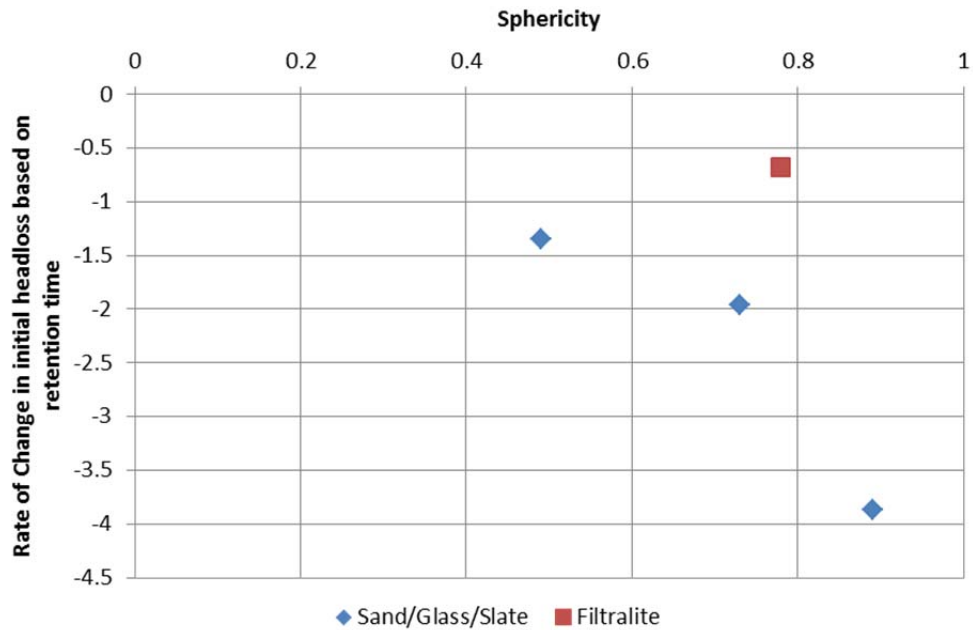


Figure 107 - Impact of sphericity on rate of change in initial headloss

Further testing using a range of media with differing sphericity is required to test these theories as at present a sample of three will not be statistically valid. However it would appear that there is a distinct variation in the sphericity region of 0.6 – 0.7 where the rate of change with sphericity beings to slow with reducing sphericity. As stated previously this is a similar pattern to the change in in initial headloss with sphericity shown in the laboratory scale testing and overturns the ideas held by Ives (1975) that a sphericity value below 0.6 would be detrimental to headloss. This also goes against the reasons for choosing well-rounded sand grains that have dominated rapid gravity filtration since their inception, especially when considered alongside the turbidity results.

7.2.4 ANALYSIS

This pilot study was affected by iron floc carryover from the hopper bottom clarifiers, this will impact the results as follows:

- Reduction in filter run-times caused by clogging of the voids in the filter bed by large floc, this will accelerate the rate of headloss accumulation.
- Turbidity removal will be improved as straining becomes a significant removal mechanism due to floc accumulation in the upper layers.

Sand was most affected by the presence of the iron floc; the outflow turbidity was lower than other identically sized media caused by increased straining. It also showed the greatest headloss accumulation caused by the small uniform pore size rapidly clogging. The opposite is true for Filtralite which unfortunately is only made in this larger size, and due to the increased size the pores were larger and capable of reducing the amount of straining occurring in the upper layers, leading to improved headloss performance but diminished turbidity removal compared to sand.

The mudballing that was observed to occur using the initial backwashing procedure will also cause problems if occurring in full scale filters as they transport contaminants through to the base of the filter bed where they are likely to be broken down and where there is the possibility of them entering the filtered water. These contaminants include pathogens such as cryptosporidium. There is also a risk from sudden change in the amount of floc carryover. Filtralite or larger media could be considered the most suitable media under the conditions experienced based on all results but it is expected that if the iron floc was removed that the turbidity removal performance would not be as good as the other media, as the fundamental transportation mechanisms cannot overcome the large pore size of the media, this has been shown in laboratory studies.

Turbidity performance was acceptable for all filter media across all flow rates. There was only one test (run 15) where the turbidity exceeded 0.1 NTU and this was for Filtralite. This followed a works shut down that led to increased clarified water turbidity. The other media also had increased turbidity but did not break above 0.1 NTU. It is expected that if contamination from the iron floc occurred, the performance of all filter media would be enhanced but headloss would increase, both because of the contribution from straining in the upper layers. Results from the pilot plant follow theories developed in laboratory testing and by Ives (1975), with angular media showing improved turbidity performance due to the torturous path through the bed. Straining led to improvements in performance in the sand

which was the smallest media and so it was difficult to determine variations due to the floc accumulation throughout a filter run but improvements in ripening before straining can become dominant also show improvements in the angular media such as slate. As predicted from laboratory studies the Filtralite with its greater particle size performed the worst although its performance was still adequate, and this does highlight the importance of optimising filtration by carefully selecting a filter media to match the clarified water quality.

Run-time and therefore operating costs would gain a significant benefit from the use of alternative filter media. Under the conditions of this pilot study at the works flowrate (5.5 m/h), Filtralite would lead to an additional 2.6 days of run-time compared to sand. Floc carryover again has influenced the results and limits their viability to HBC or similar clarifier systems upstream of the filters, however this does further show how understanding in detail the clarified water quality is key to selecting an appropriate filter media. Initial headloss performance in the media of similar particle size (sand, glass and slate) followed the same trend as in the laboratory studies with a consolidated media, with greater angularity leading to lower initial headloss. Results from the un-packed trials show glass and slate to perform nearly identically for both initial and accumulated headloss; this is expected to be due to the packing arrangement of the filter media being similar under these conditions.

Variations in clarification processes would be expected to produce a wide range of clarified water qualities, however using on-line turbidity and robotic iron detection as the dominant monitoring devices limits the ability to detect large particles as this work on-site shows. Floc carryover is unlikely to be detected at any other works using these monitoring methods and further development of the monitoring equipment beyond turbidity and soluble iron is required to gain further knowledge of the clarified water quality that modern filters must be able to deal with. Optimisation of filters is not possible without a long term and detailed analysis of the clarified water they must treat. In the conditions of this works where the floc carryover is not detected by the turbidity or soluble iron monitors a media would be specified to treat an inflow turbidity of 0.1 – 0.3 NTU with no consideration for larger particles. Under these conditions a fine media would have been suggested when in fact Filtralite has shown to be suitable based on turbidity and has significant improvements in filter run time, although with flocs it is recommended long term monitoring should form the basis of a separate study to determine if floc carryover is a continual occurrence.

The problems described by the early pioneers of filtration (circa. 1930) as described in Hendricks (2005, p. 529) are listed in the Introduction (Section 0) as:

- Maintaining effective coagulation
- Lack of laboratory control
- Education of operators
- Under-drain design
- Inadequate backwash design associated with control of mudballs and surface cracking

What has been determined from the pilot study and from discussions with various utilities is that these problems still exist in operating water works. The primary cause of the problems observed on-site is due to the clarification process not working well, either as a consequence of hydraulic balancing between tanks or from ageing and releasing floc into the post clarified water. Mudballing was observed in the pilot columns and a highly vigorous wash procedure was required to limit their creation. It is not known if they occur in the full scale filters on site as core samples would be required and this was beyond the scope of the project. Air-scour during backwashing was observed to not be evenly distributed across the full scale filters and this will be due to the under drain system being clogged or damaged, also design of the distribution pipes at the base may also be insufficient. As these problems are still evident today it highlights the lack of progress to develop effective solutions.

8 SUMMARISING DISCUSSION AND CONCLUSIONS

The aim of the work was to assess possible alternative filter media for use in rapid gravity filtration, whilst assessing their performance in relation to the fundamental theory of filtration. It is possible to recommend from this work that an understanding of which properties are beneficial to media performance can be used in future to select media to treat specific water qualities. The current generic use of a single size of sand does not account for variations in clarified water quality and other variations in upstream treatment processes that impact on the chemistry and characteristics of the water to be treated by rapid gravity filtration.

The fundamental properties of the filter media chosen were analysed based on international standard tests for filter media, and additional parameters to gain further understanding of key variations between other mineral media and sand. These criteria developed from this combination of tests were then compared with the performance of the filter media in first controlled laboratory studies and then pilot trials. These results provided additional knowledge of what filtration mechanisms were being impacted by the variations in media during these continuous trials and corroboration of the benefits they had on filtration. The ideas developed during laboratory testing were scaled up to pilot studies on selected alternative filter media to give confidence on their application in continuous trials. The pilot study also highlighted the impact of changes in water quality, and highlighted a range of areas that require further work in the future to aid in optimisation.

Not all possible alternatives have been considered in this study and there are other materials that would be worthy of further research. The media chosen were selected by the initial characterisation to have a range of properties for an academic comparison of performance and fundamental theory.

The basic properties of size and shape were found to be the most important. It was however also concluded that the negative influence of flatter (angular) media had been overestimated in previous literature; this work shows some angular variability had beneficial effects on filtration performance. It was also concluded that filter media could be adapted to improve the performance of rapid gravity filters, according to each works. The main recommendation would be that adjustments in media size should be made to match the

clarified water quality, upstream treatment processes and their variability. It is also recommended that a detailed cost/benefit analysis of dual stage filtration to replace the current universal coagulation/filtration system should be considered especially at sites that treat very low raw water turbidity. The results from this study indicate chemical coagulants could increase the solids load in these circumstances.

The factors that have been determined to impact filter performance the most from this study are given as:

- The particle size range of the filter media was confirmed as the major impactor on performance; this was expected from the literature review. The results (Filtralite) show increased media size led to lower headloss but reduced turbidity removal. It was suggested that the particle size range was an important consideration when selecting filter media and could be matched to the anticipated clarified water quality.
- Lower sphericity filter media was shown to improve turbidity removal by creating more varied and torturous flow paths through the filter bed, confirming the literature. This result was attributed to an increase in particles being transported to the media surface through the mechanism of inertia.
- Lower sphericity filter media also improved headloss performance; this was shown to be due to the creation of a varied bed porosity and permeability throughout the filter bed. This varied permeability creates preferential flowpaths through the bed that the majority of particles will flow through creating larger areas for particle accumulation without hindering flow.
- It was concluded that a lack of roughness on the surface of the glass was affecting its turbidity removal performance. The smoothness contributed to the detachment of particles as there was no effective shelter from any flow changes in the filter bed.
- In common with previous work (Mg dosing of filters) increased removal of common metals can be obtained if the filter media increases the hydroxide precipitation in the clarified water. Results with limestone showed precipitation of a range of metals

within the filter which also improved turbidity removal and could reduce the load on other treatment units e.g. reducing dependence on coagulation and GAC. These tests were at laboratory scale and further work would be needed to determine media losses and backwashing.

The overall conclusion was that the advantages of alternative media designs outweighed the disadvantages and there was potential benefit from the use of alternative media or through changes to the design of the standard sand (increased angularity) to bring about case specific improvements. A lack of long term full scale demonstration and DWI approval and therefore risk will hinder their adoption within the industry.

There is additional work needed to build upon the research conducted and the range of problems observed with the operation of rapid gravity filters. There are now opportunities to fabricate filter media to suit a particular water quality and reduce dependency on GAC or RO.

- The research has highlighted media sphericity as a key characteristic and controlled experiments are required to further the understanding of the relationship between angularity and turbidity removal and headloss. This would ideally be done through specifically designed laboratory experiments with well controlled media specifically designed for the experiment.
- Results suggested surface roughness (glass) is important in avoiding re-suspension. These experiments however need more work to quantify how much of an impact roughness versus specific surface area has. This could be provided by acid etching the surface of a media so that identical materials can have varying surface characteristics.
- Chemical coagulants have significant impact on filtration; the results show floc entering the pilot plant. The larger particle size range of Filtralite allowed it to cope with this problem, the presence of the floc in all the filters however also enhanced turbidity removal. Experiments conducted with different particle sizes of media should be carried out to create a suitable design model for treatment of a range of water characteristics. This would aid in selection of filter media in future to meet the requirements of a particular water works.
- Currently within the industry the primary methods for assessing clarified water quality are on-line turbidity and robotic coagulant monitoring (Iron or Aluminium typically). The pilot study results identified problems associated with these analytical methods which require interpretation to optimise plant performance rather than to meet the standard. Further work in the area to confirm how iron floc is to be detected and to confirm the limitations of the current monitoring equipment. In

addition an analysis of alternative methods of monitoring are required to allow for characterisation under a wider range of raw water qualities.

- Backwashing has not been considered in detail and further research is required to ascertain the impact of alternative filter media on the backwashing process. It has been observed in the pilot plant that insufficient backwashing can lead to the problems of cracking and mudballing also observed at the full scale. A balance to maintain sufficient backwashing while reducing media loss is still to be found. Based on the operational experience of the pilot plant, backwashing should be studied in a specifically designed apparatus to ensure less change in results with scale-up.
- A detailed study should be carried out to determine the current design criteria of filtration within the UK. This would require a database of filter designs managed by an independent organisation (UKWIR, ICE) and the upstream treatment processes at the works. Carrying out an industry wide survey such as this would allow for a better understanding of the variations and common water qualities filtration encounters. Analysis of the design of filters will highlight the backwashing and design limitations for alternative filter media use.

- Aksogan S, Baştürk A, Yüksel E, Akgiray Ö (2003) On the use of crushed shells of apricot stones as the upper layer in dual media filters. *Water Science and Tehcnology*. **11**(12), 497-503
- Arnepalli D N, Shanthakummar S (2008) Comparison of methods for determining specific-surface area of fine-grained soils. *Geotechnical and Geological Engineering*. **26**, 121-132.
- Albuquerque C M, Labrincha J A (2008) Removal of contaminants from aqueous solutions by beds made of rejects of the lightweight aggregates production. *Ceramics International*. **34**, 1735-1740
- American Water Works Association, 2010. *ANSI/AWWA B100-09 Granular Filter Material*, AWWA.
- Aziz H A, Smith P G (1996) Removal of manganese from water using crushed dolomite filtration technique. *Water Research*. **30**(2), 489 – 492
- Aziz H A, Adlan M N, Ariffin K S (2008) Heavy metals (Cd, Pb, Zn, Ni, Cu and Cr(III)) removal from water in Malaysia: post treatment by high quality limestone. *Bioresource Technology*. **99**, 1578-1583
- Baker M N (1948) The Quest for Pure Water. *American Water Works Association, New York*
- Baylis J R (1956) Seven years of high rate filtration. *Journal American Water Works Association*. **48**(5), 585-596.
- Beard J D, Tanaka T S (1977) A comparison of particle counting and nephelometry. *Journal of American Water Works Association*. **69**(10), 533-538.
- British Standards Institution, 2004. BS EN 12902:2004 Products used for the treatment of water intended for human consumption – Inorganic supporting and filtering materials – Methods of test. BSI.
- British Standards Institution, 2005. BS EN 12904:2005 Products used for the treatment of water intended for human consumption – Silica sand and silica gravel. BSI.

British Standards Institution, 2005. BS EN 12905:2005 Products used for the treatment of water intended for human consumption – Expanded aluminosilicate. BSI.

British Standards Institution, 2005. BS EN 12906:2005 Products used for the treatment of water intended for human consumption – Pumice. BSI.

British Standards Institution, 2005. BS EN 12907:2005 Products used for the treatment of water intended for human consumption – Pyrolyzed coal material. BSI.

British Standards Institution, 2005. BS EN 12909:2005 Products used for the treatment of water intended for human consumption – Anthracite. BSI.

British Standards Institution, 2005. BS EN 12910:2005 Products used for the treatment of water intended for human consumption – Garnet. BSI.

British Standards Institution, 2005. BS EN 12912:2005 Products used for the treatment of water intended for human consumption – Barite. BSI.

Camp T R (1964) Theory of water filtration. *Journal of Sanitation Engineering Division, Proceedings of American Society of Civil Engineers*. **90**, 1-30

Carter D L, Heilman M D, Gonzales C L (1965) Ethylene glycol monoethyl ether for determining surface area of silicate minerals. *Soil Science*. **100**(8), 356-360.

Chowdhury Z K, Moran M, Lawler D, Van Gelder A (1997) Evaluation of preservation and shipping protocols for batch counting of particles from full-scale WTP. *Proceedings of the AWWA Water Quality Technology Conference*,

Davies P, Wheatley A (2011) Alternative filter media in rapid gravity filtration of potable water. *Proceedings of IWA Young Water Professionals UK Conference 2011*, Edinburgh, UK.

Degrmont G (1979) *Water Treatment Handbook*. Firmin-Didot S.A. Paris

Elimelech M, Gregory J, Jia X, Williams R A (1995) *Particle deposition and aggregation: measurement, modelling and simulation*. Butterworth-Heinemann, Oxford

- Eikebrokk B, Saltnes T (2001) Removal of natural organic matter (NOM) using different coagulants and lightweight expanded clay aggregate filters. *Water Science and Technology: Water Supply*. **1**, 131-140
- Evans G, Dennis P, Cousins M, Campbell R (2002) Use of recycled crushed glass as a filtration medium in municipal potable water treatment plants. *Water Science and Technology: Water Supply*. **2**, 9-16
- Farizoglu B, Nuhoglu A, Yildiz E, Keskinler B (2003) The performance of pumice as a filter bed material under rapid filtration conditions. *Filtration+Separation*. **40**, 41-47
- Fitzpatrick C S B (2005) Crushed recycled glass as a filter medium. *Proceedings of IWA International Conference on Particle Separation*. Seoul, Korea.
- Galvis G, Visscher JT, Latorre J (1998) *Multi-stage filtration and innovation water treatment technology*. International reference centre for community water supply and sanitation. The Hague, Netherlands and Universidad del valle instituto CINARA, Cali, Colombia.
- Ghebremichael K A (2004) *Moringa seed and pumice as an alternative natural materials for drinking water treatment*. Ph.D. KA Royal Institute of Technology.
- Glasgow G D E (1998) *Small continuous flow rate fluctuations in rapid gravity filtration*. Ph.D. Loughborough University.
- Graetz D A, Nair V D (2000) Phosphorous Sorption Isotherm Determination. *Methods for P Analysis*, Pierzynski G M.
- Graham N J D (1988) Filter pore flocculation as a mechanism in rapid filtration. *Water Research*. **22**(10), 1229-1238
- Gray N F, Learner M A (1984) Comparative pilot-scale investigation into uprating the performance of percolating filters by partial medium treatment. *Water Research*. **18**(4), 409-422

- Hallsworth C R, Knox R W O'B (1999) (PDF) BGS Rock Classification Scheme, Volume 3, Classification of sediment and sedimentary rocks. Research Report, RR 99-03. *British Geological Survey*, Retrieved 2008-07-17
- Hargesheimer E E, McTigue N E, Mielke J L, Yee P, Elford T (1998) Tracking filter performance with particle counting. *Journal American Water Works Association*. **90(12)**, 32 – 41
- Hendricks D W (2005) *Water treatment unit processes: physical and chemical*. Boca Raton, FL: Taylor & Francis
- Horner R M W, Jarvis R J, Mackie R I (1986) Deep bed filtration: a new look at the basic equations. *Water Research*. **20(2)**, 215-220.
- Hudson H E (1963) Functional design of rapid sand filters. *Journal of the Sanitary Engineering Division, ASCE*. **89**, 17-28.
- Huisman L, Wood W E (1974) Slow Sand Filtration. *WHO, Genva, Switzerland*
- Humby M S, Fitzpatrick C S B (1996) Attrition of granular filter media during backwashing with combined air and water. *Water Research*. **30(2)**, 291-294.
- Ison C R, Ives K J (1969) Removal mechanisms in deep bed filtration. *Chemical Engineering Science*. **24**, 717-729
- Ives K J, Sholji I (1965) *Proceedings of American Society of Civil Engineers in Journal of Sanitation Engineering Directory*. **91**, 1-18.
- Ives K J (1970) Review Paper Rapid Filtration. *Water Research*. **4**, 201-223
- Ives K J (1975) Specifications for granular filter media. *Effluent and Water Treatment Journal*. **15**, 296-305
- Ives K J (1987) Filtration of clay suspensions through [quartz] sand. *Clay Minerals*. **22**, 49-61
- Ives K J (1990) Testing of Filter Media. *Aqua*. **39**, 144-151

- Judd S J, Solt G S (1991) Electrophoretically-Assisted depth filtration of aqueous suspensions through various fibrous media. *Chemical Engineering Science*. **46**(2), 419-428
- Kawamura S (2000) *Integrated Design and Operation of Water Treatment Facilities*. John Wiley & Sons, New York.
- Leclerc D (1975) Characteristics of unconsolidated filter media. In *The Scientific Basis of Filtration*, Ives K J (editor), NATO Advanced Study Institute Series, ISBN 90 286 0523 1, Noordhoff-Leyden.
- Lipp P, Schmitt A, Baldauf B (1997) Treatment of soft reservoir water by limestone filtration in combination with ultrafiltration. *Desalination*. **113**, 285 - 292
- Longsdon G S, Symons J M, Hoye R L, Arozarena M M (1981) Alternative filtration methods for removal of *Giardia sp.* cysts and cyst models. *Journal American Water Works Association*. **73**, 111-118.
- Mackie R I, Bai R (1992) Suspended particle size distribution and the performance of deep bed filters. *Water Research*. **26**(12), 1571-1575.
- Mackintosh G S, de Villiers H A (1999) Treatment of soft, acidic and ferruginous groundwaters. *IAH Groundwater Conference*. Cape Town, South Africa
- McNameee R L, Baylis J R, Borchardt J A, Cosens K W, Hazen R, Hill K V, Howard N J, Kenmir R C, Schram W B (AWWA Committee 8913 P) (1956) Filtration – Revision of Water Quality and Treatment Chapter 11. *Journal American Water Works Association*. **49**(7), 787 - 817
- Mitrouli S T, Yiantsios S G, Karabelas A J, Mitrakasa M, Follesdal M, Kjolseth P A (2008) Pretreatment or desalination of seawater from an open intake by dual-media filtration: Pilot testing and comparison of two different media. *Desalination*. **222**, 24-37
- Mitrouli S T, Karabelas A J, Yiantsios S G, Kjolseth P A (2009) New granular materials for dual-media filtration of seawater: Pilot testing. *Separation and Purification Technology*. **65**, 147-155

- Mórgeli B, Ives K J (1979) New media or effluent filtration. *Water Research*. **13**, 1001-1007
- Mulder T, Gimbel R (1991) Application of permeable collectors in deep-bed filtration. *Separations Technology*. **1**, 153-165
- O'Leary K C, Eisenor J D, Gagnon G A (2003) Examination of plant performance and filter ripening with particle counters at full-scale water treatment plants. *Environmental Technology*. **24(1)** 1 – 9
- O'Melia, Ali W (1973) The role of retained particles in deep bed filtration. *Progress in Water Technology*. **10**, 167-182
- O'Melia C R, Ali W (1978) The role of retained particles in deep bed filtration. *Progress in Water Technology*. **10**, 167-182
- O'Melia C R (1985) Particles, pretreatment, and performance in water filtration. *Journal of Environmental Engineering*. **111(6)**, 874-890
- Rooklidge S J, Ketchum J.r L H (2002) Corrosion control enhancement from a dolomite-amended slow sand filter. *Water Research*. **36**, 2689 – 2694
- Rutledge S O, Gagnon G A (2002) Comparing crushed recycled glass to silica sand for dual media filtration. *J. Environ. Eng.* **1**, 349-358
- Saltnes T, Eikebrokk B, Odegaard H (2002) Contact filtration of humic waters: performance of an expanded clay aggregate filter (Filtralite) compared to a dual anthracite/sand filter. *Water Science and Technology: Water Supply*. **2**, 17-23
- Sokolović R S, Sokolović S, Govedarica D (2009) Performance of expanded polystyrene particles in deep bed filtration. *Separation and Purification Technology*. **68**, 267-272
- Soyer E, Akgiray O, Eldem N Ö, Saatçı A (2012) Crushed recycled glass as a filter medium and comparison with silica sand. *Clean – Soil, Air, Water*. **38(10)**, 927 – 935
- Stevenson D G (1994) The Specification of Filtering Materials for Rapid-Gravity Filtration. *Water and Environmental Management*. **8**, 527-533

- Suthaker A, Smith D W, Stanley S J (1995) Evaluation of filter media for upgrading existing filter performance. *Environmental Technology*. **16**, 625-643.
- Tien C, Ramaro B V (1989) *Granular filtration of aerosols and hydrosols*. Elsevier Science, Amsterdam.
- Tobiason J E, O'Melia C R (1982) *Filtration performance in water and wastewater treatment*. Report 172: Water Resources Research Institute of the University of North Carolina
- van Olphen H (1977) *An Introduction to Clay Colloid Chemistry, 2nd edition*. John Wiley & Sons, New York
- Yao K M (1968) *Influence of suspended particle size on transport aspect of water filtration*. PhD dissertation, University of North Carolina, Chapel Hill, N.C., 1968.
- Yao K, Habibian M T, O'Melia C R (1971) Water and waste water filtration: concepts and applications. *Environmental Science & Technology*. **5**(11), 1105-1112
- Yukselen Y, Kaya A (2008) Suitability of the methylene blue test for surface area, cation exchange capacity and swell potential determination of clayey soils. *Engineering Geology*. **102**, 38-45.
- Zamani A, Maini B (2009) Flow of dispersed particles through porous media – deep bed
- Zeta Meter Inc. (1997) *Zeta potential: a complete course in 5 minutes*. [PDF] Zeta Meter Inc. Available at: <http://www.zeta-meter.com/5min.pdf> [Accessed 23 Jan 2010]

APPENDICES TO ACCOMPANY
ALTERNATIVE FILTER MEDIA IN RAPID GRAVITY
FILTRATION OF POTABLE WATER

By

PHILLIP D. DAVIES

A Doctoral Thesis Submitted in Partial Fulfillment of the Requirements for the
Award of Doctor of Philosophy of Loughborough University

June 2012

© By Phillip D. Davies (2012)

APPENDIX I

Particle Size Distribution

Particle Size Distribution Results Sheet

Material: *Leighton Buzzard Sand*

Method of Sieving: *Dry and by Hand*

d_{60} : 0.75

d_{10} : 0.59

Sieving Medium: *Woven wire cloth*

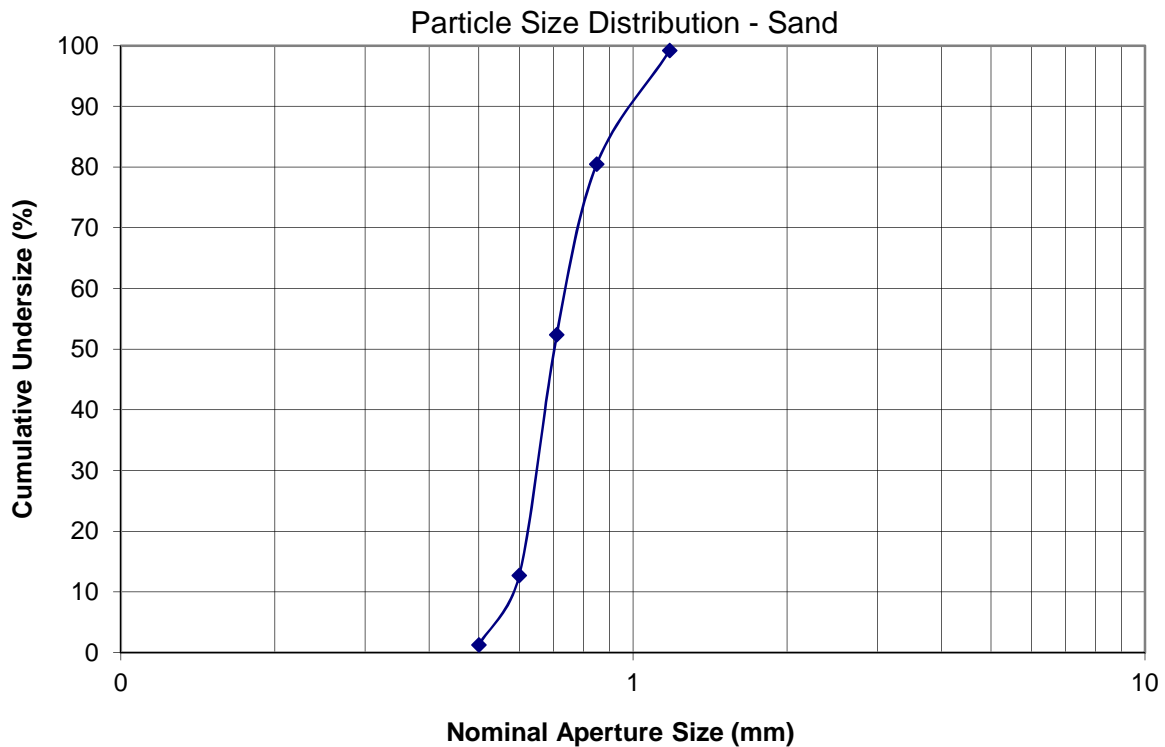
Aperture Type: *Square*

U: 1.27

eff. Size: 0.59

Duration of Sieving: *10 minutes*

1	2	3	4	5
Particle Size (d) (mm)	Sieve Fractions		Nominal Aperture Size (mm)	Cumulative Undersize %
	g	%		
$d > 2.00$	0.000	0	2.000	100
$2.00 > d > 1.18$	0.400	1	1.180	99
$1.18 > d > 0.850$	9.400	19	0.850	80
$0.850 > d > 0.710$	14.127	28	0.710	52
$0.710 > d > 0.600$	19.901	40	0.600	13
$0.600 > d > 0.500$	5.746	11	0.500	1
$d < 0.425$	0.653	1	Final Undersize	
Total	50.227	100		
Original Mass:	50.802			
Loss:	0.575	1.15		



Particle Size Distribution Results Sheet

Material: *Garside Sands Glass*

Method of Sieving: *Dry and by Hand*

d_{60} : 0.92

d_{10} : 0.76

Sieving Medium: *Woven wire cloth*

Aperture Type: *Square*

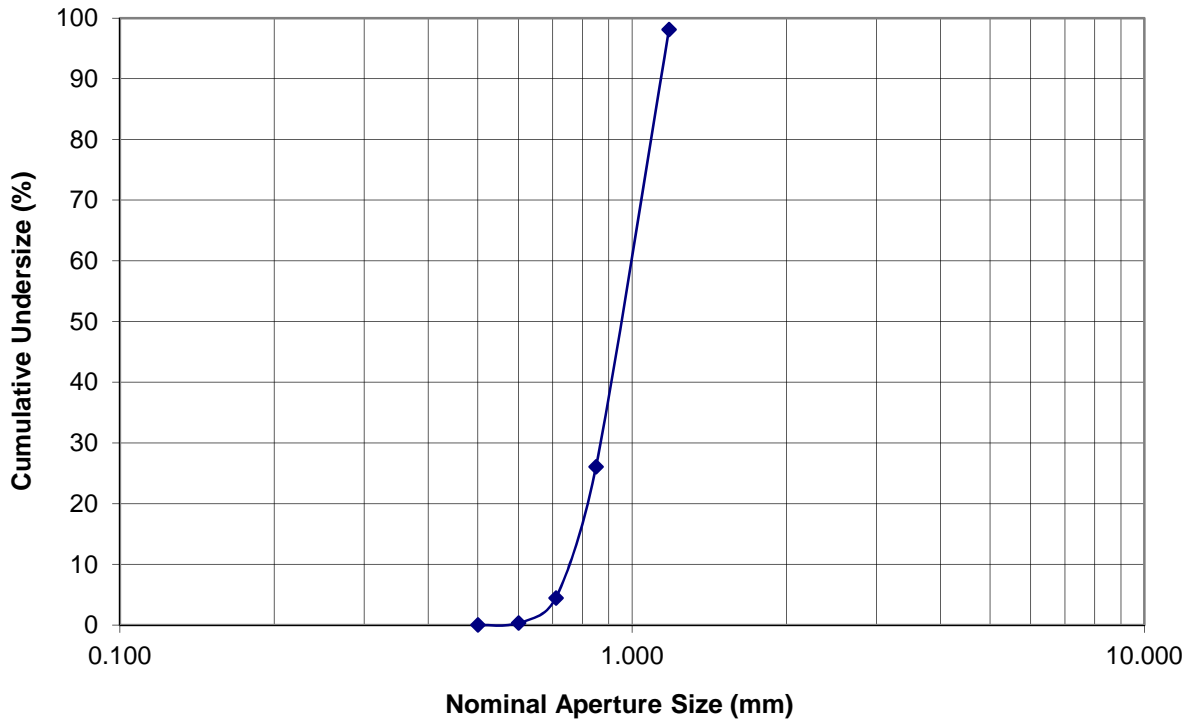
U: 1.21

eff. Size: 0.76

Duration of Sieving: *10 minutes*

1	2	3	4	5
Particle Size (d)	Sieve Fractions		Nominal Aperture Size	Cumulative Undersize
(mm)	g	%	(mm)	%
$d > 2.00$	0.000	0	2.000	100
$2.00 > d > 1.18$	1.913	2	1.180	98
$1.18 > d > 0.850$	72.079	72	0.850	26
$0.850 > d > 0.710$	21.603	22	0.710	4
$0.710 > d > 0.600$	4.132	4	0.600	0
$0.600 > d > 0.500$	0.348	0	0.500	0
$d < 0.425$	0.000	0	Final Undersize	

Total	100.073	100
Original Mass:	100.230	
Loss:	0.157	0.31



Particle Size Distribution Results Sheet

Material: *Limestone*

Method of Sieving: *Dry and by Hand*

d_{60} : 0.95

d_{10} : 0.65

Sieving Medium: *Woven wire cloth*

Aperture Type: *Square*

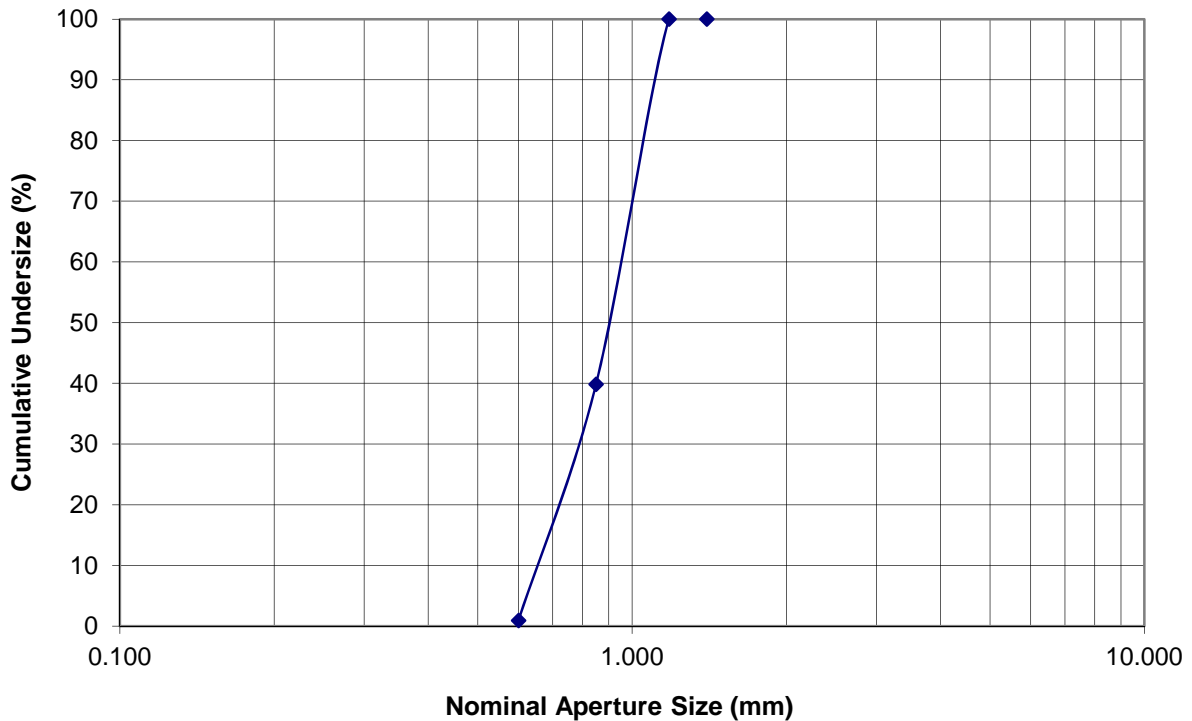
U: 1.46

eff. Size: 0.65

Duration of Sieving: *10 minutes*

1	2	3	4	5
Particle Size (d)	Sieve Fractions		Nominal Aperture Size	Cumulative Undersize
(mm)	g	%	(mm)	%
$d > 1.4$	0.000	0	1.400	100
$1.4 > d > 1.18$	0.000	0	1.180	100
$1.18 > d > 0.850$	59.997	60	0.850	40
$0.850 > d > 0.600$	38.824	39	0.600	1
$0.600 > d > 0.425$	0.916	1	Final Undersize	
Total	99.737	100		

Original Mass: 100.083
 Loss: 0.346 0.69



Particle Size Distribution Results Sheet

Material: *Filtralite*

Method of Sieving: *Dry and by Hand*

d_{60} : 1.40

d_{10} : 0.77

Sieving Medium: *Woven wire cloth*

Aperture Type: *Square*

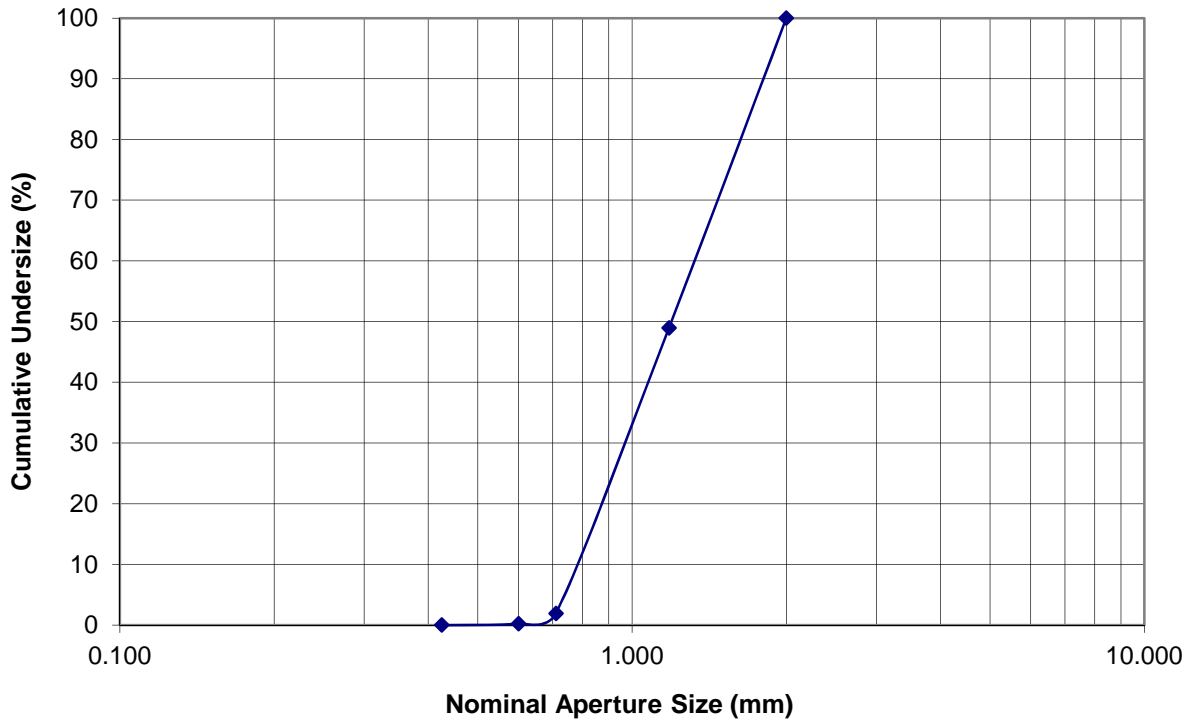
U: 1.82

eff. Size: 0.77

Duration of Sieving: *10 minutes*

1	2	3	4	5
Particle Size (d)	Sieve Fractions		Nominal Aperture Size	Cumulative Undersize
(mm)	g	%	(mm)	%
$d > 2.00$	0.000	0	2.000	100
$3.35 > d > 1.18$	42.488	51	1.180	49
$1.18 > d > 0.710$	39.123	47	0.710	2
$0.710 > d > 0.600$	1.424	2	0.600	0
$0.600 > d > 0.425$	0.195	0	0.425	0
$d < 0.425$	0.000	0	Final Undersize	
Total	83.230	100		

Original Mass: 83.333
 Loss: 0.103 0.21



Particle Size Distribution Results Sheet

Material: *Delabole Slate*

Method of Sieving: *Dry and by Hand*

d_{60} : 1.00

d_{10} : 0.58

Sieving Medium: *Woven wire cloth*

Aperture Type: *Square*

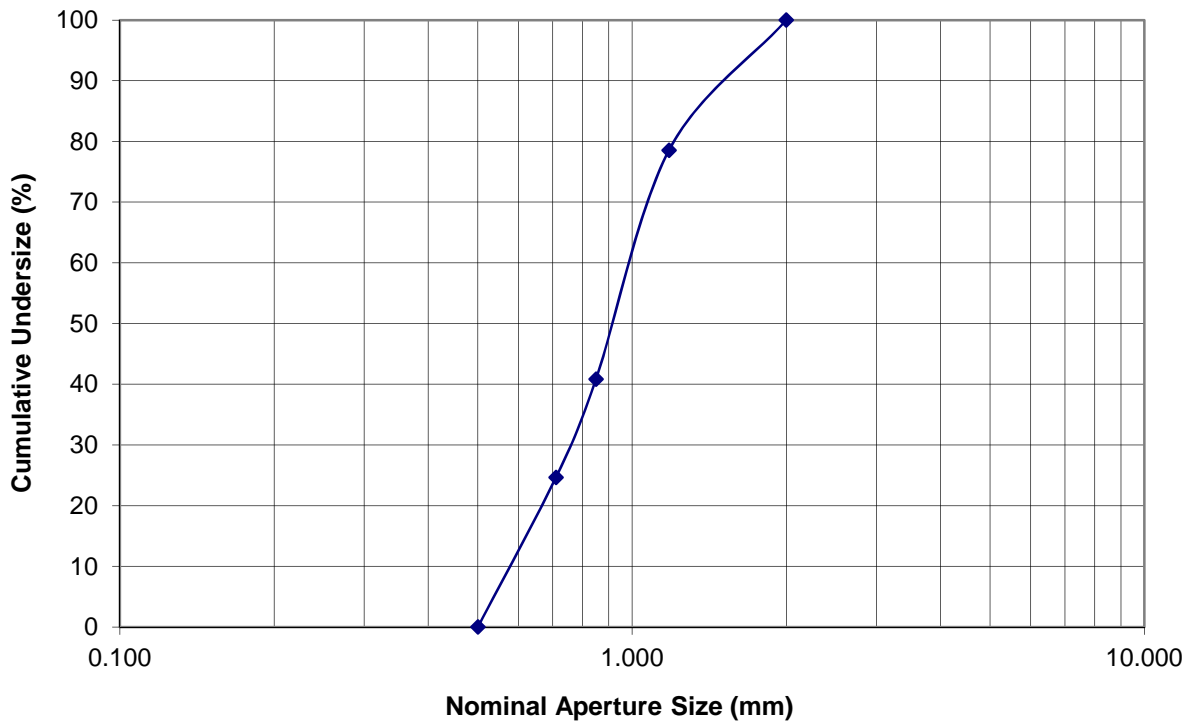
U: 1.72

eff. Size: 0.58

Duration of Sieving: *10 minutes*

1	2	3	4	5
Particle Size (d) (mm)	Sieve Fractions		Nominal Aperture Size (mm)	Cumulative Undersize (%)
	g	%		
$d > 3.35$	0	0	3.35	100
$3.35 > d > 2.0$	0.000	0	2.000	100
$2.0 > d > 1.18$	27.040	21	1.180	79
$1.18 > d > 0.850$	47.450	38	0.850	41
$0.850 > d > 0.710$	20.334	16	0.710	25
$0.710 > d > 0.500$	31.044	25	0.500	0
$d < 0.425$	0.000	0	Final Undersize	

Total	125.868	100
Original Mass:	126.900	
Loss:	1.032	2.06



Particle Size Distribution Results Sheet

Material: *Pumice - Pumex NMP9 0.2 mm - 1.4 mm*

Method of Sieving: *Dry and by Hand*

d_{60} : 0.91

d_{10} : 0.52

Sieving Medium: *Woven wire cloth*

Aperture Type: *Square*

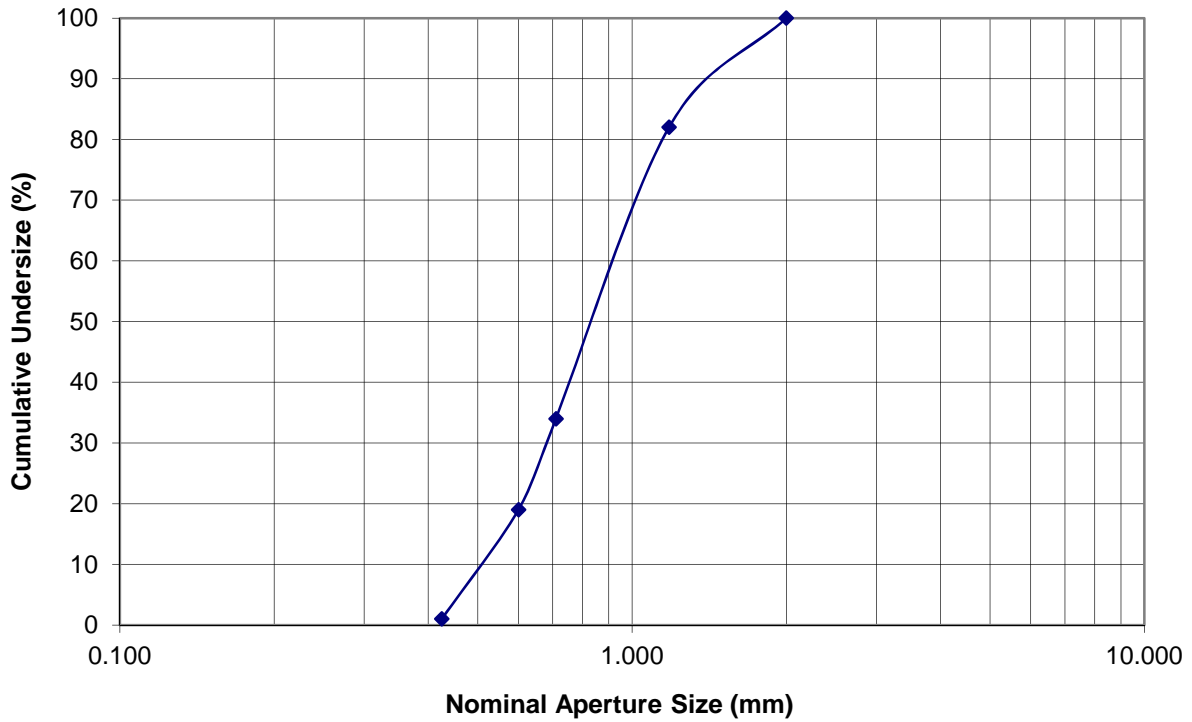
U: 1.75

eff. Size: 0.52

Duration of Sieving: *10 minutes*

1	2	3	4	5
Particle Size (d) (mm)	Sieve Fractions		Nominal Aperture Size (mm)	Cumulative Undersize (%)
	g	%		
$d > 2.00$	0.000	0	2.000	100
$3.35 > d > 1.18$	8.778	18	1.180	82
$1.18 > d > 0.710$	24.467	49	0.710	34
$0.710 > d > 0.600$	7.345	15	0.600	19
$0.600 > d > 0.425$	9.182	18	0.425	1
$d < 0.425$	0.000	0	Final Undersize	
Total	49.772	100		

Original Mass: 50.000
 Loss: 0.228 0.46



Particle Size Distribution Results Sheet

Material: *Techfil No.4 Pumice*

Method of Sieving: *Dry and by Hand*

d_{60} : 1.06

d_{10} : 0.49

Sieving Medium: *Woven wire cloth*

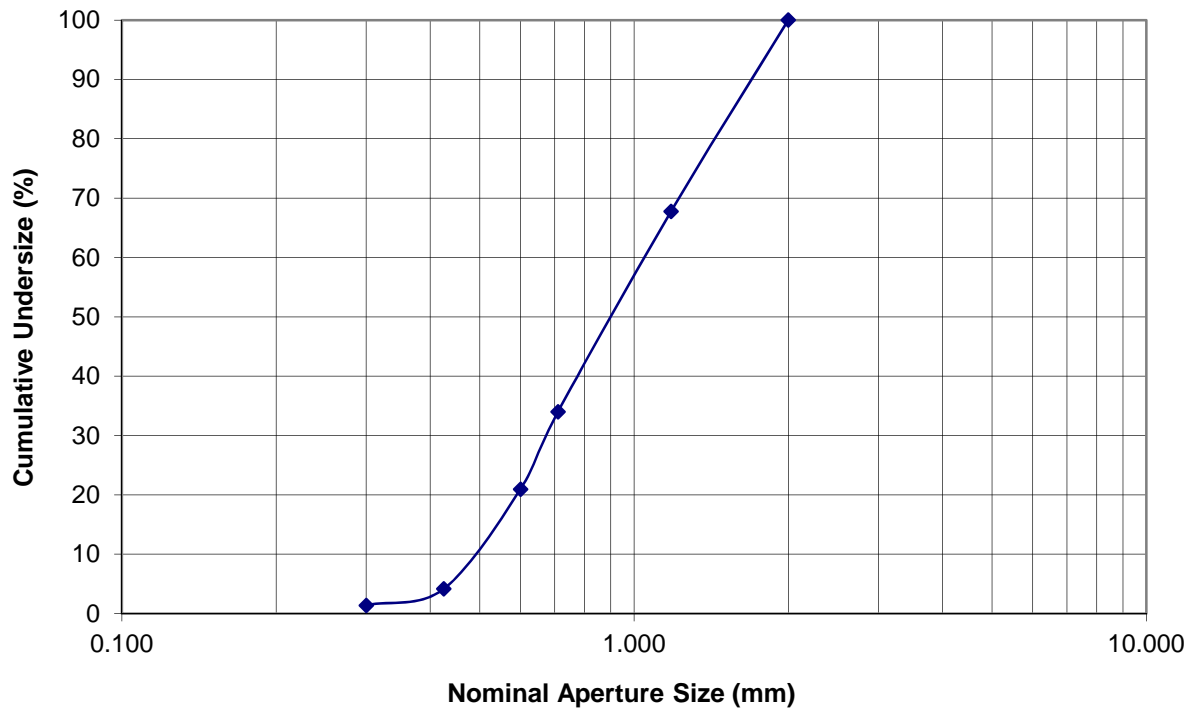
Aperture Type: *Square*

U: 2.16

eff. Size: 0.49

Duration of Sieving: *10 minutes*

1	2	3	4	5
Particle Size (d) (mm)	Sieve Fractions		Nominal Aperture Size (mm)	Cumulative Undersize (%)
	g	%		
$d > 2.00$	0.067	0	2.000	100
$2.00 > d > 1.18$	13.366	32	1.180	68
$1.18 > d > 0.710$	13.973	34	0.710	34
$0.710 > d > 0.600$	5.401	13	0.600	21
$0.600 > d > 0.425$	6.957	17	0.425	4
$0.425 > d > 0.300$	1.154	3	0.300	1
$d < 0.300$	0.094	0	Final Undersize	
Total	41.012	100		
Original Mass:	41.424			
Loss:	0.412	1.00		



Particle Size Distribution Results Sheet

Material: *S Slag*

Method of Sieving: *Dry and by Hand*

d_{60} : 0.78

d_{10} : 0.65

Sieving Medium: *Woven wire cloth*

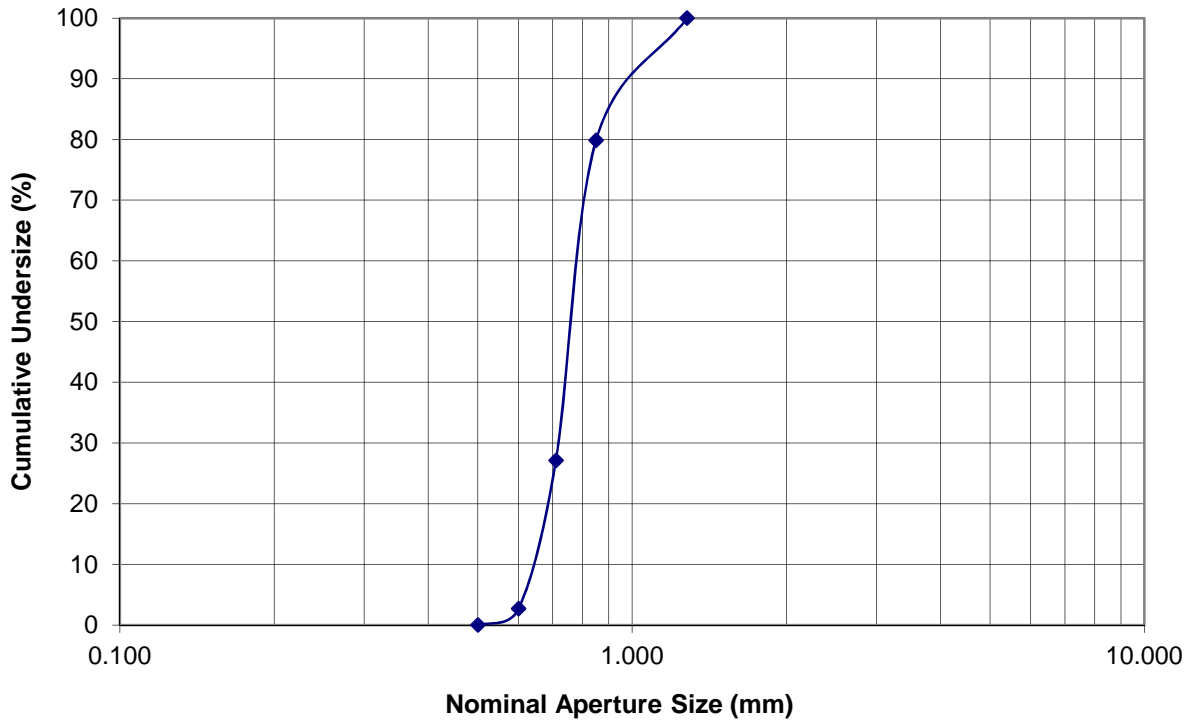
Aperture Type: *Square*

U: 1.20
eff. Size: 0.65

Duration of Sieving: *10 minutes*

1	2	3	4	5
Particle Size (d) (mm)	Sieve Fractions		Nominal Aperture Size (mm)	Cumulative Undersize (%)
	g	%		
$d > 1.180$	0.000	0	1.280	100
$1.180 > d > 0.850$	21.120	20	0.850	80
$0.850 > d > 0.600$	55.210	53	0.710	27
	25.620	24	0.600	3
$0.500 > d > 0.425$	2.820	3	0.500	0
$d < 0.425$	0.000	0	Final Undersize	
Total	104.770	100		

Original Mass: 105.210
Loss: 0.440 0.88



Particle Size Distribution Results Sheet

Material: *F Slag*

Method of Sieving: *Dry and by Hand*

d_{60} : 0.79

d_{10} : 0.64

Sieving Medium: *Woven wire cloth*

Aperture Type: *Square*

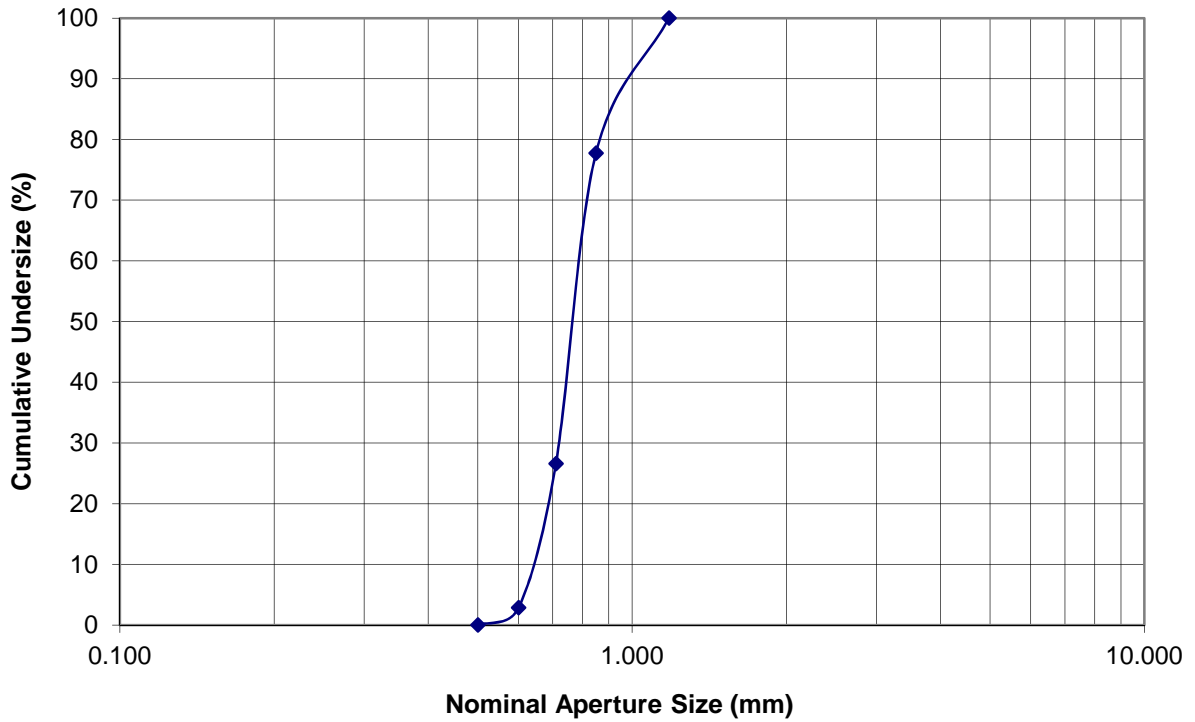
U: 1.23

eff. Size: 0.64

Duration of Sieving: *10 minutes*

1	2	3	4	5
Particle Size (d)	Sieve Fractions		Nominal Aperture Size	Cumulative Undersize
(mm)	g	%	(mm)	%
$d > 1.180$	0.000	0	1.180	100
$1.180 > d > 0.850$	22.520	22	0.850	78
$0.850 > d > 0.600$	51.820	51	0.710	27
$0.600 > d > 0.500$	24.020	24	0.600	3
$0.500 > d > 0.425$	2.890	3	0.500	0
$d < 0.425$	0.000	0	Final Undersize	
Total	101.250	100		

Original Mass: 101.970
 Loss: 0.720 1.44



Particle Size Distribution Results Sheet

Material: *P Slag*

Method of Sieving: *Dry and by Hand*

d_{60} : 0.78

d_{10} : 0.65

Sieving Medium: *Woven wire cloth*

Aperture Type: *Square*

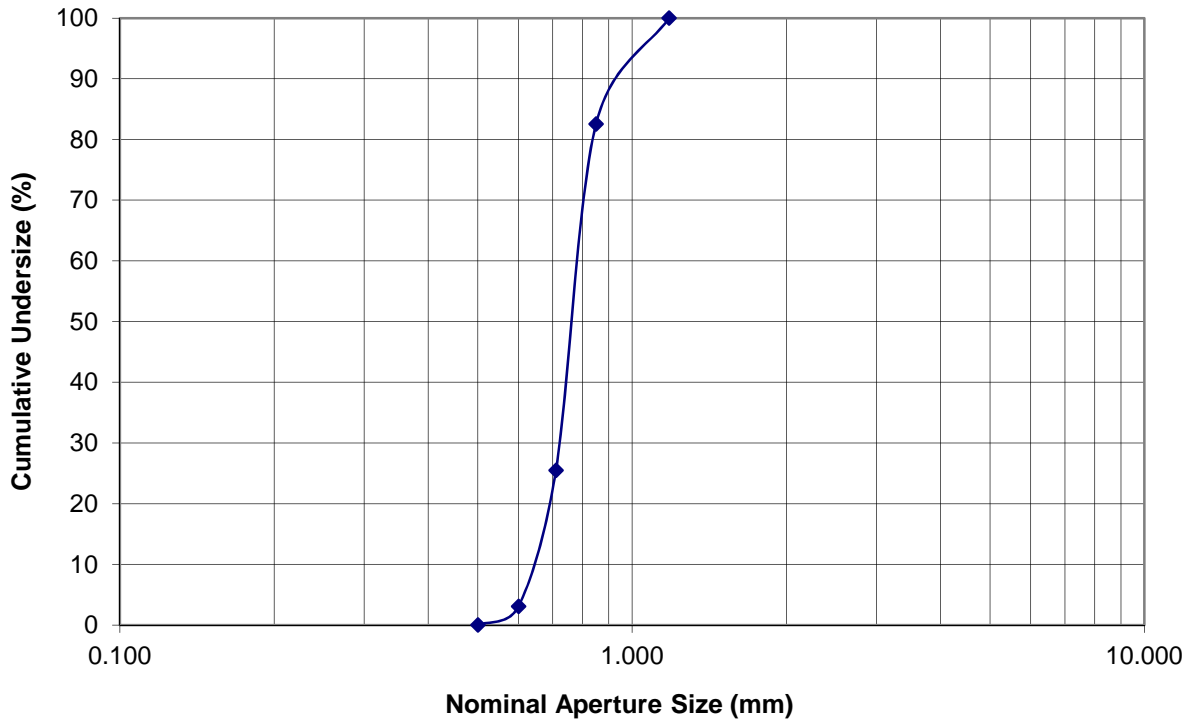
U: 1.20

eff. Size: 0.65

Duration of Sieving: *10 minutes*

1	2	3	4	5
Particle Size (d)	Sieve Fractions		Nominal Aperture Size	Cumulative Undersize
(mm)	g	%	(mm)	%
$d > 1.180$	0.000	0	1.180	100
$1.180 > d > 0.850$	18.340	17	0.850	83
$0.850 > d > 0.600$	59.910	57	0.710	25
$0.600 > d > 0.500$	23.520	22	0.600	3
$0.500 > d > 0.425$	3.250	3	0.500	0
$d < 0.425$	0.000	0	Final Undersize	
Total	105.020	100		

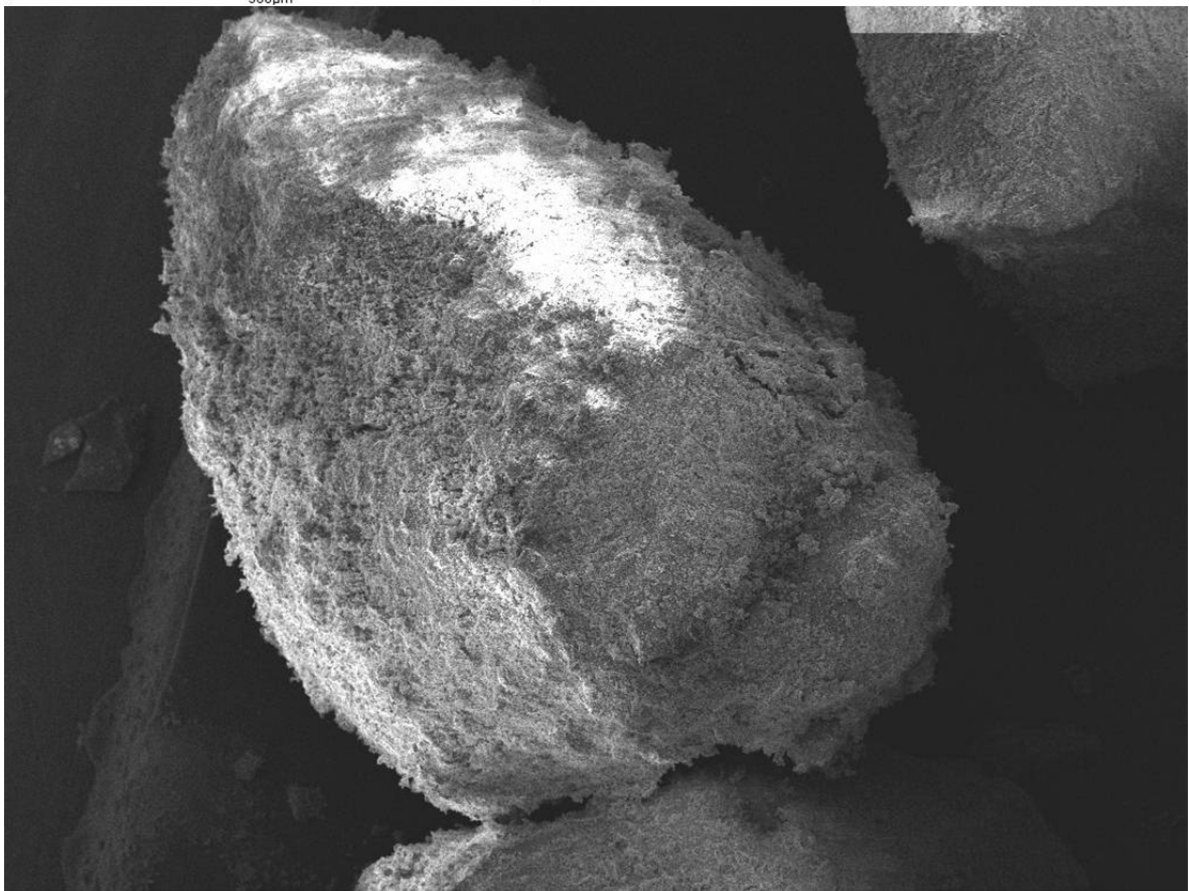
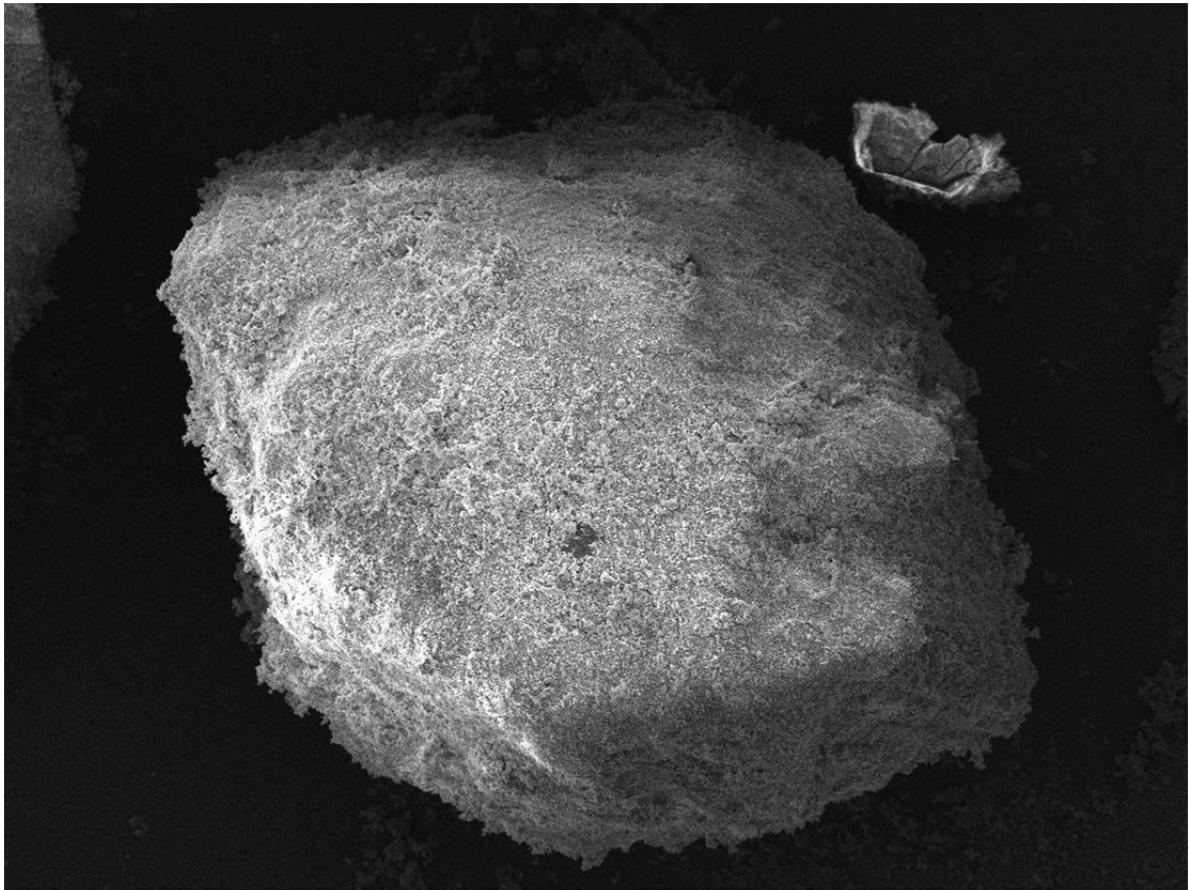
Original Mass: 105.610
 Loss: 0.590 1.18

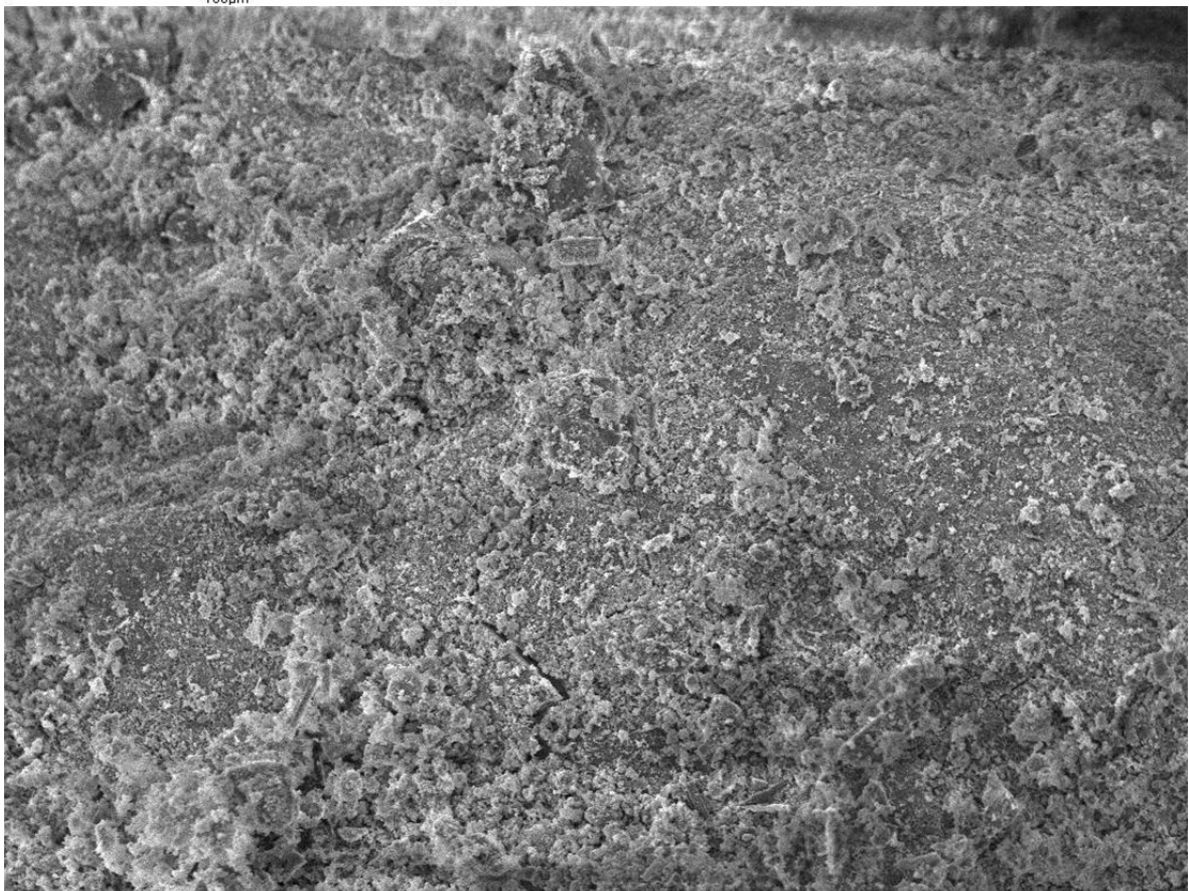
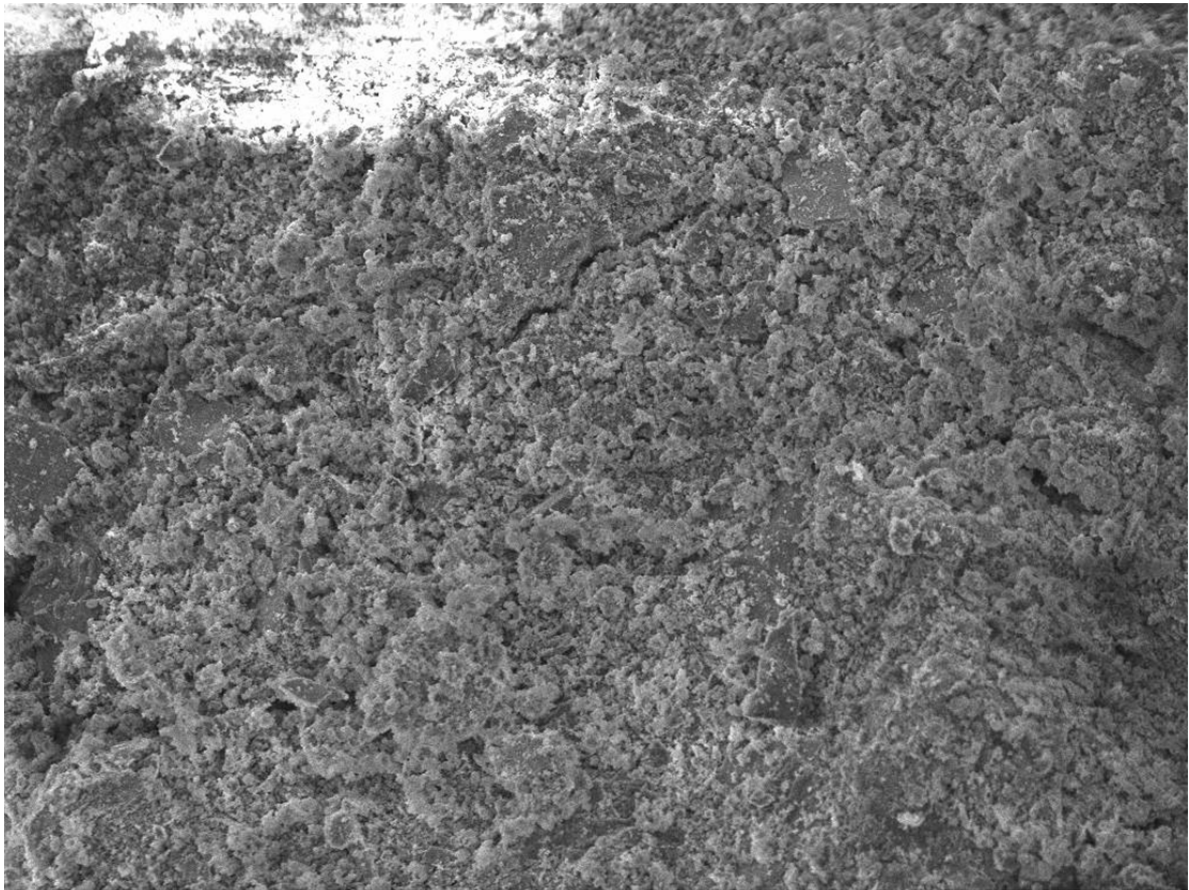


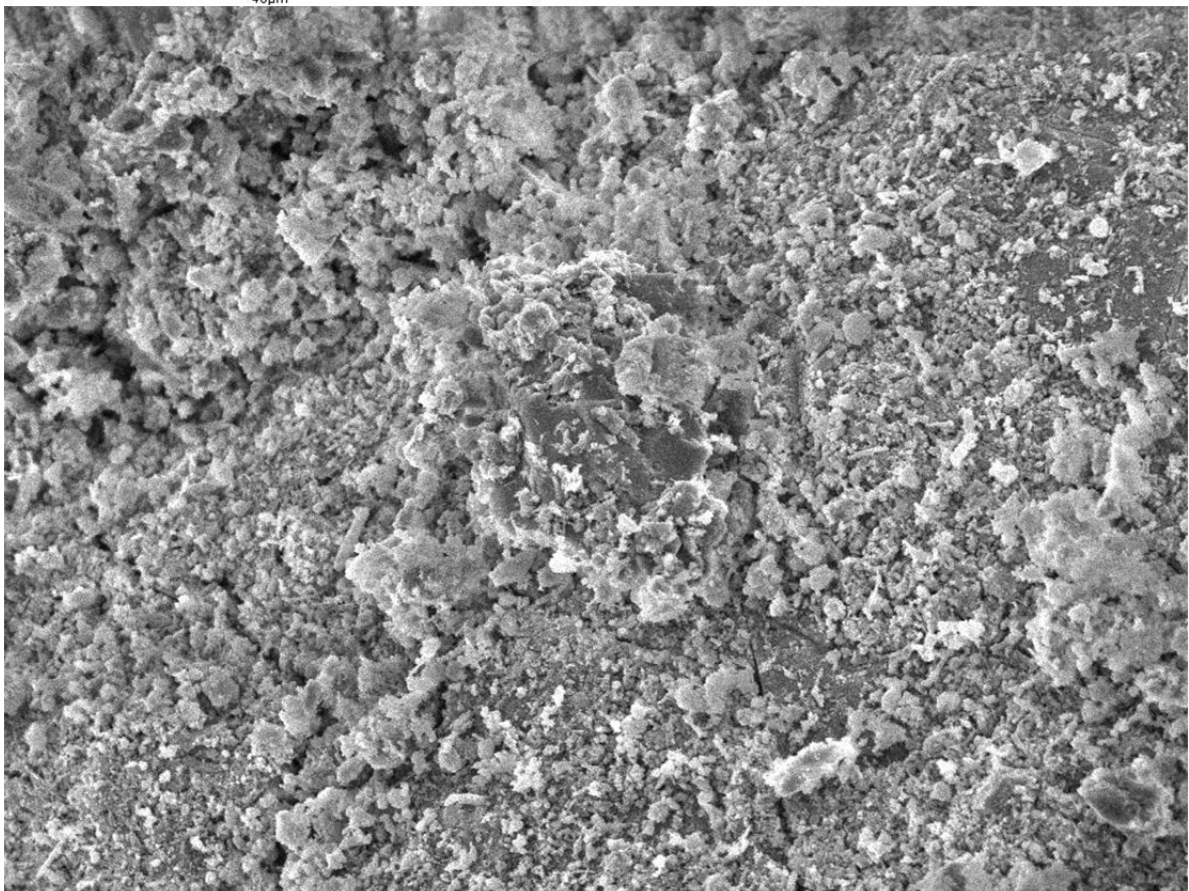
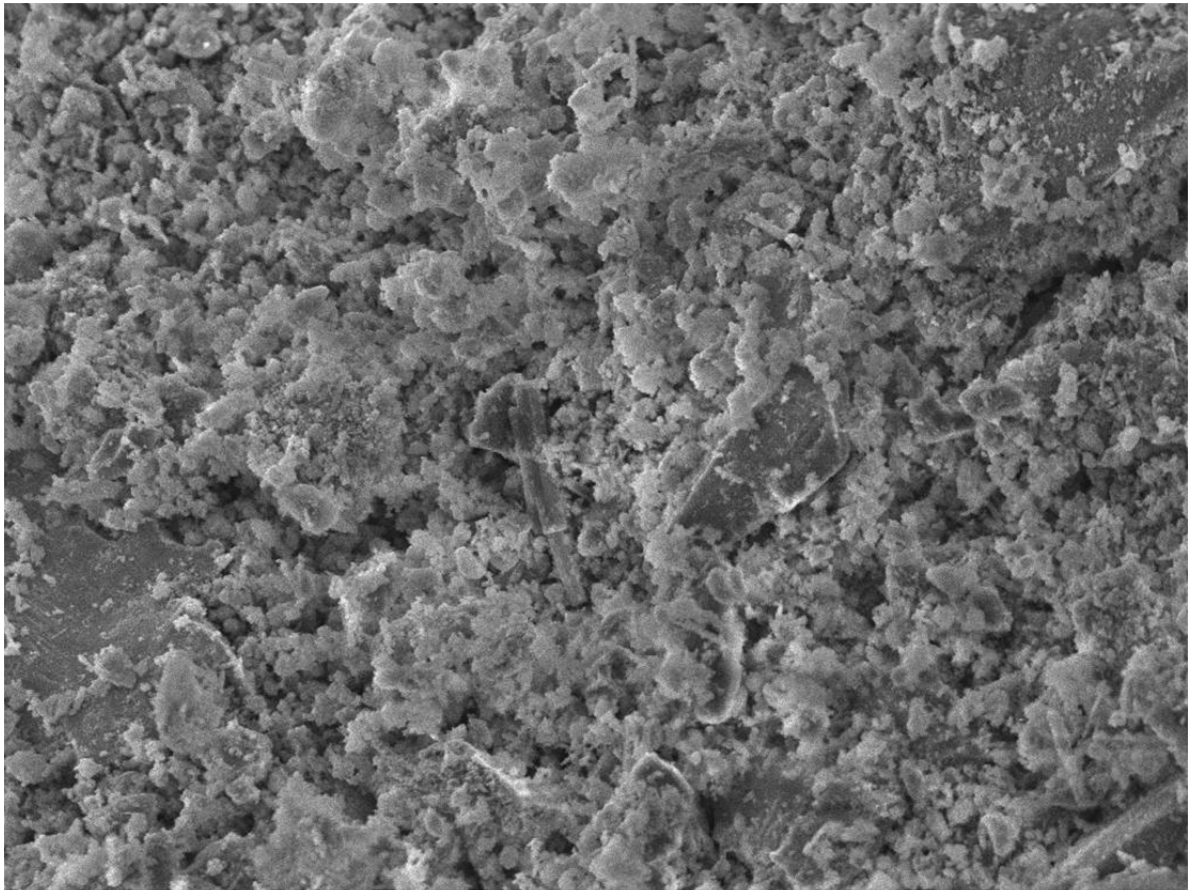
APPENDIX II

Scanning Electron Microscopy

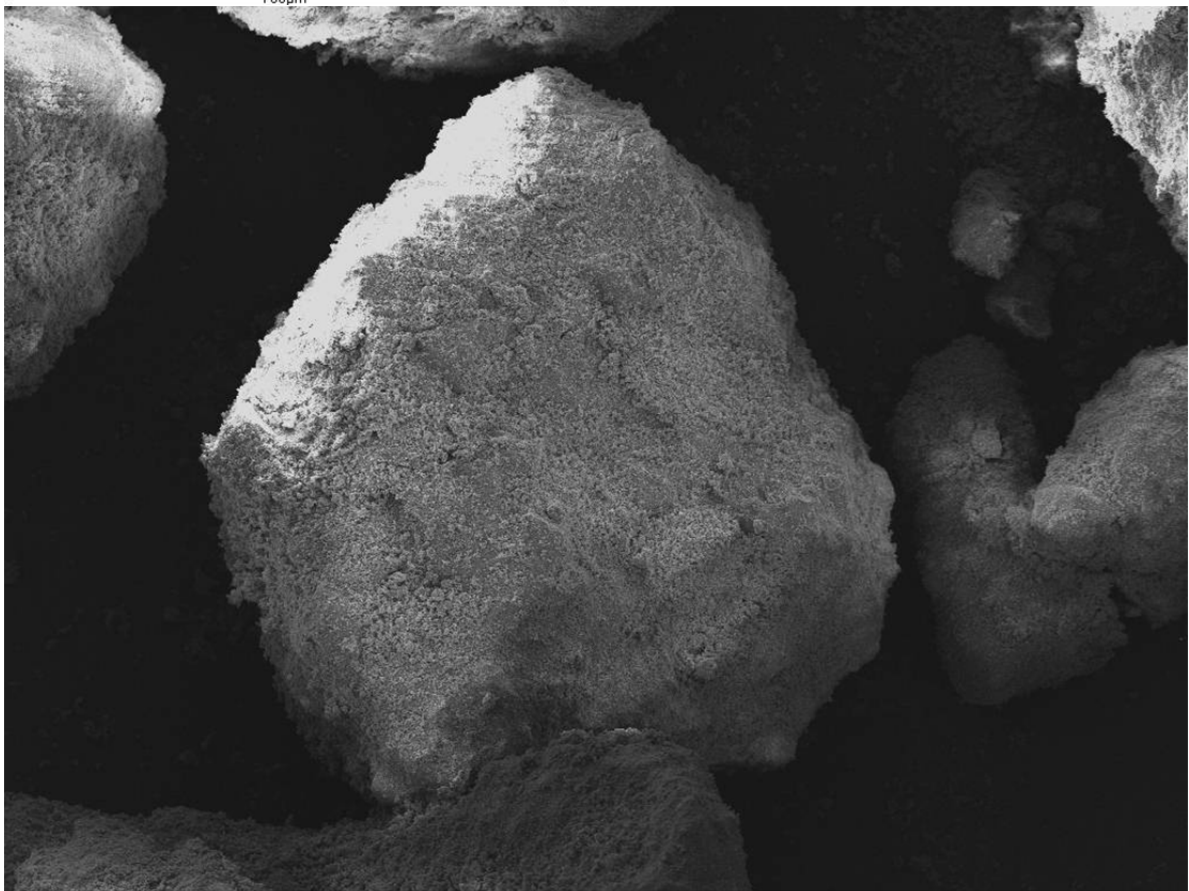
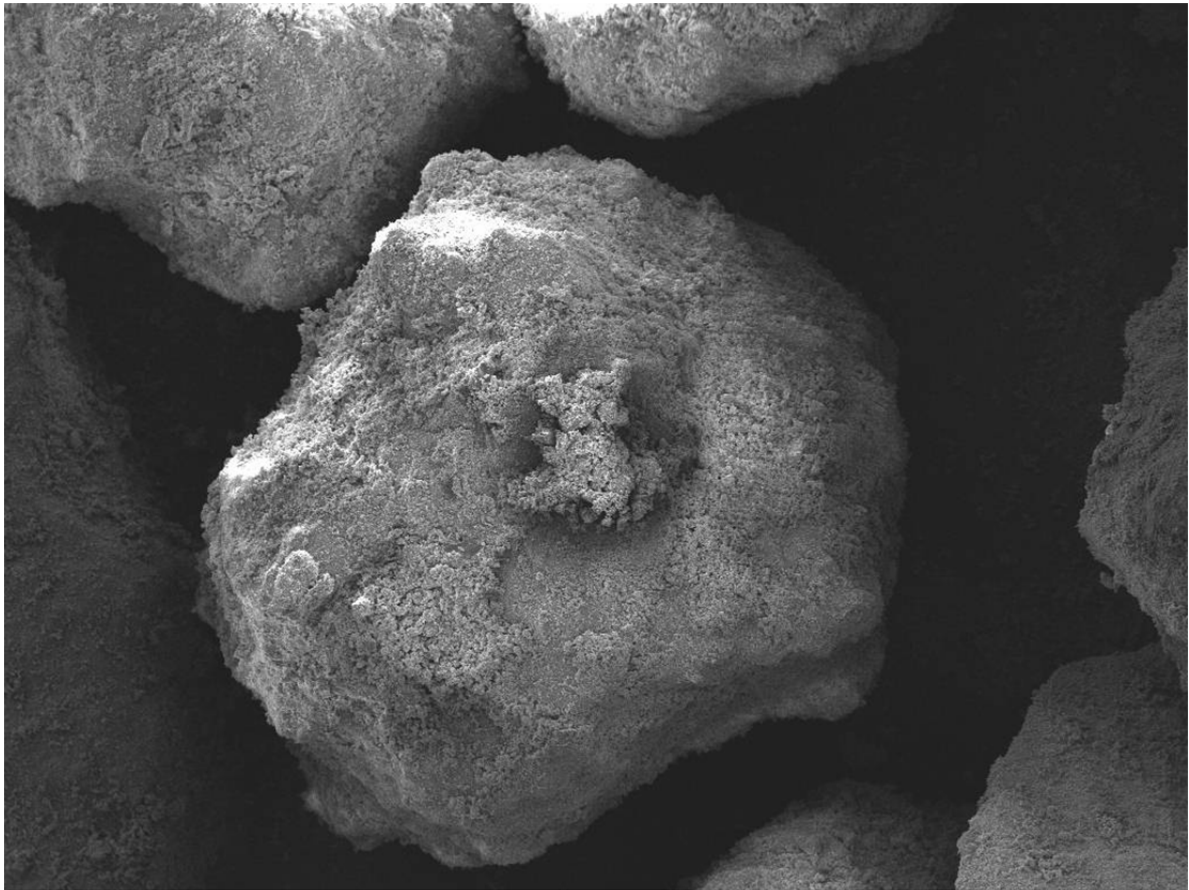
Furnace Slag SEM Images

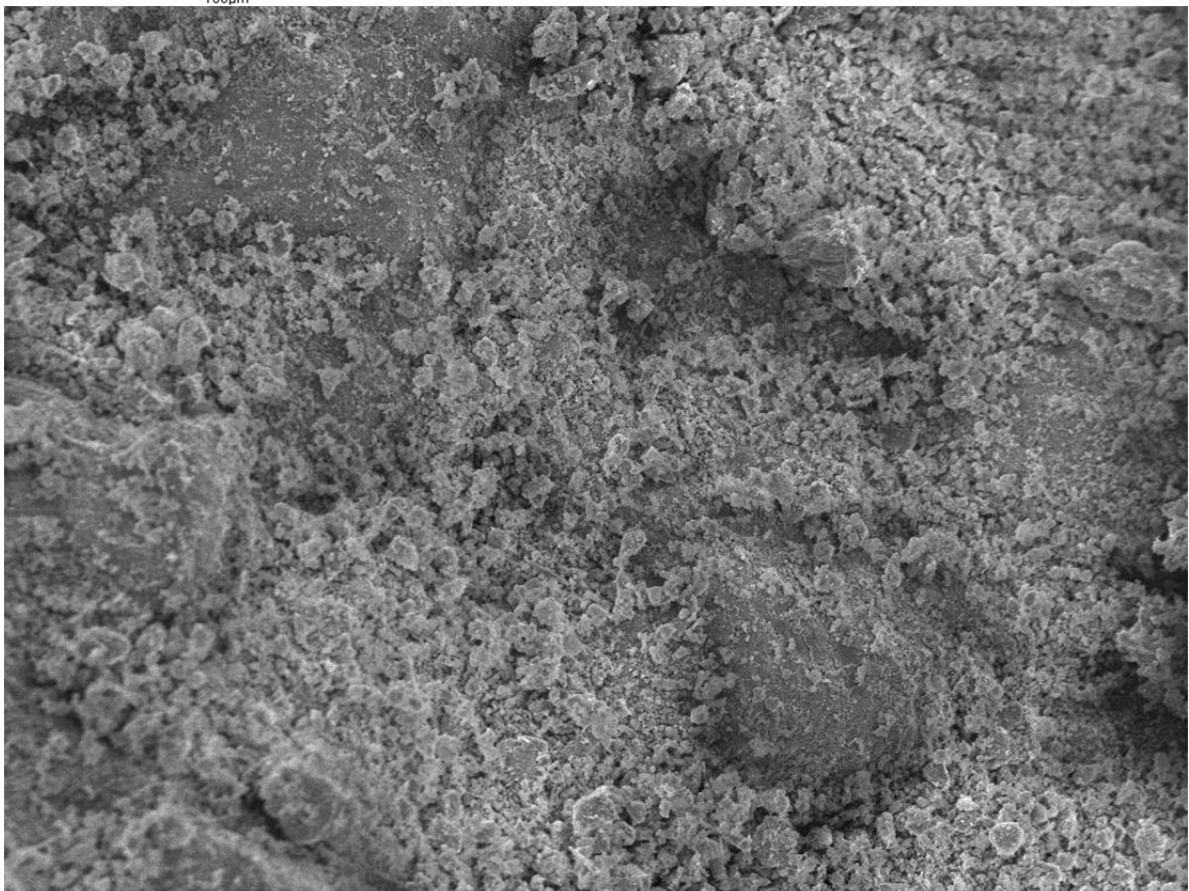
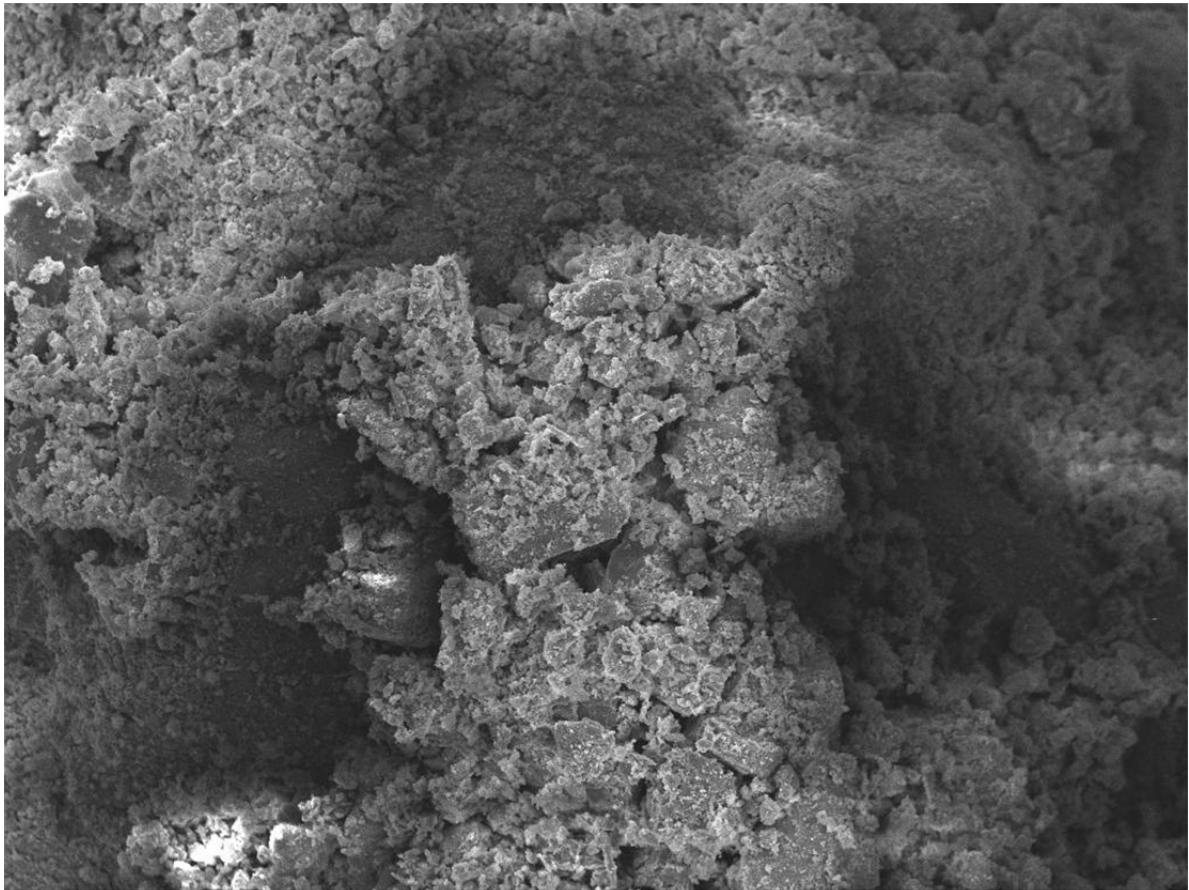


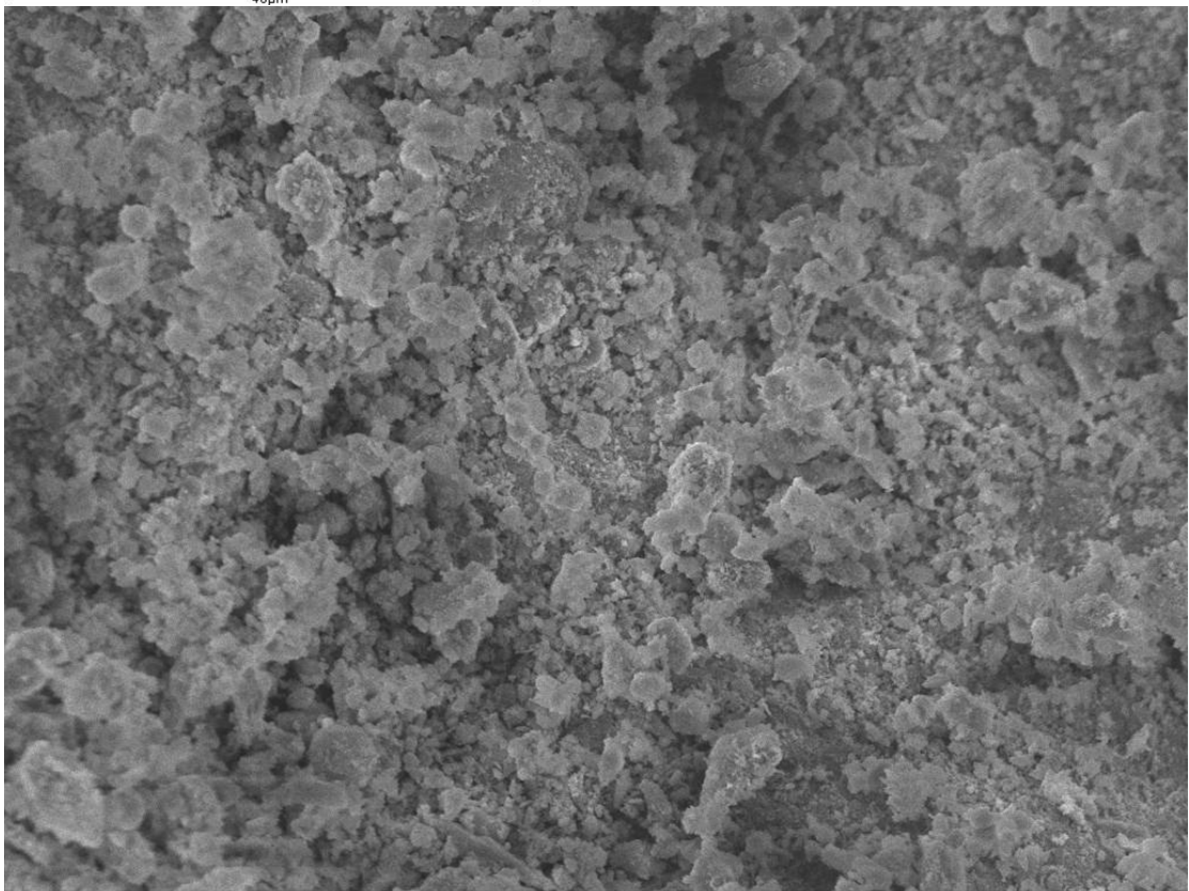
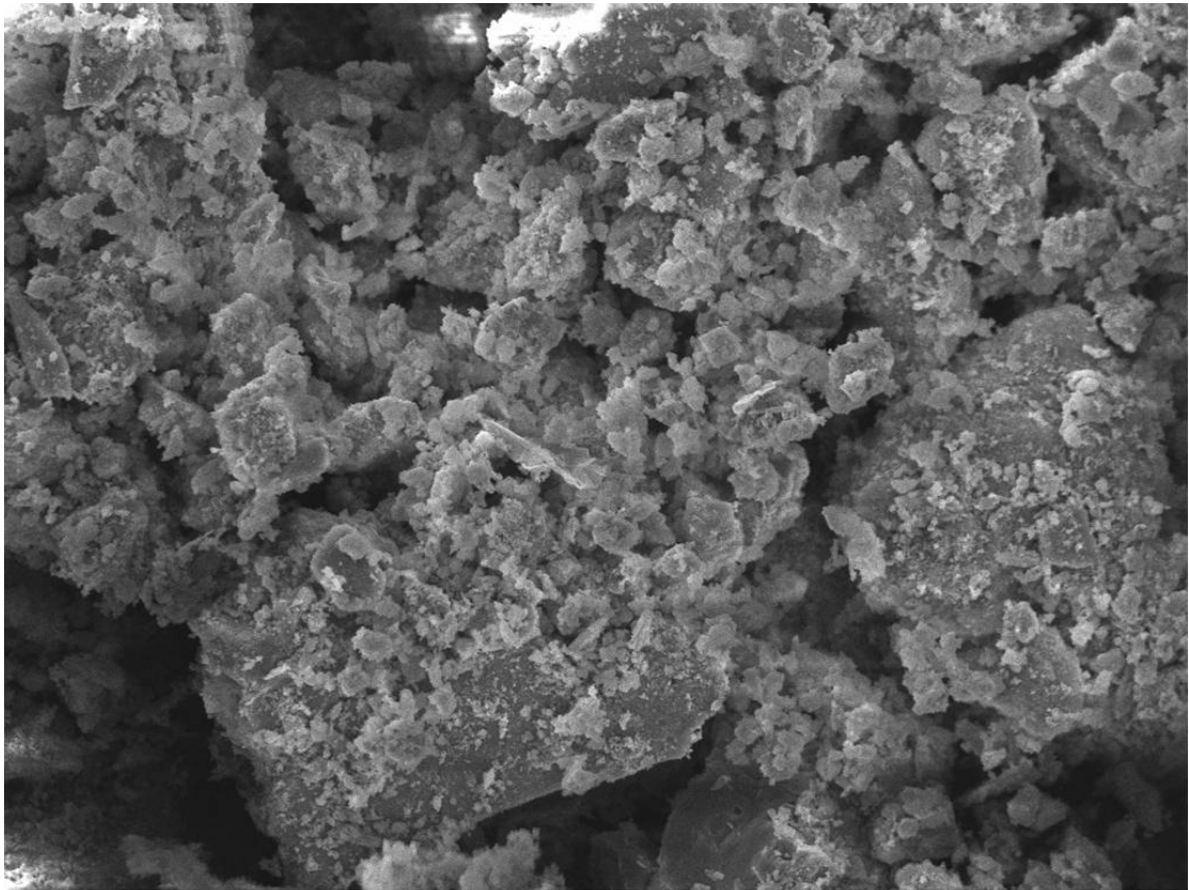




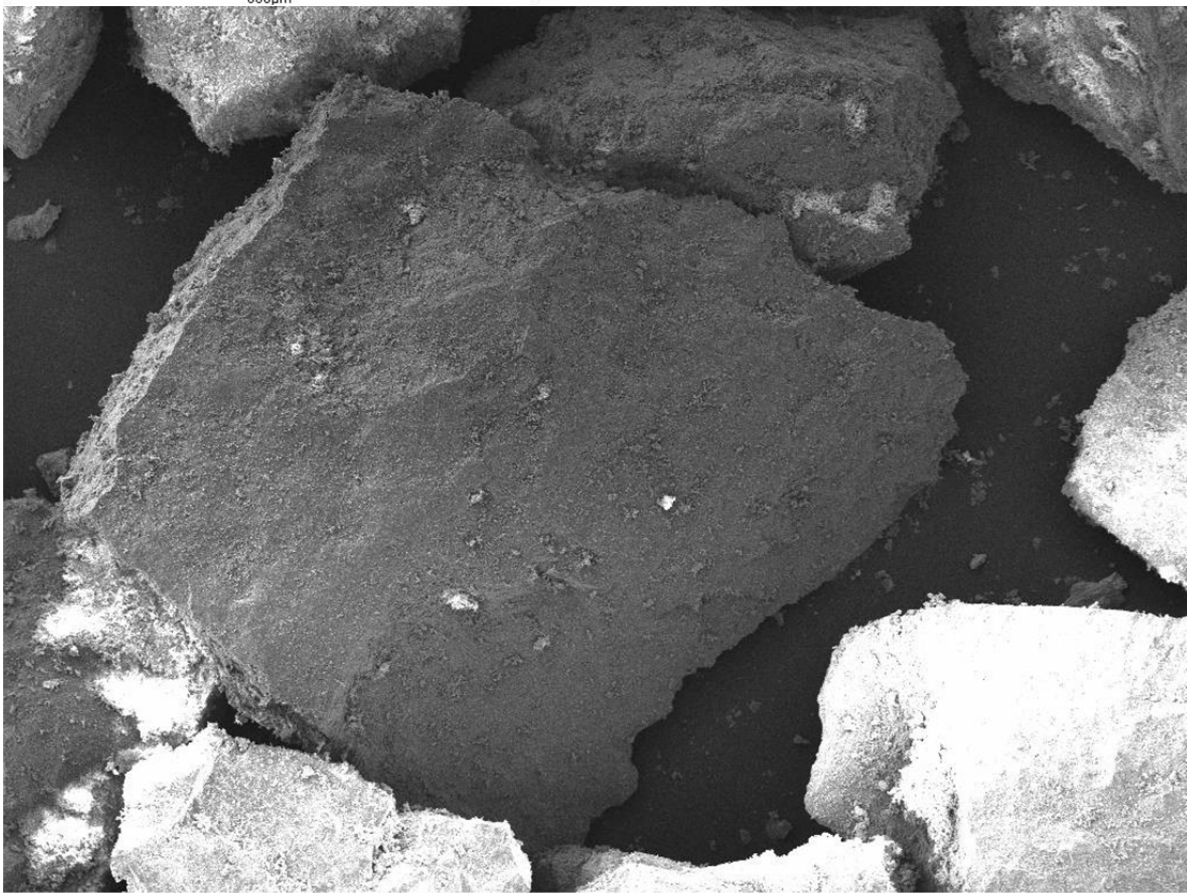
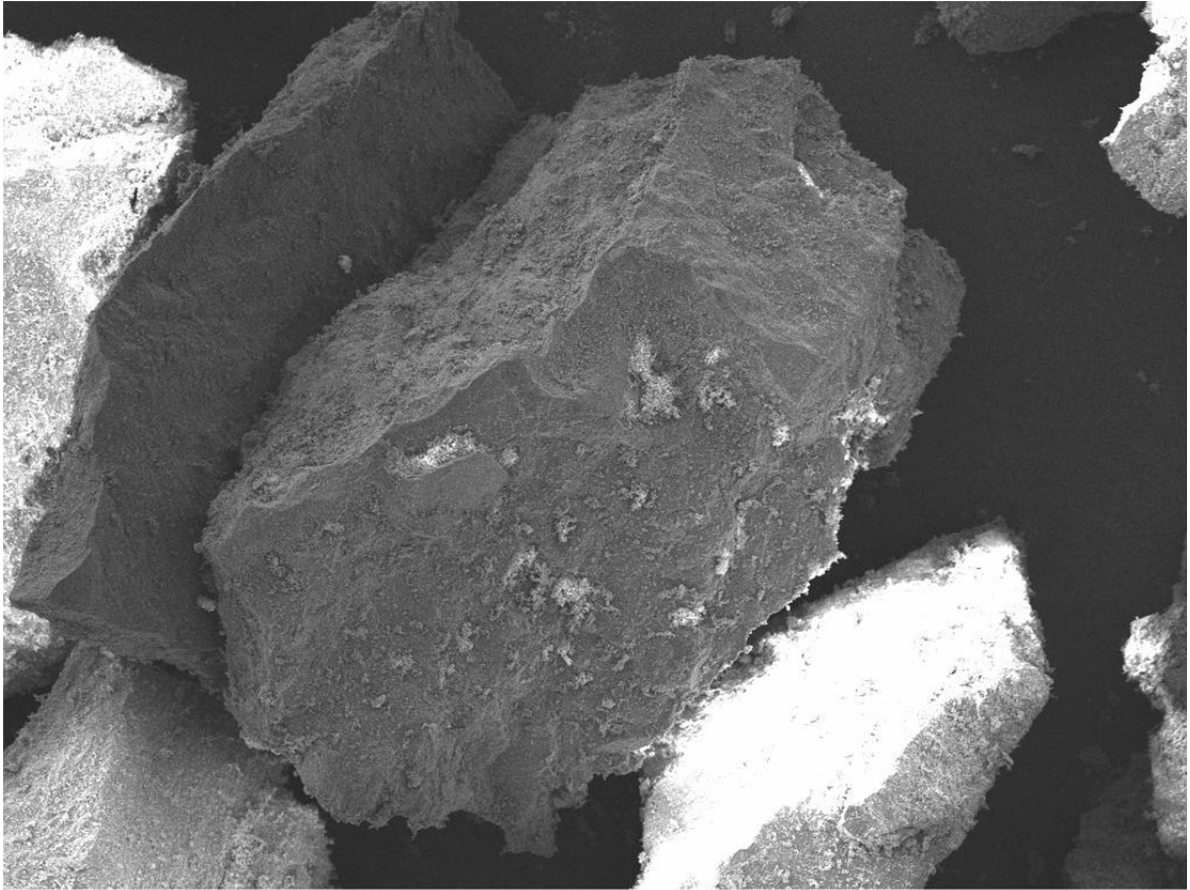
Steel Slag SEM Images

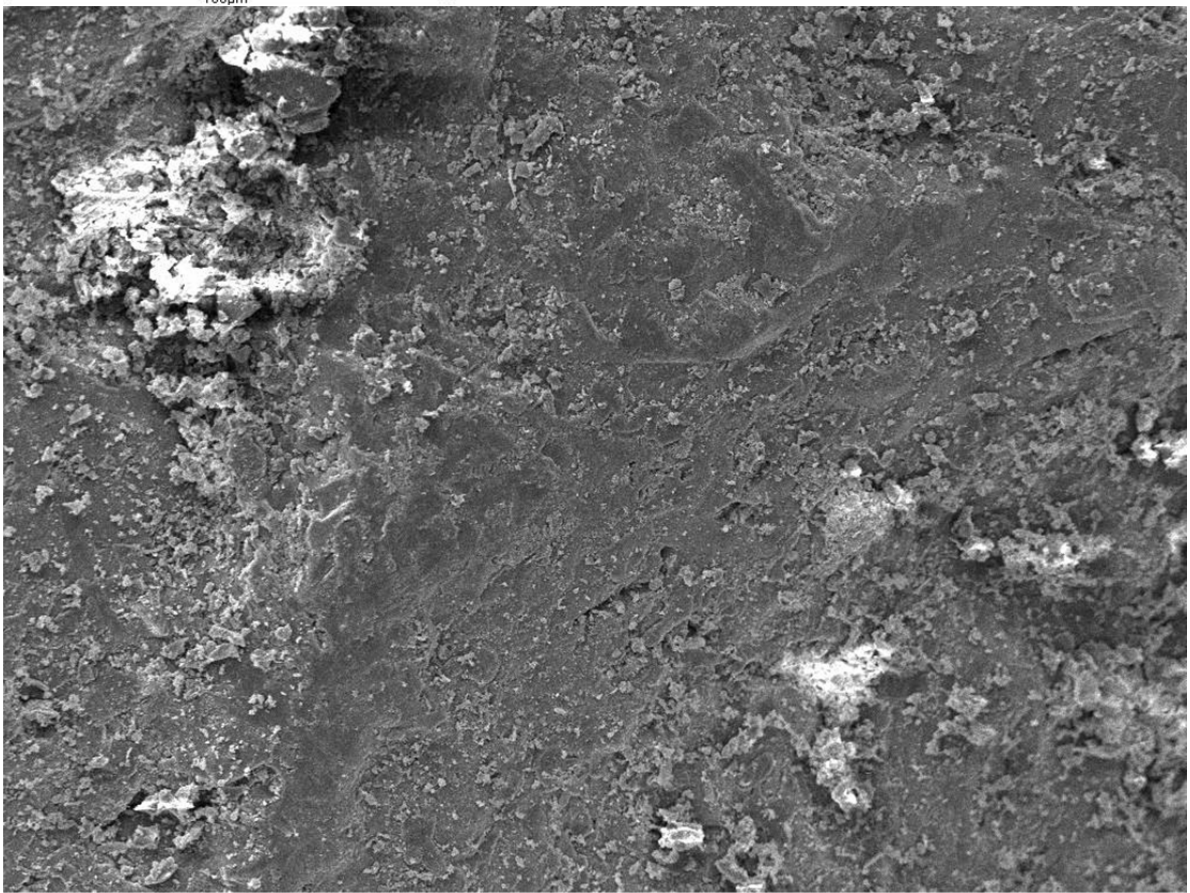
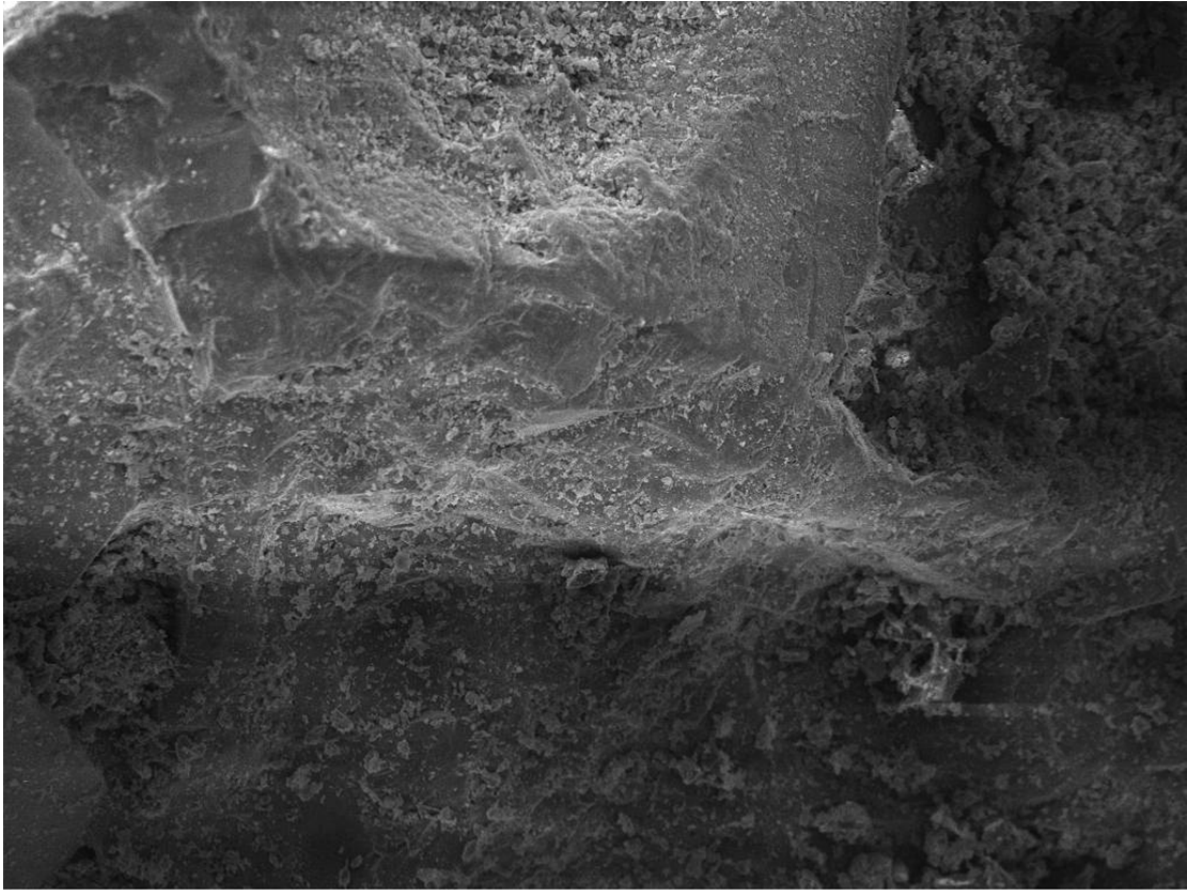


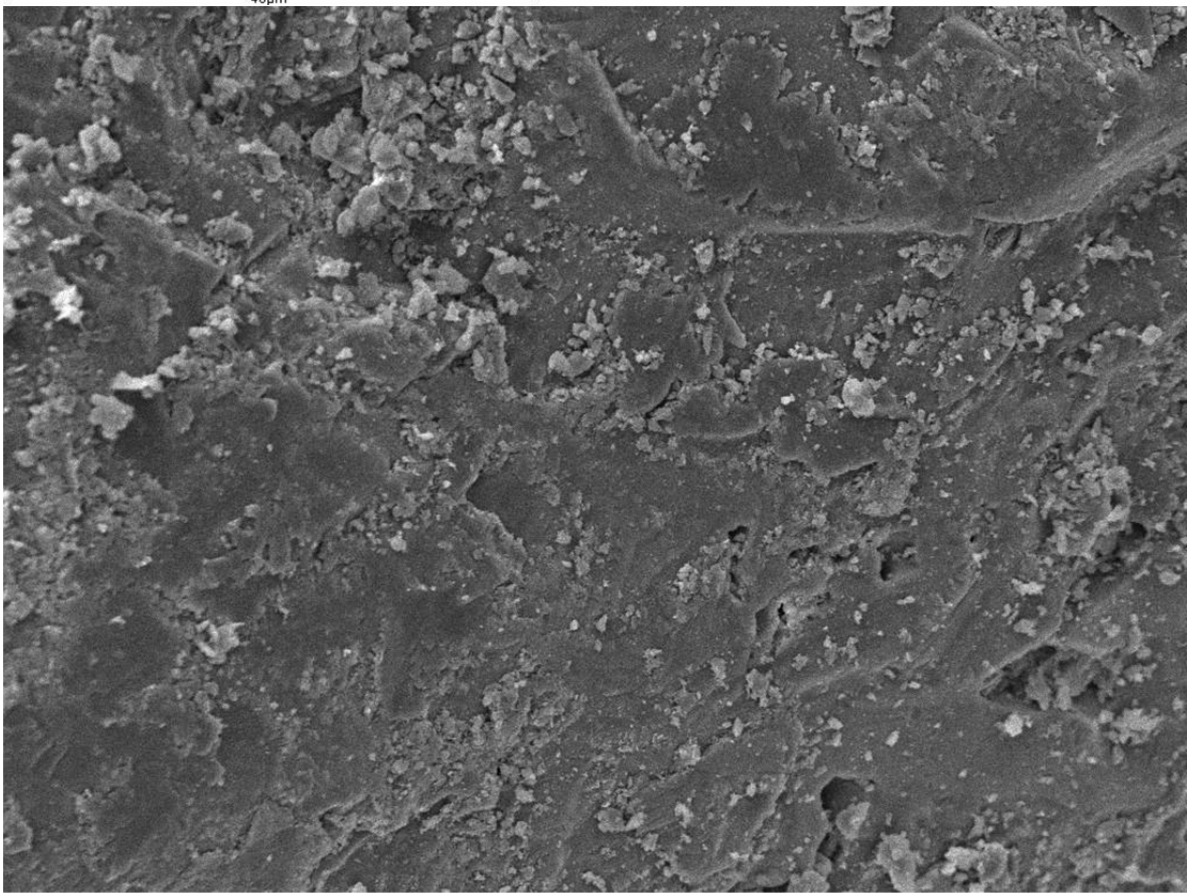
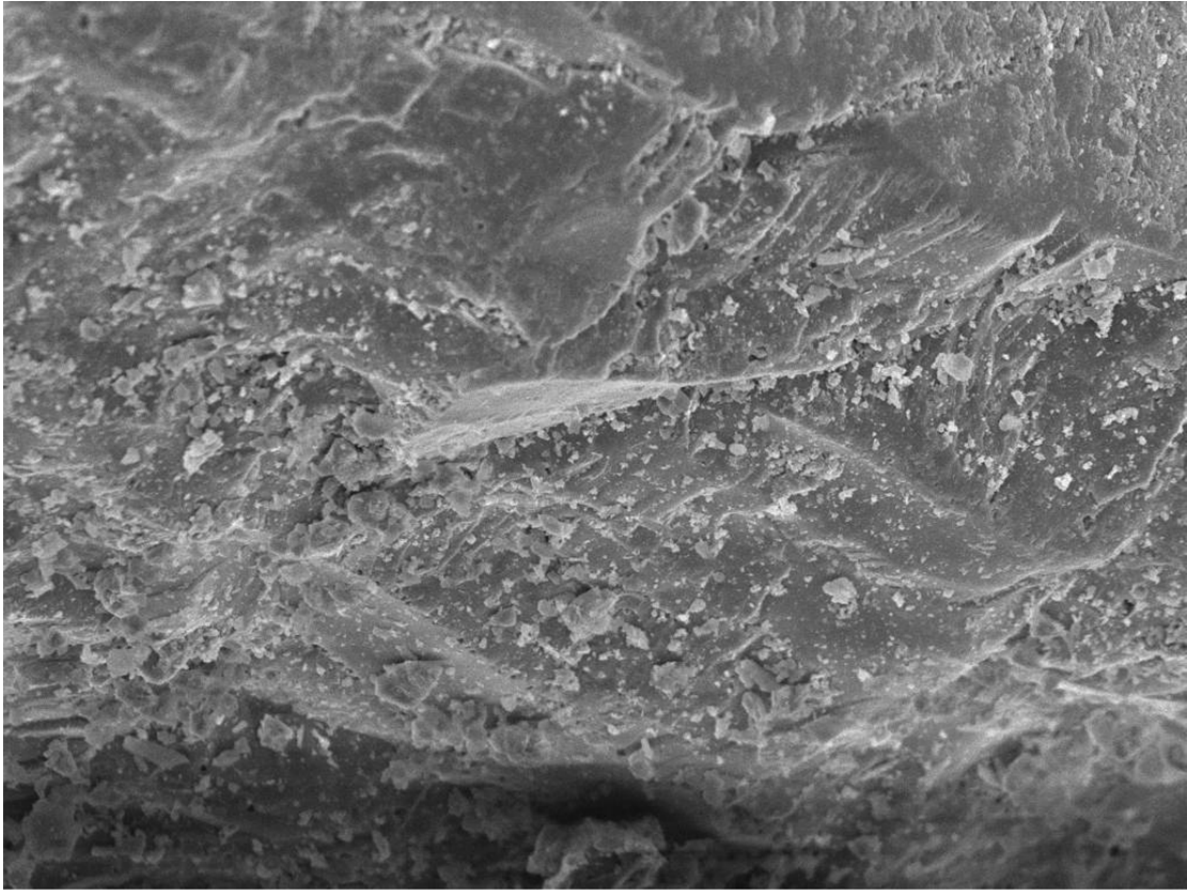




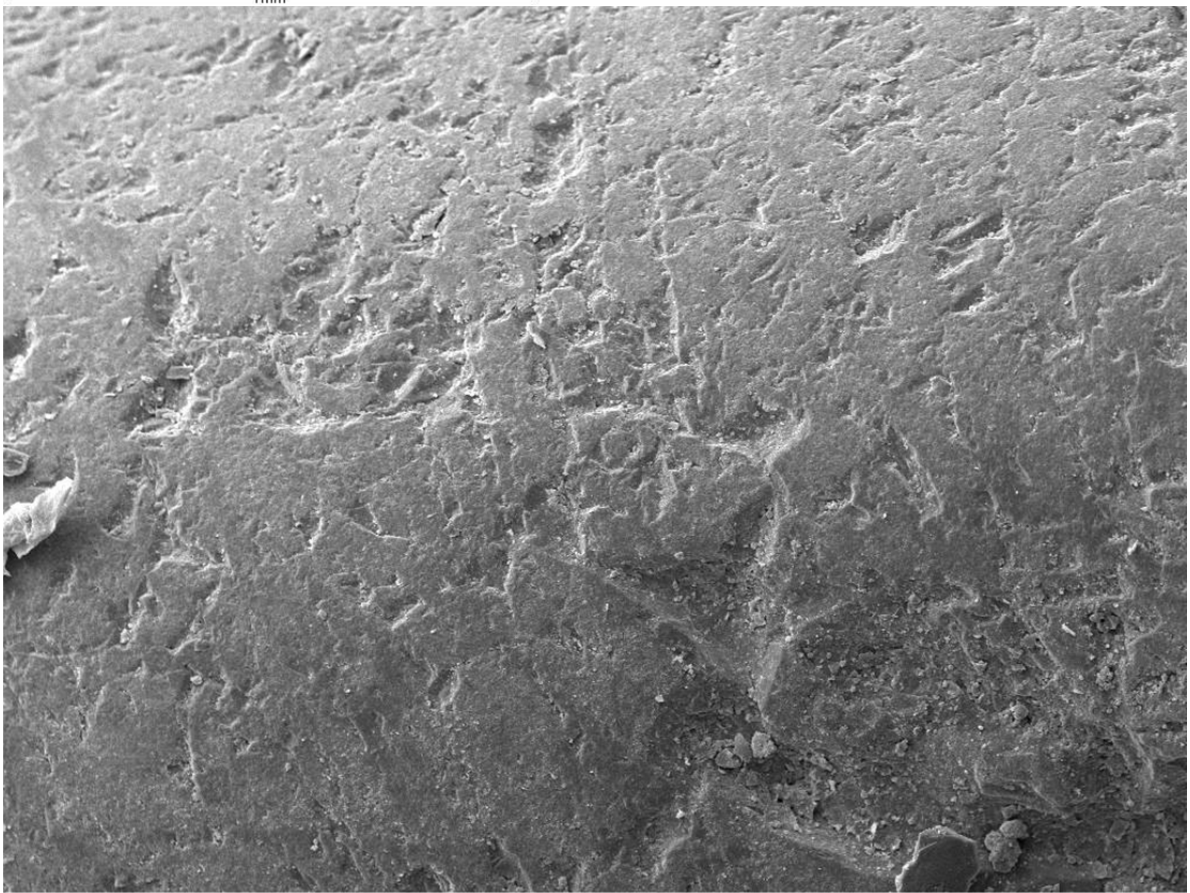
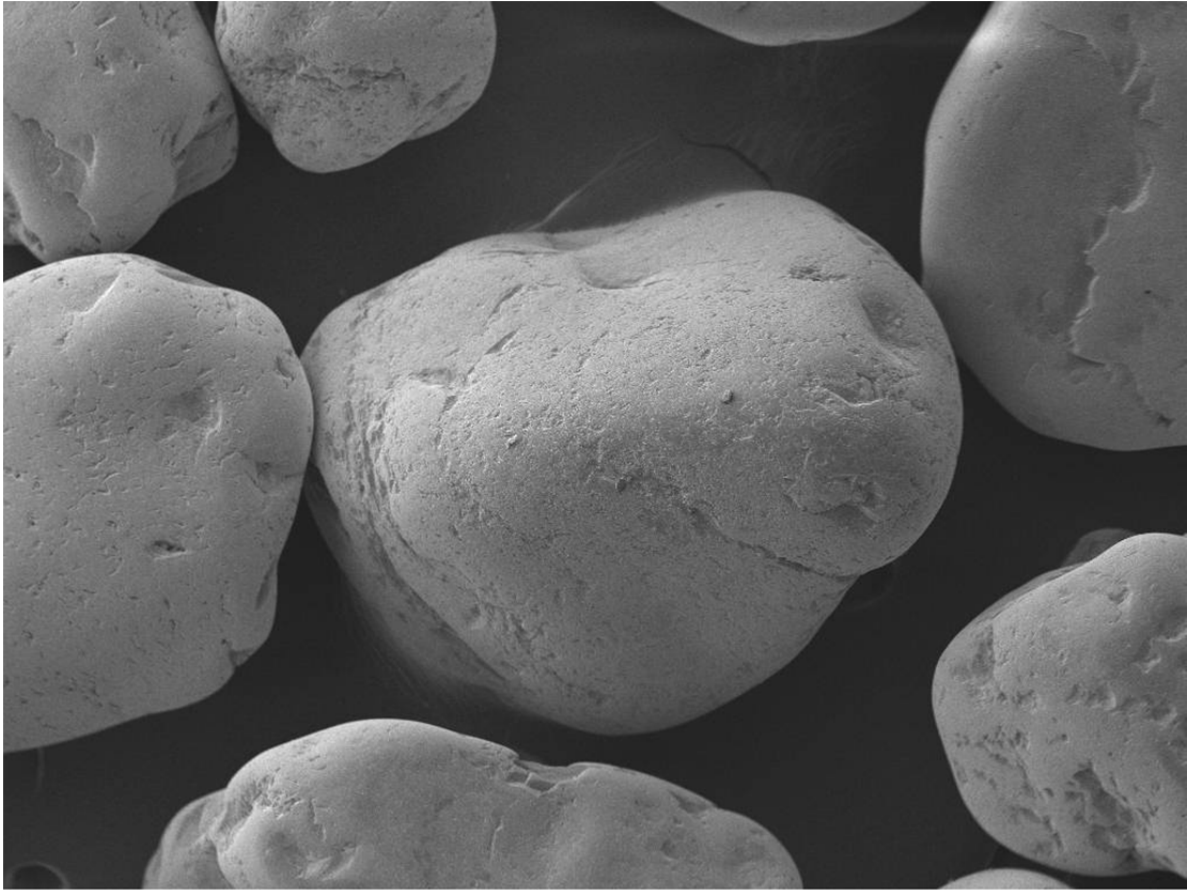
Phosphorus Slag SEM Images

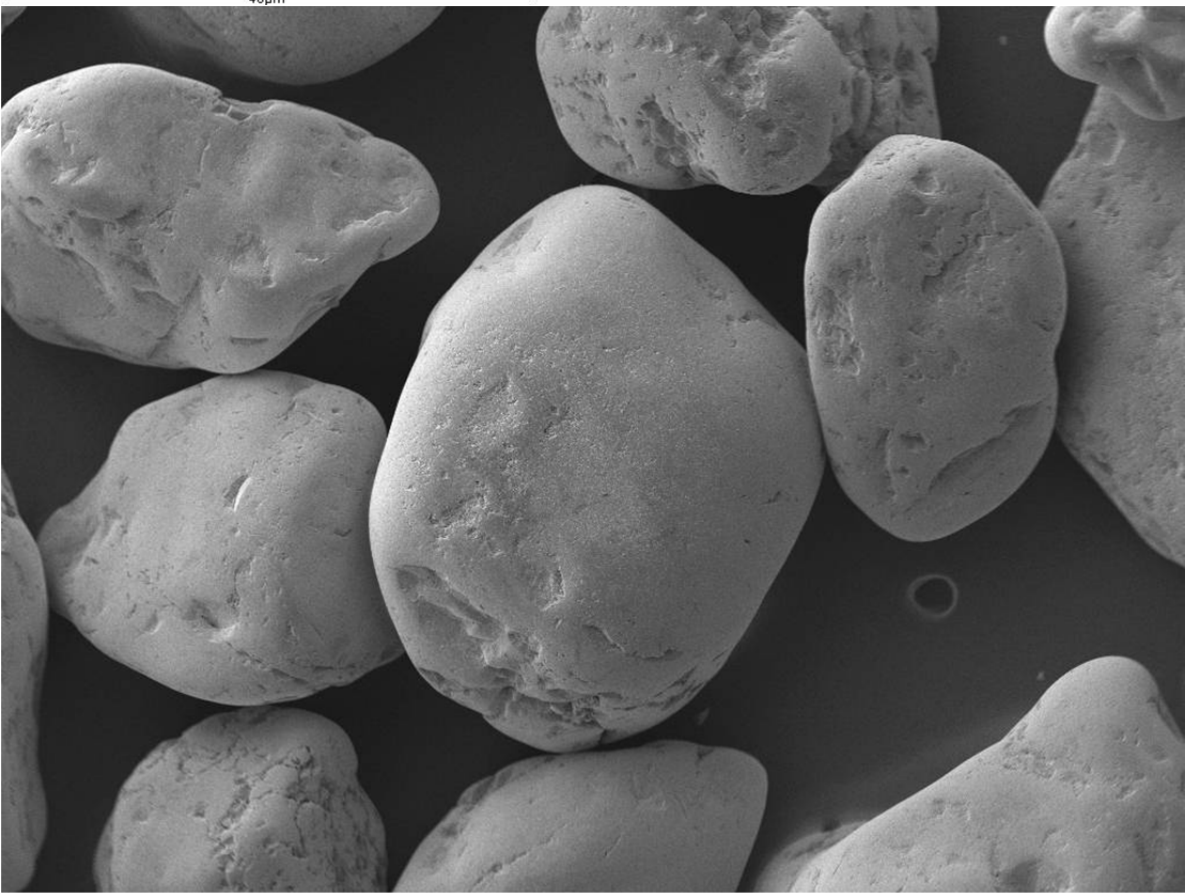
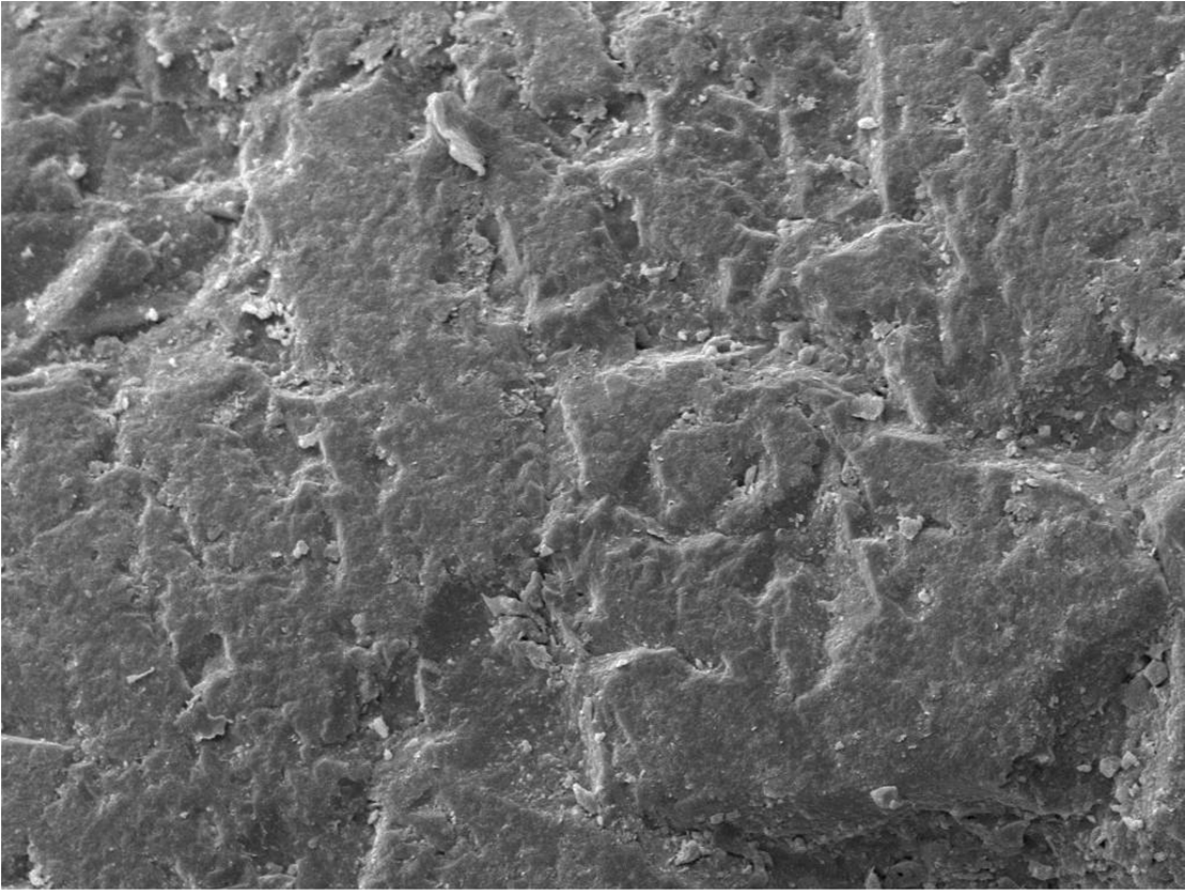


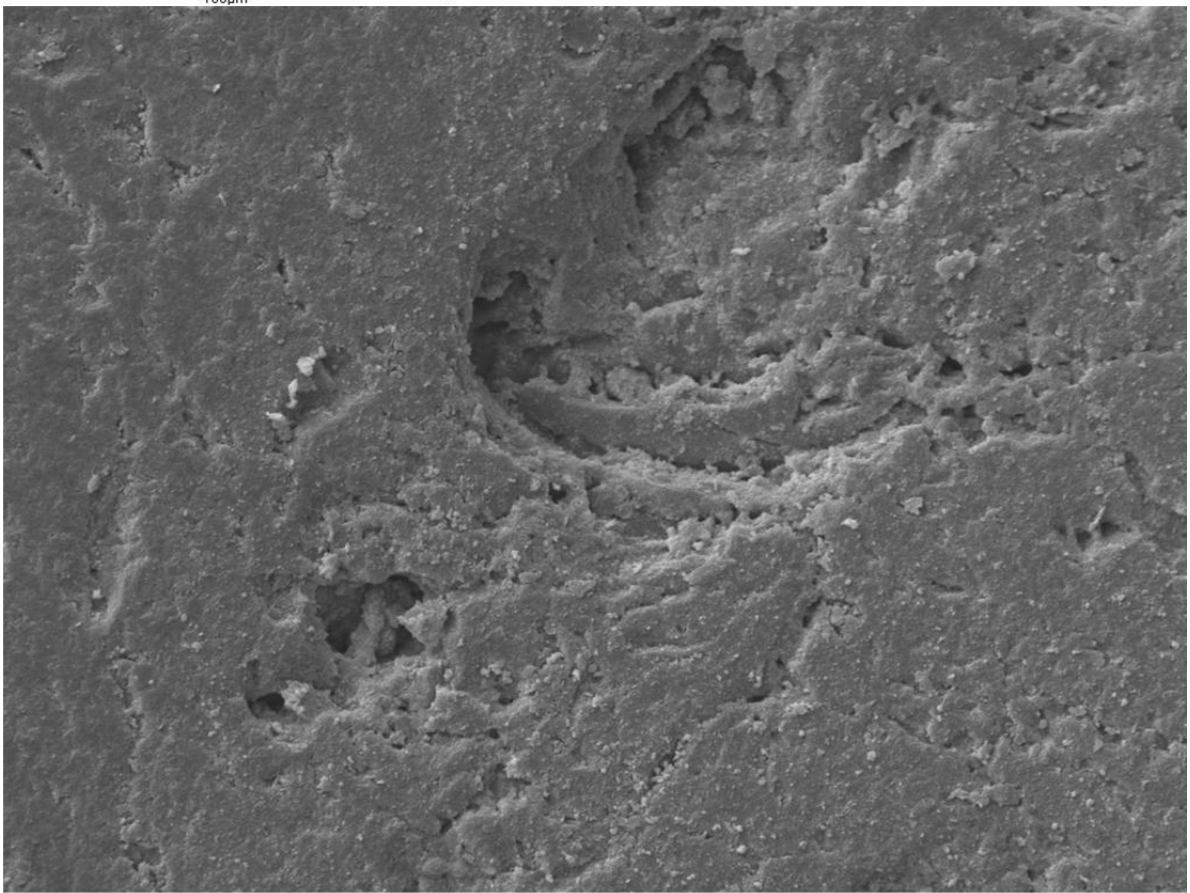
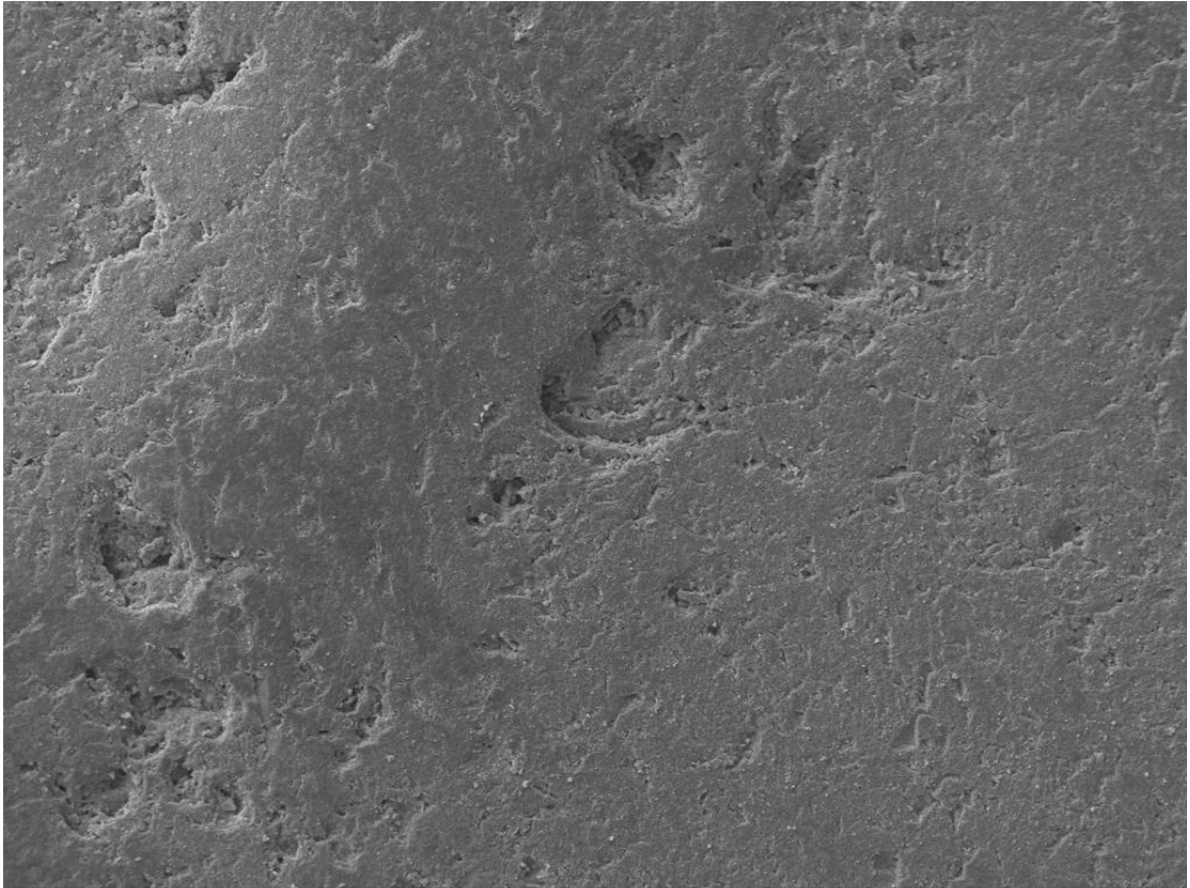


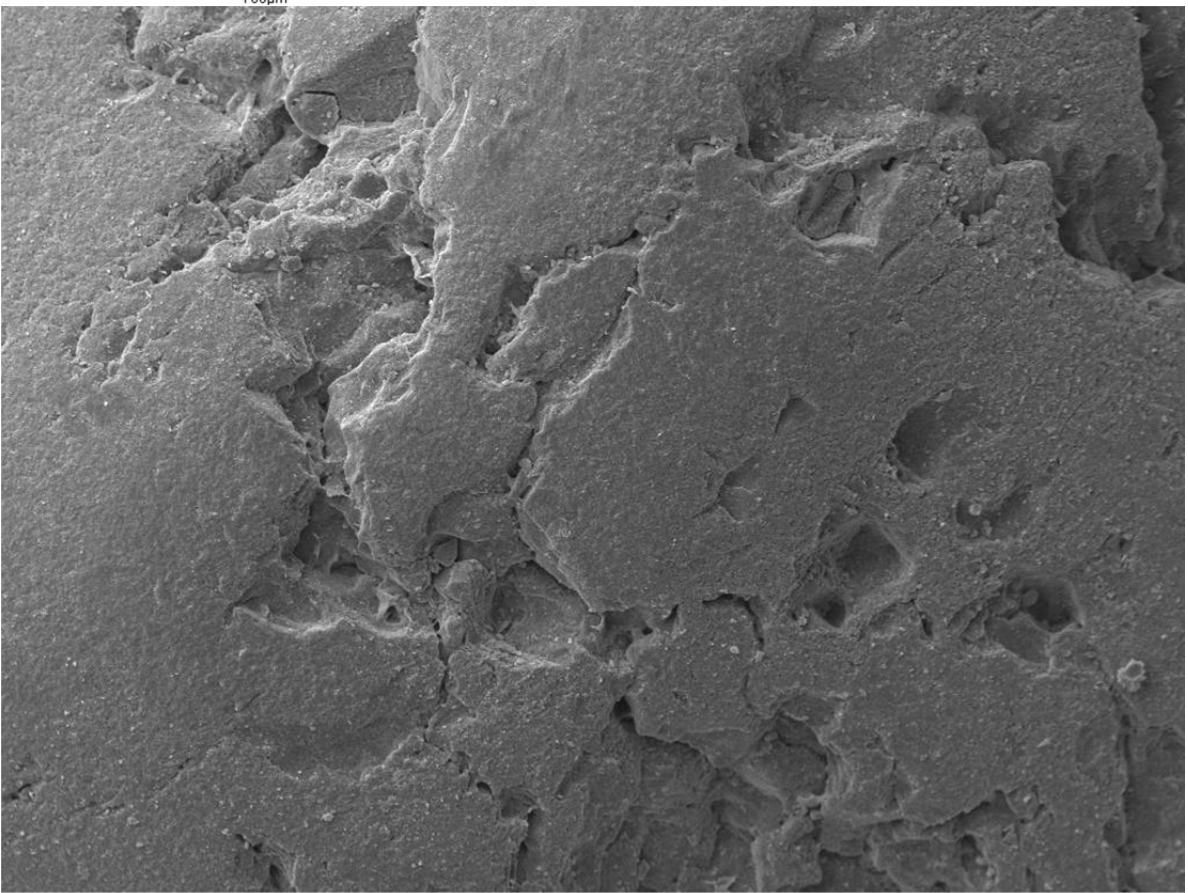
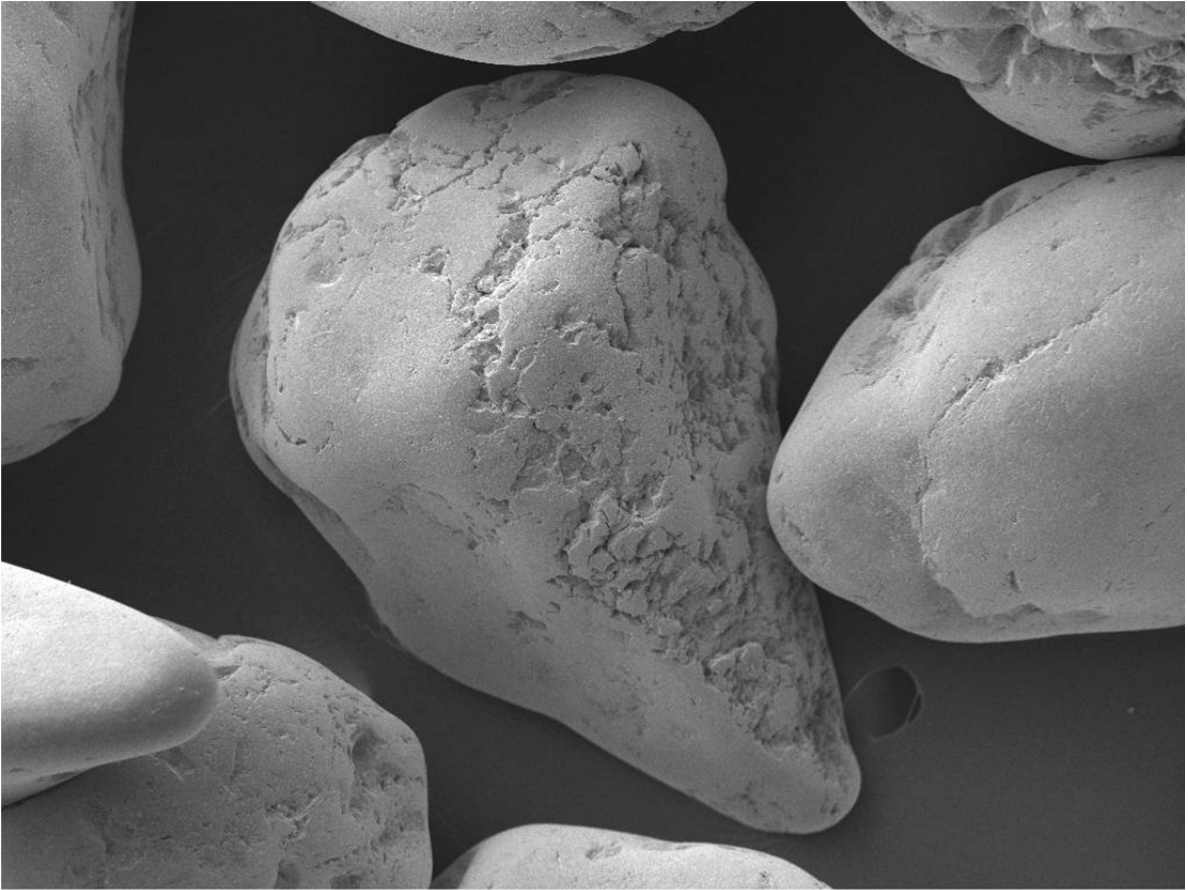


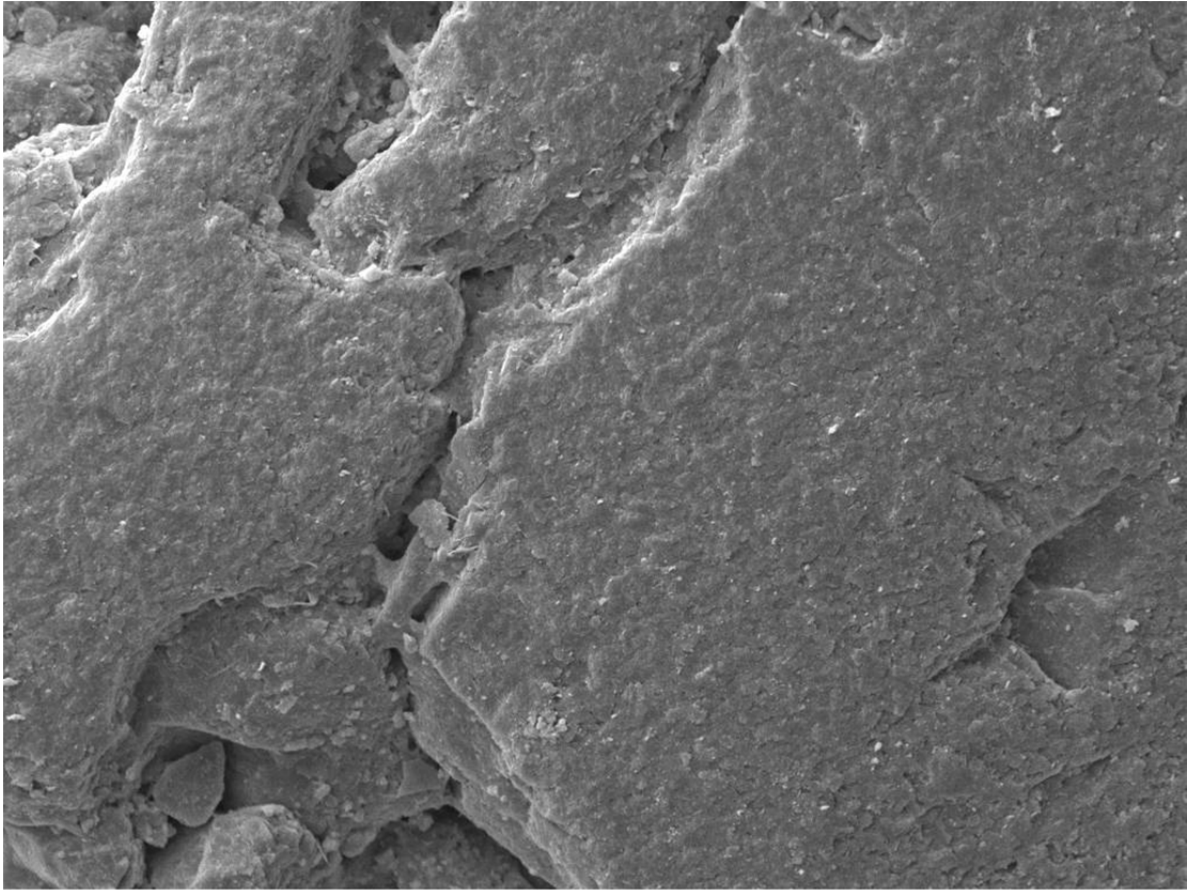
Sand SEM Images





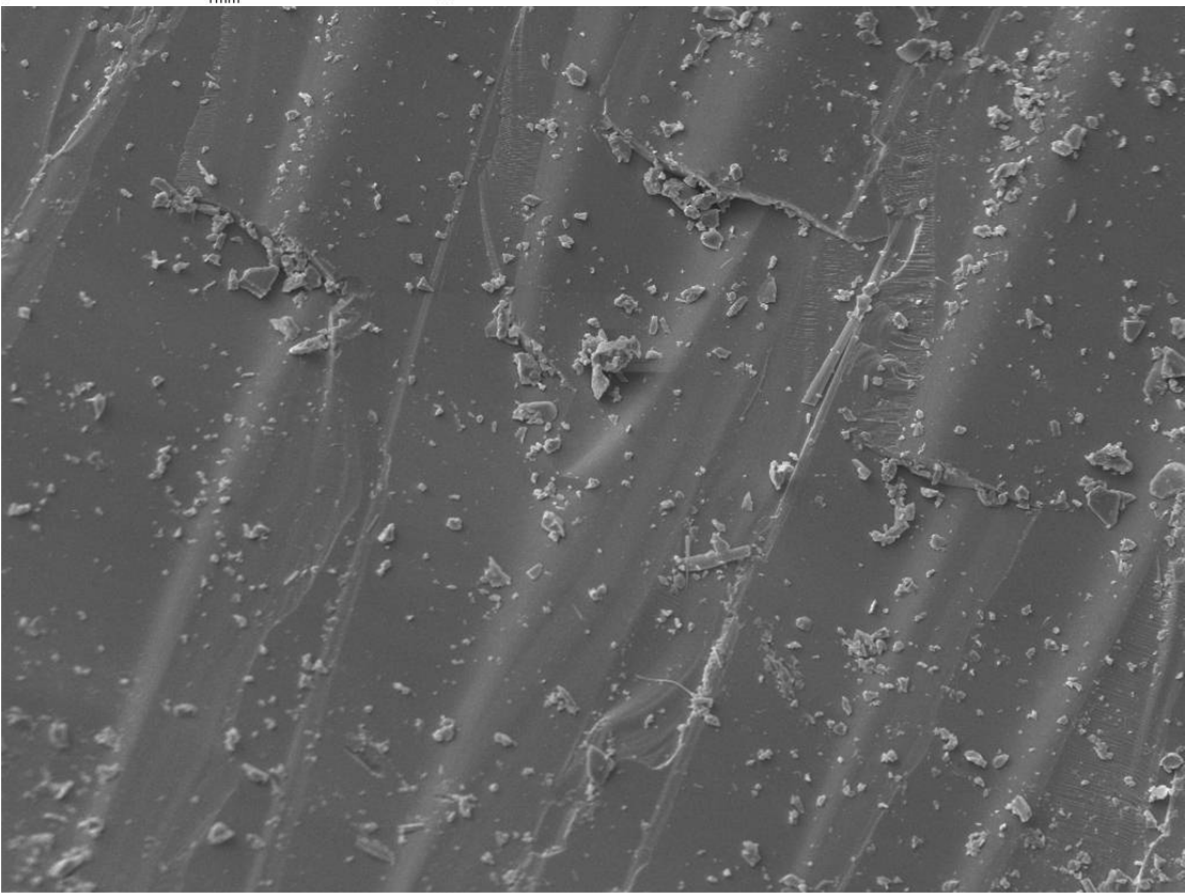
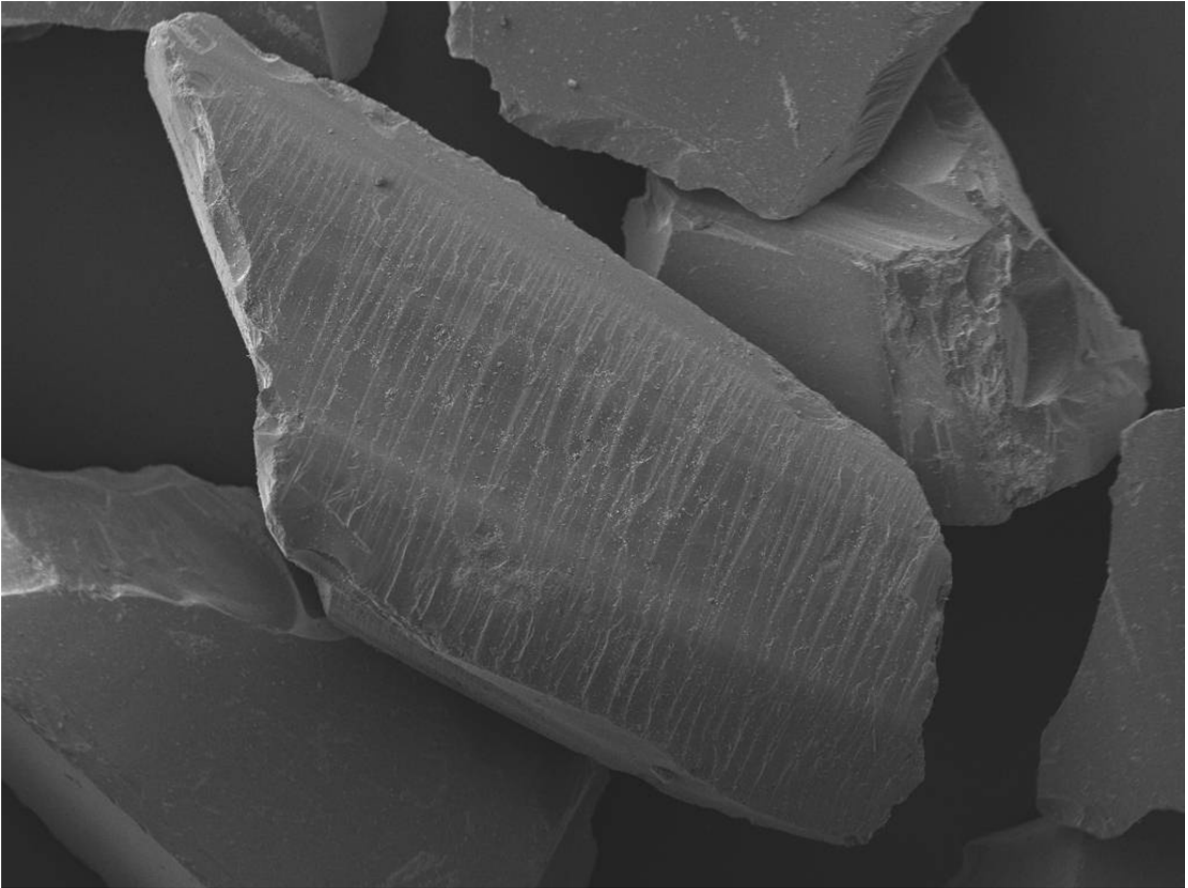


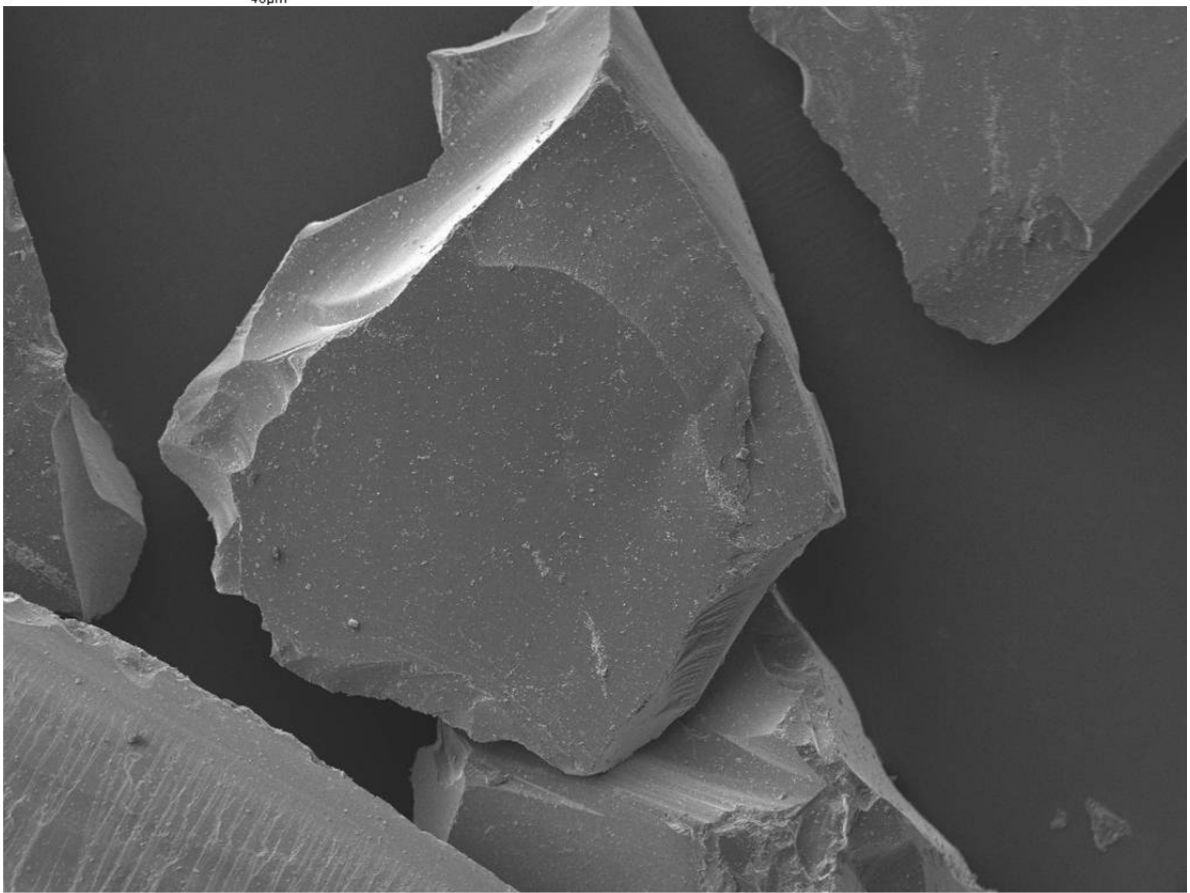
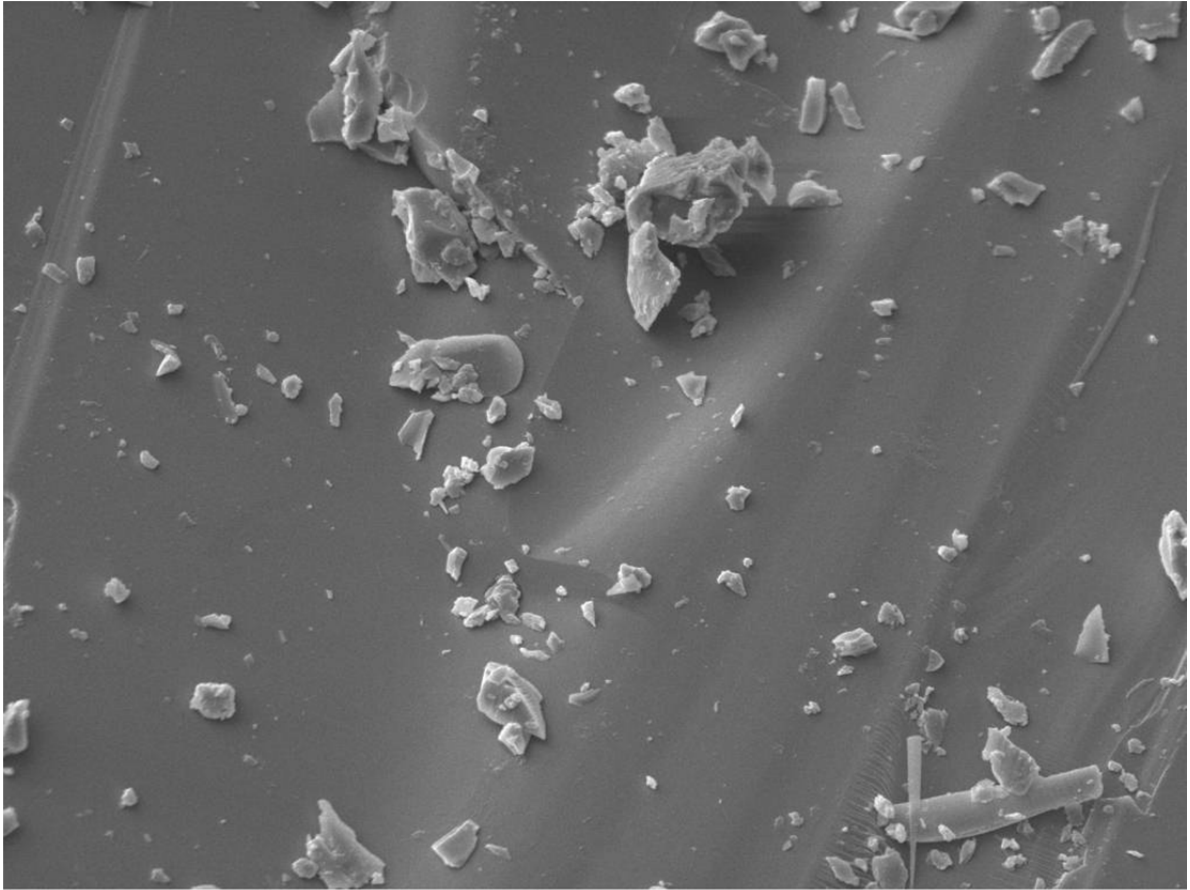


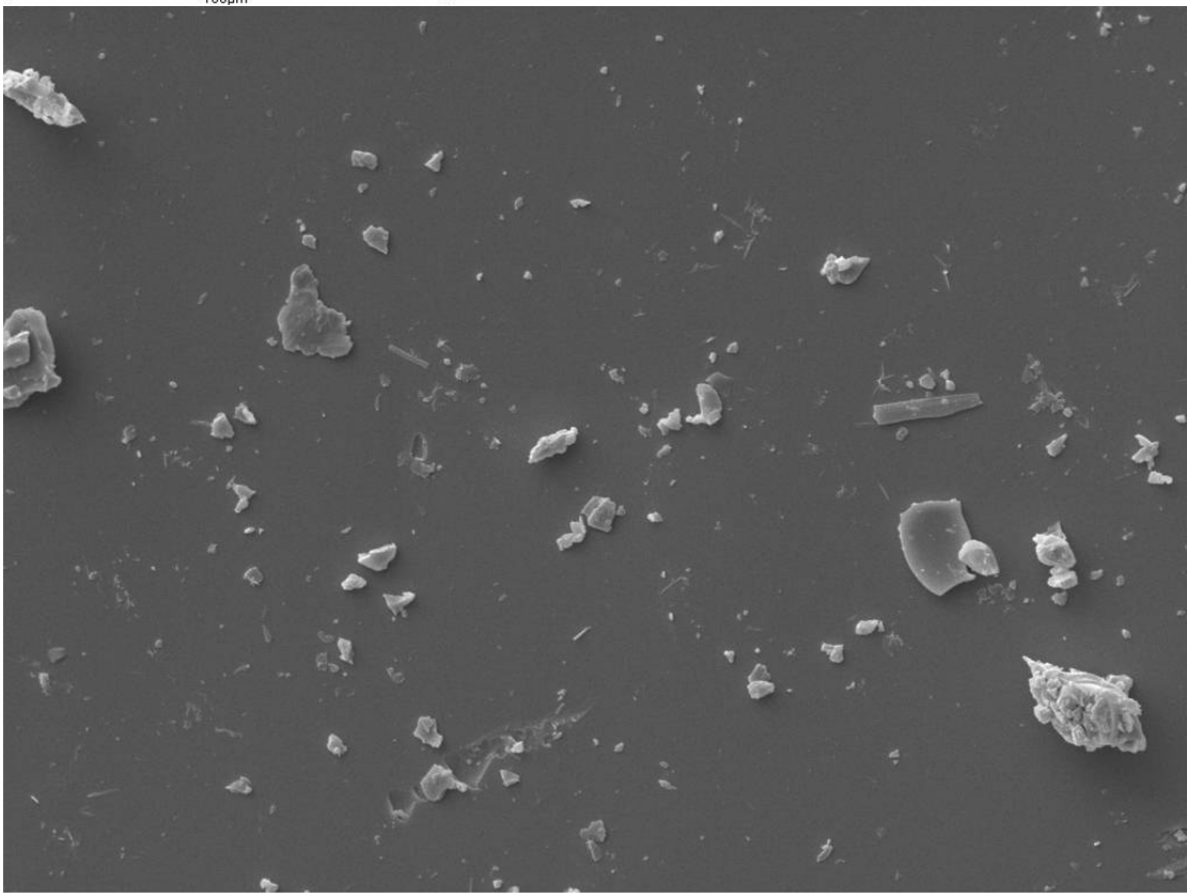
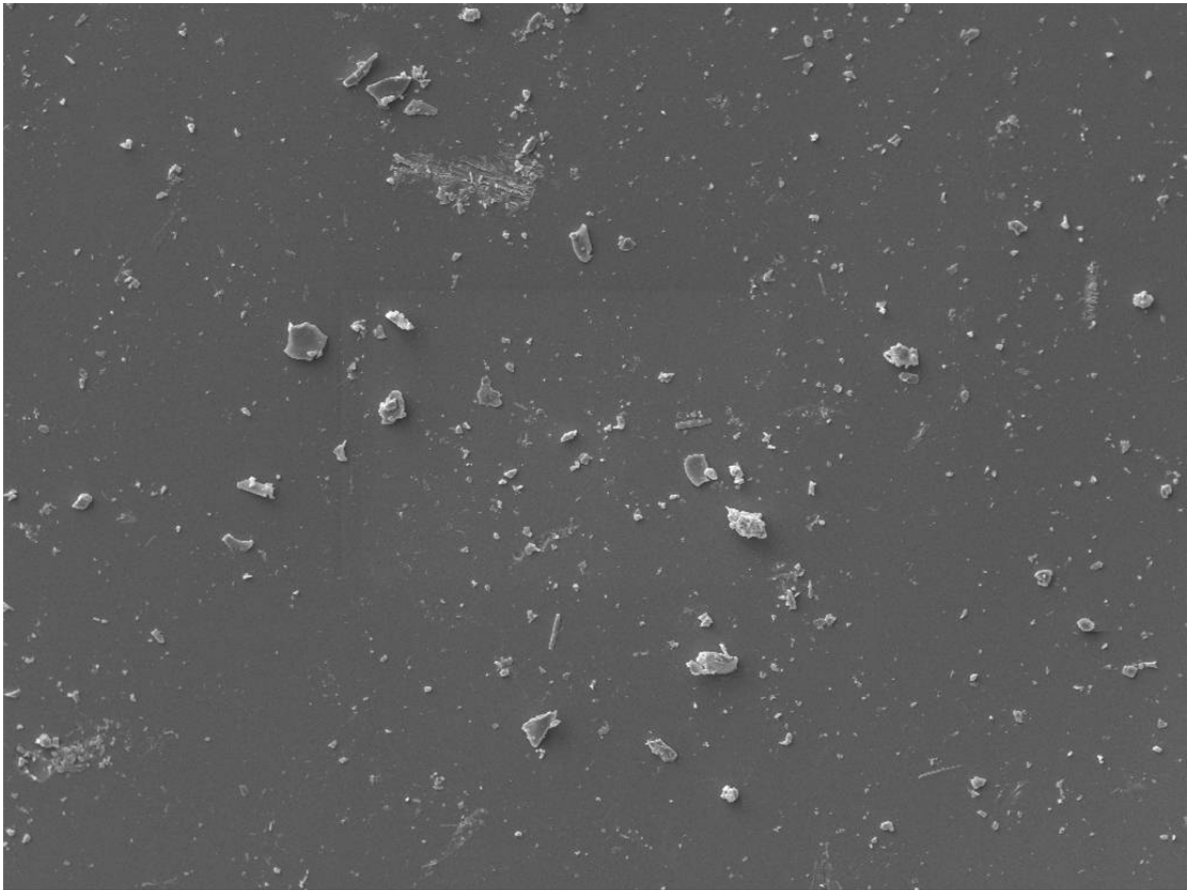


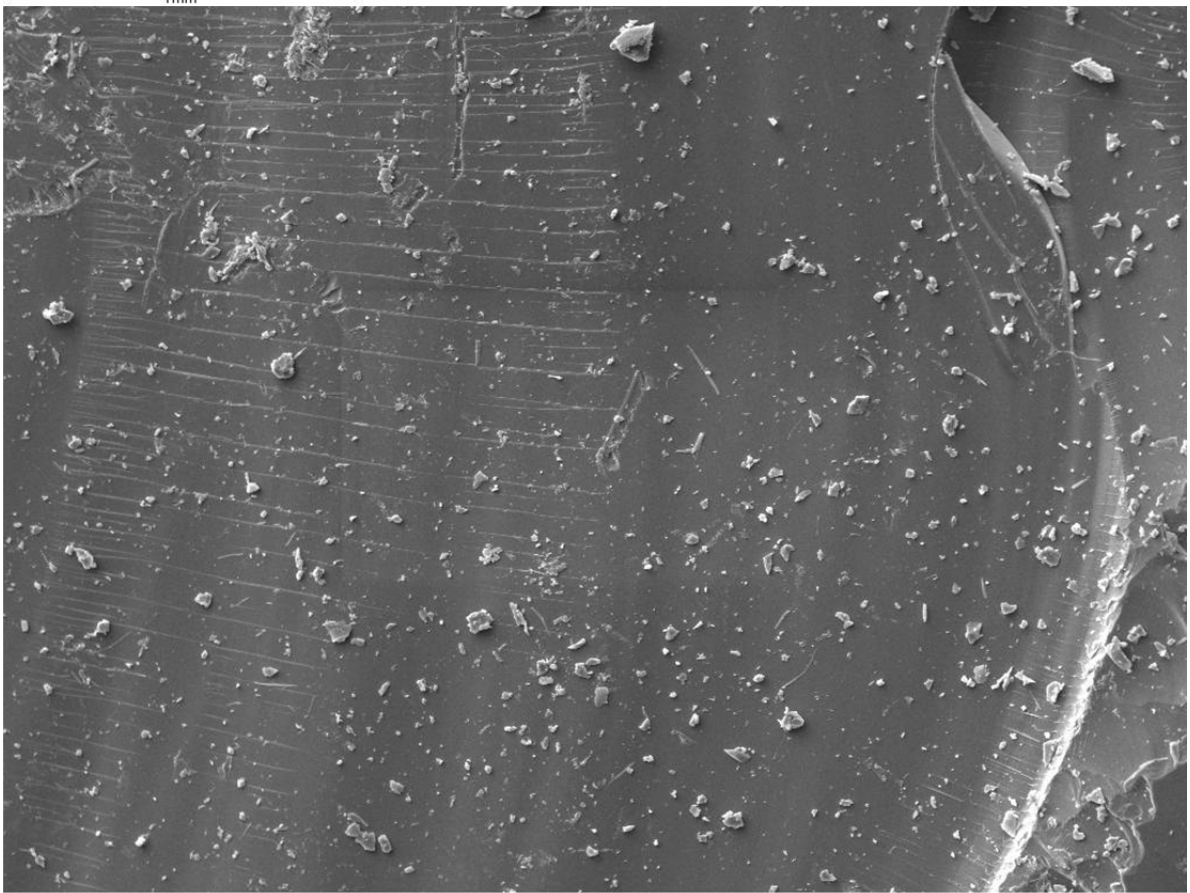
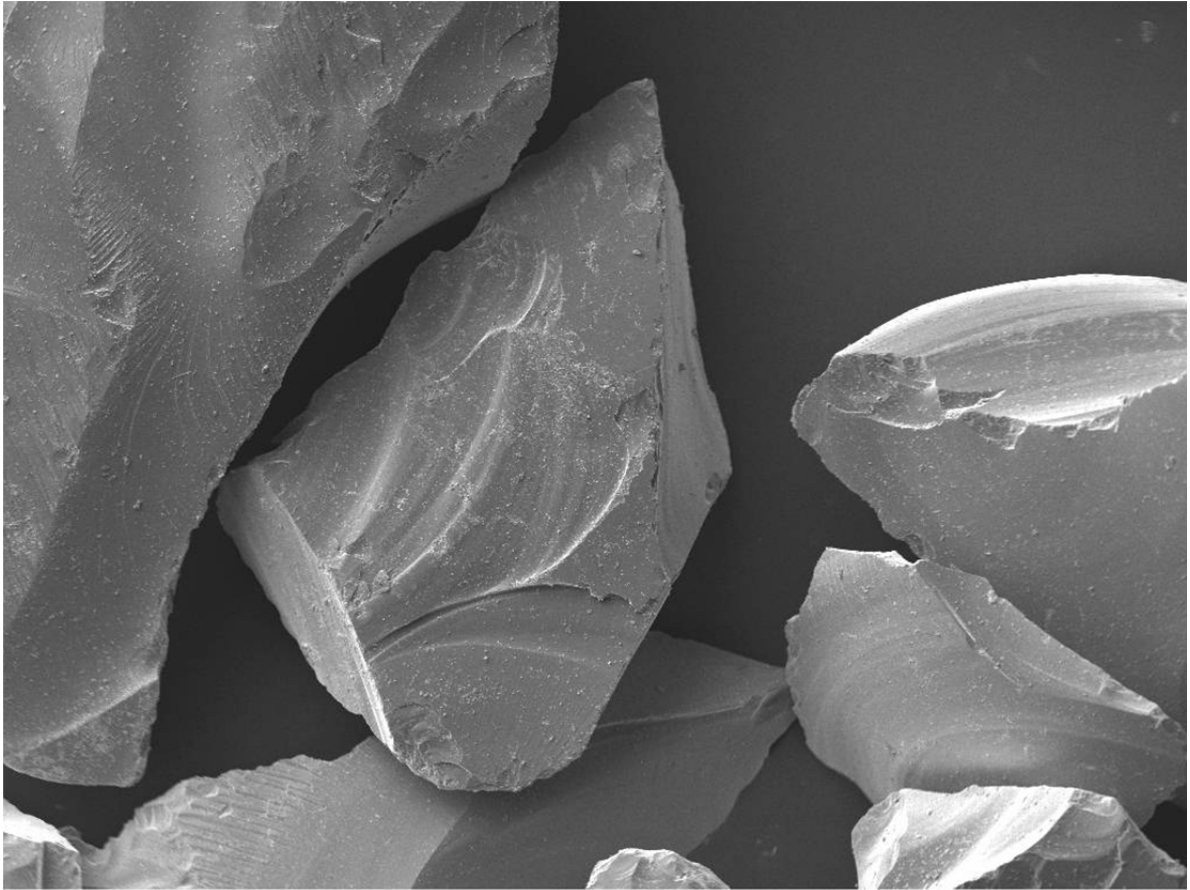
40µm

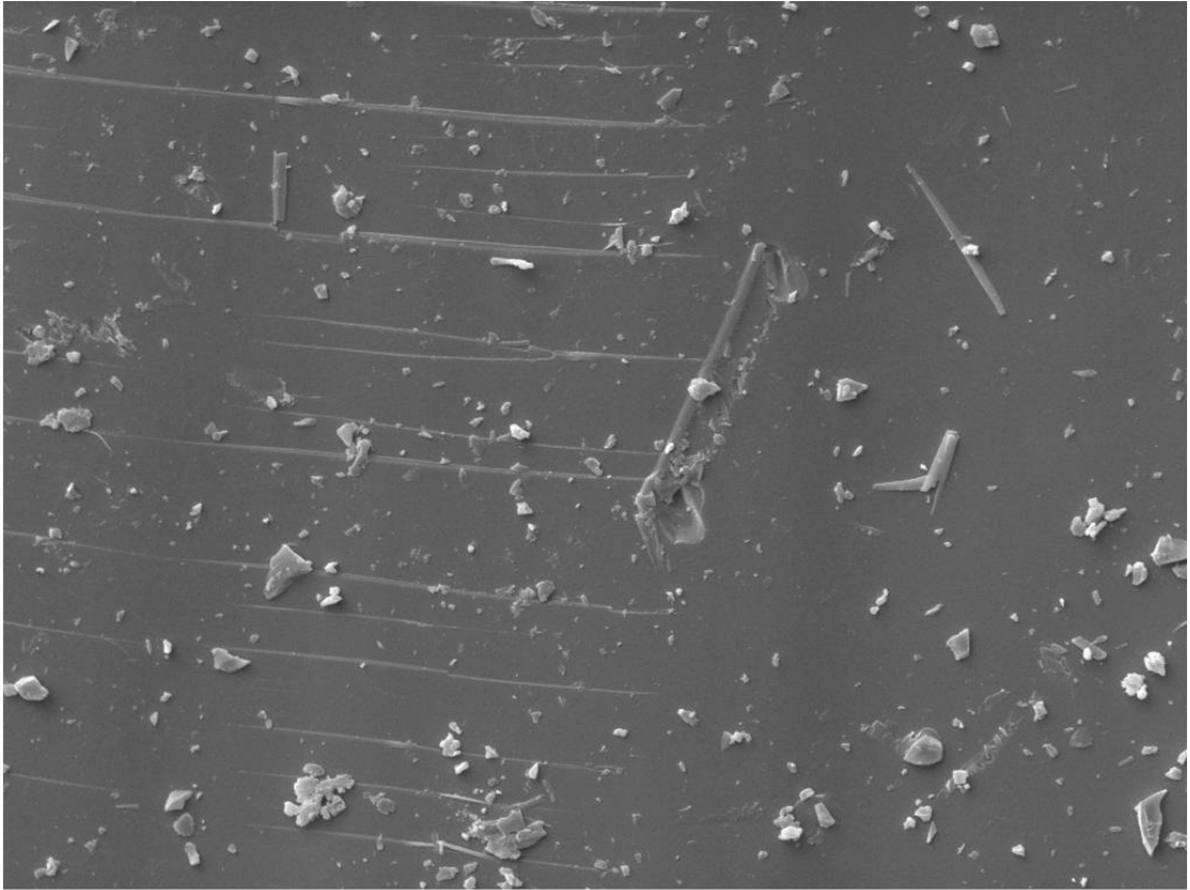
Glass SEM Images





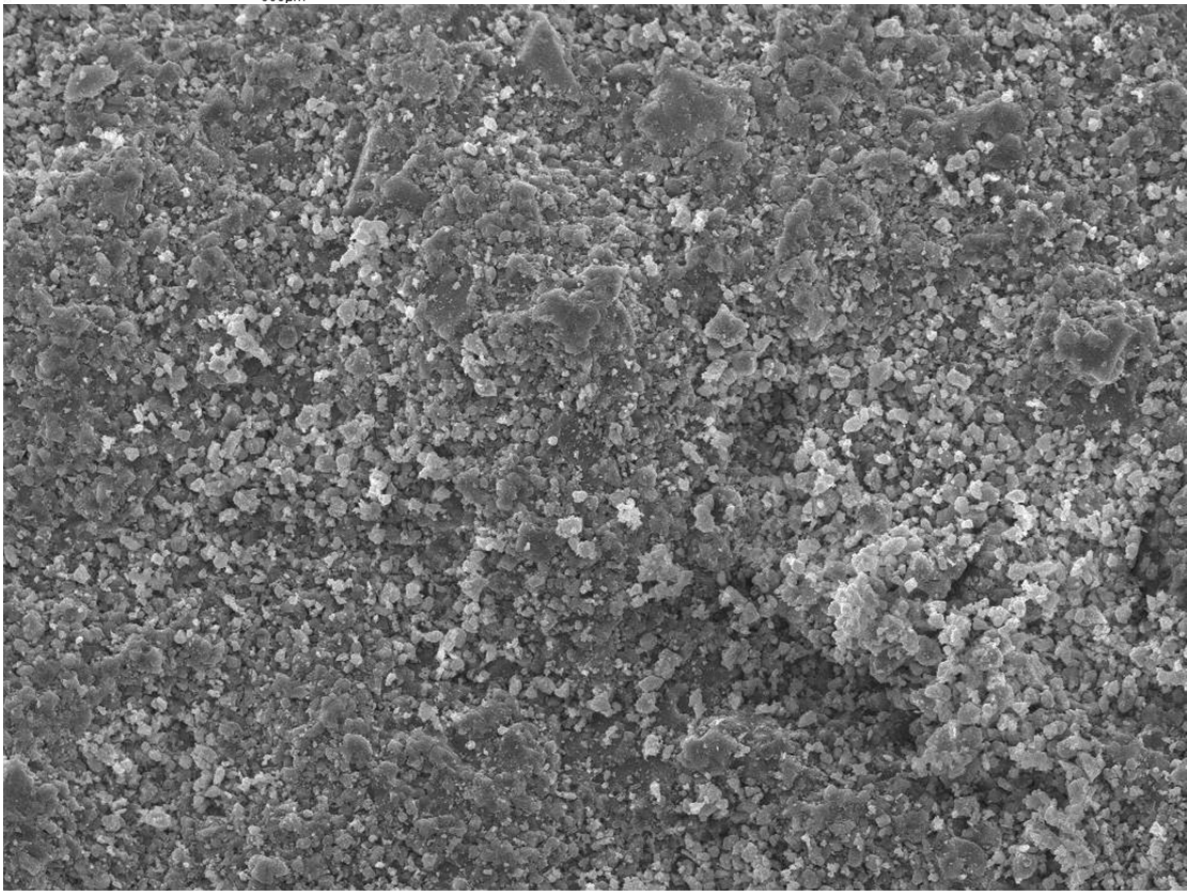
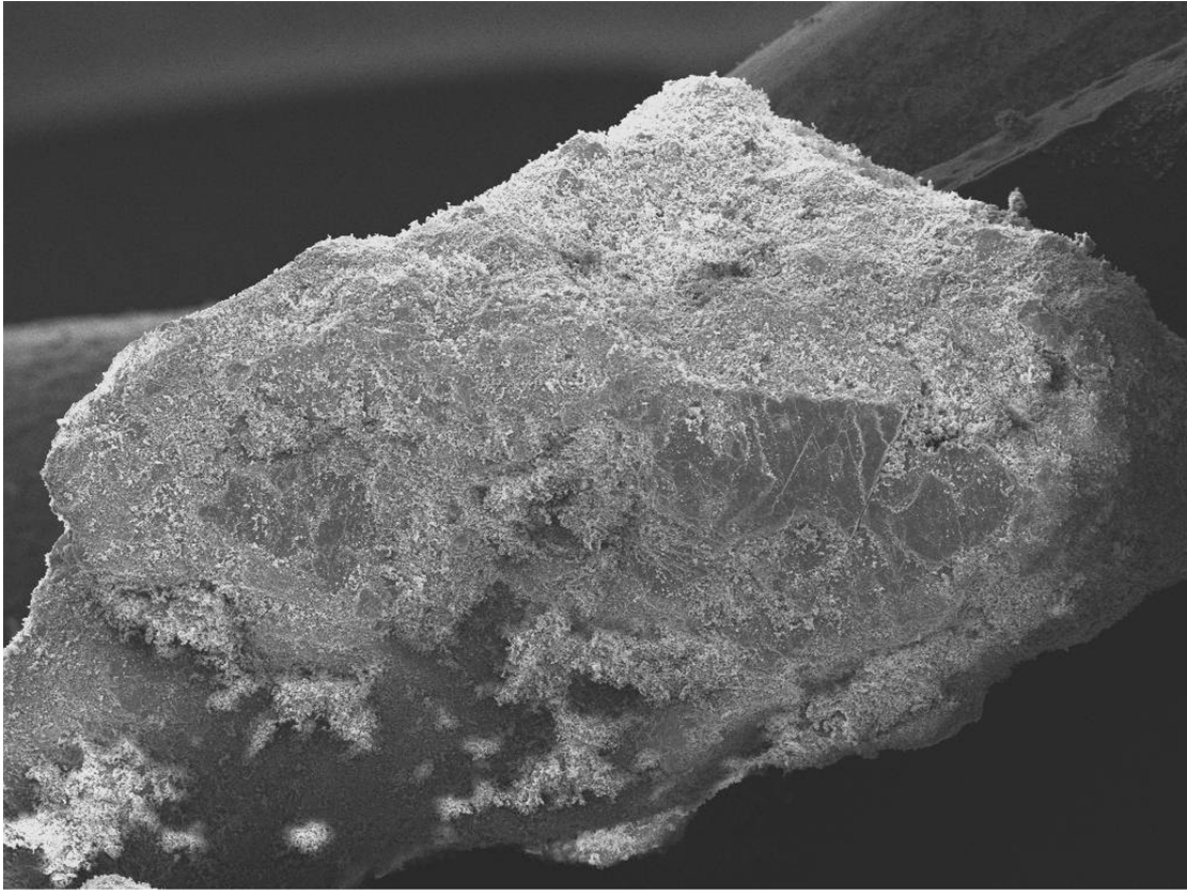


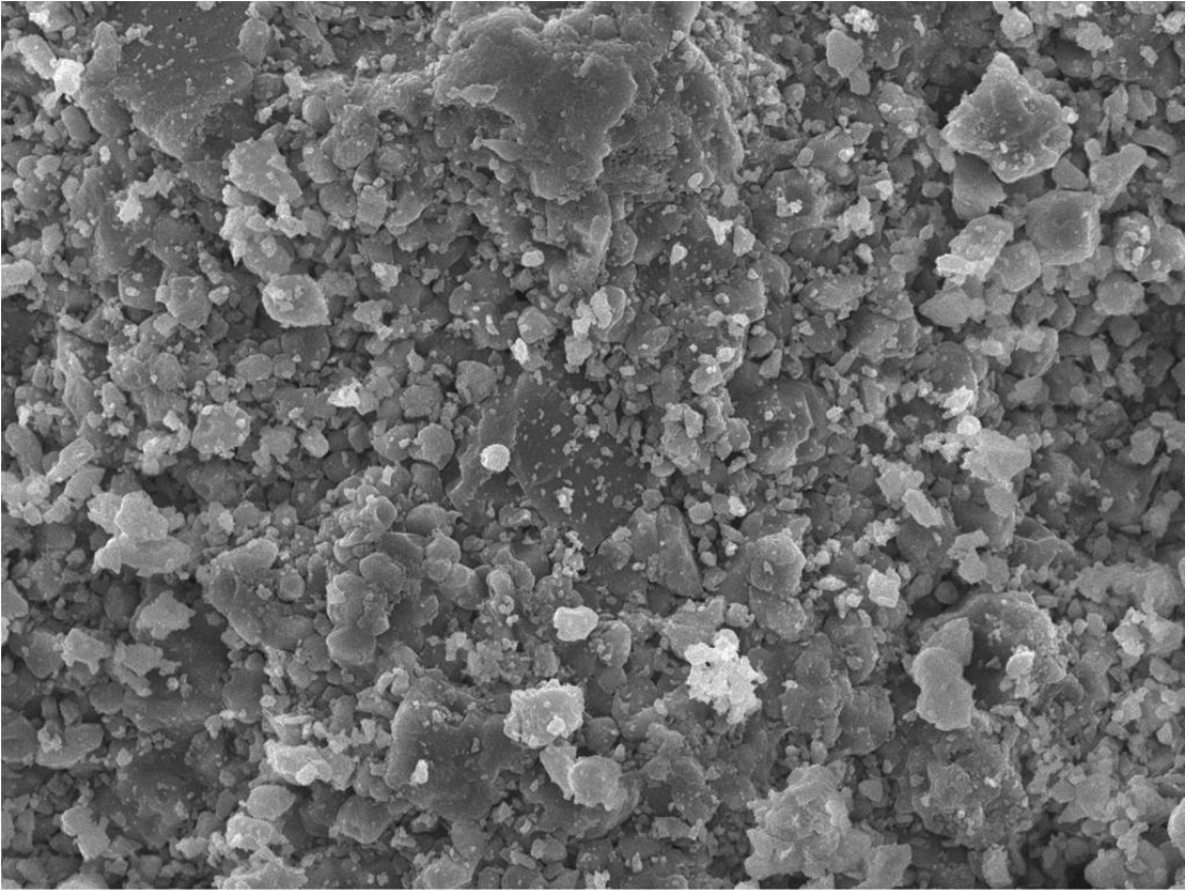




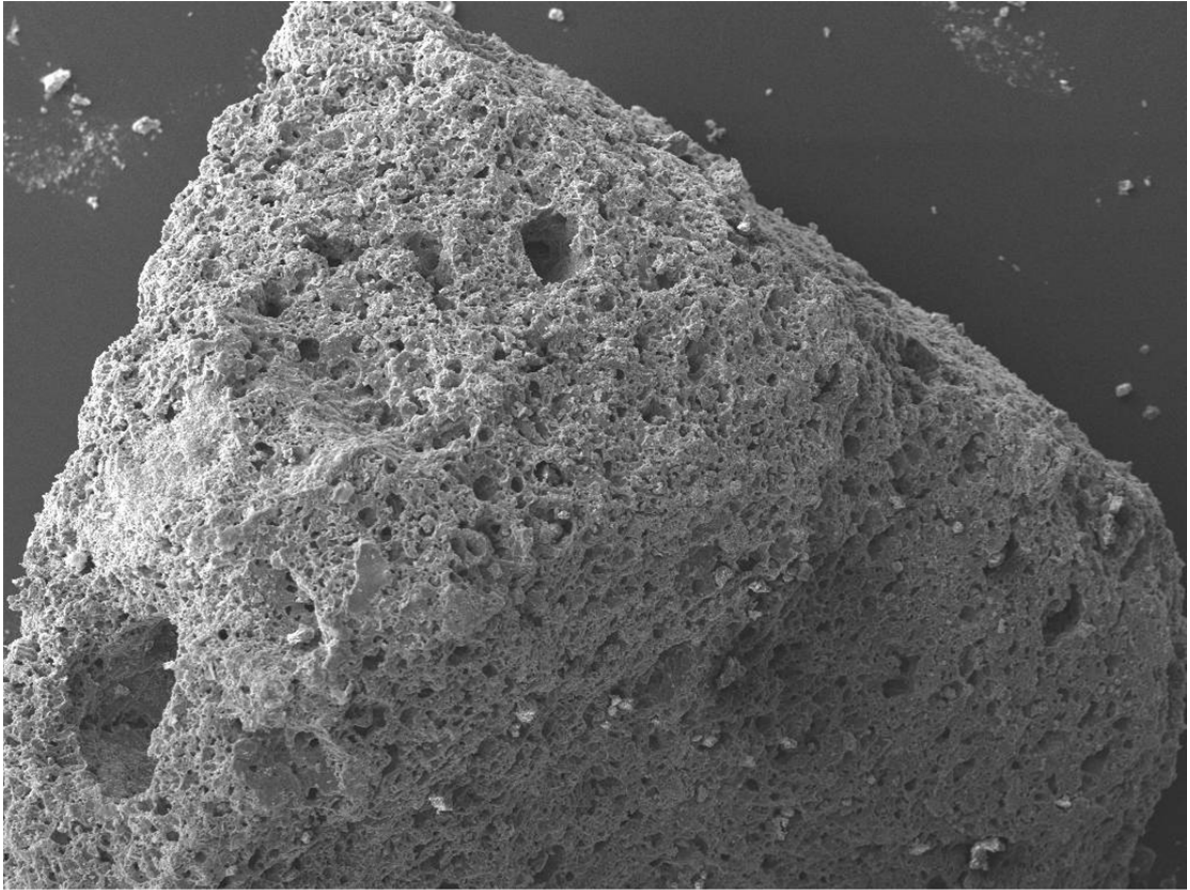
40µm

Limestone SEM Images

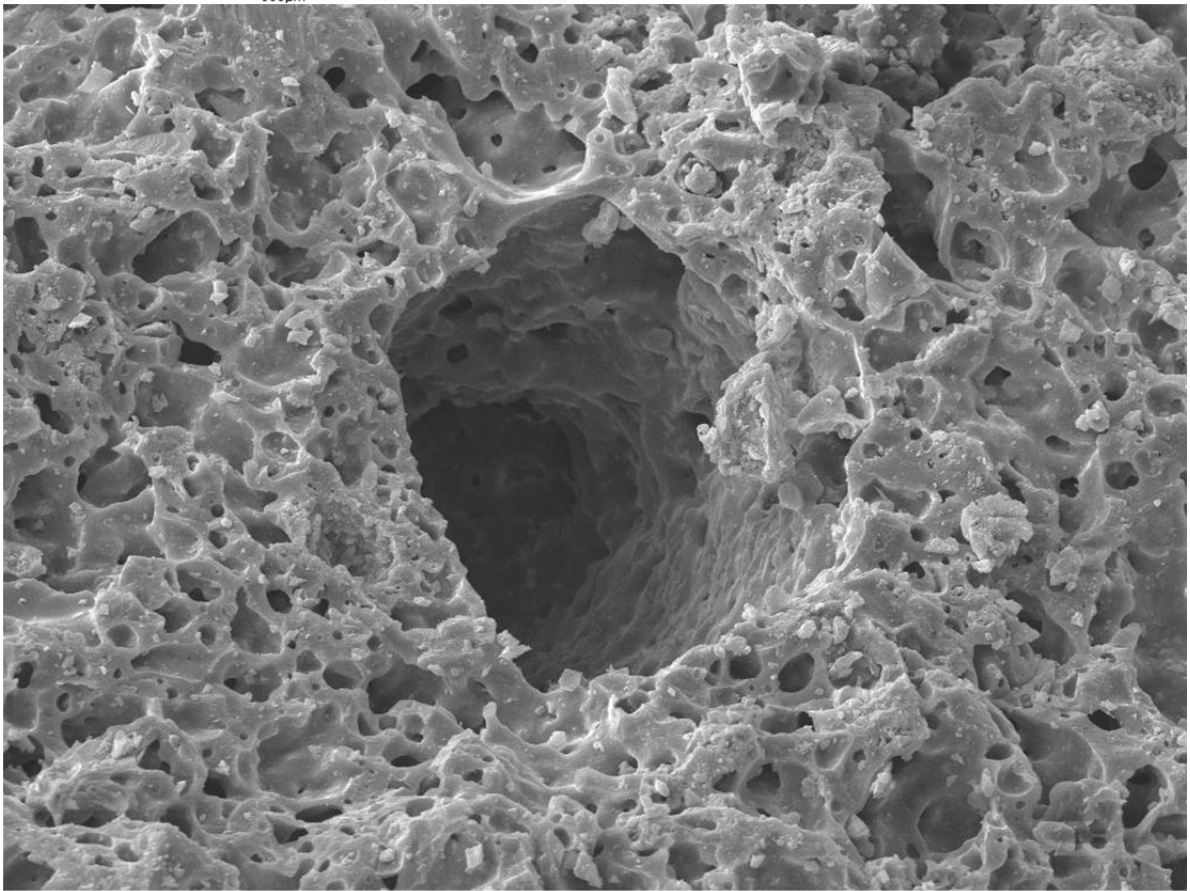




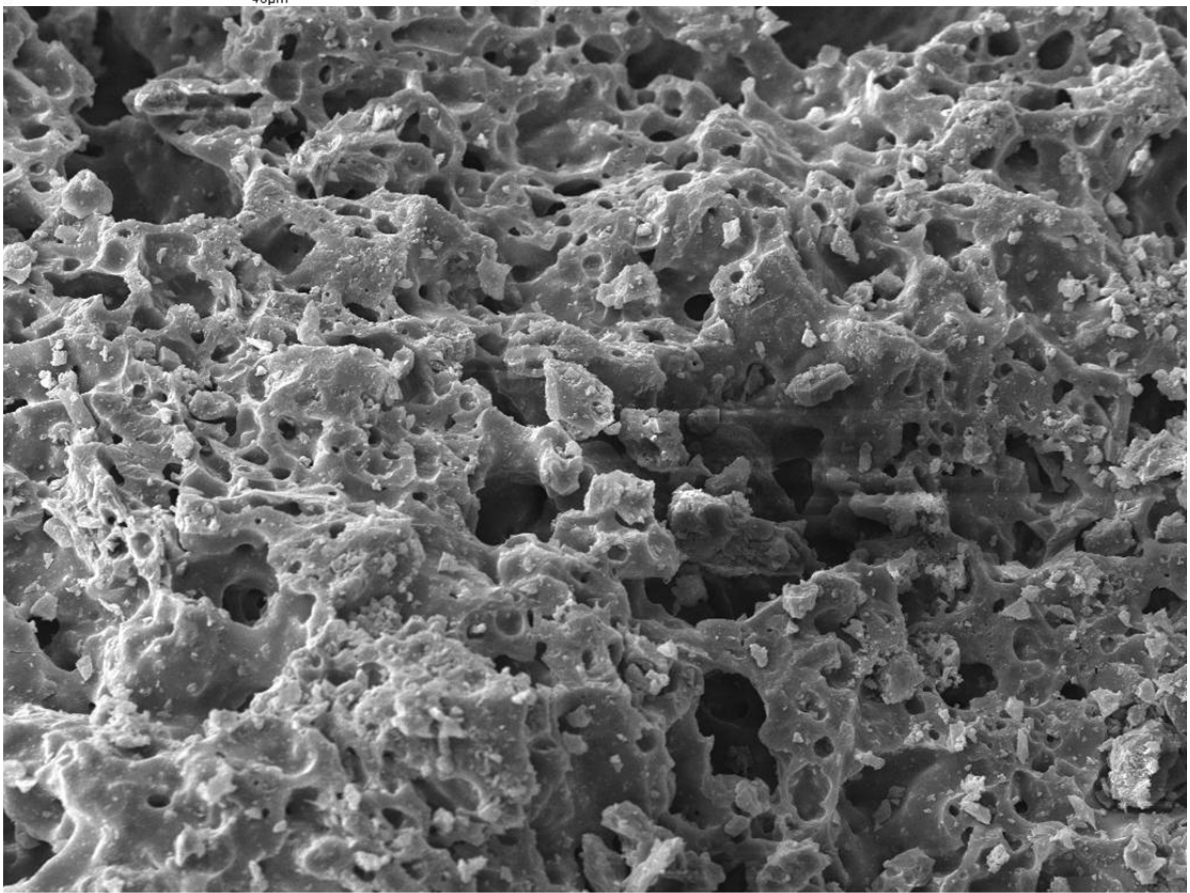
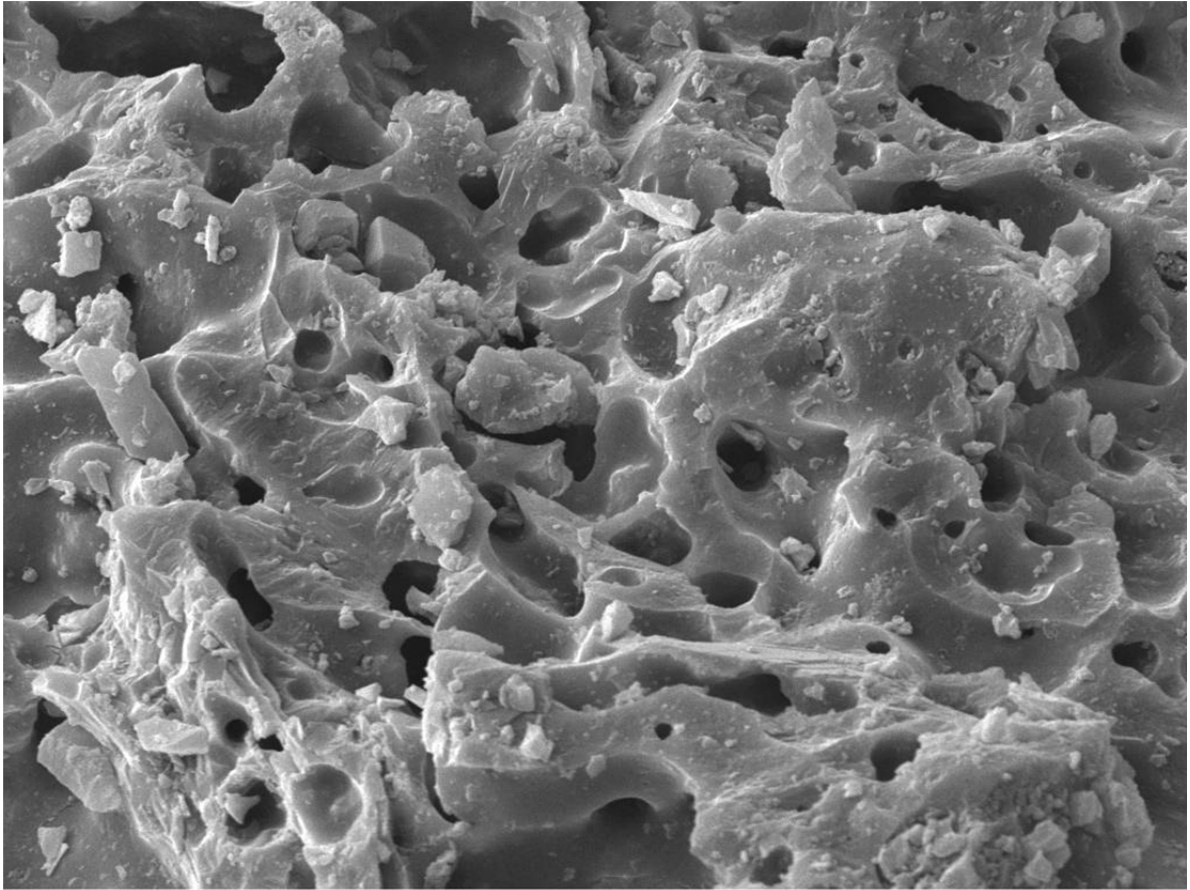
Filtralite SEM Images

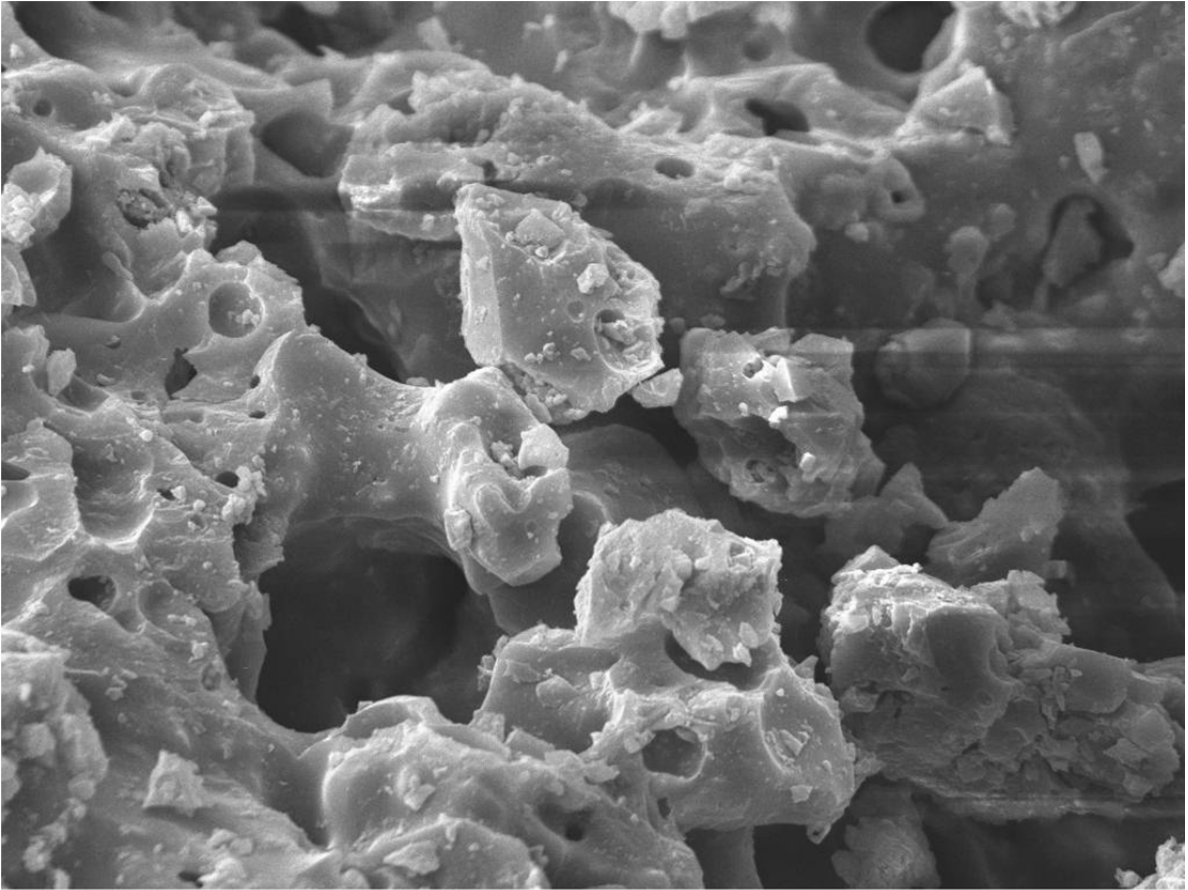


800µm



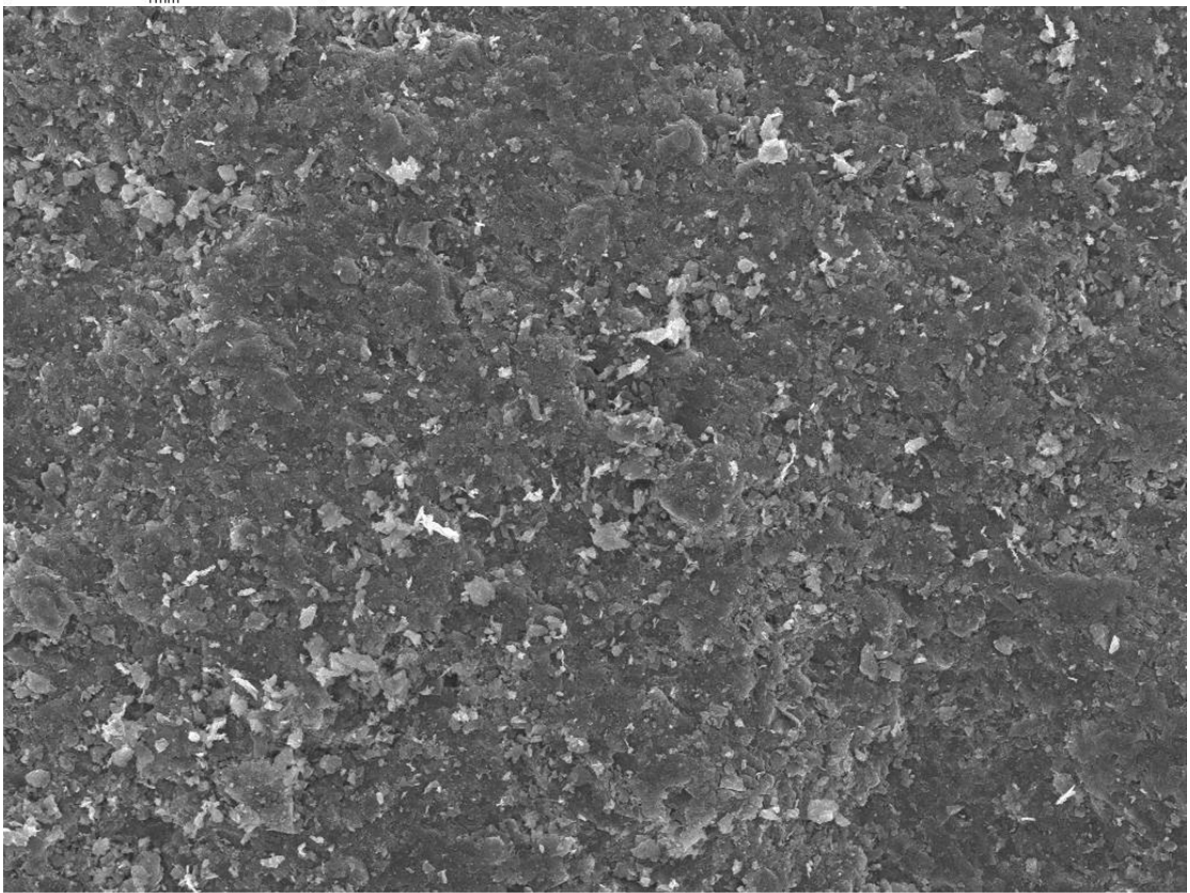
100µm

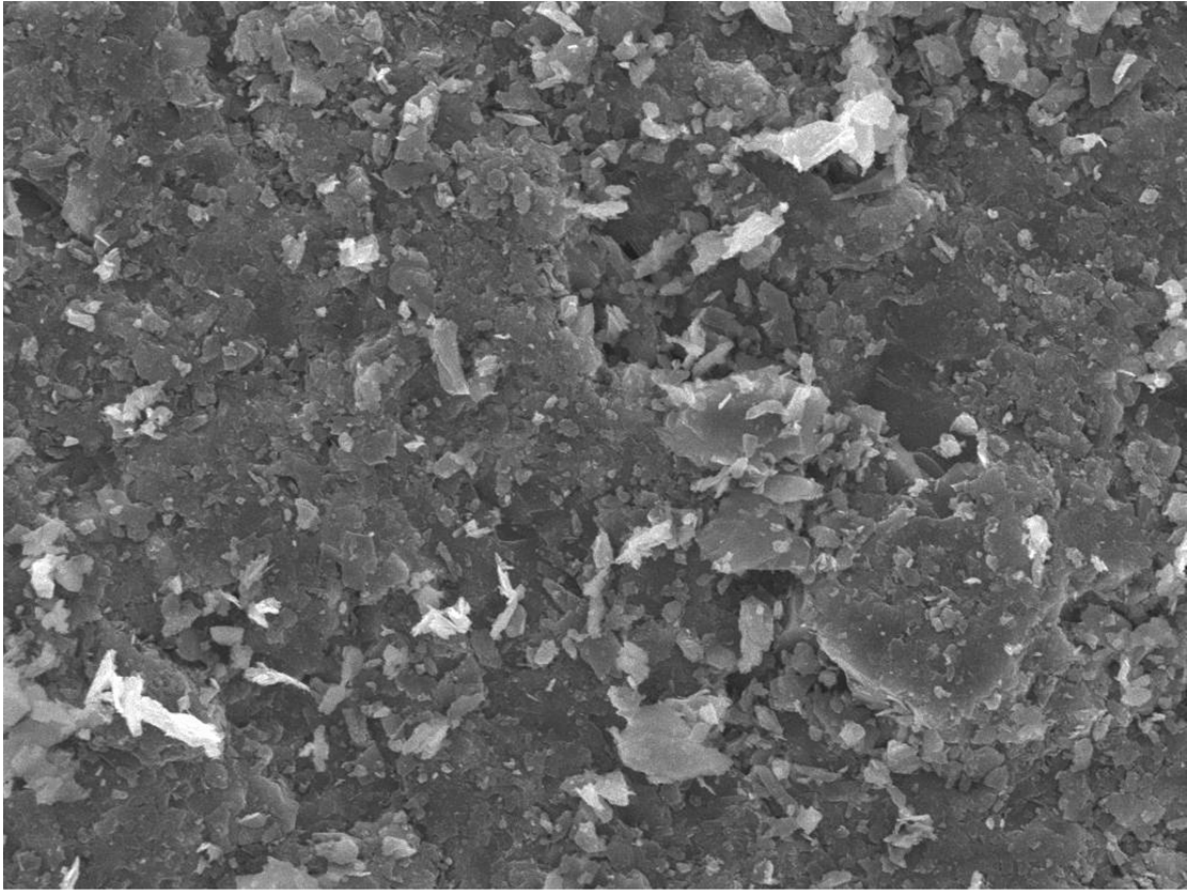




40µm

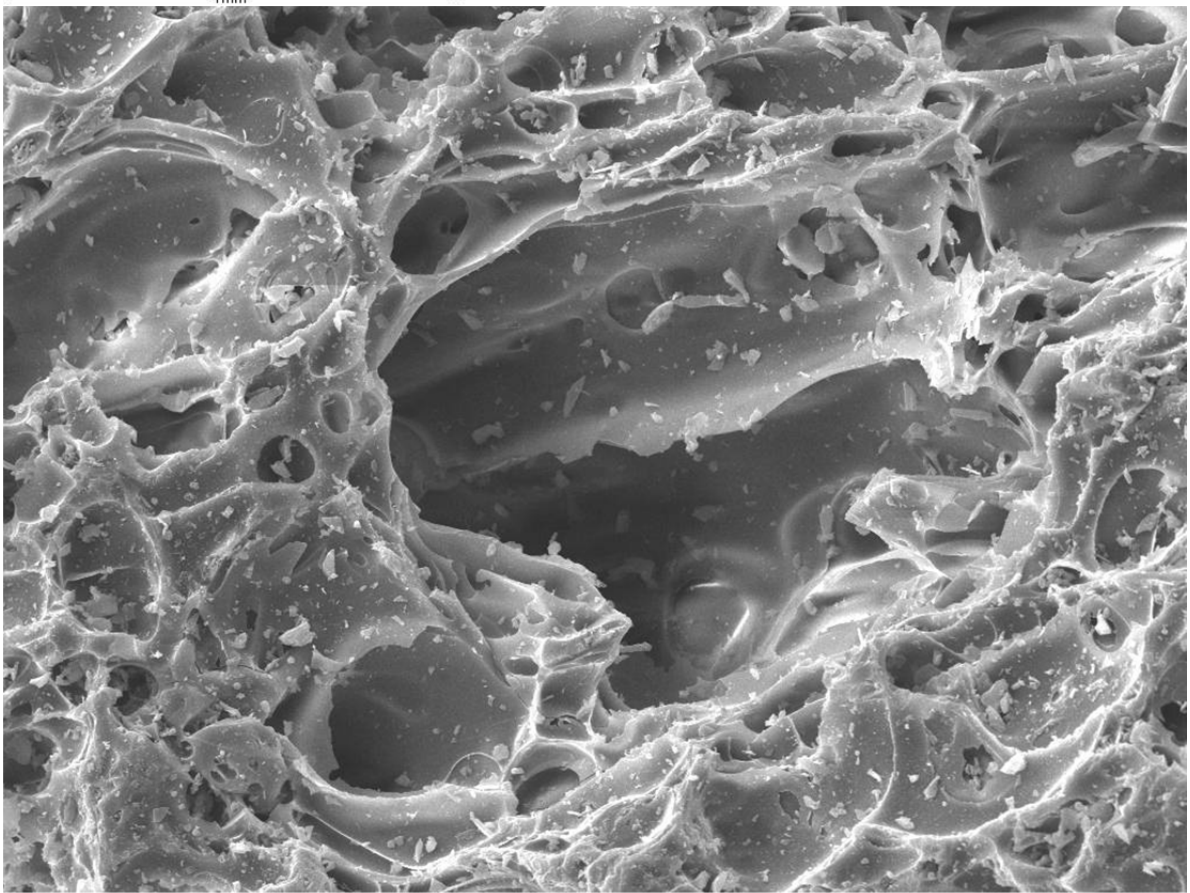
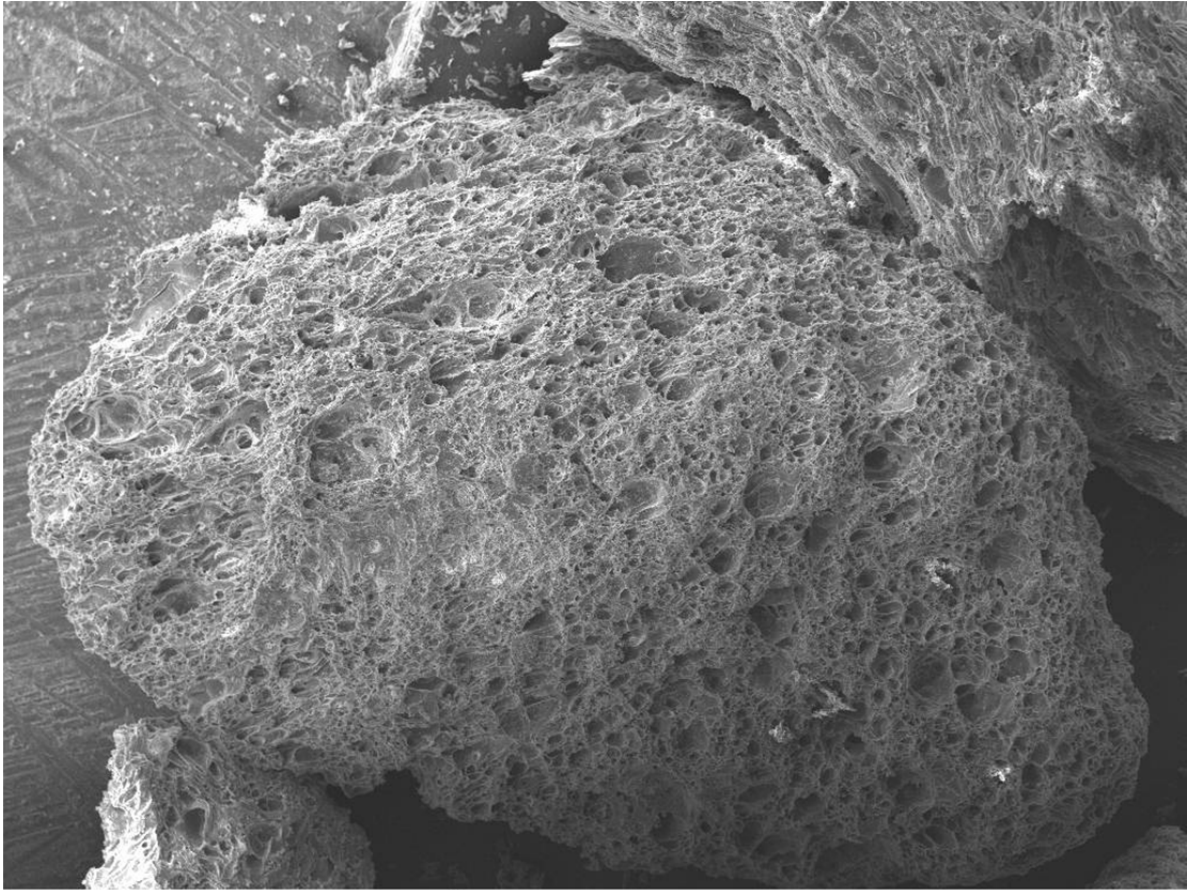
Slate SEM Images

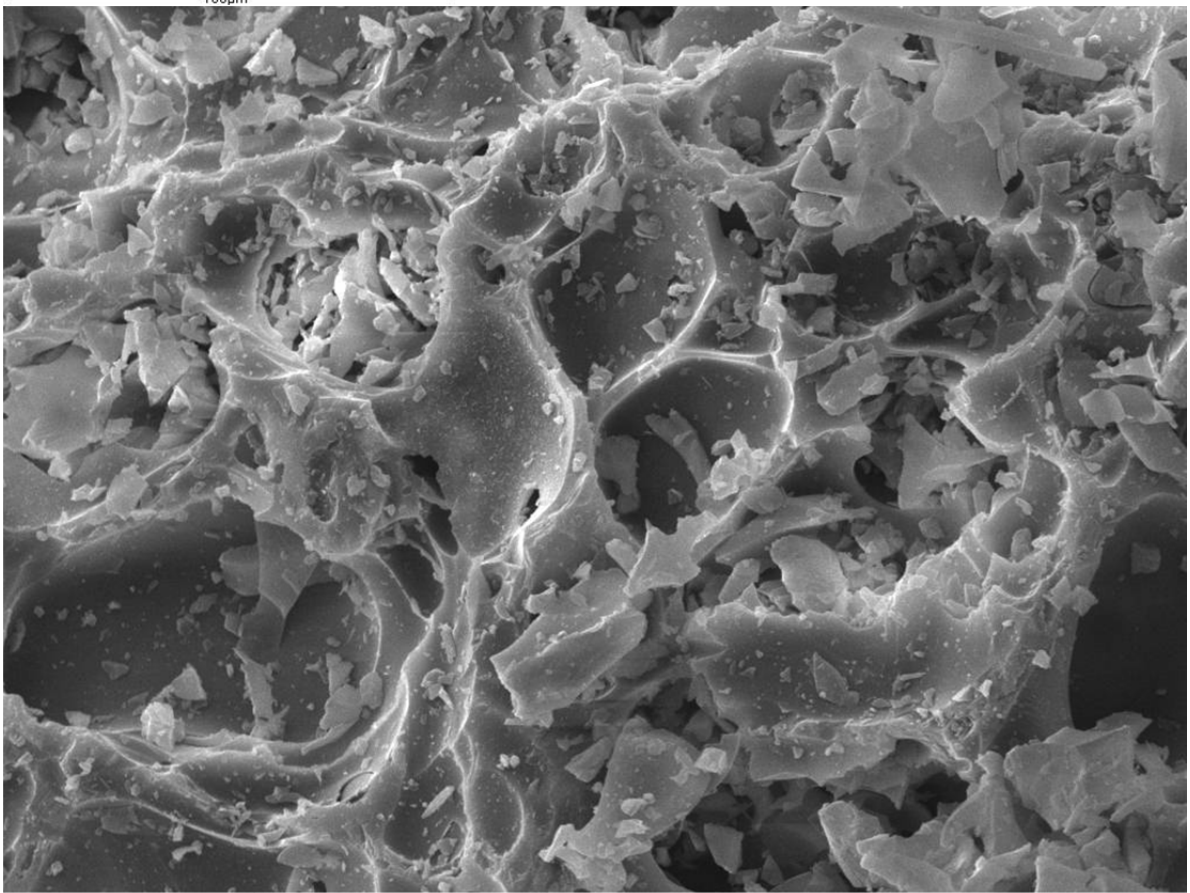
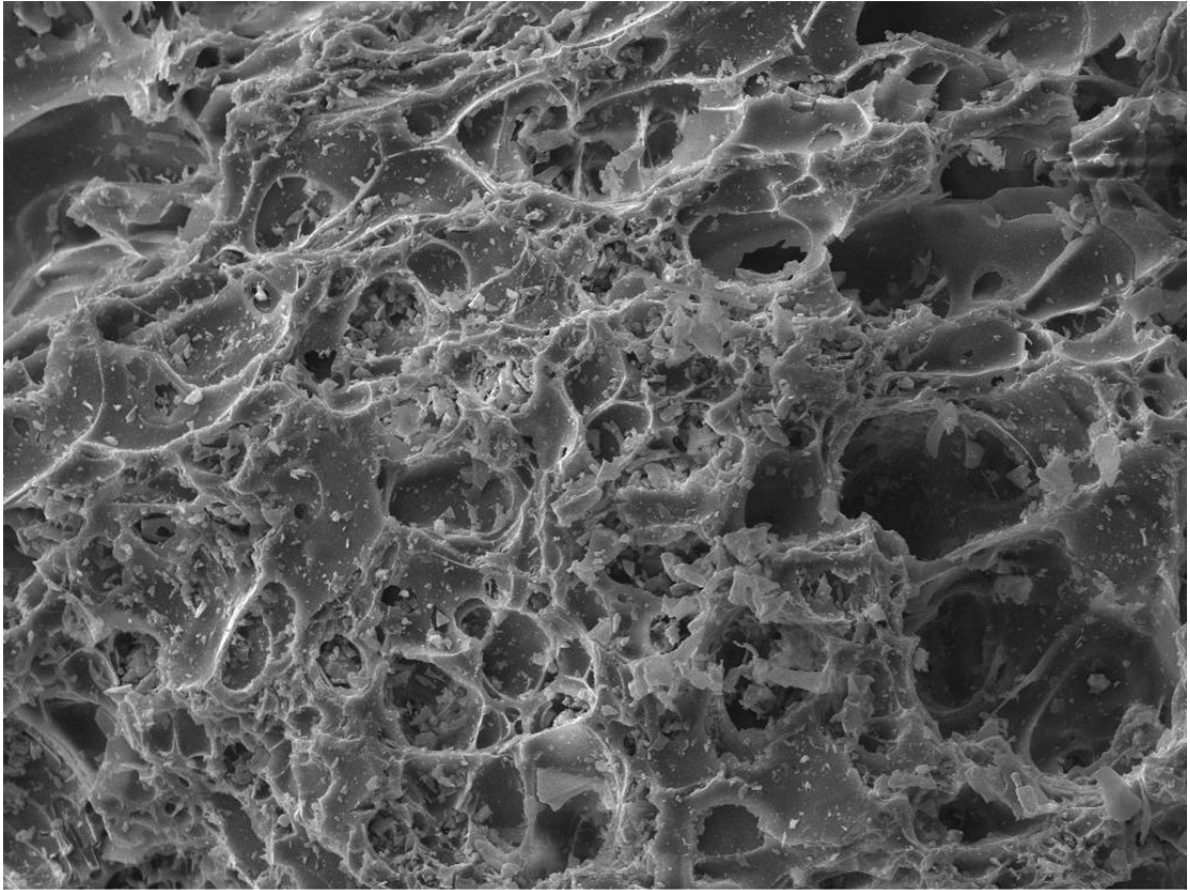




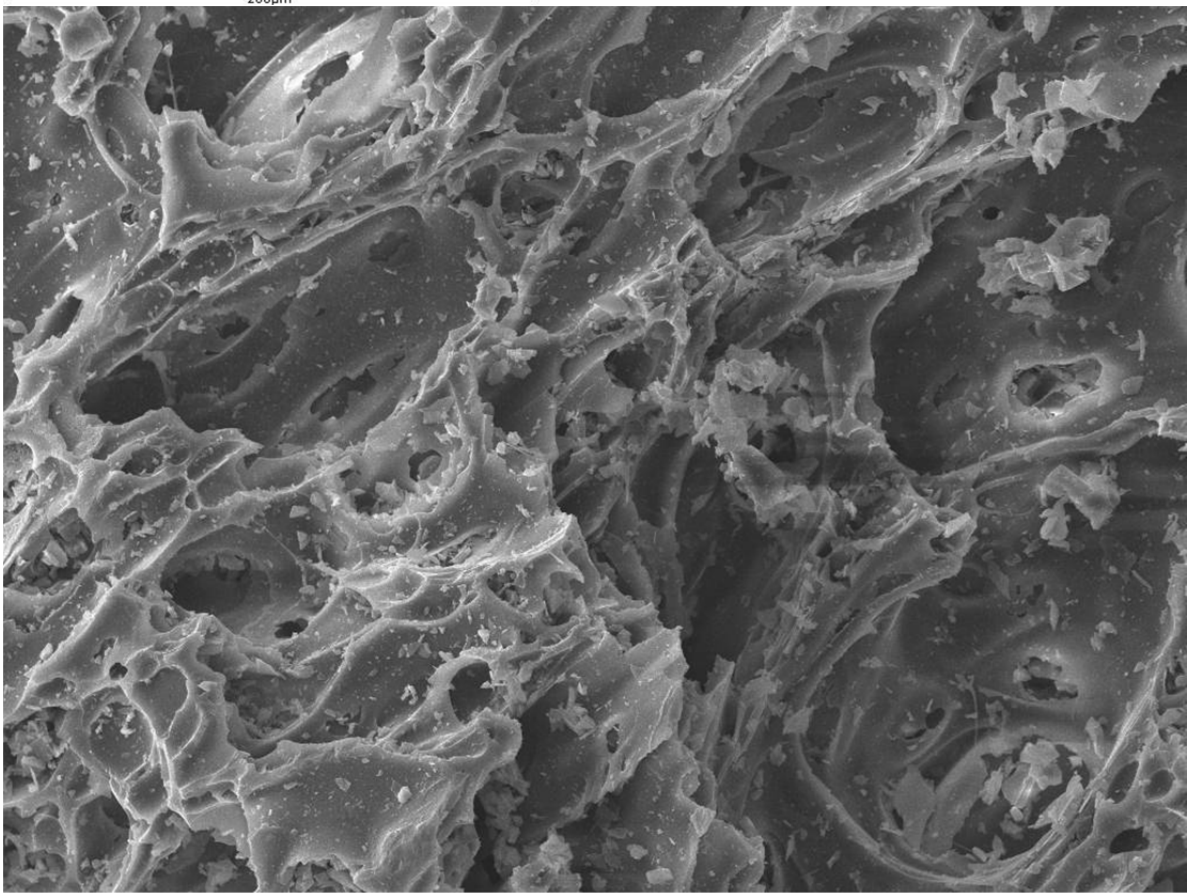
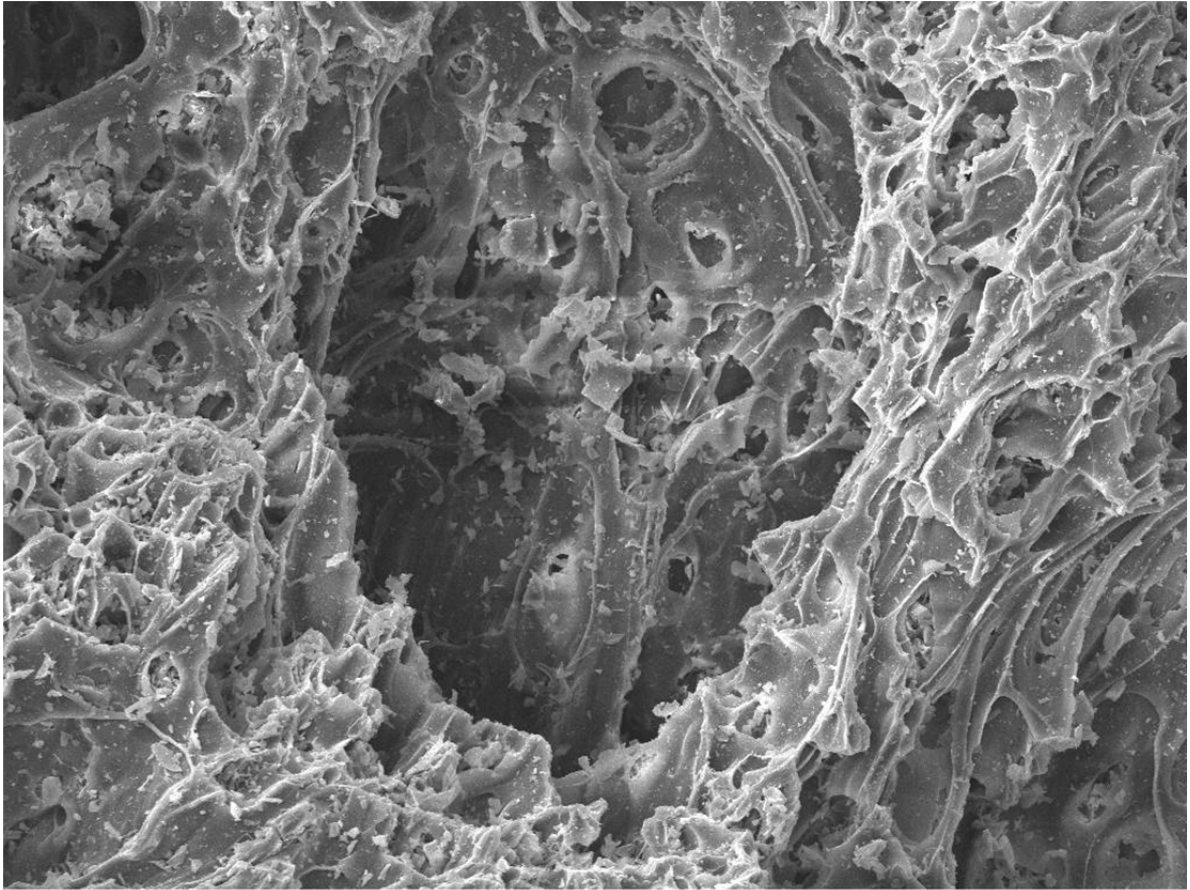
40µm

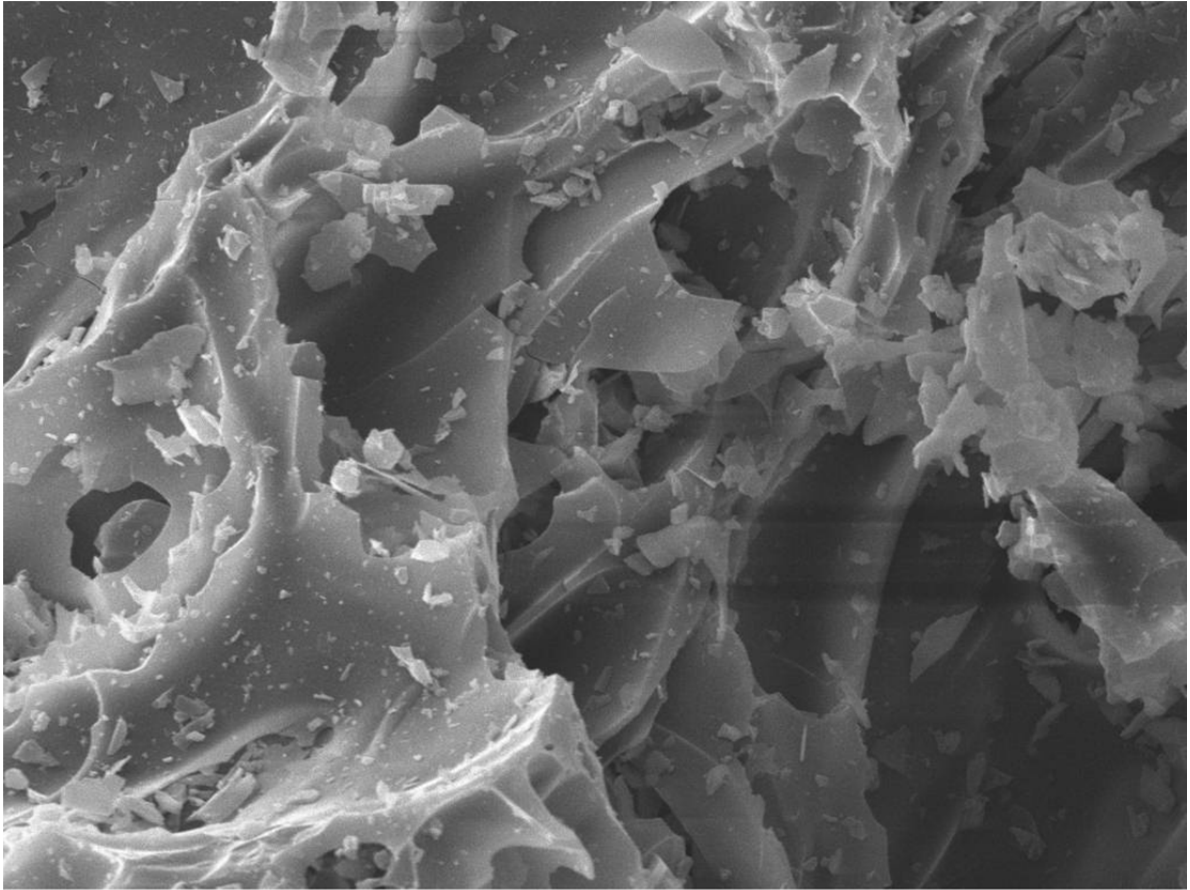
Pumex Pumice SEM Images



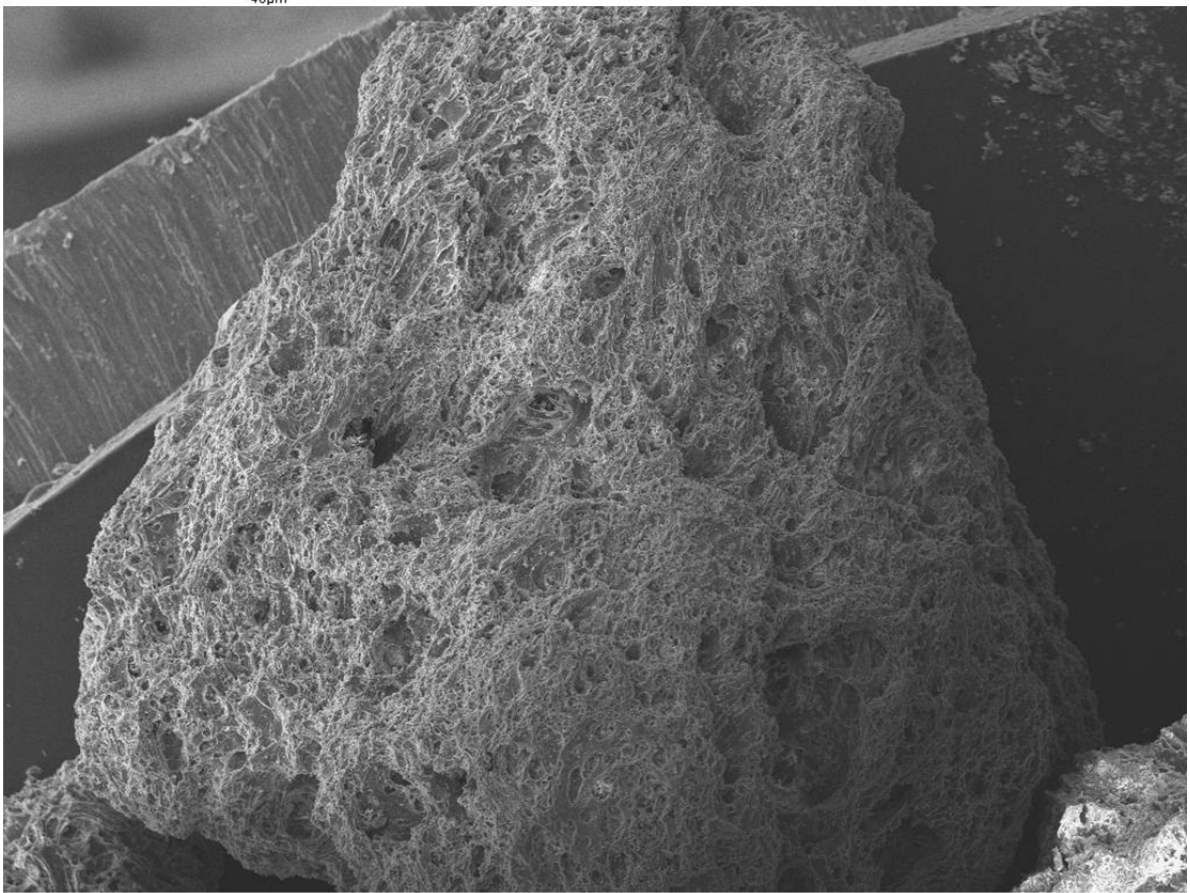


Techfil Pumice SEM Images





40µm



1mm

APPENDIX III

Laboratory Column Experiments

Flowrate – 8.6 m/h

Turbidity – 9 NTU

Sand

Time (minute)	Tests	Temperature (°C)				Head Loss (cm)	pH		Turbidity (NTU)		Conductivity		Sample No.		% Removal	C/Co
		Air	ST	HT	A		ST	A	ST	A	ST	A	ST	A		
0		15.90	13.40		9.90	74.9	7.40		9.36		510					
5								7.41		5.57		520			41	0.59
10										4.25					55	0.45
15						75.0										
20										4.06					57	0.43
25																
30						75.1				3.63					61	0.39
35																
40										3.52					62	0.38
45						75.3										
50										3.33					65	0.35
55																
60	X	15.90	14.00		14.10	75.5										
65										3.10					67	0.33
70							7.47		9.69		510					
75						75.6										
80								7.46		2.83		490			70	0.30
85																
90						75.9										
95										2.74					71	0.29
100																
105						75.9										
110										2.66					72	0.28
115																
120	X	16.10	14.50		14.70	76.4										
125										2.53					73	0.27
130							7.50		9.66		490					
135						76.5										
140								7.48		2.65		480			72	0.28

465					79.0										
470									1.53					84	0.16
475															
480	X	16.90	17.20		17.30	79.2									
485									1.56					83	0.17
490							7.62		9.42		480				
495						79.1									
500								7.61		1.51		480		84	0.16
505															
510						79.1									
515										1.51				84	0.16
520															
525						79.2									
530										1.52				84	0.16
535															
540	X	17.00	17.50		17.50	79.2									
545										1.50				84	0.16
550							7.60		9.15		480				
555						79.3									
560								7.63		1.48		480		84	0.16
565															
570						79.4									
575										1.46				84	0.16
580															
585						79.5									
590										1.54				84	0.16
595															
600	X	16.80	17.70		17.80	79.7									
605										1.57				83	0.17
610							7.64		9.16		480				
615						79.7									
620								7.65		1.49		490		84	0.16

625																
630						79.8										
635										1.62					83	0.17
640																
645						79.9										
650										1.53					84	0.16
655																
660	X	16.70	17.90		18.00	80.0										
665										1.48					84	0.16
670							7.64		9.22		470					
675						80.2										
680								7.64		1.57		480			83	0.17
685																
690						80.2										
695										1.54					84	0.16
700																
705						80.3										
710										1.49					84	0.16
715																
720	X	16.50	18.10		18.20	80.4	7.63	7.65	9.68	1.52	470	480			84	0.16

Glass

Time	Tests	Temperature (°C)				Head Loss (cm)	pH		Turbidity (NTU)		Conductivity		Sample No.		% Removal	C/Co
		Air	ST	HT	A		ST	A	ST	A	ST	A	ST	A		
0		17.70	12.00		10.60	41.5	7.17		10.70		520					
5								7.22		5.79		610			39	0.61
10						41.6										
15										5.75					40	0.60
20						41.8										
25										5.49					42	0.58
30						42.0										
35										4.97					48	0.52
40																
45						42.0										
50										3.70					61	0.39
55																
60		18.00	13.30		13.70	42.2										
65										3.84					60	0.40
70							7.23		9.96		610					
75						42.3										
80								7.30		3.56		590			63	0.37
85																
90						42.4										
95										4.23					56	0.44
100																
105						42.3										
110										3.47					64	0.36
115																
120		17.90	14.60		15.00	42.4										
125										3.36					65	0.35
130							7.29		8.78		590					
135						42.5										
140								7.34		3.58		570			62	0.38

465					44.6											
470									2.72						71	0.29
475																
480		17.60	19.20		19.30	44.8										
485									2.73						71	0.29
490							7.59		8.82		510					
495						44.8										
500								7.59		2.79		500			71	0.29
505																
510						44.8										
515										2.69					72	0.28
520																
525						44.9										
530										2.67					72	0.28
535																
540		17.40	19.50		19.60	45.0										
545										2.71					72	0.28
550							7.60		9.96		510					
555						45.1										
560								7.60		2.70		510			72	0.28
565																
570						45.2										
575										2.70					72	0.28
580																
585						45.2										
590										2.73					71	0.29
595																
600		17.30	19.80		19.80	45.3										
605										2.66					72	0.28
610							7.62		9.32		490					
615						45.5										
620								7.61		2.71		500			72	0.28

625																
630						45.5										
635										2.82					70	0.30
640																
645						45.6										
650										2.65					72	0.28
655																
660		17.30	20.00		20.00	45.7										
665										2.64					72	0.28
670							7.61		9.89		490					
675						45.7										
680								7.58		2.74		490			71	0.29
685																
690						45.8										
695										2.65					72	0.28
700																
705						45.9										
710										2.68					72	0.28
715																
720		17.20	20.10		20.20	46.0	7.63	7.60	9.00	2.61	490	480			73	0.27

Limestone

Time	Tests	Temperature (°C)				Head Loss (cm)	pH		Turbidity (NTU)		Conductivity		Sample No.		% Removal	C/Co
		Air	ST	HT	A		ST	A	ST	A	ST	A	ST	A		
0		15.40	8.40		12.00	51.1	7.21		11.50		580					
5								7.27		5.18		510			47	0.53
10						51.3										
15										5.14					48	0.52
20						51.8										
25										5.56					43	0.57
30						52.0										
35																
40										4.87					50	0.50
45						52.4										
50										4.02					59	0.41
55																
60		16.00	9.10		9.90	52.8										
65										4.09					58	0.42
70							7.28		11.10		460					
75						53.1										
80								7.38		3.35		410			66	0.34
85																
90						53.3										
95										3.04					69	0.31
100																
105						53.4										
110										3.12					68	0.32
115																
120	x	15.00	11.50		12.00	53.6										
125										2.89					71	0.29
130							7.45		9.18		410					
135						53.7										
140								7.39		2.79		410			72	0.28

465					57.9										
470									1.75					82	0.18
475															
480		17.70	14.10		14.80	58.1									
485									1.69					83	0.17
490							7.55		8.97		410				
495						58.3									
500								7.56		1.72		400		82	0.18
505															
510						58.5									
515										1.65				83	0.17
520															
525						58.6									
530										1.74				82	0.18
535															
540		17.60	14.70		15.20	58.7									
545										1.62				83	0.17
550							7.58		9.03		400				
555						58.9									
560								7.58		1.61		400		84	0.16
565															
570						59.0									
575										1.88				81	0.19
580															
585						59.2									
590										1.66				83	0.17
595															
600		17.40	15.30		15.60	59.3									
605										1.68				83	0.17
610							7.54		9.45		400				
615						59.4									
620								7.59		1.65		410		83	0.17

625															
630					59.6										
635									1.71					83	0.17
640															
645					59.7										
650									1.82					81	0.19
655															
660		17.00	15.90		16.00	59.8									
665									1.65					83	0.17
670							7.60		9.23		410				
675					59.8										
680								7.57		1.66		410		83	0.17
685															
690					60.0										
695										1.62				83	0.17
700															
705					60.2										
710										1.72				82	0.18
715															
720		17.10	16.50		16.40	60.3	7.62	7.61	9.03	1.67	410	400		83	0.17

Filtralite

Time	Tests	Temperature (°C)				Head Loss (cm)	pH		Turbidity (NTU)		Conductivity		Sample No.		% Removal	C/Co
		Air	ST	HT	A		ST	A	ST	A	ST	A	ST	A		
0		17.40	13.60		10.50	19.3	7.29		9.25		490					
5								7.30		4.39		490			53	0.47
10						19.4										
15										3.98					58	0.42
20						19.4										
25																
30						19.5				3.42					64	0.36
35																
40										3.38					64	0.36
45						19.7										
50										3.34					65	0.35
55																
60		17.40	14.10		14.50	19.7										
65										3.30					65	0.35
70							7.32		9.12		490					
75						19.8										
80								7.33		3.24		490			66	0.34
85																
90						19.9										
95										3.32					65	0.35
100																
105						20.0										
110										3.20					66	0.34
115																
120		17.60	14.70		15.00	20.2										
125										3.41					64	0.36
130							7.51		10.60		490					
135						20.4										
140								7.54		3.34		480			65	0.35

465					22.3										
470									3.11					67	0.33
475															
480		17.70	19.50		19.40	22.4									
485									3.21					66	0.34
490							7.60		9.08		490				
495						22.5									
500								7.60		3.18		490		66	0.34
505															
510						22.6									
515										3.04				68	0.32
520															
525						22.7									
530										2.98				68	0.32
535															
540		17.70	19.80		19.90	22.7									
545										2.87				70	0.30
550							7.61		8.94		500				
555						22.8									
560								7.62		2.99		490		68	0.32
565															
570						22.9									
575										2.92				69	0.31
580															
585						23.0									
590										3.02				68	0.32
595															
600		17.60	20.10		20.20	23.1									
605										3.11				67	0.33
610							7.60		9.45		490				
615						23.1									
620								7.64		3.09		480		67	0.33

625																
630					23.2											
635									2.95					69	0.31	
640																
645					23.3											
650									2.84					70	0.30	
655																
660		17.00	20.50		20.50	23.5										
665									3.05					68	0.32	
670							7.63		9.12		480					
675					23.5											
680								7.62		3.11		490		67	0.33	
685																
690					23.5											
695										3.14				67	0.33	
700																
705					23.6											
710										3.07				67	0.33	
715																
720		17.20	20.70		20.80	23.7	7.64	7.63	9.29	3.09	490	490		67	0.33	

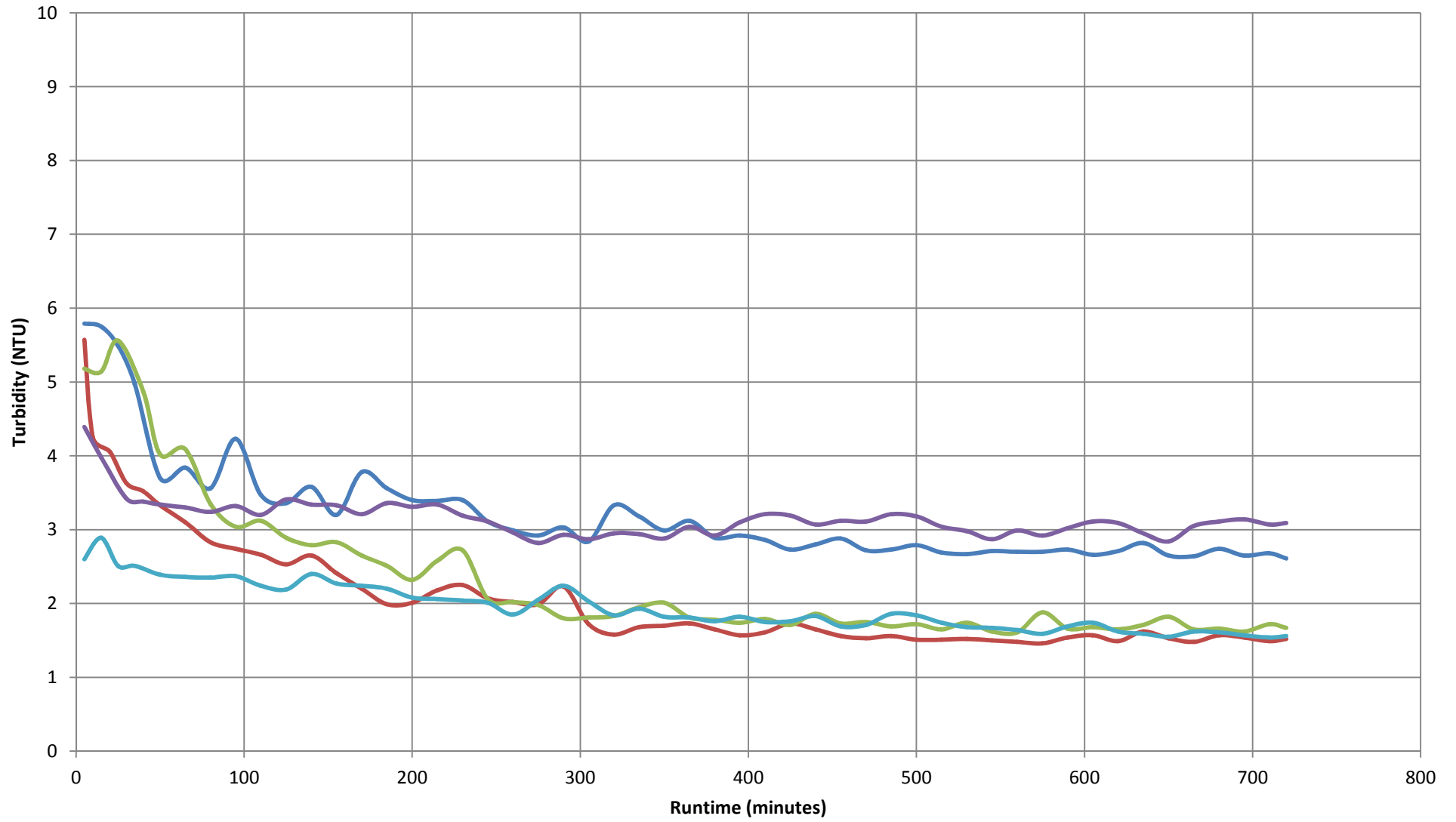
Slate

Time	Tests	Temperature (°C)				Head Loss (cm)	pH		Turbidity (NTU)		Conductivity		Sample No.		% Removal	C/Co
		Air	ST	HT	A		ST	A	ST	A	ST	A	ST	A		
0		19.20	14.20		14.80	31.7	7.40		9.28		460					
5								7.43		2.60		470			73	0.27
10																
15						32.0				2.89					69	0.31
20																
25										2.51					74	0.26
30						32.2										
35										2.51					74	0.26
40																
45						32.3										
50										2.39					75	0.25
55																
60		19.90	15.90		16.20	32.3										
65										2.36					75	0.25
70							7.50		10.50		450					
75						32.5										
80								7.46		2.35		440			75	0.25
85																
90						32.6										
95										2.37					75	0.25
100																
105						32.7										
110										2.24					76	0.24
115																
120		19.40	17.70		17.80	32.8										
125										2.19					77	0.23
130							7.51		10.14		450					
135						32.9										
140								7.43		2.40		470			75	0.25

465					35.0										
470									1.71					82	0.18
475															
480		19.30	21.70		22.10	35.0									
485									1.86					80	0.20
490							7.57		9.17		470				
495						35.1									
500								7.56		1.84		480		81	0.19
505															
510						35.1									
515										1.74				82	0.18
520															
525						35.2									
530										1.68				82	0.18
535															
540		19.10	22.00		22.40	35.3									
545										1.67				82	0.18
550								7.58		9.65		480			
555						35.4									
560								7.57		1.64		480		83	0.17
565															
570						35.4									
575										1.59				83	0.17
580															
585						35.5									
590										1.69				82	0.18
595															
600		18.70	22.20		22.50	35.6									
605										1.74				82	0.18
610								7.59		9.54		480			
615						35.7									
620								7.56		1.62		470		83	0.17

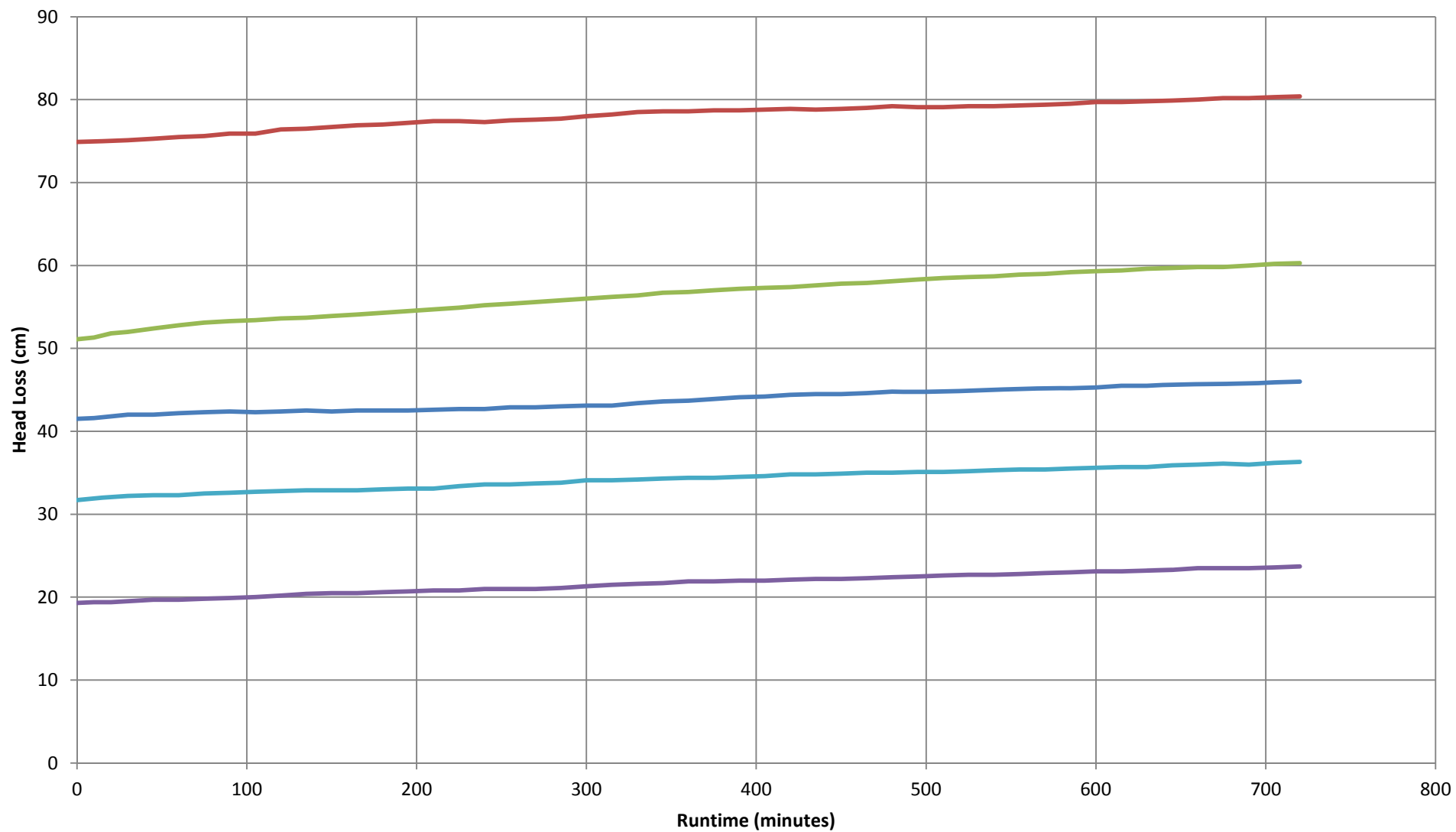
625																
630					35.7											
635									1.59					83	0.17	
640																
645					35.9											
650									1.55					84	0.16	
655																
660		18.70	22.50		22.70	36.0										
665									1.62					83	0.17	
670							7.59		9.34		470					
675					36.1											
680								7.58		1.61		470		83	0.17	
685																
690					36.0											
695										1.57				83	0.17	
700																
705					36.2											
710										1.54				84	0.16	
715																
720		18.60	22.70		22.80	36.3	7.61	7.59	9.03	1.56	470	470		84	0.16	

Turbidity



— Sand — Glass — Limestone — Filtralite — Slate

Head Loss



— Glass — Sand — Limestone — Filtralite — Slate

Flowrate – 8.6 m/h

Turbidity – 35 NTU

Sand

Time (minute)	Tests	Temperature (°C)				Head Loss (cm)	pH		Turbidity (NTU)		Conductivity		Sample No.		% Removal	C/Co
		Air	ST	HT	A		ST	A	ST	A	ST	A	ST	A		
0		11.60	9.00		10.70	93.8	7.24		35.10		540					
5								7.35		15.00		480			57	0.43
10										14.90					57	0.43
15						94.4				14.70					58	0.42
20										13.80					60	0.40
25																
30						95.1				13.20					62	0.38
35																
40										11.70					66	0.34
45						95.6										
50										10.70					69	0.31
55																
60	X	13.10	9.40		9.90	96.1										
65										11.30					68	0.32
70							7.44		36.00		470					
75						96.5										
80								7.45		10.60		440			70	0.30
85																
90						97.2										
95										9.67					72	0.28
100																
105						97.7										
110										8.41					76	0.24
115																
120	X	12.60	9.90		10.50	98.5										
125										8.27					76	0.24
130							7.44		34.30		440					
135						99.2										
140								7.45		8.60		420			75	0.25

465					116.9											
470									4.30						88	0.12
475																
480	X	13.20	12.70		13.10	117.8										
485									3.87						89	0.11
490							7.55		33.80		420					
495						118.7										
500								7.57		3.78		420			89	0.11
505																
510						119.6										
515										3.70					89	0.11
520																
525						120.7										
530										3.98					89	0.11
535																
540	X	13.30	13.30		13.50	121.8										
545										3.78					89	0.11
550							7.54		34.50		410					
555						122.7										
560								7.53		3.70		410			89	0.11
565																
570						123.6										
575										3.95					89	0.11
580																
585						124.6										
590										4.02					88	0.12
595																
600	X	13.20	13.80		13.90	125.5										
605										3.67					89	0.11
610							7.55		35.10		420					
615						126.6										
620								7.56		3.50		410			90	0.10

625															
630					127.4										
635									3.91					89	0.11
640															
645					128.3										
650									3.70					89	0.11
655															
660	X	13.10	14.20		14.40	129.2									
665									4.02					88	0.12
670							7.57		34.60		420				
675					130.2										
680							7.52		3.98		420			89	0.11
685															
690					131.0										
695									3.74					89	0.11
700															
705					131.8				3.65					90	0.10
710															
715															
720	X	13.00	14.70		14.80	132.7	7.58	7.55	35.10	3.47	420	410		90	0.10

Glass

Time	Tests	Temperature (°C)				Head Loss (cm)	pH		Turbidity (NTU)		Conductivity		Sample No.		% Removal	C/Co
		Air	ST	HT	A		ST	A	ST	A	ST	A	ST	A		
0		14.60	10.10		14.10	35.1	7.62		34.40		430					
5								7.55		16.70		440			52	0.48
10						35.9				16.10					54	0.46
15										12.60					64	0.36
20						37.4										
25										12.40					64	0.36
30						38.1										
35										10.80					69	0.31
40																
45						39.0										
50										9.96					71	0.29
55																
60		13.30	10.80		11.40	39.8										
65										9.80					72	0.28
70							7.63		35.00		420					
75						40.5										
80								7.54		9.38		420			73	0.27
85																
90						41.0										
95										9.09					74	0.26
100																
105						42.8										
110										9.17					74	0.26
115																
120		14.90	11.70		12.00	43.4										
125										7.77					78	0.22
130							7.51		34.20		390					
135						43.8										
140								7.52		7.49		400			78	0.22

465					53.5										
470									5.90					83	0.17
475															
480		14.80	15.90		15.70	53.8									
485									4.78					86	0.14
490							7.55		34.90		420				
495						54.4									
500								7.56		4.85		410		86	0.14
505															
510						54.9									
515										4.67				87	0.13
520															
525						55.4									
530										4.93				86	0.14
535															
540		15.20	16.50		16.30	55.8									
545										4.53				87	0.13
550							7.57		35.30		420				
555						56.3									
560								7.55		5.45		420		84	0.16
565															
570						56.8									
575										4.65				87	0.13
580															
585						57.2									
590										5.02				86	0.14
595															
600		14.40	17.30		16.80	57.7									
605										5.30				85	0.15
610							7.54		34.80		420				
615						58.2									
620								7.61		4.70		420		86	0.14

625															
630					58.7										
635									4.85					86	0.14
640															
645					59.3										
650									4.34					88	0.12
655															
660		13.90	17.70		17.60	59.9									
665									5.46					84	0.16
670							7.58		34.20		430				
675					60.4										
680								7.56		4.96		410		86	0.14
685															
690					61.0										
695										4.60				87	0.13
700															
705					61.6										
710										4.87				86	0.14
715															
720		14.20	18.20		18.00	62.3	7.56	7.59	34.70	4.45	420	410		87	0.13

Limestone

Time	Tests	Temperature (°C)				Head Loss (cm)	pH		Turbidity (NTU)		Conductivity		Sample No.		% Removal	C/Co
		Air	ST	HT	A		ST	A	ST	A	ST	A	ST	A		
0		15.30	7.90		9.20	49.0	7.36		34.50		510					
5						49.7		7.38		15.60		540			55	0.45
10						50.2				14.90					57	0.43
15						50.6				14.20					59	0.41
20										13.90					60	0.40
25						51.4				13.70					61	0.39
30										12.80					63	0.37
35						51.6				11.60					67	0.33
40																
45						51.5				11.20					68	0.32
50																
55										9.78					72	0.28
60		14.50	9.30		10.00	51.8										
65										11.00					68	0.32
70							7.47		33.20		510					
75						52.2										
80								7.40		10.20		510			71	0.29
85																
90						52.7										
95										9.85					72	0.28
100																
105						53.1										
110										8.64					75	0.25
115																
120		14.50	10.00		10.70	53.6										
125										8.45					76	0.24
130							7.48		35.20		460					
135						54.3										
140								7.45		8.38		480			76	0.24

465					68.4											
470									4.03						88	0.12
475																
480		15.50	14.30		14.30	68.9										
485									3.87						89	0.11
490							7.55		35.00		480					
495						69.4										
500								7.56		4.03		470			88	0.12
505																
510						69.9										
515										4.33					88	0.12
520																
525						71.4										
530										3.65					89	0.11
535																
540		15.50	14.80		14.70	71.8										
545										4.05					88	0.12
550							7.58		34.80		470					
555						72.3										
560								7.58		3.89		470			89	0.11
565																
570						72.8										
575										3.87					89	0.11
580																
585						73.3										
590										3.95					89	0.11
595																
600		15.40	15.40		15.10	73.7										
605										3.68					89	0.11
610							7.54		35.20		470					
615						74.3										
620								7.59		3.54		470			90	0.10

625															
630					74.8										
635									3.78					89	0.11
640															
645					75.5										
650									3.74					89	0.11
655															
660		15.30	15.80		15.50	76.1									
665									3.72					89	0.11
670							7.60		35.50		480				
675					77.0										
680								7.57		3.65		470		89	0.11
685															
690					77.8										
695										3.68				89	0.11
700															
705					78.5										
710										3.54				90	0.10
715															
720		15.30	16.40		16.00	79.2	7.62	7.61	34.90	3.61	470	480		90	0.10

Filtralite

Time	Tests	Temperature (°C)				Head Loss (cm)	pH		Turbidity (NTU)		Conductivity		Sample No.		% Removal	C/Co
		Air	ST	HT	A		ST	A	ST	A	ST	A	ST	A		
0		19.40	16.90		17.90	16.9	7.55		34.70		510					
5								7.58		14.70		510			58	0.42
10										9.87					71	0.29
15						17.1				8.97					74	0.26
20										8.82					75	0.25
25						17.3				8.96					74	0.26
30										8.55					75	0.25
35						17.6										
40										8.36					76	0.24
45						17.9										
50										8.19					76	0.24
55																
60		19.10	17.60		17.90	18.1										
65										8.25					76	0.24
70							7.57		35.80		500					
75						18.3										
80								7.57		8.90		500			74	0.26
85																
90						18.5										
95										8.21					76	0.24
100																
105						18.8										
110										8.20					76	0.24
115																
120		18.50	18.20		18.40	19.2										
125										8.45					76	0.24
130							7.57		33.80		510					
135						19.5										
140								7.61		8.13		490			77	0.23

465					24.7											
470									9.24						73	0.27
475																
480		18.90	20.60		24.9											
485									9.45						73	0.27
490						7.68		35.40		470						
495					25.1											
500							7.63		9.54		470				72	0.28
505																
510					25.3											
515									9.80						72	0.28
520																
525					25.6											
530									9.45						73	0.27
535																
540		19.10	20.70		25.9											
545									9.64						72	0.28
550						7.61		35.80		480						
555					26.3											
560							7.60		9.57		470				72	0.28
565																
570					26.7											
575									9.52						72	0.28
580																
585					27.1											
590									9.10						74	0.26
595																
600		19.00	20.80		27.4											
605									8.75						75	0.25
610						7.63		33.50		460						
615					27.7											
620							7.69		9.41		470				73	0.27

625															
630					28.0										
635									9.87					71	0.29
640															
645					28.4										
650									9.75					72	0.28
655															
660		18.80	20.90		28.7										
665									9.42					73	0.27
670						7.66		33.60		470					
675					29.0										
680							7.64		9.55		480			72	0.28
685															
690					29.3										
695									9.23					73	0.27
700															
705					29.7										
710									9.57					72	0.28
715															
720		18.70	21.00		30.1	7.68	7.63	34.00	9.54	470	470			72	0.28

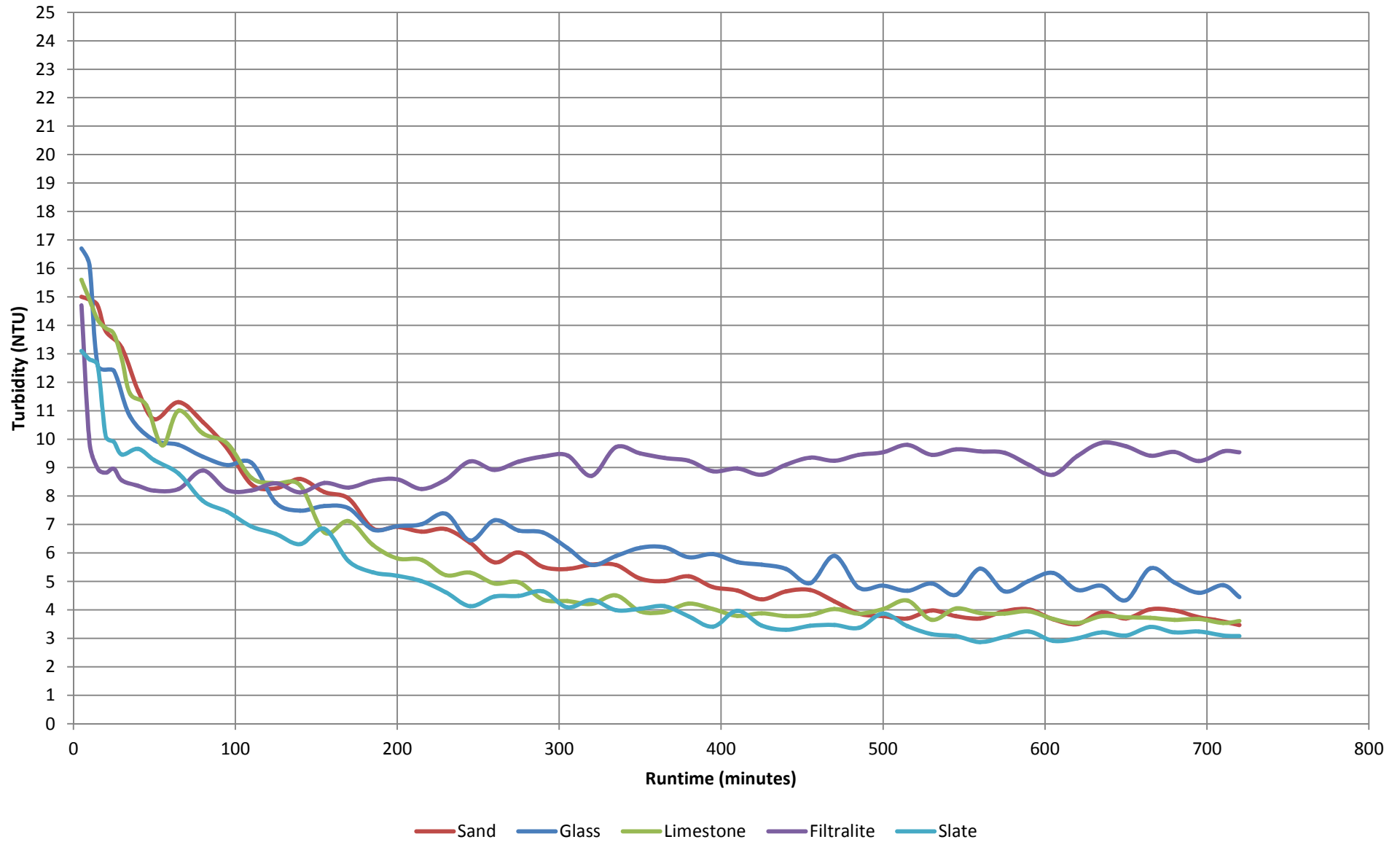
Slate

Time	Tests	Temperature (°C)				Head Loss (cm)	pH		Turbidity (NTU)		Conductivity		Sample No.		% Removal	C/Co
		Air	ST	HT	A		ST	A	ST	A	ST	A	ST	A		
0		18.90	7.90		9.70	35.3	7.39		35.30		430					
5								7.34		13.10		500			62	0.38
10						35.7				12.80					63	0.37
15										12.60					64	0.36
20						36.0				10.10					71	0.29
25										9.91					71	0.29
30						36.4				9.46					73	0.27
35																
40										9.66					72	0.28
45						36.7										
50										9.26					73	0.27
55																
60		19.40	8.70		10.00	36.9										
65										8.79					75	0.25
70							7.41		34.70		440					
75						37.1										
80								7.38		7.83		450			77	0.23
85																
90						37.4										
95										7.45					79	0.21
100																
105						37.7										
110										6.93					80	0.20
115																
120		19.20	9.60		10.90	38.0										
125										6.67					81	0.19
130							7.44		35.10		450					
135						38.4										
140								7.47		6.31		450			82	0.18

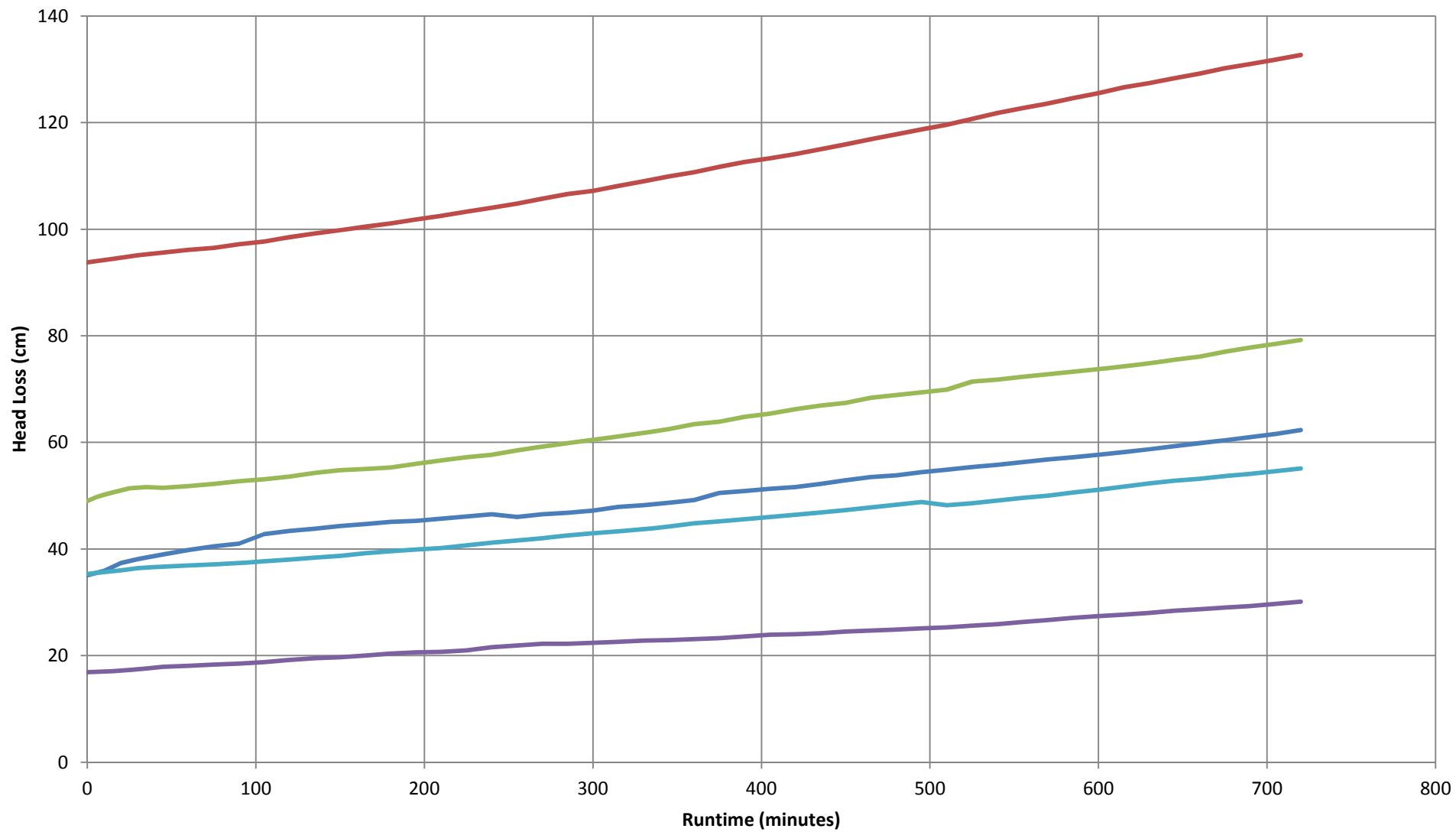
465					47.8											
470									3.47					90	0.10	
475																
480		17.90	14.70		14.90	48.3										
485									3.37					90	0.10	
490							7.54	7.55	34.20		450					
495						48.8										
500									3.87		450			89	0.11	
505																
510						48.2										
515									3.43					90	0.10	
520																
525						48.6										
530									3.15					91	0.09	
535																
540		18.00	15.50		15.70	49.1										
545									3.08					91	0.09	
550							7.53	7.50	34.50		440					
555						49.6										
560									2.87		440			92	0.08	
565																
570						50.0										
575									3.05					91	0.09	
580																
585						50.6										
590									3.24					91	0.09	
595																
600		17.80	16.20		16.30	51.1										
605									2.91					92	0.08	
610							7.58	7.55	35.50		440					
615						51.7										
620									3.00		440			91	0.09	

625																
630					52.3											
635									3.21					91	0.09	
640																
645					52.8											
650									3.10					91	0.09	
655																
660		17.70	16.70		16.80	53.2										
665									3.40					90	0.10	
670							7.57	7.60	35.20		440					
675					53.7											
680									3.21		450			91	0.09	
685																
690					54.1											
695									3.24					91	0.09	
700																
705					54.6											
710									3.10					91	0.09	
715																
720		17.80	17.20		17.30	55.1	7.54	7.57	33.90	3.08	430	440		91	0.09	

Turbidity



Head Loss



— Glass — Sand — Limestone — Filtralite — Slate

Flowrate – 11.1 m/h

Turbidity – 9 NTU

Sand

Time (minute)	Tests	Temperature (°C)				Head Loss (cm)	pH		Turbidity (NTU)		Conductivity		Sample No.		% Removal	C/Co
		Air	ST	HT	A		ST	A	ST	A	ST	A	ST	A		
0		15.00	7.90		6.20	72.6	7.37		9.60		490					
5								7.38		6.42		540			31	0.69
10										4.67					50	0.50
15						72.7										
20										4.07					56	0.44
25																
30						72.7				4.33					53	0.47
35																
40										2.99					68	0.32
45						72.6										
50										2.90					69	0.31
55																
60	X	15.70	8.40		8.90	72.6										
65										2.68					71	0.29
70							7.42		9.40		480					
75						72.8										
80								7.46		2.77		490			70	0.30
85																
90						72.6										
95										2.35					75	0.25
100																
105						72.5										
110										2.03					78	0.22
115																
120	X	15.60	8.70		9.50	72.6										
125										1.96					79	0.21
130							7.47		9.10		440					
135						72.5										
140								7.48		2.05		470			78	0.22

465					73.6										
470									1.01					89	0.11
475															
480	X	15.00	12.70		13.10	73.7									
485									1.01					89	0.11
490							7.55		9.21		460				
495						73.6									
500								7.57		1.06		420		89	0.11
505															
510						73.7									
515										1.09				88	0.12
520															
525						73.8									
530										1.14				88	0.12
535															
540	X	15.10	13.30		13.50	73.8									
545										1.05				89	0.11
550							7.54		9.34		450				
555						73.8									
560								7.53		1.11		430		88	0.12
565															
570						73.9									
575										1.04				89	0.11
580															
585						74.0									
590										1.06				89	0.11
595															
600	X	14.90	13.80		13.90	74.0									
605										0.98				89	0.11
610							7.55		9.12		440				
615						74.1									
620								7.56		1.02		410		89	0.11

625																
630						74.2										
635										1.15					88	0.12
640																
645						74.2										
650										0.97					90	0.10
655																
660	X	14.70	14.20		14.40	74.3										
665										0.98					89	0.11
670							7.57		9.54		450					
675						74.3										
680								7.52		1.04		420			89	0.11
685																
690						74.5										
695										1.06					89	0.11
700																
705						74.6				1.01					89	0.11
710																
715																
720	X	14.70	14.70		14.80	74.7	7.58	7.55	9.34	0.99	450	410			89	0.11

Glass

Time	Tests	Temperature (°C)				Head Loss (cm)	pH		Turbidity (NTU)		Conductivity		Sample No.		% Removal	C/Co
		Air	ST	HT	A		ST	A	ST	A	ST	A	ST	A		
0	X	12.30	10.70		8.40	35.8	7.54		9.07		410					
5								7.45		6.74		400			26	0.74
10						35.9										
15										5.31					42	0.58
20						36.0										
25										6.11					33	0.67
30						36.2										
35										4.46					51	0.49
40																
45						36.4										
50										4.43					51	0.49
55																
60	X	12.90	11.10		11.50	36.6										
65										4.29					53	0.47
70							7.58		9.32		410					
75						36.7										
80								7.44		3.89		390			57	0.43
85																
90						36.8										
95										2.95					68	0.32
100																
105						37.0										
110										3.52					61	0.39
115																
120	X	12.90	11.50		11.80	37.2										
125										3.18					65	0.35
130							7.56		9.20		410					
135						37.2										
140								7.52		3.02		400			67	0.33

465					38.4										
470									1.62					82	0.18
475															
480	X	13.30	14.30		14.30	38.5									
485									1.72					81	0.19
490							7.55		9.11		400				
495						38.6									
500								7.56		1.64		410		82	0.18
505															
510						38.6									
515										1.65				82	0.18
520															
525						38.7									
530										1.56				83	0.17
535															
540	X	13.00	14.60		14.70	38.7									
545										1.67				82	0.18
550							7.57		9.29		410				
555						38.8									
560								7.55		1.71		420		81	0.19
565															
570						38.9									
575										1.64				82	0.18
580															
585						39.0									
590										1.61				82	0.18
595															
600	X	12.30	14.90		14.90	39.1									
605										1.58				83	0.17
610							7.54		8.92		410				
615						39.1									
620								7.61		1.59		420		83	0.17

625																
630						39.2										
635										1.56					83	0.17
640																
645						39.2										
650										1.62					82	0.18
655																
660	X	12.90	15.20		15.30	39.3										
665										1.60					82	0.18
670							7.58		9.23		420					
675						39.4										
680								7.56		1.61		410			82	0.18
685																
690						39.5										
695										1.57					83	0.17
700																
705						39.4										
710										1.55					83	0.17
715																
720	X	12.80	15.60		15.50	39.6	7.56	7.59	9.06	1.59	410	410			83	0.17

Limestone

Time	Tests	Temperature (°C)				Head Loss (cm)	pH		Turbidity (NTU)		Conductivity		Sample No.		% Removal	C/Co
		Air	ST	HT	A		ST	A	ST	A	ST	A	ST	A		
0		13.50	9.80		8.80	36.0	7.56		9.37		410					
5								7.48		5.45		440			41	0.59
10						36.1										
15										2.81					70	0.30
20						36.0										
25										2.57					72	0.28
30						36.2										
35																
40										2.29					75	0.25
45						36.2										
50										2.18					76	0.24
55																
60		14.50	10.50		10.70	36.3										
65										1.92					79	0.21
70							7.57		9.12		410					
75						36.4										
80								7.53		1.73		420			81	0.19
85																
90						36.5										
95										1.63					82	0.18
100																
105						36.5										
110										1.68					82	0.18
115																
120	x	15.00	11.50		12.00	36.4										
125										1.65					82	0.18
130							7.56		9.67		410					
135						36.4										
140								7.55		1.56		410			83	0.17

465					36.6										
470									0.99					89	0.11
475															
480		15.20	16.40		16.40	36.6									
485									0.94					90	0.10
490							7.55		9.04		410				
495						36.7									
500								7.56		1.01		400		89	0.11
505															
510						36.7									
515										1.03				89	0.11
520															
525						36.7									
530										0.95				90	0.10
535															
540		15.30	16.90		16.90	36.7									
545										0.90				90	0.10
550							7.58		8.87		400				
555						36.8									
560								7.58		0.94		400		90	0.10
565															
570						36.8									
575										0.92				90	0.10
580															
585						36.8									
590										0.92				90	0.10
595															
600		15.00	17.40		17.50	36.6									
605										1.02				89	0.11
610							7.54		9.00		400				
615						36.8									
620								7.59		0.98		410		89	0.11

625															
630					36.8										
635									0.94					90	0.10
640															
645					36.9										
650									1.01					89	0.11
655															
660		14.80	17.80		17.80	36.9									
665									0.95					90	0.10
670							7.60		9.08		410				
675					37.0										
680								7.57		0.87		410		91	0.09
685															
690					37.0										
695										0.95				90	0.10
700															
705					36.9										
710										0.99				89	0.11
715															
720		15.10	18.20		18.30	36.7	7.62	7.61	9.23	0.94	410	400		90	0.10

Filtralite

Time	Tests	Temperature (°C)				Head Loss (cm)	pH		Turbidity (NTU)		Conductivity		Sample No.		% Removal	C/Co
		Air	ST	HT	A		ST	A	ST	A	ST	A	ST	A		
0		16.50	13.10		16.20	16.0	7.58		9.13		420					
5								7.55		3.56		440			61	0.39
10						16.1										
15										3.43					63	0.37
20						16.1										
25										3.62					61	0.39
30						16.1										
35										3.55					61	0.39
40																
45						16.1										
50										3.35					63	0.37
55																
60		15.50	14.70		14.70	16.0										
65										3.34					64	0.36
70							7.64		9.33		440					
75						16.0										
80								7.59		3.17		430			65	0.35
85																
90						16.0										
95										2.97					68	0.32
100																
105						16.2										
110										2.87					69	0.31
115																
120		15.60	15.60		15.50	16.4										
125										2.82					69	0.31
130							7.66		9.59		420					
135						16.3										
140								7.63		2.85		410			69	0.31

465					16.4										
470									2.81					69	0.31
475															
480		15.40	18.50		18.60	16.2									
485									2.74					70	0.30
490							7.63		9.20		410				
495						16.4									
500								7.57		2.69		420		71	0.29
505															
510						16.5									
515										2.68				71	0.29
520															
525						16.5									
530										2.70				71	0.29
535															
540		15.50	18.90		19.10	16.4									
545										2.81				69	0.31
550							7.66		9.17		420				
555						16.4									
560								7.59		2.69		400		71	0.29
565															
570						16.4									
575										2.74				70	0.30
580															
585						16.5									
590										2.76				70	0.30
595															
600		15.40	19.30		19.50	16.5									
605										2.70				71	0.29
610							7.62		9.02		430				
615						16.5									
620								7.64		2.81		420		69	0.31

625															
630					16.3										
635									2.73					70	0.30
640															
645					16.4										
650									2.67					71	0.29
655															
660		15.30	19.60		19.70	16.5									
665									2.71					70	0.30
670							7.61		8.87		410				
675					16.5										
680								7.62		2.65		410		71	0.29
685															
690					16.6										
695										2.73				70	0.30
700															
705					16.4										
710										2.75				70	0.30
715															
720		15.20	19.90		20.00	16.6	7.59	7.61	9.06	2.71	400	400		70	0.30

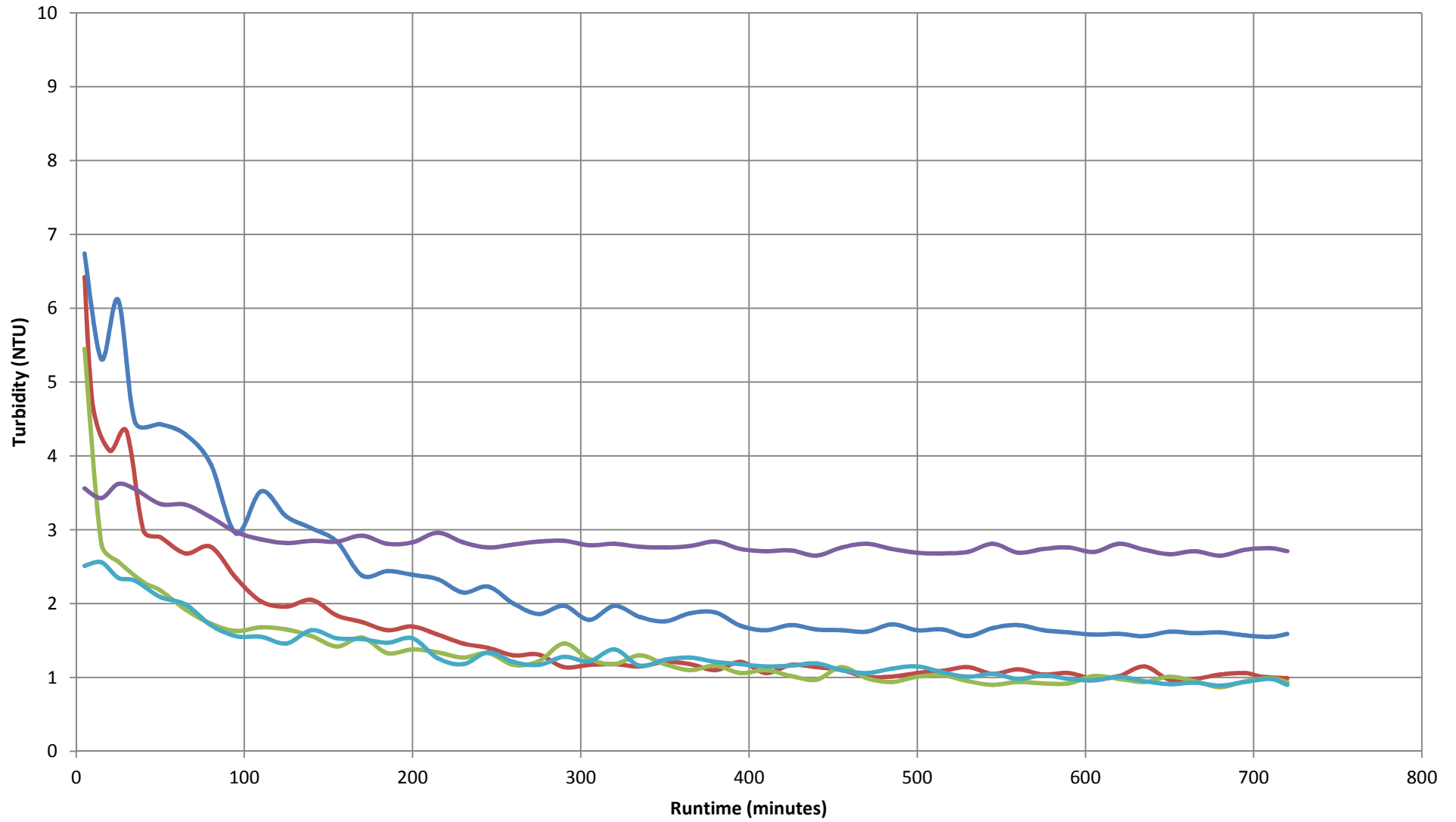
Slate

Time	Tests	Temperature (°C)				Head Loss (cm)	pH		Turbidity (NTU)		Conductivity		Sample No.		% Removal	C/Co
		Air	ST	HT	A		ST	A	ST	A	ST	A	ST	A		
0		16.90	11.10		14.70	25.8	7.29		9.79		430					
5								7.27		2.51		420			74	0.26
10						25.9										
15										2.56					73	0.27
20						26.0										
25										2.35					76	0.24
30						26.2										
35										2.31					76	0.24
40																
45						26.3										
50										2.09					78	0.22
55																
60		17.50	11.70		12.50	26.4										
65										1.99					79	0.21
70							7.38		9.77		430					
75						26.4										
80								7.50		1.71		420			82	0.18
85																
90						26.6										
95										1.56					84	0.16
100																
105						26.8										
110										1.55					84	0.16
115																
120		16.40	12.20		13.00	26.9										
125										1.46					85	0.15
130							7.44		10.10		420					
135						27.0										
140								7.43		1.64		420			83	0.17

465					29.2											
470									1.06						89	0.11
475																
480		12.40	21.50		29.3											
485									1.12						88	0.12
490																
495					29.4											
500									1.15						88	0.12
505																
510					29.6											
515									1.07						89	0.11
520																
525					29.7											
530									1.01						90	0.10
535																
540		12.20	22.00		29.8											
545									1.05						89	0.11
550																
555					29.8											
560									0.98						90	0.10
565																
570					30.0											
575									1.03						89	0.11
580																
585					30.0											
590									0.98						90	0.10
595																
600		12.10	22.50		30.1											
605									0.96						90	0.10
610																
615					30.3											
620									1.01						90	0.10

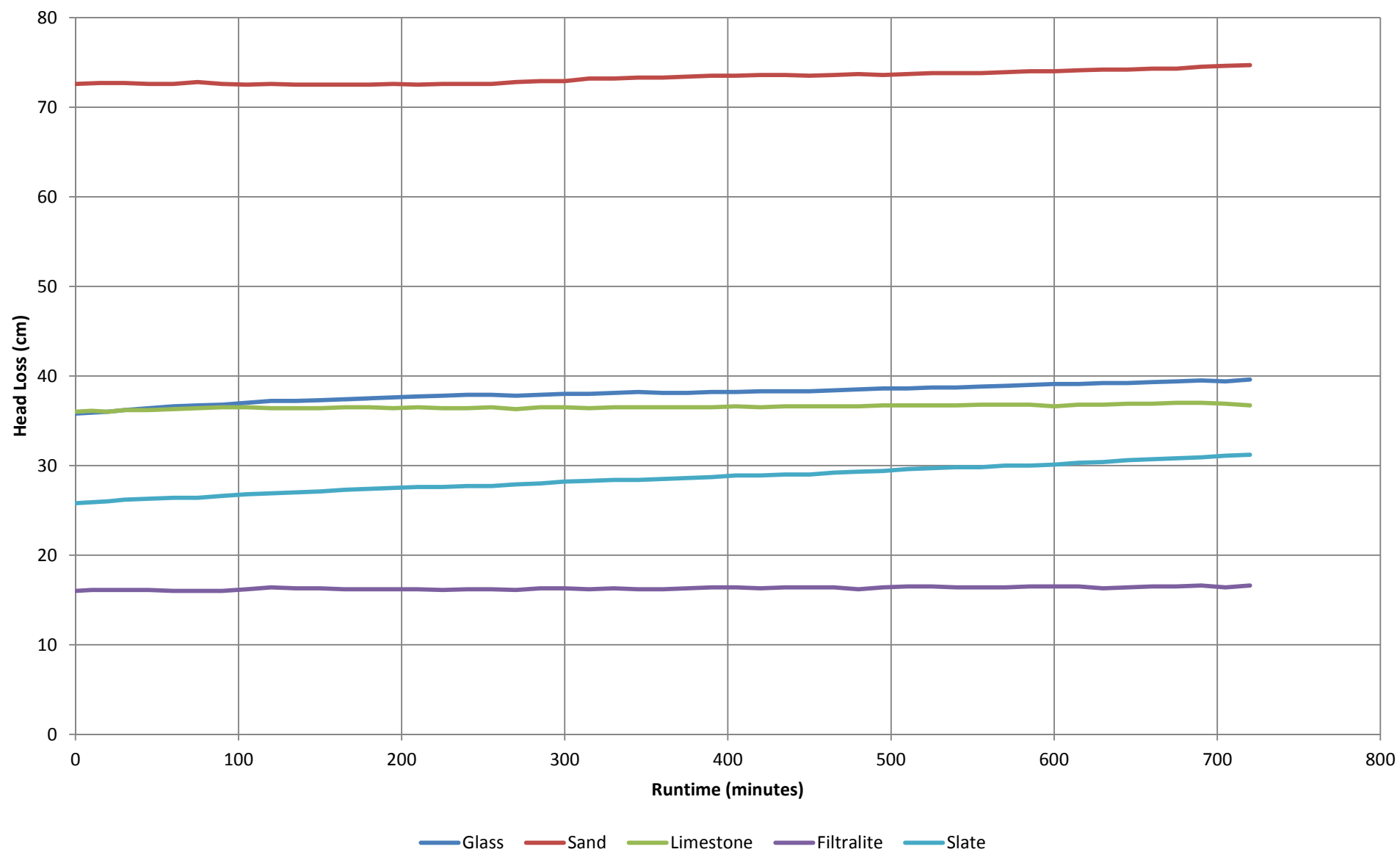
625																
630						30.4										
635										0.95					90	0.10
640																
645						30.6										
650										0.91					91	0.09
655																
660		12.00	23.00			30.7										
665										0.93					90	0.10
670																
675						30.8										
680										0.89					91	0.09
685																
690						30.9										
695										0.94					90	0.10
700																
705						31.1										
710										0.98					90	0.10
715																
720		11.90	23.40			31.2				0.90					91	0.09

Turbidity



— Sand — Glass — Limestone — Filtralite — Slate

Head Loss



Flowrate – 11.1 m/h

Turbidity – 35 NTU

Sand

Time (minute)	Tests	Temperature (°C)				Head Loss (cm)	pH		Turbidity (NTU)		Conductivity		Sample No.		% Removal	C/Co
		Air	ST	HT	A		ST	A	ST	A	ST	A	ST	A		
0		8.00	8.40		6.20	68.4	7.36		35.80		540					
5								7.36		11.10		530			68	0.32
10										9.91					72	0.28
15						68.6				8.52					76	0.24
20										8.55					75	0.25
25																
30						68.9				7.36					79	0.21
35																
40										6.58					81	0.19
45						69.5										
50										6.38					82	0.18
55																
60	X	8.90	8.90		8.60	70.1										
65										5.61					84	0.16
70							7.33		34.60		510					
75						70.8										
80								7.46		5.15		550			85	0.15
85																
90						71.3										
95										4.93					86	0.14
100																
105						71.9										
110										4.40					87	0.13
115																
120	X	9.00	9.40		9.20	72.3										
125										4.18					88	0.12
130							7.47		35.50		520					
135						73.2										
140								7.42		4.24		530			88	0.12

465					88.1										
470									2.89					92	0.08
475															
480	X	13.20	12.70		13.10	88.9									
485									2.87					92	0.08
490							7.55		33.80		490				
495						89.6									
500								7.57		3.21		420		91	0.09
505															
510						90.3									
515										3.01				91	0.09
520															
525						91.0									
530										2.87				92	0.08
535															
540	X	13.30	13.30		13.50	91.8									
545										2.94				92	0.08
550							7.54		34.50		500				
555						92.7									
560								7.53		3.01		410		91	0.09
565															
570						93.4									
575										2.86				92	0.08
580															
585						94.0									
590										2.72				92	0.08
595															
600	X	13.20	13.80		13.90	94.8									
605										2.78				92	0.08
610							7.55		35.10		490				
615						95.6									
620								7.56		2.76		410		92	0.08

625															
630					96.3										
635									3.03					91	0.09
640															
645					97.0										
650									2.87					92	0.08
655															
660	X	13.10	14.20		14.40	97.8									
665									2.82					92	0.08
670							7.57		34.60		480				
675					98.7										
680							7.52		3.23		420			91	0.09
685															
690					99.6										
695									2.75					92	0.08
700															
705					100.3				2.85					92	0.08
710															
715															
720	X	13.00	14.70		14.80	101.0	7.58	7.55	35.10	2.98	490	410		91	0.09

Glass

Time	Tests	Temperature (°C)				Head Loss (cm)	pH		Turbidity (NTU)		Conductivity		Sample No.		% Removal	C/Co
		Air	ST	HT	A		ST	A	ST	A	ST	A	ST	A		
0		9.90	10.10		7.90	36.0	7.47		34.70		530					
5								7.42		15.80		490			54	0.46
10						36.2				15.30					56	0.44
15										12.40					64	0.36
20						36.5										
25										10.20					71	0.29
30						36.8										
35										8.70					75	0.25
40																
45						37.2										
50										8.10					77	0.23
55																
60		10.50	10.90		10.80	37.6										
65										6.03					83	0.17
70							7.50		33.40		520					
75						38.1										
80								7.44		5.75		510			83	0.17
85																
90						38.4										
95										5.30					85	0.15
100																
105						38.8										
110										5.10					85	0.15
115																
120		11.00	11.70		11.50	39.2										
125										4.88					86	0.14
130							7.47		34.20		510					
135						39.6										
140								7.45		4.57		510			87	0.13

465					48.3										
470									3.94					89	0.11
475															
480		14.80	15.30		14.80	48.7									
485									4.02					88	0.12
490							7.55		34.60		480				
495						49.1									
500								7.56		3.65		460		89	0.11
505															
510						49.5									
515										3.89				89	0.11
520															
525						49.8									
530										3.14				91	0.09
535															
540		15.20	15.70		15.30	50.2									
545										3.24				91	0.09
550							7.57		35.30		470				
555						50.6									
560								7.55		3.67		470		89	0.11
565															
570						51.0									
575										4.01				88	0.12
580															
585						51.5									
590										3.79				89	0.11
595															
600		14.40	16.20		15.90	51.8									
605										3.42				90	0.10
610							7.54		34.70		470				
615						52.2									
620								7.61		3.43		480		90	0.10

625																
630					52.4											
635									3.87					89	0.11	
640																
645					52.7											
650									3.23					91	0.09	
655																
660		13.90	16.60		16.40	53.1										
665									3.45					90	0.10	
670							7.58		33.80		470					
675						53.6										
680								7.56		3.56		460		90	0.10	
685																
690						53.9										
695										3.32				90	0.10	
700																
705						54.5										
710										3.28				91	0.09	
715																
720		14.20	17.10		17.00	54.9	7.56	7.59	33.20	3.43	470	470		90	0.10	

Limestone

Time	Tests	Temperature (°C)				Head Loss (cm)	pH		Turbidity (NTU)		Conductivity		Sample No.		% Removal	C/Co
		Air	ST	HT	A		ST	A	ST	A	ST	A	ST	A		
0		12.40	7.20		6.70	36.7	7.27		35.80		380					
5								7.24		12.40		400			64	0.36
10						37.0				15.30					56	0.44
15										14.80					57	0.43
20						37.6				14.00					59	0.41
25										13.80					60	0.40
30						37.8				12.80					63	0.37
35										13.20					62	0.38
40																
45						38.2				13.10					62	0.38
50																
55										11.60					66	0.34
60		13.60	7.80		8.30	38.8										
65										11.20					67	0.33
70							7.35		33.60		420					
75						39.0										
80								7.36		11.30		380			67	0.33
85																
90						39.2										
95										10.40					70	0.30
100																
105						39.5										
110										9.70					72	0.28
115																
120	x	13.10	8.20			39.9										
125										9.50					72	0.28
130							7.38		34.10		430					
135						40.3										
140								7.40		8.20		400			76	0.24

465					49.9											
470									3.46						90	0.10
475																
480		12.00	11.40		11.80	50.5										
485									3.43						90	0.10
490							7.55		35.50		400					
495						51.0										
500								7.56		3.65		410			89	0.11
505																
510						51.5										
515										3.74					89	0.11
520																
525						51.9										
530										3.23					91	0.09
535																
540		12.00	11.80		12.10	52.4										
545										3.17					91	0.09
550								7.58		34.80		400				
555						53.0										
560								7.58		2.99		400			91	0.09
565																
570						53.4										
575										2.87					92	0.08
580																
585						53.8										
590										3.01					91	0.09
595																
600		11.80	12.30		12.50	54.3										
605										2.83					92	0.08
610								7.54		35.00		410				
615						54.8										
620								7.59		2.92		420			92	0.08

625															
630					55.3										
635									2.85					92	0.08
640															
645					55.9										
650									2.74					92	0.08
655															
660		11.90	12.60		13.00	56.3									
665									2.69					92	0.08
670							7.60		35.30		400				
675					56.8										
680								7.57		2.60		400		92	0.08
685															
690					57.3										
695										2.76				92	0.08
700															
705					57.8										
710										2.83				92	0.08
715															
720		11.70	13.00		13.20	58.4	7.62	7.61	34.60	2.93	410	400		91	0.09

Filtralite

Time	Tests	Temperature (°C)				Head Loss (cm)	pH		Turbidity (NTU)		Conductivity		Sample No.		% Removal	C/Co
		Air	ST	HT	A		ST	A	ST	A	ST	A	ST	A		
0		15.10	10.70		12.40	14.7	7.48		34.10		500					
5								7.45		13.20		490			62	0.38
10										12.10					65	0.35
15						14.8				12.30					65	0.35
20																
25						15.0				9.46					73	0.27
30																
35						15.2										
40										8.94					74	0.26
45						15.4										
50										8.87					74	0.26
55																
60		15.00	11.30		11.90	15.6										
65										9.27					73	0.27
70							7.46		33.60		470					
75						15.8										
80								7.51		7.81		430			78	0.22
85																
90						16.0										
95										7.58					78	0.22
100																
105						16.2										
110										8.20					76	0.24
115																
120		14.50	12.10		12.40	16.4										
125										7.80					78	0.22
130							7.51		36.10		430					
135						16.5										
140								7.47		8.02		400			77	0.23

465					20.0											
470									8.32						76	0.24
475																
480		15.50	15.70		15.60	20.2										
485									8.24						76	0.24
490							7.61		35.30		400					
495						20.3										
500								7.59		8.65		410			75	0.25
505																
510						20.4										
515										8.54					75	0.25
520																
525						20.4										
530										8.76					75	0.25
535																
540		15.30	16.20		16.10	20.6										
545										8.65					75	0.25
550								7.62		34.70		400				
555						20.8										
560								7.60		8.60		410			75	0.25
565																
570						21.0										
575										8.64					75	0.25
580																
585						21.2										
590										8.69					75	0.25
595																
600		15.40	16.60		16.60	21.4										
605										8.80					75	0.25
610								7.60		33.90		410				
615						21.7										
620								7.61		8.45		400			76	0.24

625															
630					21.9										
635									8.32					76	0.24
640															
645					22.0										
650									8.67					75	0.25
655															
660		15.20	16.80		16.80	22.2									
665									8.87					74	0.26
670							7.63		34.80		410				
675					22.5										
680								7.65		8.56		410		75	0.25
685															
690					22.7										
695										8.98				74	0.26
700															
705					22.9										
710										8.76				75	0.25
715															
720		15.00	17.40		17.50	23.1	7.61	7.63	34.50	8.80	410	410		75	0.25

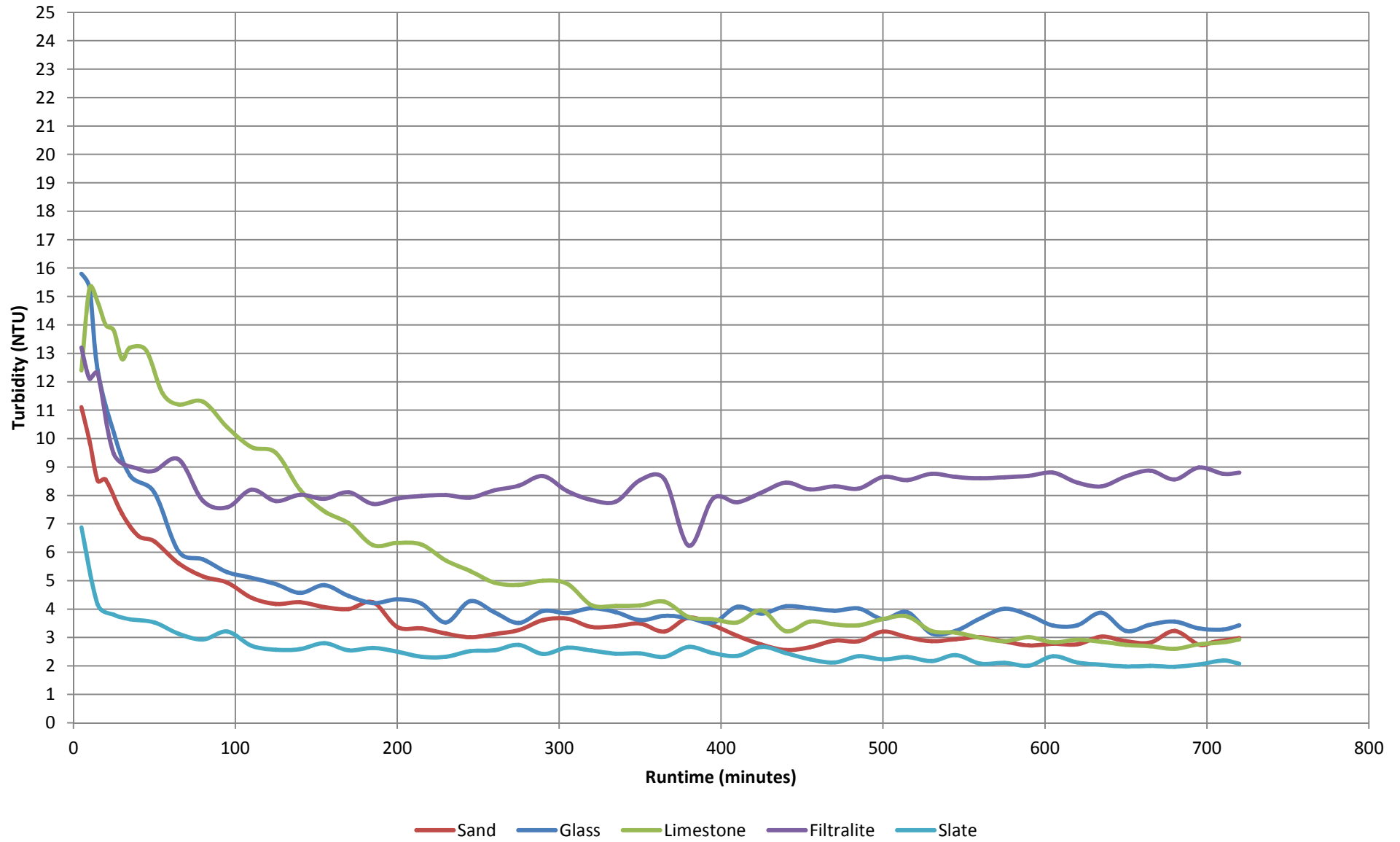
Slate

Time	Tests	Temperature (°C)				Head Loss (cm)	pH		Turbidity (NTU)		Conductivity		Sample No.		% Removal	C/Co
		Air	ST	HT	A		ST	A	ST	A	ST	A	ST	A		
0		18.80	14.10		12.10	27.6	7.47		35.50		400					
5								7.48		6.87		400			80	0.20
10																
15						28.0				4.16					88	0.12
20																
25										3.80					89	0.11
30						28.3										
35										3.64					90	0.10
40																
45						28.7										
50										3.53					90	0.10
55																
60		19.30	15.70		16.20	29.0										
65										3.13					91	0.09
70							7.54		35.40		410					
75						29.3										
80								7.50		2.93		410			92	0.08
85																
90						29.5										
95										3.21					91	0.09
100																
105						29.8										
110										2.71					92	0.08
115																
120		19.00	16.30		17.00	30.1										
125										2.57					93	0.07
130							7.56		36.30		400					
135						30.4										
140								7.54		2.59		450			93	0.07

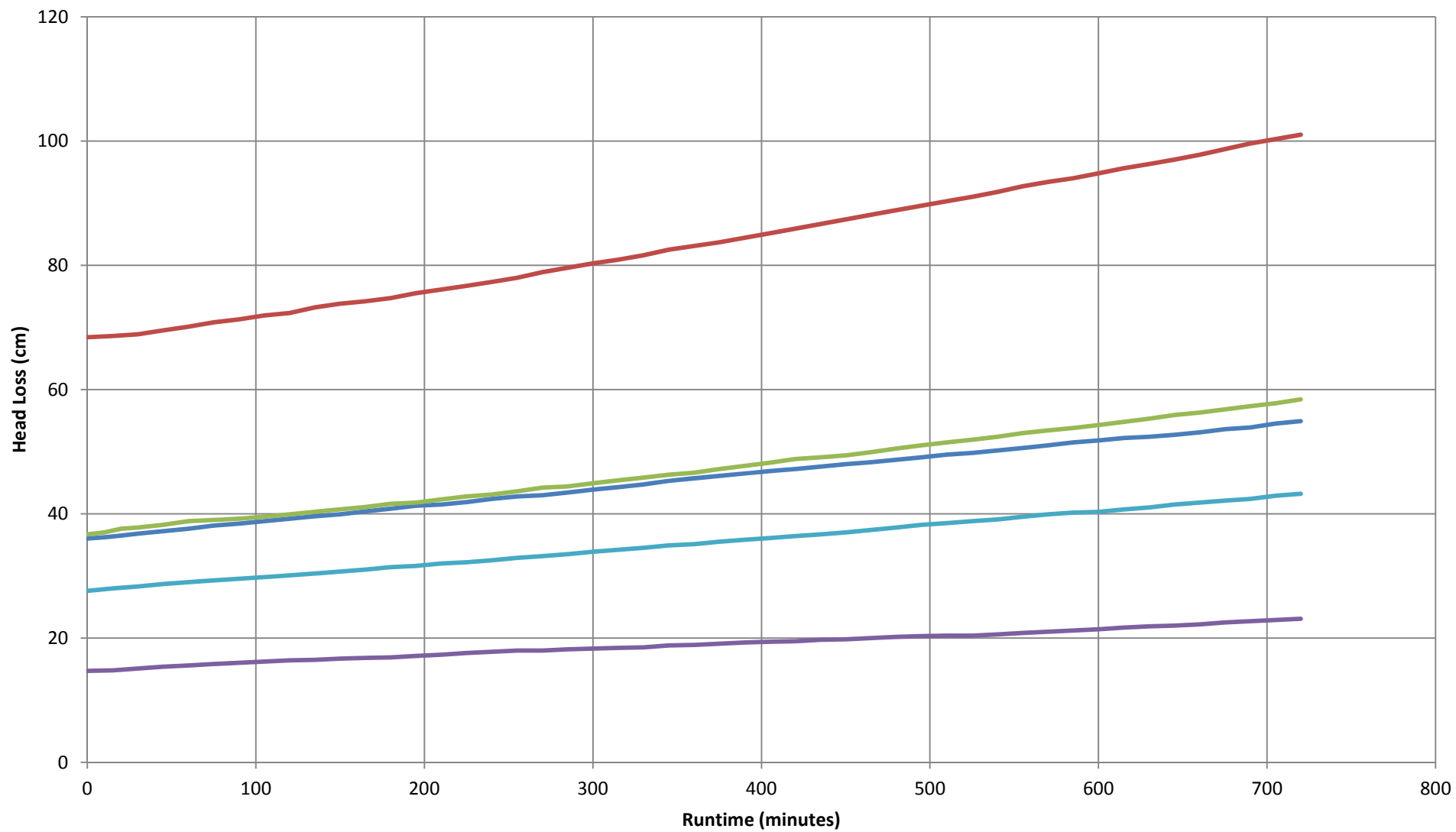
465					37.4										
470									2.12					94	0.06
475															
480		19.10	20.30		20.40	37.8									
485									2.34					93	0.07
490							7.52		34.60		430				
495						38.2									
500								7.55		2.23		440		94	0.06
505															
510						38.5									
515										2.31				93	0.07
520															
525						38.8									
530										2.17				94	0.06
535															
540		19.00	20.90		20.90	39.1									
545										2.38				93	0.07
550							7.55		34.80		430				
555						39.5									
560								7.53		2.08		420		94	0.06
565															
570						39.9									
575										2.11				94	0.06
580															
585						40.2									
590										2.01				94	0.06
595															
600		19.00	21.30		21.20	40.3									
605										2.34				93	0.07
610							7.52		35.60		440				
615						40.7									
620								7.56		2.12		430		94	0.06

625																
630						41.0										
635										2.04					94	0.06
640																
645						41.5										
650										1.98					94	0.06
655																
660		18.90	21.70		21.60	41.8										
665										2.00					94	0.06
670							7.55		35.40		440					
675						42.1										
680								7.51		1.97		440			94	0.06
685																
690						42.4										
695										2.05					94	0.06
700																
705						42.9										
710										2.19					94	0.06
715																
720		18.70	21.90		21.80	43.2	7.58	7.55	35.40	2.08	420	430			94	0.06

Turbidity



Head Loss



— Glass — Sand — Limestone — Filtralite — Slate

Flowrate – 13.5 m/h

Turbidity – 35 NTU

Sand

Time (minute)	Tests	Temperature (°C)				Head Loss (cm)	pH		Turbidity (NTU)		Conductivity		Sample No.		% Removal	C/Co
		Air	ST	HT	A		ST	A	ST	A	ST	A	ST	A		
0		19.50	12.90		17.80	95.6	7.35		8.99		470					
5								7.37		6.33		480			33	0.67
10										6.45					31	0.69
15						95.8										
20										6.60					30	0.70
25																
30						96.0				5.84					38	0.62
35																
40										5.93					37	0.63
45						96.1										
50										5.70					39	0.61
55																
60	X	19.00	13.70		14.30	96.2										
65										5.01					47	0.53
70							7.41		9.65		440					
75						96.2										
80								7.37		5.45		440			42	0.58
85																
90						96.3										
95										5.01					47	0.53
100																
105						96.3										
110										4.34					54	0.46
115																
120	X	19.60	14.70		15.20	96.4										
125										4.21					55	0.45
130							7.51		11.40		450					
135						96.4										
140								7.54		4.07		460			57	0.43

465					99.0											
470									2.19						77	0.23
475																
480	X	20.20	18.70		18.80	99.1										
485									2.25						76	0.24
490							7.57		8.70		470					
495						99.2										
500								7.57		2.45		470			74	0.26
505																
510						99.4										
515										2.27					76	0.24
520																
525						99.5										
530										2.41					74	0.26
535																
540	X	20.00	19.10		19.20	99.6										
545										2.39					75	0.25
550							7.58		9.43		480					
555						99.7										
560								7.58		2.22		470			76	0.24
565																
570						99.8										
575										2.18					77	0.23
580																
585						100.0										
590										2.29					76	0.24
595																
600	X	20.10	19.50		19.70	100.0										
605										2.34					75	0.25
610							7.59		9.19		480					
615						100.1										
620								7.57		2.27		480			76	0.24

625																
630						100.2										
635										2.19					77	0.23
640																
645						100.3										
650										2.20					77	0.23
655																
660	X	19.90	19.80		19.90	100.5										
665										2.17					77	0.23
670							7.62		9.15		480					
675						100.6										
680								7.59		2.18		470			77	0.23
685																
690						100.7										
695										2.26					76	0.24
700																
705						100.8										
710										2.19					77	0.23
715																
720	X	19.70	20.10		20.30	100.9	7.61	7.60	9.24	2.32	470	470			75	0.25

Glass

Time	Tests	Temperature (°C)				Head Loss (cm)	pH		Turbidity (NTU)		Conductivity		Sample No.		% Removal	C/Co
		Air	ST	HT	A		ST	A	ST	A	ST	A	ST	A		
0		17.80	15.50		13.70	48.0	7.46		10.60		470					
5								7.68		8.62		470			12	0.88
10						48.1										
15										8.26					16	0.84
20						48.2										
25										7.28					26	0.74
30						48.4										
35										6.50					34	0.66
40																
45						48.6										
50										6.53					33	0.67
55																
60		18.20	16.30		16.60	48.6										
65										5.81					41	0.59
70							7.54		10.50		460					
75						48.7										
80								7.53		5.41		430			45	0.55
85																
90						48.8										
95										5.20					47	0.53
100																
105						49.0										
110										4.91					50	0.50
115																
120		18.50	17.10		17.50	49.2										
125										4.74					52	0.48
130							7.51		9.71		460					
135						49.3										
140								7.63		5.24		460			47	0.53

465					51.9											
470									3.08						69	0.31
475																
480		19.50	20.90		20.80	52.1										
485									3.15						68	0.32
490							7.63				470					
495						52.2										
500								7.60		3.12		470			68	0.32
505																
510						52.3										
515										3.12					68	0.32
520																
525						52.4										
530										3.08					69	0.31
535																
540		19.40	21.40		21.50	52.5										
545										3.04					69	0.31
550								7.62				480				
555						52.6										
560								7.61		3.26		480			67	0.33
565																
570						52.8										
575										2.98					70	0.30
580																
585						52.9										
590										2.97					70	0.30
595																
600		19.60	21.80		21.90	53.0										
605										2.95					70	0.30
610								7.64				480				
615						53.2										
620								7.63		3.00		470			69	0.31

625															
630					53.3										
635									2.93					70	0.30
640															
645					53.4										
650									2.94					70	0.30
655															
660		19.30	22.10		22.00	53.5									
665									2.86					71	0.29
670							7.62			460					
675					53.6										
680								7.63	2.97		470			70	0.30
685															
690					53.8										
695									2.92					70	0.30
700															
705					53.9										
710									2.91					70	0.30
715															
720		19.40	22.40		22.20	54.0	7.63	7.62	2.87	470	480			71	0.29

Limestone

Time	Tests	Temperature (°C)				Head Loss (cm)	pH		Turbidity (NTU)		Conductivity		Sample No.		% Removal	C/Co
		Air	ST	HT	A		ST	A	ST	A	ST	A	ST	A		
0		19.80	14.10		14.20	54.8	7.34		11.70		530					
5								7.34		4.83		530			51	0.49
10						54.9										
15										4.60					53	0.47
20						55.3										
25										4.45					55	0.45
30						55.6										
35																
40										3.85					61	0.39
45						56.0										
50										3.59					63	0.37
55																
60		20.60	14.90		15.40	56.4										
65										3.41					65	0.35
70							7.37		10.50		530					
75						56.7										
80								7.41		3.38		510			66	0.34
85																
90						56.9										
95										3.82					61	0.39
100																
105						57.1										
110										3.35					66	0.34
115																
120	x	20.80	15.70		16.30	57.3										
125										3.30					66	0.34
130							7.41		9.73		490					
135						57.6										
140								7.43		3.45		490			65	0.35

465					64.1											
470									2.05						79	0.21
475																
480		20.20	19.50		19.50	64.3										
485									2.06						79	0.21
490							7.55		9.45		500					
495						64.5										
500								7.55		1.99		490			80	0.20
505																
510						64.6										
515										2.07					79	0.21
520																
525						64.8										
530										2.04					79	0.21
535																
540		20.10	20.00		20.10	64.9										
545										1.98					80	0.20
550							7.56		9.26		510					
555						65.1										
560								7.54		1.98		480			80	0.20
565																
570						65.4										
575										1.99					80	0.20
580																
585						65.6										
590										1.94					80	0.20
595																
600		20.10	20.40		20.40	65.8										
605										1.92					80	0.20
610							7.57		9.00		490					
615						66.0										
620								7.58		1.98		500			80	0.20

625															
630					66.1										
635									1.89					81	0.19
640															
645					66.3										
650									1.93					80	0.20
655															
660		19.90	20.80		20.70	66.5									
665									2.04					79	0.21
670							7.58		9.68		490				
675						66.9									
680								7.57		1.91		490		81	0.19
685															
690						67.2									
695										2.04				79	0.21
700															
705						67.4									
710										1.98				80	0.20
715															
720		19.60	21.10		21.00	67.6	7.59	7.60	9.34	1.90	490	490		81	0.19

Filtralite

Time	Tests	Temperature (°C)				Head Loss (cm)	pH		Turbidity (NTU)		Conductivity		Sample No.		% Removal	C/Co
		Air	ST	HT	A		ST	A	ST	A	ST	A	ST	A		
0		19.40	15.70		15.30	23.4	7.35		9.55		540					
5								7.41		5.02		580			47	0.53
10																
15						23.6				4.45					53	0.47
20																
25										4.12					57	0.43
30						24.0										
35										3.82					60	0.40
40																
45						24.1										
50										3.83					60	0.40
55																
60		19.70	16.40		16.90	24.2										
65										3.74					61	0.39
70							7.41		9.55		500					
75						24.4										
80								7.43		3.75		530			60	0.40
85																
90						24.6										
95										3.65					62	0.38
100																
105						24.7										
110										3.54					63	0.37
115																
120		19.70	17.20		17.60	24.8										
125										3.67					61	0.39
130							7.48		10.10		510					
135						24.8										
140								7.47		3.48		510			63	0.37

465					26.5											
470									3.54						63	0.37
475																
480		20.30	20.40		20.40	26.4										
485									3.58						62	0.38
490							7.59		9.19		500					
495						26.6										
500								7.59		3.65		510			62	0.38
505																
510						26.7										
515										3.69					61	0.39
520																
525						26.8										
530										3.48					63	0.37
535																
540		20.40	20.80		20.70	26.8										
545										3.51					63	0.37
550							7.61		9.24		510					
555						26.8										
560								7.60		3.45		520			64	0.36
565																
570						26.9										
575										3.44					64	0.36
580																
585						27.0										
590										3.25					66	0.34
595																
600		20.10	21.10		21.00	27.0										
605										3.65					62	0.38
610							7.61		9.68		510					
615						27.1										
620								7.62		3.45		510			64	0.36

625																
630					27.1											
635									3.61					62	0.38	
640																
645					27.2											
650									3.58					62	0.38	
655																
660		20.00	21.40		21.20	27.3										
665									3.58					62	0.38	
670						7.63		9.35		510						
675					27.3											
680							7.62		3.54		500			63	0.37	
685																
690					27.4											
695									3.64					62	0.38	
700																
705					27.4											
710									3.35					65	0.35	
715																
720		19.80	21.60		21.40	27.5	7.62	7.61	9.21	3.48	510	500		63	0.37	

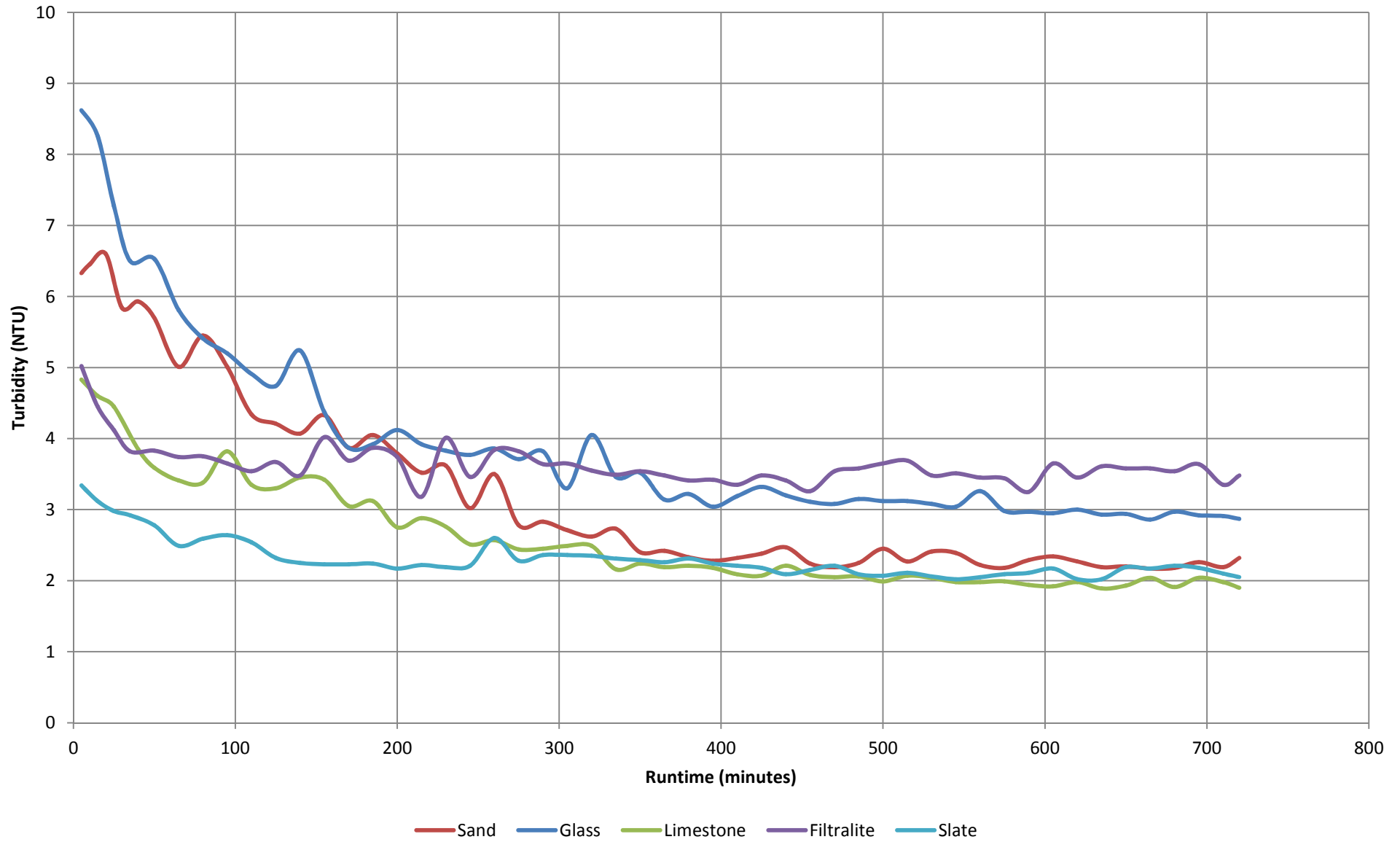
Slate

Time	Tests	Temperature (°C)				Head Loss (cm)	pH		Turbidity (NTU)		Conductivity		Sample No.		% Removal	C/Co
		Air	ST	HT	A		ST	A	ST	A	ST	A	ST	A		
0		18.90	16.90		20.60	42.1	7.38		9.52		560					
5								7.44		3.34		570			63	0.37
10						42.4										
15										3.12					66	0.34
20						42.5										
25										2.98					67	0.33
30						42.5										
35										2.92					68	0.32
40																
45						42.5										
50										2.78					70	0.30
55																
60		19.20	17.90		18.20	42.6										
65										2.49					73	0.27
70							7.48		8.86		570					
75						42.7										
80								7.50		2.59		510			72	0.28
85																
90						42.8										
95										2.64					71	0.29
100																
105						42.8										
110										2.54					72	0.28
115																
120		20.00	18.60		18.40	43.0										
125										2.32					75	0.25
130							7.53		8.54		490					
135						43.2										
140								7.52		2.25		460			75	0.25

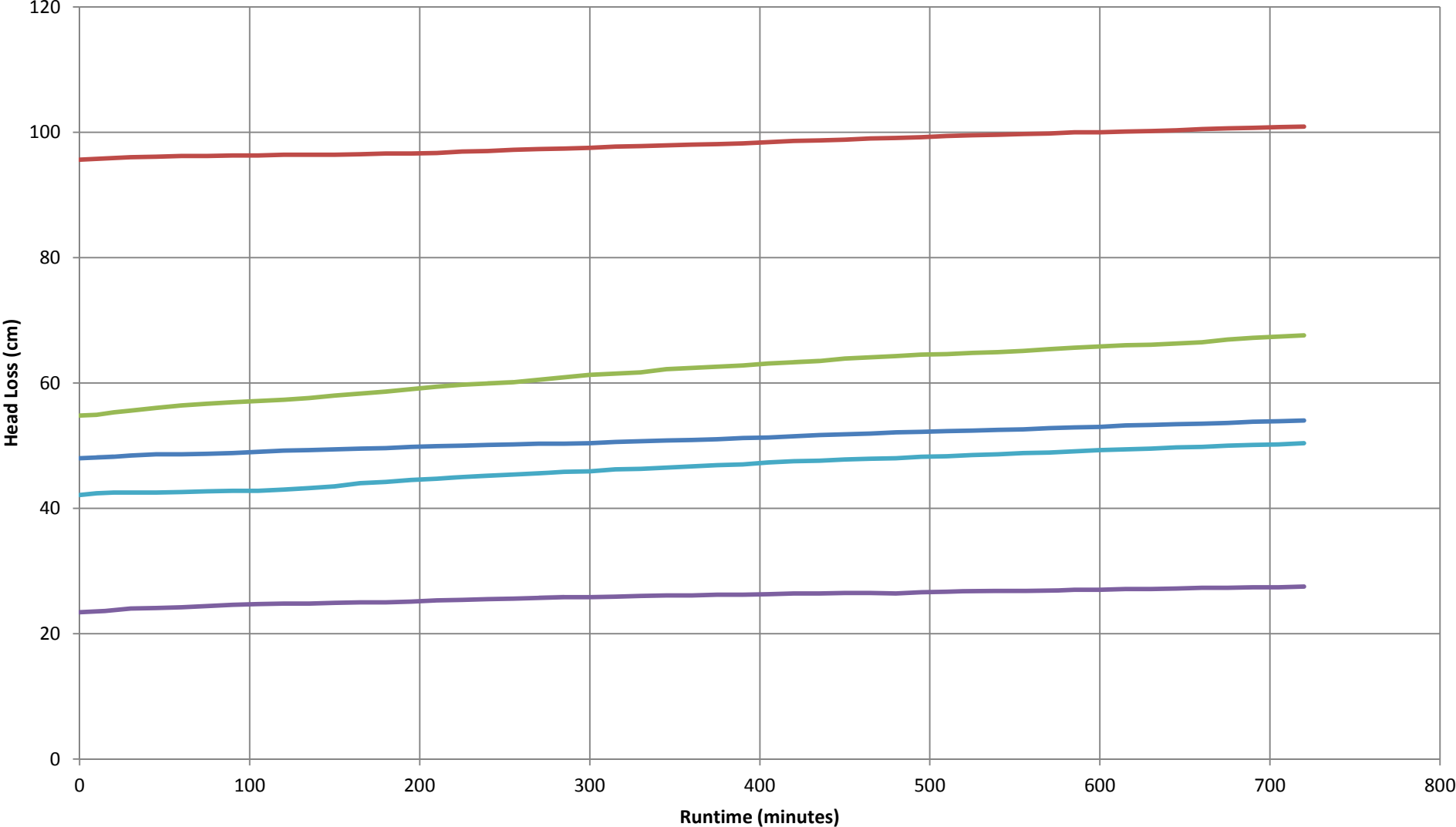
465					47.9										
470									2.21					76	0.24
475															
480		20.70	21.50		21.50	48.0									
485									2.09					77	0.23
490							7.58		8.99		510				
495						48.2									
500								7.59		2.07		510		77	0.23
505															
510						48.3									
515										2.11				77	0.23
520															
525						48.5									
530										2.06				77	0.23
535															
540		20.60	21.90		22.00	48.6									
545										2.02				78	0.22
550							7.59		9.42		510				
555						48.8									
560								7.60		2.05		500		78	0.22
565															
570						48.9									
575										2.09				77	0.23
580															
585						49.1									
590										2.11				77	0.23
595															
600		20.40	22.30		22.40	49.3									
605										2.17				76	0.24
610							7.61		9.35		510				
615						49.4									
620								7.61		2.02		510		78	0.22

625															
630					49.5										
635									2.02					78	0.22
640															
645					49.7										
650									2.19					76	0.24
655															
660		20.40	22.60		22.70	49.8									
665									2.17					76	0.24
670							7.62		9.45		500				
675					50.0										
680								7.61		2.21		500		76	0.24
685															
690					50.1										
695										2.18				76	0.24
700															
705					50.2										
710										2.10				77	0.23
715															
720		20.30	22.80		22.90	50.4	7.62	7.60	9.08	2.05	500	510		78	0.22

Turbidity



Head Loss



— Glass — Sand — Limestone — Filtralite — Slate

Flowrate – 13.5 m/h

Turbidity – 9 NTU

Sand

Time (minute)	Tests	Temperature (°C)				Head Loss (cm)	pH		Turbidity (NTU)		Conductivity		Sample No.		% Removal	C/Co
		Air	ST	HT	A		ST	A	ST	A	ST	A	ST	A		
0		19.10	15.30			95.2	7.58		34.50		520					
5		19.10	15.50		15.90	95.8		7.47		18.10		520			48	0.52
10										16.70					52	0.48
15		19.20	15.60		15.90	96.5			34.70	15.50	520				56	0.44
20						96.7		7.54		14.30					59	0.41
25						96.8				14.00	520				60	0.40
30		19.40	15.90		16.10	97.0	7.64		35.10	13.00					63	0.37
35						97.4				12.70					64	0.36
40						97.5		7.56		12.30					65	0.35
45							7.64		34.60	12.40					64	0.36
50						98.0				12.10	520	510			65	0.35
55		19.60	16.10		15.90	98.3				11.80					66	0.34
60																
65						98.4				11.50					67	0.33
70																
75		19.70				98.5	7.67	7.55	34.00	10.90	510	530			69	0.31
80			16.30		16.50											
85										10.40					70	0.30
90						99.1										
95										10.60					70	0.30
100		19.90	16.60		16.90	99.6										
105						100.0	7.64	7.61	34.10	9.55	510	520			73	0.27
110																
115										9.64					72	0.28
120																
125																
130		19.30	17.00		17.30	101.8	7.52	7.61	35.30	9.52	510	530			73	0.27
135																
140						102.2				9.18					74	0.26

465					118.8											
470									6.72						81	0.19
475																
480		19.70	20.00		20.00	119.5										
485									6.67						81	0.19
490							7.72		33.80		520					
495						120.3										
500								7.67		6.84		530			80	0.20
505																
510						121.3										
515										7.32					79	0.21
520																
525						122.3										
530										7.28					79	0.21
535																
540		19.70	20.50		20.50											
545										6.01					83	0.17
550						123.4	7.73		35.50		510					
555																
560								7.62		6.98		520			80	0.20
565																
570						124.1										
575										6.35					82	0.18
580																
585						125.0										
590										6.84					80	0.20
595																
600						125.8										
605		19.90	20.40		20.40											
610										6.26					82	0.18
615						126.6	7.67		36.10		530					
620								7.63		7.03		520			80	0.20

625																
630					127.4											
635									6.26					82	0.18	
640																
645					128.4											
650									5.87					83	0.17	
655																
660		20.10	20.60		20.60	129.0										
665									5.96					83	0.17	
670							7.72		34.70		530					
675					129.8											
680							7.78		5.60		530			84	0.16	
685																
690					130.7											
695									6.66					81	0.19	
700																
705					131.6				5.66					84	0.16	
710																
715																
720		20.20	20.50		20.70	132.5	7.69	7.71	35.20	5.96	530	520		83	0.17	

Glass

Time	Tests	Temperature (°C)				Head Loss (cm)	pH		Turbidity (NTU)		Conductivity		Sample No.		% Removal	C/Co
		Air	ST	HT	A		ST	A	ST	A	ST	A	ST	A		
0		15.10	12.90		14.20	46.7			35.40							
5						47.0	7.29			22.50					35	0.65
10						47.3		7.33		19.90					43	0.57
15						47.7				18.30	420	500			47	0.53
20						47.9			35.50	17.60					50	0.50
25										16.40					53	0.47
30		15.40	13.10		13.50	48.4				15.50					56	0.44
35										15.10					57	0.43
40						48.9			34.80		430					
45								7.44		14.00					60	0.40
50						49.4	7.39				480					
55						49.6				13.60					61	0.39
60		14.70	13.40		14.20	49.8			34.60							
65										12.80					63	0.37
70							7.45		35.50		410					
75						50.5										
80								7.46		12.70		410			64	0.36
85																
90						50.9										
95										11.70					66	0.34
100																
105						51.4										
110										11.10					68	0.32
115																
120		14.10	13.80		14.00	52.0										
125										10.50					70	0.30
130							7.40		35.70		430					
135						52.6										
140								7.43		10.60		420			70	0.30

465					66.4											
470									8.16						77	0.23
475																
480		15.10	16.80		16.50	67.1										
485									7.65						78	0.22
490							7.59		35.60		420					
495																
500						67.8		7.64		8.53		430			76	0.24
505																
510						68.4										
515										8.63					75	0.25
520																
525						68.9										
530										8.38					76	0.24
535																
540		15.20	17.30		16.70	69.3										
545										8.20					76	0.24
550							7.62		34.20		430					
555						69.8										
560								7.65		8.30		410			76	0.24
565																
570						70.4										
575										8.81					75	0.25
580																
585						70.9										
590										9.30					73	0.27
595																
600		14.40	17.70		17.30	71.4										
605										8.93					74	0.26
610							7.63		34.50		430					
615						72.1										
620								7.60		9.13		430			74	0.26

625															
630					72.5										
635									9.26					73	0.27
640															
645					73.1										
650									8.29					76	0.24
655															
660		13.90	18.10		17.80	73.5									
665									8.79					75	0.25
670							7.65		34.20		440				
675					74.0										
680							7.65		9.57		440			73	0.27
685															
690					74.4										
695									8.69					75	0.25
700															
705					75.2										
710									8.72					75	0.25
715															
720		14.20	18.30		18.00	75.9	7.64	7.62	35.20	8.64	440	430		75	0.25

Limestone

Time	Tests	Temperature (°C)				Head Loss (cm)	pH		Turbidity (NTU)		Conductivity		Sample No.		% Removal	C/Co
		Air	ST	HT	A		ST	A	ST	A	ST	A	ST	A		
0		15.50	11.70		13.60	20.5	7.50		35.70							
5								7.53		17.60					50	0.50
10						22.5				16.60		520			52	0.48
15						23.6				14.40		430			59	0.41
20						25.4				13.80					60	0.40
25						26.6				13.60					61	0.39
30						27.4			34.30	13.00					63	0.37
35						28.3				12.80					63	0.37
40																
45						30.9				12.40					64	0.36
50																
55						32.4				12.20					65	0.35
60		14.40	12.30		12.70	33.8										
65										10.90					69	0.31
70							7.43		35.70			460				
75						36.1										
80								7.45		10.50		440			70	0.30
85																
90						38.4										
95										10.40					70	0.30
100																
105						40.6										
110										10.30					70	0.30
115																
120		15.00	12.90		13.20											
125						43.6				9.90					72	0.28
130							7.53		35.90			440				
135						45.2										
140								7.46		10.00		450			71	0.29

465					80.1											
470									7.42						79	0.21
475																
480		14.60	16.30		16.00	81.6										
485									7.23						79	0.21
490							7.53		34.70		470					
495						82.7										
500								7.48		7.64		460			78	0.22
505																
510						84.2										
515										7.76					78	0.22
520																
525						85.7										
530										6.92					80	0.20
535																
540		14.00	16.80		16.70	87.0										
545										6.84					80	0.20
550								7.51		34.40		460				
555						88.3										
560								7.51		7.85		470			78	0.22
565																
570						89.6										
575										7.89					77	0.23
580																
585						91.5										
590										8.02					77	0.23
595																
600		14.30	17.50		17.10	92.7										
605										7.56					78	0.22
610								7.56		33.20		480				
615						94.0										
620								7.52		7.42		450			79	0.21

625															
630					95.6										
635									7.80					78	0.22
640															
645					96.9										
650									6.72					81	0.19
655															
660		14.30	17.90		17.70	98.4									
665									7.35					79	0.21
670							7.54		35.70		460				
675					99.8										
680								7.51		7.66		460		78	0.22
685															
690					101.4										
695										6.56				81	0.19
700															
705					102.8										
710										6.98				80	0.20
715															
720		14.20	18.20		18.00	104.1	7.57	7.53	34.40	7.32	470	460		79	0.21

Filtralite

Time	Tests	Temperature (°C)				Head Loss (cm)	pH		Turbidity (NTU)		Conductivity		Sample No.		% Removal	C/Co
		Air	ST	HT	A		ST	A	ST	A	ST	A	ST	A		
0		13.50	11.90		12.60	25.0	7.40		34.20		430					
5									17.30					50	0.50	
10						25.5		7.47		15.50		490		56	0.44	
15										14.90				57	0.43	
20						26.0				14.40				59	0.41	
25										13.90				60	0.40	
30						26.4				13.40				62	0.38	
35																
40										13.20				62	0.38	
45						26.7										
50										13.10				62	0.38	
55																
60		13.50	12.30		12.60	27.2										
65										13.50				61	0.39	
70							7.40		34.90		470					
75						27.6										
80								7.45		13.30		430		62	0.38	
85																
90						27.9										
95										13.50				61	0.39	
100																
105						28.2										
110										13.70				61	0.39	
115																
120		13.30	12.80		13.00	28.6										
125										12.80				63	0.37	
130							7.43		35.60		420					
135						29.0										
140								7.48		13.70		420		61	0.39	

465					35.5											
470									13.40						62	0.38
475																
480		15.70	16.30		16.30	35.7										
485									14.60						58	0.42
490							7.50		36.20		410					
495						36.0										
500								7.57		14.70		410			58	0.42
505																
510						36.3										
515										14.40					59	0.41
520																
525						36.6										
530										14.20					59	0.41
535																
540		15.50	17.00		17.00	36.7										
545										14.00					60	0.40
550								7.51		34.90		420				
555						36.9										
560								7.57		12.90		410			63	0.37
565																
570						37.2										
575										14.40					59	0.41
580																
585						37.4										
590										14.10					60	0.40
595																
600		15.70	17.60		17.70	37.6										
605										13.50					61	0.39
610								7.56		33.90		420				
615						37.9										
620								7.52		14.90		420			57	0.43

625															
630					38.2										
635									14.50					58	0.42
640															
645					38.4										
650									14.00					60	0.40
655															
660		14.40	18.00		17.80	38.7									
665									14.30					59	0.41
670							7.53		35.50		420				
675					38.9										
680								7.57		13.80		420		60	0.40
685															
690					39.2										
695										14.20				59	0.41
700															
705					39.4										
710										14.70				58	0.42
715															
720		14.20	18.10		17.90	39.6	7.55	7.53	34.60	14.40	410	420		59	0.41

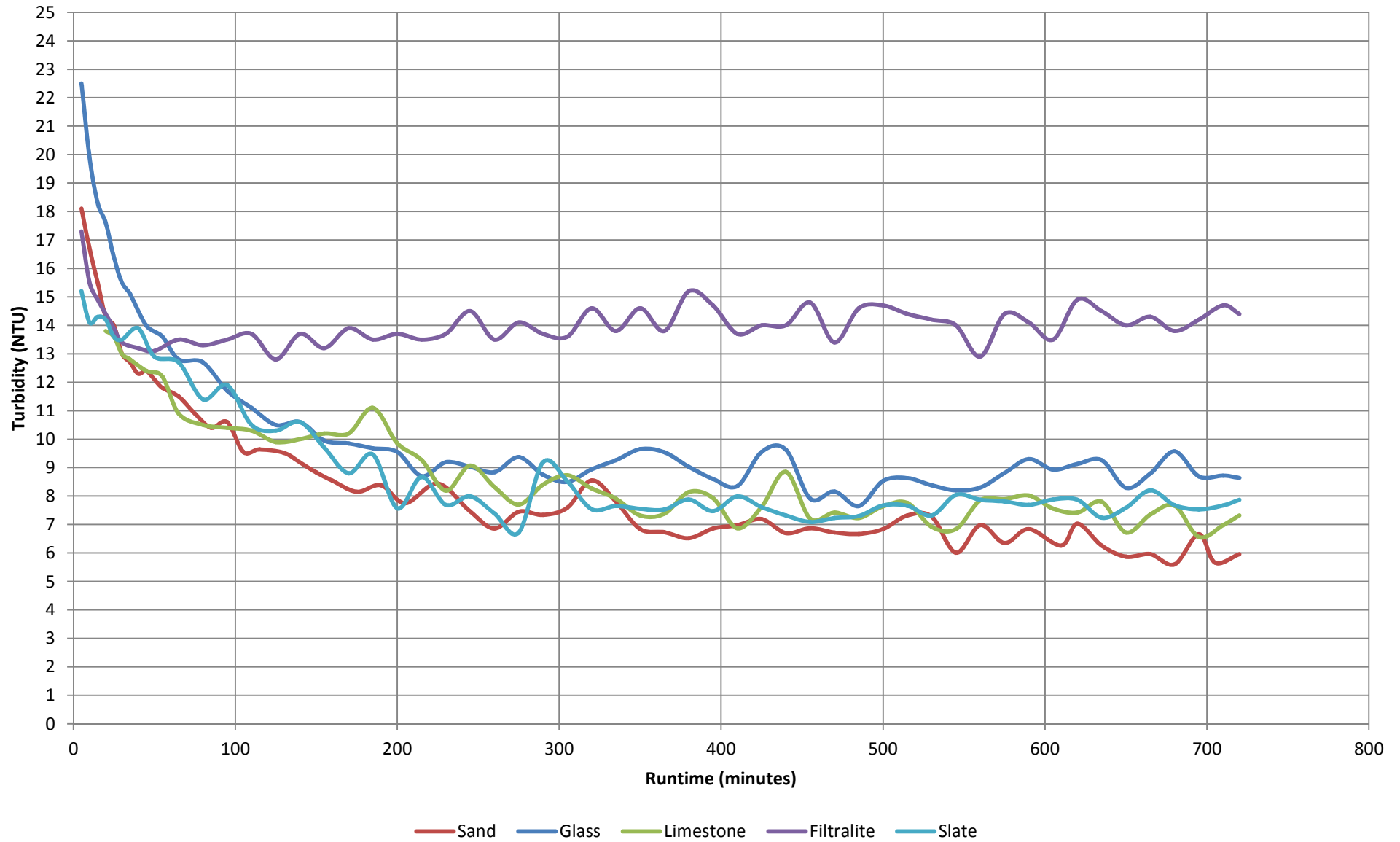
Slate

Time	Tests	Temperature (°C)				Head Loss (cm)	pH		Turbidity (NTU)		Conductivity		Sample No.		% Removal	C/Co
		Air	ST	HT	A		ST	A	ST	A	ST	A	ST	A		
0		12.50	9.60		9.90	40.0	7.35		34.80		410					
5										15.20				56	0.44	
10						40.6		7.35		14.10		390		59	0.41	
15										14.30				59	0.41	
20						41.0				14.20				59	0.41	
25										13.60				61	0.39	
30						41.4				13.50				61	0.39	
35																
40										13.90				60	0.40	
45						41.8										
50										12.90				63	0.37	
55																
60		11.70	9.90		10.30	42.2										
65										12.70				63	0.37	
70							7.41		36.10		400					
75						42.6										
80								7.36		11.40		380		67	0.33	
85																
90						43.1										
95										11.90				66	0.34	
100																
105						43.5										
110										10.50				70	0.30	
115																
120		12.30	10.30		10.70	43.9										
125										10.30				70	0.30	
130							7.39		35.30		400					
135						44.4										
140								7.36		10.60		390		70	0.30	

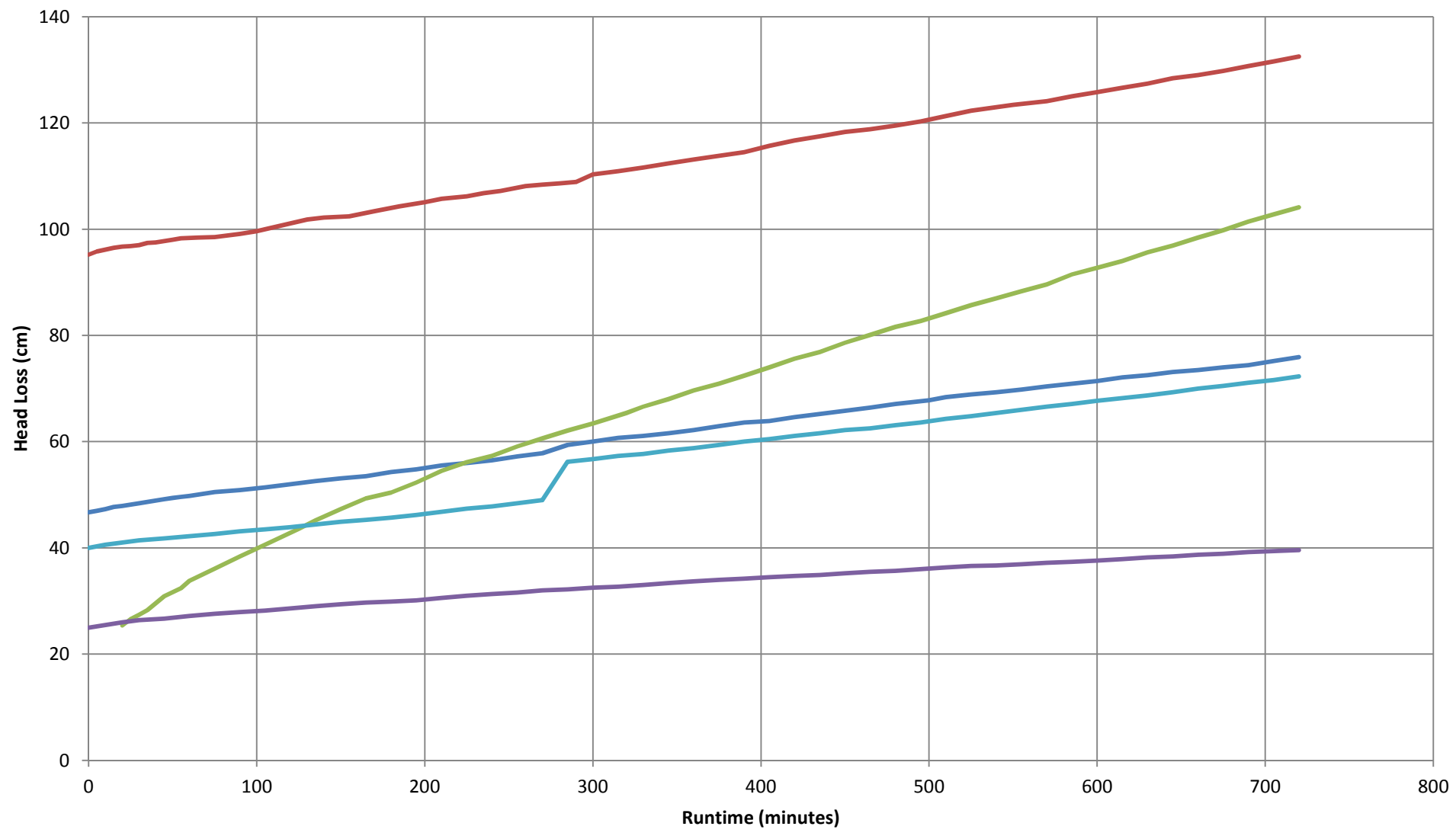
465					62.5											
470									7.23						79	0.21
475																
480		12.40	13.70		14.30	63.1										
485									7.30						79	0.21
490							7.52		34.00		400					
495						63.6										
500								7.53		7.67		410			78	0.22
505																
510						64.3										
515										7.66					78	0.22
520																
525						64.8										
530										7.32					79	0.21
535																
540		12.20	14.20		14.10	65.4										
545										8.04					77	0.23
550							7.56		32.90		410					
555						66.0										
560								7.50		7.87		410			77	0.23
565																
570						66.6										
575										7.81					78	0.22
580																
585						67.1										
590										7.69					78	0.22
595																
600		12.10	14.60		14.00	67.7										
605										7.88					77	0.23
610							7.55		34.70		410					
615						68.2										
620								7.51		7.87		420			77	0.23

625															
630					68.7										
635									7.24					79	0.21
640															
645					69.3										
650									7.59					78	0.22
655															
660		12.00	15.00		14.10	70.0									
665									8.20					76	0.24
670							7.53		34.10		400				
675					70.5										
680								7.48		7.68		410		78	0.22
685															
690					71.1										
695										7.53				78	0.22
700															
705					71.6										
710										7.67				78	0.22
715															
720		11.90	15.50		14.20	72.3	7.56	7.53		7.87	410	410		77	0.23

Turbidity



Head Loss



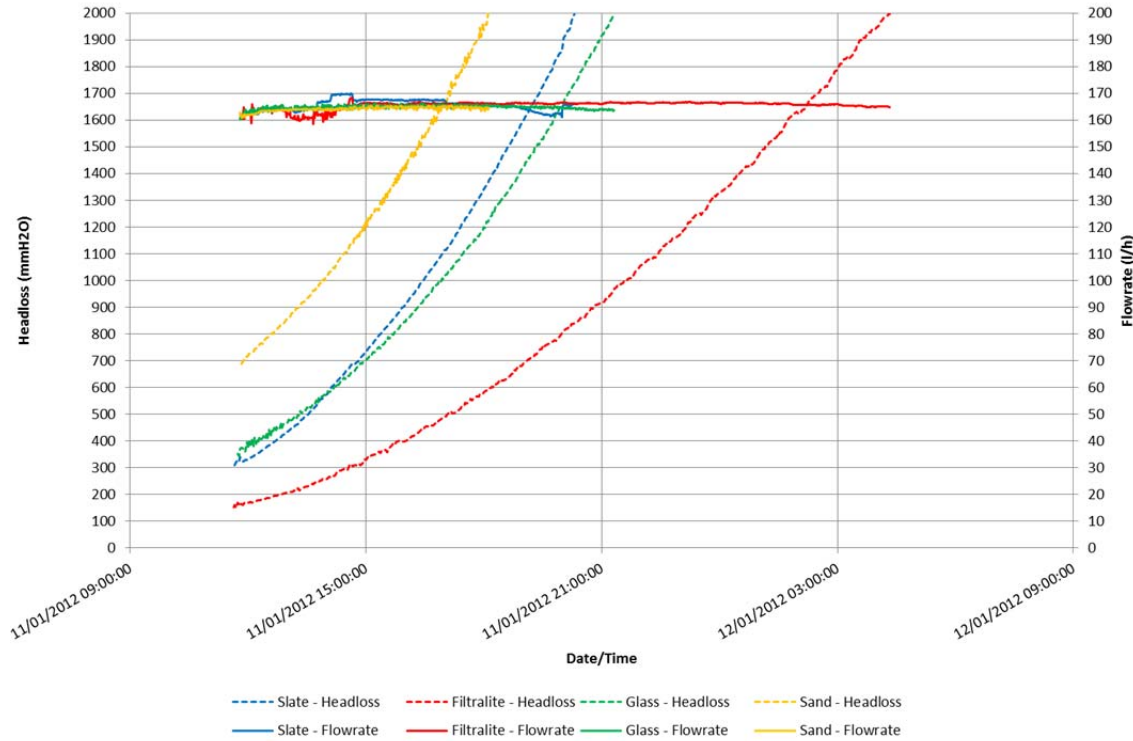
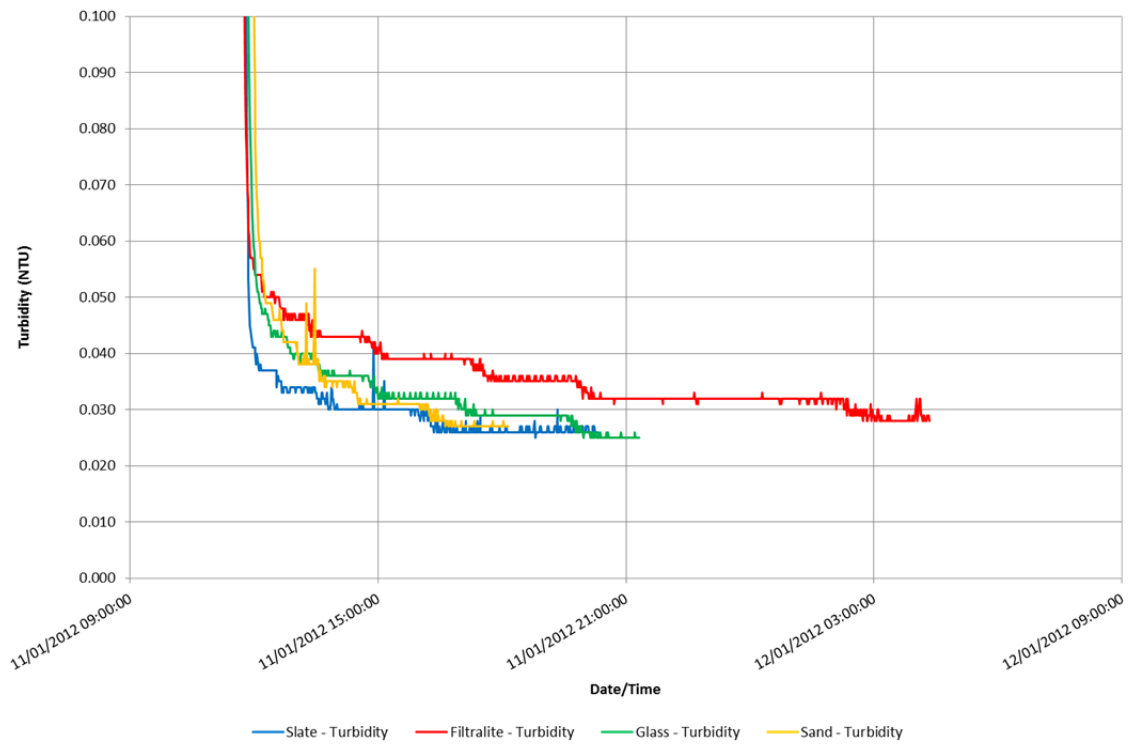
— Glass — Sand — Limestone — Filtralite — Slate

APPENDIX IV

Pilot Plant Study

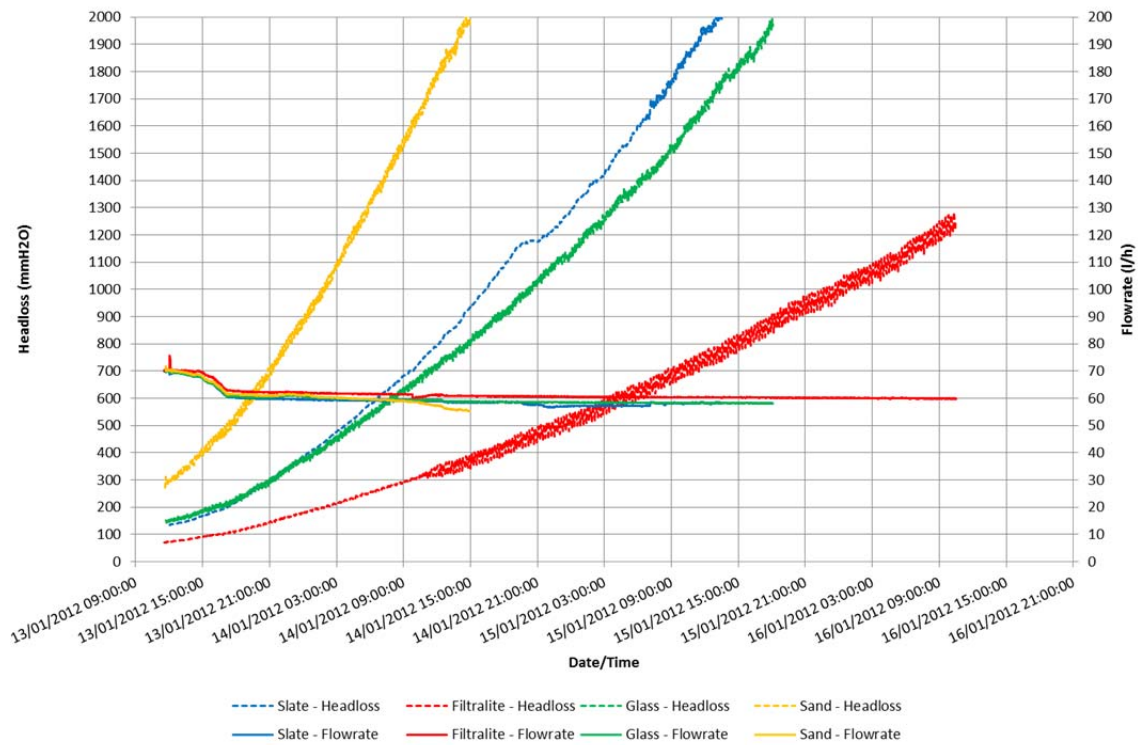
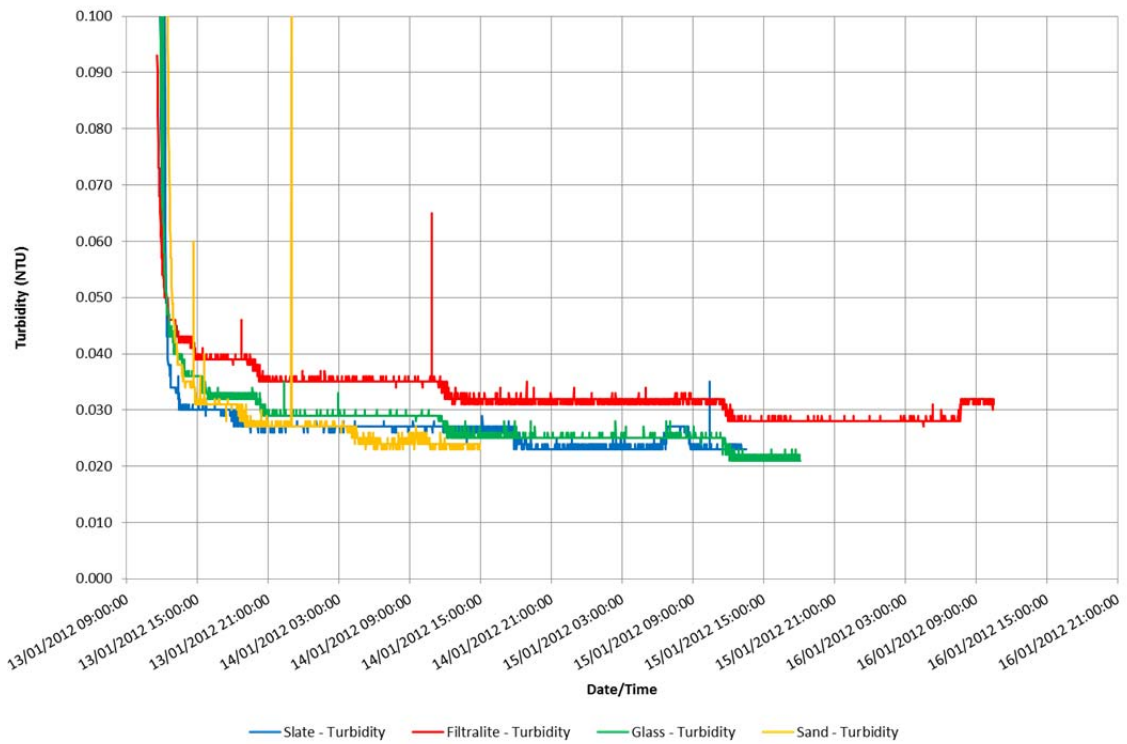
Test Run 1 – 11/01/2012

Flowrate – 9.34 m/h



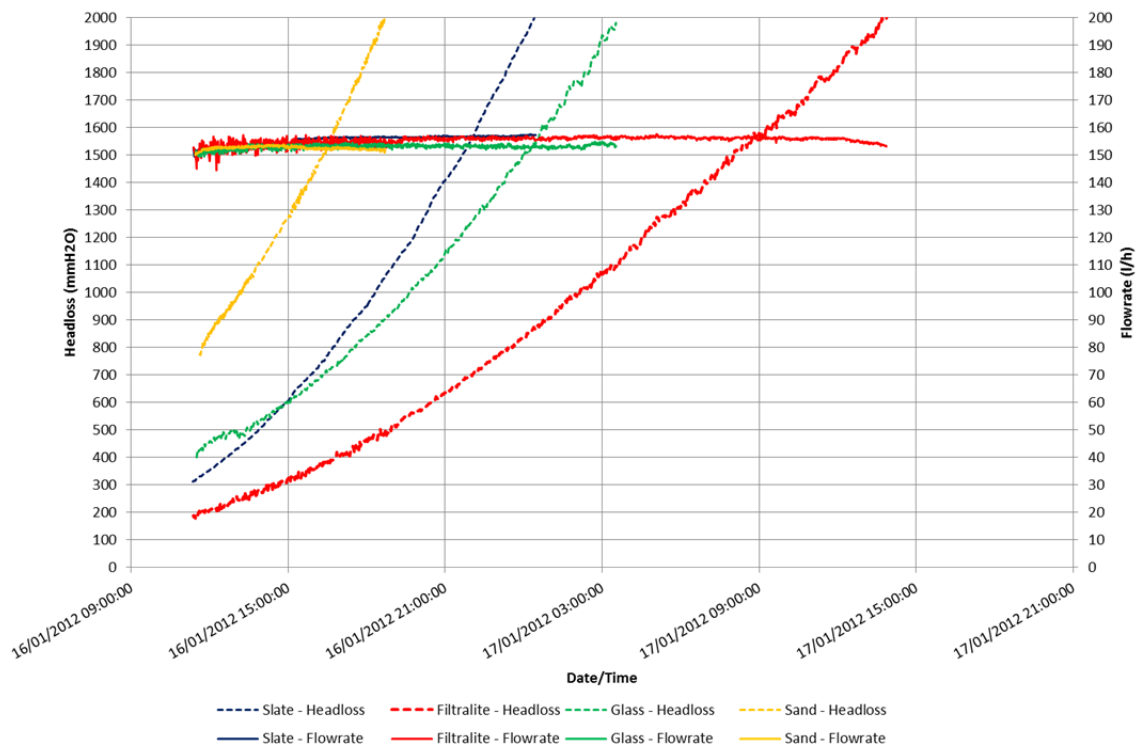
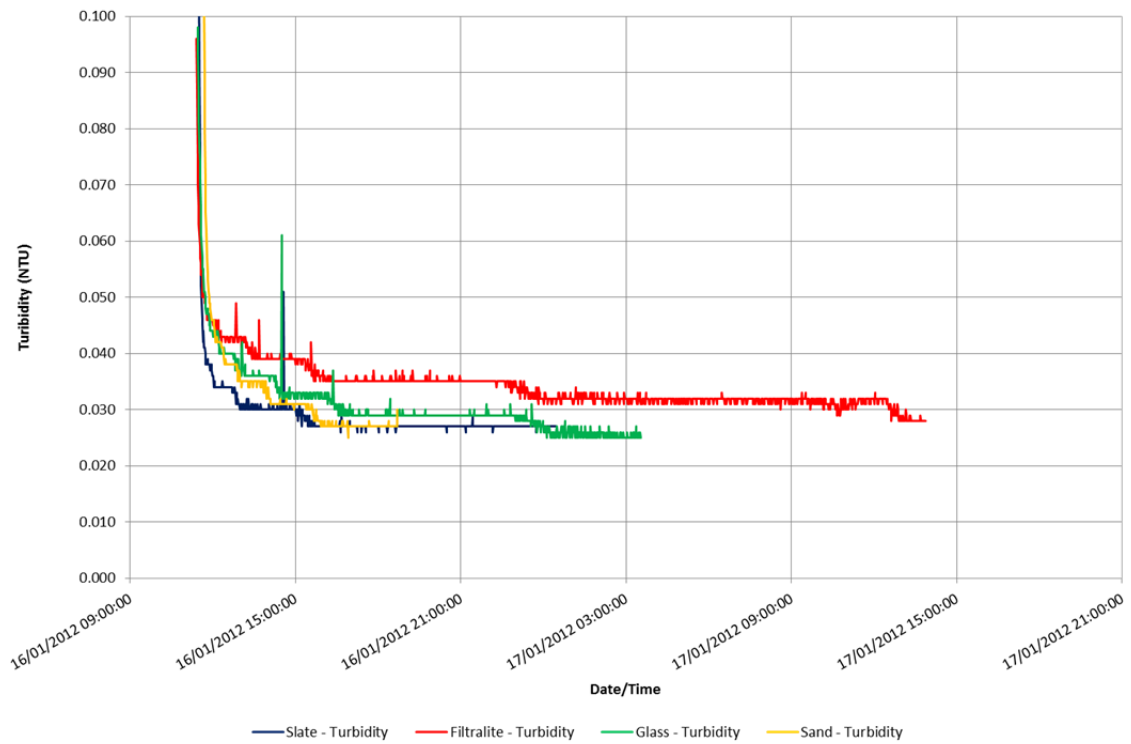
Test Run 2 – 13/01/2012

Flowrate – 3.43 m/h



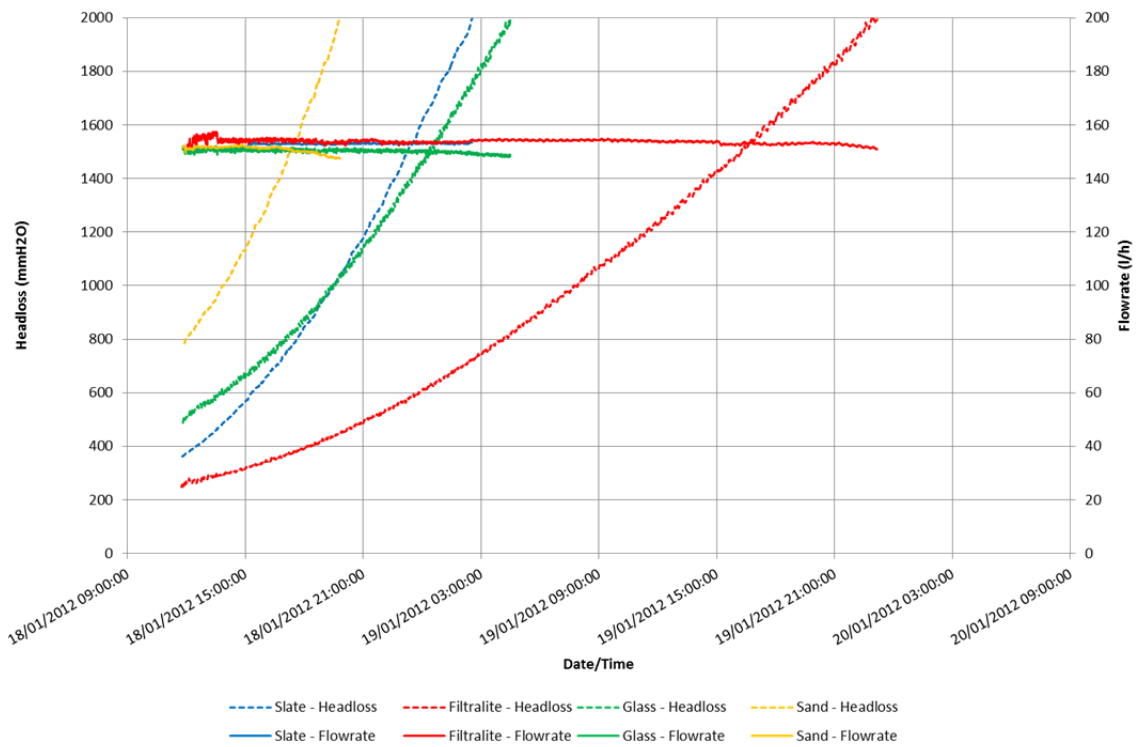
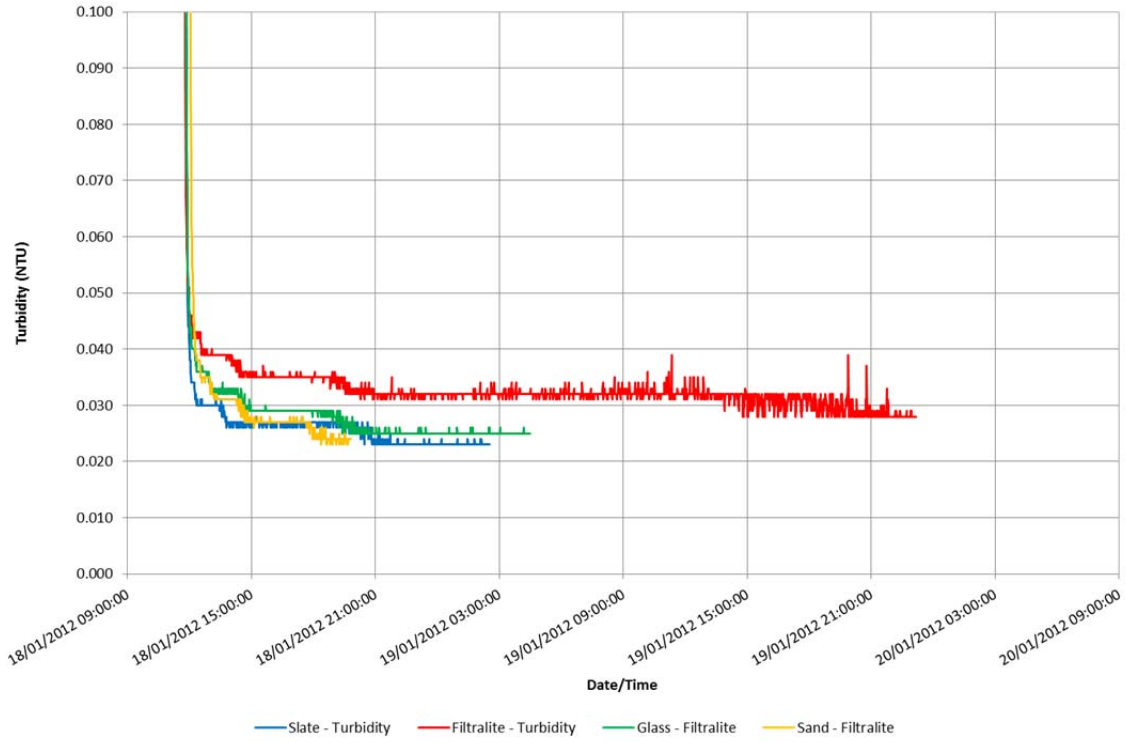
Test Run 3 – 16/01/2012

Flowrate – 8.73 m/h



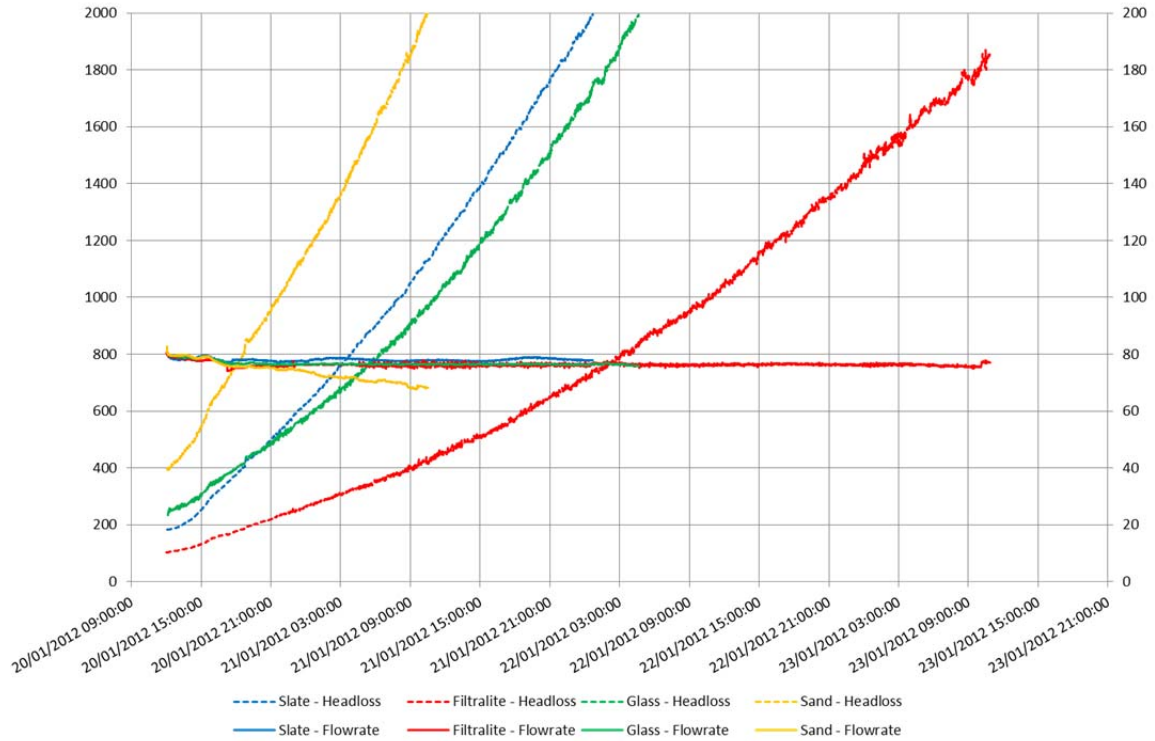
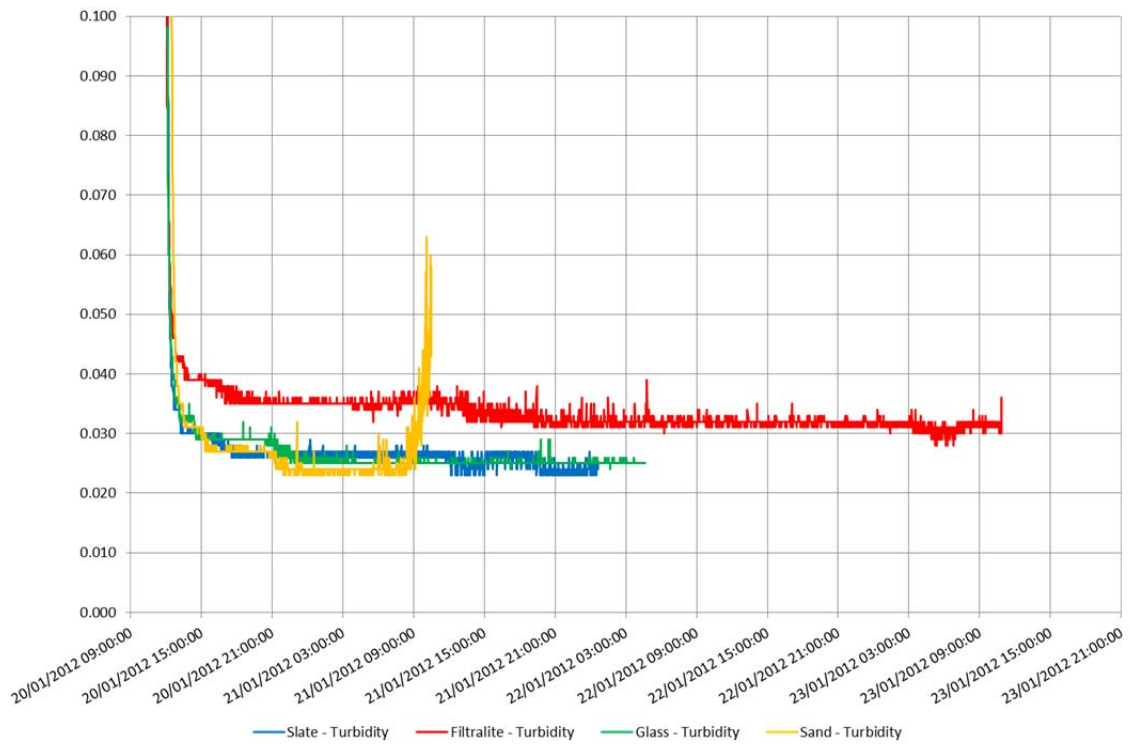
Test Run 4 – 18/01/2012

Flowrate – 8.59 m/h



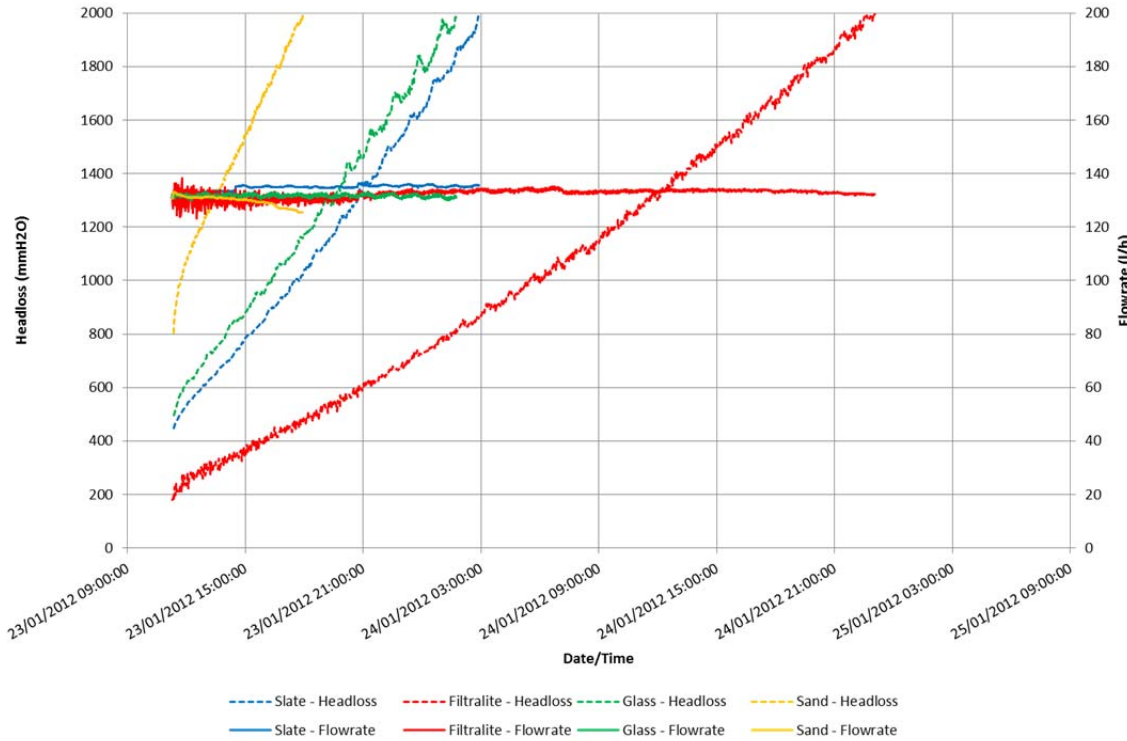
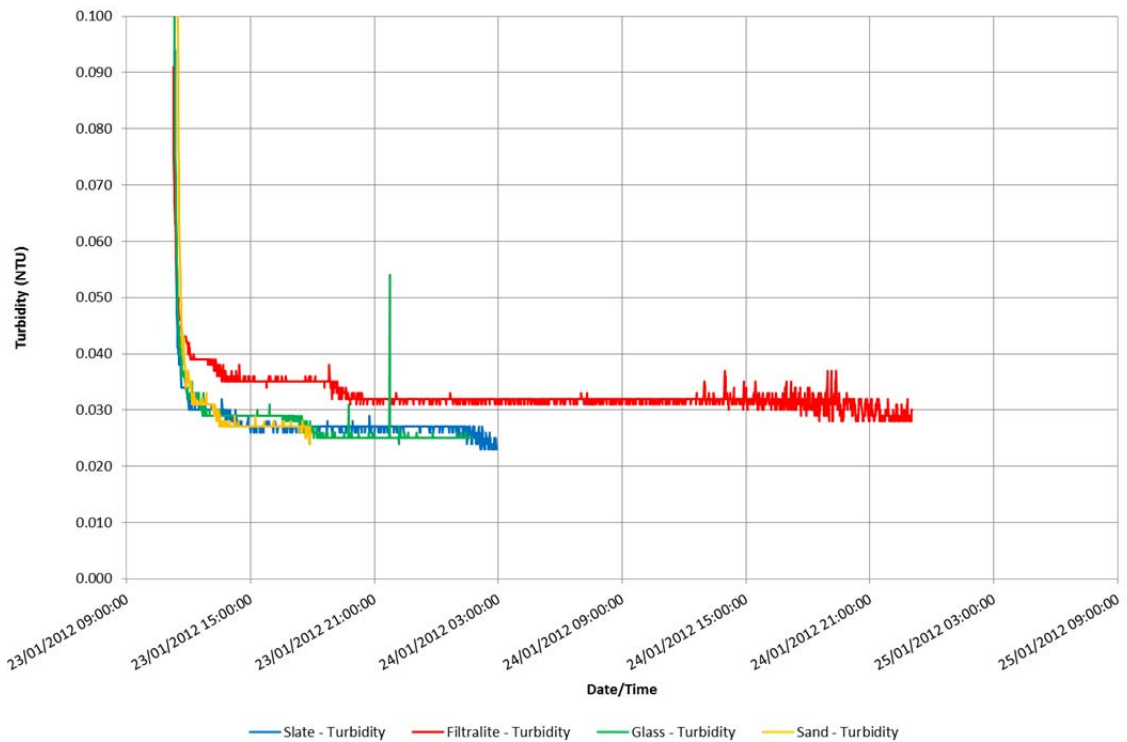
Test Run 5 – 20/01/2012

Flowrate – 4.32 m/h



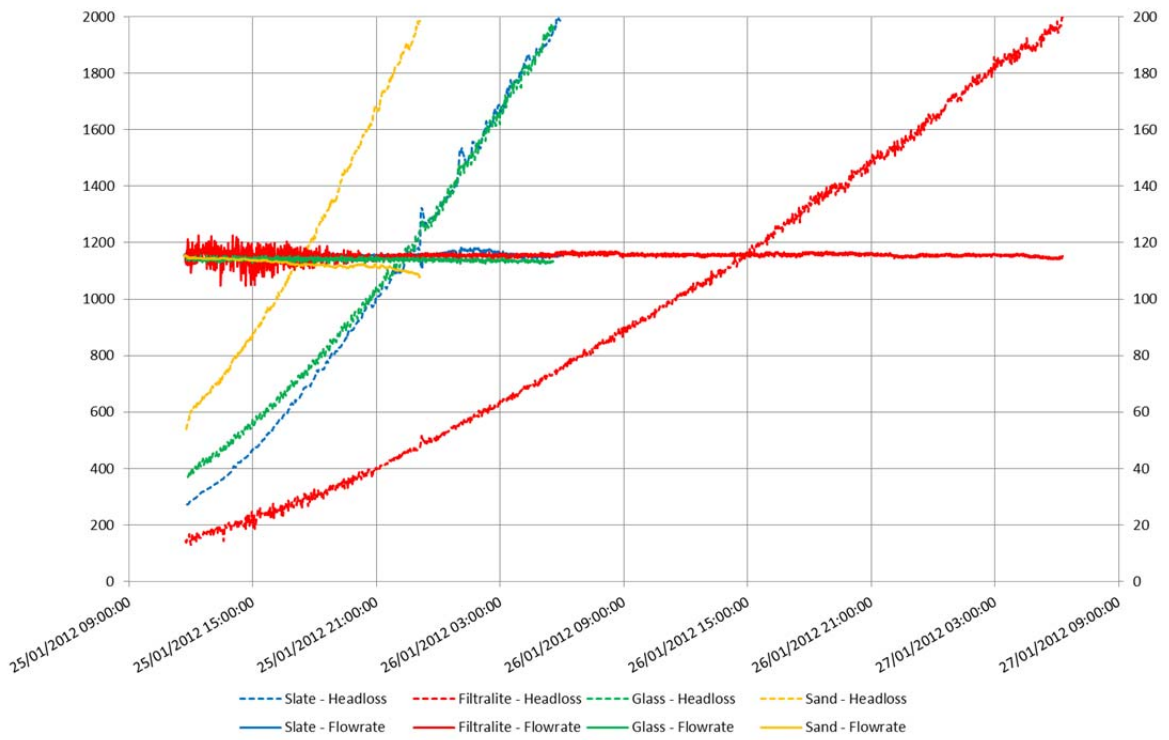
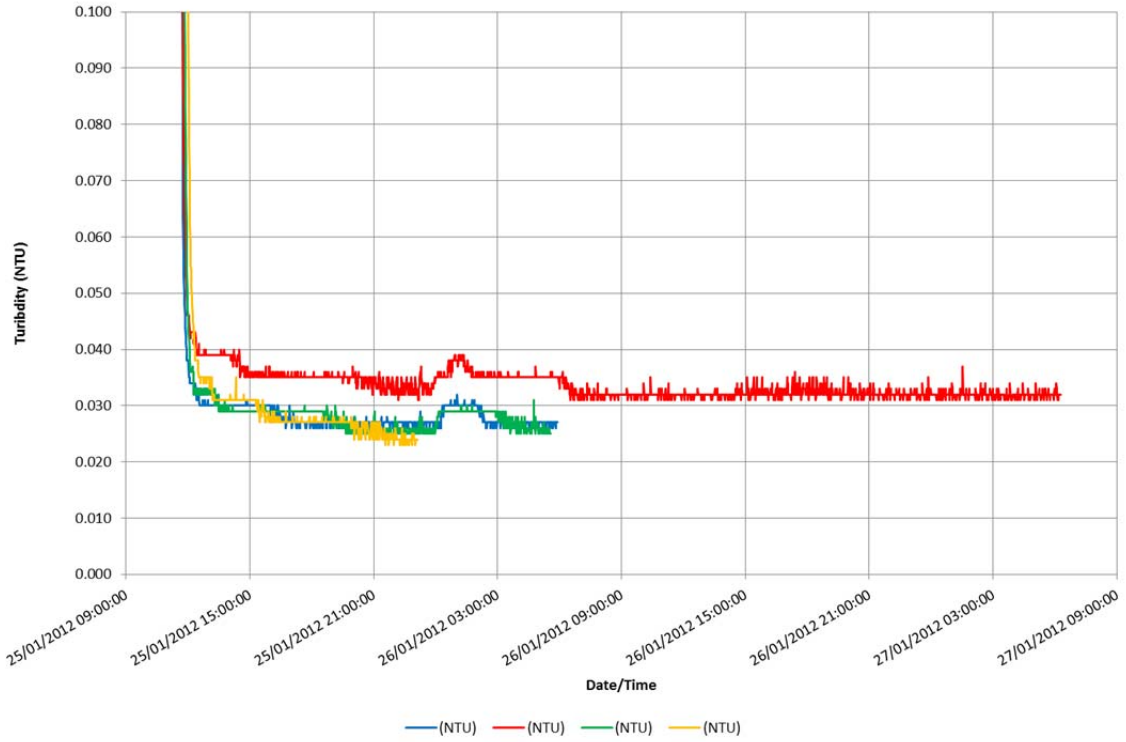
Test Run 6 – 23/01/2012

Flowrate – 7.48 m/h



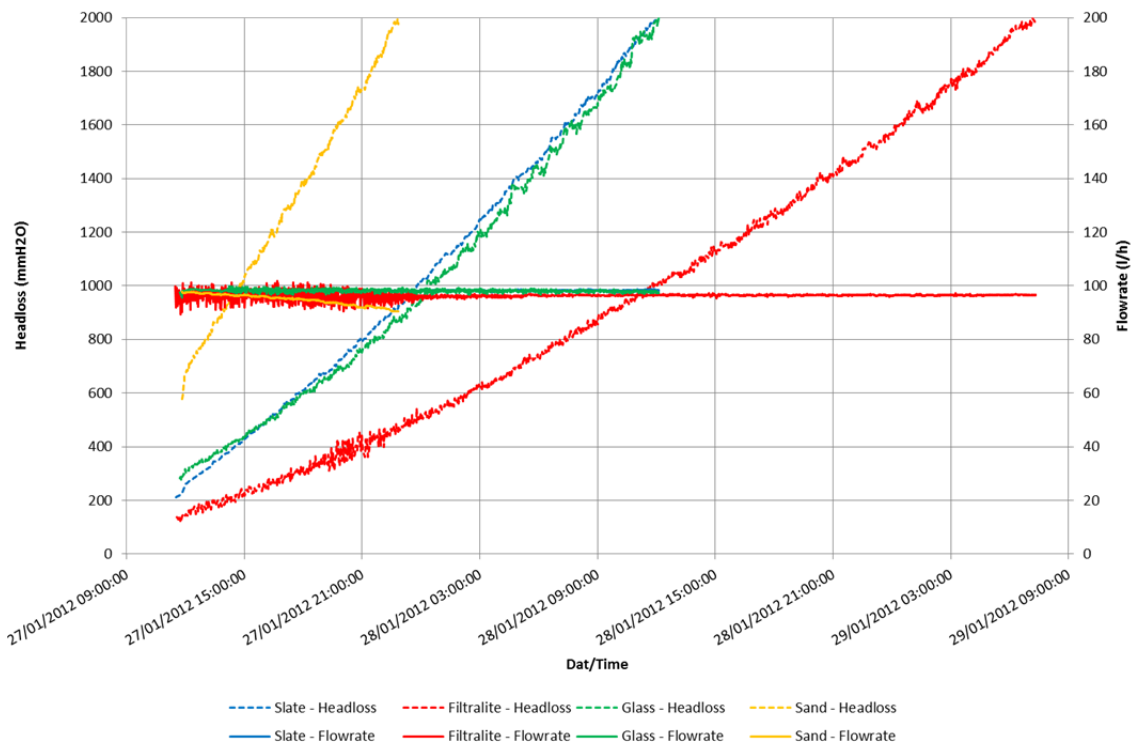
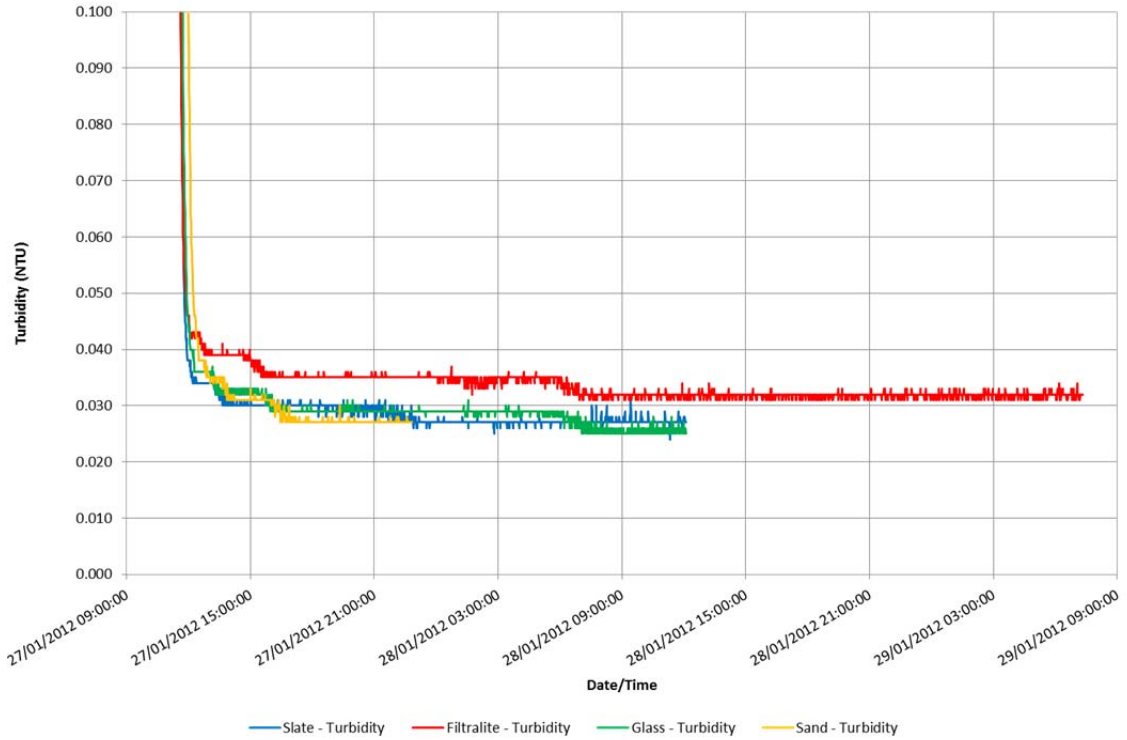
Test Run 7 – 25/01/2012

Flowrate – 6.47 m/h



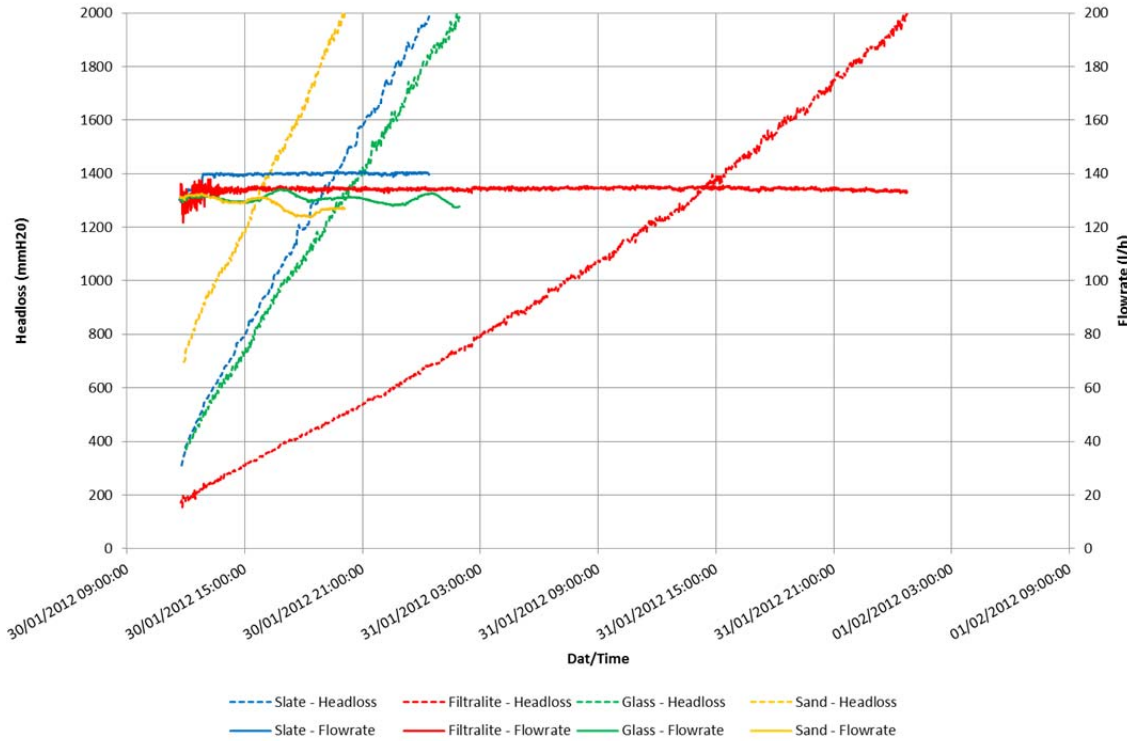
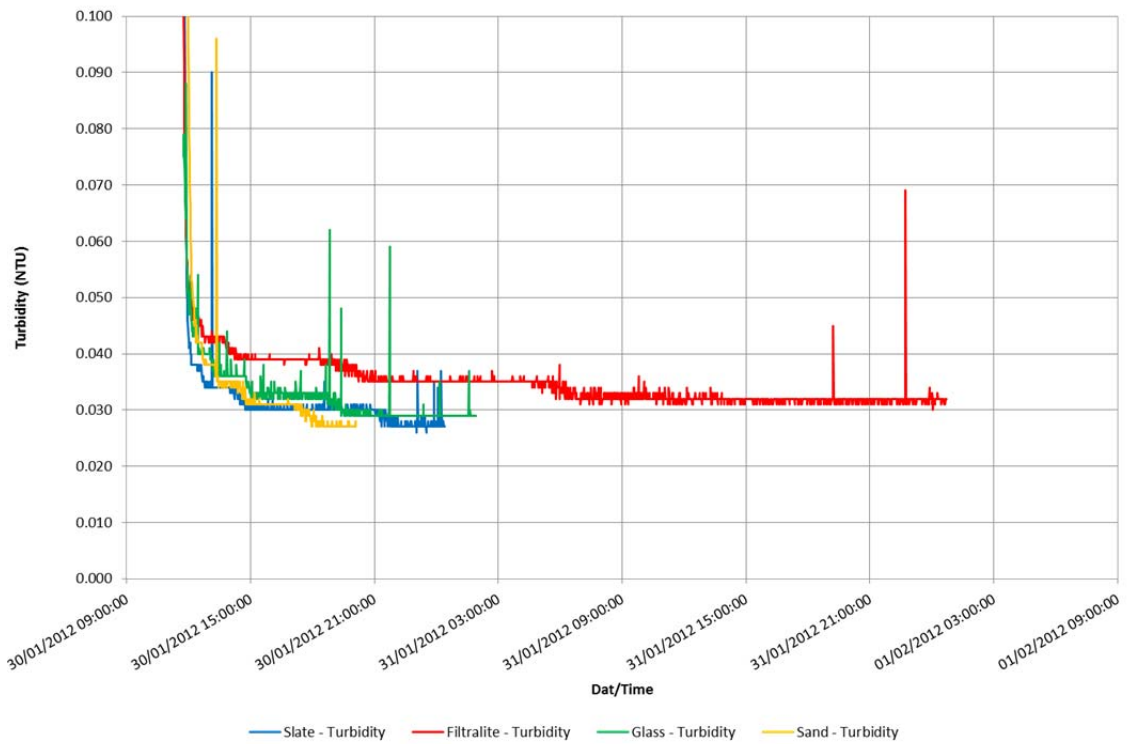
Test Run 8 – 27/01/2012

Flowrate – 5.48 m/h



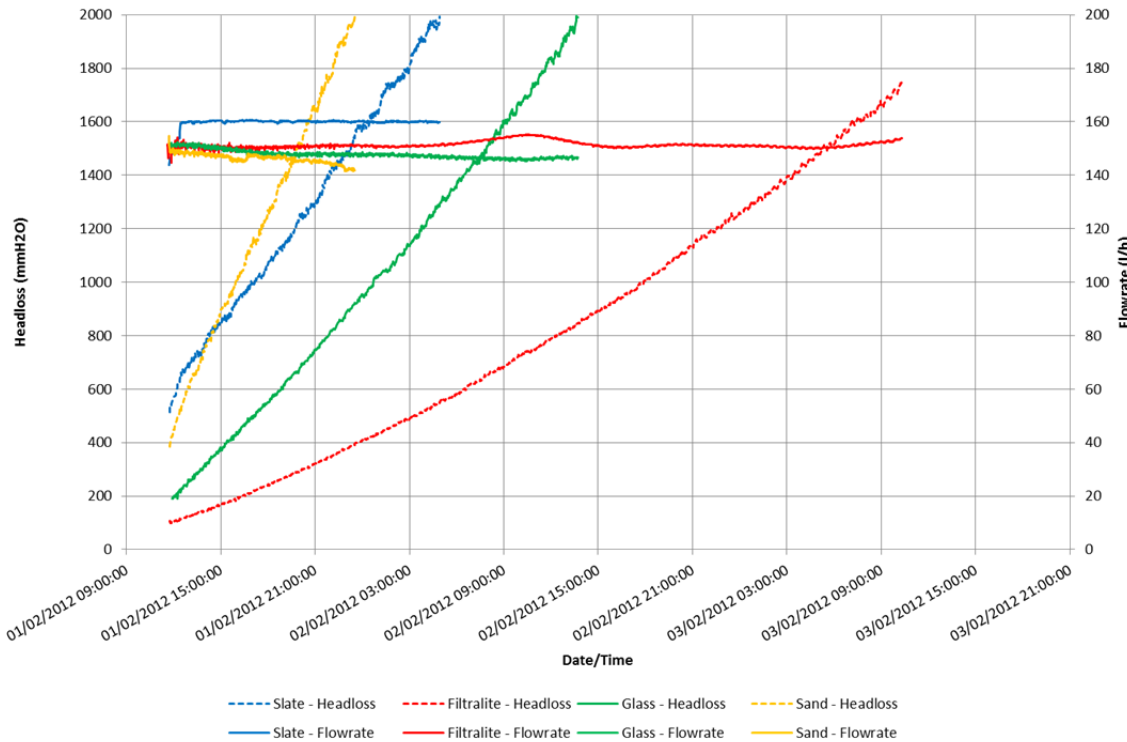
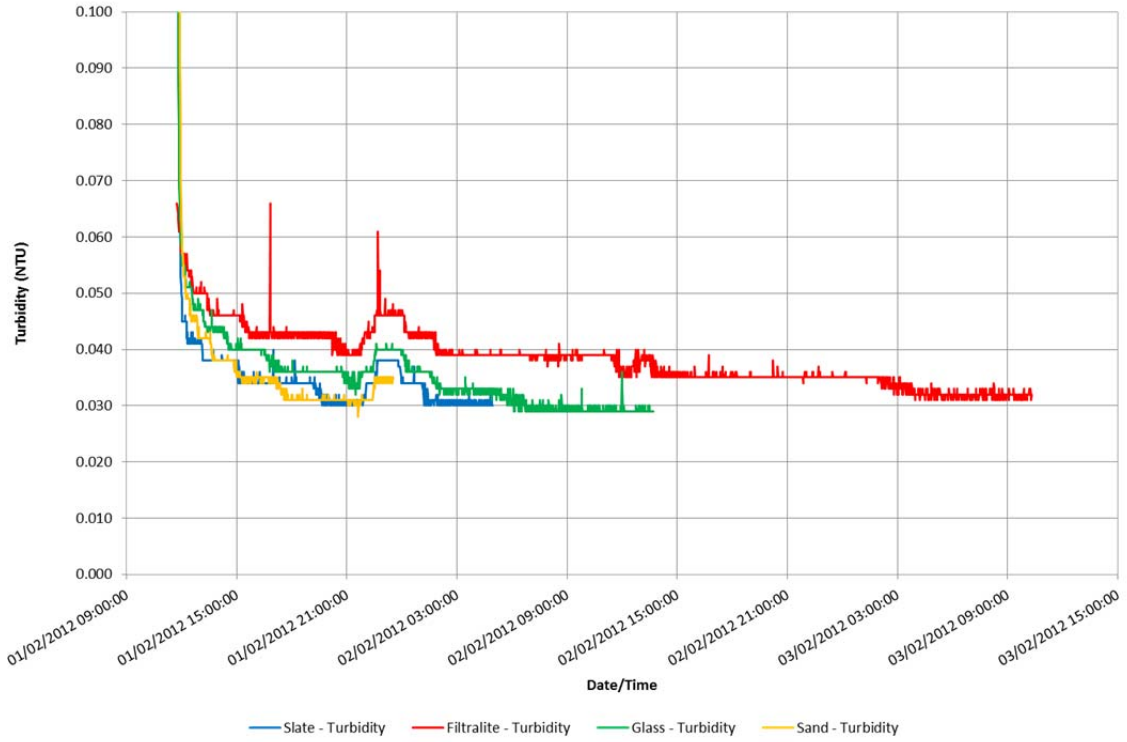
Test Run 9 – 30/01/2012

Flowrate – 7.54 m/h



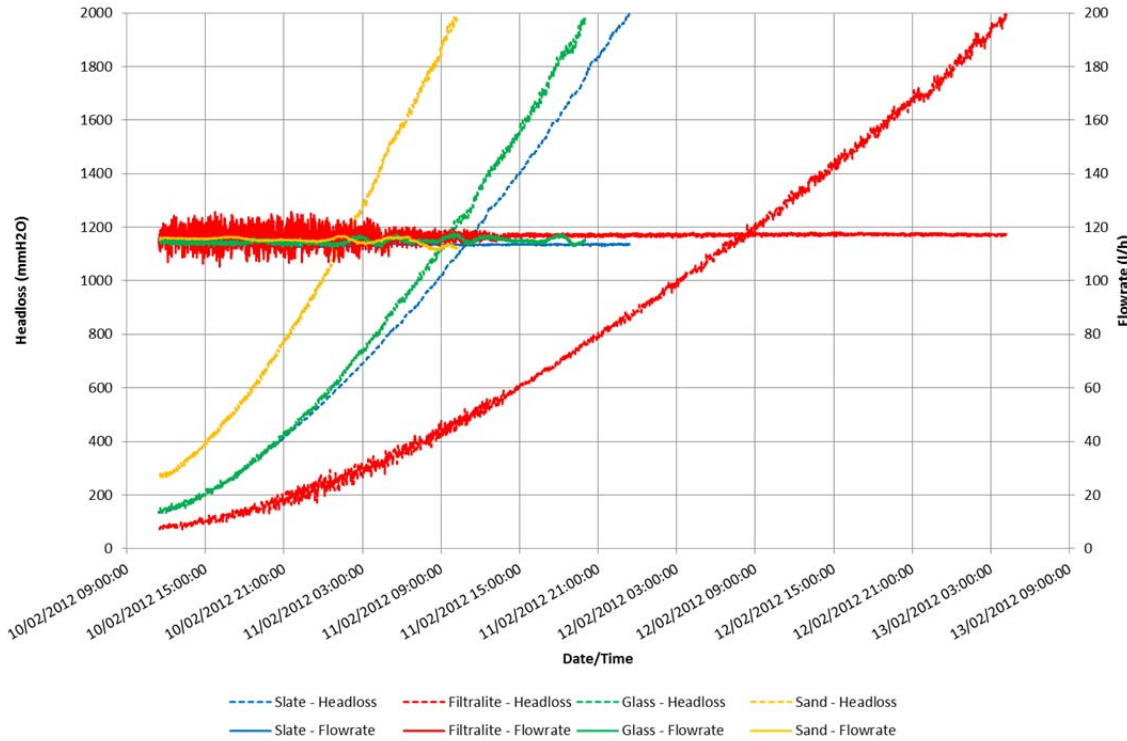
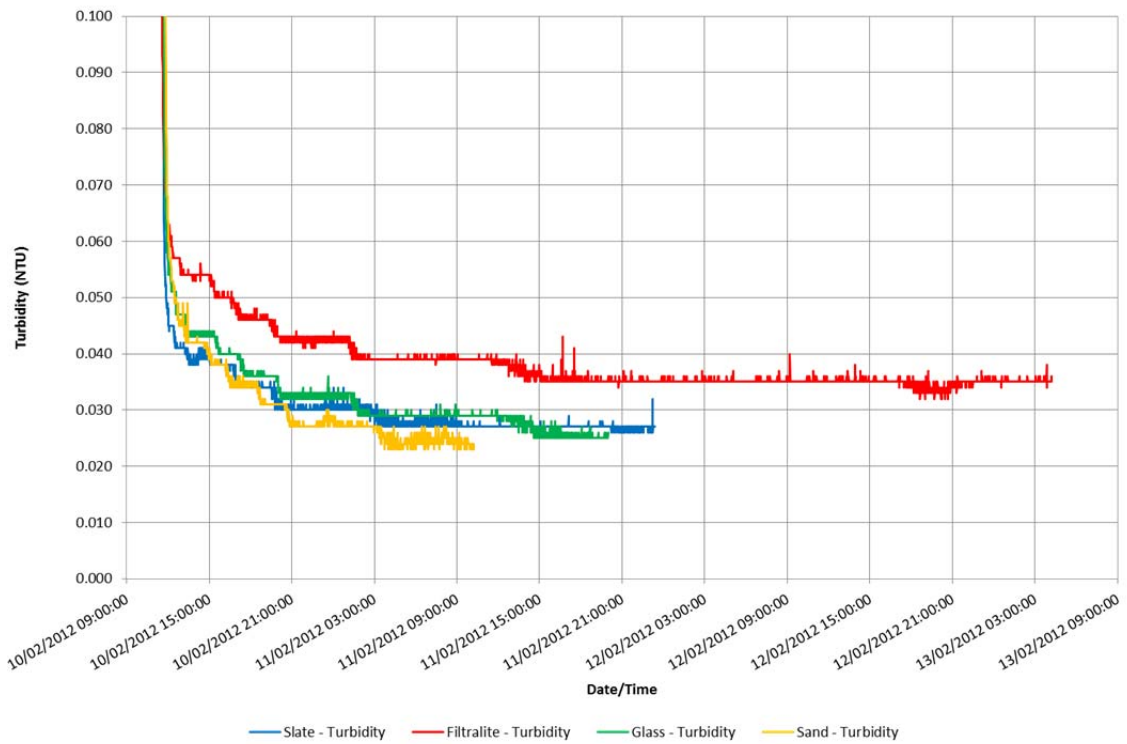
Test Run 10 – 01/02/2012

Flowrate – 8.56 m/h



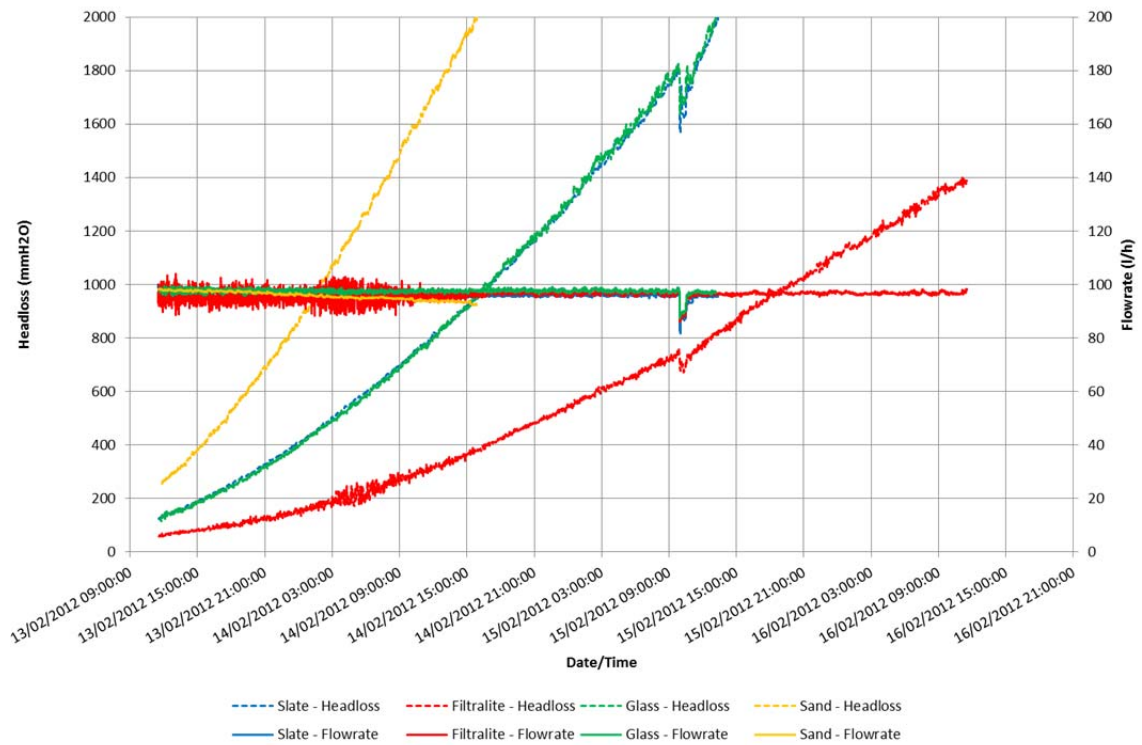
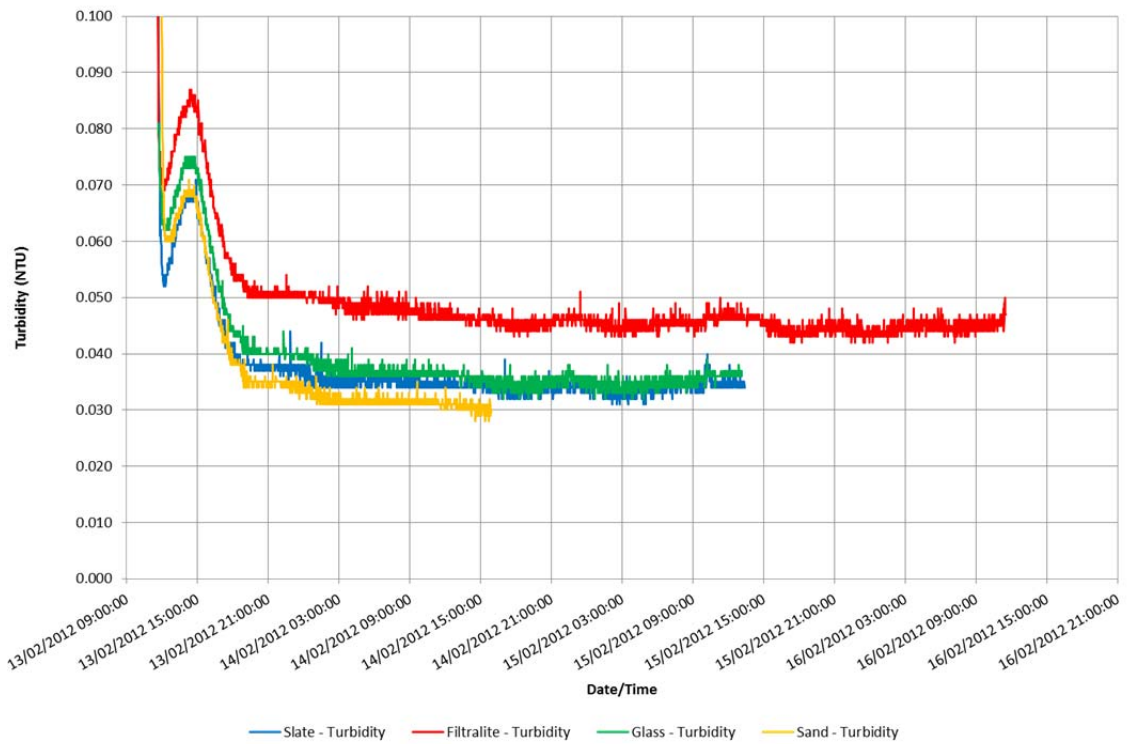
Test Run 12 – 10/02/2012

Flowrate – 6.51 m/h



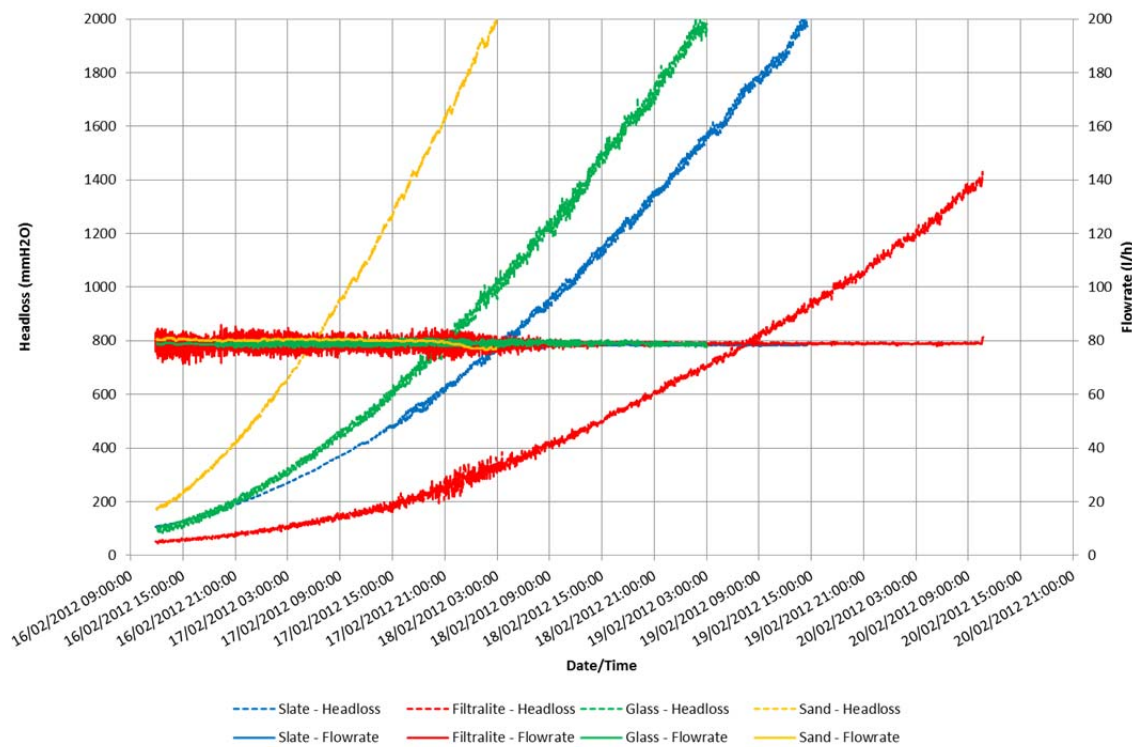
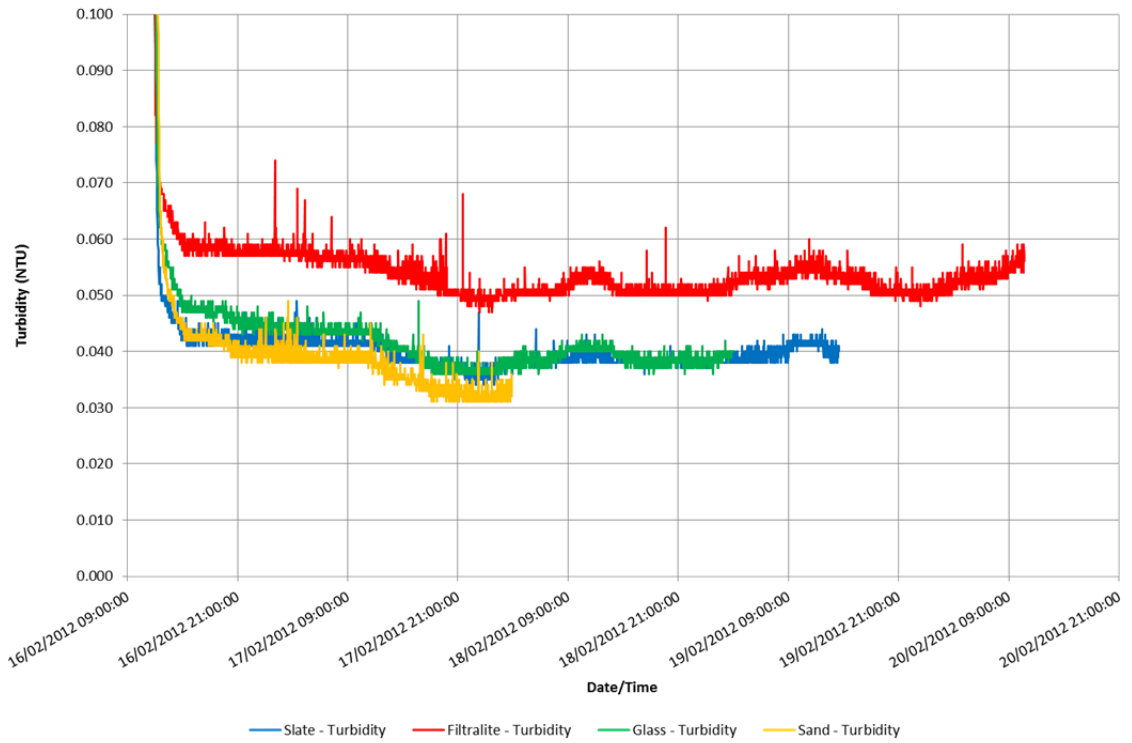
Test Run 13 – 13/02/2012

Flowrate – 5.45 m/h



Test Run 14 – 16/02/2012

Flowrate – 4.46 m/h



Test Run 15 – 20/02/2012

Flowrate – 2.88 m/h

